

UCLA

UCLA Electronic Theses and Dissertations

Title

Nickel-Catalyzed Cross-Coupling of Phenol Derivatives and Total Synthesis of Welwitindolinone Natural Products

Permalink

<https://escholarship.org/uc/item/8xk21825>

Author

Quasdorf, Kyle

Publication Date

2012

Peer reviewed|Thesis/dissertation

UNIVERSITY OF CALIFORNIA

Los Angeles

Nickel-Catalyzed Cross-Coupling of Phenol Derivatives and
Total Synthesis of Welwitindolinone Natural Products

A dissertation submitted in partial satisfaction of the
requirements for the degree Doctor of Philosophy
in Chemistry

by

Kyle Wayne Quasdorf

2012

© Copyright by
Kyle Wayne Quasdorf
2012

ABSTRACT OF THE DISSERTATION

Nickel-Catalyzed Cross-Coupling of Phenol Derivatives and Total Synthesis of Welwitindolinone Natural Products

by

Kyle Wayne Quasdorf

Doctor of Philosophy in Chemistry

University of California, Los Angeles, 2012

Professor Neil K. Garg, Chair

Chapter one provides a survey of the wide variety of unconventional phenol derivatives that are now available for use in traditional cross-coupling reactions. Emphasis is given to carbon-carbon (C-C) bond forming reactions with a brief discussion of other transformations. Chapters two and three are a discussion of our work in the field of nickel-catalyzed cross-coupling reactions of phenol derivatives. The use of aryl pivalates, sulfamates, carbamates, and carbonates in the nickel-catalyzed Suzuki-Miyaura coupling is described, along with synthetic applications utilizing these phenol derivatives. A computational and experimental mechanistic study for the cross-coupling of aryl sulfamates and carbamates is also reported.

Chapters four and five detail our efforts in the total synthesis of the welwitindolinone natural products. The enantiospecific total syntheses of (-)-*N*-methylwelwitindolinone C isothiocyanate and (-)-*N*-methylwelwitindolinone C isonitrile, as well as their respective C3-

hydroxylated analogs are reported. The synthetic routes feature an aryne cyclization to rapidly construct the [4.3.1]-bicyclic core of these molecules, as well as a late-stage intramolecular nitrene insertion to functionalize a bridgehead carbon. The strategic use of a deuterium kinetic isotope effect to improve the efficiency of the nitrene insertion is also discussed. A computational prediction for the stereochemical configuration at C3 of the hydroxylated welwitindolinones is presented, which was subsequently confirmed by experimental studies.

The dissertation of Kyle Wayne Quasdorf is approved.

Kendall N. Houk

Catherine F. Clarke

Yi Tang

Neil K. Garg, Committee Chair

University of California, Los Angeles

2012

For my parents, Don and Sheri Quasdorf

TABLE OF CONTENTS

Abstract.....	ii
Committee Page.....	iv
Dedication Page.....	v
Table of Contents.....	vi
List of Figures.....	xi
List of Schemes.....	xxi
List of Tables.....	xxvi
List of Abbreviations.....	xxviii
Acknowledgments.....	xxxii
Biographical Sketch.....	xxxvi
CHAPTER ONE: Nickel-Catalyzed Cross-Couplings of Unconventional Phenol Derivatives.....	1
1.1 Abstract.....	1
1.2 Introduction.....	1
1.3 Nickel-Catalyzed Cross-Couplings of Ethers.....	3
1.3.1 Kumada Couplings.....	3
1.3.2 Suzuki–Miyaura Couplings.....	8
1.4 Nickel-Catalyzed Cross-Couplings of Aryl and Vinyl Phosphates.....	10
1.4.1 Kumada Couplings.....	10
1.4.2 Suzuki–Miyaura Couplings.....	14
1.4.3 Negishi Couplings.....	17
1.5 Nickel-Catalyzed Cross-Couplings of Aryl and Vinyl Mesylates and Tosylates.....	18

1.5.1 Kumada Couplings.....	18
1.5.2 Suzuki–Miyaura Couplings.....	18
1.5.3 Heck Couplings.....	21
1.6 Nickel-Catalyzed Cross-Couplings of Aryl and Vinyl Esters.....	21
1.6.1 Suzuki–Miyaura Couplings.....	21
1.6.2 Negishi Couplings.....	27
1.6.3 Heck Couplings.....	27
1.6.4 C–H Azole Couplings.....	28
1.6.5 Palladium-Catalyzed Suzuki–Miyaura Couplings.....	28
1.7 Nickel-Catalyzed Cross-Couplings of Aryl and Vinyl Sulfamates.....	29
1.7.1 Kumada Couplings.....	29
1.7.2 Suzuki–Miyaura Couplings.....	31
1.8 Nickel-Catalyzed Cross-Couplings of Aryl and Vinyl Carbamates and Carbonates.....	34
1.8.1 Kumada Couplings.....	34
1.8.2 Suzuki–Miyaura Couplings.....	35
1.8.3 Negishi Couplings.....	38
1.9 Nickel-Catalyzed Cross-Couplings of Phenols.....	38
1.9.1 Kumada Couplings.....	38
1.9.2 Suzuki–Miyaura Couplings.....	39
1.10 Non Carbon–Carbon Bond Forming Reactions.....	40
1.10.1 Amination Reactions.....	40
1.10.2 Deoxygenation Reactions.....	46
1.10.3 Borylation Reactions.....	49

1.10.4 Phosphonylation Reactions.....	51
1.11 Conclusion.....	51
1.12 Notes and References.....	53
 CHAPTER TWO: Cross-Coupling Reactions of Aryl Pivalates with Boronic Acids	
2.1 Abstract.....	60
2.2 Introduction.....	60
2.3 Substrate Scope With Respect to the Pivalate Component.....	62
2.4 Substrate Scope With Respect to the Arylboronic Acid Component.....	64
2.5 One Pot Acylation / Cross-Coupling and Orthogonal Cross-Coupling Reactions.....	65
2.6 Conclusion.....	66
2.7 Experimental Section.....	67
2.7.1 Materials and Methods.....	67
2.7.2 Experimental Procedures.....	68
2.8 Notes and References.....	87
 APPENDIX ONE: Spectra Relevant to Chapter Two.....	
	91
 CHAPTER THREE: Suzuki–Miyaura Cross-Coupling of Aryl Carbamates and Sulfamates: Experimental and Computational Studies.....	
	133
3.1 Abstract.....	133
3.2 Introduction.....	134
3.3 Suzuki–Miyaura Cross-Coupling Reactions of Aryl <i>O</i> -Carbamates.....	136

3.4 Suzuki–Miyaura Cross-Coupling Reactions of Aryl <i>O</i> -Sulfamates.....	142
3.5 Suzuki–Miyaura Cross-Coupling Reactions of Heterocyclic <i>O</i> -Sulfamates.....	149
3.6 Mechanistic Studies.....	152
3.7 Synthetic Applications.....	159
3.8 Conclusion.....	164
3.9 Experimental Section.....	166
3.9.1 Materials and Methods.....	166
3.9.2 Experimental Procedures.....	167
3.10 Notes and References.....	185
APPENDIX TWO: Spectra Relevant to Chapter Three.....	195
CHAPTER FOUR: Total Synthesis of (–)- <i>N</i> -Methylwelwitindolinone C Isothiocyanate.....	237
4.1 Abstract.....	237
4.2 Introduction.....	237
4.3 Retrosynthetic Analysis of (–)- <i>N</i> -Methylwelwitindolinone C Isothiocyanate.....	238
4.4 Construction of the [4.3.1]-Bicyclic Framework.....	239
4.5 Introduction of the Vinyl Chloride and Oxindole Moieties.....	240
4.6 Completion of (–)- <i>N</i> -Methylwelwitindolinone C Isothiocyanate.....	241
4.7 Conclusion.....	243
4.8 Experimental Section.....	244
4.8.1 Materials and Methods.....	244
4.8.2 Experimental Procedures.....	245

4.9 Notes and References.....	262
APPENDIX THREE: Spectra Relevant to Chapter Four.....	267
CHAPTER FIVE: Total Synthesis of Oxidized Welwitindolinones and (-)- <i>N</i> - Methylwelwitindolinone C Isonitrile.....	295
5.1 Abstract.....	295
5.2 Introduction.....	295
5.3 Previous Total Synthesis of (-)- <i>N</i> -Methylwelwitindolinone C Isothiocyanate.....	296
5.4 Optimization of Nitrene Insertion.....	297
5.5 Syntheses of <i>N</i> -Methylwelwitindolinone C Isothiocyanate and <i>N</i> - Methylwelwitindolinone Isonitrile.....	299
5.6 Syntheses of the C3-hydroxylated Welwitindolinones.....	300
5.7 Computational and Experimental Studies to Establish the Stereochemistry of the C3- hydroxylated Welwitindolinones.....	301
5.8 Conclusion.....	303
5.9 Experimental Section.....	304
5.9.1 Materials and Methods.....	304
5.9.2 Experimental Procedures.....	305
5.9.3 Computational Data.....	314
5.10 Notes and References.....	344
APPENDIX FOUR: Spectra Relevant to Chapter Five.....	350

LIST OF FIGURES

CHAPTER ONE

Figure 1.1	Unconventional phenol derivatives in Ni-catalyzed cross-couplings.....	2
------------	--	---

CHAPTER TWO

Figure 2.1	Cross-coupling of <i>O</i> -acylated phenol derivatives.....	61
Figure 2.2	One-pot acylation/cross-coupling sequence and orthogonal cross-coupling reactions.....	66

APPENDIX ONE

Figure A1.1	¹ H NMR (500 MHz, CDCl ₃) of compound 2.1	92
Figure A1.2	Infrared spectrum of compound 2.1	93
Figure A1.3	¹³ C NMR (125 MHz, CDCl ₃) of compound 2.1	93
Figure A1.4	¹ H NMR (500 MHz, CDCl ₃) of compound 2.9	94
Figure A1.5	¹ H NMR (500 MHz, CDCl ₃) of compound 2.10	95
Figure A1.6	Infrared spectrum of compound 2.10	96
Figure A1.7	¹³ C NMR (125 MHz, CDCl ₃) of compound 2.10	96
Figure A1.8	¹ H NMR (500 MHz, CDCl ₃) of compound 2.11	97
Figure A1.9	Infrared spectrum of compound 2.11	98
Figure A1.10	¹³ C NMR (125 MHz, CDCl ₃) of compound 2.11	98
Figure A1.11	¹ H NMR (300 MHz, CDCl ₃) of compound 2.12	99
Figure A1.12	¹ H NMR (500 MHz, CDCl ₃) of compound 2.13	100

Figure A1.13	^1H NMR (500 MHz, CDCl_3) of compound 2.14	101
Figure A1.14	Infrared spectrum of compound 2.14	102
Figure A1.15	^{13}C NMR (125 MHz, CDCl_3) of compound 2.14	102
Figure A1.16	^1H NMR (500 MHz, CDCl_3) of compound 2.16	103
Figure A1.17	Infrared spectrum of compound 2.16	104
Figure A1.18	^{13}C NMR (125 MHz, CDCl_3) of compound 2.16	104
Figure A1.19	^1H NMR (500 MHz, CDCl_3) of compound 2.17	105
Figure A1.20	Infrared spectrum of compound 2.17	106
Figure A1.21	^{13}C NMR (125 MHz, CDCl_3) of compound 2.17	106
Figure A1.22	^1H NMR (500 MHz, CDCl_3) of compound 2.19	107
Figure A1.23	Infrared spectrum of compound 2.19	108
Figure A1.24	^{13}C NMR (125 MHz, CDCl_3) of compound 2.19	108
Figure A1.25	^1H NMR (500 MHz, CDCl_3) of compound 2.3a	109
Figure A1.26	^1H NMR (500 MHz, CDCl_3) of compound 2.21	110
Figure A1.27	^1H NMR (500 MHz, CDCl_3) of compound 2.22	111
Figure A1.28	Infrared spectrum of compound 2.22	112
Figure A1.29	^{13}C NMR (125 MHz, CDCl_3) of compound 2.22	112
Figure A1.30	^1H NMR (500 MHz, CDCl_3) of compound 2.23	113
Figure A1.31	Infrared spectrum of compound 2.23	114
Figure A1.32	^{13}C NMR (125 MHz, CDCl_3) of compound 2.23	114
Figure A1.33	^1H NMR (500 MHz, CDCl_3) of compound 2.24	115
Figure A1.34	^1H NMR (500 MHz, CDCl_3) of compound 2.25	116
Figure A1.35	^1H NMR (500 MHz, CDCl_3) of compound 2.26	117

Figure A1.36	^1H NMR (500 MHz, CDCl_3) of compound 2.27	118
Figure A1.37	^1H NMR (500 MHz, CDCl_3) of compound 2.28	119
Figure A1.38	^1H NMR (500 MHz, CDCl_3) of compound 2.3b	120
Figure A1.39	^1H NMR (500 MHz, CDCl_3) of compound 2.3c	121
Figure A1.40	^1H NMR (500 MHz, CDCl_3) of compound 2.3d	122
Figure A1.41	^1H NMR (500 MHz, CDCl_3) of compound 2.3e	123
Figure A1.42	^1H NMR (500 MHz, CDCl_3) of compound 2.3f	124
Figure A1.43	^1H NMR (500 MHz, CDCl_3) of compound 2.5	125
Figure A1.44	Infrared spectrum of compound 2.5	126
Figure A1.45	^{13}C NMR (125 MHz, CDCl_3) of compound 2.5	126
Figure A1.46	^1H NMR (500 MHz, CDCl_3) of compound 2.6	127
Figure A1.47	Infrared spectrum of compound 2.6	128
Figure A1.48	^{13}C NMR (125 MHz, CDCl_3) of compound 2.6	128
Figure A1.49	^1H NMR (500 MHz, CDCl_3) of compound 2.7	129
Figure A1.50	Infrared spectrum of compound 2.7	130
Figure A1.51	^{13}C NMR (125 MHz, CDCl_3) of compound 2.7	130
Figure A1.52	^1H NMR (500 MHz, CDCl_3) of compound 2.8	131
Figure A1.53	Infrared spectrum of compound 2.8	132
Figure A1.54	^{13}C NMR (125 MHz, CDCl_3) of compound 2.8	132

CHAPTER THREE

Figure 3.1	Phenol-based cross-coupling partners.....	134
------------	---	-----

Figure 3.2	Gibbs free energy profile of Ni-catalyzed Suzuki–Miyaura cross-coupling reaction of phenyl <i>N,N</i> -dimethyl <i>O</i> -carbamate 3.15 with phenylboronic acid.....	153
Figure 3.3	Gibbs free energy profile of the Ni-catalyzed Suzuki–Miyaura cross-coupling reaction of <i>N,N</i> -dimethyl phenyl <i>O</i> -sulfamate with phenylboronic acid.....	156
Figure 3.4	Transition state structures of Ni-catalyzed oxidative additions of (a) <i>N,N</i> -dimethyl phenyl <i>O</i> -carbamate and (b) <i>N,N</i> -dimethyl phenyl <i>O</i> -sulfamate.....	157
Figure 3.5	Qualitative relative rates of cross-coupling depending on boronic acid..	158
Figure 3.6	Intermolecular competition experiments of aryl sulfamates and aryl carbamates.....	164

APPENDIX TWO

Figure A2.1	¹ H NMR (500 MHz, CDCl ₃) of compound 3.57	196
Figure A2.2	Infrared spectrum of compound 3.57	197
Figure A2.3	¹³ C NMR (125 MHz, CDCl ₃) of compound 3.57	197
Figure A2.4	¹ H NMR (500 MHz, CDCl ₃) of compound 3.61	198
Figure A2.5	Infrared spectrum of compound 3.61	199
Figure A2.6	¹³ C NMR (125 MHz, CDCl ₃) of compound 3.61	199
Figure A2.7	¹ H NMR (500 MHz, CDCl ₃) of compound 3.62	200
Figure A2.8	¹ H NMR (500 MHz, CDCl ₃) of compound 3.63	201
Figure A2.9	Infrared spectrum of compound 3.63	202

Figure A2.10	^{13}C NMR (125 MHz, CDCl_3) of compound 3.63	202
Figure A2.11	^1H NMR (500 MHz, CDCl_3) of compound 3.65	203
Figure A2.12	Infrared spectrum of compound 3.65	204
Figure A2.13	^{13}C NMR (125 MHz, CDCl_3) of compound 3.65	204
Figure A2.14	^1H NMR (500 MHz, CDCl_3) of compound 3.12	205
Figure A2.15	Infrared spectrum of compound 3.12	206
Figure A2.16	^{13}C NMR (125 MHz, CDCl_3) of compound 3.12	206
Figure A2.17	^1H NMR (500 MHz, CDCl_3) of compound 3.66	207
Figure A2.18	Infrared spectrum of compound 3.66	208
Figure A2.19	^{13}C NMR (125 MHz, CDCl_3) of compound 3.66	208
Figure A2.20	^1H NMR (500 MHz, CDCl_3) of compound 3.67	209
Figure A2.21	^1H NMR (500 MHz, CDCl_3) of compound 3.68	210
Figure A2.22	^1H NMR (500 MHz, CDCl_3) of compound 3.59	211
Figure A2.23	^1H NMR (500 MHz, CDCl_3) of compound 3.70	212
Figure A2.24	^1H NMR (500 MHz, C_6D_6) of compound 3.72	213
Figure A2.25	Infrared spectrum of compound 3.72	214
Figure A2.26	^{13}C NMR (125 MHz, C_6D_6) of compound 3.72	214
Figure A2.27	^1H NMR (400 MHz, CDCl_3) of compound 3.73	215
Figure A2.28	^1H NMR (500 MHz, CDCl_3) of compound 3.75	216
Figure A2.29	Infrared spectrum of compound 3.75	217
Figure A2.30	^{13}C NMR (125 MHz, CDCl_3) of compound 3.75	217
Figure A2.31	^1H NMR (500 MHz, CDCl_3) of compound 3.77	218
Figure A2.32	Infrared spectrum of compound 3.77	219

Figure A2.33	^{13}C NMR (125 MHz, CDCl_3) of compound 3.77	219
Figure A2.34	^1H NMR (500 MHz, CDCl_3) of compound 3.78	220
Figure A2.35	Infrared spectrum of compound 3.78	221
Figure A2.36	^{13}C NMR (125 MHz, CDCl_3) of compound 3.78	221
Figure A2.37	^1H NMR (500 MHz, CDCl_3) of compound 3.79	222
Figure A2.38	^1H NMR (400 MHz, CDCl_3) of compound 3.80	223
Figure A2.39	^1H NMR (500 MHz, CDCl_3) of compound 3.81	224
Figure A2.40	^1H NMR (400 MHz, CDCl_3) of compound 3.82	225
Figure A2.41	^1H NMR (400 MHz, CDCl_3) of compound 3.83	226
Figure A2.42	Infrared spectrum of compound 3.83	227
Figure A2.43	^{13}C NMR (100 MHz, CDCl_3) of compound 3.83	227
Figure A2.44	^1H NMR (400 MHz, CDCl_3) of compound 3.86	228
Figure A2.45	Infrared spectrum of compound 3.86	229
Figure A2.46	^{13}C NMR (125 MHz, CDCl_3) of compound 3.86	229
Figure A2.47	^1H NMR (400 MHz, CDCl_3) of compound 3.88	230
Figure A2.48	^1H NMR (400 MHz, CDCl_3) of compound 3.90	231
Figure A2.49	Infrared spectrum of compound 3.90	232
Figure A2.50	^{13}C NMR (125 MHz, CDCl_3) of compound 3.90	232
Figure A2.51	^1H NMR (500 MHz, CDCl_3) of compound 3.91	233
Figure A2.52	Infrared spectrum of compound 3.91	234
Figure A2.53	^{13}C NMR (125 MHz, CDCl_3) of compound 3.91	234
Figure A2.54	^1H NMR (500 MHz, CDCl_3) of compound 3.14	235
Figure A2.55	Infrared spectrum of compound 3.14	236

Figure A2.56	^{13}C NMR (125 MHz, CDCl_3) of compound 3.14	236
--------------	---	-----

CHAPTER FOUR

Figure 4.1	[4.3.1]-Bicyclic welwitindolinones 4.1–4.3	238
------------	---	-----

APPENDIX THREE

Figure A3.1	^1H NMR (500 MHz, CDCl_3) of compound 4.11	268
Figure A3.2	Infrared spectrum of compound 4.11	269
Figure A3.3	^{13}C NMR (125 MHz, CDCl_3) of compound 4.11	269
Figure A3.4	^1H NMR (500 MHz, CDCl_3) of compound 4.12	270
Figure A3.5	Infrared spectrum of compound 4.12	271
Figure A3.6	^{13}C NMR (125 MHz, CDCl_3) of compound 4.12	271
Figure A3.7	^1H NMR (500 MHz, CDCl_3) of compound 4.13	272
Figure A3.8	Infrared spectrum of compound 4.13	273
Figure A3.9	^{13}C NMR (125 MHz, CDCl_3) of compound 4.13	273
Figure A3.10	^1H NMR (500 MHz, CDCl_3) of compound 4.14	274
Figure A3.11	Infrared spectrum of compound 4.14	275
Figure A3.12	^{13}C NMR (125 MHz, CDCl_3) of compound 4.14	275
Figure A3.13	^1H NMR (500 MHz, CDCl_3) of compound 4.23	276
Figure A3.14	^1H NMR (500 MHz, CDCl_3) of compound 4.16	277
Figure A3.15	Infrared spectrum of compound 4.16	278
Figure A3.16	^{13}C NMR (125 MHz, CDCl_3) of compound 4.16	278
Figure A3.17	^1H NMR (500 MHz, CDCl_3) of compound 4.24	279

Figure A3.18	^1H NMR (500 MHz, CDCl_3) of compound 4.17	280
Figure A3.19	Infrared spectrum of compound 4.17	281
Figure A3.20	^{13}C NMR (125 MHz, CDCl_3) of compound 4.17	281
Figure A3.21	^1H NMR (500 MHz, CDCl_3) of compound 4.18	282
Figure A3.22	Infrared spectrum of compound 4.18	283
Figure A3.23	^{13}C NMR (125 MHz, CDCl_3) of compound 4.18	283
Figure A3.24	^1H NMR (500 MHz, CDCl_3) of compound 4.4	284
Figure A3.25	Infrared spectrum of compound 4.4	285
Figure A3.26	^{13}C NMR (125 MHz, CDCl_3) of compound 4.4	285
Figure A3.27	^1H NMR (500 MHz, CDCl_3) of compound 4.25	286
Figure A3.28	^1H NMR (500 MHz, CDCl_3) of compound 4.19	287
Figure A3.29	Infrared spectrum of compound 4.19	288
Figure A3.30	^{13}C NMR (125 MHz, CDCl_3) of compound 4.19	288
Figure A3.31	^1H NMR (500 MHz, CDCl_3) of compound 4.20	289
Figure A3.32	Infrared spectrum of compound 4.20	290
Figure A3.33	^{13}C NMR (125 MHz, CDCl_3) of compound 4.20	290
Figure A3.34	^1H NMR (500 MHz, CDCl_3) of compound 4.21	291
Figure A3.35	Infrared spectrum of compound 4.21	292
Figure A3.36	^{13}C NMR (125 MHz, CDCl_3) of compound 4.21	292
Figure A3.37	^1H NMR (500 MHz, CDCl_3) of compound 4.1	293
Figure A3.38	Infrared spectrum of compound 4.1	294
Figure A3.39	^{13}C NMR (125 MHz, CDCl_3) of compound 4.1	294

CHAPTER FIVE

Figure 5.1	Welwitindolinones 5.1–5.5	296
Figure 5.2	Nitrene insertion of substrates 5.10a and 5.10b	298
Figure 5.3	Total synthesis of oxidized welwitindolinones 5.3 and 5.4	301
Figure 5.4	Structures of 5.3 and 5.4 , in addition to C3 epimers, and summary of computational findings.....	302

APPENDIX FOUR

Figure A4.1	¹ H NMR (500 MHz, CDCl ₃) of compound 5.9	351
Figure A4.2	Infrared spectrum of compound 5.9	352
Figure A4.3	¹³ C NMR (125 MHz, CDCl ₃) of compound 5.9	352
Figure A4.4	¹ H NMR (500 MHz, CDCl ₃) of compound 5.15	353
Figure A4.5	¹ H NMR (500 MHz, CDCl ₃) of compound 5.10b	354
Figure A4.6	² H NMR (77 MHz, CDCl ₃) of compound 5.10b	355
Figure A4.7	Infrared spectrum of compound 5.10b	356
Figure A4.8	¹³ C NMR (125 MHz, CDCl ₃) of compound 5.10b	356
Figure A4.9	¹ H NMR (500 MHz, CDCl ₃) of compounds 5.11b	357
Figure A4.10	² H NMR (77 MHz, CDCl ₃) of compound 5.11b	358
Figure A4.11	Infrared spectrum of compound 5.11b	359
Figure A4.12	¹³ C NMR (125 MHz, CDCl ₃) of compound 5.11b	359
Figure A4.13	¹ H NMR (500 MHz, CDCl ₃) of compound 5.12	360
Figure A4.14	Infrared spectrum of compound 5.12	361
Figure A4.15	¹³ C NMR (125 MHz, CDCl ₃) of compound 5.12	361

Figure A4.16	^1H NMR (500 MHz, CDCl_3) of compound 5.2	362
Figure A4.17	Infrared spectrum of compound 5.2	363
Figure A4.18	^{13}C NMR (125 MHz, CDCl_3) of compound 5.2	363
Figure A4.19	^1H NMR (500 MHz, CD_2Cl_2) of compound 5.4	364
Figure A4.20	Infrared spectrum of compound 5.4	365
Figure A4.21	^{13}C NMR (125 MHz, C_6D_6) of compound 5.4	365
Figure A4.22	^1H NMR (500 MHz, CD_2Cl_2) of compound 5.3	366
Figure A4.23	Infrared spectrum of compound 5.3	367
Figure A4.24	^{13}C NMR (125 MHz, CD_2Cl_2) of compound 5.3	367
Figure A4.25	^1H NMR (500 MHz, CDCl_3) of compound 5.14	368
Figure A4.26	Infrared spectrum of compound 5.14	369
Figure A4.27	^{13}C NMR (125 MHz, CDCl_3) of compound 5.14	369

LIST OF SCHEMES

CHAPTER ONE

Scheme 1.1	Wenkert's Kumada coupling of aryl and vinyl ethers.....	3
Scheme 1.2	Dankwardt's Kumada coupling of aryl ethers.....	4
Scheme 1.3	Shi's Kumada coupling of aryl ethers.....	5
Scheme 1.4	Shi's Kumada coupling of benzylic ethers.....	6
Scheme 1.5	Wang's Kumada coupling of aryl and alkenyl ethers.....	7
Scheme 1.6	Kumada's coupling of aryl silyl ethers.....	8
Scheme 1.7	Chatani's Suzuki–Miyaura coupling of aryl ethers.....	8
Scheme 1.8	Doyle's Suzuki–Miyaura coupling of styrenyl epoxides.....	9
Scheme 1.9	Doyle's Suzuki–Miyaura coupling of <i>N,O</i> - and chromene acetals.....	10
Scheme 1.10	Kumada's coupling of vinyl phosphates.....	11
Scheme 1.11	Kumada's coupling of aryl phosphates.....	11
Scheme 1.12	Nakamura's Kumada coupling of aryl phosphates.....	12
Scheme 1.13	Kumada couplings of phosphates in drug discovery.....	13
Scheme 1.14	Yamada's fuscol synthesis.....	14
Scheme 1.15	Lu's cryptotanshinone and tanshinone IIA synthesis.....	14
Scheme 1.16	Nan and Yang's Suzuki–Miyaura coupling of vinyl phosphates.....	15
Scheme 1.17	Skrydstrup's Suzuki–Miyaura coupling of vinyl phosphates.....	15
Scheme 1.18	Zhao and Cheng's Suzuki–Miyaura coupling of aryl phosphates.....	16
Scheme 1.19	Han's Suzuki–Miyaura coupling of aryl phosphoramides.....	17
Scheme 1.20	Wu and Yang's Negishi coupling of coumarin derived phosphates.....	17

Scheme 1.21	Percec's Kumada coupling of aryl mesylates.....	18
Scheme 1.22	Percec's Suzuki–Miyaura coupling of aryl mesylates.....	19
Scheme 1.23	Zim and Monterio's Suzuki–Miyaura coupling of aryl tosylates.....	19
Scheme 1.24	Yang's Suzuki–Miyaura coupling of aryl tosylates.....	20
Scheme 1.25	Skrydstrup's Heck coupling of aryl sulfonates.....	21
Scheme 1.26	Garg's Suzuki–Miyaura coupling of aryl pivalates.....	22
Scheme 1.27	Shi's Suzuki–Miyaura coupling of aryl esters.....	23
Scheme 1.28	Shi's Suzuki–Miyaura coupling of aryl pivalates.....	23
Scheme 1.29	Shi's triaryl synthesis.....	24
Scheme 1.30	Garg's triaryl synthesis.....	25
Scheme 1.31	Garg and Shi's Suzuki–Miyaura coupling of vinyl esters.....	26
Scheme 1.32	Shi's Suzuki–Miyaura coupling of α -pivaloxyl ketones.....	26
Scheme 1.33	Shi's Negishi coupling of aryl pivalates.....	27
Scheme 1.34	Watson's Heck coupling of aryl pivalates.....	28
Scheme 1.35	Itami's azole coupling with aryl pivalates.....	28
Scheme 1.36	Li's Pd-catalyzed Suzuki–Miyaura coupling of quinoline benzoates.....	29
Scheme 1.37	Snieckus' Kumada coupling of aryl sulfamates.....	30
Scheme 1.38	Du Bois' Kumada coupling of aryl cyclic sulfamates.....	31
Scheme 1.39	Garg's Suzuki–Miyaura coupling of aryl sulfamates.....	31
Scheme 1.40	Garg's flurbiprofen synthesis.....	32
Scheme 1.41	Garg and Snieckus' Suzuki–Miyaura coupling of heterocyclic sulfamates.....	32

Scheme 1.42	Competition experiments for the Suzuki–Miyaura coupling of aryl sulfamates and carbamates.....	33
Scheme 1.43	Kappe’s Suzuki–Miyaura coupling of aryl sulfamates and carbamates....	33
Scheme 1.44	Kocienski and Dixon’s Kumada coupling of vinyl carbamates.....	34
Scheme 1.45	Snieckus’ Kumada coupling of aryl carbamates.....	35
Scheme 1.46	Garg’s Suzuki–Miyaura coupling of aryl carbamates.....	36
Scheme 1.47	Snieckus’ Suzuki–Miyaura coupling of aryl carbamates.....	37
Scheme 1.48	Kuwano and Shimizu’s Suzuki–Miyaura coupling of aryl carbonates.....	37
Scheme 1.49	Fu’s Negishi coupling of propargylic carbonates.....	38
Scheme 1.50	Shi’s Kumada coupling of 2-naphthols.....	39
Scheme 1.51	Shi’s Suzuki–Miyaura coupling of 2-naphthol.....	40
Scheme 1.52	Chatani’s amination of aryl ethers.....	41
Scheme 1.53	Huang and Yang’s amination of aryl phosphates.....	41
Scheme 1.54	Bolm’s amination of aryl tosylates.....	42
Scheme 1.55	Yang’s amination of aryl tosylates.....	42
Scheme 1.56	Chatani’s amination of aryl pivalates.....	43
Scheme 1.57	Garg’s amination of aryl sulfamates.....	44
Scheme 1.58	Garg’s linezolid synthesis.....	44
Scheme 1.59	Ackermann’s amination of aryl sulfamates.....	45
Scheme 1.60	Garg’s amination of aryl carbamates.....	46
Scheme 1.61	Sasaki’s reduction of aryl mesylates.....	46
Scheme 1.62	Kogan’s reduction of aryl tosylates.....	47
Scheme 1.63	Lipshutz’s reduction of aryl tosylates.....	48

Scheme 1.64	Álvarez-Bercedo and Martin's reduction of aryl ethers.....	48
Scheme 1.65	Chatani's reduction of aryl pivalates.....	49
Scheme 1.66	Percec's borylation of aryl mesylates.....	50
Scheme 1.67	Shi's borylation of aryl carbamates.....	50
Scheme 1.68	Zhang's phosphorylation of aryl tosylates.....	51

CHAPTER TWO

Scheme 2.1	Coupling of 1-naphthylpivalate with phenyl boronic acid.....	62
------------	--	----

CHAPTER THREE

Scheme 3.1	Cross-coupling reactions involving carbamates and sulfamates.....	135
Scheme 3.2	<i>Ortho</i> -functionalization of phenyl sulfamate.....	146
Scheme 3.3	Suzuki–Miyaura coupling of a heterocyclic sulfamate with a heterocyclic boronic acid.....	152
Scheme 3.4	Synthesis of 5-phenyl-2 <i>H</i> -chromene.....	160
Scheme 3.5	Substituted benzofuran synthesis.....	161
Scheme 3.6	Substituted pyridine synthesis.....	162
Scheme 3.7	Synthesis of flurbiprofen.....	163

CHAPTER FOUR

Scheme 4.1	Retrosynthetic analysis of 4.1	239
Scheme 4.2	Synthesis of [4.3.1]-bicycle 4.14	240
Scheme 4.3	Synthesis of oxindole 4.4	241

Scheme 4.4	Synthesis of (-)- <i>N</i> -methylwelwitindolinone C isothiocyanate (4.1).....	243
------------	---	-----

CHAPTER FIVE

Scheme 5.1	Summary for the total synthesis of (-)- <i>N</i> -methylwelwitindolinone C isothiocyanate (5.1).....	297
Scheme 5.2	Synthesis of (-)- <i>N</i> -methylwelwitindolinone isonitrile (5.2).....	299
Scheme 5.3	Synthesis of 5.3 and NOESY correlation.....	303

LIST OF TABLES

CHAPTER TWO

Table 2.1	Cross-couplings of various aryl pivalates with arylboronic acids 2.2a or 2.2b	63
Table 2.2	Cross-coupling of pivalate 2.1 with various arylboronic acids.....	65

CHAPTER THREE

Table 3.1	Cross-coupling of aryl carbamates with arylboronic acids.....	137
Table 3.2	Optimization studies for naphthyl 2- <i>O</i> -carbamate coupling.....	138
Table 3.3	Cross-coupling of aryl carbamates under improved conditions.....	139
Table 3.4	Cross-coupling of <i>ortho</i> -substituted aryl <i>O</i> -carbamates.....	140
Table 3.5	Cross-coupling of heterocyclic aryl <i>O</i> -carbamates and scope of aryl boronates.....	141
Table 3.6	Cross-coupling of aryl sulfamates.....	143
Table 3.7	Cross-coupling of <i>ortho</i> -substituted aryl sulfamates.....	145
Table 3.8	Scope of boronic acid in the Suzuki–Miyaura cross-coupling of aryl <i>O</i> -sulfamates.....	148
Table 3.9	Cross-coupling of heterocyclic aryl <i>O</i> -sulfamates with phenyl boronic acid.....	150
Table 3.10	Cross-coupling of 1-naphthyl- <i>O</i> -sulfamates with heterocyclic aryl boronic acids.....	151

CHAPTER FIVE

Table 5.1	Comparison of Experimental and Computed NMR Chemical Shifts for Structure 5.4	314
Table 5.2	Comparison of Experimental and Computed NMR Chemical Shifts for Structure 5.3	315

LIST OF ABBREVIATIONS

‡	transition state
$[\alpha]_D$	specific rotation at wavelength of sodium D line
Ac	acetyl, acetate
acac	acetylacetonate
AcOH	acetic acid
app.	apparent
aq.	aqueous
atm	atmosphere
B3LYP	Becke, 3-parameter, Lee–Yang (functional)
BINAP	2,2'-bis(diphenylphosphino)-1,1'-binaphthyl
bipyr	2,2'-bipyridine
Bn	benzyl
Boc	<i>tert</i> -butyloxycarbonyl
br	broad
Bu	butyl
<i>i</i> -Bu	<i>iso</i> -butyl
<i>n</i> -Bu	butyl
<i>t</i> -Bu	<i>tert</i> -butyl
<i>n</i> -BuLi	butyl lithium
<i>s</i> -BuLi	<i>sec</i> -butyl lithium
<i>t</i> -BuLi	<i>tert</i> -butyl lithium
<i>t</i> -BuOH	<i>tert</i> -butyl alcohol
<i>c</i>	concentration for specific rotation measurements
°C	degrees Celsius
calc'd	calculated
CCDC	Cambridge Crystallographic Data Centre
CI	chemical ionization
COD	1,5-cyclooctadiene
Cy	cyclohexyl
d	doublet
dba	dibenzylideneacetone
DCE	1,2-dichloroethane

dec	decomposition
DFT	density functional theorem
DIPEA	<i>N,N</i> -diisopropylethylamine
DMA	dimethylacetamide
DMAP	4-dimethylaminopyridine
DME	1,2-dimethoxyethane
DMF	<i>N,N</i> -dimethylformamide
DMSO	dimethyl sulfoxide
DoM	directed ortho metalation
dppb	1,4-bis(diphenylphosphino)butane
dppe	1,2-bis(diphenylphosphino)ethane
dppf	1,1'-bis(diphenylphosphino)ferrocene
dppp	1,3-bis(diphenylphosphino)propane
EC ₅₀	50% effective concentration
ee	enantiomeric excess
equiv	equivalent
ESI	electrospray ionization
Et	ethyl
FAB	fast atom bombardment
g	gram(s)
G	Gibbs free energy
gCOSY	gradient-selected Correlation Spectroscopy
h	hour(s)
HRMS	high resolution mass spectroscopy
HPLC	high performance liquid chromatography
hν	light
Hz	hertz
IBX	2-iodoxybenzoic acid
IR	infrared (spectroscopy)
<i>J</i>	coupling constant
K ₃ PO ₄	potassium phosphate (tribasic)
kcal/mol	kilocalories to mole ratio
KHMDS	potassium hexamethyldisilazane
λ	wavelength
L	liter

LANL2DZ	Los Alamos National Laboratory 2 double ζ (basis set)
LDA	lithium diisopropylamide
LiHMDS	lithium hexamethyldisilazane
m	multiplet or milli
<i>m</i>	meta
<i>m/z</i>	mass to charge ratio
μ	micro
Me	methyl
MHz	megahertz
min	minute(s)
mol	mole(s)
MOM	methoxymethyl ether
mp	melting point
Ms	methanesulfonyl (mesyl)
MS	molecular sieves
MW	microwave
NBS	<i>N</i> -bromosuccinimide
NIS	<i>N</i> -iodosuccinimide
NMR	nuclear magnetic resonance
NOE	Nuclear Overhauser Effect
NOESY	Nuclear Overhauser Enhancement Spectroscopy
[O]	oxidation
<i>p</i>	para
PCy ₃	tricyclohexylphosphine
Ph	phenyl
pH	hydrogen ion concentration in aqueous solution
PhH	benzene
Piv	pivaloyl
PivCl	pivaloyl chloride
PPh ₃	triphenylphosphine
ppm	parts per million
PP	protein phosphatase
Pr	propyl
<i>i</i> -Pr	isopropyl

pyr	pyridine
q	quartet
rt	room temperature
R_f	retention factor
s	singlet or strong
SEM	(trimethylsilyl)ethoxymethyl
t	triplet
TBAF	tetrabutylammonium fluoride
TBS	<i>tert</i> -butyldimethylsilyl
TBSCl	<i>tert</i> -butyldimethylsilyl chloride
Tf	trifluoromethanesulfonyl (trifyl)
TFA	trifluoroacetic acid
THF	tetrahydrofuran
TIPS	triisopropylsilyl
TLC	thin layer chromatography
TMDSO	tetramethyldisiloxane
TMEDA	tetramethylethylenediamine
TMS	trimethylsilyl
TMSCl	trimethylsilyl chloride
Ts	<i>p</i> -toluenesulfonyl (tosyl)
TS	transition state
UV	ultraviolet
w	weak

ACKNOWLEDGEMENTS

I would first like to thank Professor Neil Garg for his support and mentorship. I felt very fortunate to have been accepted into UCLA, and to have the opportunity to begin working in his laboratory my first summer here. From the start, his enthusiasm and dedication for research has been very inspiring, and his constant optimistic attitude and guidance has helped dramatically in times where research looked to be at a dead-end. I'm very grateful for all his support, assistance, and advice as a mentor and teacher over the last five years.

I would also like to thank several other professors at UCLA whose support has been greatly appreciated over the years. Professor Ken Houk has been extremely kind and supportive, and I am extremely thankful. His endless knowledge of organic chemistry is very inspiring and impressive, and I feel very fortunate to have had the opportunity to participate in collaborative efforts with his laboratory. Professor Miguel Garcia-Garibay has also been extremely generous over the years, both in allowing use of his laboratory equipment and also in his support. I would also like to thank the other members of my thesis committee Professor Catherine Clarke and Professor Yi Tang for taking time to serve on my committee.

I would also like to acknowledge and thank several professors from my time as an undergraduate at Iowa State, beginning with Professor Richard Larock. I really enjoyed and learned a lot from his classes at Iowa State. It was those experiences that are responsible for developing my interest in organic chemistry. His continuing support over the years has been greatly appreciated. I would also like to extend a very special thanks to Professor Walter S. Trahanovksy. I'm extremely thankful for his kindness as both an academic and research advisor

in my time at Iowa State. Had it not been for the experience and skills that I learned from him while working in his laboratory, I never would have considered going to graduate school.

I would also like to thank all members of the Garg group that I've been fortunate enough to work with over the years, beginning with Dr. Xia Tian. My experience working with him on the nickel-catalyzed pivalate couplings during my first year was a very rewarding one. During that time of having to balance labwork, along with all the other responsibilities that come in your first year, it was extremely helpful to have someone like Xia to work with. I learned a lot from him through both our chemistry and non-chemistry related discussions. All of the other members that have been part of the nickel catalysis project including, Stephen Ramgren, Amanda Silberstein, and Anna Komaromi, have also been great to work with. Collaborations outside the Garg lab involving the nickel catalysis project proved to be very rewarding. Computations carried out by Peng Lui in the Houk lab at UCLA proved to be extremely insightful and important in understanding the mechanism of the reaction, and experimental studies in collaboration with Aurora Antoft-Finch and Tom Blackburn from the Snieckus lab at Queen's University really helped to strengthen the methodology. It was also a great pleasure to interact and meet with Professor Snieckus on a professional and social level. Finally, Brad Rosen, Daniell Wilson, Na Zhang, and Ana-Maria Resmerita from the Percec lab at the University of Pennsylvania were tremendously helpful in writing the review on nickel-catalyzed cross-couplings. In my last couple of years I really had a great time working with Alex Hutters and Evan Styduhar on the welwitindolinone project.

I would also like to thank all of the members of the Garg lab for making it such a great place to work. I would especially like to thank Alex Schammel, Ben Boal, Sarah Bronner, and Tehetena Mesganaw who were also here from the very beginning. I've really enjoyed working

with them over the last five years. I would particularly like to thank Alex Schammel and Ben Boal. I've really enjoyed having them as lab mates, and their friendship has meant a lot over the last five years.

Finally, I would like to thank all my friends and family back home. Most of all, I would like to thank my parents Don and Sheri Quasdorf. Their love and support have made everything possible.

Chapter 1 is a version of Rosen, B. M.; Quasdorf, K. W.; Wilson, D. A.; Zhang, N.; Resmerita, A.-M.; Garg, N. K.; Percec, V. *Chem. Rev.* **2011**, *111*, 1346–1416. This work was done in collaboration with Brad M. Rosen, Daniella A Wilson, Na Zhang, Ana-Maria Resmerita, and Virgil Percec from the University of Pennsylvania. Rosen, Quasdorf, Zhang, Resmerita, Garg, and Percec were responsible for writing the manuscript.

Chapter 2 is a version of Quasdorf, K. W.; Tian, X.; Garg, N. K. *J. Am. Chem. Soc.* **2008**, *130*, 14422–14423. Quasdorf, Tian, and Garg were responsible for experimental work.

Chapter 3 is a version Quasdorf, K. W.; Antoft-Finch, A.; Liu, P.; Silberstein, A. L.; Komaromi, A.; Blackburn, T.; Ramgren, S. D.; Houk, K. N.; Snieckus, V.; Garg, N. K. *J. Am. Chem. Soc.* **2011**, *133*, 6352–6363. This work was done in collaboration with Peng Liu and Kendall N. Houk from the University of California, Los Angeles and Aurora Antoft-Finch, Tom Blackburn, and Victor Snieckus from Queen's University. Quasdorf, Antoft-Finch, Silberstein, Komaromi, Blackburn, and Ramgren were responsible for experimental work. Liu and Houk were responsible for computational work. This chapter also includes portions of Quasdorf, K. W.; Reiner, M.; Petrova, K. V.; Garg, N. K. *J. Am. Chem. Soc.* **2009**, *131*, 17748–17749. Quasdorf, Reiner, and Petrova were responsible for experimental work.

Chapter 4 is a version of Hutters, A. D.; Quasdorf, K. W.; Styduhar, E. D.; Garg, N. K. *J. Am. Chem. Soc.* **2011**, *133*, 15797–15799. Hutters, Quasdorf, and Styduhar were responsible for experimental work.

Chapter 5 is a version of Quasdorf, K. W.; Hutters, A. D.; Lodewyk, M. W.; Tantillo, D. J. Garg, N. K. *J. Am. Chem. Soc.* **2012**, *134*, 1396–1399. This work was done in collaboration with Michael W. Lodewyk and Dean J. Tantillo at the University of California, Davis. Quasdorf and Hutters were responsible for experimental work. Lodewyk and Tantillo were responsible for computational work.

BIOGRAPHICAL SKETCH

Education:

Iowa State University, Ames, IA

- Bachelor of Science Degree in Chemistry, May 2007

Professional and Academic Experience:

Graduate Research Assistant: University of California, Los Angeles, CA

- July 2007 to current (Ph. D expected spring 2012)
- Reported the first Suzuki–Miyaura cross-couplings of aryl pivalates, as a graduate student in the laboratory of Professor Neil K. Garg.
- Demonstrated the first Suzuki–Miyaura cross-couplings of aryl carbamates, carbonates, sulfamates, and highlighted this methodology in a synthesis of the anti-inflammatory drug flurbiprofen.
- Completed the enantiospecific total syntheses of (–)-*N*-methylwelwitindolinone C isothiocyanate and (–)-*N*-methylwelwitindolinone C isonitrile and their C-3 hydroxylated analogs.

Undergraduate Research Assistant: Ames Laboratory, Ames, IA

- November 2005 to December 2006
- Performed research in organic synthesis and prepared novel copper complexes under the direction of Dr. John Fielden and Dr. Paul Kögerler.

Undergraduate Research Assistant: Iowa State University, Ames, IA

- May 2006 to July 2007
- Performed undergraduate research in flash vacuum pyrolysis and reactions in supercritical alcohols under the guidance of Professor Walter Trahanovsky.

Honors and Awards:

- Iowa State University Academic Excellence Award, 2004–2007
- Plagens Undergraduate Research Fellowship, 2006
- UCLA Excellence in First Year Academics and Research Award, 2008
- UCLA Christopher S. Foote Graduate Fellowship in Organic Chemistry, 2010
- ACS Division of Organic Chemistry Graduate Fellowship, 2010
- UCLA Majeti–Alapati Graduate Fellowship for Excellence in Research, 2010
- Bristol-Myers Squibb Graduate Fellowship in Synthetic Organic Chemistry, 2011
- Chemical Science Poster Prize at Organic Reactions and Processes GRC, 2011

Publications:

1. **Cross-Coupling Reactions of Aryl Pivalates with Boronic Acids.** Kyle W. Quasdorf, Xia Tian, and Neil K. Garg. *J. Am. Chem. Soc.* **2008**, *130*, 14422.
2. **Cross-Coupling of Phenolic Derivatives.** Neil K. Garg, Kyle W. Quasdorf, and Xia Tian. U.S. Patent 2011077406, March 31, 2011.

3. **A Homochiral 2D Copper(II) Coordination Framework.** John Fielden, Kyle W. Quasdorf, Arkady Ellern, and Paul Kögerler. *Eur. J. Inorg. Chem.* **2009**, 717.
4. **Suzuki–Miyaura Coupling of Aryl Carbamates, Carbonates, and Sulfamates.** Kyle W. Quasdorf, Michelle Reiner, Krastina V. Petrova, and Neil K. Garg. *J. Am. Chem. Soc.* **2009**, *131*, 17748.
5. **Bis(tricyclohexylphosphine)dichloronickel.** Kyle W. Quasdorf and Neil K. Garg. *Encyclopedia of Reagents for Organic Synthesis*, **2010**.
6. **Nickel-Catalyzed Cross-Couplings Involving Carbon–Oxygen Bonds.** Brad M. Rosen, Kyle W. Quasdorf, Daniella A. Wilson, Na Zhang, Ana-Maria Resmerita, Neil K. Garg, and Virgil Percec. *Chem. Rev.* **2011**, *111*, 1346.
7. **Suzuki–Miyaura Cross-Coupling of Aryl Carbamates and Sulfamates: Experimental and Computational Studies.** Kyle W. Quasdorf, Aurora Antoft-Finch, Peng Liu, Amanda L. Silberstein, Anna Komaromi, Tom Blackburn, Stephen D. Ramgren, K. N. Houk, Victor Snieckus, and Neil K. Garg. *J. Am. Chem. Soc.* **2011**, *133*, 6352.
8. **Amination of Aryl Alcohol Derivatives.** Neil K. Garg, Stephen D. Ramgren, Amanda L. Silberstein, and Kyle W. Quasdorf. US Patent Application, *filing in progress*.
9. **Total Synthesis of (–)-N-Methylwelwitindolinone C Isothiocyanate.** Alexander D. Hutters, Kyle W. Quasdorf, Evan D. Styduhar, and Neil K. Garg. *J. Am. Chem. Soc.* **2011**, *133*, 15797.
10. **Total Synthesis of Oxidized Welwitindolinones and (–)-N-Methylwelwitindolinone C Isonitrile.** Kyle W. Quasdorf, Alexander D. Hutters, Michael W. Lodewyk, Dean J. Tantillo, and Neil K. Garg. *J. Am. Chem. Soc.* **2012**, *134*, 1396.

Posters or Presentations at Meetings or Conferences:

1. **Suzuki-Miyaura coupling of aryl pivalates, sulfamates, carbamates, and carbonates.** Kyle W. Quasdorf and Neil K. Garg. *239th ACS National Meeting*. **2010**, ORGN-1007 (poster).
2. **Suzuki-Miyaura coupling of aryl pivalates, sulfamates, carbamates, and carbonates.** Kyle W. Quasdorf and Neil K. Garg. *241st ACS National Meeting*. **2011**, ORGN-94 (oral).
3. **Progress toward the total synthesis of N-methylwelwitindolinone C isothiocyanate.** Alexander D. Hutters, Kyle W. Quasdorf and Neil K. Garg. *241st ACS National Meeting*. **2011**, ORGN-747 (poster).
4. **Conversion of cellulosic materials to ethylene glycol, propylene glycol, and glycerol by supercritical alcohols.** Walter S. Trahanovsky, Ronald C. Holton, Kyle W. Quasdorf, Alyse A. Hurd, Joseph A. Marshall and Norman K. Olson. *241st ACS National Meeting*. **2011**, FUEL-99.
5. **Nickel-catalyzed cross-couplings of phenol derivatives and progress toward the total synthesis of N-methylwelwitindolinone C isothiocyanate.** Kyle W. Quasdorf and Neil K. Garg. *42nd National Organic Chemistry Symposium*. **2011** (poster).
6. **Nickel-catalyzed cross-couplings of phenol derivatives and progress toward the total synthesis of N-methylwelwitindolinone C isothiocyanate.** Kyle W. Quasdorf and Neil K. Garg. *Gordon Research Conference: Organic Reactions & Processes*. **2011** (poster and short-talk).

CHAPTER ONE

Nickel-Catalyzed Cross-Couplings of Unconventional Phenol Derivatives

In part, adapted from: Brad M. Rosen, Kyle W. Quasdorf, Daniella A. Wilson,

Na Zhang, Ana-Maria Resmerita, Neil K. Garg, and Virgil Percec

Chem. Rev. **2011**, *111*, 1346–1416.

1.1 Abstract

The number of methods for the Ni-catalyzed cross-coupling of unconventional phenol derivatives has grown dramatically in recent years. This chapter provides a survey of the wide variety of unconventional phenol derivatives that are now available for use in traditional cross-coupling reactions. The particular focus is Ni-catalyzed cross-couplings involving carbon–oxygen (C–O) bonds in new carbon–carbon (C–C) bond forming reactions.

1.2 Introduction

Transition metal-catalyzed cross-coupling reactions have emerged as one of the most powerful methods for constructing carbon–carbon (C–C) and carbon–heteroatom (C–X) bonds.¹ Whereas methodologies for the cross-coupling of aryl halides have significantly improved in the past decade,^{1,2} less progress has been made toward the coupling of the corresponding phenol derivatives.¹ Given that phenols are cheap and readily available, and that oxygenation can be used to direct the installation of functional groups on an aromatic ring, practical methods that allow for the cross-coupling of phenol derivatives are extremely attractive.

Figure 1.1 depicts a number of phenol derivatives that can now be utilized in nickel-catalyzed cross-coupling reactions. Aryl ethers, which are quite atom economical are some of the most attractive coupling partners. However, their limited reactivity in the more functional group tolerant coupling reactions (i.e., Suzuki–Miyaura couplings) and limited directing group ability dampens their synthetic utility. Vinyl phosphate esters have proven to be efficient coupling partners; however, the extension of such methodologies to the coupling of aryl phosphate esters has remained limited. The coupling of tosylates and mesylates to forge C–C bonds generally proceeds in good yields with a wide substrate scope, although their relative instability and poor directing group ability restricts their use in multistep synthesis. Esters, carbamates, and sulfamates, as will be described in Chapter 2 and 3, have emerged as powerful partners in many nickel-catalyzed cross-coupling reactions in recent years. Their superior directing group ability in *ortho*-metalation reactions^{3,4,5} and pronounced stability, including low reactivity toward Pd catalysis, makes them very effective substrates for the synthesis of polysubstituted aromatic compounds.

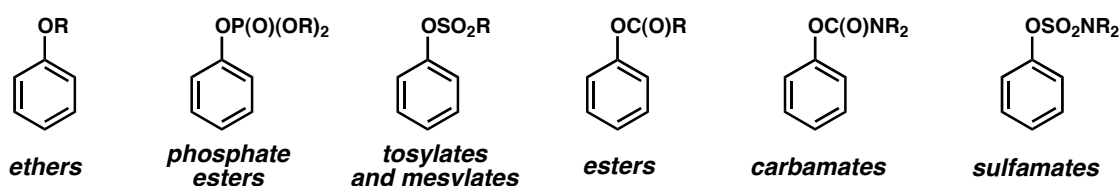


Figure 1.1. Unconventional phenol derivatives in Ni-catalyzed cross-couplings

Several comprehensive reviews have been written in recent years devoted to nickel-catalyzed cross-coupling reactions involving aryl C–O bonds.^{6,7} This chapter will discuss only a

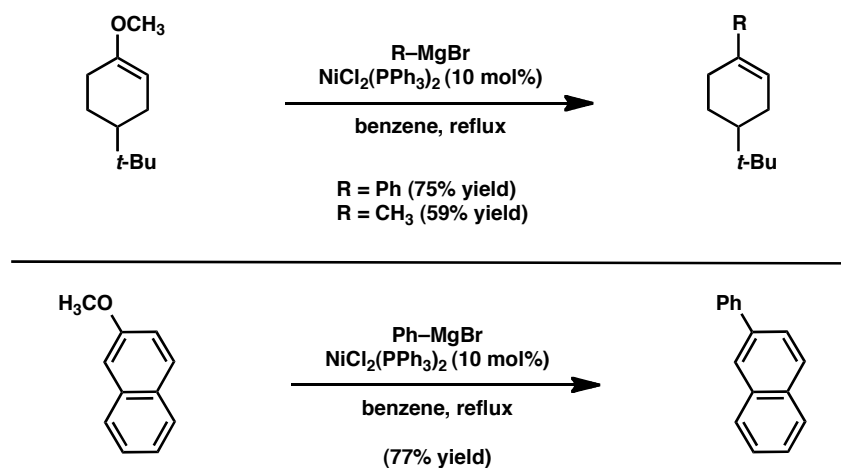
portion of the material covered in the reviews, with emphasis on the formation of carbon–carbon bonds.

1.3 Nickel-Catalyzed Cross-Couplings of Ethers

1.3.1 Kumada Couplings

Aryl and vinyl ethers, although typically consider “inert”, were actually some of the first substrates to be utilized in Ni-catalyzed Kumada couplings by Wenkert in 1979.⁸ In this seminal contribution, vinyl methyl ethers were shown to undergo Kumada couplings with methyl and phenyl Grignard reagents in the presence of a catalytic amount of $\text{NiCl}_2(\text{PPh}_3)_2$ (Scheme 1.1). The coupling of the corresponding aryl methyl ethers could also be achieved, although the scope was limited to the use of phenyl Grignard reagents. In subsequent studies, Wenkert et al. further explored the Kumada coupling of enol and aryl ethers paying particular attention to the stereochemistry associated with the ring-opening of dihydropyrans and dihydrofurans.⁹

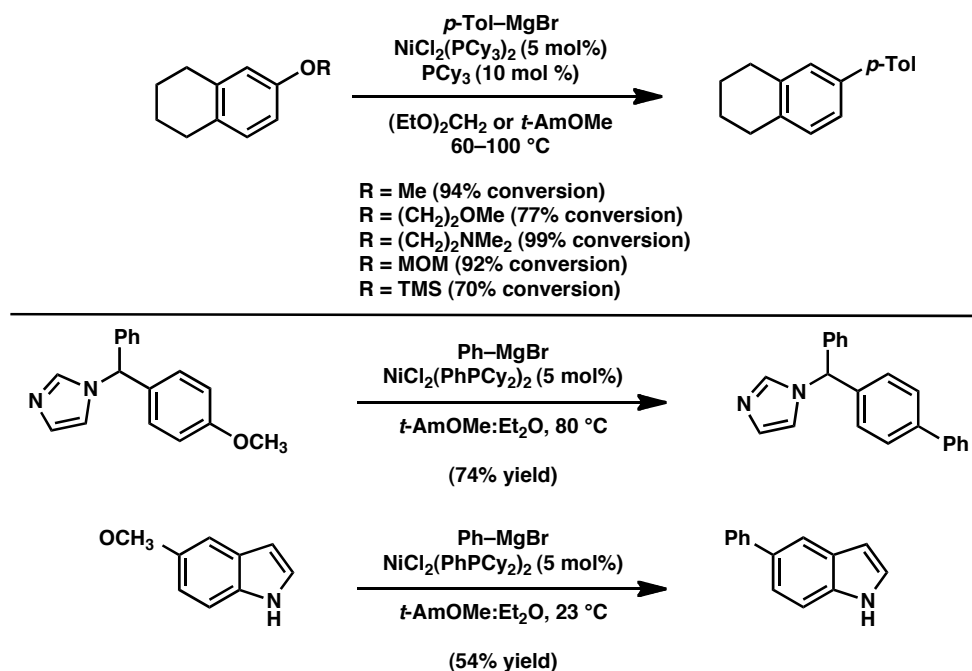
Scheme 1.1



In 2004, Dankwardt significantly expanded the scope of aryl ether cross-couplings by switching ligands to either PCy_3 or PhPCy_2 and shifting to ethereal solvents (Scheme 1.2).¹⁰

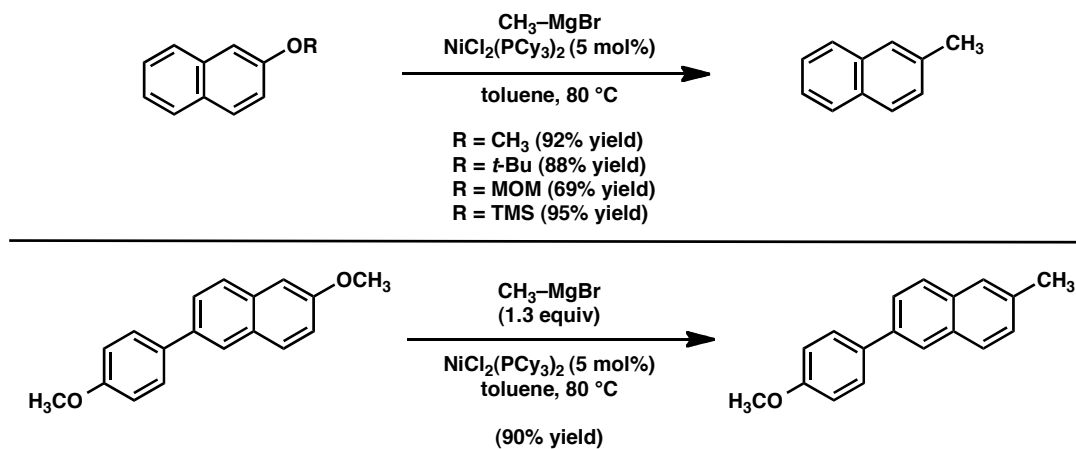
Using this modified protocol, a range of simple aryl ethers, including a tetramethylsilane (TMS) ether, were converted to biaryl products in good to excellent yield. The reaction also proved to be tolerant of free hydroxyl groups, as well as number of heterocyclic compounds, including imidazole and indole containing substrates.

Scheme 1.2



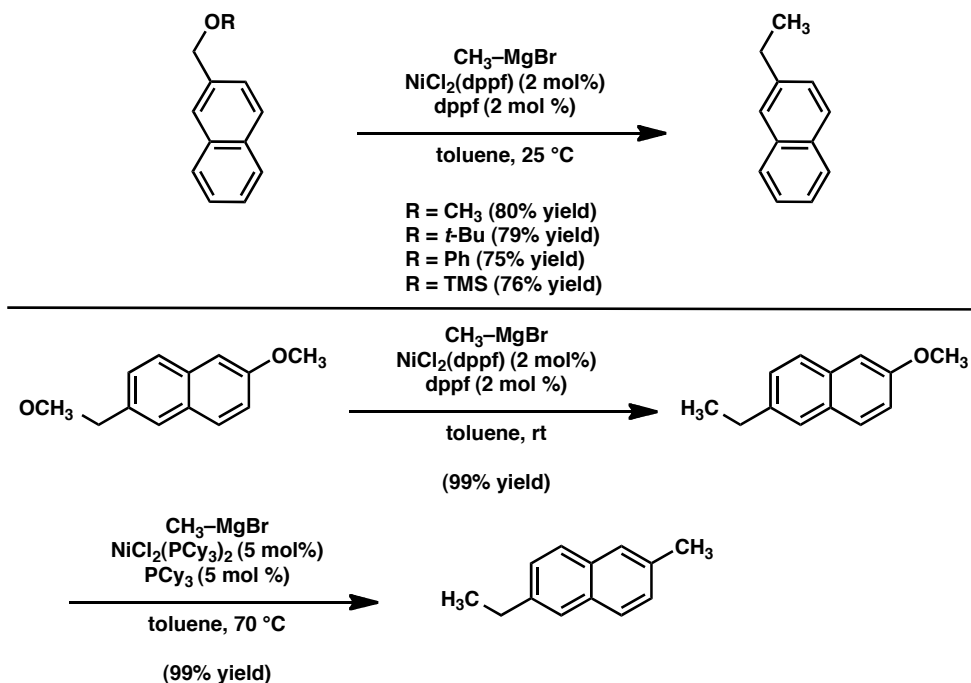
Shi's group has recently discovered conditions that allow for the cross-coupling of aryl ethers with methyl Grignard reagents, thus enabling the formation of $\text{sp}^3\text{--sp}^2$ C–C bonds (Scheme 1.3).¹¹ Fused aromatics, such as a variety of ethers derived from 2-naphthol coupled smoothly, while non-fused substrates coupled less effectively. Indeed, in a competition experiment it was shown that a methyl aryl ether of a fused aromatic could be coupled with excellent selectivity in the presence a methyl ether derived from a non-fused aromatic.

Scheme 1.3



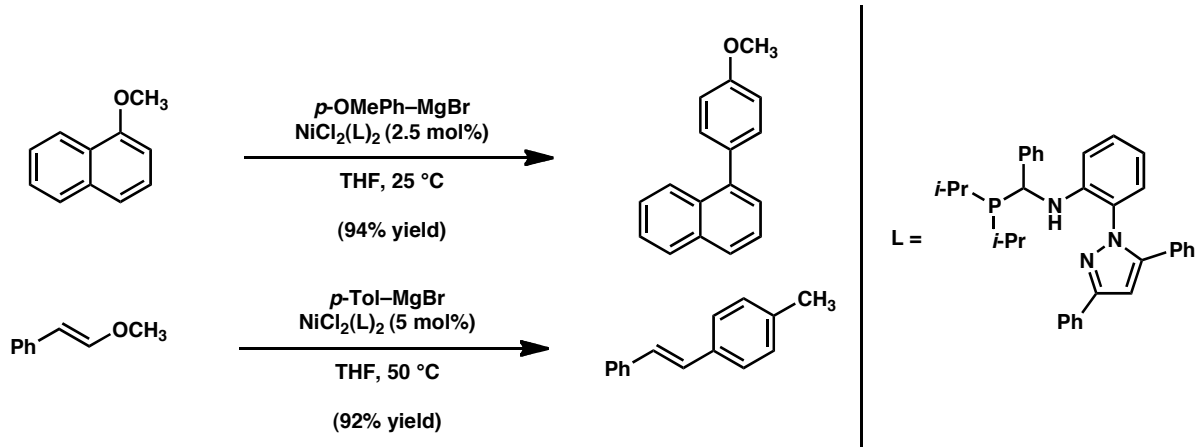
Shi's group has also extended the reaction scope to allow for the coupling of benzylic ethers, thus offering a unique Ni-catalyzed method for the formation of $\text{sp}^3\text{-sp}^3$ C-C bonds (Scheme 1.4).¹² A number of ethers including methyl, *t*-butyl, phenyl, and trimethylsilyl all proved to be competent coupling partners at ambient temperatures by using the dppf ligand. Also demonstrated was the sequential and selective cross-coupling of a benzylic ether followed by an aryl ether controlled by the choice of Ni-catalyst.

Scheme 1.4



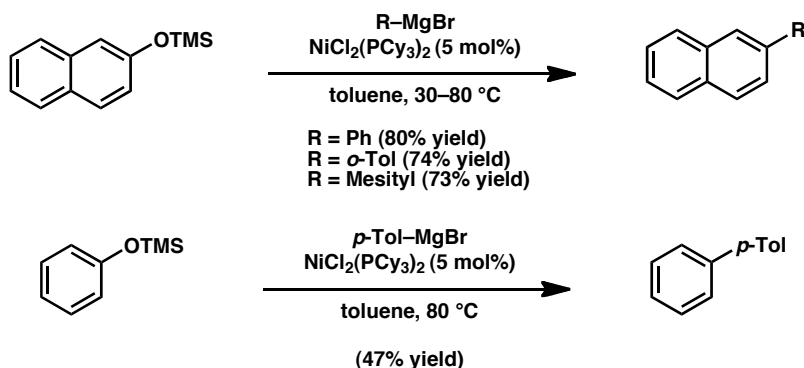
Utilizing a number of novel Ni-complexes Wang has reported conditions for the coupling of a variety of aryl and alkenyl ethers with aryl Grignard reagents (Scheme 1.5).¹³ Reactions of naphthol derived substrates typically proceeded at ambient temperature, while the use of simple phenyl and alkenyl ethers or sterically hindered Grignard reagents required the use of elevated temperatures.

Scheme 1.5



Other classes of aryl and vinyl ethers have also found use as electrophiles in Ni-catalyzed Kumada couplings. In 1980, Kumada and co-workers described the cross-couplings of silyl enon ethers with Grignard reagents using a various nickel complexes as catalysts.¹⁴ Later, Johnstone and McClean observed that Ni-catalyzed Kumada coupling of aryl 5-1-phenyltetrazolyl ethers proceeded smoothly with the use of both alkyl and aryl Grignard reagents.¹⁵ Recently the Shi group has also reported the Kumada coupling of silyl ethers using $\text{NiCl}_2(\text{PCy}_3)_2$ (Scheme 1.6).¹⁶ The reaction proceeded in excellent yield on naphthyl derived substrates, and also worked on phenyl and vinyl substrates although in diminished yield.

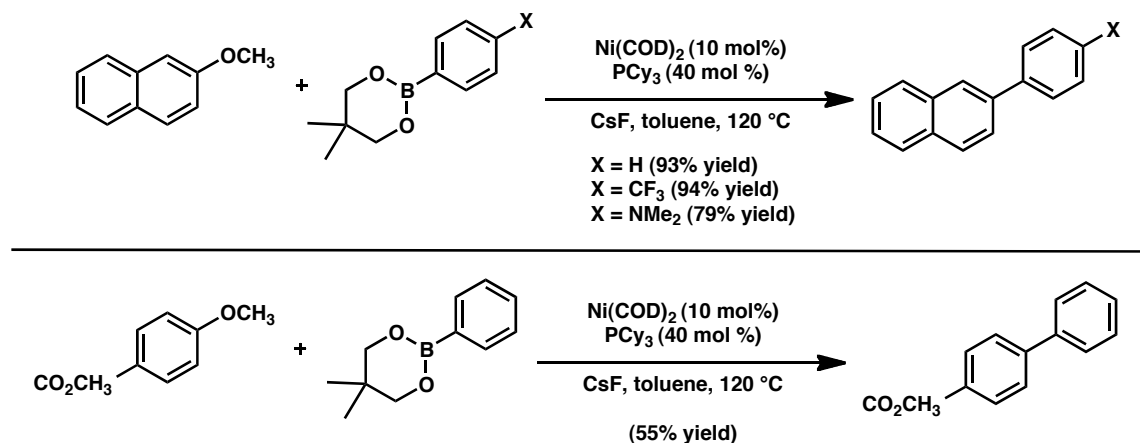
Scheme 1.6



1.3.2 Suzuki–Miyaura Couplings

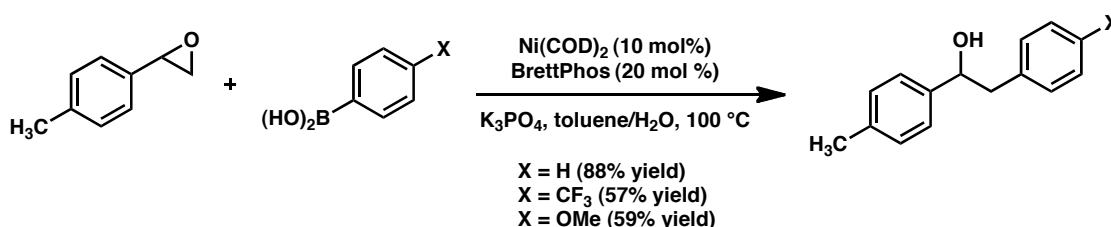
In 2008, Chatani and co-workers demonstrated the first Suzuki–Miyaura coupling of aryl ethers.¹⁷ By using a $\text{Ni}(\text{COD})_2/\text{PCy}_3$ catalyst system, methyl ethers were cross-coupled with aryl boronic esters to give biaryl products. The transformation proceeded most efficiently with fused aromatic substrates, as well as electron-deficient phenol derivatives (Scheme 1.7). The scope of the reaction was later expanded to facilitate the Suzuki–Miyaura coupling of vinyl methyl ethers.¹⁸

Scheme 1.7



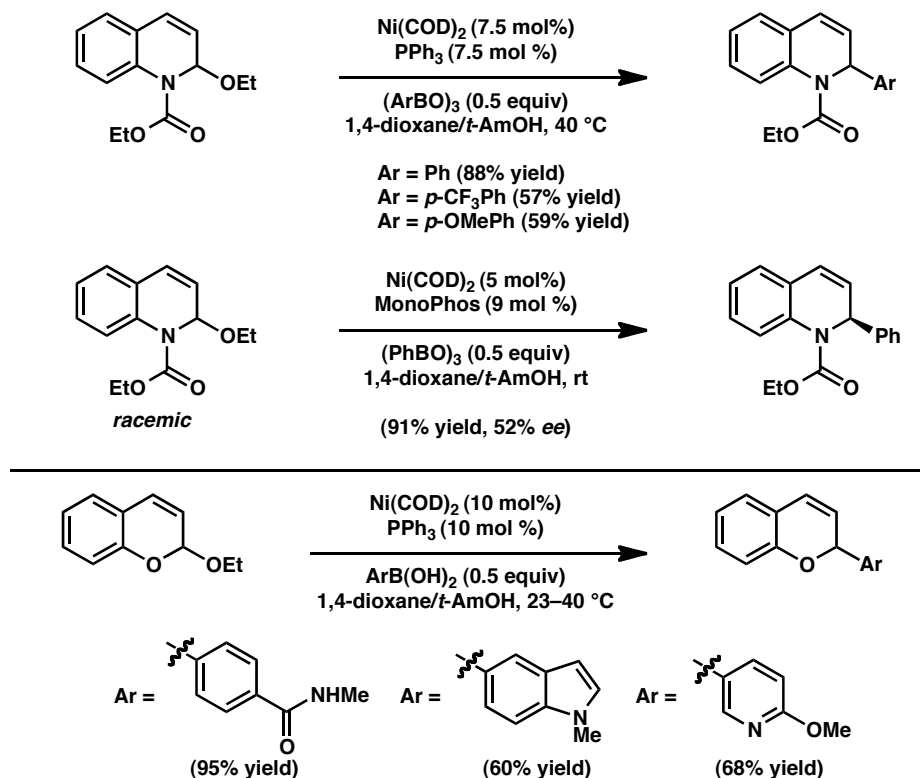
Recently, the Doyle laboratory has shown that a number of activated ether substrates participate in Ni-catalyzed Suzuki–Miyaura couplings. Styrenyl epoxides were found to undergo Suzuki–Miyaura coupling in the presence of Ni(COD)₂/BrettPhos catalyst system (Scheme 1.8).¹⁹ Coupling occurs with good yield and regioselectivity, and both electron-rich and deficient boronic acids could be used in this transformation.

Scheme 1.8



Doyle has also reported the coupling of quinoline or isoquinoline derived *N,O*-acetals,²⁰ along with the chromene acetals²¹ using Ni(COD)₂/PPh₃. The *N,O*-acetal couplings were shown to occur with excellent regioselectivity and the transformation could achieve moderate enantioselectivity with the use of a chiral ligand. The conditions for the *N,O*-acetal Suzuki–Miyaura couplings were also found to facilitate the coupling of chromene derived acetals. A wide scope of boronic acids, included those containing heterocyclic components, furnished coupled products in good yield (Scheme 1.9).

Scheme 1.9



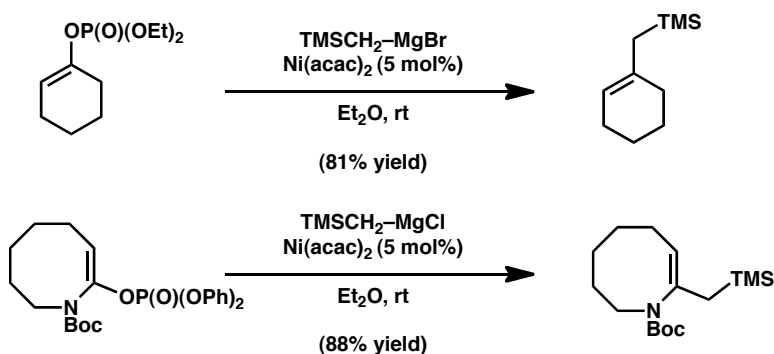
1.4 Nickel-Catalyzed Cross-Couplings of Aryl and Vinyl Phosphates

1.4.1 Kumada Couplings

One of the earliest reports of the Ni-catalyzed cross-coupling of phenolic derivatives was published in 1981.²² In this seminal study, Kumada and co-workers demonstrated that vinyl phosphates could be coupled with trimethylsilylmethyl magnesium halides in the presence of a Ni(acac)₂ catalyst. For example, a vinyl phosphate readily prepared from cyclohexanone was converted to the corresponding allylsilane in 81% yield (Scheme 1.10). The methodology was also tolerant of acyclic vinyl phosphate substrates. Since Kumada and co-workers' report, Claesson and co-workers²³ and Bäckvall and co-workers²⁴ have expanded the scope of this methodology to include the cross-coupling of dienyl phosphates with aryl and alkyl Grignard

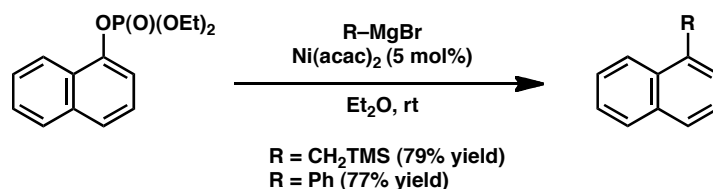
reagents. Nicolaou et al. have also demonstrated the nickel-catalyzed Kumada coupling of a lactam-derived ketene aminal phosphate with trimethylsilylmethyl magnesium chloride.²⁵

Scheme 1.10



Kumada and co-workers' conditions for vinyl phosphate coupling also proved amenable to the corresponding reactions of aryl phosphates.²⁶ As shown in Scheme 1.11, a naphthyl phosphate underwent Ni-catalyzed Kumada coupling to deliver arylated products. Both aryl and alkyl Grignard reagents could be utilized in this methodology.

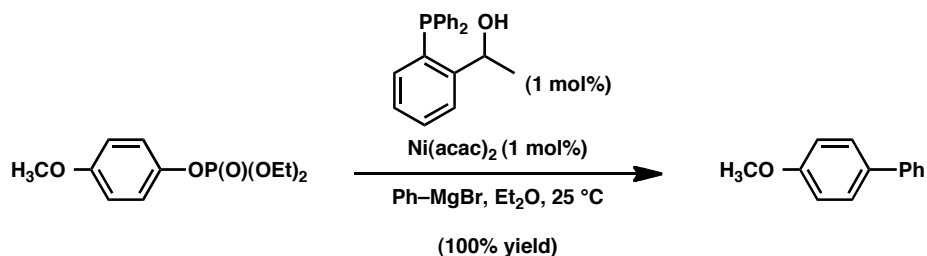
Scheme 1.11



Nakamura and co-workers have recently reported the Kumada coupling of aryl phosphates using a versatile hydroxyphosphine ligand (Scheme 1.12).²⁷ Even electron-rich substrates and *ortho*-substituted derivatives could be used with this methodology. On the basis of

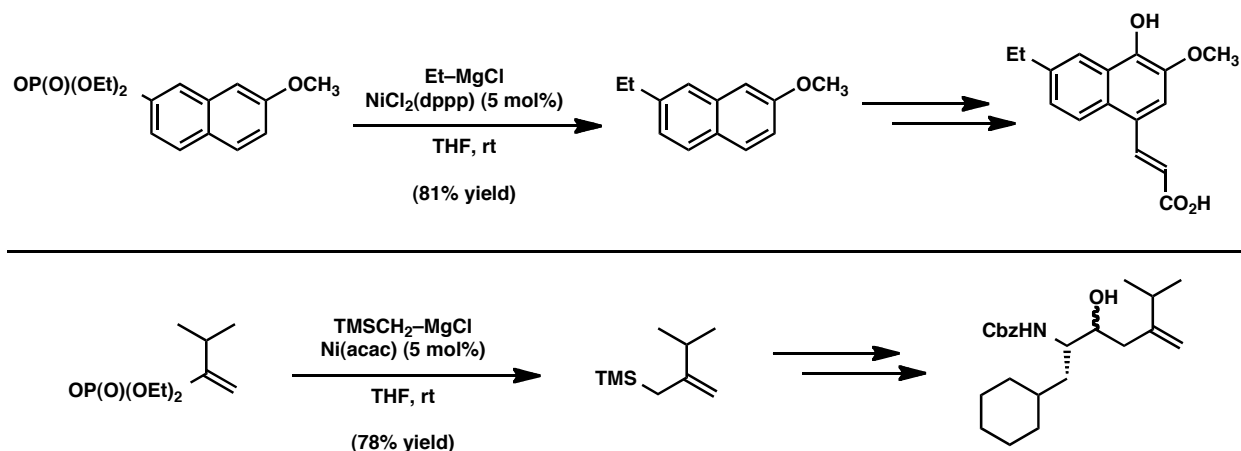
experimental and computational studies, the authors attribute the high catalytic activity to an in situ formed bimetallic species derived from the nickel precatalyst, the hydroxyphosphine ligand, and the Grignard reagent.

Scheme 1.12



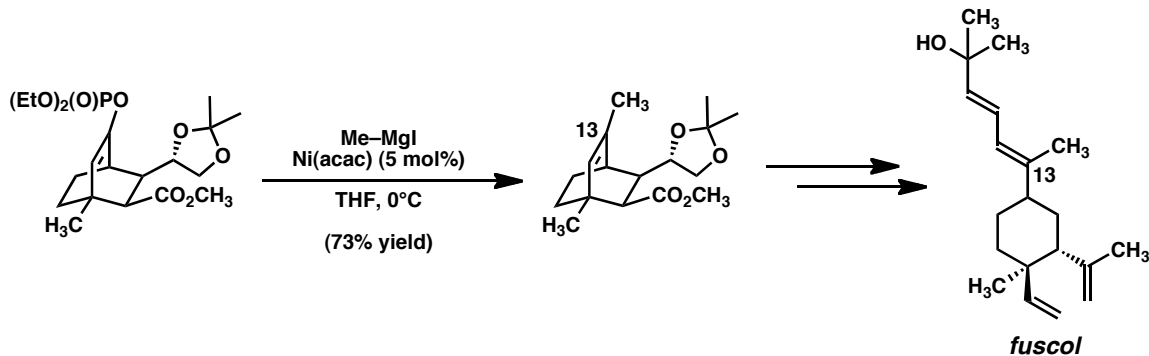
The Kumada coupling of aryl and vinyl phosphates has been used in drug discovery (Scheme 1.13). Tsukuba Research Laboratories carried out the nickel-catalyzed cross-coupling of an aryl phosphate with ethylmagnesium chloride to deliver the alkylated product in 81% yield.²⁸ In turn, the alkylated product served as a precursor to a series of compounds, that were found to inhibit the generation of the interleukin-1 (IL-1) cytokine. Subsequently, scientists at Abbott Laboratories reported the conversion of a vinylphosphate to an allylsilane using nickel catalysis.²⁹ The allylsilane was elaborated to the depicted homoallylic alcohol, en route to a class of hydroxyethylene dipeptide isosteres.

Scheme 1.13

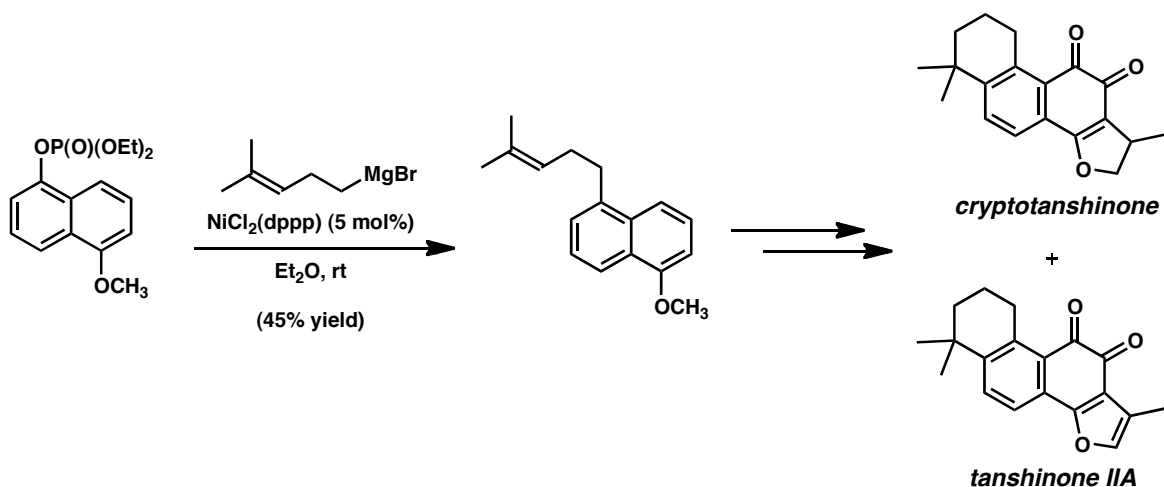


Nickel-catalyzed Kumada couplings of phosphate derivatives have also been utilized in natural product total synthesis (Schemes 1.14 and 1.15). In their synthesis of the diterpene fuscol, Yamada and co-workers reported the coupling of a vinyl phosphate substrate with methyl magnesium iodide using $\text{Ni}(\text{acac})_2$ as a catalyst.³⁰ The transformation proceeded readily at 0 °C, thus providing an efficient means to install the C13 methyl group of the natural product. In 2003, Lu and co-workers demonstrated the use of an aryl phosphate ester in natural product synthesis (Scheme 1.15).³¹ The aryl phosphate was converted to the corresponding alkylated product under nickel-catalyzed Kumada conditions. This intermediate could be used to access both cryptotanshinone and tanshinone IIA, natural products that were being examined for their ability to inhibit *cdc25* protein phosphatases.³²

Scheme 1.14



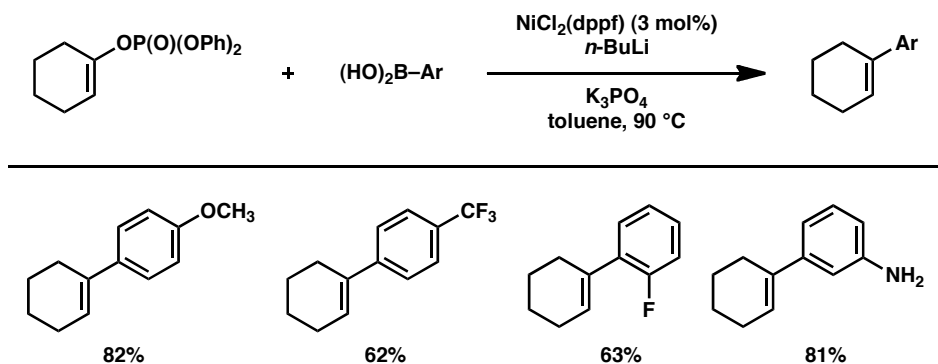
Scheme 1.15



1.4.2 Suzuki–Miyaura Couplings

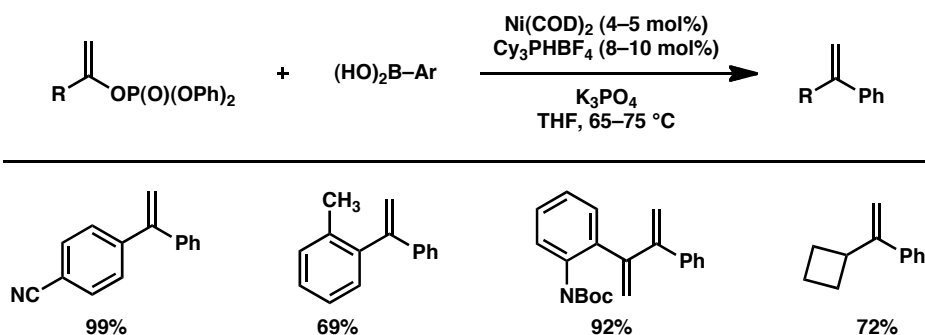
In contrast to the nickel-catalyzed Kumada coupling of phosphate esters, reports of the analogous Suzuki–Miyaura coupling are relatively scarce. The first nickel-catalyzed Suzuki–Miyaura coupling of a vinyl phosphate was described by Nan and Yang in 1999.³³ It was shown that cyclohexenylphosphate underwent smooth cross-coupling with a variety of arylboronic acids to deliver arylated products in good yield (Scheme 1.16). In all cases, the requisite Ni^0 catalyst was generated by mixing $\text{NiCl}_2(\text{dppf})$ with *n*-butyllithium prior to the cross-coupling reaction.

Scheme 1.16



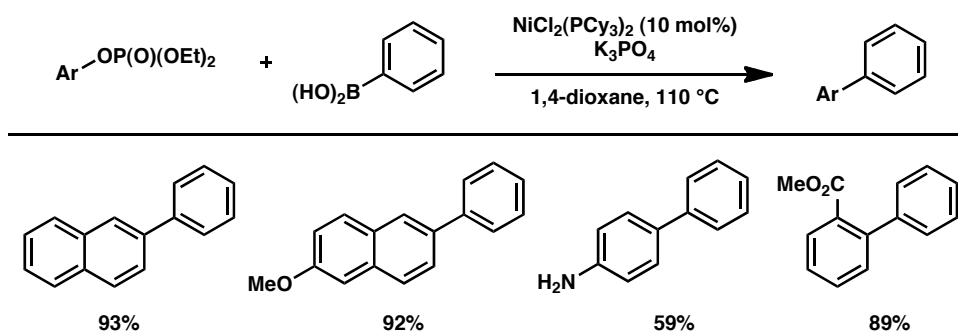
Skrydstrup and co-workers later expanded the scope of the vinyl phosphate Suzuki–Miyaura coupling.^{34,35} The nickel-catalyzed coupling of vinyl phosphates with aryl boronic acids proceeds most efficiently with the PCy_3 ligand to deliver a variety of 1,1-disubstituted alkenes (Scheme 1.17). The scope of the transformation was found to be broad with respect to the vinyl phosphate substituents, as a number of functionalized aromatics could be used, in addition to heterocycles and alkyl substituents. Considerable variation in the aryl boronic acid fragment was also tolerated.

Scheme 1.17



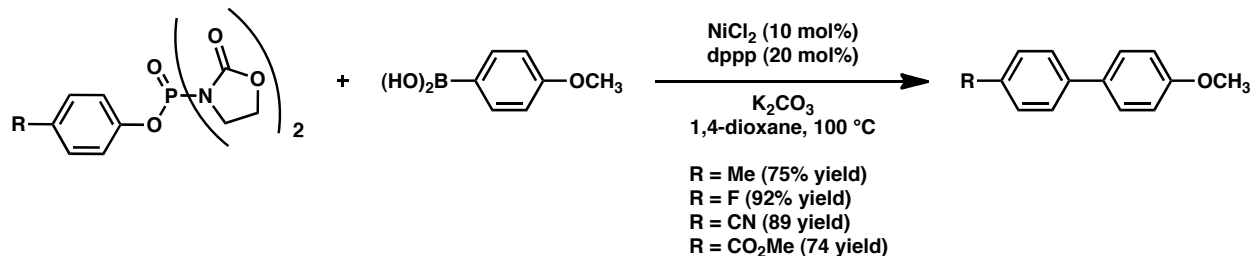
In 2011 Zhao and Cheng reported the first Suzuki–Miyaura coupling of aryl phosphates.³⁶ Utilizing $\text{NiCl}_2(\text{PCy}_3)_2$ as a Ni^{II} precatalyst, both fused and phenyl derived phosphates coupled in good yield (Scheme 1.18). The substrate scope was also quite broad with respect to the boronic acid component.

Scheme 1.18



Han and co-workers have also recently achieved the cross-coupling of a related electrophilic species, namely, the aryl phosphoramidate group.³⁷ In this study, aryl “BOP” coupling partners were readily derived from phenols and bis(2-oxo-3-oxazolidinyl)phosphinic chloride (Scheme 1.19). Suzuki–Miyaura coupling of various substrates afforded biaryl products in high yield. Of note, naphthyl derivatives and heterocyclic substrates derived from 3- and 4-hydroxypyridine could also be cross-coupled efficiently using this methodology.

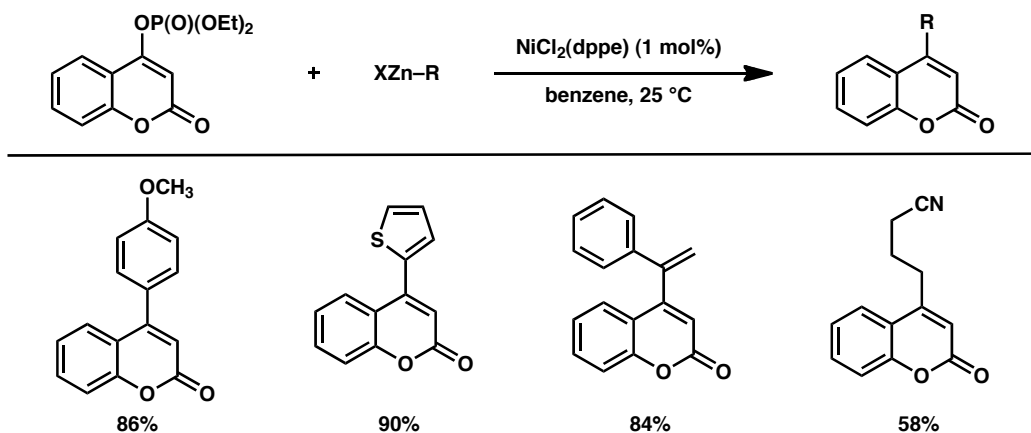
Scheme 1.19



1.4.3 Negishi Couplings

The nickel-catalyzed Negishi coupling of vinyl phosphates has been reported as a tool to synthesize a number of substituted coumarins.³⁸ Upon examining several Pd and Ni catalyst, Wu and Yang found that 1% $\text{NiCl}_2(\text{dppe})$ enabled the desired cross-coupling, which proceeded at ambient temperatures (Scheme 1.20). A range of organozinc reagents could be utilized, including aryl-, heteroaryl-, vinyl-, and alkylzinc species, to deliver cross-coupled products in synthetically useful yields.

Scheme 1.20

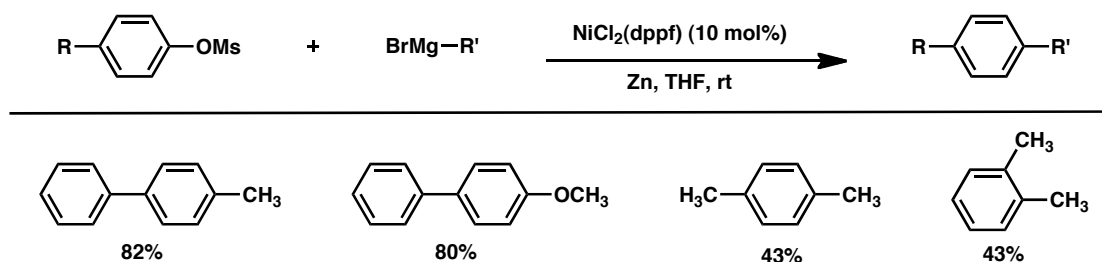


1.5 Nickel-Catalyzed Cross-Couplings of Aryl and Vinyl Mesylates and Tosylates

1.5.1 Kumada Couplings

Although aryl halide and triflate electrophiles were known to be effective in Kumada cross-coupling, aryl mesylates were generally regarded as inactive. In 1995, Percec et al. demonstrated the efficient nickel-catalyzed coupling of aryl mesylates with Grignard reagents to produce biaryl products in good yields (Scheme 1.21).³⁹ Recently Wu and co-workers have also disclosed conditions for the coupling of aryl tosylates and mesylates with organoindium reagents.⁴⁰

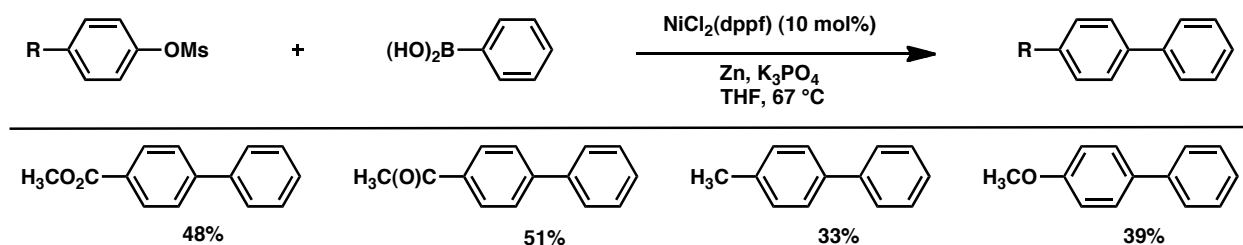
Scheme 1.21



1.5.2 Suzuki–Miyaura Couplings

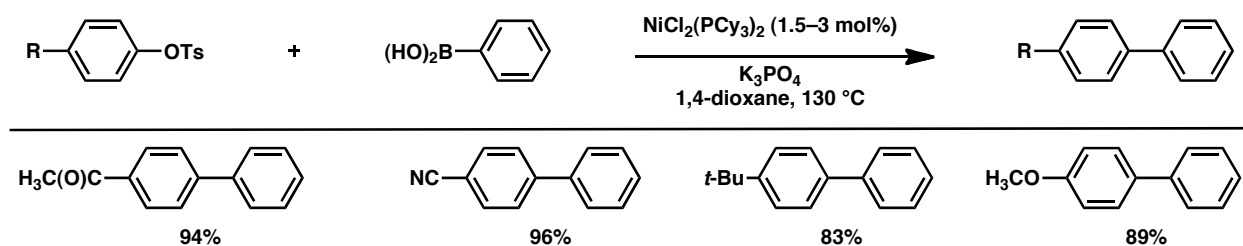
In a seminal 1995 report, Percec et al. reported the first nickel-catalyzed Suzuki–Miyaura coupling of aryl mesylates.⁴¹ Utilizing NiCl₂(dppf) as a Ni^{II} precatalyst that undergoes in situ reduction by zinc powder to Ni⁰, aryl mesylates could be coupled to produce biaryl products in moderate yields (Scheme 1.22). The choice of K₃PO₄ as base was also an important factor in the success of the reaction.

Scheme 1.22



Realizing the use of external reducing agents is often undesirable, a number of groups have explored conditions to promote the nickel-catalyzed Suzuki–Miyaura coupling without the need to add external reducing agents. The first report of such reactions came from Kobayashi and co-workers using lithium aryl⁴² or alkenyl⁴³ organoborates as coupling partners. In 2001, Zim and Monterio expanded the use of $\text{NiCl}_2(\text{PCy}_3)_2$ as an efficient external reducing agent free catalyst for the Suzuki–Miyaura cross-coupling of aryl tosylates (Scheme 1.23).⁴⁴ Using this catalyst system, simple phenyl tosylates coupled in excellent yields. In subsequent work by Hu and Tang $\text{Ni}(\text{COD})_2/\text{PCy}_3$ catalyst system was shown promote the coupling of aryl tosylates at ambient temperatures.⁴⁵

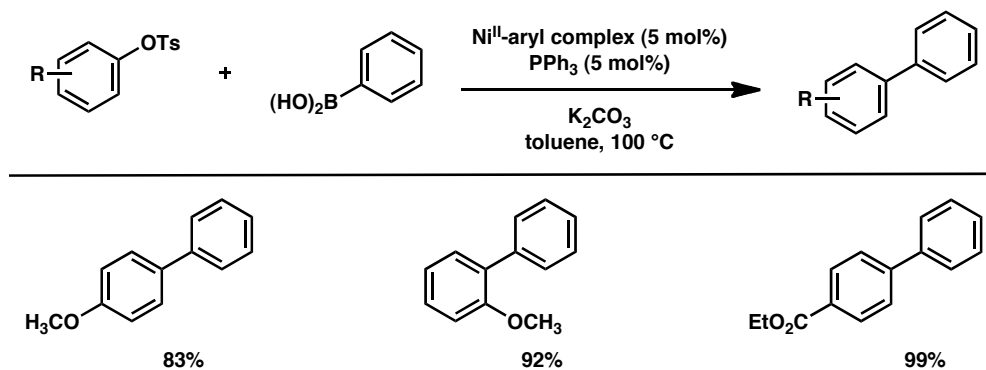
Scheme 1.23



In 2004, Percec et al. reported the use of the $\text{NiCl}_2(\text{dppe})/\text{dppe}$ catalyst system for the coupling aryl mesylates and tosylates.⁴⁶ While this system proved sufficient for electron-deficient substrates, a mixed ligand catalyst system of $\text{NiCl}_2(\text{dppe})/\text{PPh}_3$ proved to be high yielding across both electron-rich and deficient substrates. Recently Percec and co-workers have also reported a comprehensive study comparing many C–O electrophiles in nickel-catalyzed Suzuki–Miyaura couplings.⁴⁷

The use of a Ni^{II} -aryl complex as a catalyst in the Suzuki–Miyaura coupling for aryl tosylates has been described by Yang and co-workers.⁴⁸ High yields were obtained for both electron-rich and electron-deficient aryl tosylates, with high functional group tolerance except for aldehydes and nitro-bearing substrates (Scheme 1.24). Percec et al. have also employed Ni^{II} -aryl complexes in the Suzuki–Miyaura coupling of neopentylglycolboronates with aryl mesylates to afford biaryl products in good yields.⁴⁹

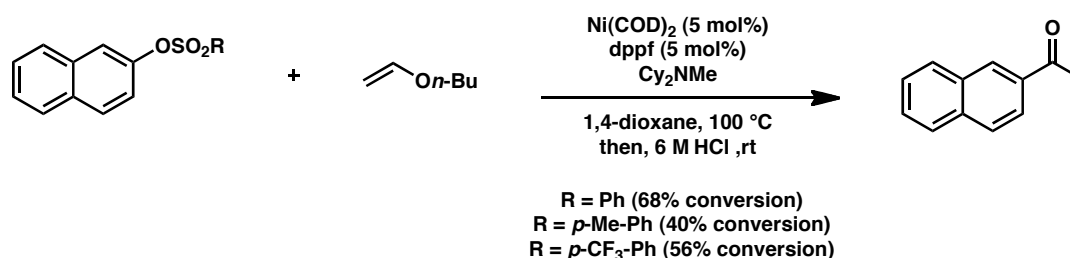
Scheme 1.24



1.5.3 Heck Couplings

In 2012, Skrydstrup and co-workers reported the first example for a Heck coupling of an aryl tosylate.⁵⁰ Using a Ni(COD)₂/dppf catalyst system, aryl sulfonates were found to undergo Heck coupling with alkyl enol ethers to afford after hydrolysis, aryl ketones in moderate yield (Scheme 1.25).

Scheme 1.25



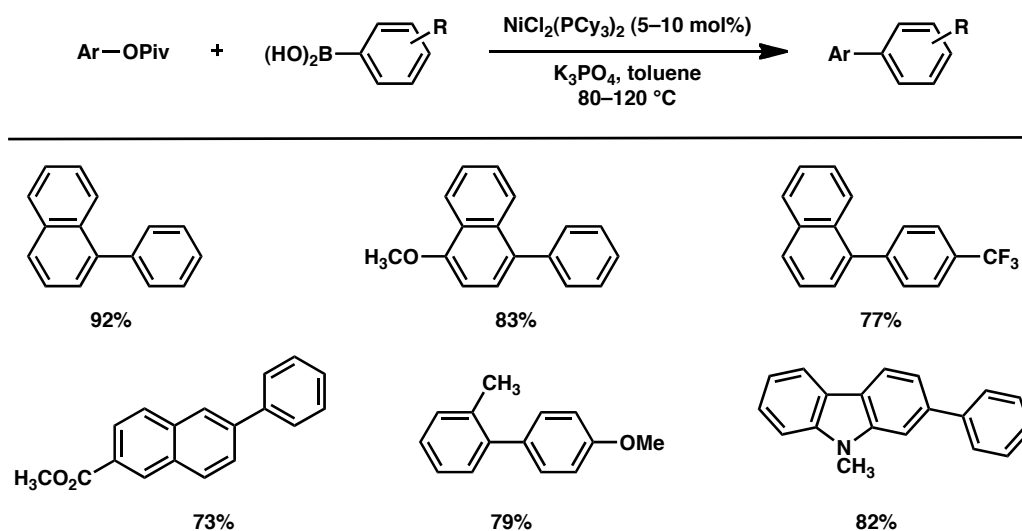
1.6 Nickel-Catalyzed Cross-Couplings of Aryl and Vinyl Esters

1.6.1 Suzuki–Miyaura Couplings

In 2008, the Garg and Shi laboratories simultaneously reported the Suzuki–Miyaura coupling of esters derived from phenols and naphthols.^{51,52,53} The two methodologies operate under similar conditions, although Garg's method utilizes aryl boronic acid coupling partners, whereas Shi's technology uses aryl boroxines. In Garg's studies, it was found that aryl pivalates were optimal substrates for the coupling with boronic acid (Scheme 1.26). Naphthyl, phenyl, and heterocyclic pivalates could be utilized in this methodology. The scope with respect to the aryl boronic acid component was also shown to be fairly broad. It should be noted that the precatalyst used, NiCl₂(PCy₃)₂,^{54,55} is commercially available, air-stable, and bench top friendly.⁵⁶ Moreover,

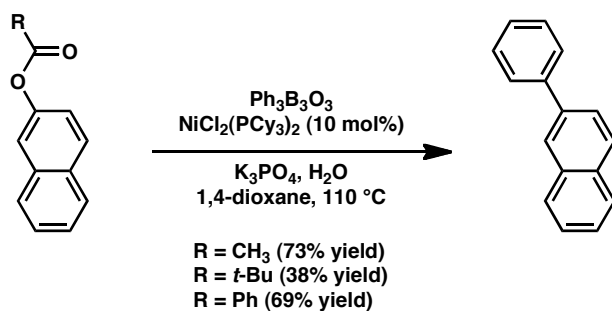
a tandem acylation / cross-coupling variation of this transformation was developed, which allowed for the one-pot conversion of 1-naphthol to a biaryl product.⁵¹

Scheme 1.26

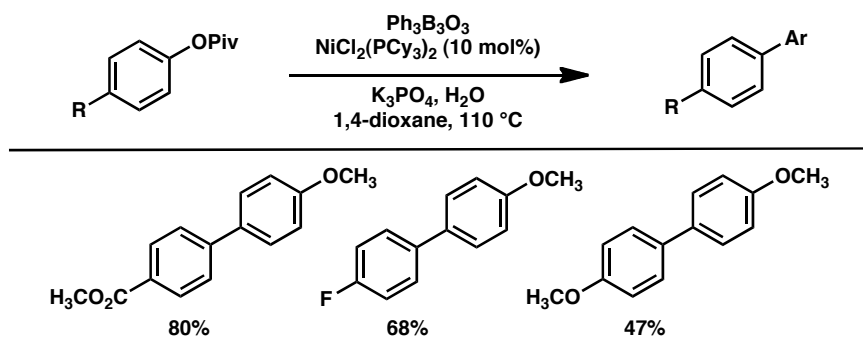


As mentioned above, Shi's protocol for the Suzuki–Miyaura coupling of phenolic esters utilized aryl boroxines instead of aryl boronic acids.⁵² Under optimal conditions, with 0.88 equiv of water, acetate, pivalate, and benzoate ester derivatives could be cross-coupled with aryl boroxines (Scheme 1.27). Nonfused aromatic substrates were also tolerated, provided that pivalate esters were used as the substrates (Scheme 1.28). A computational mechanistic study on the nickel-catalyzed cross-coupling of aryl esters is available, which suggests that transmetalation is likely the rate-determining step in these processes.⁵⁷ Recently, Molander and Beaumard have reported that, in addition to boronic acids and boroximes, aryl and heteroaryl potassium trifluoroborate salts were effective partners for Ni(COD)₂/PCy₃HBF₄-catalyzed cross-coupling of aryl pivalates.⁵⁸

Scheme 1.27

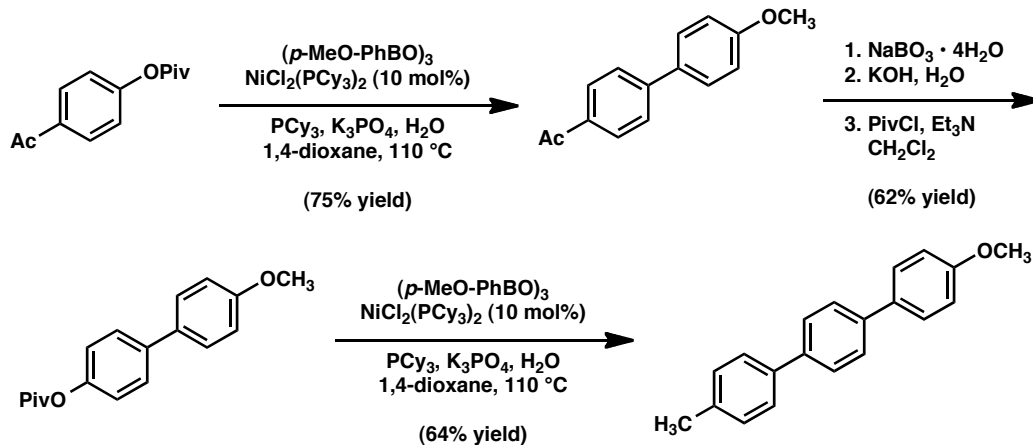


Scheme 1.28



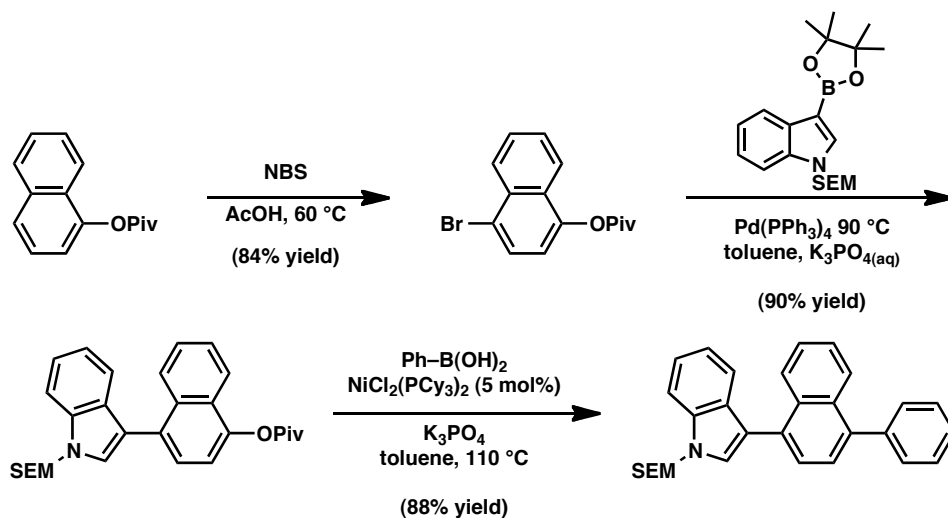
The Garg and Shi laboratories have independently demonstrated the utility of aryl ester cross-couplings through sequential cross-coupling sequences. In Shi and co-workers' example,⁵² Suzuki–Miyaura coupling of a readily available aryl pivalate furnished the biaryl product in 75% yield (Scheme 1.29). Subsequent Baeyer–Villiger oxidation, hydrolysis, and acylation provided a new aryl pivalate substrate in 62% yield over 3 steps. Finally, Ni-catalyzed Suzuki–Miyaura coupling of the aryl pivalate gave rise to a triaryl product.

Scheme 1.29



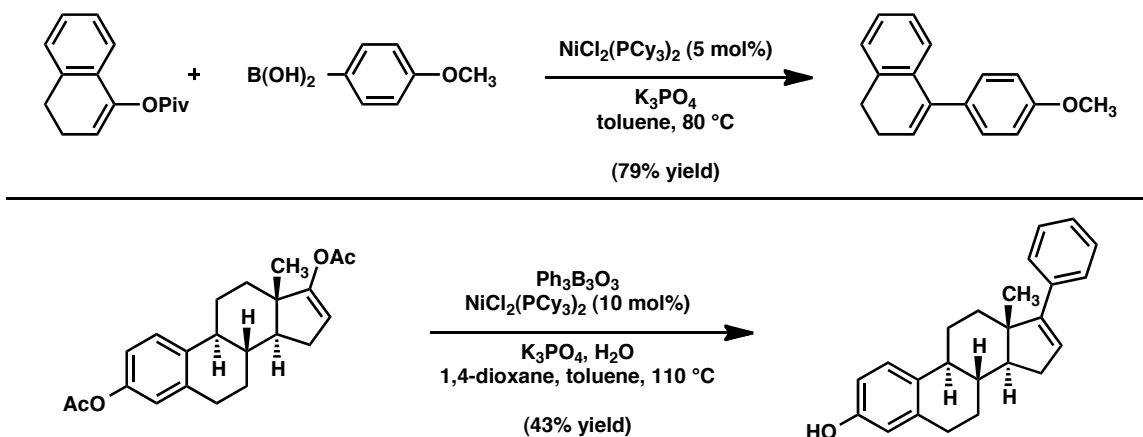
Garg and co-workers' example showcased the directing ability of aryl pivalates, in addition to the low reactivity of these substrates toward Pd^0 (Scheme 1.30).⁵¹ A naphthyl pivalate underwent regioselective *para*-bromination. Exposure of the resulting bromopivalate to Pd-catalyzed Suzuki–Miyaura coupling conditions with an indolylboronic ester led to selective coupling of the aryl bromide. Of note, the robust pivalate group remained intact, despite the harsh basic conditions used (i.e., aqueous K_3PO_4 , 90 °C). Next, the aryl pivalate underwent Suzuki–Miyaura coupling under nickel-catalyzed conditions to afford a triaryl product in 88% yield.

Scheme 1.30



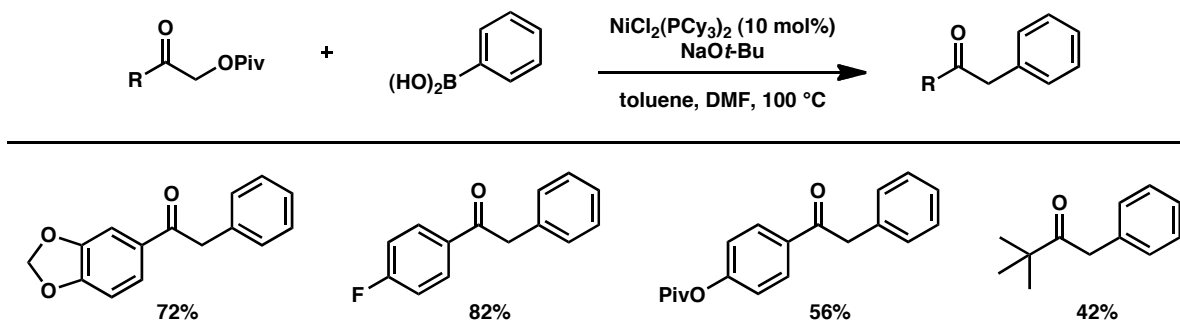
The scope of the nickel-catalyzed ester coupling extends beyond aryl systems, as demonstrated by the cross-coupling of vinyl acetates and pivalates. For example, the pivalate derived from α -tetralone was cross-coupled in 79% yield (Scheme 1.31). Although most examples of vinyl acetate and pivalate coupling involve styrenyl systems, an estrone-derived vinyl acetate has also been coupled under Shi's Suzuki–Miyaura conditions.⁵⁹ Interestingly, in this latter example, the *aryl* acetate moiety in the substrate underwent hydrolysis rather than cross-coupling.

Scheme 1.31



The Shi group has also reported the Suzuki–Miyaura coupling of α -pivaloxyl ketones using $\text{NiCl}_2(\text{PCy}_3)_2$ as an effective Ni^{II} precatalyst, thus allowing for the construction $\text{sp}^2\text{-sp}^3$ C–C bonds.⁶⁰ A wide variety of benzylic α -pivaloxyl ketones proved to be viable partners in the coupling reaction, as did a *t*-butyl α -pivaloxyl ketone (Scheme 1.32). Also of note was the coupling of an α -pivaloxyl ketone in the presence of an aryl pivalate. Either aryl boronic acids or aryl boroxines could be used in this transformation.

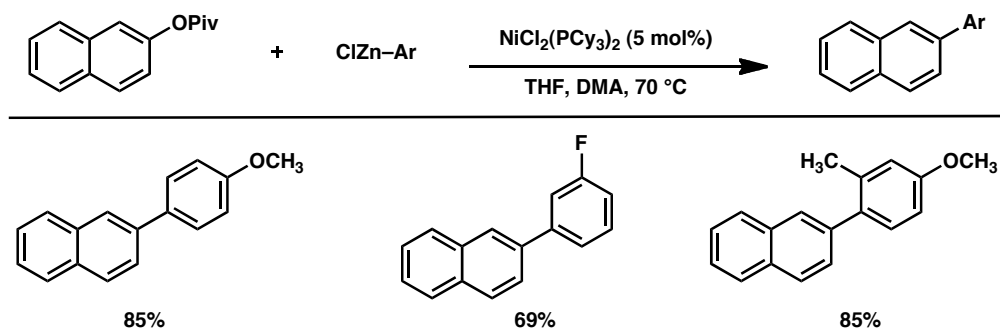
Scheme 1.32



1.6.2 Negishi Couplings

The scope of pivalate cross-coupling has been extended by the Shi group to include the Negishi coupling of 2-naphthol derivatives and electron-deficient aryl pivalates (Scheme 1.33).⁶¹ For example, 2-naphthylpivalate could be cross-coupled with a range of aryl zinc reagents to furnish 2-aryl naphthalenes. The corresponding arylation of styrenyl vinyl pivalates was also demonstrated.

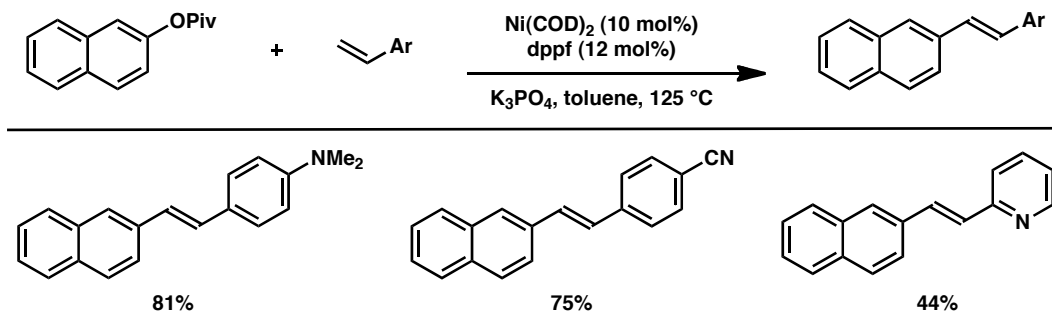
Scheme 1.33



1.6.3 Heck Couplings

Watson and co-workers have recently described the first Heck coupling of aryl pivalates.⁶² Coupling of 2-naphthylpivalate with various styrenyl derivatives provided products in excellent yield (Scheme 1.34). The scope included phenyl and heterocyclic pivalates. Of note, of the many phenol derivatives examined (i.e. OTs, OMs, OAc, OMe), aryl pivalates proved to be the optimal substrate for this transformation under the developed reaction conditions.

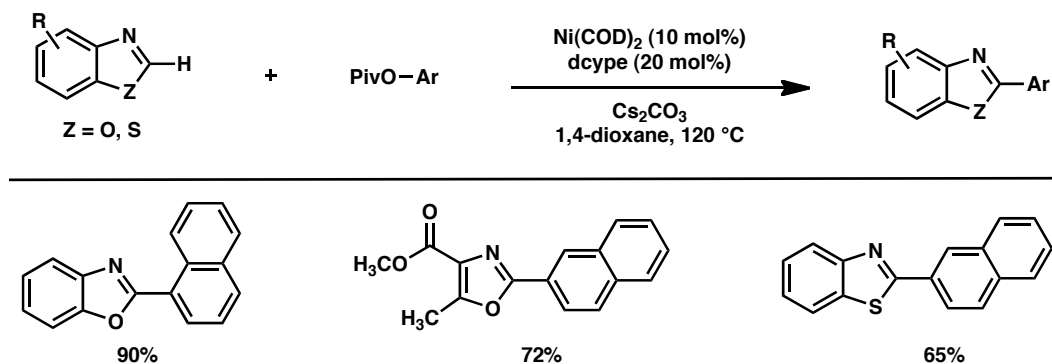
Scheme 1.34



1.6.4 C–H Azole Couplings

The nickel-catalyzed coupling of azoles with phenol derivatives has been reported by the Itami laboratory.⁶³ A number of phenol derivatives, including triflates, sulfamates, and carbamates could be used; however, in most instances the coupling was performed with aryl pivalates. Variation in the both the azole and aryl pivalate were well tolerated in the reaction (Scheme 1.35). Interestingly, ligands commonly employed in nickel-catalyzed reactions involving aryl C–O bonds were completely ineffective in this transformation and 1,2-bis(dicyclohexylphosphino)ethane (dcype) was found to be the ligand of choice.

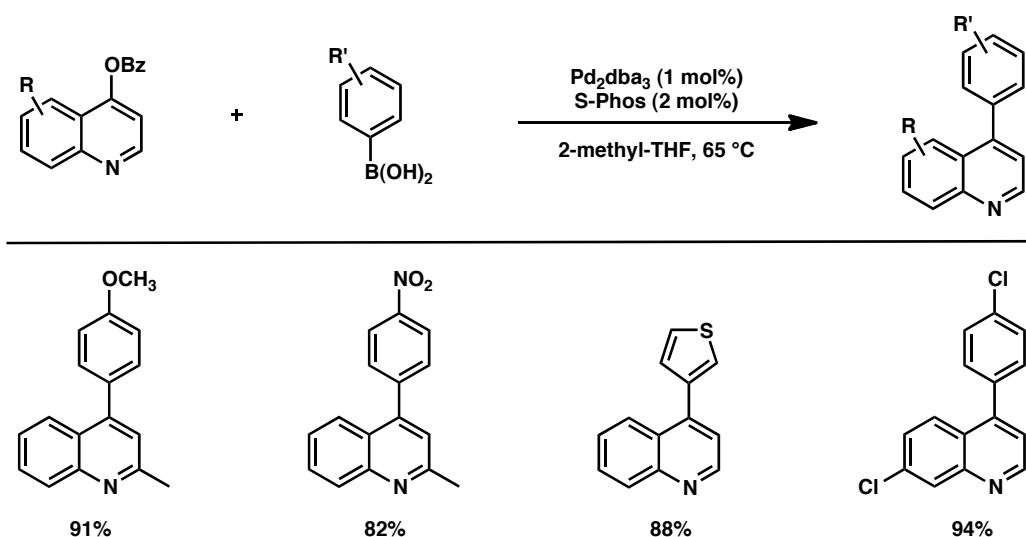
Scheme 1.35



1.6.5 Palladium-Catalyzed Suzuki–Miyaura Couplings

Although aryl esters are typically thought to be inert toward palladium catalysis, a report from Li and co-workers at Boehringer-Ingelheim pharmaceuticals describes the palladium-catalyzed Suzuki–Miyaura coupling of quinoline-derived benzoates (Scheme 1.36).⁶⁴ A wide variety of benzoate esters derived from 4-hydroxyquinoline underwent coupling with a range of aryl boronic acids in excellent yield. Of note, is the transformation proceeds in the absence of base.

Scheme 1.36



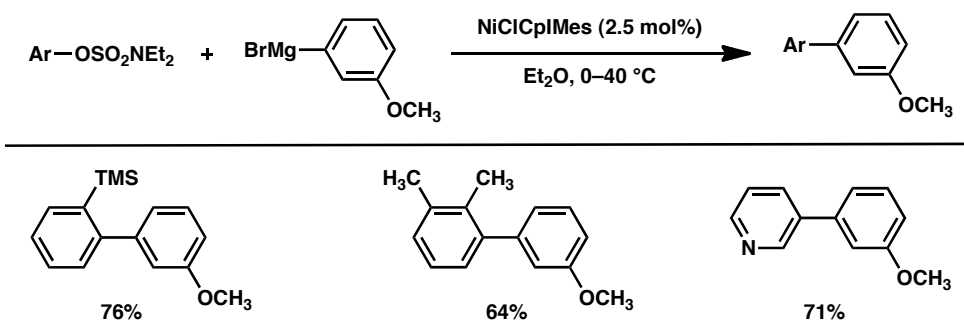
1.7 Nickel-Catalyzed Cross-Couplings of Aryl and Vinyl Sulfamates

1.7.1 Kumada Couplings

Snieckus and co-workers have shown that the *O*-sulfamate moiety is an effective group for directed *ortho*-metalation (DoM) and use in nickel-catalyzed Kumada couplings. In an early report,⁶⁵ the Snieckus laboratory found that the Ni–NHC complex, NiClCpIMes, was an extraordinarily efficient catalyst for the cross-coupling of aryl sulfamates with aryl Grignard

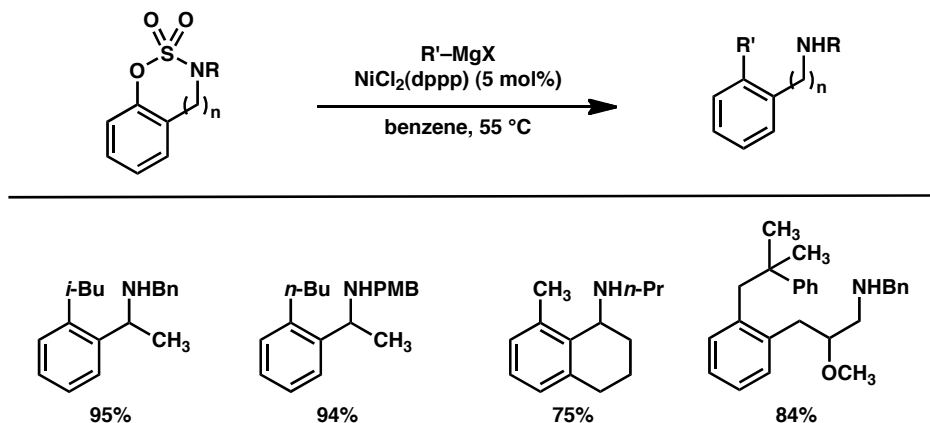
reagents. As shown in Scheme 1.37, this allowed for the construction of biaryl products, including *ortho*-substituted biaryls, in good to excellent yield.

Scheme 1.37



Wehn and Du Bois have reported the nickel-catalyzed Kumada coupling of cyclic sulfamate derivatives.⁶⁶ In this methodology the cyclic sulfamates were constructed via a rhodium-catalyzed nitrene C–H insertion reaction, and then subjected to conditions for the nickel-catalyzed Kumada coupling. This allowed for the construction of functionalized aromatics starting from simple *ortho*-substituted phenols. Variation in the nitrogen substituent, and Grignard reagent was well tolerated (Scheme 1.38).

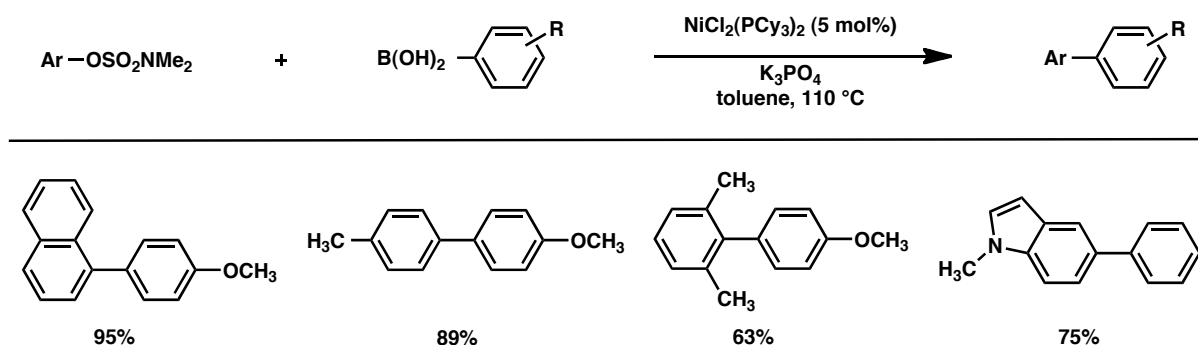
Scheme 1.38



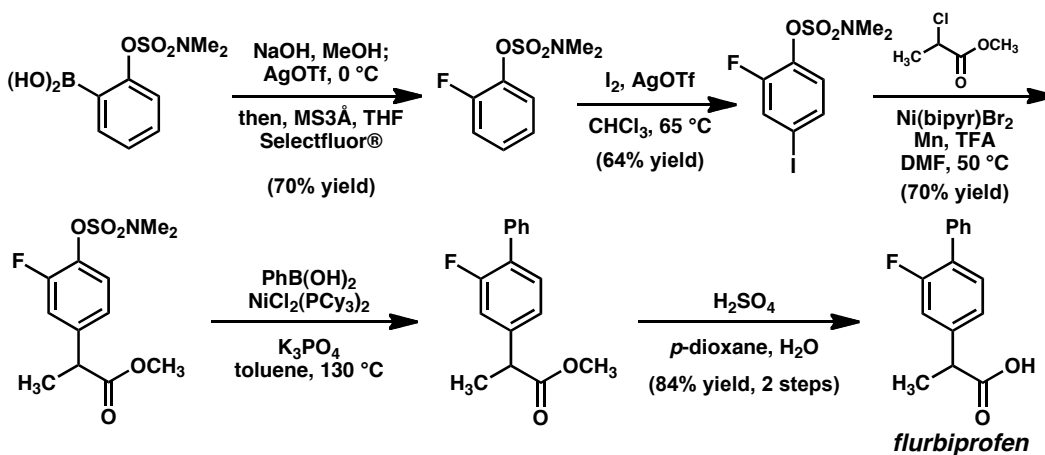
1.7.2 Suzuki–Miyaura Couplings

Garg recently reported the first successful Suzuki–Miyaura cross-coupling of aryl sulfamates (Scheme 1.39).⁶⁷ Naphthyl, nonfused aromatic, heterocyclic, and vinyl sulfamates were converted to biaryl products in good yields. The coupling of sterically hindered or *ortho*-substituted sulfamates could be overcome at elevated temperatures. This Ni-catalyzed cross-coupling of sulfamates was applied to the synthesis of the anti-inflammatory drug flurbiprofen, highlighting the ability of the sulfamate to serve as a powerful directing group and as a competent coupling partner (Scheme 1.40).

Scheme 1.39

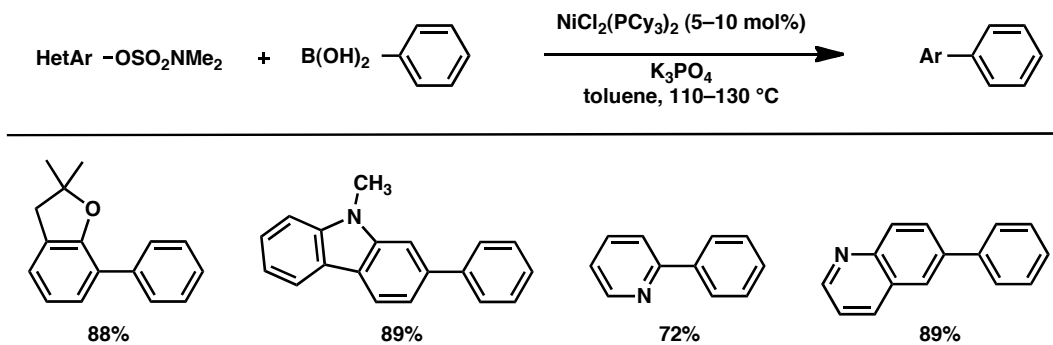


Scheme 1.40

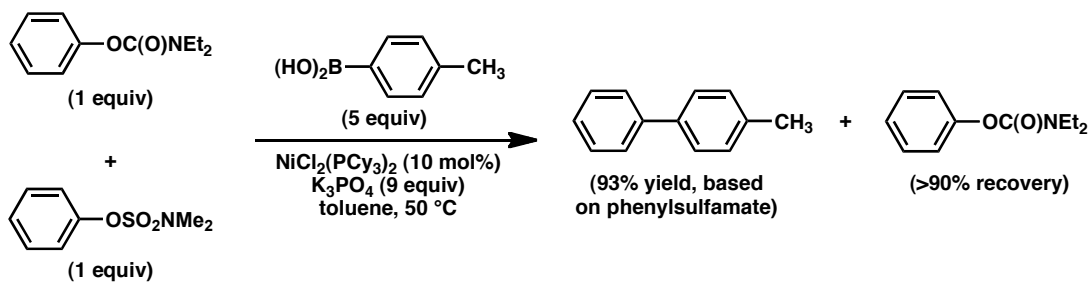


Subsequently, Garg and Snieckus extended the scope of aryl sulfamate Suzuki–Miyaura couplings to allow for the coupling of a wider variety of heterocyclic substrates (Scheme 1.41).⁶⁸ It was also demonstrated that an aryl sulfamate could be coupled in the presence of an aryl carbamates with high selectivity (Scheme 1.42). Computational and experimental mechanistic studies provided evidence that transmetalation is likely the rate-determining step in the catalytic cycle, in the Suzuki–Miyaura coupling of aryl sulfamate.

Scheme 1.41

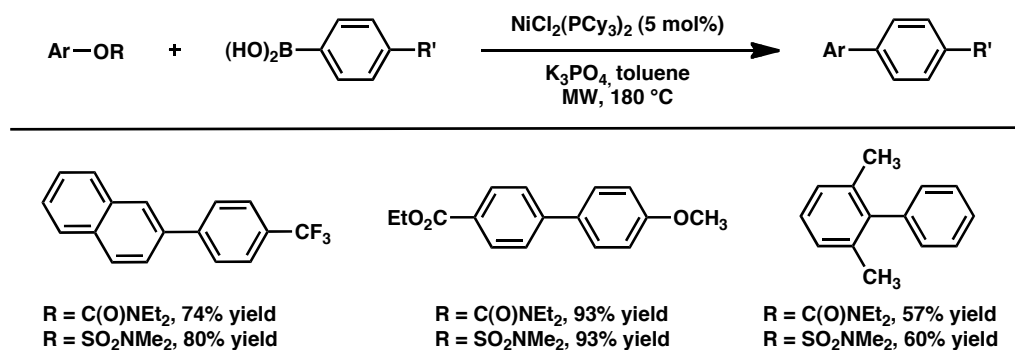


Scheme 1.42



The Suzuki–Miyaura coupling of aryl sulfamates and carbamates has also been explored by Kappe and co-workers using microwave conditions.⁶⁹ The substrate scope and yields using the microwave conditions proved comparable to those found using conventional thermal conditions (Scheme 1.43). It was found that reaction times were very quick, usually on the order of 10 minutes, and that the reaction could be scaled up to a 375 mmol scale without an appreciable loss in yield.

Scheme 1.43

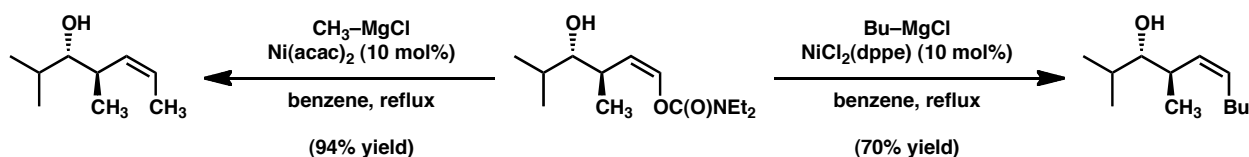


1.8 Nickel-Catalyzed Cross-Couplings of Aryl and Vinyl Carbamates and Carbonates

1.8.1 Kumada Couplings

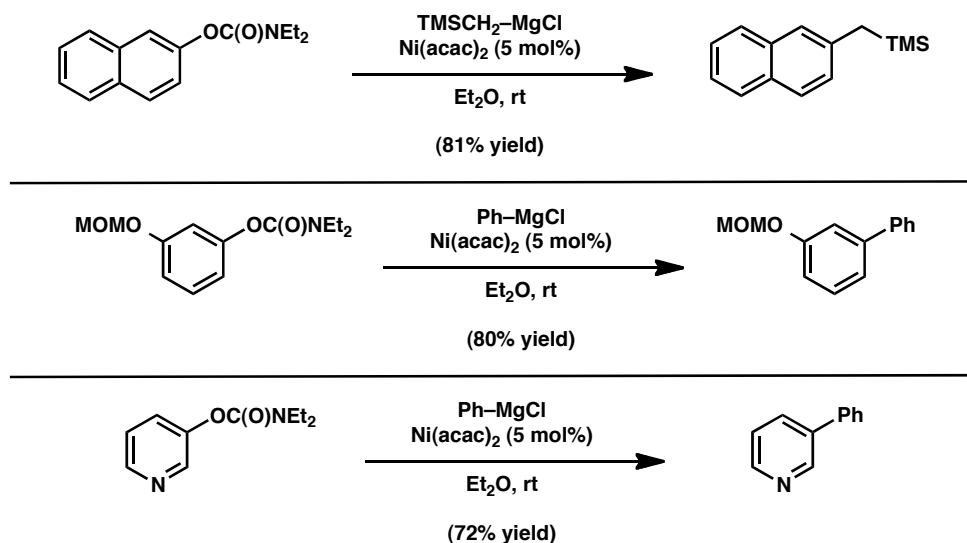
Although typically considered inert substrates, aryl and vinyl carbamates participate in cross-coupling reactions. The earliest examples of carbamate couplings were described by Kocienski and Dixon in 1989.⁷⁰ The authors found that a vinyl carbamate substrate could be coupled with alkyl Grignard reagents in the presence of Ni^{II} precatalysts (Scheme 1.44). Methylation and butylation delivered the corresponding olefins with retention of alkene stereochemistry. In the latter case, the NiCl₂(dppe) complex was found to suppress undesired reduction of the substrate that had been observed when using Ni(acac)₂. Betzer and co-workers have reported similar results using vinyl, aryl, and alkyl Grignard reagents, where the identity of the Ni^{II} precatalyst was found to influence product distribution (i.e., desired cross-coupling versus reduction or homocoupling).⁷¹

Scheme 1.44



Snieckus and co-workers have demonstrated that aryl carbamates undergo Kumada coupling with aryl and alkyl Grignard reagents under conditions similar to those utilized for vinyl carbamate coupling.⁷² The transformation is tolerant of fused aromatic carbamate substrates, in addition to nonfused aromatic derivatives and heterocycles (Scheme 1.45). Of note, the authors found that *ortho*-substituted aryl carbamates are easily accessible through directed-metalation chemistry⁵ and, more recently, via Pd-mediated C–H functionalization.⁴

Scheme 1.45



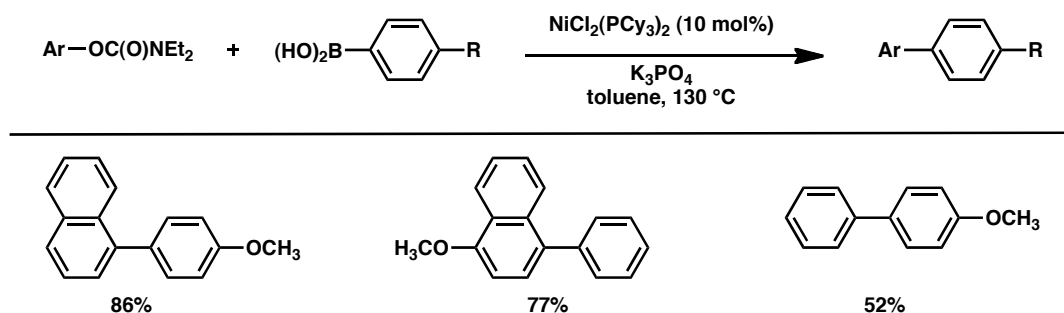
Snieckus and co-workers' methodology has proven quite robust and scalable, as demonstrated in a high-yielding synthesis of 2,7-dimethylnaphthalene beginning from 2,7-dihydroxynaphthalene, which was carried out on a 200 mmol scale.⁷³ Recently, Nakamura and co-workers have utilized a hydroxyphosphine ligand to achieve aryl carbamate Kumada couplings.²⁷

1.8.2 Suzuki–Miyaura Couplings

The Garg and Snieckus laboratories simultaneously reported the nickel-catalyzed Suzuki–Miyaura coupling of aryl carbamates.^{67,68,74} Garg's method allows for the cross-coupling of aryl carbamates with aryl boronic acids to deliver biaryls (Scheme 1.46). Fused aromatic substrates provided the highest yields, whereas nonfused aromatics typically afforded products in ca. 50% yield. The optimal reaction conditions also facilitated the Suzuki–Miyaura coupling of naphthyl carbonates. As described by Kappe, microwave conditions that proved successful for

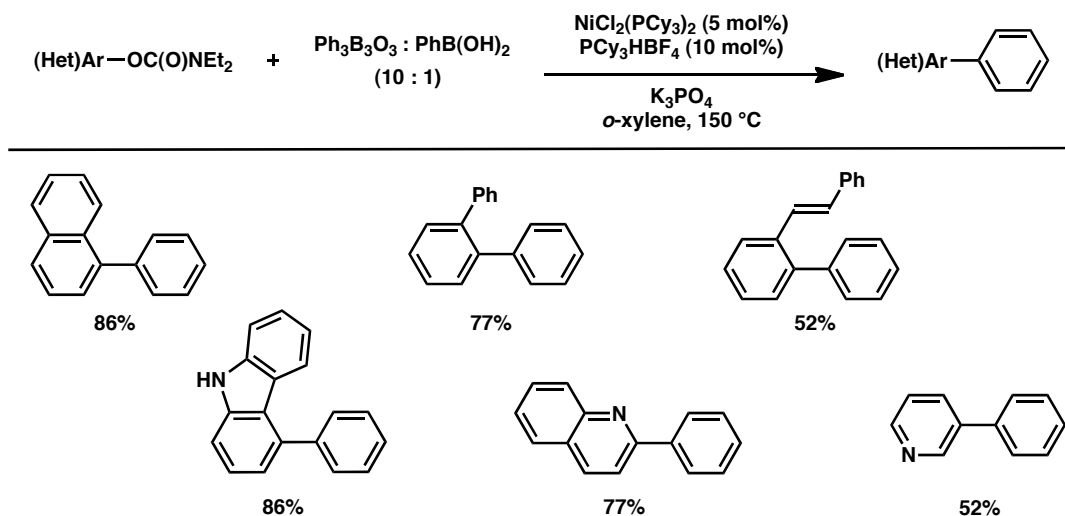
the coupling of aryl sulfamates also proved applicable to the Suzuki–Miyaura coupling of aryl carbamates.⁶⁹

Scheme 1.46



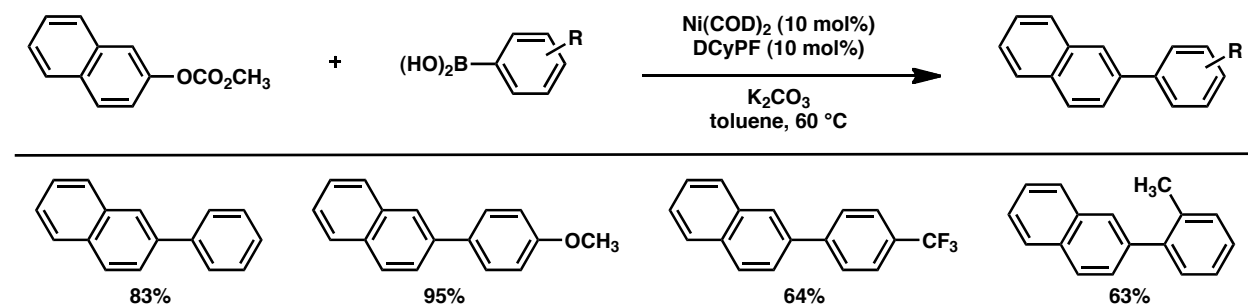
Snieckus' variant of the aryl carbamate Suzuki–Miyaura coupling possesses a wide substrate scope.⁶⁸ By using a mixture of triaryl boroxine and aryl boronic acid (10:1 ratio) at $150\text{ }^\circ\text{C}$, naphthyl substrates, nonfused aromatics, and heterocyclic substrates could be used in the methodology (Scheme 1.47). Most strikingly, several *ortho*-substituted aromatics could be cross-coupled in synthetically useful yields. This tactic, prefaced by the introduction of *ortho*-substituents using directed metalation, provided access to several polysubstituted aromatic and heteroaromatic compounds. More recently, Shi and co-workers have disclosed an alternative protocol for the Suzuki–Miyaura coupling of aryl carbamates using triaryl boroxines and 1 equiv of water.⁷⁵ The modified protocol functioned at lower temperatures (i.e., $110\text{ }^\circ\text{C}$), provided biaryls in high yields ranging from 62–95%, and proved amenable to the corresponding cross-coupling of vinyl carbamate substrates.

Scheme 1.47



Recently Kuwano and Shimizu have reported an improved protocol for the coupling of aryl carbonates.⁷⁶ Imperative to the success of the reaction is the use of the 1,1'-bis(dicyclohexylphosphino)ferrocene (DCyPF) ligand. Under optimized reaction conditions, aryl carbonates were coupled to afford biaryl products in good yield (Scheme 1.48).

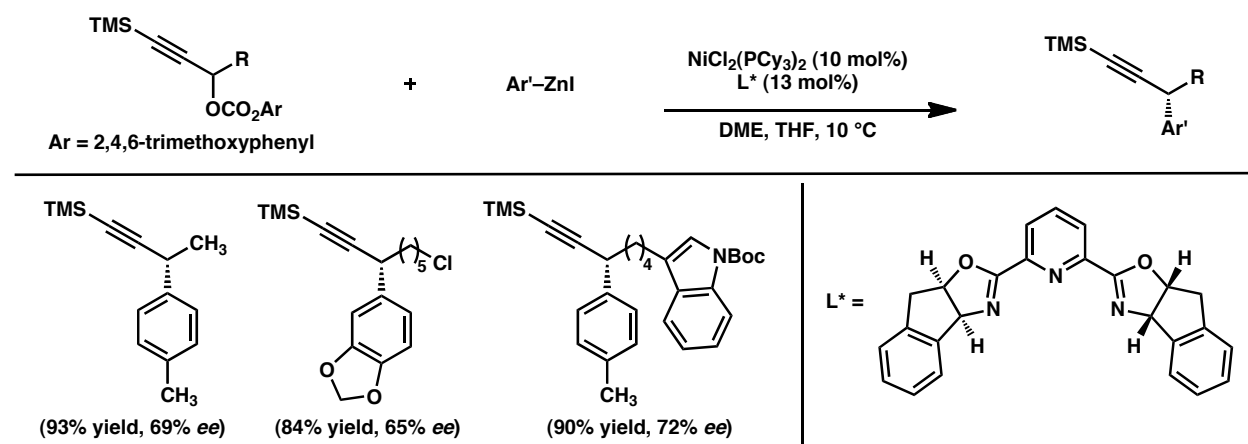
Scheme 1.48



1.8.3 Negishi Couplings

In 2012, Fu and co-workers reported the first nickel-catalyzed Negishi coupling of propargylic carbonates.⁷⁷ It was shown that racemic propargylic carbonates could be coupled with a wide scope of aryl zinc reagents to afford products in good yield and excellent *ee* (Scheme 1.49). This methodology is particularly noteworthy given its ability to construct sp^2 - sp^3 C-C bonds in an asymmetric fashion utilizing an unconventional coupling partner.

Scheme 1.49



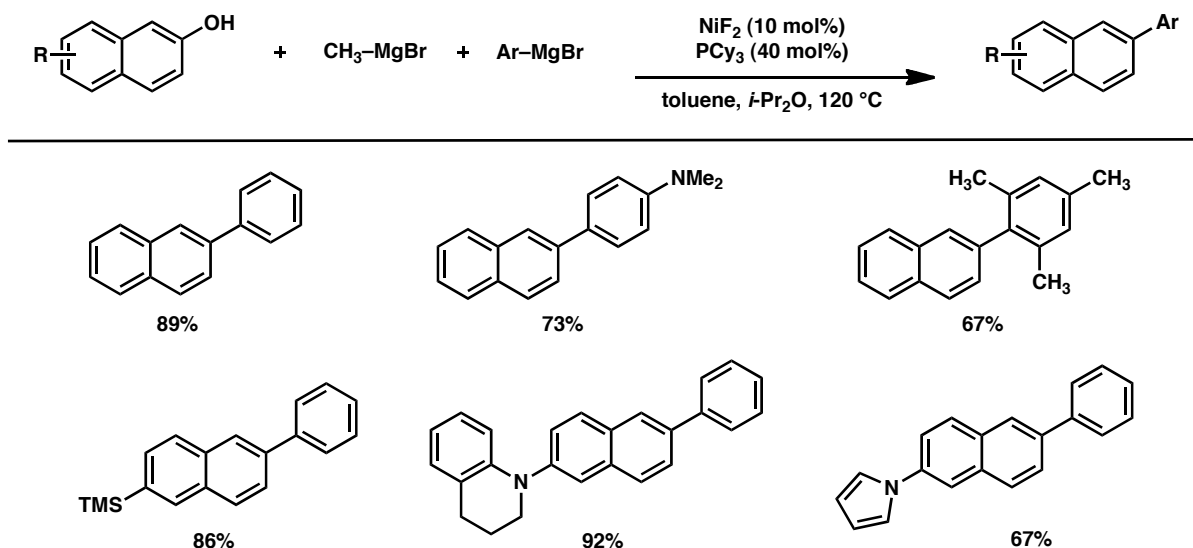
1.9 Nickel-Catalyzed Cross-Couplings of Phenols

1.9.1 Kumada Couplings

Shi and co-workers recently described the unprecedented cross-coupling of 2-naphthol derivatives.⁷⁸ In this transformation, 2-naphthol derivatives were treated sequentially with methyl magnesium bromide and an aryl Grignard reagent in the presence of NiF_2 and PCy_3 at 120 °C to deliver arylated products (Scheme 1.50). Although the reaction only proceeds with 2-naphthol derivatives, the scope with respect to substituents on the naphthol is quite broad, as is the range with respect to the aryl Grignard reagents. Cross-coupled products were obtained in 67–92%

yield depending on the nature of the substrate. Several phenoxide substrates were tested, and it was found that bulky substituents decreased the rate of the reaction, thus resulting in lower yields.

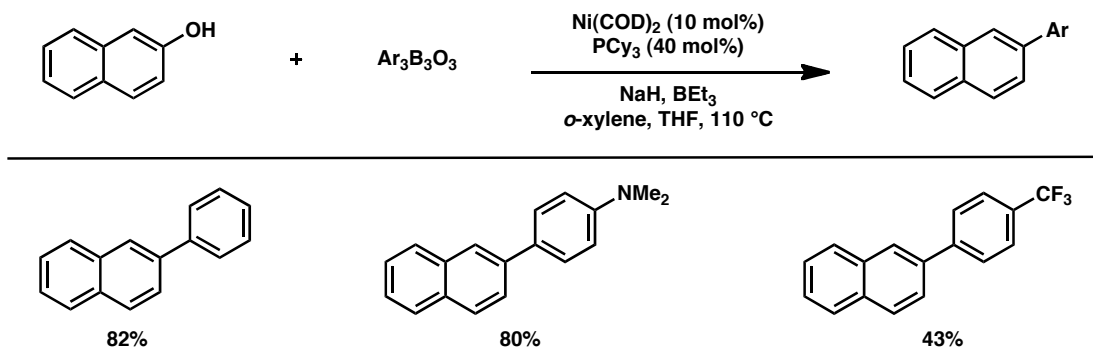
Scheme 1.50



1.9.2 Suzuki–Miyaura Couplings

Shi has also extended the scope of phenol couplings to include the Suzuki–Miyaura coupling.⁷⁹ As seen in earlier examples involving Kumada couplings, the best yields were obtained using 2-naphthol (Scheme 1.51). However, in the case of the Suzuki–Miyaura couplings the substrate scope was expanded to include other polycyclic phenols. Attempts to couple simple phenol derivatives proved difficult and afforded the desired biaryl products in low yield.

Scheme 1.51

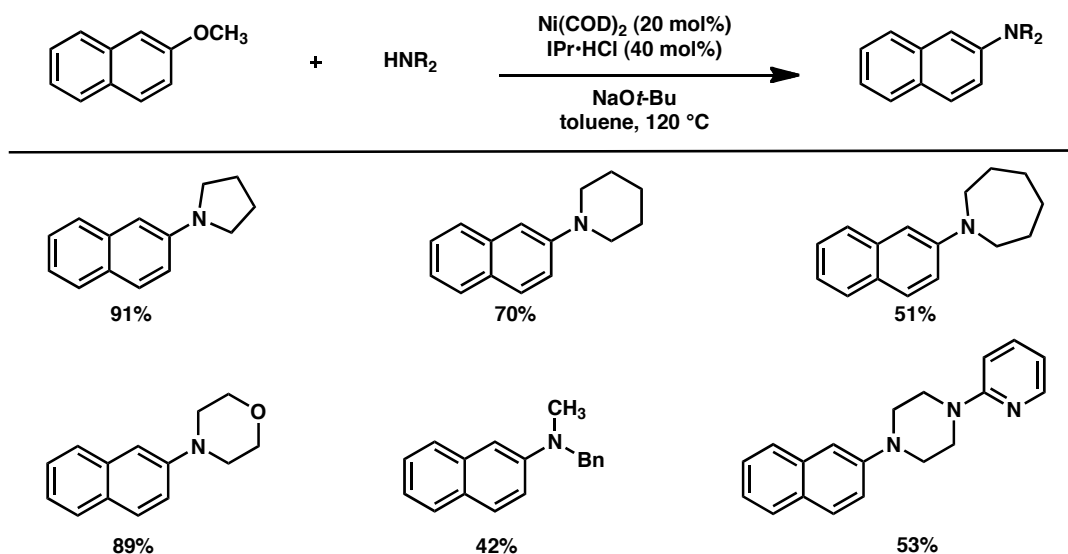


1.10 Non Carbon–Carbon Bond Forming Reactions

1.10.1 Amination Reactions

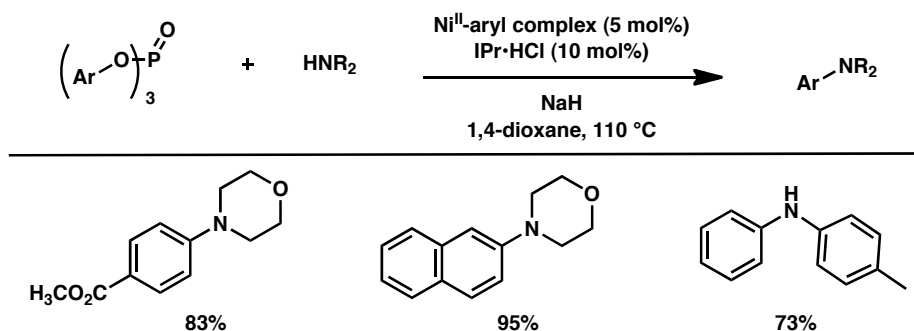
Chatani and co-workers have discovered conditions that enable the amination of methyl ethers using nickel catalysis. The amination of 2-methoxynaphthalene proceeds readily using $\text{Ni}(\text{COD})_2$ and the *N*-heterocyclic carbene ligand IPr in toluene at $120\text{ }^\circ\text{C}$ (Scheme 1.52).⁸⁰ Cyclic amines of varying sizes were tolerated, as were acyclic amines and substrates possessing additional heteroatoms. Phenolic methyl ethers could also be used in the amination reaction, albeit with lower yields (ca. 40%).

Scheme 1.52



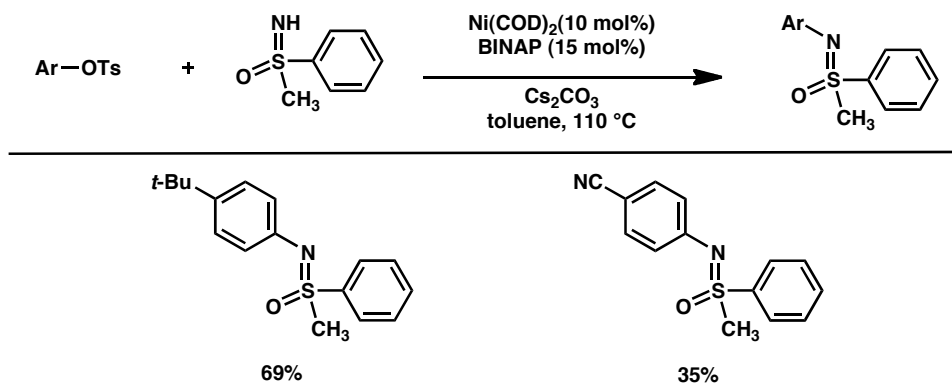
The amination of aryl phosphates using nickel-catalysis was reported by Huang and Yang in 2011 (Scheme 1.53).⁸¹ The methodology relies on the use of a Ni^{II} -aryl complex as a precatalyst that is reduced in situ to the active Ni^0 catalyst. This in conjunction with the *N*-heterocyclic carbene ligand *IPr*, allows for the coupling of aryl phosphates in good yield. Both phenyl and fused aromatic phosphates were competent coupling partners, and the scope with respect to amine was also broad.

Scheme 1.53



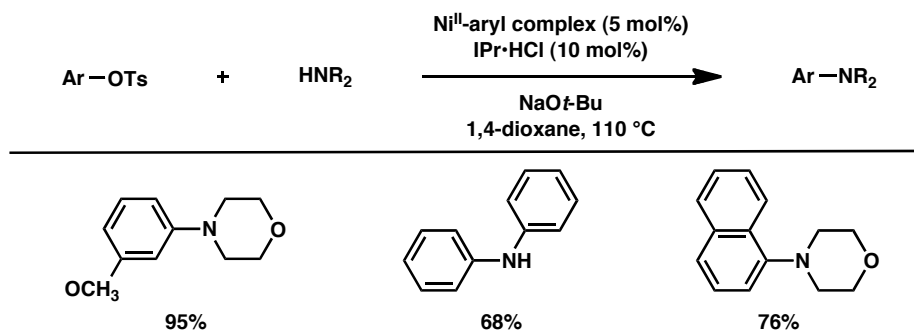
In 2000, Bolm et al. reported the first nickel-catalyzed C–N bond forming reaction of aryl tosylates with *N*-aryl sulfoximines (Scheme 1.54).⁸² A Ni(COD)₂/BINAP catalyst system was found to be effective for promoting the desired transformation.

Scheme 1.54



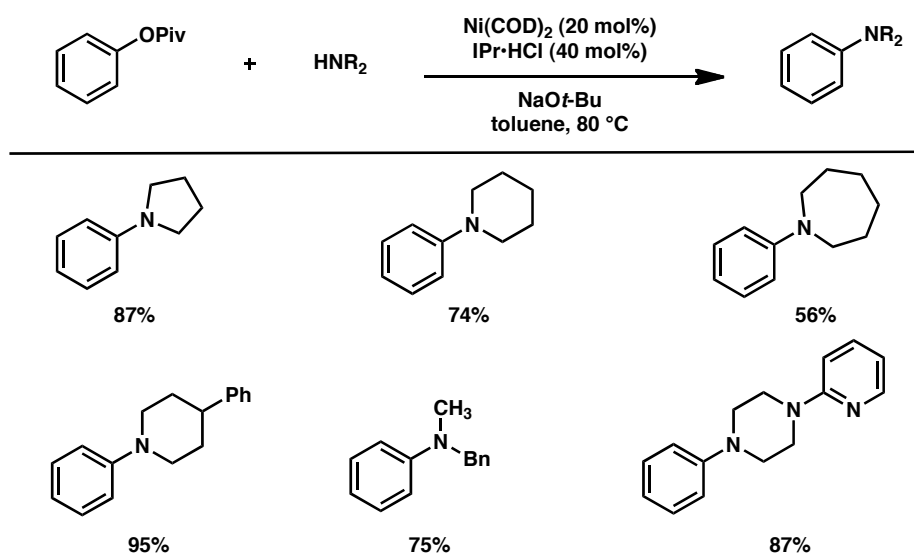
In 2008, Yang and co-workers extended the amination of aryl tosylates to include secondary amines and aniline derivatives (Scheme 1.55).⁸³ Using Ni^{II}-aryl complexes and NaO*t*-Bu as base, a number of aryl tosylates could be coupled to deliver aminated products in good yield.

Scheme 1.55



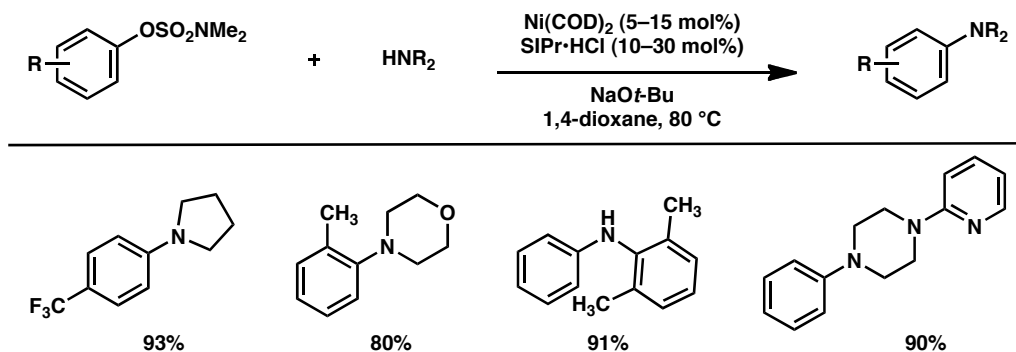
In addition to serving as tools for carbon–carbon bond formation, aryl pivalates have been utilized to access carbon–nitrogen bonds using methodology disclosed by Chatani and co-workers (Scheme 1.56).⁸⁴ The use of Ni(COD)₂ and the *N*-heterocyclic carbene ligand IPr facilitated the desired transformation. The scope of the methodology was broad with respect to both the pivalate and amine coupling partners.

Scheme 1.56

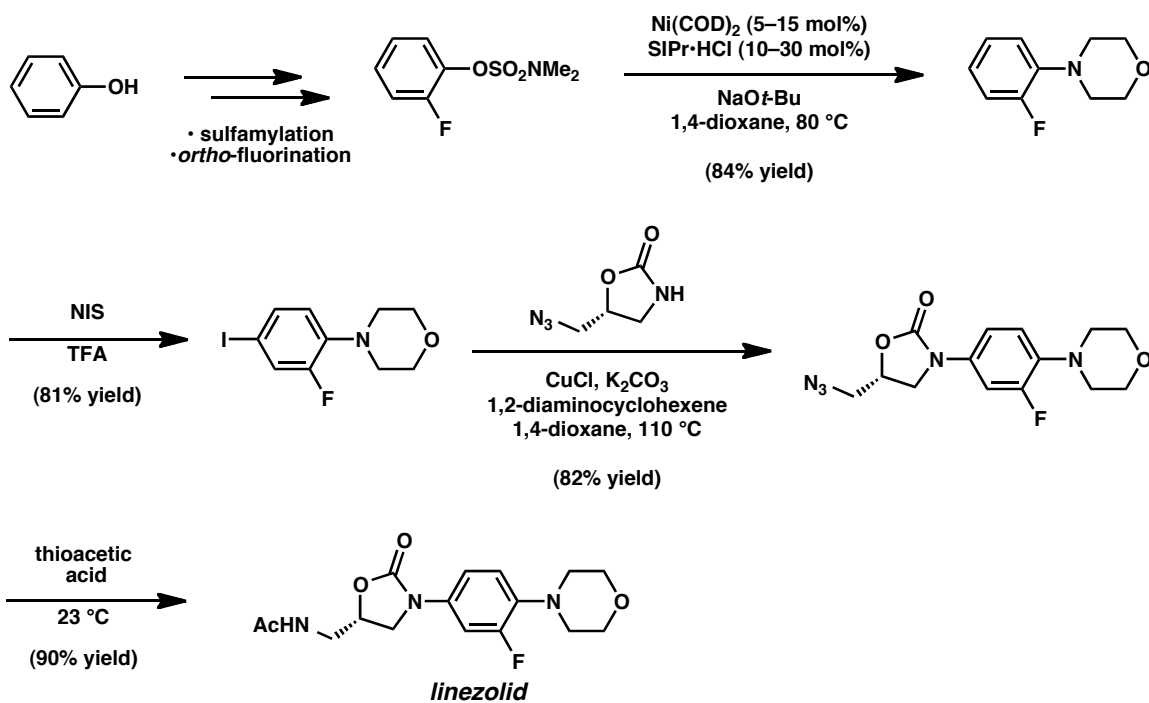


The first nickel-catalyzed amination of sulfamates was reported by Garg and co-workers (Scheme 1.57). It was shown that aryl sulfamates, including many *ortho*-substituted compounds, would undergo amination with both cyclic and acyclic amines, as well as aniline derivatives, using a Ni(COD)₂/SIPr catalyst system.⁸⁵ Showcasing the unique ability of the sulfamate for the construction of polysubstituted aromatics, a concise synthesis of the antibacterial drug linezolid was also demonstrated (Scheme 1.58).

Scheme 1.57



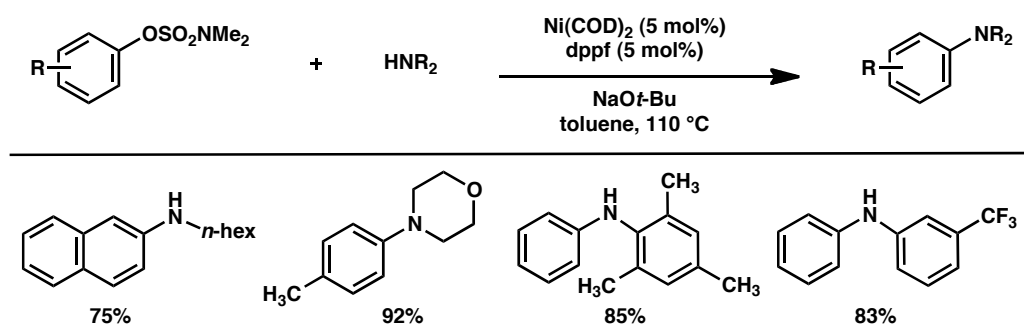
Scheme 1.58



Ackermann and co-workers have also explored the amination of aryl sulfamates (Scheme 1.59).⁸⁶ In contrast to many other nickel-catalyzed aminations, this method relies on the use of dppe as a ligand instead of a *N*-heterocyclic carbene. Nonetheless, the substrate scope is

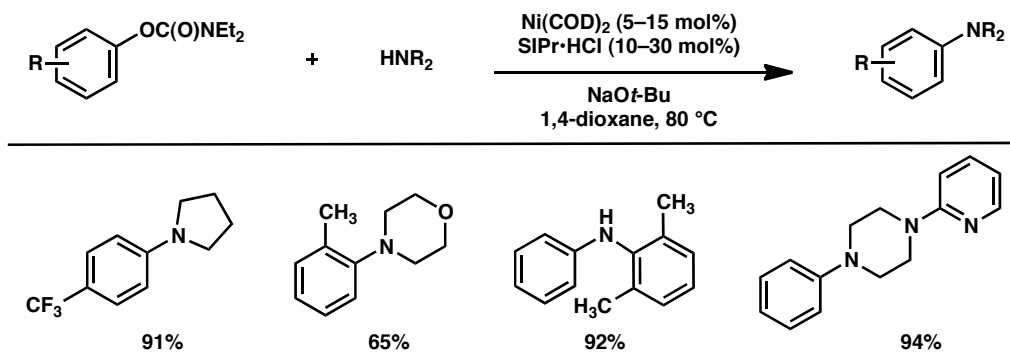
comparable with aniline derivatives and both cyclic and acyclic amines undergoing efficient coupling.

Scheme 1.59



The first carbamate amination was a single example reported in Chatani and co-workers' study of aryl pivalate amination.⁸⁴ Garg later disclosed a general method for aryl carbamate amination.⁸⁷ It was found that conditions that promoted the amination of aryl sulfamates could also be applied to the amination of aryl carbamates. Reactions had a wide substrate scope with respect to both the aryl carbamate and amine coupling partners (Scheme 1.60). A computational study was also conducted, which suggested that reductive elimination was the rate-determining step in the catalytic cycle.

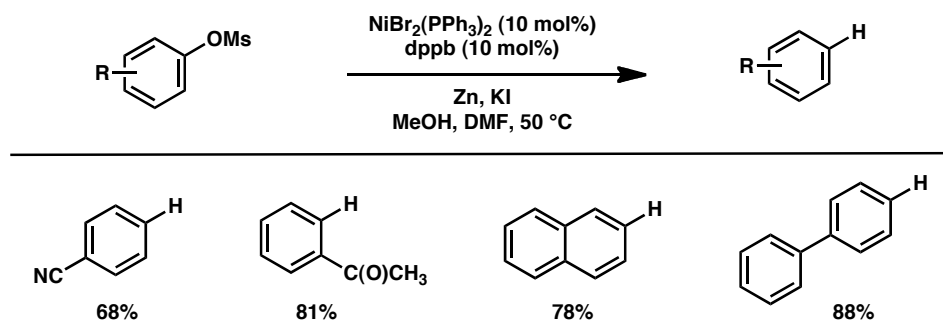
Scheme 1.60



1.10.2 Deoxygenation Reactions

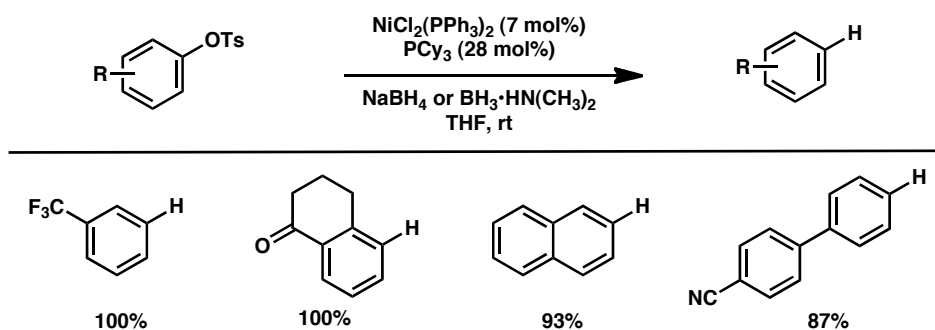
Sasaki and co-workers reported the first conditions for the deoxygenation of aryl mesylates.⁸⁸ Conditions using a $\text{NiBr}_2(\text{PPh}_3)_2/\text{dppb}$ catalyst system in MeOH/DMF afforded reduced products in good yields (Scheme 1.61). Reductions can also be expanded to include alkyl mesylates as described by Alonso and Yus with the use of a $\text{NiCl}_2\cdot 2\text{H}_2\text{O}/\text{Li-DTBB}$ catalyst system.⁸⁹

Scheme 1.61



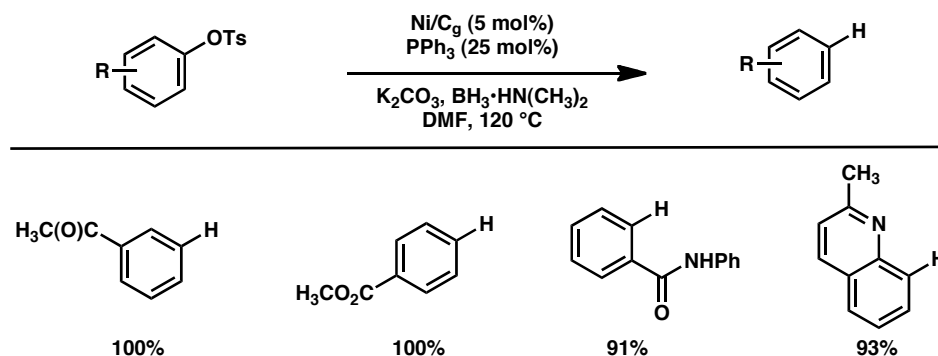
Aryl tosylates also undergo deoxygenation reactions as describe by Kogan.⁹⁰ Using NaBH_4 , or $\text{BH}_3 \cdot \text{HN}(\text{CH}_3)_2$ in cases where other functional groups were sensitive to reduction, aryl tosylates could be reduced in excellent yield (Scheme 1.62).

Scheme 1.62



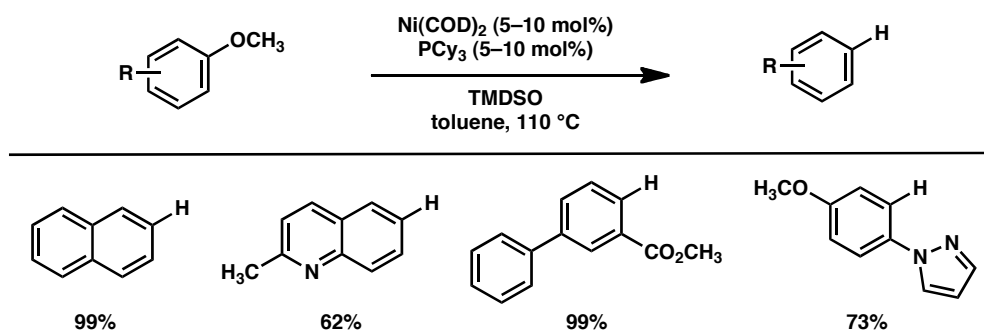
Lipshutz et al. have tested their heterogeneous Ni/C catalyst in the reduction of aryl mesylates and tosylates.⁹¹ The Ni/C catalyst was prepared using $\text{BH}_3 \cdot \text{HN}(\text{CH}_3)_2$ as reducing agent and PPh_3 as a ligand. Microwave irradiation decreased the reaction time considerably (ca. 45 minutes) and in some case provide quantitative reduction (Scheme 1.63). This mild reaction showed very good tolerance to other sensitive functional groups such as esters, amides, and ketones.

Scheme 1.63



In a recent report, Álvarez-Bercedo and Martín⁹² found that aryl methyl ethers could be reduced to the corresponding arenes by using catalytic Ni(COD)₂/PCy₃ in the presence of stoichiometric tetramethyldisiloxane (TMDSO) as a hydride source (Scheme 1.64). This technique can be broadly applied to substituted arenes, naphthalenes, biaryls, or heterobiaryls and provides a useful approach toward removing methoxy groups from a substrate after their use as *ortho*-directing groups has been fulfilled.

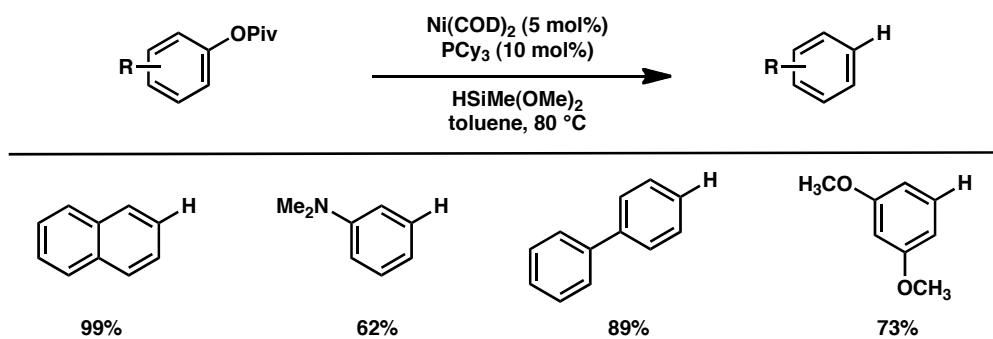
Scheme 1.64



Chatani and co-workers have also reported the nickel-catalyzed reduction of aryl methyl ethers, and have also applied the methodology to the reduction of aryl pivalate esters as (Scheme

1.65).⁹³ Both fused aromatic and phenyl methyl ethers could be reduced to the corresponding arene in good yields. Aryl pivalates proved to be excellent substrates as, affording good yields of the desired product across a wide variety of substrates.

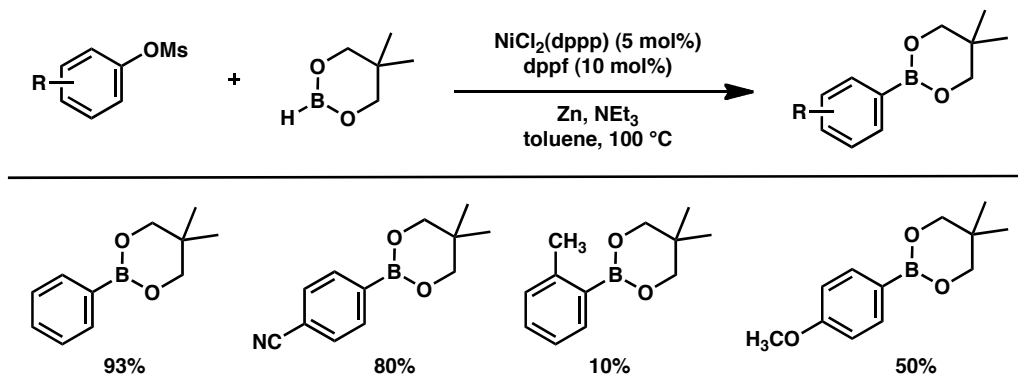
Scheme 1.65



1.10.3 Borylation Reactions

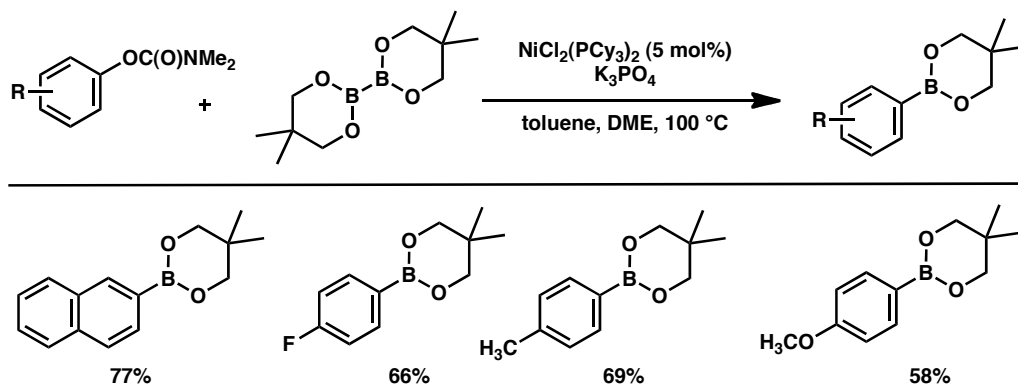
The first example for the borylation of an aryl mesylate was reported by Percec, although the transformation proceeded in only 8% yield.⁹⁴ In subsequent efforts, Percec and co-workers have developed an improved procedure utilizing a mixed catalyst system of NiCl₂(dppp)/dppf for the neopentylglycolborylation of aryl mesylates and tosylates to deliver aryl boronic esters in moderate yields. In the case of *ortho*-substituted compounds, yields were generally diminished (Scheme 1.66).⁹⁵

Scheme 1.66



The neopentylglycolborylation of aryl carbamates has recently been reported by Shi and co-workers (Scheme 1.67).⁹⁶ Carbamates derived from both fused and phenyl substrates provided borylated products in good yields. The use of a diboron reagent in this transformation also prevented the need to add an external reducing agent for the reduction of the Ni^{II} precatalyst to the active Ni⁰ catalyst.

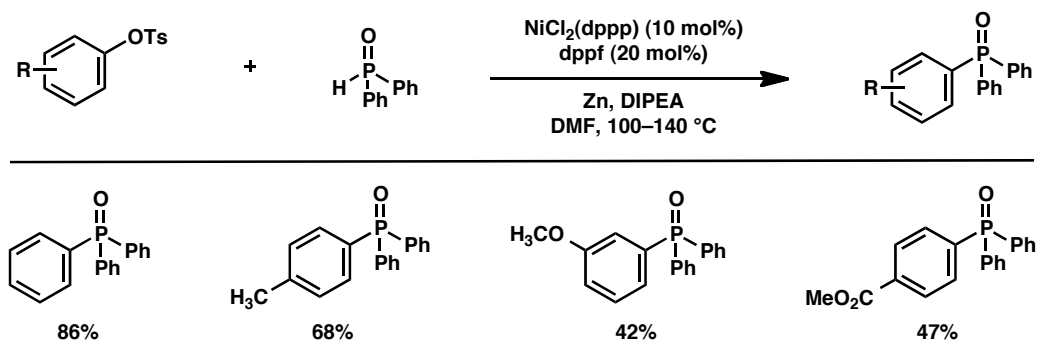
Scheme 1.67



1.10.4 Phosphonylation Reactions

The Zhang laboratory has shown that the nickel-catalyzed phosphonylation of aryl tosylates and mesylates affords aryl phosphine oxides in moderate to good yields (Scheme 1.68).⁹⁷ Among the catalyst systems tested, the NiCl₂(dppf)/dppf catalyst system was uniquely effective for the transformation.

Scheme 1.68



1.11 Conclusion

As discussed above, the use of nickel in transition metal-catalyzed reactions has become an extremely popular and rapidly expanding field of research. In large part this is due to the unique ability of nickel to activate unconventional C–O electrophiles for use in cross-coupling reactions. Often times, these C–O electrophiles are more readily available than the corresponding organic halides, and may have improved stability to a variety of reaction conditions. For instance the low reactivity of aryl pivalates, carbamates, and sulfamates toward Pd catalysis provides the opportunity for sequential site selective couplings. Several of the C–O electrophiles also serve as powerful directing groups for the synthesis of complex polysubstituted aromatic compounds. It is

expected that the use of nickel in transition metal catalysis will continue to grow in the coming years as new, practical, and innovative methods are discovered.

1.12 Notes and References

- (1) (a) *Metal-Catalyzed Cross-Coupling Reactions*; Diederich, F., Meijere, A., Eds.; Wiley-VCH: Weinheim, 2004. (b) Hassan, J.; Sévignon, M.; Gozzi, C.; Schulz, E.; Lemaire, M. *Chem. Rev.* **2002**, *102*, 1359–1469. (c) *Topics in Current Chemistry*; Miyaura, N., Ed.; Vol. 219; Springer-Verlag: New York, 2002. (d) Corbet, J.; Mignani, G. *Chem. Rev.* **2006**, *106*, 2651–2710. (e) Negishi, E. *Bull. Chem. Soc. Jpn.* **2007**, *80*, 233–257.
- (2) For a pertinent review, see: Littke, A. F.; Fu, G. C. *Angew. Chem. Int. Ed.* **2002**, *41*, 4176–4211.
- (3) For a Pd-based method for ester-directed arene functionalization, see: Xiao, B.; Fu, Y.; Xu, J.; Gong, T.-J.; Dai, J.-J.; Yi, J.; Liu, L. *J. Am. Chem. Soc.* **2010**, *132*, 468–469.
- (4) For Pd-, Ir-, or Rh-based methods for carbamate-directed arene functionalization, see: (a) Bedford, R. B.; Webster, R. L.; Mitchell, C. J. *Org. Biomol. Chem.* **2009**, *7*, 4853–4857. (b) Zhao, X.; Yeung, C. S.; Dong, V. M. *J. Am. Chem. Soc.* **2010**, *132*, 5837–5844. (c) Nishikata, T.; Abela, A. R.; Huang, S.; Lipshutz, B. H. *J. Am. Chem. Soc.* **2010**, *132*, 4978–4979. (d) Yamazaki, K.; Kawamorita, S.; Ohmiya, H.; Sawamura, M. *Org. Lett.* **2010**, *12*, 3978–3981. (e) Feng, C.; Loh, T.-P. *Chem. Commun.* **2011**, *47*, 10458–10460. (f) Gong, T.-J.; Xiao, B.; Liu, Z.-J.; Wan, J.; Xu, J.; Luo, D.-F.; Fu, Y.; Liu, L. *Org. Lett.* **2011**, *13*, 3235–3237.
- (5) Snieckus, V. *Chem. Rev.* **1990**, *90*, 879–933.
- (6) Rosen, B. M.; Quasdorf, K. W.; Wilson, D. A.; Zhang, N.; Resmerita, A.-M.; Garg, N. K.; Percec, V. *Chem. Rev.* **2011**, *111*, 1346–1416.
- (7) Yu, D.-G.; Li, B.-J.; Shi, Z.-J. *Acc. Chem. Res.* **2010**, *43*, 1486–1495.

- (8) Wenkert, E.; Michelotti, E. L.; Swindell, C. S. *J. Am. Chem. Soc.* **1979**, *101*, 2246–2247.
- (9) Wenkert, E.; Michelotti, E. L.; Swindell, C. S.; Tingoli, M. *J. Org. Chem.* **1984**, *49*, 4894–4899.
- (10) Dankwardt, J. W. *Angew. Chem., Int. Ed.* **2004**, *43*, 2428–2432.
- (11) Guan, B.-T.; Xiang, S.-K.; Wu, T.; Sun, Z.-P.; Wang, B.-Q.; Zhao, K.-Q.; Shi, Z.-J. *Chem. Commun.* **2008**, 1437–1439.
- (12) Guan, B.-T.; Xiang, S.-K.; Wang, B.-Q.; Sun, Z.-P.; Wang, Y.; Zhao, K.-Q.; Shi, Z.-J. *J. Am. Chem. Soc.* **2008**, *130*, 3268–3269.
- (13) Xie, L.-G.; Wang, Z.-X. *Chem.—Eur. J.* **2011**, *17*, 4972–4975.
- (14) Hayashi, T.; Katsuro, Y.; Kumada, M. *Tetrahedron Lett.* **1980**, *21*, 3915–3918.
- (15) Johnstone, R. A. W.; McClean, W. N. *Tetrahedron Lett.* **1988**, *29*, 5553–5556.
- (16) Zhao, F.; Yu, D.-G.; Zhu, R.-Y.; Xi, Z.; Shi, Z.-J. *Chem. Lett.* **2011**, *40*, 1001–1003.
- (17) Tobisu, M.; Shimasaki, T.; Chatani, N. *Angew. Chem., Int. Ed.* **2008**, *47*, 4866–4869.
- (18) Shimasaki, T.; Konno, Y.; Tobisu, M.; Chatani, N. *Org. Lett.* **2009**, *11*, 4890–4892.
- (19) Nielsen, D. A.; Doyle, A. G. *Angew. Chem. Int. Ed.* **2011**, *50*, 6056–6059.
- (20) Graham, T. J. A.; Shields, J. D.; Doyle, A. G. *Chem. Sci.*, **2011**, *2*, 980–984.
- (21) Graham, T. J. A.; Doyle, A. G.; *Org. Lett.* **2012**, *14*, 1616–1619.
- (22) Hayashi, T.; Fujiwa, T.; Okamoto, Y.; Katsuro, Y.; Kumada, M. *Synthesis* **1981**, 1001–1002.
- (23) Sahlberg, C.; Quader, A.; Claesson, A. *Tetrahedron Lett.* **1983**, *24*, 5137–5138.
- (24) Sofia, A.; Karlström, E.; Itami, K.; Bäckvall, J.-E. *J. Org. Chem.* **1999**, *64*, 1745–1749.
- (25) Nicolaou, K. C.; Shi, G.-Q.; Namoto, K.; Bernal, F. *Chem. Commun.* **1998**, 1757–1758.

- (26) Hayashi, T.; Katsuro, Y.; Okamoto, Y.; Kumada, M. *Tetrahedron Lett.* **1981**, *22*, 4449–4452.
- (27) Yoshikai, N.; Matsuda, H.; Nakamura, E. *J. Am. Chem. Soc.* **2009**, *131*, 9590–9599.
- (28) Tanaka, M.; Chiba, K.-I.; Okita, M.; Kaneko, T.; Tagami, K.; Hibi, S.; Okamoto, Y.; Shirota, H.; Goto, M.; Obaishi, H.; Sakurai, H.; Machida, Y.; Yamatsu, I. *J. Med. Chem.* **1992**, *35*, 4665–4675.
- (29) Baker, W. R.; Pratt, J. K. *Tetrahedron* **1993**, *49*, 8739–8756.
- (30) Iwashima, M.; Nagaoka, H.; Kobayashi, K.; Yamada, Y. *Tetrahedron Lett.* **1992**, *33*, 81–82.
- (31) Jiang, Y.-Y.; Li, Q.; Lu, W.; Cai, J.-C. *Tetrahedron Lett.* **2003**, *44*, 2073–2075.
- (32) Huang, W. G.; Jiang, Y.-Y.; Li, Q.; Li, J. Y.; Lu, W.; Cai, J.-C. *Tetrahedron* **2005**, *61*, 1863–1870.
- (33) Nan, Y.; Yang, Z. *Tetrahedron Lett.* **1999**, *40*, 3321–3324.
- (34) Hansen, A. L.; Ebran, J.-P.; Gøgsig, T. M.; Skrydstrup, T. *Chem. Commun.* **2006**, 4137–4139.
- (35) Hansen, A. L.; Ebran, J.-P.; Gøgsig, T. M.; Skrydstrup, T. *J. Org. Chem.* **2007**, *72*, 6464–6472.
- (36) Chen, H.; Huang, Z.; Hu, X.; Tang, G.; Xu, P.; Zhao, Y.; Chen, C.-H. *J. Org. Chem.* **2011**, *76*, 2338–2344.
- (37) Zhao, Y.-L.; Li, Y.; Li, Y.; Gao, L.-X.; Han, F.-S. *Chem.—Eur. J.* **2010**, *16*, 4991–4194.
- (38) Wu, J.; Yang, Z. *J. Org. Chem.* **2001**, *66*, 7875–7878.
- (39) Percec, V.; Bae, J. Y.; Hill, D. H. *J. Org. Chem.* **1995**, *60*, 6895–6903.
- (40) Zhang, L.; Luo, Y.; Wu, J. *Synlett* **2012**, *12*, 1845–1848.

- (41) Percec, V.; Bae, J. Y.; Hill, D. H. *J. Org. Chem.* **1995**, *60*, 1060–1065.
- (42) Kobayashi, Y.; Mizojiri, R. *Tetrahedron Lett.* **1996**, *37*, 8531–8534.
- (43) Kobayashi, Y.; William, A. D.; Mizojiri, R. *J. Organomet. Chem.* **2002**, *653*, 91–97.
- (44) Zim, D.; Monteiro, A. L. *Org. Lett.* **2001**, *3*, 3049–3051.
- (45) Tang, Z.-Y.; Hu, Q.-S. *J. Am. Chem. Soc.* **2004**, *126*, 3058–3059.
- (46) Percec, V.; Golding, G. M.; Smidrkal, J.; Weichold, O. *J. Org. Chem.* **2004**, *69*, 3447–3452.
- (47) Leowanawat, P.; Zhang, N.; Percec, V. *J. Org. Chem.*, **2012**, *77*, 1018–1025
- (48) Fan, X.-H.; Yang, L.-M. *Eur. J. Org. Chem.* **2010**, 2457–2460.
- (49) Leowanawat, P.; Zhang, N.; Safi, M.; Hoffman, D. J.; Fryberger, M. C.; George, A.; Percec V. *J. Org. Chem.* **2012**, *77*, 2885–2892.
- (50) Gøgsig, T. M.; Kleimark, J.; Nilsson Lill, S. O.; Korsager, S.; Lindhardt, A. T.; Norrby, P.-O.; Skrydstrup, T. *J. Am. Chem. Soc.* **2012**, *134*, 443–452.
- (51) Quasdorf, K. W.; Tian, X.; Garg, N. K. *J. Am. Chem. Soc.* **2008**, *130*, 14422–14423.
- (52) Guan, B.-T.; Wang, Y.; Li, B.-J.; Yu, D.-G.; Shi, Z.-J. *J. Am. Chem. Soc.* **2008**, *130*, 14468–14470.
- (53) Gooßen, L. J.; Gooßen, K.; Stanciu, C. *Angew. Chem., Int. Ed.* **2009**, *48*, 3569–3571.
- (54) Stone, P. J.; Dori, Z. *Inorg. Chim. Acta* **1971**, *5*, 434–438.
- (55) Barnett, K. W. *J. Chem. Educ.* **1974**, *51*, 422–423.
- (56) Quasdorf, K. W.; Garg, N. K. *Encyclopedia of Reagents for Organic Synthesis*, DOI: 10.1002/047084289X.rn01201.
- (57) Li, Z.; Zhang, S.-L.; Fu, Y.; Guo, Q.-X.; Liu, L. *J. Am. Chem. Soc.* **2009**, *131*, 8815–8823.
- (58) Molander, G. A.; Beaumard, F. *Org. Lett.* **2010**, *12*, 4022–4025.

- (59) Sun, C.-L.; Wang, Y.; Zhou, X.; Wu, Z.-H.; Li, B.-J.; Guan, B.-T.; Shi, Z.-J. *Chem.—Eur. J.* **2010**, *16*, 5844–5847.
- (60) Huang, K.; Li, G.; Haung, W.-P.; Yu, D.-G.; Shi, Z.-J. *Chem. Commun.* **2011**, *47*, 7224–7226.
- (61) Li, B.-J.; Li, Y.-Z.; Lu, X.-Y.; Liu, J.; Guan, B.-T.; Shi, Z.-J. *Angew. Chem., Int. Ed.* **2008**, *47*, 10124–10127.
- (62) Ehle, A. R.; Zhou, Q.; Watson, M. P. *Org. Lett.* **2012**, *14*, 1202–1205.
- (63) Muto, K.; Yamaguchi, J.; Itami, K. *J. Am. Chem. Soc.* **2012**, *134*, 169–172.
- (64) Li, W.; Gao, J. J.; Zhang, Y.; Tang, W.; Lee, H.; Fandrick, K. R.; Lu, B.; Senanayake, C. H. *Adv. Synth. Catal.* **2011**, *353*, 1671–1675.
- (65) Macklin, T. K.; Snieckus, V. *Org. Lett.* **2005**, *7*, 2519–2522.
- (66) Wehn, P. M.; Du Bois, J. *Org. Lett.* **2005**, *7*, 4685–4688.
- (67) Quasdorf, K. W.; Reiner, M.; Petrova, K. V.; Garg, N. K. *J. Am. Chem. Soc.* **2009**, *131*, 17748–17749.
- (68) Quasdorf, K. W.; Antoft-Finch, A.; Liu, P.; Silberstein, A. L.; Komaromi, A.; Blackburn, T.; Ramgren, S. D.; Houk, K. N.; Snieckus, V.; Garg, N. K. *J. Am. Chem. Soc.* **2011**, *133*, 6352–6363.
- (69) Baghbanzadeh, M.; Pilger, C.; Kappe C. O. *J. Org. Chem.* **2011**, *76*, 1507–1510.
- (70) Kocienski, P.; Dixon, N. J. *Synlett* **1989**, 52–53.
- (71) Porée, F.-H.; Clavel, A.; Betzer, J.-F.; Pancrazi, A.; Ardisson, J. *Tetrahedron Lett.* **2003**, *44*, 7553–7556.

- (72) Sengupta, S.; Leite, M.; Raslan, D. S.; Quesnelle, C.; Snieckus, V. *J. Org. Chem.* **1992**, *57*, 4066–4068.
- (73) Dallaire, C.; Kolber, I.; Gingras, M. *Org. Synth.* **2002**, *78*, 42–43.
- (74) Antoft-Finch, A.; Blackburn, T.; Snieckus, V. *J. Am. Chem. Soc.* **2009**, *131*, 17750–17752.
- (75) Xi, L.; Li, B.-J.; Wu, Z.-H.; Lu, X.-Y.; Guan, B.-T.; Wang, B.-Q.; Zhao, K.-Q.; Shi, Z.-J. *Org. Lett.* **2010**, *12*, 884–887.
- (76) Kuwano, R.; Shimizu, R. *Chem. Lett.* **2011**, *40*, 913–915.
- (77) Oelke, A. J.; Sun, J.; Fu, G. C. *J. Am. Chem. Soc.* **2012**, *134*, 2966–2969.
- (78) Yu, D.-G.; Li, B.-J.; Zheng, S.-F.; Guan, B.-T.; Wang, B.-Q.; Shi, Z.-J. *Angew. Chem., Int. Ed.* **2010**, *49*, 4566–4570.
- (79) Yu, D.-G.; Shi, Z.-J. *Angew. Chem. Int. Ed.* **2011**, *50*, 7097–7100.
- (80) Tobisu, M.; Shimasaki, T.; Chatani, N. *Chem. Lett.* **2009**, *38*, 710–711.
- (81) Huang, J.-H.; Yang, L.-M. *Org. Lett.* **2011**, *13*, 3750–3753.
- (82) Bolm, C.; Hildebrand, J. P.; Rudolph, J. *Synthesis* **2000**, 911–913.
- (83) Gao, C. Y.; Yang, L. M. *J. Org. Chem.* **2008**, *73*, 1624–1627.
- (84) Shimasaki, T.; Tobisu, M.; Chatani, N. *Angew. Chem., Int. Ed.* **2010**, *49*, 2929–2932.
- (85) Ramgren, S. D.; Silberstein, A. L.; Yang, Y.; Garg, N. K. *Angew. Chem. Int. Ed.* **2011**, *50*, 2171–2173.
- (86) Ackermann, L.; Sandmann, R.; Song, W. *Org. Lett.* **2011**, *13*, 1784–1786.
- (87) Mesganaw, T.; Silberstein, A. L.; Ramgren, S. D.; Fine Nathel, N. F.; Hong, X.; Liu, P.; Garg, N. K. *Chem. Sci.* **2011**, *2*, 1766–1771.
- (88) Sasaki, K.; Kubo, T.; Sakai, M.; Kuroda, Y. *Chem. Lett.* **1997**, *26*, 617–618.

- (89) Alonso, F.; Yus, M. *Chem. Soc. Rev.* **2004**, *33*, 284–293.
- (90) Kogan, V. *Tetrahedron Lett.* **2006**, *47*, 7515–7518.
- (91) Lipshutz, B. H.; Frieman, B. A.; Butler, T.; Kogan, V. *Angew. Chem., Int. Ed.* **2006**, *45*, 800–803.
- (92) Álvarez-Bercedo, P.; Martin, R. *J. Am. Chem. Soc.* **2010**, *132*, 17352–17353.
- (93) Tobisu, M.; Yamakawa, K.; Shimasaki, T.; Chatani, N. *Chem. Commun.* **2011**, *47*, 2946–2948.
- (94) Wilson, D. A.; Wilson, C. J.; Rosen, B. M.; Percec, V. *Org. Lett.* **2008**, *10*, 4879–4882.
- (95) Wilson, D. A.; Wilson, C. J.; Moldoveanu, C.; Resmerita, A.-M.; Corcoran, P.; Hoang, L. A.; Rosen, B. M.; Percec, V. *J. Am. Chem. Soc.* **2010**, *132*, 1800–1801.
- (96) Huang, K.; Yu, D.-G.; Zheng, S.-F.; Wu, Z.-H.; Shi, Z.-J. *Chem.—Eur. J.* **2011**, *17*, 786–791.
- (97) Shen, C.; Yang, G.; Zhang, W. *Org. Biomol. Chem.* **2012**, DOI: 10.1039/c2ob25225b.

CHAPTER TWO

Cross-Coupling Reactions of Aryl Pivalates with Boronic Acids

Kyle W. Quasdorf, Xia Tian, and Neil K. Garg.

J. Am. Chem. Soc. **2008**, *130*, 14422–14223.

2.1 Abstract

The first cross-coupling of acylated phenol derivatives has been achieved. In the presence of an air-stable Ni(II) complex, readily accessible aryl pivalates participate in the Suzuki–Miyaura coupling with arylboronic acids. The process is tolerant of considerable variation in each of the cross-coupling components. In addition, a one-pot acylation/cross-coupling sequence has been developed. The potential to utilize an aryl pivalate as a directing group has also been demonstrated, along with the ability to sequentially cross-couple an aryl bromide followed by an aryl pivalate, using palladium and nickel catalysis, respectively.

2.2 Introduction

Transition metal-catalyzed cross-coupling reactions have emerged as one of the most powerful methods for constructing carbon–carbon (C–C) and carbon–heteroatom (C–X) bonds.¹ Whereas methodologies for the cross-coupling of aryl halides have significantly improved in the past decade,^{1,2} less progress has been made toward the coupling of the corresponding phenol derivatives.¹ Given that phenols are cheap and readily available, and that oxygenation can be used to direct the installation of functional groups on an aromatic ring, practical methods that allow for the cross-coupling of phenol derivatives are extremely attractive.

Of the known methods for cross-coupling phenol derivatives,^{1,3,4,5} there are no examples that utilize simple *O*-acylated phenols.⁶ Such a process would be of great value, given that *O*-acylated phenols are: a) exceedingly simple to prepare, b) among the most affordable phenol derivatives available,⁷ c) stable to a variety of reaction conditions, and d) able to direct the installation of other functional groups onto an aromatic ring. Furthermore, this cross-coupling would presumably begin by the selective oxidative addition of a metal into the aryl C–O bond of the *O*-acylated phenol (Figure 2.1), a transformation that has never been achieved.⁸ In this Communication, we describe the first cross-coupling reactions of *O*-acylated phenol derivatives, involving the Ni-catalyzed reaction of aryl pivalates.

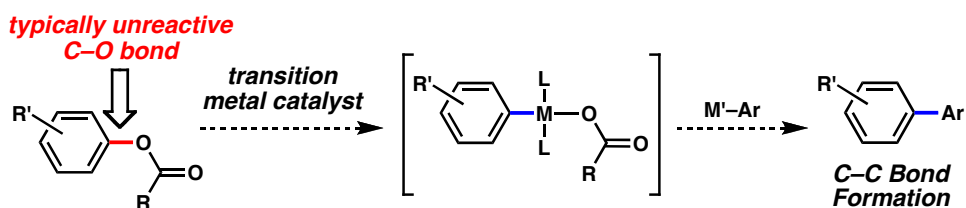


Figure 2.1. Cross-coupling of *O*-acylated phenol derivatives.

Of the vast array of cross-coupling reactions known, Suzuki–Miyaura couplings were chosen as the starting point for our studies because of the numerous advantages that pertain to using boronic acids (i.e., low toxicity, wide availability, stability to water and air, and high functional group tolerance).^{1,9} Several challenges were apparent from the outset of our endeavors. First, the *O*-acylated phenol substrates we intended to employ could be prone to hydrolysis under typical Suzuki–Miyaura conditions involving strong base. Thus, robust pivalate esters (–OC(O)CMe₃) were selected as the acylated phenol derivatives of choice. In addition, we postulated that the activation energy for oxidative addition between a transition metal and the

aryl C–O bond of an acylated phenol derivative would be fairly high. Since fused aromatic systems are generally activated toward oxidative addition,^{1a,4} a naphthol derivative was first examined.

2.3 Substrate Scope With Respect to the Pivalate Component

An extensive survey of various reaction parameters (e.g., choice of metal,¹⁰ ligand,¹¹ solvent, base, additives, and temperature) led to the identification of a catalyst system that facilitates the desired cross-coupling. Under optimal conditions (i.e., $\text{NiCl}_2(\text{PCy}_3)_2$ (5 mol%) and K_3PO_4 (4.5 equiv) in toluene at 80 °C), coupling of naphthyl pivalate **2.1** and phenylboronic acid (**2.2a**)¹² afforded biaryl product **2.3a** in 92% yield (Scheme 2.1). The Ni(II) precatalyst¹³ of choice is readily available¹⁴ and also shows marked stability to air. Therefore, all reactions are routinely carried out on the bench-top rather than in a glovebox, circumventing a common limitation of related Ni(0) processes.^{3b,4}

Scheme 2.1

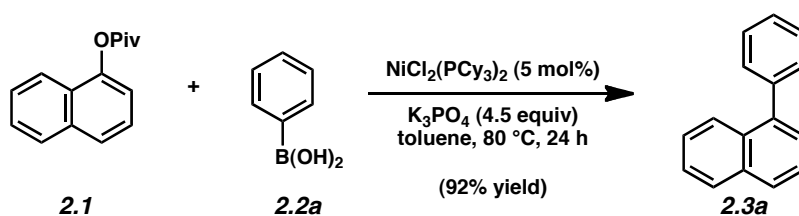


Table 2.1. Cross-couplings of various aryl pivalates with arylboronic acids **2.2a** or **2.2b**.^a

entry	Ar-OPiv	(HO) ₂ B-Ar	product	yield ^b
1				92%
2		2.2a		73%
3		2.2a		83%
4		2.2b		65% ^c
5		2.2b		79% ^c
6		2.2a		58% ^c
7		2.2a		82%
8		2.2b		79% ^d

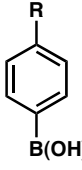
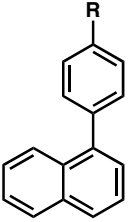
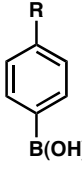
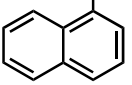
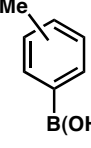
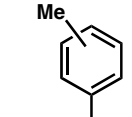
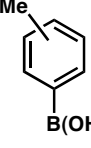
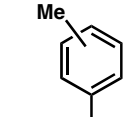
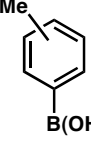
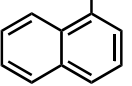
^a Conditions: NiCl₂(PCy₃)₂ (5 mol%), ArB(OH)₂ (4 equiv), K₃PO₄ (7.2 equiv), toluene (0.3 M), 110 °C, 24 h. ^b Isolated yields. ^c Conditions: NiCl₂(PCy₃)₂ (10 mol%), ArB(OH)₂ (5 equiv), K₃PO₄ (9 equiv), toluene (0.3 M), 110 °C, 24 h. ^d Conditions: NiCl₂(PCy₃)₂ (5 mol%), ArB(OH)₂ (2.5 equiv), K₃PO₄ (4.5 equiv), toluene (0.3 M), 80 °C, 24 h.

The scope of this methodology was first examined by varying the aryl pivalate component (Table 2.1). Cross-coupling of *p*-methoxyphenylboronic acid (**2.2b**) with the pivalate derivative of 2-naphthol proceeded in 92% yield (entry 1). In addition, the reaction proved tolerant of an electron-withdrawing group (–CO₂Me, entry 2) and an electron-donating group (–OMe, entry 3) on the naphthyl ring. The corresponding reactions of non-fused aryl pivalates proved more challenging. Nonetheless, employing additional equivalents of boronic acid and increasing catalyst loading to 10 mol%, significantly improved the yields of cross-coupled products. For instance, *p*- and *o*-tolyl pivalates afforded products in 65% and 79% yields (entries 4 and 5), respectively. A non-fused aromatic substrate bearing a *p*-methoxy substituent also participated in the cross-coupling reaction (entry 6). Finally, a substrate derived from *N*-methyl-2-hydroxycarbazole underwent smooth cross-coupling (entry 7), as did a vinyl pivalate derived from tetralone (entry 8).

2.4 Substrate Scope With Respect to the Arylboronic Acid Component

We have also found that a range of arylboronic acids participate in the Ni-catalyzed cross-coupling of naphthyl pivalate **2.1** (Table 2.2). For instance, cross-coupling of electron-rich boronic acid **2.2b**, bearing a *p*-methoxy substituent, furnished biaryl adduct **2.3b** in 95% yield (entry 1). Electron-deficient boronic acid **2.2c** can also be utilized in the desired cross-coupling reaction (entry 2). Finally, Me-substitution is tolerated at the *p*, *m*, and *o*-positions as demonstrated by the coupling of substrates **2.2d-f**, respectively (entries 3–5), although the *o*-substituted substrate (entry 5) requires elevated temperatures and proceeds in modest yield.

Table 2.2. Cross-coupling of pivalate **2.1** with various arylboronic acids.^a

entry	ArB(OH) ₂	temp (°C)	product	yield ^b
1	 R = OMe 2.2b	80 °C	 2.3b	95%
2	 R = CF ₃ 2.2c	120 °C	 2.3c	77%
3	 <i>para</i> 2.2d	80 °C	 2.3d	91%
4	 <i>meta</i> 2.2e	80 °C	 2.3e	99%
5	 <i>ortho</i> 2.2f	130 °C	 2.3f	58%

^a Conditions: Pivalate **2.1** (1 equiv), NiCl₂(PCy₃)₂ (5 mol%), ArB(OH)₂ (2.5 equiv), K₃PO₄ (4.5 equiv), toluene (0.3 M), 24 h. ^b Isolated yields.

2.5 One Pot Acylation / Cross-Coupling and Orthogonal Cross-Coupling Reactions

Figure 2.2 highlights two unprecedented and powerful variations of the cross-coupling methods described herein. As pivalylation protocols typically proceed quantitatively and with minimal byproduct formation, we hypothesized that a one-pot acylation/cross-coupling sequence of phenol derivatives could be possible. Gratifyingly, our efforts to achieve the one-pot conversion of 1-naphthol (**2.4**) to biaryl adduct **2.3b** were successful, affording the desired product in 86% yield. Next, to demonstrate the directing ability of aryl pivalates,¹⁵ naphthyl pivalate **2.1** was selectively brominated at C4 to afford bromopivalate **2.5** in 84% yield.¹⁶ Postulating that the pivalate functional group of **2.5** would not be reactive toward Pd(0), we next attempted to carry out orthogonal cross-coupling reactions of the bromide and pivalate groups. In the first cross-coupling, treatment of substrate **2.5** with indolylboronic ester **2.6** under Pd-catalysis led to the selective reaction of the aryl bromide to afford biaryl product **2.7**, with the robust pivalate group remaining intact, despite the harsh basic conditions employed (i.e., aqueous

K_3PO_4 , 90 °C). Next, aryl pivalate **2.7** underwent smooth cross-coupling under our nickel-catalyzed conditions to afford triaryl product **2.8** in 88% yield.

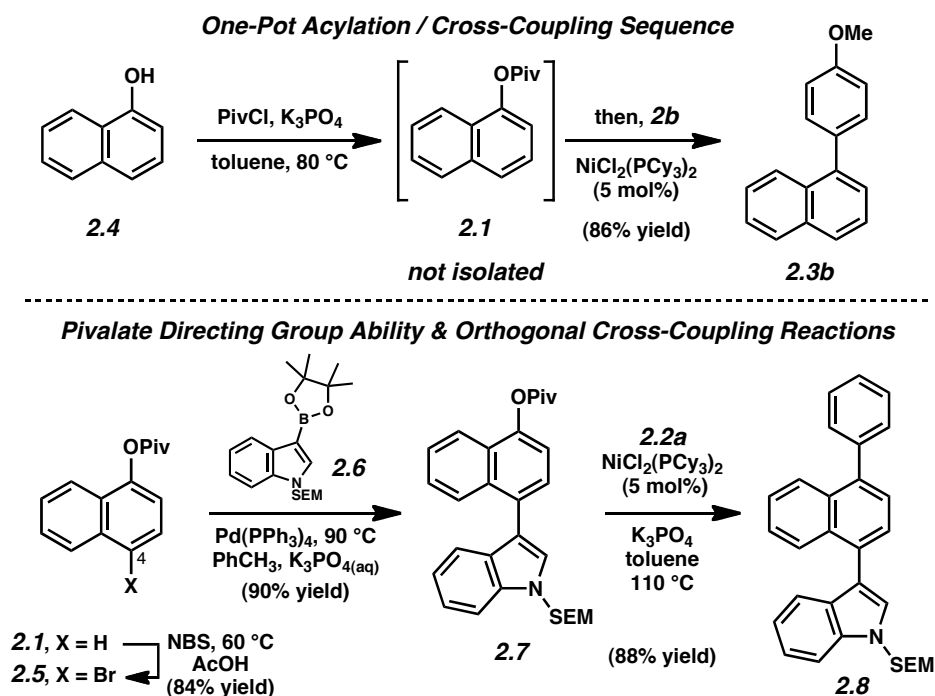


Figure 2.2. One-pot acylation/cross-coupling sequence and orthogonal cross-coupling reactions.

2.6 Conclusion

In summary, we have discovered the first cross-coupling reactions of *O*-acylated phenol derivatives. The method described relies on the use of a readily available, air-stable Ni(II) complex to facilitate the Suzuki–Miyaura coupling of aryl pivalates. In addition, a one-pot acylation/cross-coupling sequence has been developed. Moreover, the potential to utilize an aryl pivalate as a directing group has been demonstrated, along with the ability to sequentially cross-couple an aryl bromide followed by an aryl pivalate. Studies aimed at probing mechanistic aspects of these findings are currently underway.

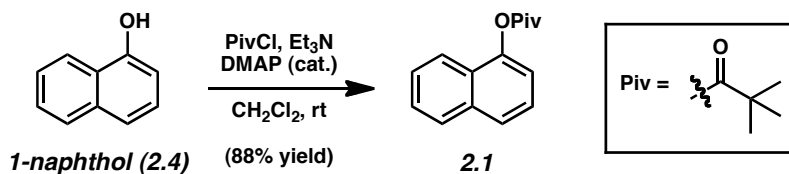
2.7 Experimental Section

2.7.1 Materials and Methods

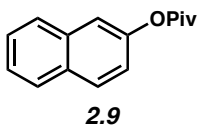
Unless stated otherwise, reactions were conducted in flame-dried glassware under an atmosphere of nitrogen using anhydrous solvents (either freshly distilled or passed through activated alumina columns). All commercially obtained reagents were used as received. NiCl₂ (anhydrous) and PCy₃ were obtained from Strem Chemicals. Finely powdered anhydrous K₃PO₄ was obtained from Acros (*note: non-powdered K₃PO₄ obtained from Sigma-Aldrich, Strem Chemicals, or Pfaltz & Bauer was not effective*). Boronic acids were obtained from either Oakwood Products (**2.2b–2.2f**), Sigma-Aldrich (**2.2a**), or TCI (**2.2a**, **2.2b**). Reaction temperatures were controlled using an IKAmag temperature modulator, and unless stated otherwise, reactions were performed at room temperature (rt, approximately 23 °C). Thin-layer chromatography (TLC) was conducted with EMD gel 60 F254 pre-coated plates (0.25 mm) and visualized using a combination of UV, anisaldehyde, ceric ammonium molybdate, and potassium permanganate staining. EMD silica gel 60 (particle size 0.040–0.063 mm) was used for flash column chromatography. ¹H NMR spectra were recorded on Bruker spectrometers (at 500 MHz) and are reported relative to deuterated solvent signals. Data for ¹H NMR spectra are reported as follows: chemical shift (δ ppm), multiplicity, coupling constant (Hz) and integration. ¹³C NMR spectra were recorded on Bruker Spectrometers (at 125 MHz). Data for ¹³C NMR spectra are reported in terms of chemical shift. IR spectra were recorded on a Perkin-Elmer 100 spectrometer and are reported in terms of frequency of absorption (cm⁻¹). Melting points are uncorrected and were obtained on a Laboratory Devices Mel-Temp II instrument. High resolution mass spectra were obtained from the UC Irvine Mass Spectrometry Facility.

2.7.2 Experimental Procedures

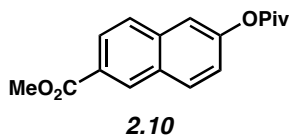
A. Synthesis of Aryl Pivalates



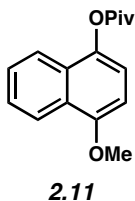
Representative Procedure (naphthyl pivalate 2.1 is used as an example). To a solution of 1-naphthol (**2.4**) (6.32 g, 43.9 mmol, 1 equiv) in CH₂Cl₂ (150 mL) at 23 °C was added triethylamine (7.32 mL, 52.6 mmol, 1.2 equiv) and DMAP (536 mg, 4.39 mmol, 0.1 equiv). Pivaloyl chloride (6.44 mL, 52.6 mmol, 1.2 equiv) was then added dropwise over 5 min. After stirring for 4 h the reaction was quenched with a solution of aqueous NaHSO₄ (0.5 M, 75 mL) and the layers were separated. The aqueous layer was extracted with CH₂Cl₂ (2 x 50 mL) and the combined organic layers were dried over MgSO₄. Following evaporation of the solvent under reduced pressure, the crude residue was purified by flash chromatography (2:1 Hexanes:EtOAc) to yield **2.1** as a yellow oil (8.84 g, 88% yield). *R_f* 0.35 (4:1 Hexanes:EtOAc); ¹H NMR (500 MHz, CDCl₃): δ 7.90-7.88 (m, 2H), 7.76 (d, *J* = 8.3, 1H), 7.57-7.51 (m, 2H), 7.49 (t, *J* = 7.8, 1H), 7.24 (dd, *J* = 7.5, 0.6, 1H), 1.53 (s, 9H); ¹³C NMR (125 MHz, CDCl₃): δ 177.2, 147.1, 134.9, 128.2, 127.2, 126.6, 126.5, 126.0, 125.6, 121.2, 118.1, 39.7, 27.6; IR (film): 2976, 2937, 1742, 1388, 1225 cm⁻¹; HRMS-ESI (*m/z*) [M + Na]⁺ calcd for C₁₅H₁₆O₂Na, 251.1048; found, 251.1046.



Pivalate 2.9 (Table 2.1, entry 1). Purification by flash chromatography (6:1 Hexanes:EtOAc) afforded **2.9** as a white solid (92% yield). R_f 0.68 (4:1 Hexanes:EtOAc); $^1\text{H NMR}$ (500 MHz, CDCl_3): δ 7.89-7.83 (m, 2H), 7.80 (d, $J = 7.7$, 1H), 7.54 (d, $J = 2.4$, 1H), 7.52-7.44 (m, 2H), 7.21 (dd, $J = 8.9, 2.3$, 1H), 1.42 (s, 9H). Spectral data for **2.9** match those previously reported.¹⁷

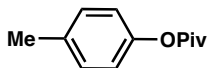


Pivalate 2.10 (Table 2.1, entry 2). Purification by flash chromatography (4:1 Hexanes:Et₂O) afforded **2.10** as a white solid (93% yield). R_f 0.6 (1:1 Hexanes:Et₂O); $^1\text{H NMR}$ (500 MHz, CDCl_3): δ 8.61 (s, 1H), 8.07 (dd, $J = 8.5, 1.5$, 1H), 7.96 (d, $J = 9.0$, 1H), 7.83 (d, $J = 8.5$, 1H), 7.58 (d, $J = 2.0$, 1H), 7.28 (d, $J = 2.0$, 1H), 3.98 (s, 3H), 1.41 (s, 9H); $^{13}\text{C NMR}$ (125 MHz, CDCl_3): δ 176.8, 166.8, 150.5, 135.9, 130.7, 130.6, 130.2, 127.6, 127.0, 125.7, 121.9, 118.2, 52.0, 39.0, 27.0; IR (film): 2965, 1749, 1711, 1474, 1286 cm^{-1} ; m.p. 103-104 °C; HRMS-ESI (m/z) [$\text{M} + \text{Na}$]⁺ calcd for C₁₇H₁₈O₄Na, 309.1103; found, 309.1106.



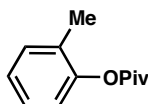
Pivalate 2.11 (Table 2.1, entry 3). Purification by flash chromatography (3:1 Benzene:Hexanes) afforded **2.11** as a white solid (98% yield). R_f 0.5 (2:1 Hexanes:Et₂O); $^1\text{H NMR}$ (500 MHz, CDCl_3): δ 8.28 (d, $J = 8.2$, 1H), 7.78 (d, $J = 7.5$, 1H), 7.58-7.44 (m, 2H), 7.11 (d, $J = 8.0$, 1H),

6.77 (d, $J = 8.5$ 1H), 4.01 (s, 3H), 1.50 (s, 9H); ^{13}C NMR (125 MHz, CDCl_3): δ 177.6, 153.4, 140.4, 127.9, 127.1, 126.4, 125.8, 122.6, 121.0, 117.7, 103.1, 55.9, 39.6, 27.6; IR (film): 2978, 2956, 1746, 1583, 1390, 1264 cm^{-1} ; m.p. 67-69 $^\circ\text{C}$; HRMS-ESI (m/z) $[\text{M} + \text{Na}]^+$ calcd for $\text{C}_{16}\text{H}_{18}\text{O}_3\text{Na}$, 281.1154; found, 281.1152.



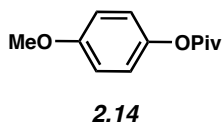
2.12

Pivalate 2.12 (Table 2.1, entry 4). Purification by flash chromatography (9:1 Hexanes: Et_2O) afforded **2.12** as a white solid (89% yield). R_f 0.7 (4:1 Hexanes: Et_2O); ^1H NMR (500 MHz, CDCl_3): δ 7.16 (d, $J = 8$, 2H), 6.93 (d, $J = 8$, 2H), 2.34 (s, 3H), 1.35 (s, 9H). Spectral data match those previously reported.¹⁸

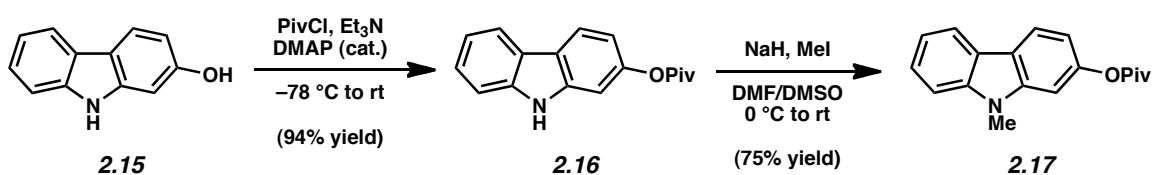


2.13

Pivalate 2.13 (Table 2.1, entry 5). Purification by flash chromatography (19:1 Hexanes: Et_2O) afforded **2.13** as a colorless oil (64% yield). R_f 0.6 (4:1 Hexanes: Et_2O); ^1H NMR (500 MHz, CDCl_3): δ 7.23-7.18 (m, 2H), 7.13 (t, $J = 7.5$, 1H), 6.96 (d, $J = 8.0$, 1H), 2.17 (s, 3H), 1.39 (s, 9H). Spectral data match those previously reported.¹⁹



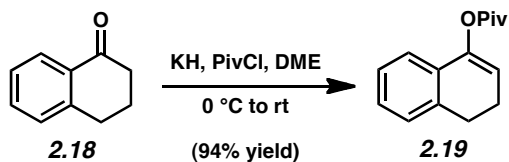
Pivalate 2.14 (Table 2.1, entry 6). Purification by flash chromatography (4:1 Hexanes:Et₂O) afforded **2.14** as a colorless oil (99% yield). *R_f* 0.3 (4:1 Hexanes:CH₂Cl₂); ¹H NMR (500 MHz, CDCl₃): δ 6.98 (d, *J* = 9.2, 2H), 6.89 (d, *J* = 9.1, 2H), 3.80 (s, 3H), 1.36 (s, 9H); ¹³C NMR (125 MHz, CDCl₃): δ 177.6, 157.3, 144.8, 122.4, 114.6, 55.8, 39.2, 27.3; HRMS-ESI (*m/z*) [*M* + Na]⁺ calcd for C₁₂H₁₆O₃Na, 231.0997; found, 231.0993. Spectral data match those previously reported.²⁰



Carbazole substrate 2.17 (Table 2.1, entry 7). To a mixture of 2-hydroxycarbazole (**2.15**) (1.00 g, 5.45 mmol, 1 equiv) and triethylamine (0.830 mL, 6.00 mmol, 1.1 equiv) in CH₂Cl₂ (18 mL) at –78 °C was added pivaloyl chloride (0.700 mL, 5.72 mmol, 1.05 equiv) dropwise over 1 min. The reaction mixture was allowed to warm to 23 °C. After 12 h, the resulting heterogeneous mixture was filtered to remove the triethylammonium salt and the filtrate was concentrated under reduced pressure. The crude residue was purified by flash chromatography (10%→20% EtOAc/Hexanes) to afford pivalate **2.16** as a white powder (1.38 g, 94% yield). *R_f* 0.56 (4:1 Hexanes:EtOAc); ¹H NMR (500 MHz, CDCl₃): δ 8.10 (s, 1H), 7.94 (d, *J* = 7.7, 1H), 7.91 (d, *J* = 8.4, 1H), 7.35 (dd, *J* = 7, 7, 1H), 7.29 (d, *J* = 8, 1H), 7.21 (dd, *J* = 7.8, 7.8, 1H), 7.07 (d, *J* = 2, 1H), 6.88 (dd, *J* = 2, 8.4, 1H), 1.44 (s, 9H); ¹³C NMR (125 MHz, CDCl₃): δ 177.9, 149.4, 140.0, 139.8, 125.4, 122.8, 121.0, 120.6, 120.0, 119.5, 113.0, 110.6, 103.7, 39.1, 27.2; IR (film): 3405,

2985, 2870, 1732, 1444 cm^{-1} ; m.p. 205-207 $^{\circ}\text{C}$; HRMS-ESI (m/z) [$\text{M} + \text{Na}$] $^{+}$ calcd for $\text{C}_{17}\text{H}_{17}\text{NO}_2\text{Na}$, 290.1157; found, 290.1150.

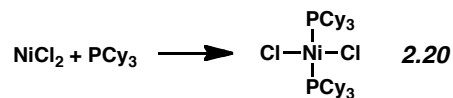
To a suspension of NaH (142 mg, 3.55 mmol, 1.2 equiv) in DMF (5 mL) and DMSO (0.67 mL) at 0 $^{\circ}\text{C}$ was added a solution of pivalate **2.16** (789 mg, 2.95 mmol, 1 equiv) in DMF (1.67 mL) dropwise over 5 min. After stirring for 30 min, MeI (0.221 mL, 3.55 mmol, 1.2 equiv) was added and the cooling bath was removed. After an additional 30 min of stirring, saturated aqueous NH_4Cl (15 mL) was added dropwise and the aqueous layer was extracted with EtOAc (2 x 15 mL). The combined organic layers were washed with brine (20 mL), dried over Na_2SO_4 and concentrated under reduced pressure. The crude residue was purified by flash chromatography (10% $\text{CH}_2\text{Cl}_2/\text{Hexanes}$) to give pivalate **2.17** as a white powder (620 mg, 75% yield). R_f 0.54 (1:1 Hexanes: CH_2Cl_2); ^1H NMR (500 MHz, CDCl_3): δ 8.18 (d, $J = 7.5$, 1H), 8.17 (d, $J = 8.5$, 1H), 7.59 (ddd, $J = 8.5$, 8.2, 1.5, 1H), 7.50 (d, $J = 8$, 1H), 7.37 (t, $J = 7$, 1H), 7.24 (d, $J = 2$, 1H), 7.05 (dd, $J = 8.5$, 2, 1H), 3.92 (s, 3H), 1.56 (s, 9H); ^{13}C NMR (125 MHz, CDCl_3): δ 177.5, 149.7, 141.44, 141.38, 125.4, 122.4, 120.7, 120.5, 120.1, 119.1, 112.6, 108.4, 101.7, 39.1, 29.1, 27.2; IR (film): 2986, 2956, 1750, 1598, 1466, 1451 cm^{-1} ; m.p. 135-136 $^{\circ}\text{C}$; HRMS-ESI (m/z) [$\text{M} + \text{Na}$] $^{+}$ calcd for $\text{C}_{18}\text{H}_{19}\text{NO}_2\text{Na}$, 304.1313; found, 304.1308.



Vinyl pivalate 2.19 (Table 2.1, entry 8). A 60% suspension of KH in mineral oil was added to a round bottom flask under N_2 . The suspension was then washed with pentane (3 x 15 mL) to give dry KH (1.01 g, 25.3 mmol, 2 equiv) as a grey powder. The flask was then cooled to 0 $^{\circ}\text{C}$ in an ice bath and DME (30 mL) was added. A solution of α -tetralone (**2.18**) (1.67 mL, 12.6 mmol, 1

equiv) in DME (6 mL) was then added dropwise to the suspension of KH in DME over 5 min. The reaction was then stirred for 30 min, warmed to rt, then stirred for an additional 30 min. The flask was then cooled to 0 °C and a solution of pivaloyl chloride (2.57 mL, 21.0 mmol, 1.67 equiv) in DME (6 mL) was added dropwise. The ice bath was then removed and the reaction was stirred at 23 °C for 1 h. The resulting mixture was cooled to 0 °C and slowly quenched with a solution of aqueous NaHSO₄ (0.5 M, 30 mL). Ether (25 mL) was then added and the layers separated. The aqueous layer was extracted with ether (3 x 25 mL) and the combined organic layers were dried over MgSO₄ and concentrated under reduced pressure. The crude residue was purified by flash chromatography (9:1 Hexanes:EtOAc) to yield pivalate **2.19** as a yellow oil (2.72 g, 94% yield). *R_f* 0.43 (9:1 Hexanes: EtOAc); ¹H NMR (500 MHz, CDCl₃): δ 7.23-7.14 (m, 3H), 7.14-7.07 (m, 1H), 5.70 (t, *J* = 4.5, 1H), 2.89 (t, *J* = 8.0, 2H), 2.52-2.41 (m, 2H), 1.41 (s, 9H); ¹³C NMR (125 MHz, CDCl₃): δ 177.0, 145.9, 136.6, 130.9, 128.0, 127.7, 126.5, 120.7, 115.2, 39.4, 27.7, 27.5, 22.2; IR (film): 2973, 2936, 1750, 1479, 1181 cm⁻¹; HRMS-ESI (*m/z*) [*M* + Na]⁺ calcd for C₁₅H₁₈O₂Na, 253.1204; found, 253.1205.

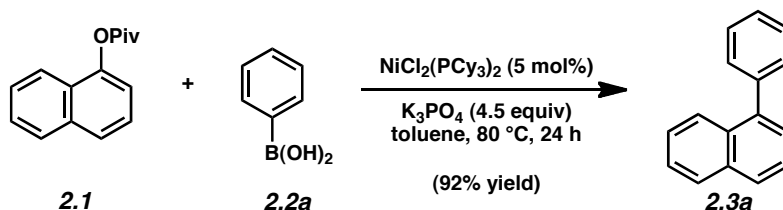
B. Preparation of NiCl₂(PCy₃)₂



NiCl₂(PCy₃)₂ (2.20). This catalyst was prepared following the procedures previously described in the literature.²¹ In a glove box, two separate flasks were charged with NiCl₂ (2.50 g, 19.4 mmol, 1 equiv) and PCy₃ (14.2 g, 50.8 mmol, 2.62 equiv), respectively. The flasks were removed from the glove box, placed under a positive pressure of N₂, and degassed EtOH (sparged with N₂ for 15 min) was added to each flask (50 mL each). The solution of NiCl₂ was heated

(approximately 70 °C) until a yellow homogeneous solution was obtained, which was then transferred via cannula into the solution of PCy₃ in EtOH, with stirring. The resulting purple heterogeneous mixture was gently refluxed for 1 h and then allowed to cool to 23 °C. The solid that formed was collected by filtration, washed sequentially with ice cold EtOH (50 mL) and ice cold Et₂O (50 mL), then dried under reduced pressure for 12 h, to afford NiCl₂(PCy₃)₂ (**2.20**) as a reddish-purple powder (10.20 g, 76% yield). This complex could be stored in a scintillation vial on the bench-top, protected from light, for several months without loss of purity or catalytic activity. m.p. 227–231 °C decomp.; literature m.p. 227 °C.

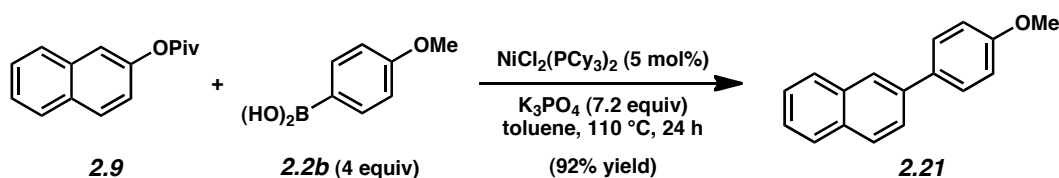
C. Cross-Coupling Reactions



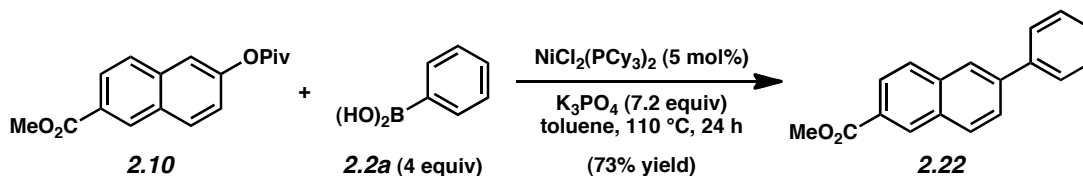
Representative Procedure (coupling of naphthyl pivalate **2.1 and phenylboronic acid **2.2a** is used as an example).** A 1-dram vial was charged with anhydrous powdered K₃PO₄ (418 mg, 1.98 mmol, 4.5 equiv, *obtained from Acros*) and a magnetic stir bar. The vial and contents were flame-dried under reduced pressure, then allowed to cool under N₂. Phenylboronic acid **2.2a** (134 mg, 1.10 mmol, 2.5 equiv), NiCl₂(PCy₃)₂ (15 mg, 0.022 mmol, 5 mol%), and pivalate substrate **1** (100 mg, 0.439 mmol, 1 equiv) were added. The vial was then evacuated and backfilled with N₂. Toluene (1.46 mL) was added and the vial was sealed with a Teflon-lined screw cap. The heterogeneous mixture was allowed to stir at 23 °C for 1 h, then heated to 80 °C for 24 h. The reaction vessel was cooled to 23 °C and then transferred to a round bottom flask containing

CH₂Cl₂ (20 mL). Silica gel (3 mL) was added and the solvent was removed under reduced pressure to afford a free-flowing powder. This powder was then dry-loaded onto a silica gel column (2.5 x 7.5 cm) and purified by flash chromatography (100% Hexanes) to yield 88 mg of a mixture (14.5 to 1) of biaryl product **2.3a** (82 mg, 92% yield) and biphenyl.²² R_f 0.39 (Hexanes); ¹H NMR (500 MHz, CDCl₃): δ 7.95 (d, *J* = 8.5, 2H), 7.90 (d, *J* = 8.5, 1H), 7.59-7.44 (m, 9H). Spectral data match authentic sample obtained from Alfa Aesar.

Any modifications of the conditions shown in this representative procedure are specified in the following schemes, which depict all Table 2.1 and Table 2.2 cross-coupling reactions.

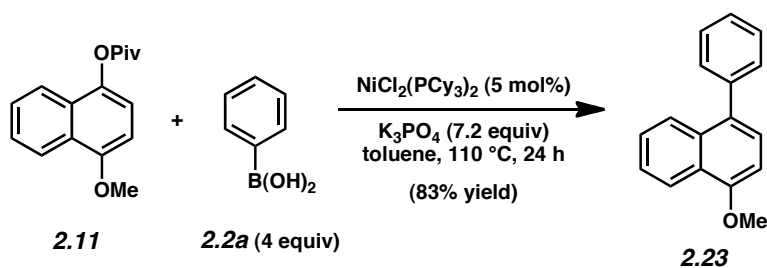


Biaryl 2.21 (Table 2.1, entry 1). Purification by flash chromatography (2:1 Hexanes:Benzenes) afforded **2.21** as a white solid (92% yield). R_f 0.28 (2:1 Hexanes:Benzenes); ¹H NMR (500 MHz, CDCl₃): δ 8.00 (s, 1H), 7.90 (t, *J* = 8.5, 2H), 7.86 (d, *J* = 8.0, 1H), 7.73 (dd, *J* = 8.5, 1.5, 1H), 7.68 (d, *J* = 9.0, 2H), 7.52-7.45 (m, 2H), 7.04 (d, *J* = 8.5, 2H), 3.89 (s, 3H). Spectral data match those previously reported.²³

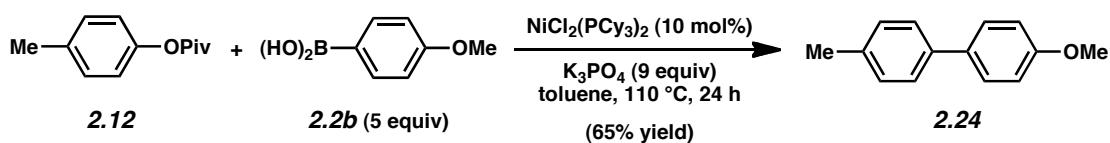


Biaryl 2.22 (Table 2.1, entry 2). Purification by flash chromatography (10%→15% Et₂O/Hexanes) afforded **2.22** as a white solid (73% yield). R_f 0.5 (2:1 Hexanes:Et₂O); ¹H NMR (500 MHz, CDCl₃): δ 8.64 (s, 1H), 8.10 (dd, *J* = 9.0, 1.5, 1H), 8.06 (s, 1H), 8.01 (d, *J* = 8.5, 1H),

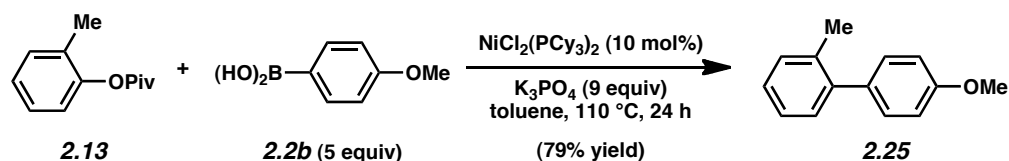
7.92 (d, $J = 8.5$, 1H), 7.81 (dd, $J = 9.0$, 1.5, 1H), 7.73 (d, $J = 7.5$, 2H), 7.51 (t, $J = 7.5$, 2H), 7.42 (t, $J = 7.5$, 1H), 3.99 (s, 3H); ^{13}C NMR (125 MHz, CDCl_3): δ 167.2, 140.9, 140.5, 135.7, 131.6, 130.8, 129.8, 128.9, 128.3, 127.8, 127.4, 127.3, 126.3, 125.6, 125.5, 52.2; IR (film): 2947, 2846, 1709, 1436, 1292, 1095 cm^{-1} ; m.p. 170-172 $^\circ\text{C}$; HRMS-ESI (m/z) $[\text{M} + \text{Na}]^+$ calcd for $\text{C}_{18}\text{H}_{14}\text{O}_2\text{Na}$, 285.0891; found, 285.0893.



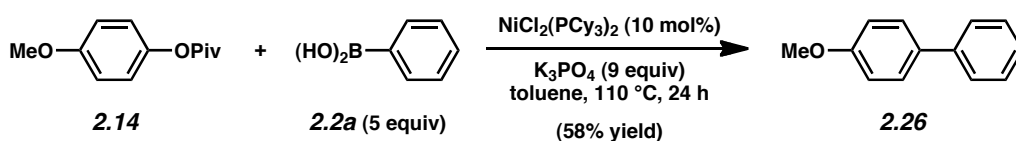
Biaryl 2.23 (Table 2.1, entry 3). Purification by flash chromatography (5%→10% $\text{CH}_2\text{Cl}_2/\text{Hexanes}$) afforded **2.23** as a colorless oil (83% yield). R_f 0.64 (2:1 Hexanes: Et_2O); ^1H NMR (500 MHz, CDCl_3): δ 8.42 (d, $J = 8.0$, 1H), 7.93 (d, $J = 8.5$, 1H), 7.57-7.43 (m, 7H), 7.39 (d, $J = 8.0$, 1H), 6.91 (d, $J = 7.5$, 1H), 4.08 (s, 3H); ^{13}C NMR (125 MHz, CDCl_3): δ 155.1, 141.1, 132.9, 132.7, 130.5, 128.4, 127.1, 126.7, 125.94, 125.85, 125.3, 122.4, 103.6, 55.7. Spectral data match those previously reported.²⁴



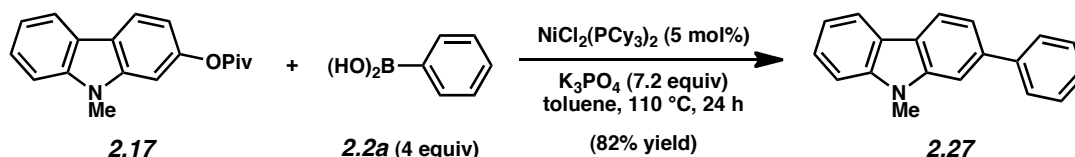
Biaryl 2.24 (Table 2.1, entry 4). Purification by flash chromatography (5%→10% $\text{CH}_2\text{Cl}_2/\text{Hexanes}$) afforded **2.24** as a white solid (65% yield). R_f 0.65 (2:1 Hexanes: Et_2O); ^1H NMR (500 MHz, CDCl_3): δ 7.51 (d, $J = 9.5$, 2H), 7.45 (d, $J = 8$, 2H), 7.22 (d, $J = 8$, 2H), 6.96 (d, $J = 7$, 2H), 3.85 (s, 3H), 2.38 (s, 3H). Spectral data match those previously reported.²⁵



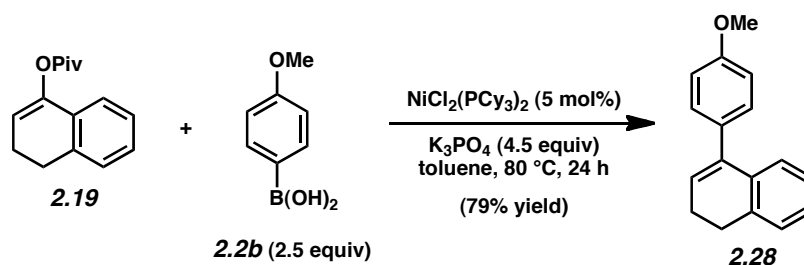
Biaryl 2.25 (Table 2.1, entry 5). Purification by flash chromatography (5%→10% CH₂Cl₂/Hexanes) afforded **2.25** as a colorless oil (79% yield). *R_f* 0.68 (2:1 Hexanes:Et₂O); ¹H NMR (500 MHz, CDCl₃): δ 7.34-7.30 (m, 6H), 7.03 (d, *J* = 8.5, 2H), 3.91 (s, 3H), 2.36 (s, 3H). Spectral data match those previously reported.²⁶



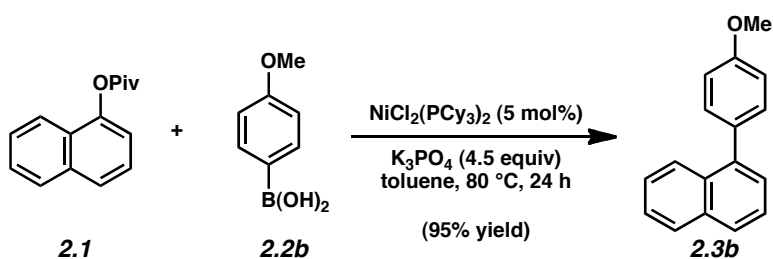
Biaryl 2.26 (Table 2.1, entry 6). Purification by flash chromatography (5%→10% CH₂Cl₂/Hexanes) afforded **2.26** as a white solid (58% yield). *R_f* 0.59 (2:1 Hexanes:CH₂Cl₂); ¹H NMR (500 MHz, CDCl₃): δ 7.57-7.53 (m, 4H), 7.42 (t, *J* = 7.5, 2H), 7.31 (t, *J* = 7.5, 1H), 6.98 (d, *J* = 8.5, 2H), 3.86 (s, 3H); Spectral data match those previously reported.²⁷



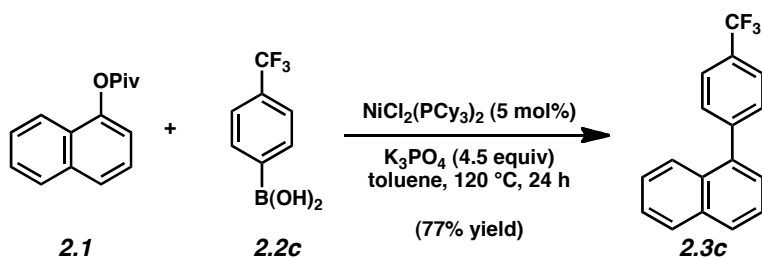
Biaryl 2.27 (Table 2.1, entry 7). Purification by flash chromatography (5%→15% CH₂Cl₂/Hexanes) afforded **2.27** as a white solid (82% yield). *R_f* 0.71 (2:1 Hexanes:Et₂O); ¹H NMR (500 MHz, CDCl₃): δ 8.19 (t, *J* = 8.5, 2H), 7.83 (d, *J* = 8.5, 2H), 7.64 (s, 1H), 7.59-7.54 (m, 4H), 7.48-7.43 (m, 2H), 7.34 (t, *J* = 7.5, 1H), 3.88 (s, 3H). Spectral data match those previously reported.²⁸



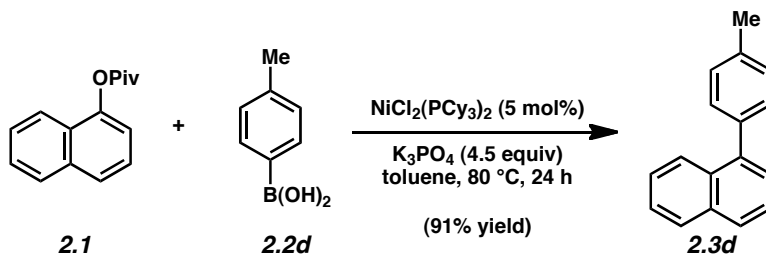
Biaryl 2.28 (Table 2.1, entry 8). Purification by flash chromatography (1:1 Hexanes:Benzene) afforded **2.28** as a white solid (79% yield). R_f 0.6 (1:1 Hexanes:Benzene); $^1\text{H NMR}$ (500 MHz, CDCl_3): δ 7.31 (d, $J = 8.6$, 2H), 7.23 (d, $J = 7.2$, 1H), 7.19 (t, $J = 7.8$, 1H), 7.15 (t, $J = 7.6$, 1H), 7.06 (d, $J = 7.4$, 1H), 6.95 (d, $J = 8.6$, 2H), 6.08 (t, $J = 4.5$, 1H), 3.89 (s, 3H), 2.88 (t, $J = 8.0$, 2H), 2.44-2.40 (m, 2H). Spectral data matches those previously reported.²⁹



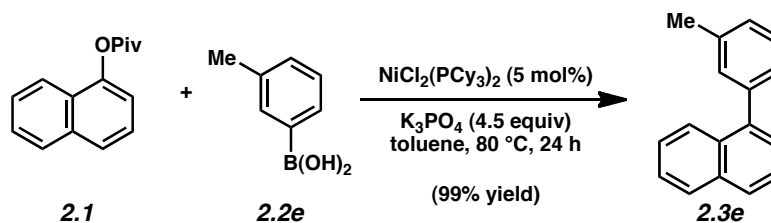
Biaryl 2.3b (Table 2.2, entry 1). Purification by flash chromatography (2:1 Hexanes:Benzene) afforded **2.3b** as a white solid (95% yield). R_f 0.4 (2:1 Hexanes:Benzene); $^1\text{H NMR}$ (500 MHz, CDCl_3): δ 7.95 (d, $J = 8.5$, 1H), 7.92 (d, $J = 8.5$, 1H), 7.86 (d, $J = 8.5$, 1H), 7.57-7.48 (m, 2H), 7.48-7.39 (m, 4H), 7.06 (d, $J = 8.5$, 2H), 3.92 (s, 3H). Spectral data match those previously reported.³⁰



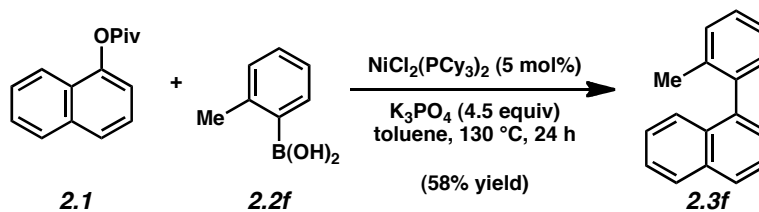
Biaryl 2.3c (Table 2.2, entry 2). Purification by flash chromatography (2:1 Hexanes:Benzene) afforded a mixture (16.7 to 1) of biaryl product **2.3c** (77% yield) and 4,4'-bis(trifluoromethyl)biphenyl.²² R_f 0.72 (2:1 Hexanes:Benzene); $^1\text{H NMR}$ (500 MHz, CDCl_3): δ 7.95 (d, $J = 8.5$, 1H), 7.93 (d, $J = 8.5$, 1H), 7.84 (d, $J = 9.5$, 1H), 7.78 (d, $J = 6.5$, 2H), 7.64 (d, $J = 9.0$, 2H), 7.58-7.53 (m, 2H), 7.48 (t, $J = 8.0$, 1H), 7.42 (d, $J = 8.0$, 1H). Spectral data match those previously reported.³¹



Biaryl 2.3d (Table 2.2, entry 3). Purification by flash chromatography (100% Hexanes) afforded a mixture (28.6 to 1) of biaryl product **2.3d** (91% yield) and 4,4'-dimethylbiphenyl.²² R_f 0.77 (9:1 Hexanes:EtOAc); $^1\text{H NMR}$ (500 MHz, CDCl_3): δ 8.04 (d, $J = 8.5$, 1H), 7.99 (d, $J = 8.0$, 1H), 7.93 (d, $J = 8.5$, 1H), 7.64-7.54 (m, 2H), 7.54-7.46 (m, 4H), 7.39 (d, $J = 8$, 2H), 2.55 (s, 3H). Spectral data match those previously reported.³²

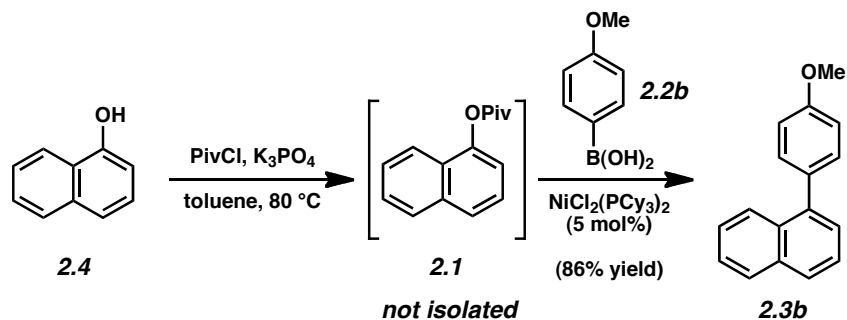


Biaryl 2.3e (Table 2.2, entry 4). Purification by flash chromatography (100% Hexanes) afforded a mixture (38.4 to 1) of biaryl product **2.3e** (99% yield) and 3,3'-dimethylbiphenyl.²² R_f 0.78 (9:1 Hexanes:EtOAc); $^1\text{H NMR}$ (500 MHz, CDCl_3): δ 7.94 (t, $J = 8.0$, 2H), 7.88 (d, $J = 8.0$, 1H), 7.58-7.50 (m, 2H), 7.46 (dt, $J = 8.0$, 1.5, 2H), 7.42 (t, $J = 7.5$, 1H), 7.38-7.31 (m, 2H), 7.30-7.26 (m, 1H), 2.48 (s, 3H). Spectral data match those previously reported.³³



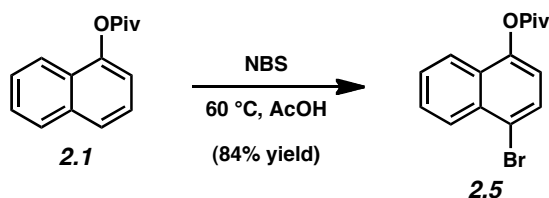
Biaryl 2.3f (Table 2.2, entry 5). Purification by flash chromatography (100% Hexanes) afforded a mixture (25.6 to 1) of biaryl product **2.3f** (58% yield) and 2,2'-dimethylbiphenyl.²² R_f 0.80 (9:1 Hexanes:EtOAc); $^1\text{H NMR}$ (500 MHz, CDCl_3): δ 7.94 (d, $J = 8.0$, 1H), 7.91 (d, $J = 8.0$, 1H), 7.60-7.54 (m, 1H), 7.54-7.48 (m, 2H), 7.45-7.36 (m, 4H), 7.34 (dt, $J = 5.0$, 2.0, 1H), 7.32-7.27 (m, 1H), 2.07 (s, 3H). Spectral data match those previously reported.¹⁸

D. One-Pot Acylation/Cross-Coupling Sequence

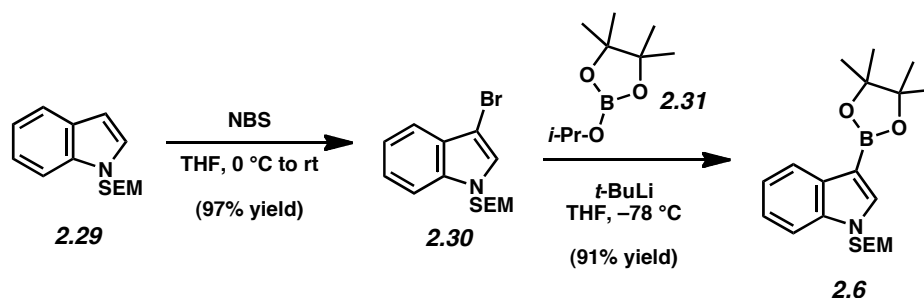


Procedure for one-pot conversion of 2.4→2.3b. A 1-dram vial was charged with anhydrous powdered K_3PO_4 (0.511g, 2.41 mmol, 5.5 equiv, *obtained from Acros*) and a magnetic stir bar. The vial and contents were flame-dried under reduced pressure, then allowed to cool under N_2 . 1-naphthol (**2.4**) (63.0 mg, 0.439 mmol, 1 equiv) and toluene (1.5 mL) were added, followed by pivaloyl chloride (62 μ L, 0.505 mmol, 1.15 equiv). The vial was purged with N_2 , heated at 80 °C for 24 h, then cooled to 23 °C. The vial was opened, then boronic acid **2.2b** (167 mg, 1.10 mmol, 2.5 equiv) and $NiCl_2(PCy_3)_2$ (15 mg, 0.022 mmol, 0.05 equiv) were added sequentially. The vial was then purged with N_2 for 5 min then sealed with a Teflon-lined screw cap. The heterogeneous mixture was allowed to stir at 23 °C for 1 h, then heated to 80 °C for 24 h. The reaction vessel was cooled to 23 °C and then transferred to a round bottom flask containing CH_2Cl_2 (20 mL). Silica gel (3 mL) was added and the solvent was removed under reduced pressure to afford a free-flowing powder. This powder was then dry-loaded onto a silica gel column and purified by flash chromatography (2:1 Hexanes:Benzene) to yield biaryl product **2.3b** as a white solid (88 mg, 86% yield).

E. Pivalate Directing Ability & Orthogonal Cross-Coupling Reactions



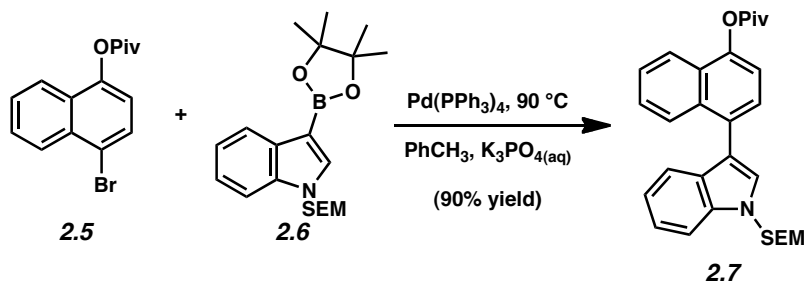
Bromide 2.5. To a solution of pivalate ester **2.1** (1.77 g, 7.76 mmol, 1 equiv) in glacial acetic acid (8 mL) was added NBS (1.46 g, 8.20 mmol, 1.06 equiv) in one portion. The reaction was then heated to 60 °C for 6 h, then cooled to 23 °C. Ether (50 mL) was added and the mixture was washed sequentially with water (2 x 20 mL), saturated aqueous NaHCO₃ (2 x 20 mL), saturated aqueous Na₂SO₃ (2 x 20 mL), and brine (20 mL). The combined organic layers were dried over Na₂SO₄ and concentrated under reduced pressure. The crude residue was purified by flash chromatography (5% CH₂Cl₂/Hexanes) to give bromide **2.5** as a white solid (1.99 g, 84% yield). *R_f* 0.38 (4:1 Hexanes:CH₂Cl₂); ¹H NMR (500 MHz, CDCl₃): δ 8.25 (d, *J* = 8.5, 1H), 7.88 (d, *J* = 8.5, 1H), 7.77 (d, *J* = 8.0, 1H), 7.64 (t, *J* = 7.0, 1H), 7.58 (t, *J* = 7.0, 1H), 7.10 (d, *J* = 8.0, 1H), 1.50 (s, 9H); ¹³C NMR (125 MHz, CDCl₃): δ 177.0, 146.8, 133.0, 129.5, 128.4, 128.0, 127.8, 127.4, 121.7, 119.7, 118.7, 39.7, 27.5; IR (film): 2980, 2959, 1747, 1120 cm⁻¹; m.p. 102-103 °C; HRMS-ESI (*m/z*) [M + Na]⁺ calcd for C₁₅H₁₅BrO₂Na, 329.0153; found, 329.0149.



Boronic Ester 2.6. To a solution of indole³⁴ **2.29** (500 mg, 2.0 mmol, 1 equiv) in THF (20 mL) at 0 °C was added NBS (360 mg, 2.0 mmol, 1 equiv) in one portion. The mixture was stirred for 15 min, then diluted with saturated aqueous Na₂SO₃ (10 mL). The aqueous layer was extracted with ether (25 mL) and the combined organic fractions were dried over Na₂SO₄, then concentrated under reduced pressure. The crude residue was purified by flash chromatography (10% CH₂Cl₂/Hexanes) to afford bromoindole **2.30** (630 mg, 97% yield), which was used immediately in the subsequent transformation.

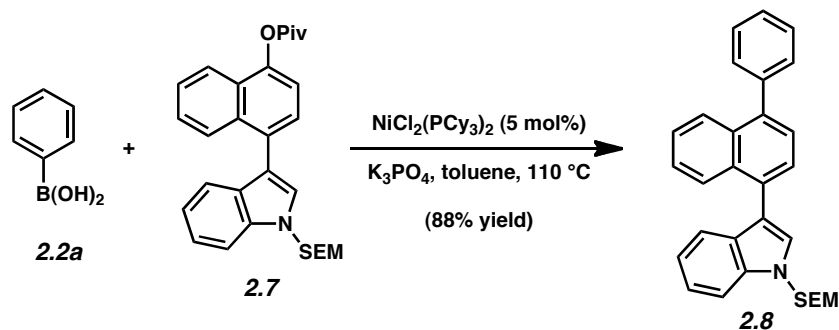
To a solution of bromoindole **2.30** (1.86 g, 5.72 mmol, 1 equiv) in THF (57 mL) at -78 °C was added *t*-BuLi (8.00 mL, 12.6 mmol, 2.2 equiv) dropwise down the side of the flask over 5 min. After stirring the reaction mixture for 10 min, **2.31** (2.30 mL, 11.4 mmol, 2 equiv) was added dropwise over 1 min. The reaction was stirred for 2 h, quenched with saturated aqueous NH₄Cl (10 mL), and allowed to warm to 23 °C. The solution was diluted with brine (10 mL) and extracted with ether (3 x 20 mL). The combined organic layers were dried over Na₂SO₄ and concentrated under reduced pressure. The crude residue was purified by flash chromatography (5% to 10% Et₂O/Hexanes) to afford boronic ester **2.6** as a yellow oil (1.95 g, 91% yield). *R*_f 0.62 (2:1 Hexanes:Et₂O); ¹H NMR (500 MHz, CDCl₃): δ 8.06 (d, *J* = 8, 1H), 7.63 (s, 1H), 7.51 (d, *J* = 7.9, 1H), 7.26 (dd, *J* = 8, 8, 1H), 7.23 (dd, *J* = 8, 8, 1H), 5.49 (s, 2H), 3.48 (t, *J* = 8.1, 2H), 1.39 (s, 12H), 0.89 (t, *J* = 8.1, 2H), -0.03 (s, 9H); ¹³C NMR (125 MHz, CDCl₃): δ 137.5, 137.2, 132.8, 122.6, 122.2, 120.8, 110.0, 82.8, 75.9, 65.8, 24.8, 17.6, 15.2, -1.5; IR (film): 2977, 2953,

1614, 1537, 1143, 1093 cm^{-1} ; HRMS-ESI (m/z) [$M + \text{Na}$] $^+$ calcd for $\text{C}_{20}\text{H}_{32}\text{BNO}_3\text{SiNa}$, 396.2146; found, 396.2141.



Indole Pivalate 2.7. A 20 ml scintillation vial was charged with a magnetic stir bar, K_3PO_4 (2.07 g, 9.78 mmol, 6 equiv), H_2O (5 mL, sparged with N_2 for 30 min), and toluene (5 mL). The resulting mixture was stirred until all solids had dissolved. To the resulting biphasic mixture, bromide **2.5** (500 mg, 1.63 mmol, 1 equiv) and boronic ester **2.6** (912 mg, 2.45 mmol, 1.5 equiv) were added, followed by $\text{Pd}(\text{PPh}_3)_4$ (188 mg, 0.163 mmol, 0.1 equiv). The vial was sealed with a Teflon-coated screw-cap and heated at $90\text{ }^\circ\text{C}$ for 14 h. After cooling to $23\text{ }^\circ\text{C}$, the reaction mixture was extracted with EtOAc (3 x 10 mL). The combined organic layers were dried over Na_2SO_4 and concentrated under reduced pressure. The crude residue was purified by flash chromatography (10% to 30% $\text{CH}_2\text{Cl}_2/\text{Hexanes}$) to give indolyl pivalate **2.7** as a white foam (712 mg, 90%). R_f 0.67 (1:2 Hexanes: CH_2Cl_2); ^1H NMR (500 MHz, CDCl_3): δ 8.13 (d, $J = 8.5$, 1H), 8.02 (d, $J = 8.3$, 1H), 7.65 (d, $J = 8.3$, 1H), 7.63 (d, $J = 7.7$, 1H), 7.58 (dd, $J = 7.1$, 7.1, 1H), 7.53 (d, $J = 7.7$, 1H), 7.47 (dd, $J = 8.2$, 8.2, 1H), 7.39-7.34 (m, 3H), 7.21 (dd, $J = 7.3$, 7.3, 1H), 5.61 (s, 2H), 3.65 (t, $J = 8$, 2H), 1.60 (s, 9H), 1.01 (t, $J = 8$, 2H), 0.04 (s, 9H); ^{13}C NMR (125 MHz, CDCl_3): δ 177.1, 146.0, 136.5, 133.5, 130.6, 128.8, 127.4, 127.3, 127.2, 126.8, 126.2, 126.1, 122.5, 121.1, 120.4, 120.3, 117.6, 115.7, 110.0, 75.6, 65.8, 39.4, 27.4, 17.7, -1.46; IR (film):

2955, 1751, 1460, 1218, 1013 cm^{-1} ; HRMS-ESI (m/z) $[\text{M} + \text{Na}]^+$ calcd for $\text{C}_{29}\text{H}_{35}\text{NO}_3\text{SiNa}$, 496.2284; found, 496.2277.



Indole 2.8. A 1-dram vial was charged with anhydrous powdered K_3PO_4 (322 mg, 1.52 mmol, 7.2 equiv), celite (100 mg, to prevent clumping), and a magnetic stir bar. The vial and contents were flame-dried under reduced pressure, then allowed to cool under N_2 . Phenylboronic acid **2.2a** (103 mg, 0.844 mmol, 4 equiv), $\text{NiCl}_2(\text{PCy}_3)_2$ (7 mg, 0.0106 mmol, 5 mol%), and pivalate substrate **2.7** (100 mg, 0.211 mmol, 1 equiv) were added. The vial was then evacuated and backfilled with N_2 . Toluene (0.8 mL) was added and the vial was sealed with a Teflon-lined screw cap. The heterogeneous mixture was allowed to stir at rt for 1 h, then heated to 110 °C for 24 h. The reaction vessel was cooled to rt and then transferred to a round bottom flask containing CH_2Cl_2 (10 mL). Silica gel (3 mL) was added and the solvent was removed under reduced pressure to afford a free-flowing powder. This powder was then dry-loaded onto a silica gel column (2.5 x 7 cm) and purified by flash chromatography (10% to 20% CH_2Cl_2 :Hexanes) to yield product **2.8** as a white solid (83 mg, 88% yield). R_f 0.59 (2:1 Hexanes:Et₂O); ^1H NMR (500 MHz, CDCl_3): δ 8.03 (d, $J = 8$, 1H), 7.88 (d, $J = 9$, 1H), 7.52-7.28 (m, 12H), 7.21 (t, $J = 7.5$, 1H), 7.05 (t, $J = 7$, 1H), 5.48 (s, 2H), 3.49 (t, $J = 8$, 2H), 0.84 (t, $J = 8$, 2H), -0.14 (s, 9H); ^{13}C NMR (125 MHz, CDCl_3): δ 140.9, 139.3, 136.6, 132.7, 132.2, 132.0, 130.1, 128.9, 128.2, 127.4,

127.23, 127.15, 126.8, 126.7, 126.3, 125.8, 125.5, 122.5, 120.5, 120.4, 116.3, 110.2, 75.7, 65.9, 17.8, -1.4; IR (film): 3053, 2951, 1464, 1246, 1073 cm^{-1} ; HRMS-ESI (m/z) $[\text{M} + \text{Na}]^+$ calcd for $\text{C}_{30}\text{H}_{31}\text{NOSiNa}$, 472.2073; found, 472.2073.

2.8 Notes and References

- (1) (a) *Metal-Catalyzed Cross-Coupling Reactions*; Diederich, F., Meijere, A., Eds.; Wiley-VCH: Weinheim, 2004. (b) Hassan, J.; Sévignon, M.; Gozzi, C.; Schulz, E.; Lemaire, M. *Chem. Rev.* **2002**, *102*, 1359–1469. (c) *Topics in Current Chemistry*; Miyaura, N., Ed.; Vol. 219; Springer-Verlag: New York, 2002. (d) Corbet, J.; Mignani, G. *Chem. Rev.* **2006**, *106*, 2651–2710. (e) Negishi, E. *Bull. Chem. Soc. Jpn.* **2007**, *80*, 233–257.
- (2) For a pertinent review, see: Littke, A. F.; Fu, G. C. *Angew. Chem. Int. Ed.* **2002**, *41*, 4176–4211.
- (3) For aryl mesylate and tosylate cross-couplings, see: (a) Zim, D.; Lando, V. R.; Dupont, J.; Monteiro, A. L. *Org. Lett.* **2001**, *3*, 3049–3051. (b) Tang, Z.; Hu, Q. *J. Am. Chem. Soc.* **2004**, *126*, 3058–3059. (c) Percec, V.; Golding, G. M.; Smidrkal, J.; Weichold, O. *J. Org. Chem.* **2004**, *69*, 3447–3452. (d) Zhang, L.; Meng, T.; Wu, J. *J. Org. Chem.* **2007**, *72*, 9346–9349. (e) Munday, R. H.; Martinelli, J. R.; Buchwald, S. L. *J. Am. Chem. Soc.* **2008**, *130*, 2754–2755; see also references therein.
- (4) The Suzuki–Miyaura coupling of electron-deficient aryl methyl ethers was recently reported; see: Tobisu, M.; Shimasaki, T.; Chatani, N. *Angew. Chem. Int. Ed.* **2008**, *47*, 4866–4869.
- (5) Of the known methods for phenol coupling, the most common involves formation and reaction of the corresponding aryl triflates. However, these species are somewhat costly to prepare (see reference 7b), unable to serve as directing groups, and are susceptible to base-promoted hydrolysis. Aryl mesylates and tosylates can also be utilized, although their utility does not yet appear to be general.

- (6) For unsuccessful attempts to effect the cross-coupling of *O*-acetylated phenols using Ni-catalysis, see: Guan, B.; Xiang, S.; Wu, T.; Sun, Z.; Wang, B.; Zhao, K.; Shi, Z. *Chem. Commun.* **2008**, 1437–1439; see also reference 4.
- (7) Approximate reagent costs by Aldrich Chemical Company, Inc. are: (a) Trimethylacetyl chloride (pivaloyl chloride)=\$10 per mol. (b) Triflic anhydride=\$310 per mol. (c) methanesulfonyl chloride=\$10 per mol). (d) iodomethane=\$24 per mol.
- (8) For the insertion of Ni(0) into the *acyl* C–O bond of acylated phenols, see: Yamamoto, T.; Ishizu, J.; Kohara, T.; Komiya, S.; Yamamoto, A. *J. Am. Chem. Soc.* **1980**, *102*, 3758–3764.
- (9) (a) Miyaura, N.; Suzuki, A. *Chem. Rev.* **1995**, *95*, 2457–2483. (b) Suzuki, A. *Chem. Commun.* **2005**, 4759–4763. (c) Doucet, H. *Eur. J. Org. Chem.* **2008**, 2013–2030.
- (10) The more expensive and commonly used d⁸ transition metal, palladium, was completely ineffective at promoting the desired transformation under a variety of reaction conditions.
- (11) In the presence of Ni(0), other ligands such as PPh₃, dppe, dppf, and dppp provided trace amounts of cross-coupled products.
- (12) Excess of the arylboronic acid component is required because the trimeric boroxine, which comprises between 30 and 60% of commercially available arylboronic acids, is completely unreactive under these anhydrous reactions.
- (13) In the presence of excess arylboronic acid, NiCl₂(PCy₃)₂ is thought to undergo reduction to an active Ni(0) catalyst; see reference 3a.
- (14) NiCl₂(PCy₃)₂, is commercially available from Strem Chemicals Inc., or can be prepared in multigram quantities following a simple one-step protocol; see: (a) Stone, P. J.; Dori, Z. *Inorg. Chim. Acta* **1970**, *5*, 434–438. (b) Barnett, K. W. *J. Chem. Educ.* **1974**, *51*, 422–423.

- (15) Arenes that possess an $-OC(O)R$ substituent are known to undergo electrophilic aromatic substitution to afford *ortho/para* substituted products; see: Smith, M. B.; March, J. *March's Advanced Organic Chemistry*; 6th ed.; John Wiley & Sons, Inc.: New Jersey, 2007; p 668.
- ¹⁶ The formation of *ortho*-brominated products was not observed, likely because of the steric bulk imposed by the pivalate group.
- (17) Chen, C. T.; Kuo, J. H.; Pawar, V. D.; Munot, Y. S.; Weng, S. S.; Ku, C. H.; Liu, C. Y. *J. Org. Chem.* **2005**, *70*, 1188–1197.
- (18) Dalpozzo, R.; Nino, A.; Maiuolo, L.; Oliverio, M.; Porcopio, A.; Russo, B.; Tocci, A. *Australian J. Chem.* **2007**, *60*, 75–79.
- (19) Martin, R. *Bull. Soc. Chim. Fr.* **1979**, 373–380.
- (20) (a) Miyashita, M.; Shiina, I.; Miyoshi, S.; Mukaiyama, T. *Bull. Chem. Soc. Jpn.* **1993**, *66*, 1516–1527. (b) Sloan, K. B.; Koch, A. M. *J. Org. Chem.* **1983**, *48*, 3777–3783.
- (21) (a) Stone, P. J.; Dori, Z. *Inorg. Chim. Acta* **1970**, *5*, 434–438. (b) Barnett, K. W. *J. Chem. Educ.* **1974**, *51*, 422–423.
- (22) Biaryl products that form are the result of homocoupling of the arylboronic acid, which occurs during the reduction of the Ni(II) precatalyst to Ni(0).
- (23) Shen, H. C.; Pal, S.; Lian, J. J.; Liu, R. S. *J. Am. Chem. Soc.* **2003**, *125*, 15762–15763.
- (24) Repinskaya, I. B.; Shakirov, M. M.; Kultunov, K. Y.; Koptuyug, V. A. *J. Org. Chem. USSR* **1988**, *24*, 1719–1727.
- (25) Moore, L. R.; Shaughnessy, K. H. *Org. Lett.* **2004**, *6*, 225–228.
- (26) Tao, B.; Boykin, D. W. *J. Org. Chem.* **2004**, *69*, 4330–4335.
- (27) Riggleman, S.; DeShong, P. *J. Org. Chem.* **2003**, *68*, 8106–8109.

- (28) Kong, A.; Han, X.; Lu, X. *Org. Lett.* **2006**, *8*, 1339–1342.
- (29) Alcock, N. J.; Mann, I.; Peach, P.; Wills, M. *Tetrahedron Asymm.* **2002**, *13*, 2485–2490.
- (30) Denmark, S. E.; Ober, M. H. *Org. Lett.* **2003**, *5*, 1357–1360.
- (31) Song, C.; Ma, Y.; Chai, Q.; Ma, C.; Jiang, W.; Andrus, M. B. *Tetrahedron* **2005**, *61*, 7438–7446.
- (32) Mino, T.; Shirae, Y.; Sakamoto, M.; Fujita, T. *J. Org. Chem.* **2005**, *70*, 2191–2194.
- (33) Zhang, L.; Cheng, J.; Zhang, W.; Lin, B.; Pan, C.; Chen, J. *Synth. Commun.* **2007**, *37*, 3809–3814.
- (34) Denmark, S. E.; Baird, J. D.; Regens, C. S. *J. Org. Chem.* **2008**, *73*, 1440–1455.

APPENDIX ONE

Spectra Relevant to Chapter Two:

Cross-Coupling Reactions of Aryl Pivalates with Boronic Acids

Kyle W. Quasdorf, Xia Tian, and Neil K. Garg.

J. Am. Chem. Soc. **2008**, *130*, 14422–14223.

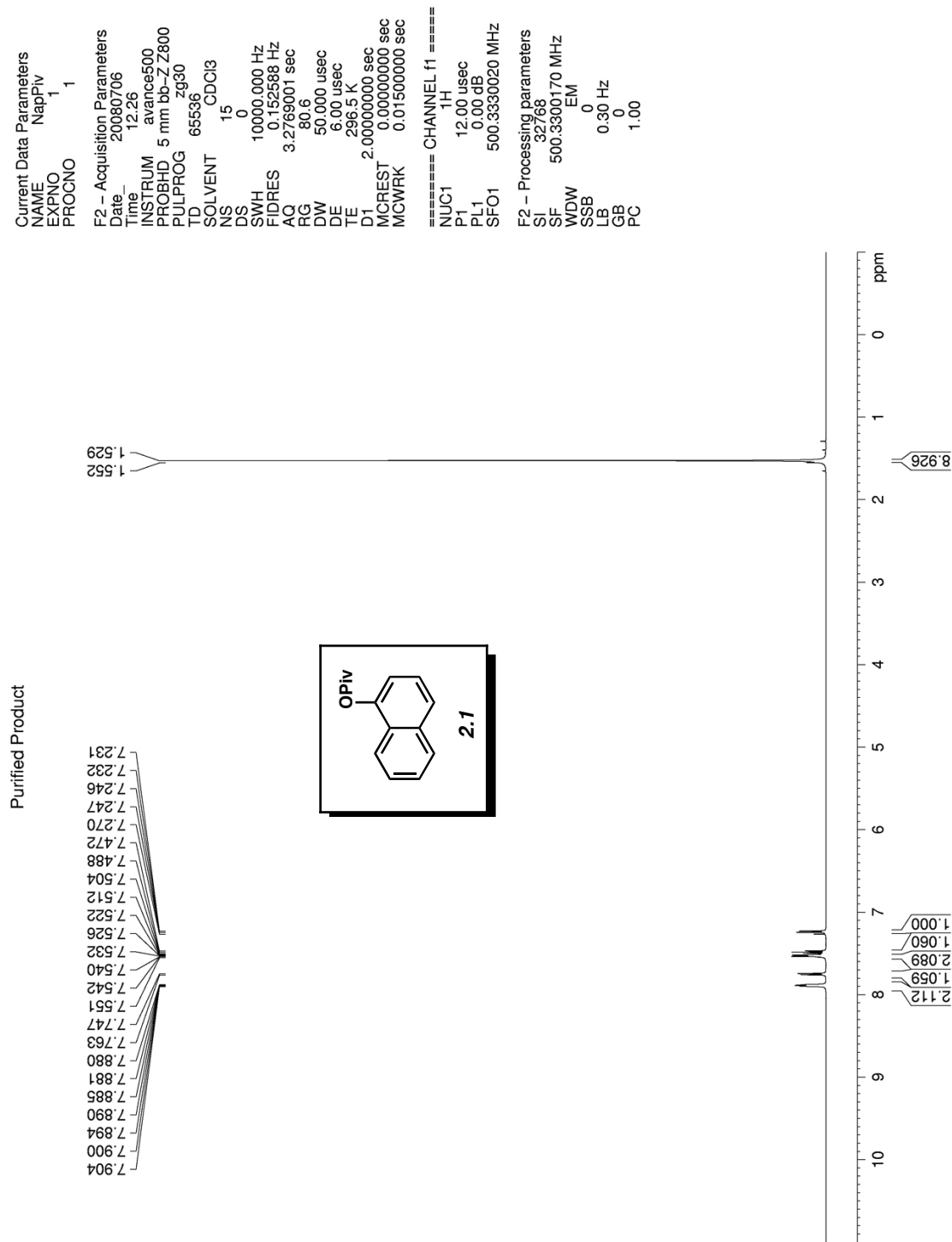


Figure A1.1 ¹H NMR (500 MHz, CDCl₃) of compound 2.1.

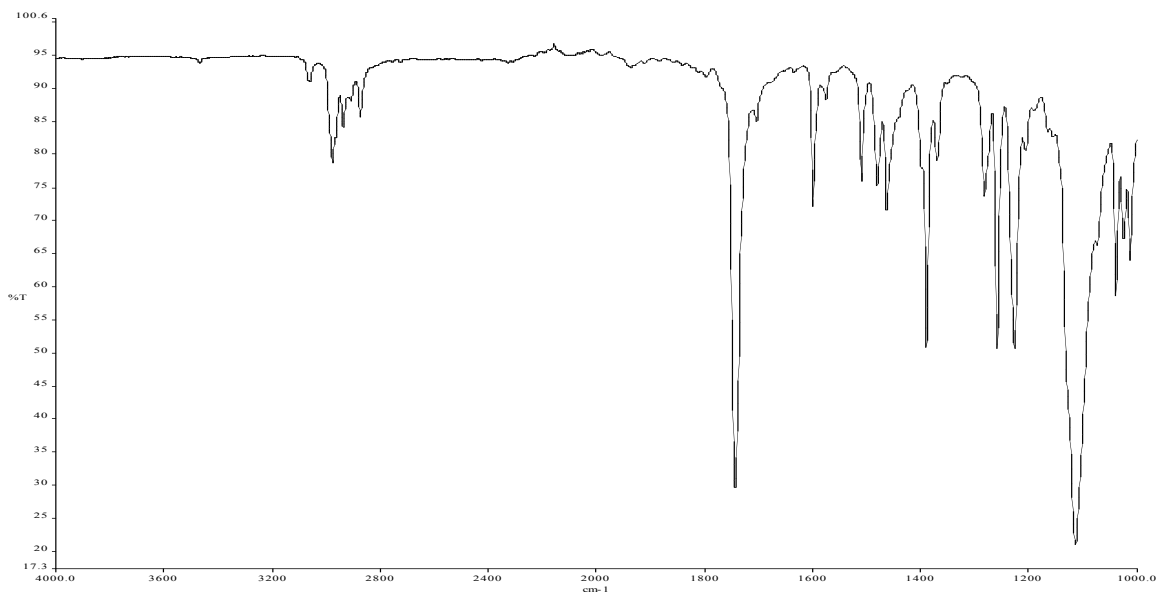


Figure A1.2 Infrared spectrum of compound **2.1**.

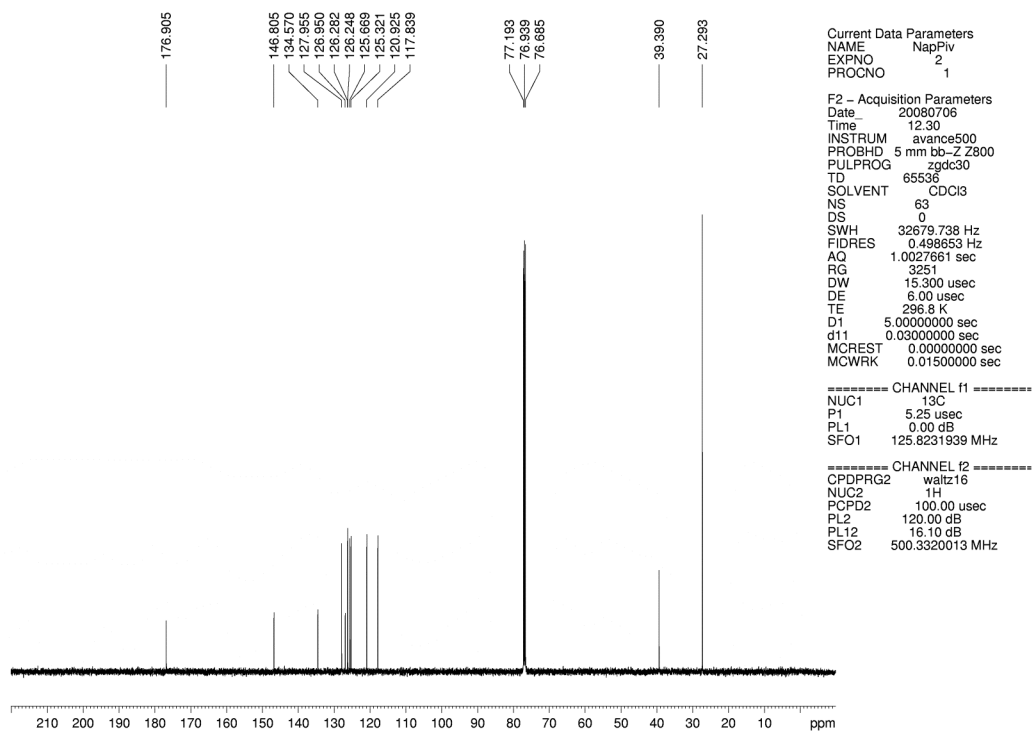
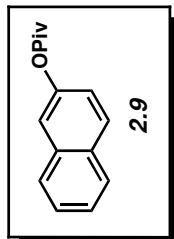


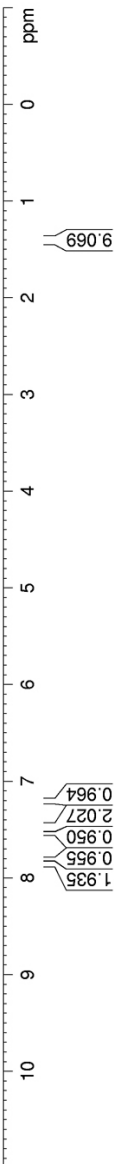
Figure A1.3 ^{13}C NMR (125 MHz, CDCl_3) of compound **2.1**.

Purified Product

7.868
7.861
7.851
7.812
7.797
7.797
7.542
7.538
7.513
7.511
7.499
7.497
7.484
7.480
7.467
7.453
7.270
7.219
7.214
7.201
7.197



1.553
1.421



Current Data Parameters
NAME KQ2-49Pure
EXPNO 1
PROCNO 1

F2 - Acquisition Parameters
Date_ 20080606
Time 17.29
INSTRUM arx500
PROBHD 5 mm broadband
PULPROG zg30
TD 65536
SOLVENT CDCl3
NS 13
DS 0
SWH 10000.000 Hz
FIDRES 0.152588 Hz
AQ 3.2768500 sec
RG 2048
DW 50.000 usec
DE 71.43 usec
TE 300.0 K
D1 2.0000000 sec
P1 11.00 usec
SFO1 500.1330008 MHz
NUCLEUS 1H

F2 - Processing parameters
SI 32768
SF 500.1300190 MHz
WDW EM
SSB 0
LB 0.30 Hz
GB 0
PC 1.00

Figure A1.4 ¹H NMR (500 MHz, CDCl₃) of compound 2.9.

Current Data Parameters
 NAME xt2-35
 EXPNO 1
 PROCNO 1

F2 - Acquisition Parameters
 Date_ 20080625
 Time_ 10.42
 INSTRUM avance500
 PROBHD 5 mm bb-Z800
 PULPROG zg30
 TD 32768
 SOLVENT CDCI3
 NS 8
 DS 0
 SWH 10000.000 Hz
 FIDRES 0.305176 Hz
 AQC 1.6385000 sec
 RG 256
 DW 50.000 usec
 DE 6.00 usec
 TE 296.2 K
 D1 2.0000000 sec
 MCREST 0.0000000 sec
 MCWRK 0.01500000 sec

===== CHANNEL f1 =====
 NUC1 1H
 P1 12.00 usec
 PL1 0.00 dB
 SFO1 500.3330020 MHz

F2 - Processing parameters
 SI 32768
 SF 500.3299873 MHz
 WDW EM
 SSB 0
 LB 0.30 Hz
 GB 0
 PC 1.00

default proton parameters

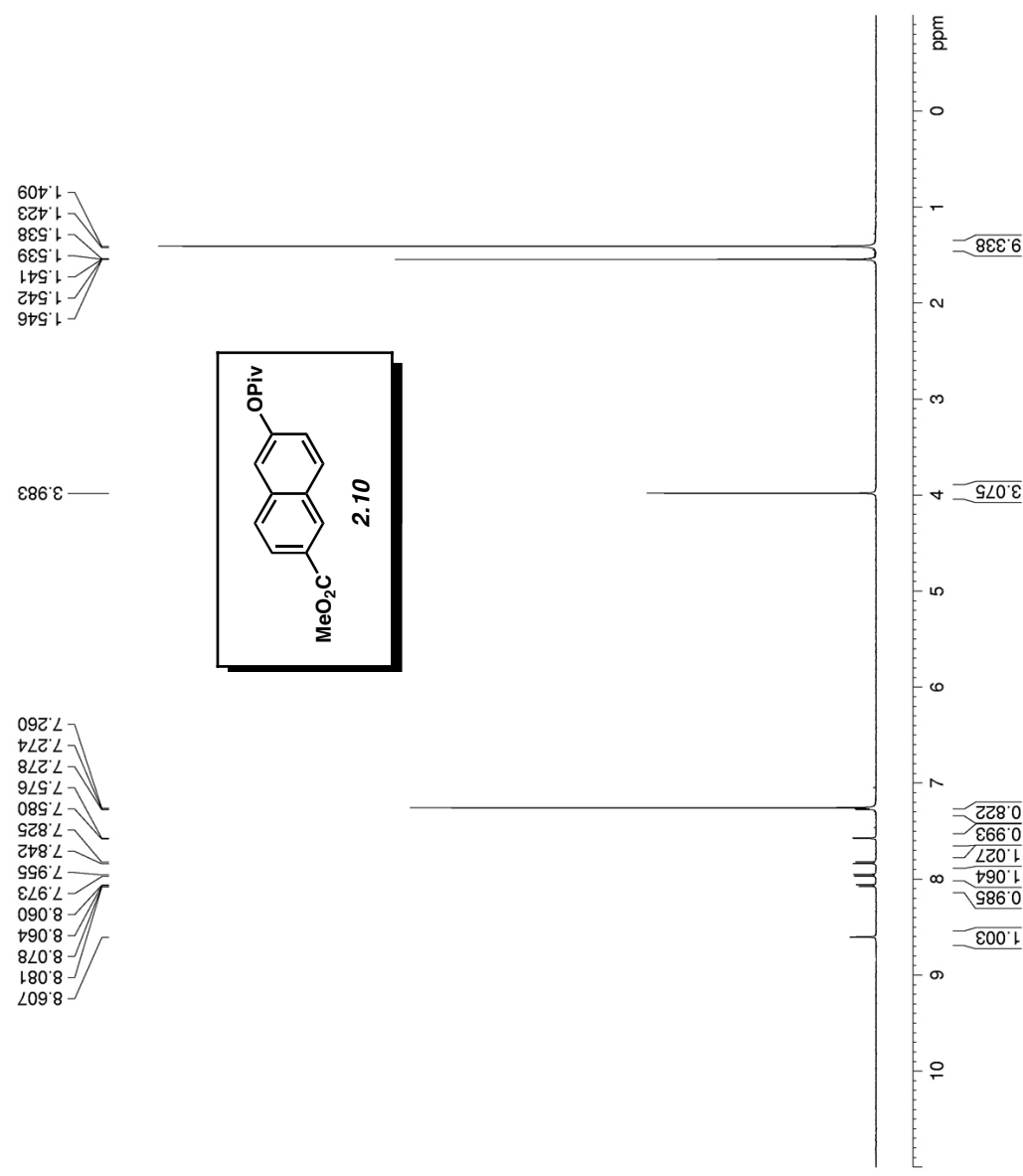


Figure A1.5 ¹H NMR (500 MHz, CDCl₃) of compound 2.10.

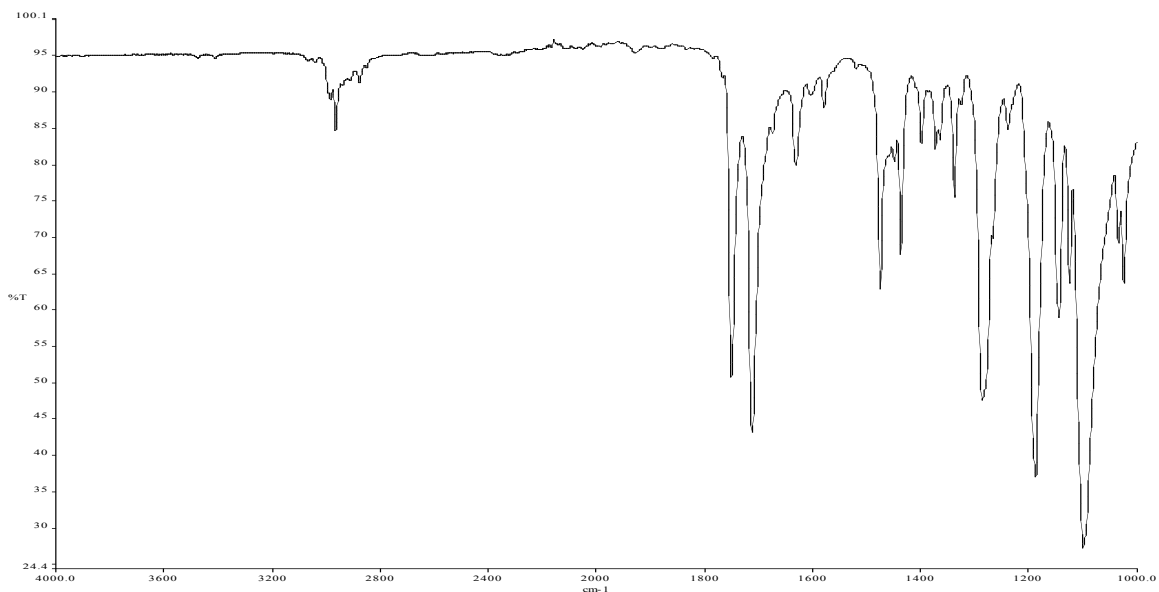


Figure A1.6 Infrared spectrum of compound **2.10**.

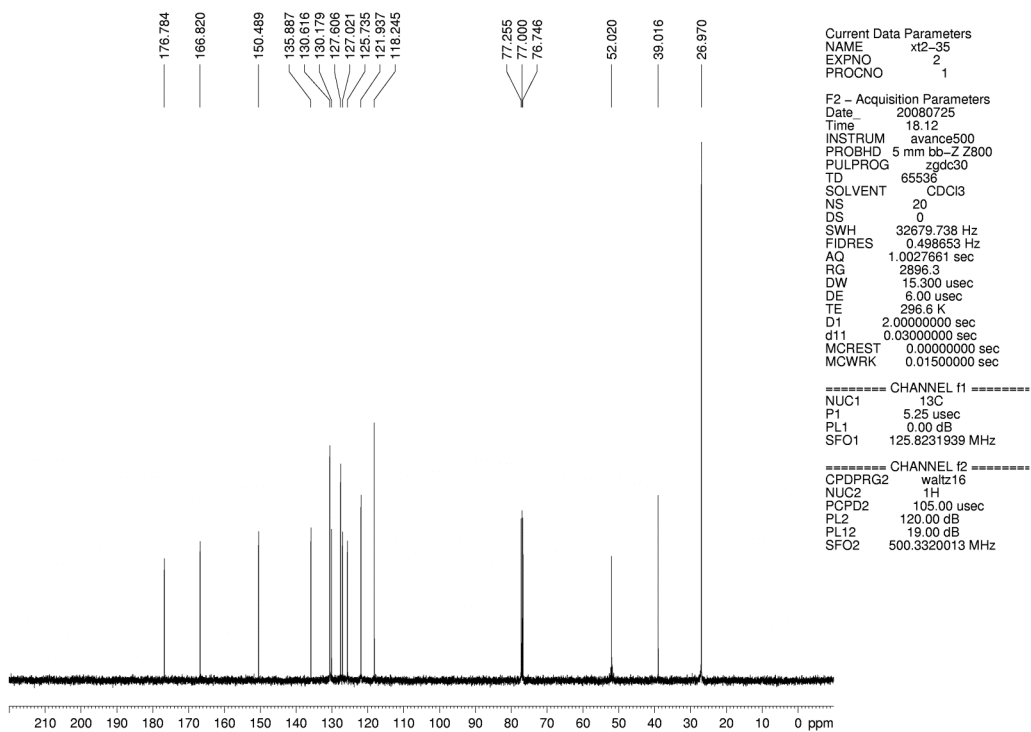


Figure A1.7 ^{13}C NMR (125 MHz, CDCl_3) of compound **2.10**.

Current Data Parameters
 NAME KQ2-69Purified
 EXPNO 1
 PROCNO 1

F2 - Acquisition Parameters
 Date_ 20080621
 Time 13:23
 INSTRUM av500
 PROBHD 5 mm broadband
 PULPROG zg30
 TD 65536
 SOLVENT CDCl3
 NS 26
 DS 0
 SWH 10000.000 Hz
 FIDRES 0.152588 Hz
 AQ 3.2768500 sec
 RG 1430
 DW 50.000 usec
 DE 71.43 usec
 TE 300.0 K
 D1 2.0000000 sec
 P1 11.00 usec
 SFO1 500.1330008 MHz
 NUCLEUS 1H

F2 - Processing parameters
 SI 32768
 SF 500.1300195 MHz
 WDW EM
 SSB 0
 LB 0.30 Hz
 GB 0
 PC 1.00

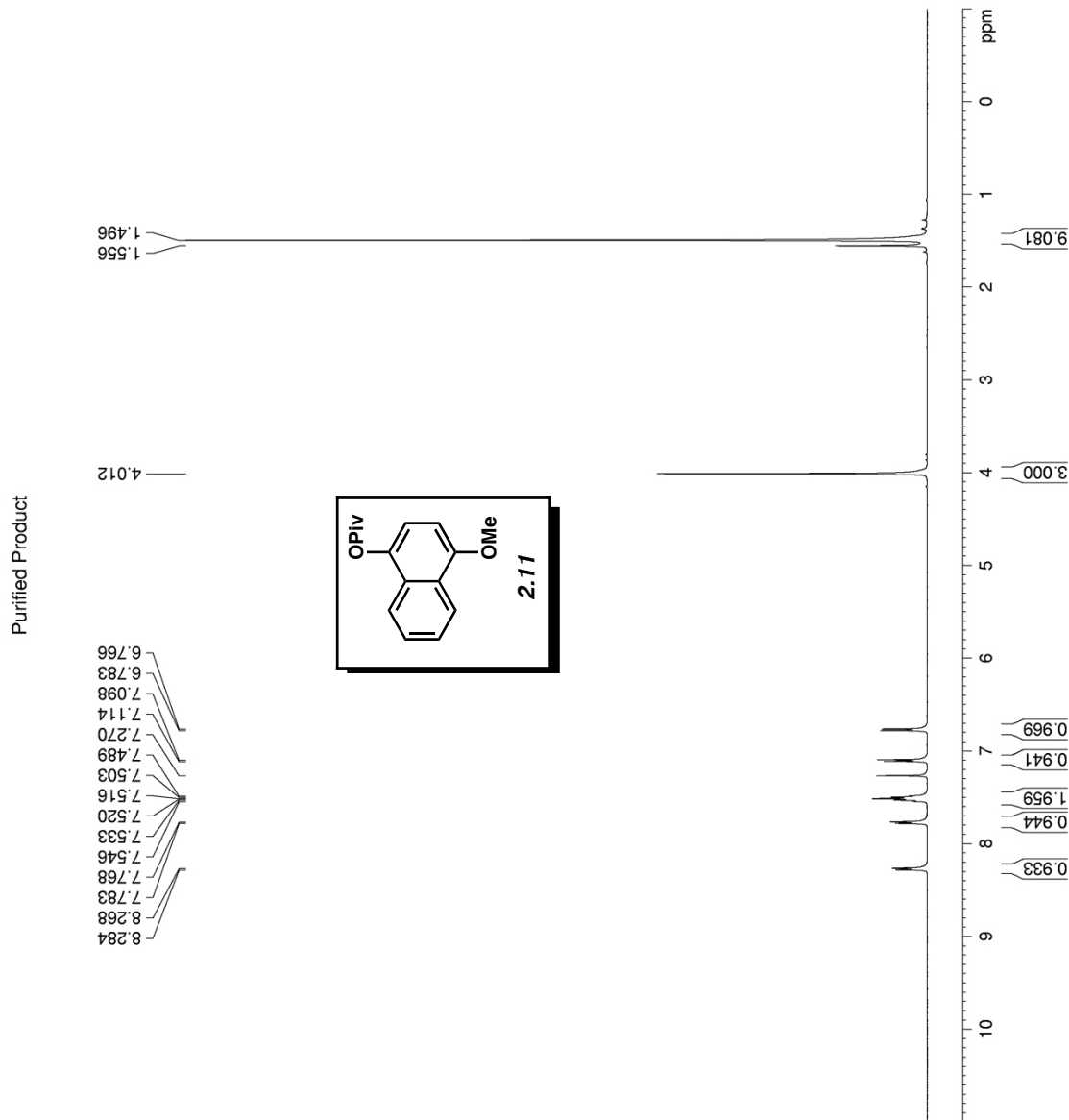


Figure A1.8 ¹H NMR (500 MHz, CDCl₃) of compound 2.11.

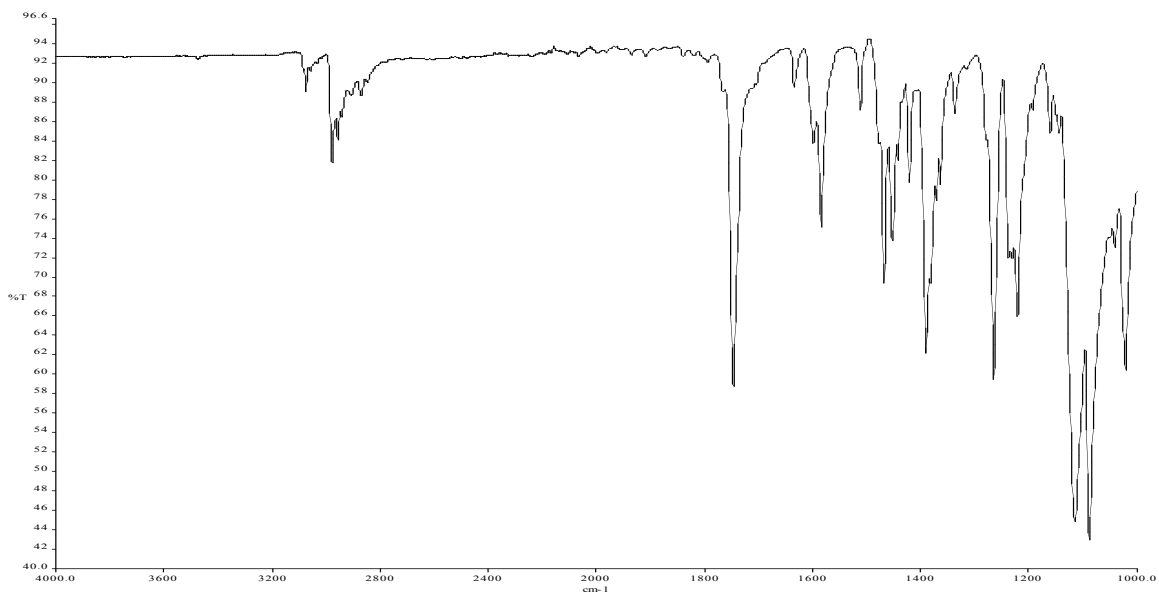


Figure A1.9 Infrared spectrum of compound **2.11**.

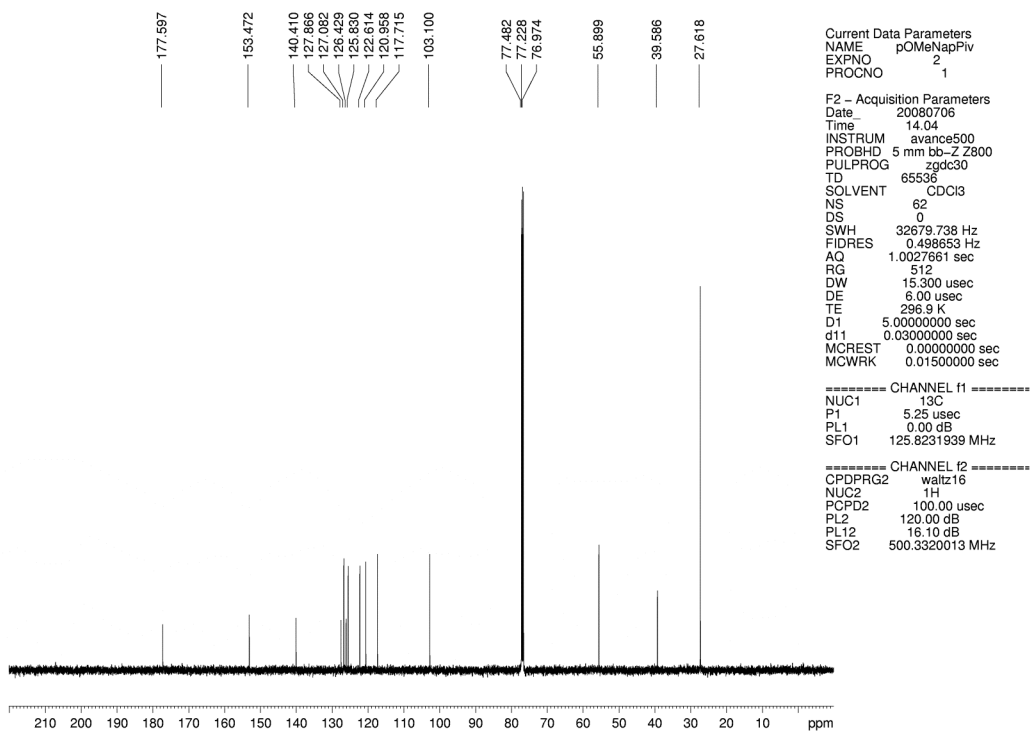


Figure A1.10 ^{13}C NMR (125 MHz, CDCl_3) of compound **2.11**.

default proton parameters

```
Current Data Parameters
NAME      XT1-97
EXPNO     1
PROCNO    1

F2 - Acquisition Parameters
Date_     20080804
Time      20:57
INSTRUM   av300
PROBHD    5 mm PABBO BB-
PULPROG   zg30
TD         65536
SOLVENT   CDCl3
NS         8
DS         0
SWH        5995.204 Hz
FIDRES     0.091480 Hz
AQ         5.4657526 sec
RG         812.7
DW         83.400 usec
DE         6.00 usec
TE         297.9 K
D1         2.0000000 sec
TD0        1

===== CHANNEL f1 =====
NUC1       1H
P1         14.00 usec
PL1        -2.00 dB
SFO1       300.1318008 MHz

F2 - Processing parameters
SI         65536
SF         300.1300131 MHz
WDW        EM
SSB        0
LB         0.30 Hz
GB         0
PC         1.40
```

7.258
7.172
7.144
7.144
6.939
6.910

2.336
1.535
1.347

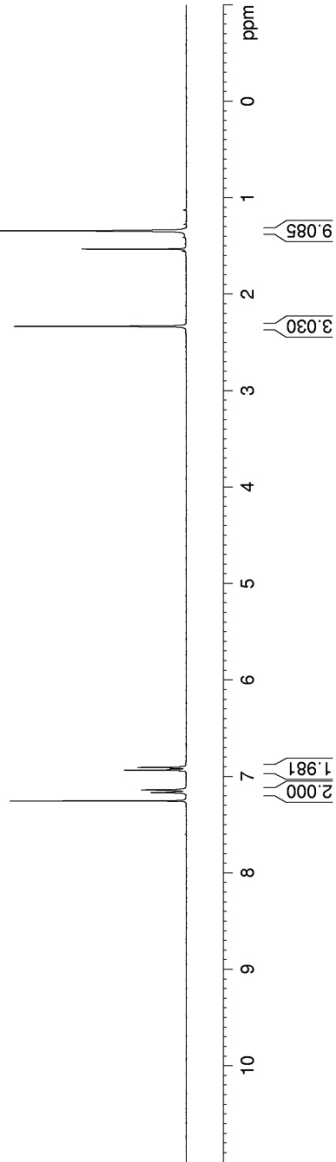
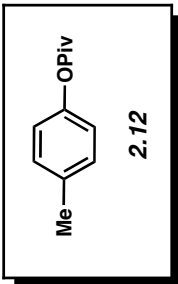


Figure A1.11 ¹H NMR (300 MHz, CDCl₃) of compound 2.12.

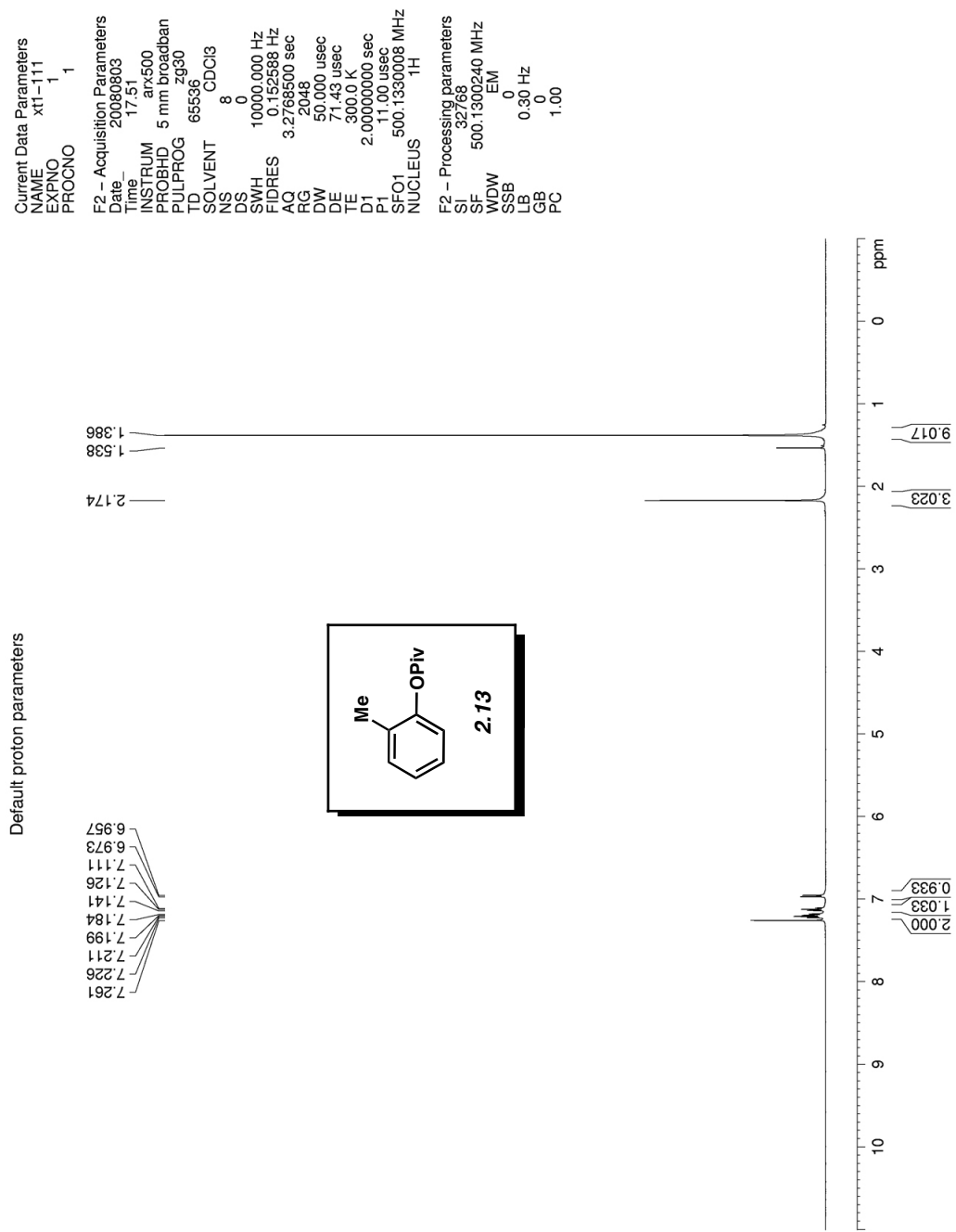


Figure A1.12 ¹H NMR (500 MHz, CDCl₃) of compound **2.13**.

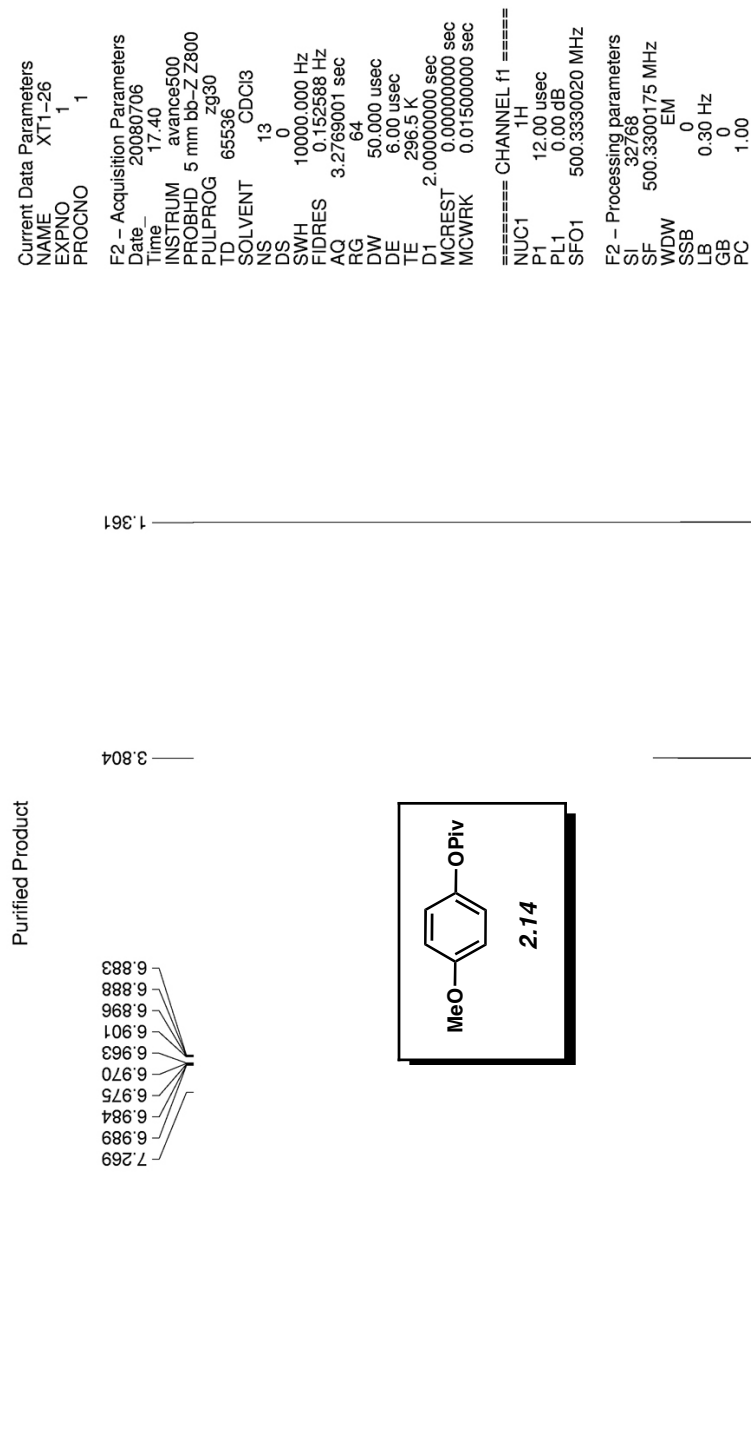


Figure A1.13 ¹H NMR (500 MHz, CDCl₃) of compound 2.14.

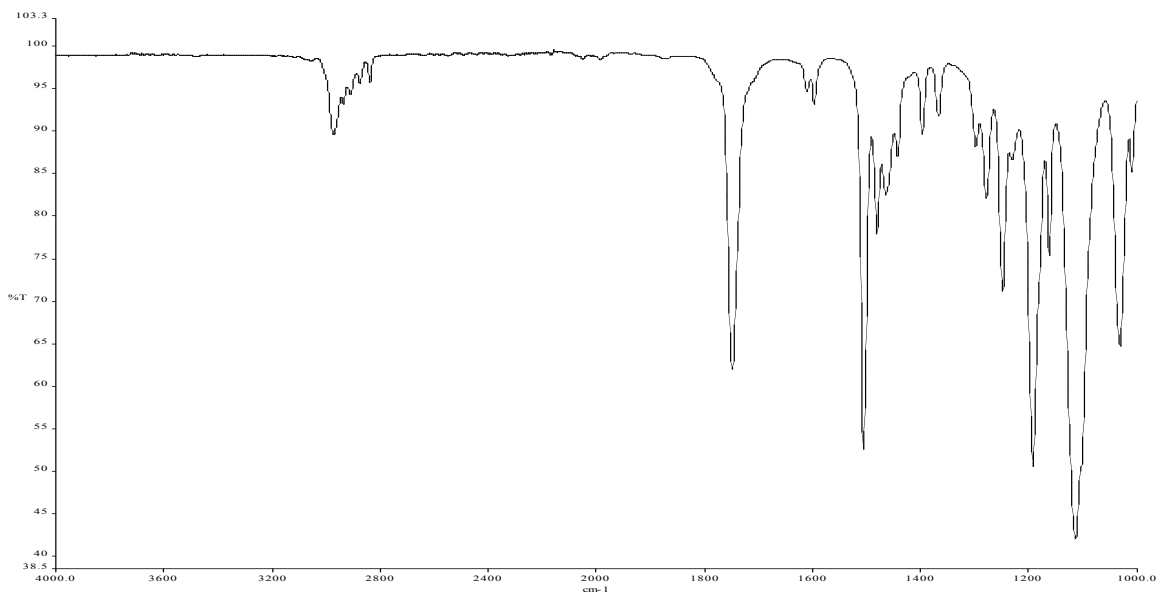


Figure A1.14 Infrared spectrum of compound 2.14.

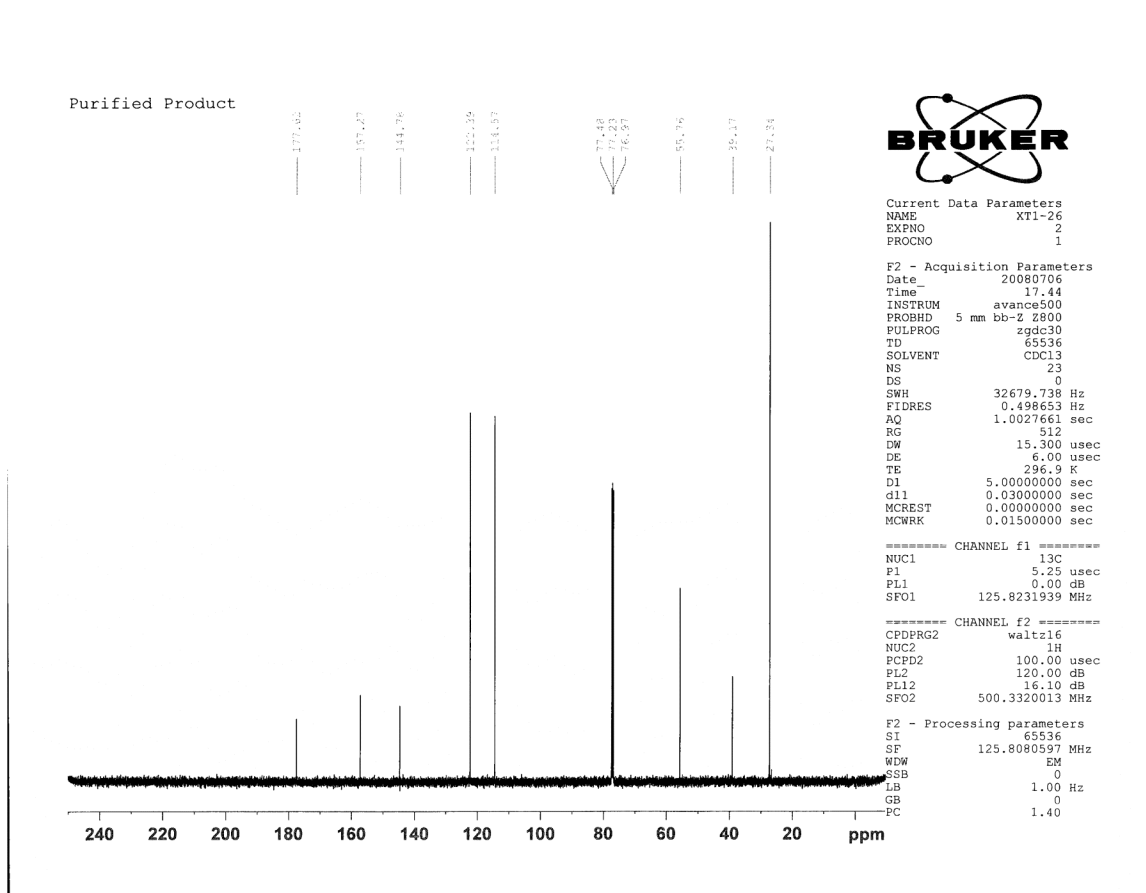
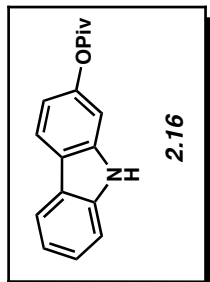


Figure A1.15 ^{13}C NMR (125 MHz, CDCl_3) of compound 2.14.

default proton parameters

8.095
7.948
7.932
7.919
7.902
7.375
7.372
7.358
7.356
7.344
7.342
7.297
7.281
7.260
7.221
7.219
7.205
7.191
7.070
7.066
6.899
6.895
6.882
6.878



Current Data Parameters
NAME xt2-14
EXPNO 1
PROCNO 1

F2 - Acquisition Parameters
Date_ 20080730
Time_ 5.36
INSTRUM avance500
PROBHD 5 mm bb-ZZ800
PULPROG zg30
TD 65536
SOLVENT CDCI3
NS 8
DS 0
SWH 10000.000 Hz
FIDRES 0.152588 Hz
AQ 3.2769001 sec
RG 114
DW 50.000 usec
DE 6.00 usec
TE 296.3 K
D1 2.0000000 sec
MCREST 0.0000000 sec
MCWRK 0.01500000 sec

===== CHANNEL f1 =====
NUC1 1H
P1 12.00 usec
PL1 0.00 dB
SFO1 500.3330020 MHz

F2 - Processing parameters
SI 32768
SF 500.3300219 MHz
WDW EM
SSB 0
LB 0.30 Hz
GB 0
PC 1.00

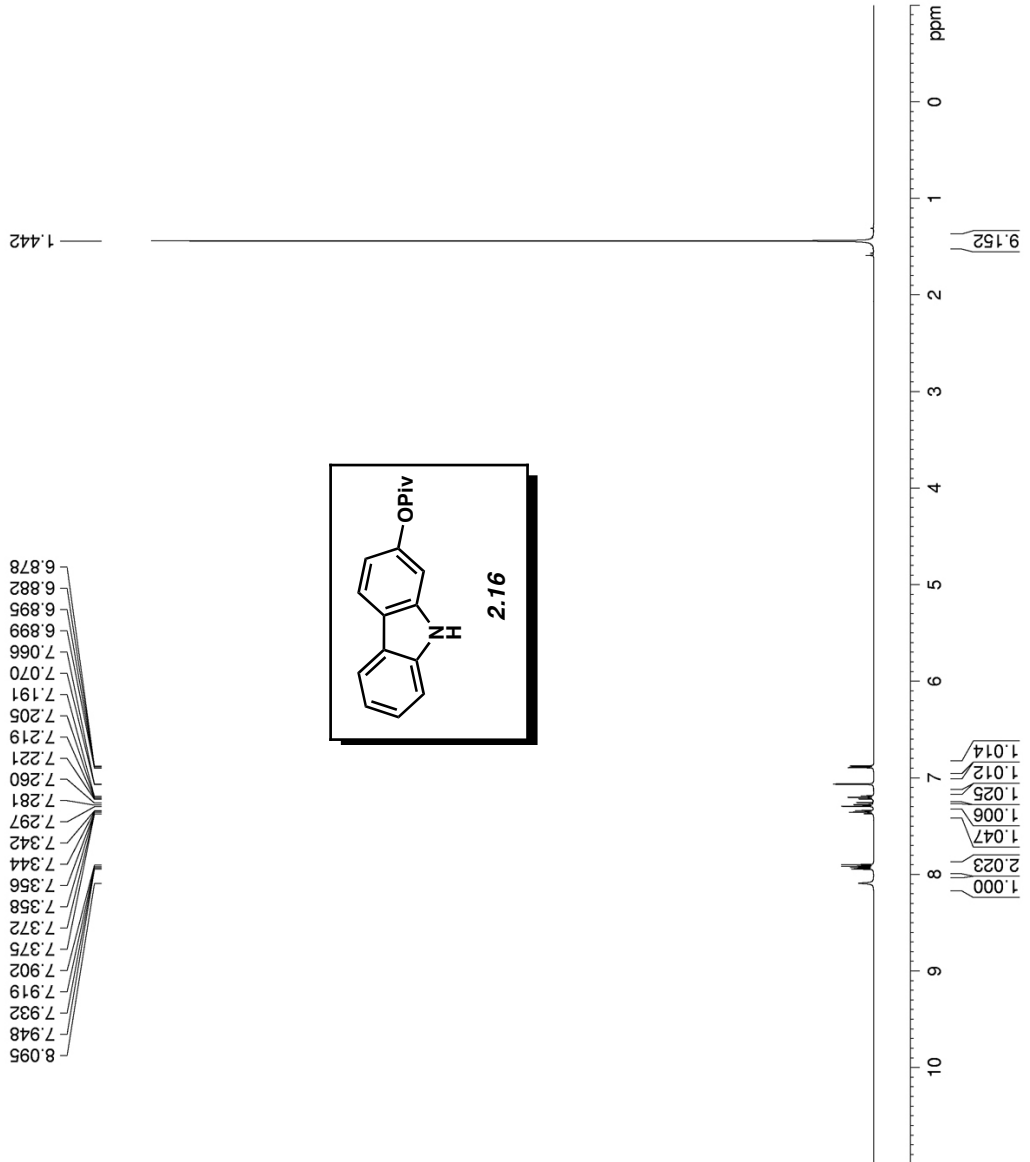


Figure A1.16 ¹H NMR (500 MHz, CDCl₃) of compound 2.16.

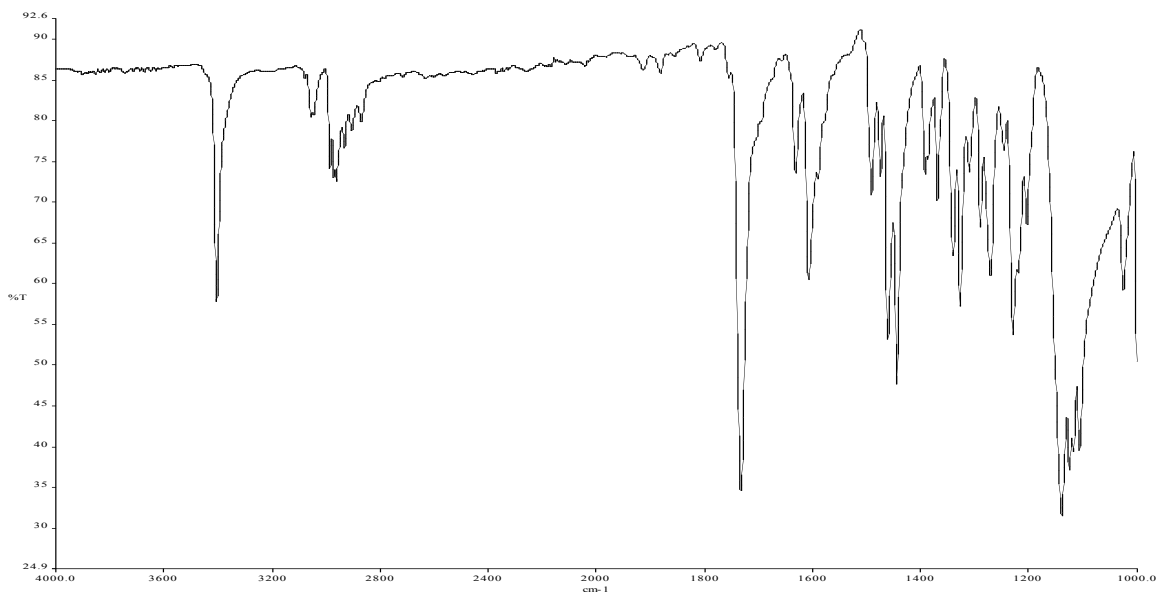


Figure A1.17 Infrared spectrum of compound **2.16**.

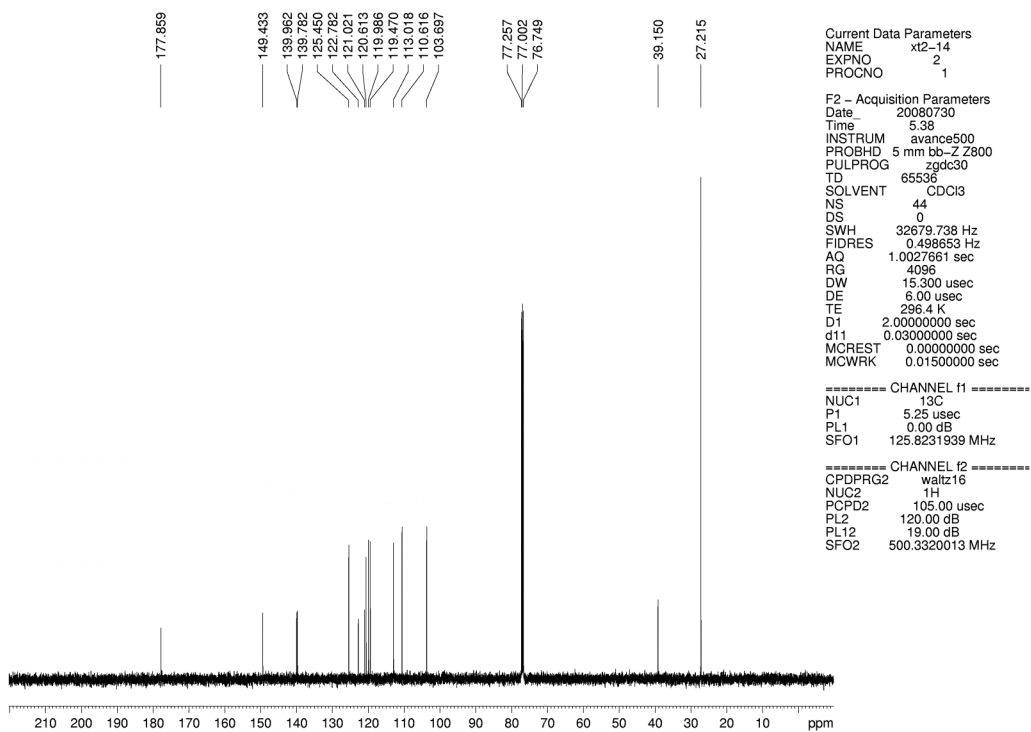


Figure A1.18 ^{13}C NMR (125 MHz, CDCl_3) of compound **2.16**.

Current Data Parameters
 NAME xt2-15
 EXPNO 1
 PROCNO 1

F2 - Acquisition Parameters
 Date_ 20080725
 Time_ 18.05
 INSTRUM avance500
 PROBHD 5 mm bb-ZZ800
 PULPROG zg30
 TD 65536
 SOLVENT CDCl3
 NS 5
 DS 0
 SWH 10000.000 Hz
 FIDRES 0.152588 Hz
 AQ 3.2769001 sec
 RG 143.7
 DW 50.000 usec
 DE 6.00 usec
 TE 296.4 K
 D1 2.0000000 sec
 MCREST 0.0000000 sec
 MCWRK 0.01500000 sec

===== CHANNEL f1 =====
 NUC1 1H
 P1 12.00 usec
 PL1 0.00 dB
 SFO1 500.3330020 MHz

F2 - Processing parameters
 SI 32768
 SF 500.3299690 MHz
 WDW EM
 SSB 0
 LB 0.30 Hz
 GB 0
 PC 1.00

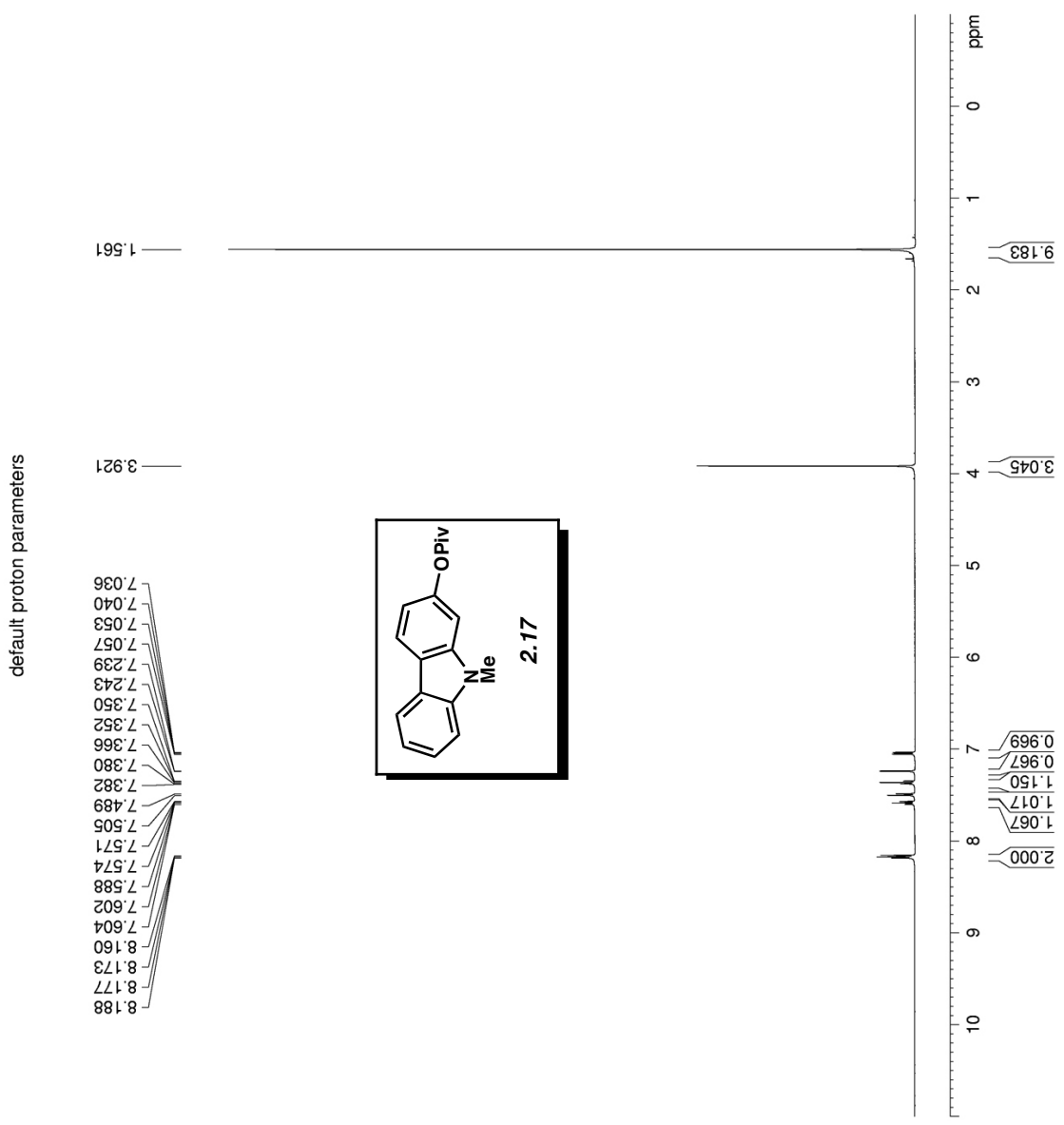


Figure A1.19 ¹H NMR (500 MHz, CDCl₃) of compound 2.17.

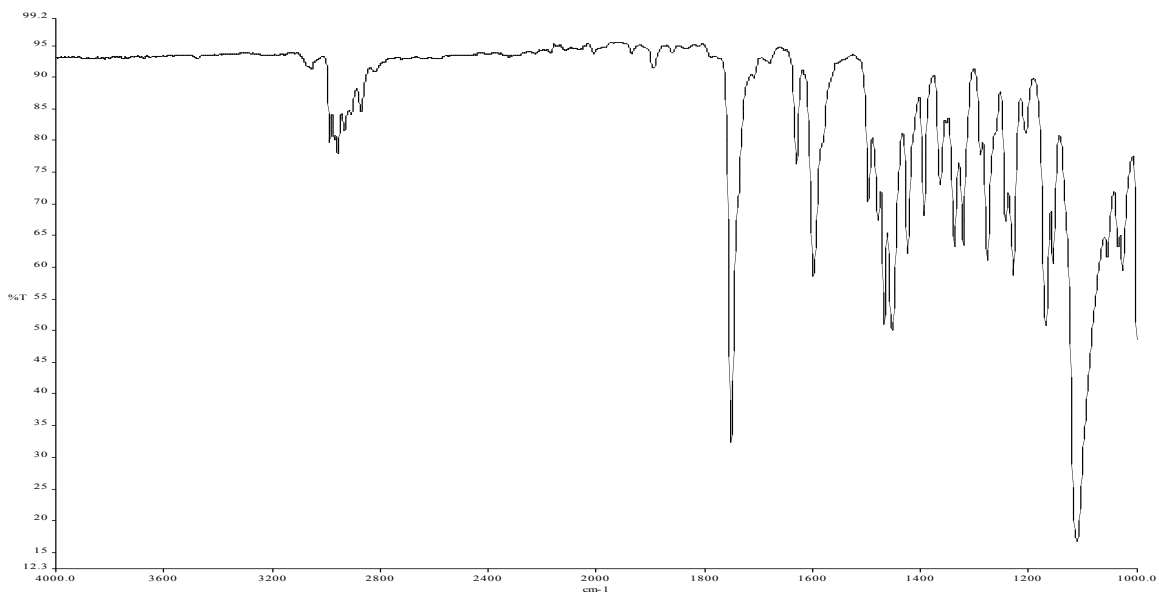


Figure A1.20 Infrared spectrum of compound **2.17**.

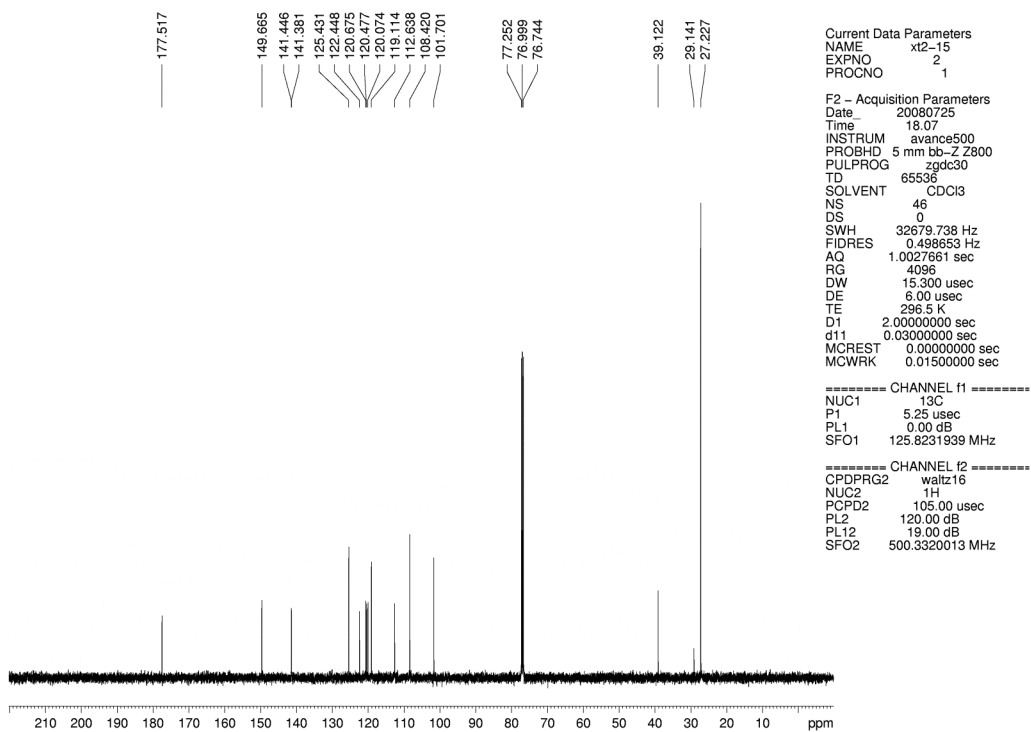


Figure A1.21 ^{13}C NMR (125 MHz, CDCl_3) of compound **2.17**.

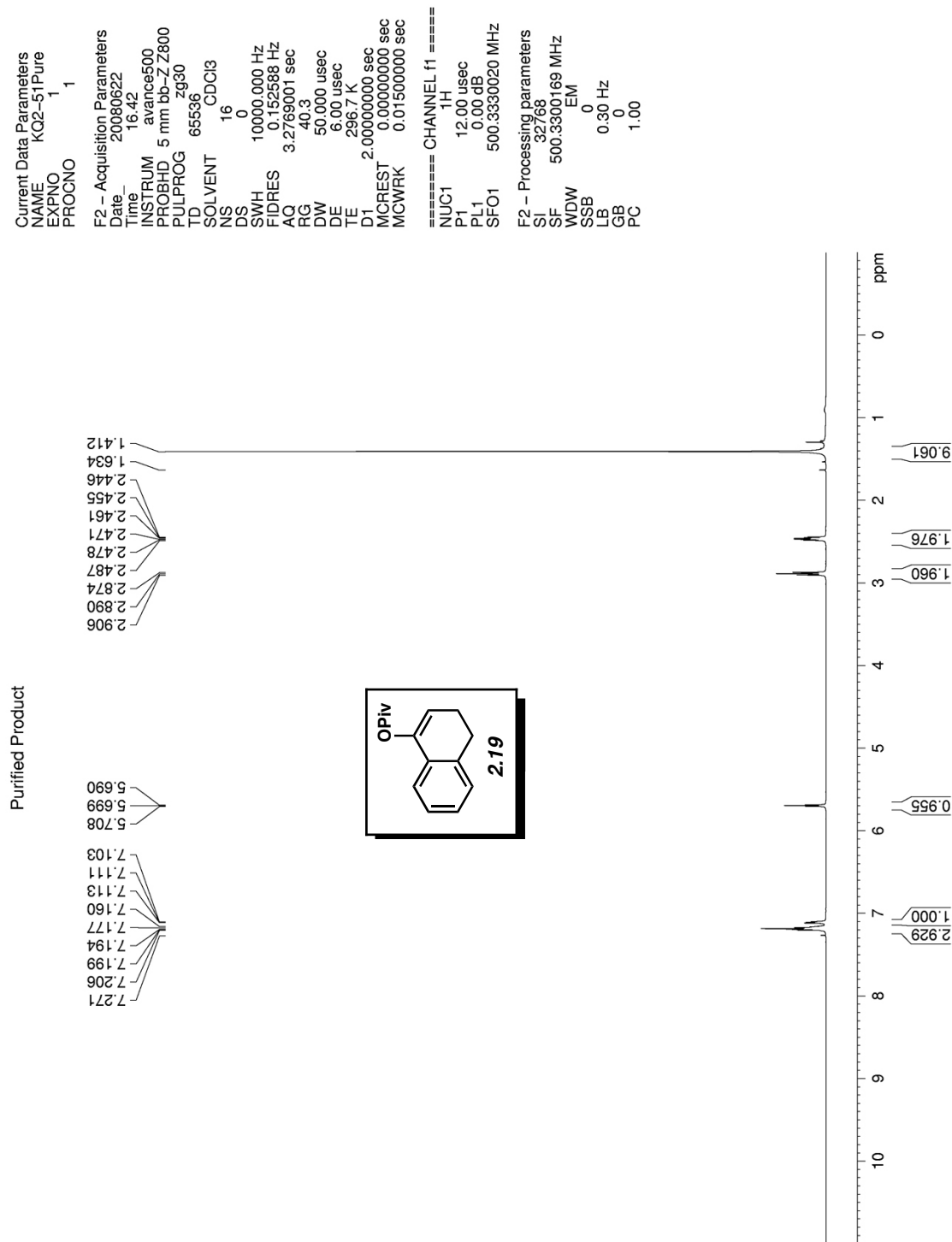


Figure A1.22 ¹H NMR (500 MHz, CDCl₃) of compound 2.19.

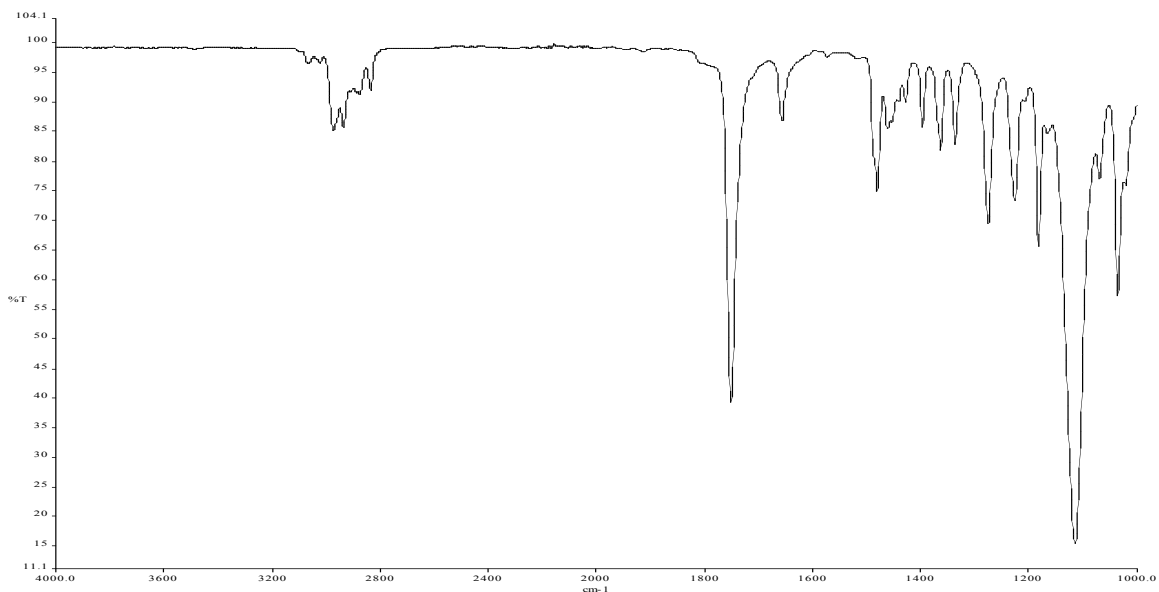


Figure A1.23 Infrared spectrum of compound **2.19**.

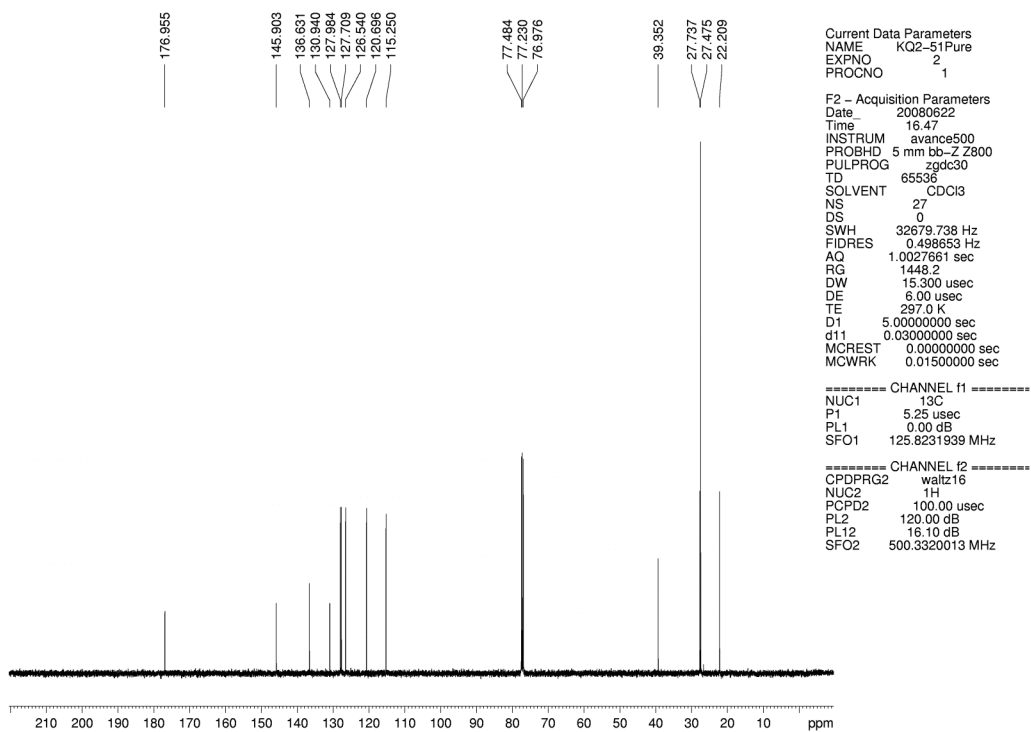


Figure A1.24 ¹³C NMR (125 MHz, CDCl₃) of compound **2.19**.

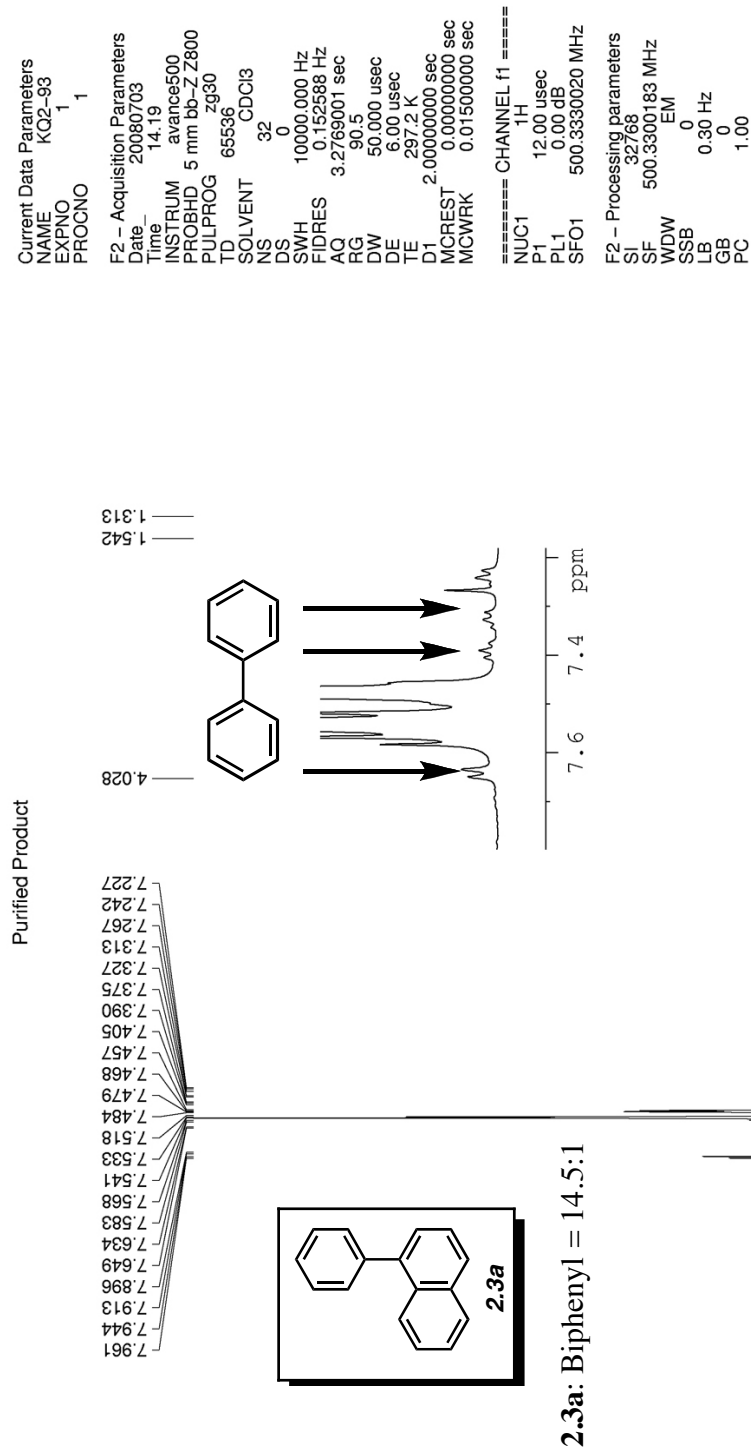


Figure A1.25 ¹H NMR (500 MHz, CDCl₃) of compound **2.3a**.

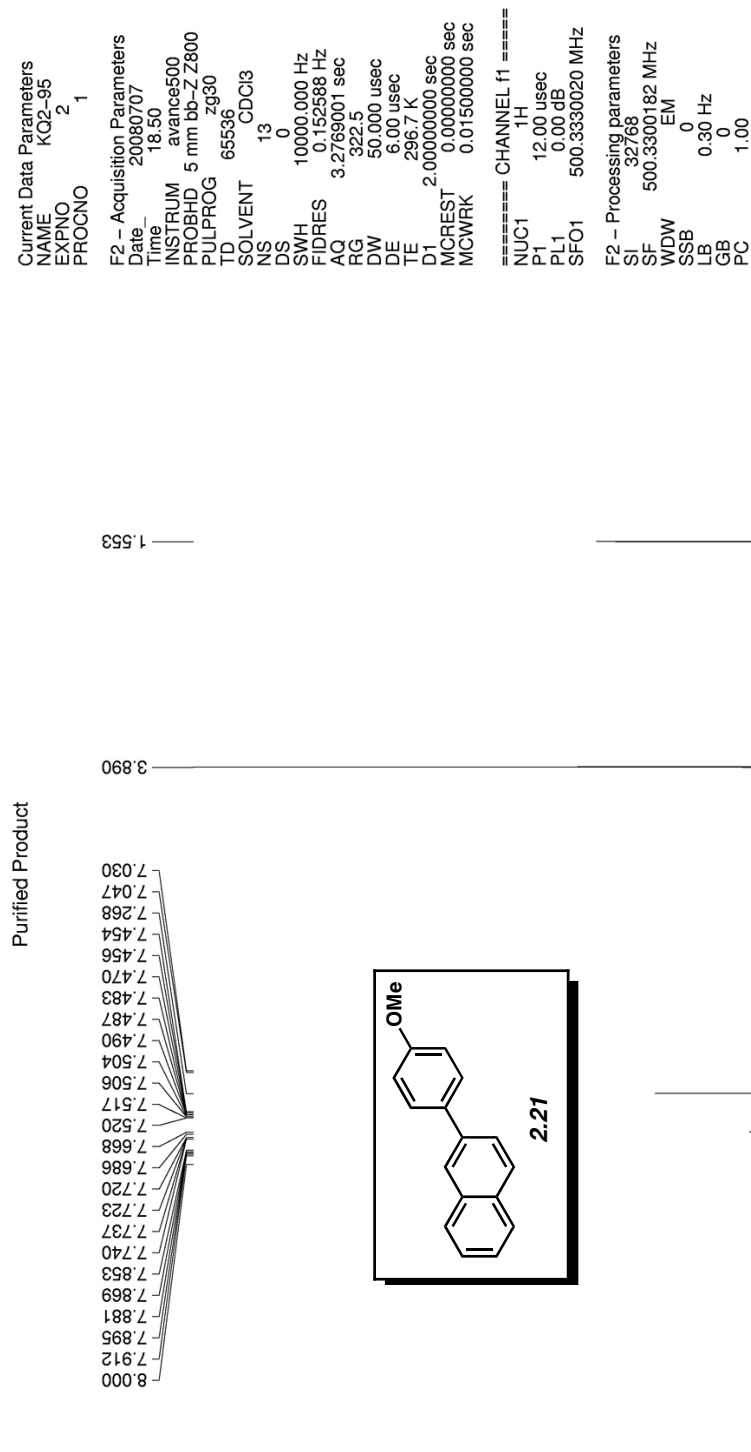


Figure A1.26 ¹H NMR (500 MHz, CDCl₃) of compound 2.21.

default proton parameters

Current Data Parameters
NAME x12-117
EXPNO 1
PROCNO 1

F2 - Acquisition Parameters
Date_ 20080725
Time 18.46
INSTRUM avance500
PROBHD 5 mm bb-ZZ800
PULPROG zg30
TD 32768
SOLVENT CDCI3
NS 8
DS 0
SWH 10000.000 Hz
FIDRES 0.305176 Hz
AQ 1.6385000 sec
RG 143.7
DW 50.000 usec
DE 6.00 usec
TE 296.5 K
D1 2.0000000 sec
MCREST 0.0000000 sec
MCWRK 0.01500000 sec

===== CHANNEL f1 =====
NUC1 1H
P1 12.00 usec
PL1 0.00 dB
SFO1 500.3330020 MHz

F2 - Processing parameters
SI 32768
SF 500.3300220 MHz
WDW EM
SSB 0
LB 0.30 Hz
GB 0
PC 1.00

8.635
8.107
8.104
8.089
8.086
8.063
8.021
8.004
7.931
7.914
7.816
7.813
7.799
7.795
7.738
7.723
7.525
7.510
7.494
7.434
7.420
7.405
7.259

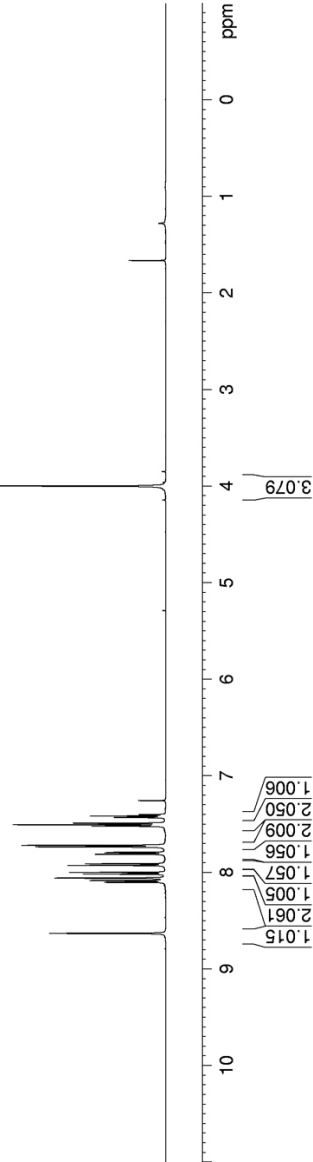
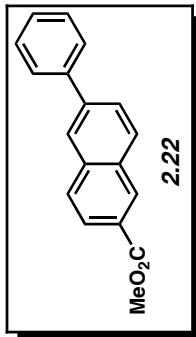


Figure A1.27 ¹H NMR (500 MHz, CDCl₃) of compound 2.22.

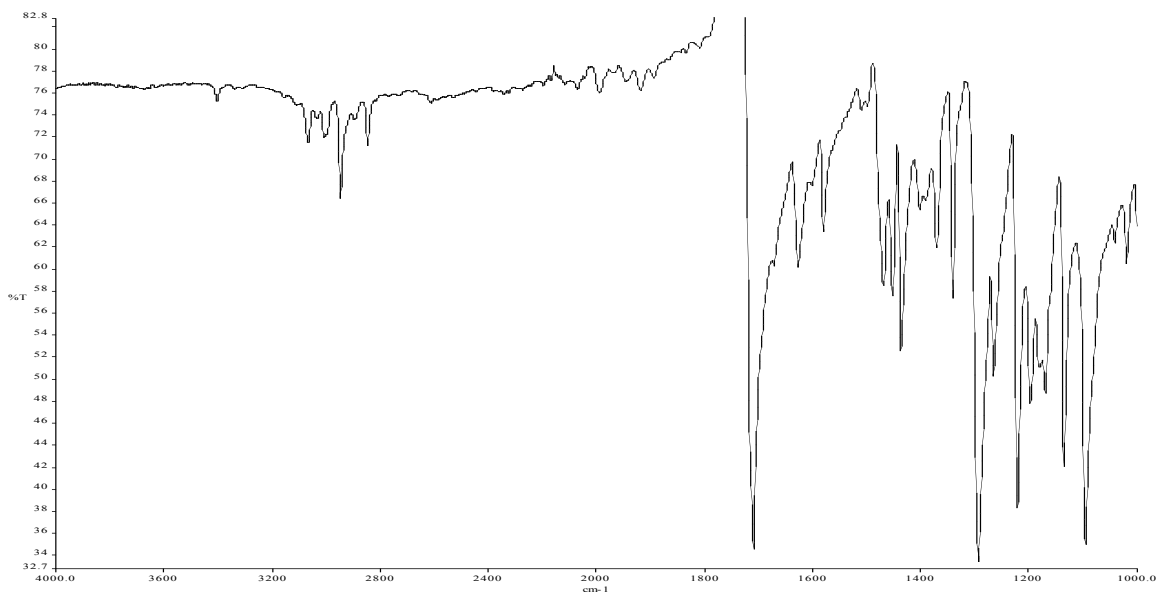


Figure A1.28 Infrared spectrum of compound **2.22**.

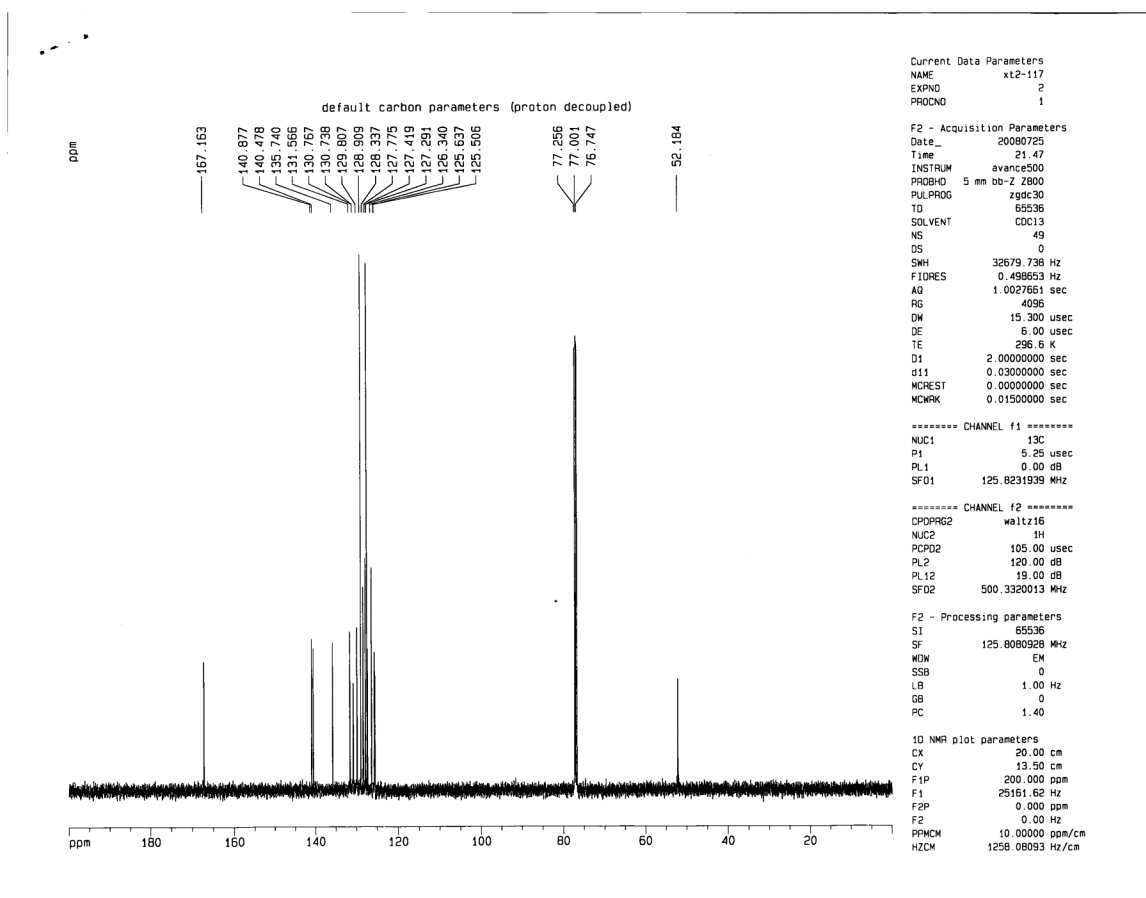


Figure A1.29 ^{13}C NMR (125 MHz, CDCl_3) of compound **2.22**.

Current Data Parameters
 NAME KQ2-117
 EXPNO 1
 PROCNO 1

F2 - Acquisition Parameters
 Date_ 20080720
 Time_ 17.21
 INSTRUM avance500
 PROBHD 5 mm bb-ZZ800
 PULPROG zg30
 TD 65536
 SOLVENT CDCl3
 NS 10
 DS 0
 SWH 10000.000 Hz
 FIDRES 0.152588 Hz
 AQ 3.2769001 sec
 RG 90.5
 DW 50.000 usec
 DE 6.00 usec
 TE 296.4 K
 D1 2.0000000 sec
 MCREST 0.0000000 sec
 MCWRK 0.01500000 sec

===== CHANNEL f1 =====
 NUC1 1H
 P1 12.00 usec
 PL1 0.00 dB
 SFO1 500.3330020 MHz

F2 - Processing parameters
 SI 32768
 SF 500.3300220 MHz
 WDW EM
 SSB 0
 LB 0.30 Hz
 GB 0
 PC 1.00

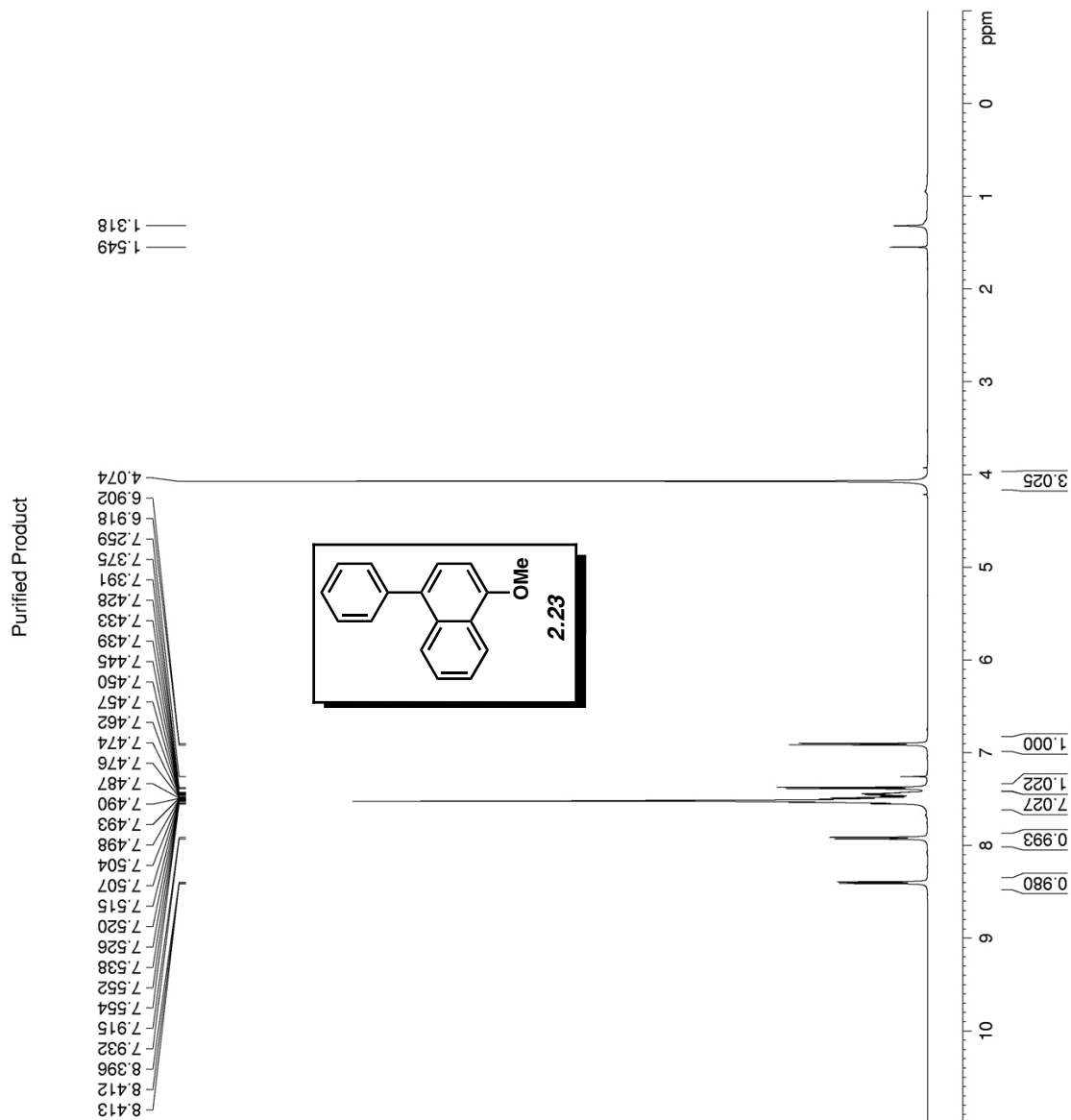


Figure A1. ^1H NMR (500 MHz, CDCl_3) of compound 2.23.

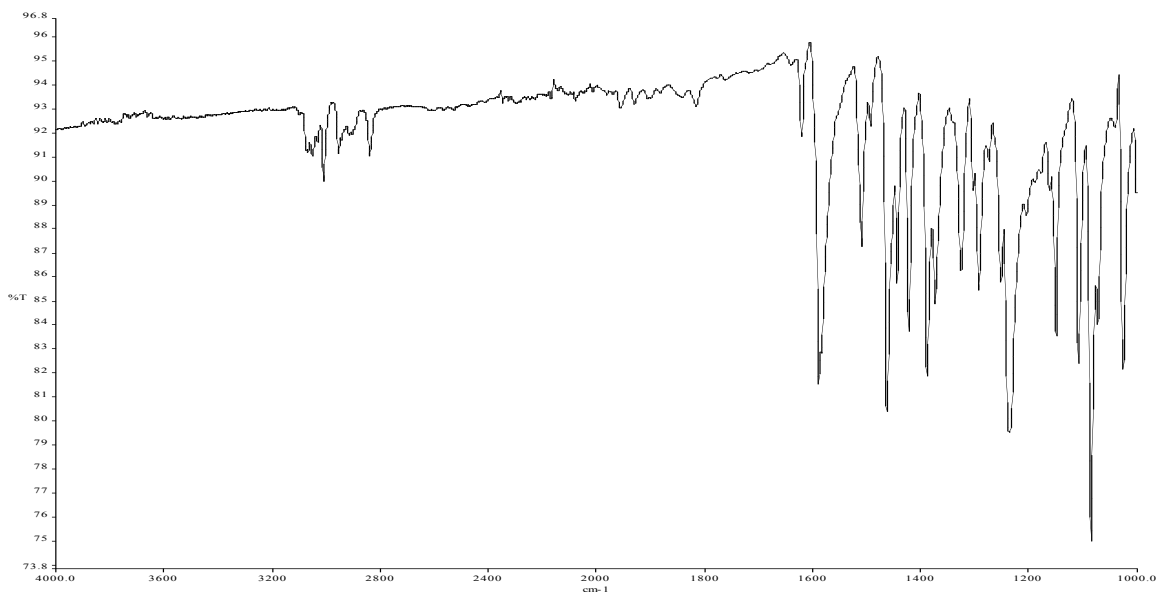


Figure A1.31 Infrared spectrum of compound **2.23**.

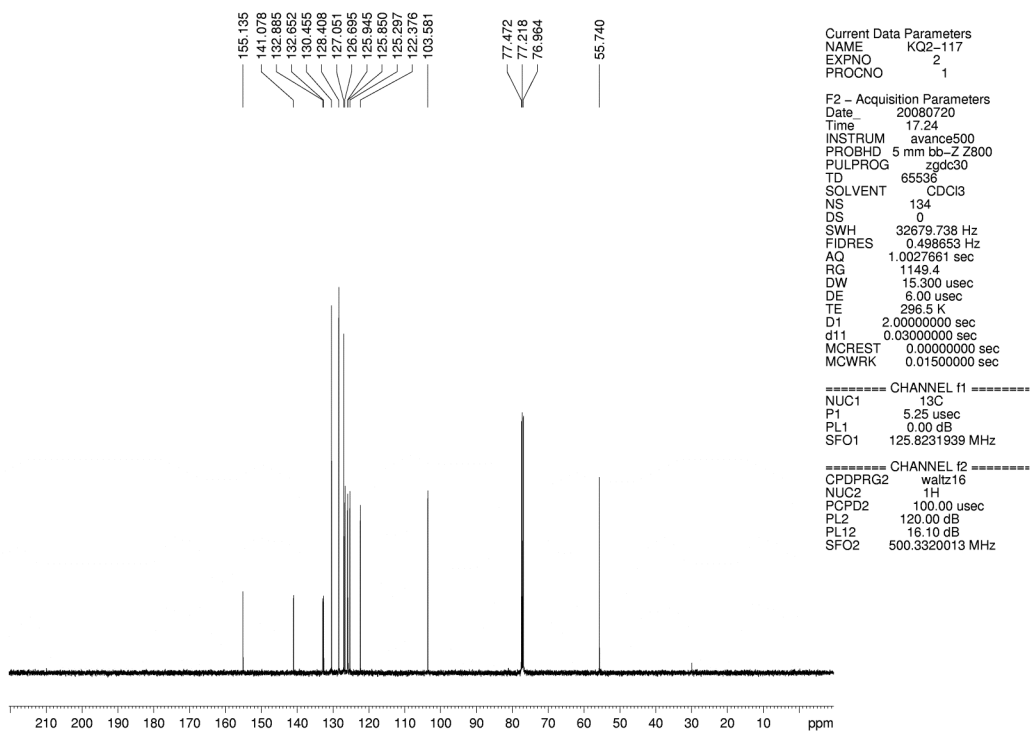


Figure A1.32 ^{13}C NMR (125 MHz, CDCl_3) of compound **2.23**.

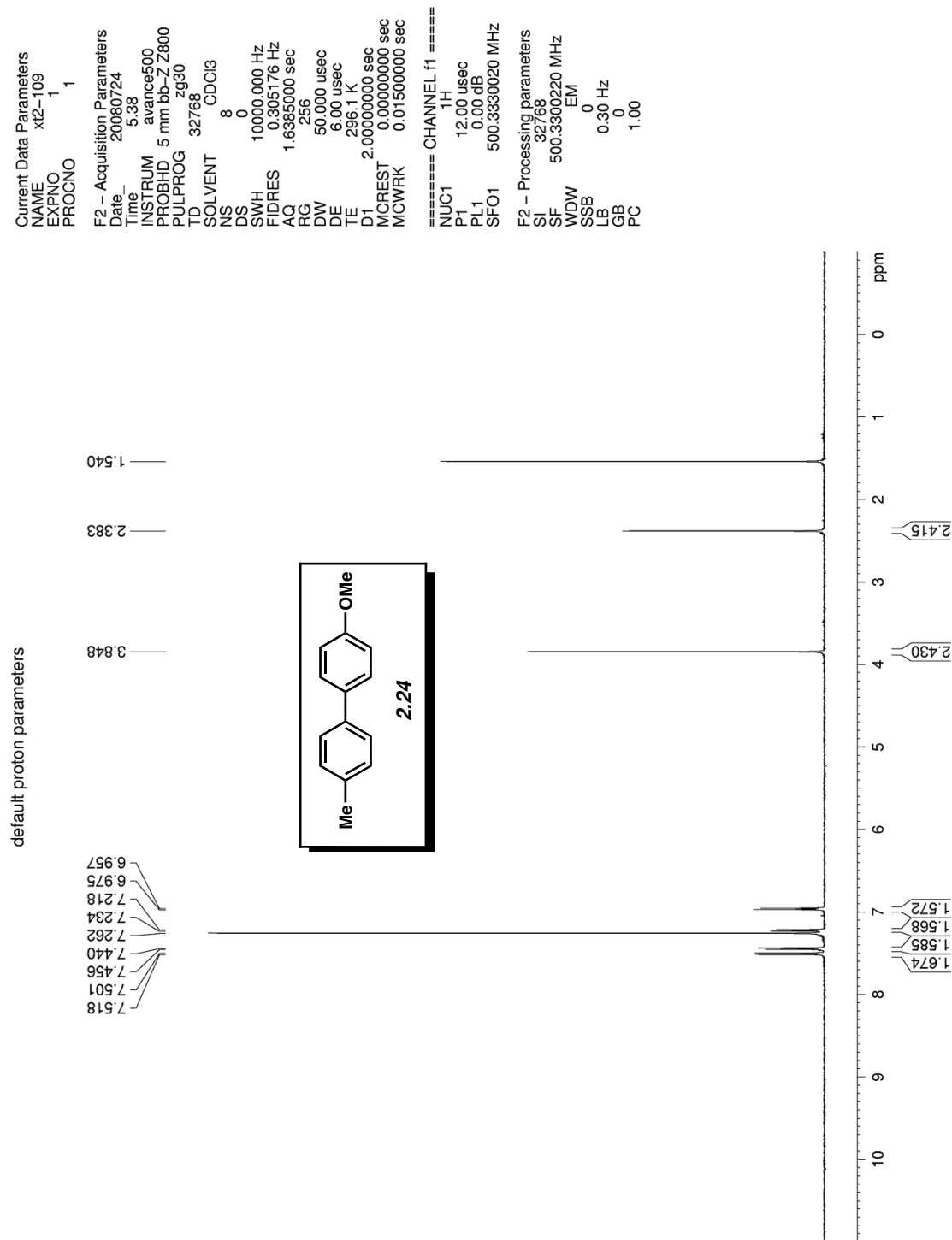


Figure A1.33 ¹H NMR (500 MHz, CDCl₃) of compound 2.24.

Current Data Parameters
 NAME x12-115
 EXPNO 1
 PROCNO 1

F2 - Acquisition Parameters
 Date_ 20080725
 Time_ 18.37
 INSTRUM avance500
 PROBHD 5 mm bb-Z800
 PULPROG zg30
 TD 65536
 SOLVENT CDCl3
 NS 8
 DS 0
 SWH 10000.000 Hz
 FIDRES 0.152588 Hz
 AQ 3.2769001 sec
 RG 90.5
 DW 50.000 usec
 DE 6.00 usec
 TE 296.5 K
 D1 2.0000000 sec
 MCREST 0.0000000 sec
 MCWRK 0.01500000 sec

===== CHANNEL f1 =====
 NUC1 1H
 P1 12.00 usec
 PL1 0.00 dB
 SFO1 500.3330020 MHz

F2 - Processing parameters
 SI 32768
 SF 500.3300220 MHz
 WDW EM
 SSB 0
 LB 0.30 Hz
 GB 0
 PC 1.00

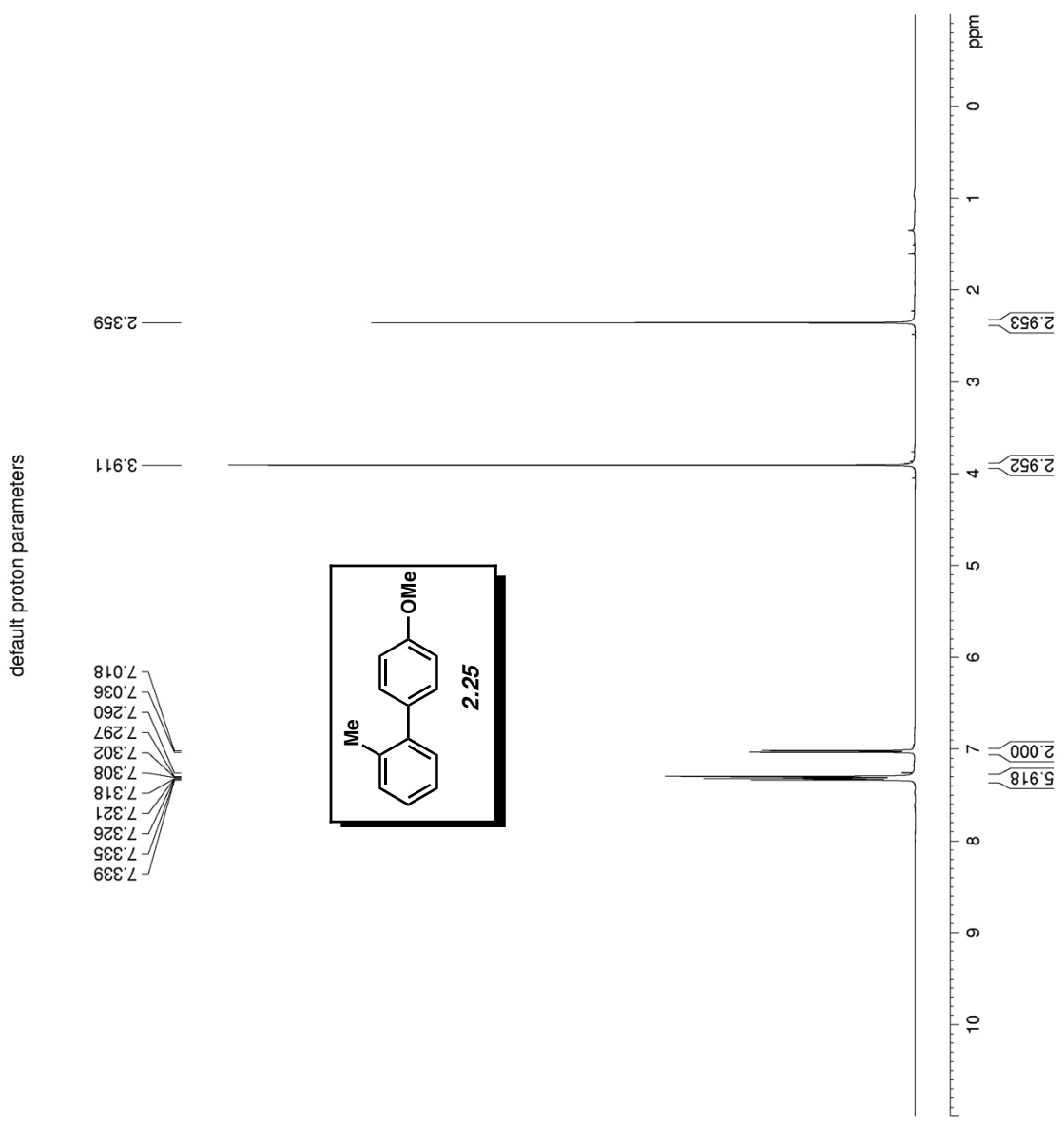


Figure A1.34 ¹H NMR (500 MHz, CDCl₃) of compound 2.25.

Current Data Parameters
 NAME xt2-25
 EXPNO 1
 PROCNO 1

F2 - Acquisition Parameters
 Date_ 20080619
 Time_ 12.17
 INSTRUM avance500
 PROBHD 5 mm bb-Z800
 PULPROG zg30
 TD 65536
 SOLVENT CDCl3
 NS 8
 DS 0
 SWH 10000.000 Hz
 FIDRES 0.152588 Hz
 AQ 3.2769001 sec
 RG 203.2
 DW 50.000 usec
 DE 6.00 usec
 TE 296.2 K
 D1 2.0000000 sec
 MCREST 0.0000000 sec
 MCWRK 0.01500000 sec

===== CHANNEL f1 =====
 NUC1 1H
 P1 12.00 usec
 PL1 0.00 dB
 SFO1 500.3330020 MHz

F2 - Processing parameters
 SI 32768
 SF 500.3300221 MHz
 WDW EM
 SSB 0
 LB 0.30 Hz
 GB 0
 PC 1.00

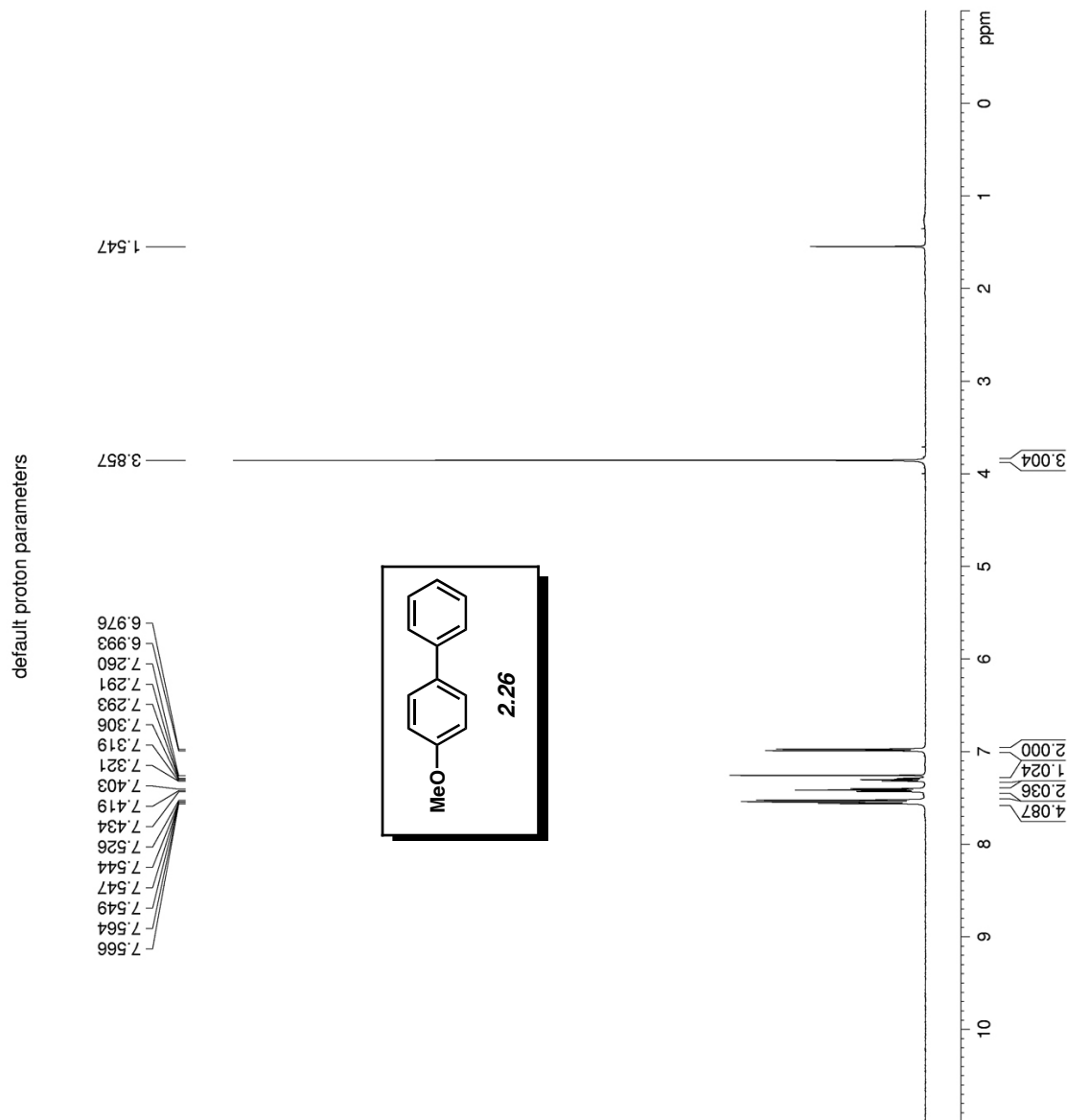
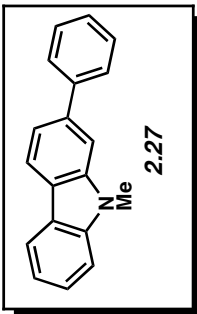


Figure A1.35 ¹H NMR (500 MHz, CDCl₃) of compound 2.26.

default proton parameters

8.209
8.192
8.175
8.158
8.141
8.124
8.107
8.090
8.073
8.056
8.039
8.022
8.005
7.988
7.971
7.954
7.937
7.920
7.903
7.886
7.869
7.852
7.835
7.818
7.801
7.784
7.767
7.750
7.733
7.716
7.699
7.682
7.665
7.648
7.631
7.614
7.597
7.580
7.563
7.546
7.529
7.512
7.495
7.478
7.461
7.444
7.427
7.410
7.393
7.376
7.359
7.342
7.325
7.308
7.291
7.274
7.257
7.240
7.223
7.206
7.189
7.172
7.155
7.138
7.121
7.104
7.087
7.070
7.053
7.036
7.019
7.002
6.985
6.968
6.951
6.934
6.917
6.900
6.883
6.866
6.849
6.832
6.815
6.798
6.781
6.764
6.747
6.730
6.713
6.696
6.679
6.662
6.645
6.628
6.611
6.594
6.577
6.560
6.543
6.526
6.509
6.492
6.475
6.458
6.441
6.424
6.407
6.390
6.373
6.356
6.339
6.322
6.305
6.288
6.271
6.254
6.237
6.220
6.203
6.186
6.169
6.152
6.135
6.118
6.101
6.084
6.067
6.050
6.033
6.016
5.999
5.982
5.965
5.948
5.931
5.914
5.897
5.880
5.863
5.846
5.829
5.812
5.795
5.778
5.761
5.744
5.727
5.710
5.693
5.676
5.659
5.642
5.625
5.608
5.591
5.574
5.557
5.540
5.523
5.506
5.489
5.472
5.455
5.438
5.421
5.404
5.387
5.370
5.353
5.336
5.319
5.302
5.285
5.268
5.251
5.234
5.217
5.200
5.183
5.166
5.149
5.132
5.115
5.098
5.081
5.064
5.047
5.030
5.013
4.996
4.979
4.962
4.945
4.928
4.911
4.894
4.877
4.860
4.843
4.826
4.809
4.792
4.775
4.758
4.741
4.724
4.707
4.690
4.673
4.656
4.639
4.622
4.605
4.588
4.571
4.554
4.537
4.520
4.503
4.486
4.469
4.452
4.435
4.418
4.401
4.384
4.367
4.350
4.333
4.316
4.299
4.282
4.265
4.248
4.231
4.214
4.197
4.180
4.163
4.146
4.129
4.112
4.095
4.078
4.061
4.044
4.027
4.010
3.993
3.976
3.959
3.942
3.925
3.908
3.891
3.874
3.857
3.840
3.823
3.806
3.789
3.772
3.755
3.738
3.721
3.704
3.687
3.670
3.653
3.636
3.619
3.602
3.585
3.568
3.551
3.534
3.517
3.500
3.483
3.466
3.449
3.432
3.415
3.398
3.381
3.364
3.347
3.330
3.313
3.296
3.279
3.262
3.245
3.228
3.211
3.194
3.177
3.160
3.143
3.126
3.109
3.092
3.075
3.058
3.041
3.024
3.007
2.990
2.973
2.956
2.939
2.922
2.905
2.888
2.871
2.854
2.837
2.820
2.803
2.786
2.769
2.752
2.735
2.718
2.701
2.684
2.667
2.650
2.633
2.616
2.599
2.582
2.565
2.548
2.531
2.514
2.497
2.480
2.463
2.446
2.429
2.412
2.395
2.378
2.361
2.344
2.327
2.310
2.293
2.276
2.259
2.242
2.225
2.208
2.191
2.174
2.157
2.140
2.123
2.106
2.089
2.072
2.055
2.038
2.021
2.004
1.987
1.970
1.953
1.936
1.919
1.902
1.885
1.868
1.851
1.834
1.817
1.800
1.783
1.766
1.749
1.732
1.715
1.698
1.681
1.664
1.647
1.630
1.613
1.596
1.579
1.562
1.545
1.528
1.511
1.494
1.477
1.460
1.443
1.426
1.409
1.392
1.375
1.358
1.341
1.324
1.307
1.290
1.273
1.256
1.239
1.222
1.205
1.188
1.171
1.154
1.137
1.120
1.103
1.086
1.069
1.052
1.035
1.018
1.001
0.984
0.967
0.950
0.933
0.916
0.899
0.882
0.865
0.848
0.831
0.814
0.797
0.780
0.763
0.746
0.729
0.712
0.695
0.678
0.661
0.644
0.627
0.610
0.593
0.576
0.559
0.542
0.525
0.508
0.491
0.474
0.457
0.440
0.423
0.406
0.389
0.372
0.355
0.338
0.321
0.304
0.287
0.270
0.253
0.236
0.219
0.202
0.185
0.168
0.151
0.134
0.117
0.100
0.083
0.066
0.049
0.032
0.015
-0.002
-0.019
-0.036
-0.053
-0.070
-0.087
-0.104
-0.121
-0.138
-0.155
-0.172
-0.189
-0.206
-0.223
-0.240
-0.257
-0.274
-0.291
-0.308
-0.325
-0.342
-0.359
-0.376
-0.393
-0.410
-0.427
-0.444
-0.461
-0.478
-0.495
-0.512
-0.529
-0.546
-0.563
-0.580
-0.597
-0.614
-0.631
-0.648
-0.665
-0.682
-0.699
-0.716
-0.733
-0.750
-0.767
-0.784
-0.801
-0.818
-0.835
-0.852
-0.869
-0.886
-0.903
-0.920
-0.937
-0.954
-0.971
-0.988
-1.005
-1.022
-1.039
-1.056
-1.073
-1.090
-1.107
-1.124
-1.141
-1.158
-1.175
-1.192
-1.209
-1.226
-1.243
-1.260
-1.277
-1.294
-1.311
-1.328
-1.345
-1.362
-1.379
-1.396
-1.413
-1.430
-1.447
-1.464
-1.481
-1.498
-1.515
-1.532
-1.549
-1.566
-1.583
-1.600
-1.617
-1.634
-1.651
-1.668
-1.685
-1.702
-1.719
-1.736
-1.753
-1.770
-1.787
-1.804
-1.821
-1.838
-1.855
-1.872
-1.889
-1.906
-1.923
-1.940
-1.957
-1.974
-1.991
-2.008
-2.025
-2.042
-2.059
-2.076
-2.093
-2.110
-2.127
-2.144
-2.161
-2.178
-2.195
-2.212
-2.229
-2.246
-2.263
-2.280
-2.297
-2.314
-2.331
-2.348
-2.365
-2.382
-2.399
-2.416
-2.433
-2.450
-2.467
-2.484
-2.501
-2.518
-2.535
-2.552
-2.569
-2.586
-2.603
-2.620
-2.637
-2.654
-2.671
-2.688
-2.705
-2.722
-2.739
-2.756
-2.773
-2.790
-2.807
-2.824
-2.841
-2.858
-2.875
-2.892
-2.909
-2.926
-2.943
-2.960
-2.977
-2.994
-3.011
-3.028
-3.045
-3.062
-3.079
-3.096
-3.113
-3.130
-3.147
-3.164
-3.181
-3.198
-3.215
-3.232
-3.249
-3.266
-3.283
-3.300
-3.317
-3.334
-3.351
-3.368
-3.385
-3.402
-3.419
-3.436
-3.453
-3.470
-3.487
-3.504
-3.521
-3.538
-3.555
-3.572
-3.589
-3.606
-3.623
-3.640
-3.657
-3.674
-3.691
-3.708
-3.725
-3.742
-3.759
-3.776
-3.793
-3.810
-3.827
-3.844
-3.861
-3.878
-3.895
-3.912
-3.929
-3.946
-3.963
-3.980
-3.997
-4.014
-4.031
-4.048
-4.065
-4.082
-4.099
-4.116
-4.133
-4.150
-4.167
-4.184
-4.201
-4.218
-4.235
-4.252
-4.269
-4.286
-4.303
-4.320
-4.337
-4.354
-4.371
-4.388
-4.405
-4.422
-4.439
-4.456
-4.473
-4.490
-4.507
-4.524
-4.541
-4.558
-4.575
-4.592
-4.609
-4.626
-4.643
-4.660
-4.677
-4.694
-4.711
-4.728
-4.745
-4.762
-4.779
-4.796
-4.813
-4.830
-4.847
-4.864
-4.881
-4.898
-4.915
-4.932
-4.949
-4.966
-4.983
-5.000
-5.017
-5.034
-5.051
-5.068
-5.085
-5.102
-5.119
-5.136
-5.153
-5.170
-5.187
-5.204
-5.221
-5.238
-5.255
-5.272
-5.289
-5.306
-5.323
-5.340
-5.357
-5.374
-5.391
-5.408
-5.425
-5.442
-5.459
-5.476
-5.493
-5.510
-5.527
-5.544
-5.561
-5.578
-5.595
-5.612
-5.629
-5.646
-5.663
-5.680
-5.697
-5.714
-5.731
-5.748
-5.765
-5.782
-5.799
-5.816
-5.833
-5.850
-5.867
-5.884
-5.901
-5.918
-5.935
-5.952
-5.969
-5.986
-6.003
-6.020
-6.037
-6.054
-6.071
-6.088
-6.105
-6.122
-6.139
-6.156
-6.173
-6.190
-6.207
-6.224
-6.241
-6.258
-6.275
-6.292
-6.309
-6.326
-6.343
-6.360
-6.377
-6.394
-6.411
-6.428
-6.445
-6.462
-6.479
-6.496
-6.513
-6.530
-6.547
-6.564
-6.581
-6.598
-6.615
-6.632
-6.649
-6.666
-6.683
-6.700
-6.717
-6.734
-6.751
-6.768
-6.785
-6.802
-6.819
-6.836
-6.853
-6.870
-6.887
-6.904
-6.921
-6.938
-6.955
-6.972
-6.989
-7.006
-7.023
-7.040
-7.057
-7.074
-7.091
-7.108
-7.125
-7.142
-7.159
-7.176
-7.193
-7.210
-7.227
-7.244
-7.261
-7.278
-7.295
-7.312
-7.329
-7.346
-7.363
-7.380
-7.397
-7.414
-7.431
-7.448
-7.465
-7.482
-7.499
-7.516
-7.533
-7.550
-7.567
-7.584
-7.601
-7.618
-7.635
-7.652
-7.669
-7.686
-7.703
-7.720
-7.737
-7.754
-7.771
-7.788
-7.805
-7.822
-7.839
-7.856
-7.873
-7.890
-7.907
-7.924
-7.941
-7.958
-7.975
-7.992
-8.009
-8.026
-8.043
-8.060
-8.077
-8.094
-8.111
-8.128
-8.145
-8.162
-8.179
-8.196
-8.213
-8.230
-8.247
-8.264
-8.281
-8.298
-8.315
-8.332
-8.349
-8.366
-8.383
-8.400
-8.417
-8.434
-8.451
-8.468
-8.485
-8.502
-8.519
-8.536
-8.553
-8.570
-8.587
-8.604
-8.621
-8.638
-8.655
-8.672
-8.689
-8.706
-8.723
-8.740
-8.757
-8.774
-8.791
-8.808
-8.825
-8.842
-8.859
-8.876
-8.893
-8.910
-8.927
-8.944
-8.961
-8.978
-8.995
-9.012
-9.029
-9.046
-9.063
-9.080
-9.097
-9.114
-9.131
-9.148
-9.165
-9.182
-9.199
-9.216
-9.233
-9.250
-9.267
-9.284
-9.301
-9.318
-9.335
-9.352
-9.369
-9.386
-9.403
-9.420
-9.437
-9.454
-9.471
-9.488
-9.505
-9.522
-9.539
-9.556
-9.573
-9.590
-9.607
-9.624
-9.641
-9.658
-9.675
-9.692
-9.709
-9.726
-9.743
-9.760
-9.777
-9.794
-9.811
-9.828
-9.845
-9.862
-9.879
-9.896
-9.913
-9.930
-9.947
-9.964
-9.981
-10.000



Current Data Parameters
NAME x12-116
EXPNO 1
PROCNO 1
F2 - Acquisition Parameters
Date_ 20080725
Time_ 18.41
INSTRUM avance500
PROBHD 5 mm bb-Z800
PULPROG zg30
TD 65536
SOLVENT CDCI3
NS 4
DS 0
SWH 10000.000 Hz
FIDRES 0.152588 Hz
AQ 3.2769001 sec
RG 114
DW 50.000 usec
DE 6.00 usec
TE 296.5 K
D1 2.0000000 sec
MCREST 0.0000000 sec
MCWRK 0.01500000 sec
===== CHANNEL f1 =====
NUC1 1H
P1 12.00 usec
PL1 0.00 dB
SFO1 500.3330020 MHz
F2 - Processing parameters
SI 32768
SF 500.3300220 MHz
WDW EM
SSB 0
LB 0.30 Hz
GB 0
PC 1.00

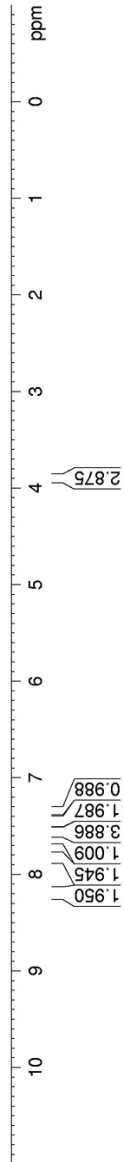


Figure A1.36 ¹H NMR (500 MHz, CDCl₃) of compound 2.27.

Current Data Parameters
 NAME KQ2-59Pure
 EXPNO 1
 PROCNO 1

F2 - Acquisition Parameters
 Date_ 20080620
 Time_ 8.30
 INSTRUM avance500
 PROBHD 5 mm bb-Z800
 PULPROG zg30
 TD 65536
 SOLVENT CDCl3
 NS 12
 DS 0
 SWH 10000.000 Hz
 FIDRES 0.152588 Hz
 AQ 3.2769001 sec
 RG 90.5
 DW 50.000 usec
 DE 6.00 usec
 TE 296.2 K
 D1 2.0000000 sec
 MCREST 0.0000000 sec
 MCWRK 0.01500000 sec

===== CHANNEL f1 =====
 NUC1 1H
 P1 12.00 usec
 PL1 0.00 dB
 SFO1 500.3330020 MHz

F2 - Processing parameters
 SI 32768
 SF 500.3300171 MHz
 WDW EM
 SSB 0
 LB 0.30 Hz
 GB 0
 PC 1.00

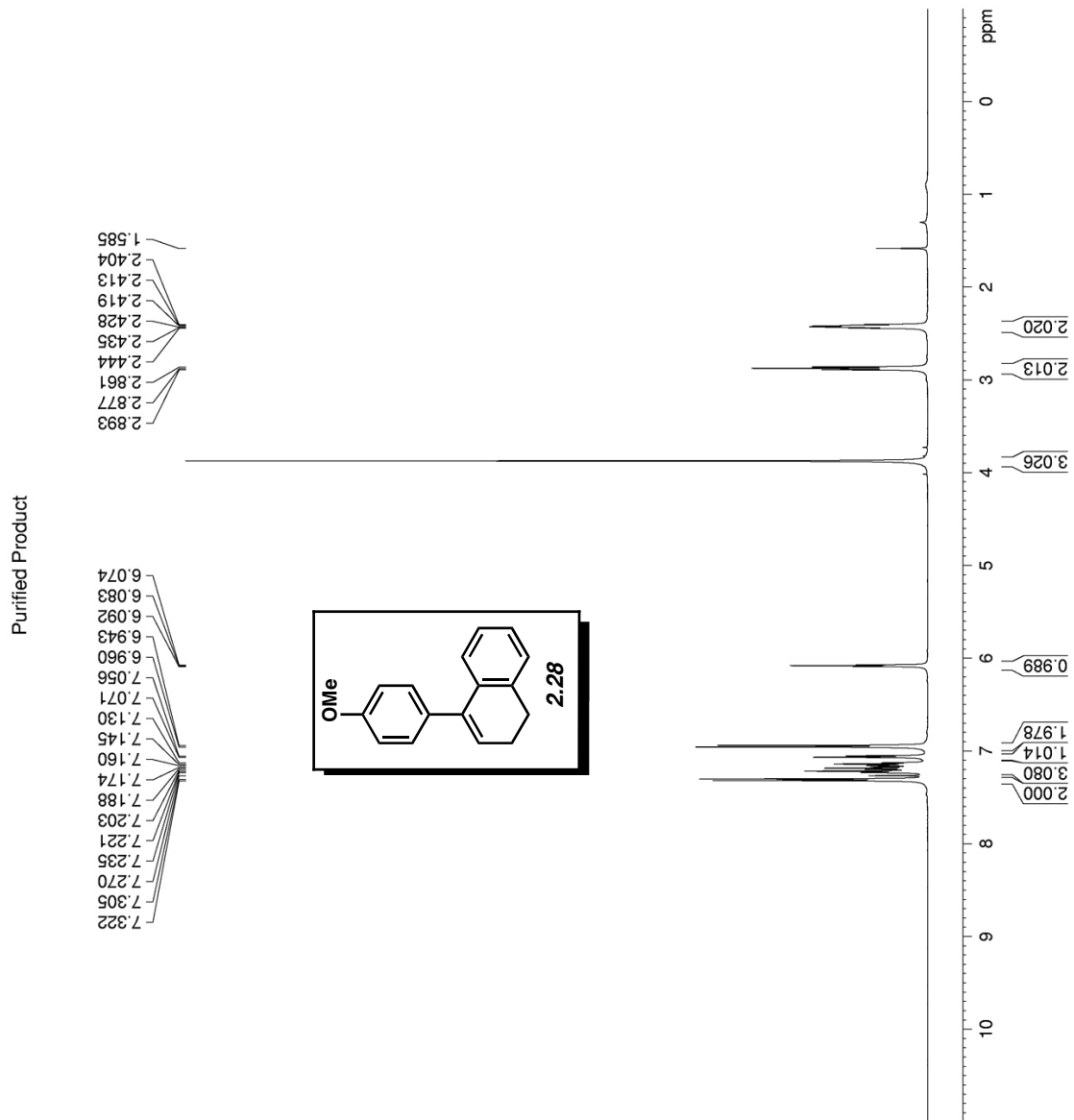


Figure A1.37 ¹H NMR (500 MHz, CDCl₃) of compound 2.28.

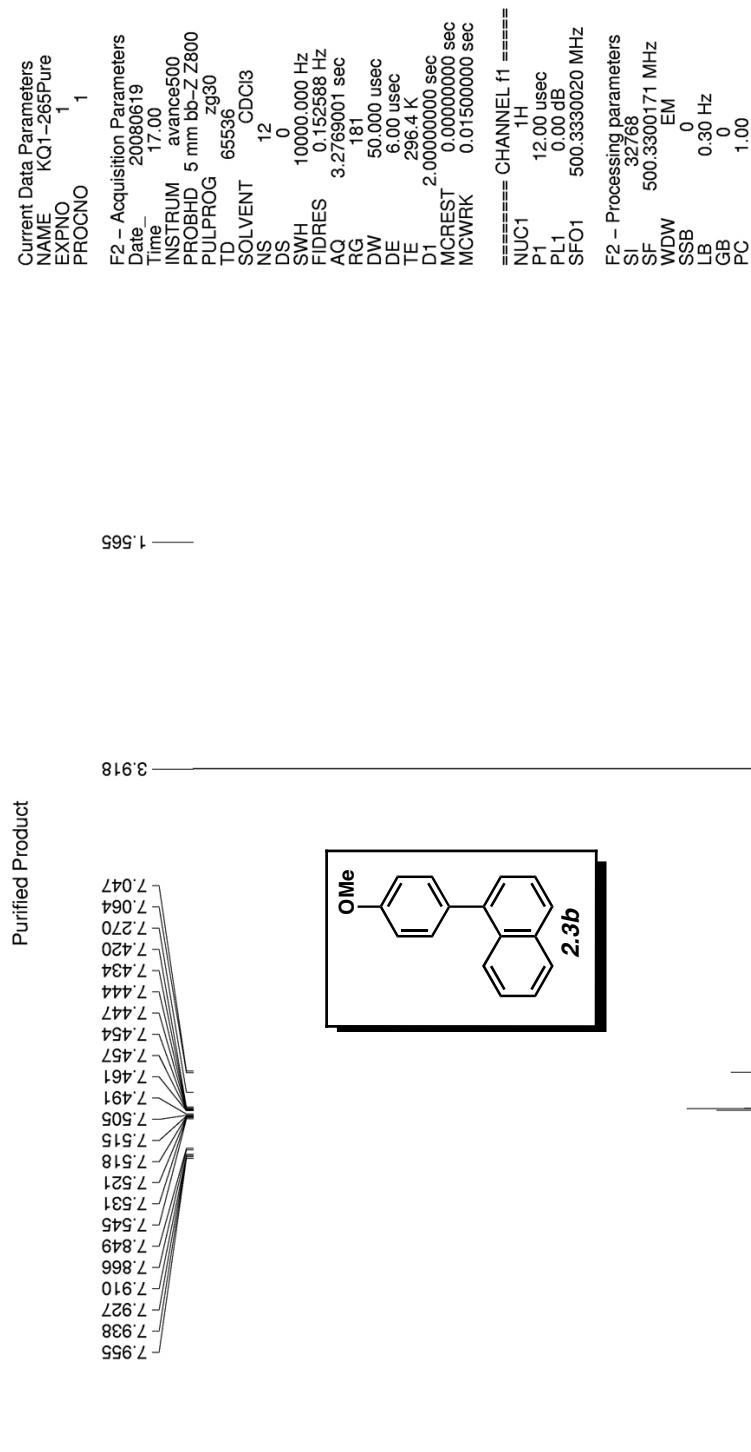


Figure A1.38 ¹H NMR (500 MHz, CDCl₃) of compound **2.3b**.

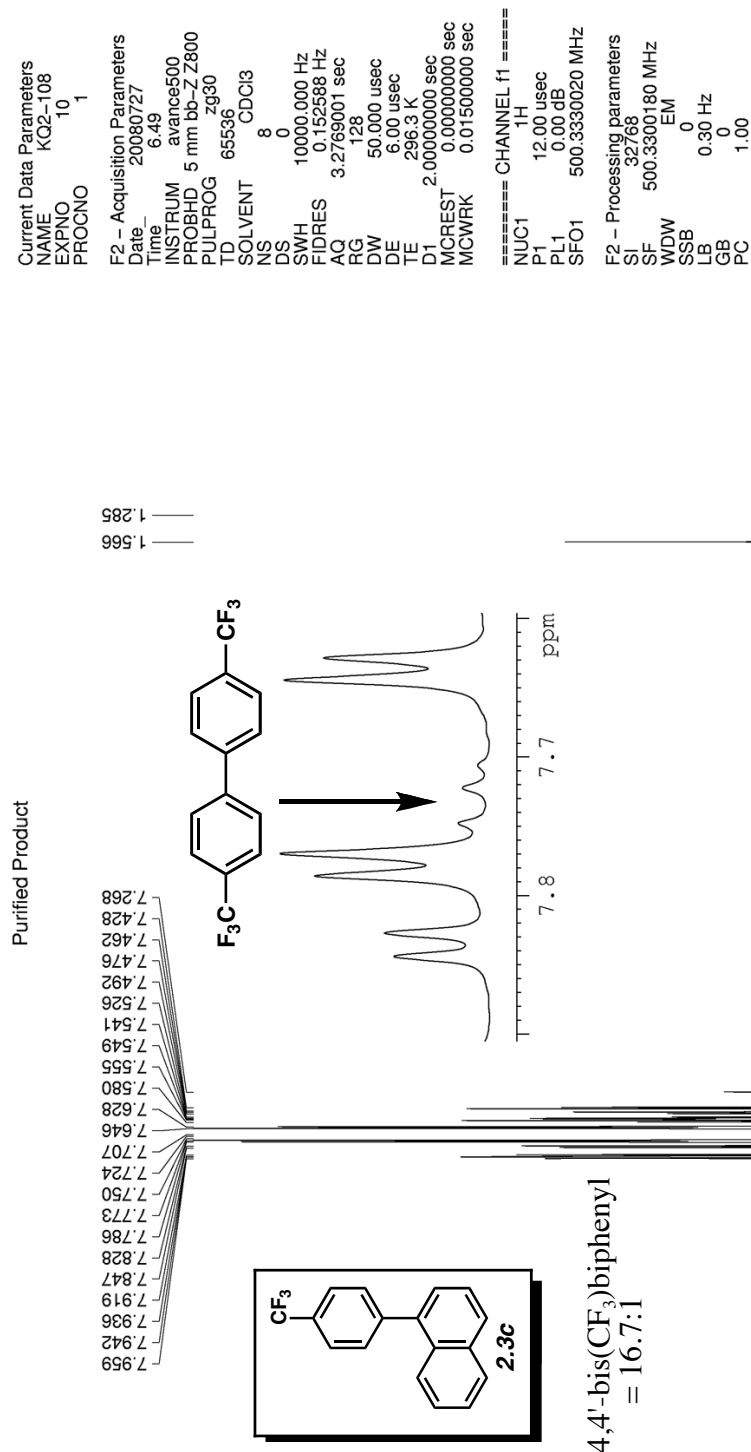


Figure A1.39 ¹H NMR (500 MHz, CDCl₃) of compound **2.3c**.

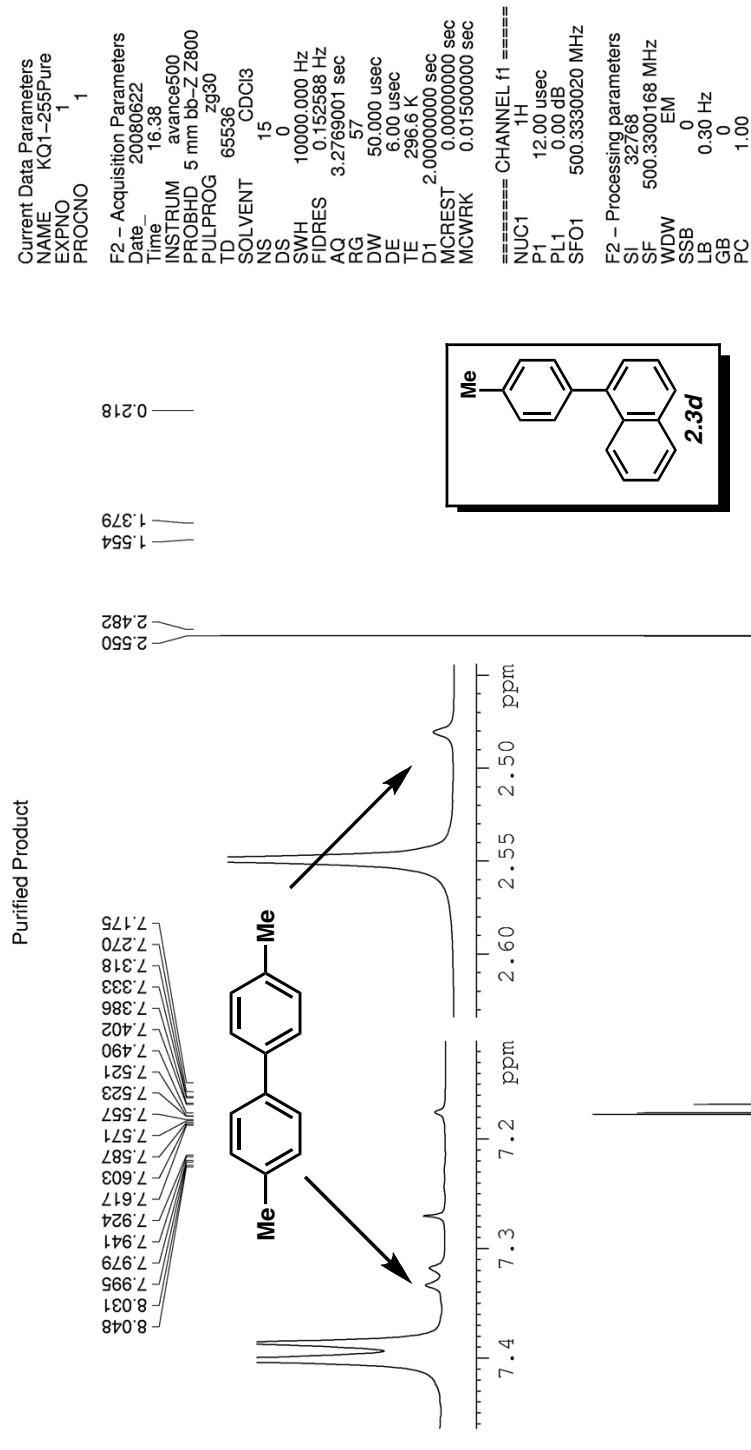


Figure A1.40 ¹H NMR (500 MHz, CDCl₃) of compound **2.3d**.

Current Data Parameters
 NAME XT1-144Purified
 EXPNO 1
 PROCNO 1

F2 - Acquisition Parameters
 Date 20080415
 Time 14.09
 INSTRUM avance500
 PROBHD 5 mm bb-Z800
 PULPROG zg30
 TD 65536
 SOLVENT CDCl3
 NS 13
 DS 0
 SWH 10000.000 Hz
 FIDRES 0.152588 Hz
 AQC 3.2769001 sec
 RG 114
 DW 50.000 usec
 DE 6.00 usec
 TE 296.0 K
 D1 2.0000000 sec
 MCREST 0.0000000 sec
 MCWRK 0.01500000 sec

===== CHANNEL f1 =====
 NUC1 1H
 P1 12.00 usec
 PL1 0.00 dB
 SFO1 500.3330020 MHz

F2 - Processing parameters
 SI 32768
 SF 500.3300170 MHz
 WDW EM
 SSB 0
 LB 0.30 Hz
 GB 0
 PC 1.00

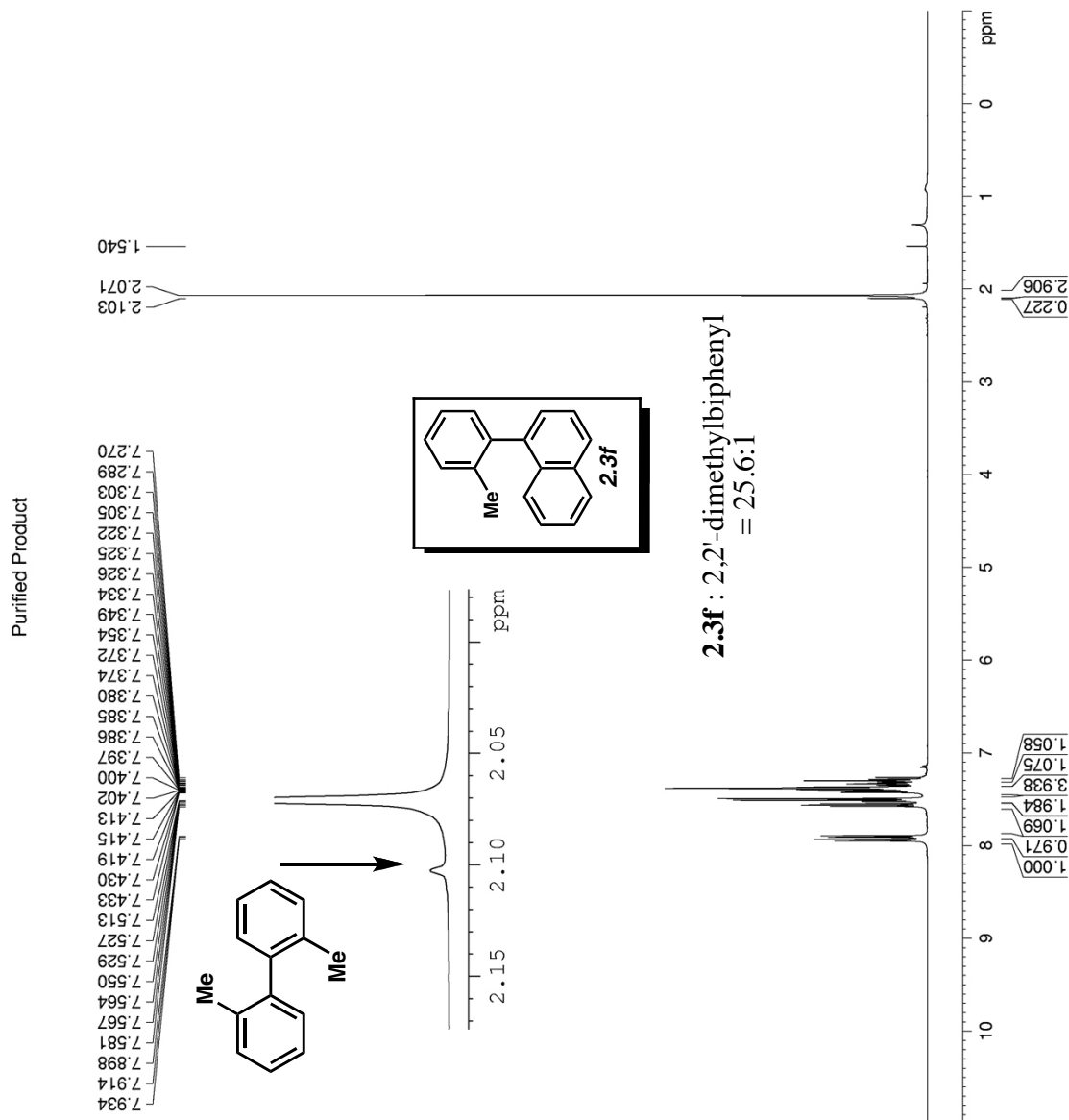
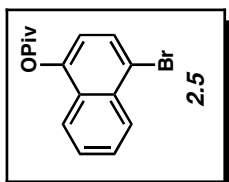


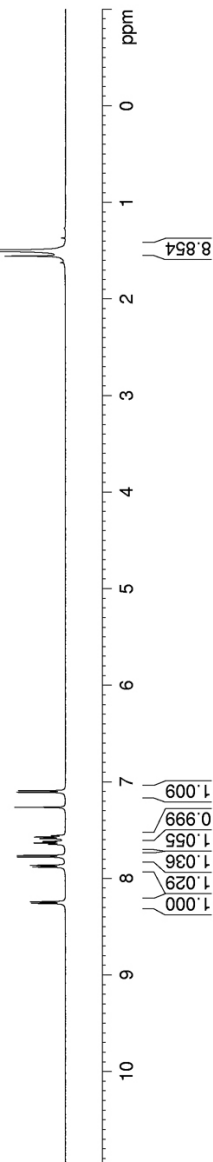
Figure A1.42 ¹H NMR (500 MHz, CDCl₃) of compound **2.3f**.

Purified Product

8.263
8.246
7.886
7.869
7.782
7.766
7.650
7.636
7.622
7.620
7.590
7.576
7.561
7.268
7.112
7.096



1.560
1.502



Current Data Parameters
NAME KQ2-76
EXPNO 10
PROCNO 1

F2 - Acquisition Parameters
Date_ 20080727
Time_ 10.57
INSTRUM avance500
PROBHD 5 mm bb-ZZ800
PULPROG zg30
TD 65536
SOLVENT CDCl3
NS 8
DS 0
SWH 10000.000 Hz
FIDRES 0.152588 Hz
AQ 3.2769001 sec
RG 181
DW 50.000 usec
DE 6.00 usec
TE 296.3 K
D1 2.0000000 sec
MCREST 0.0000000 sec
MCWRK 0.01500000 sec

===== CHANNEL f1 =====
NUC1 1H
P1 12.00 usec
PL1 0.00 dB
SFO1 500.3330020 MHz

F2 - Processing parameters
SI 32768
SF 500.3300182 MHz
WDW EM
SSB 0
LB 0.30 Hz
GB 0
PC 1.00

Figure A1.43 ¹H NMR (500 MHz, CDCl₃) of compound 2.5.

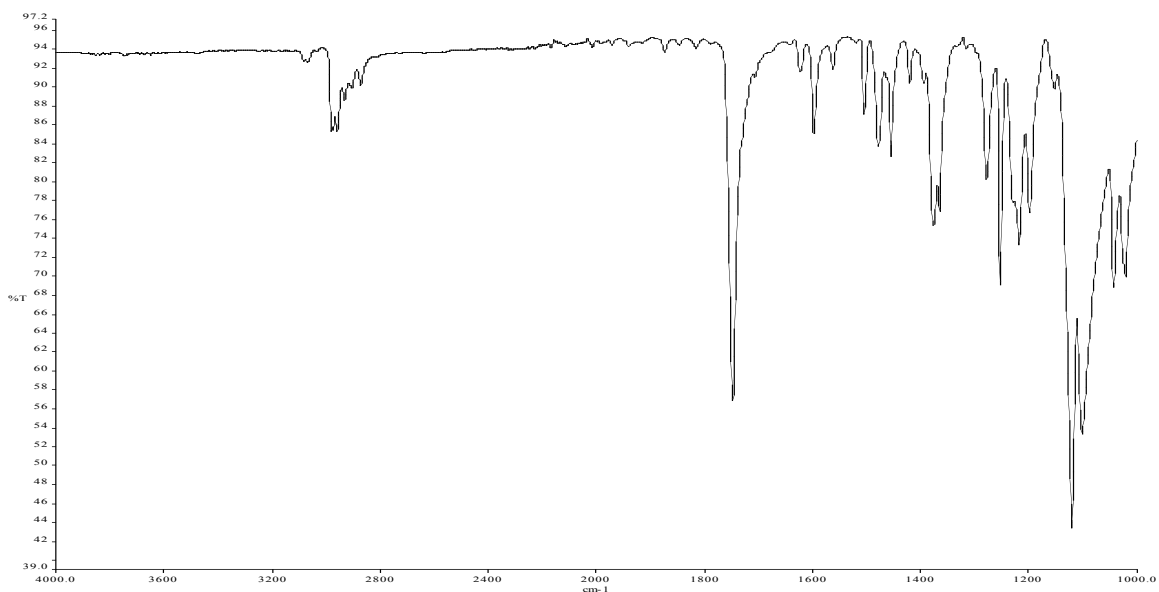


Figure A1.44 Infrared spectrum of compound **2.5**.

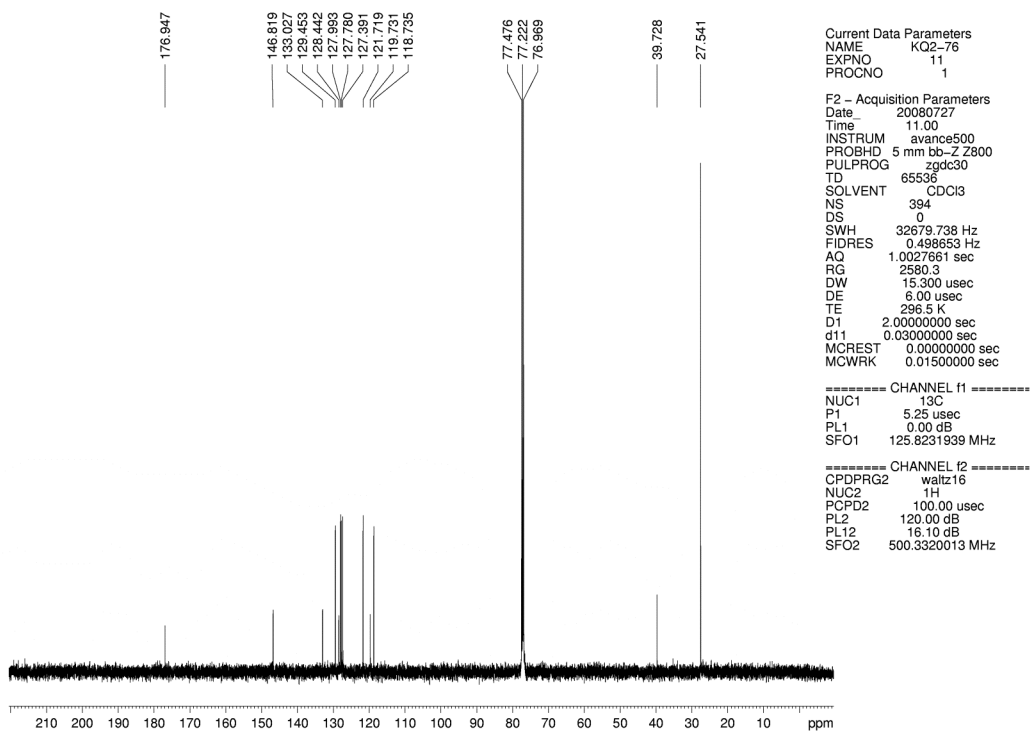


Figure A1.45 ^{13}C NMR (125 MHz, CDCl_3) of compound **2.5**.

Current Data Parameters
 NAME xt2-81
 EXPNO 1
 PROCNO 1

F2 - Acquisition Parameters
 Date_ 20080730
 Time_ 5.42
 INSTRUM avance500
 PROBHD 5 mm bb-ZZ800
 PULPROG zg30
 TD 65536
 SOLVENT CDCI3
 NS 7
 DS 0
 SWH 10000.000 Hz
 FIDRES 0.152588 Hz
 AQC 3.2769001 sec
 RG 64
 DW 50.000 usec
 DE 6.00 usec
 TE 296.2 K
 D1 2.00000000 sec
 MCREST 0.00000000 sec
 MCWRK 0.01500000 sec

===== CHANNEL f1 =====
 NUC1 1H
 P1 12.00 usec
 PL1 0.00 dB
 SFO1 500.3330020 MHz

F2 - Processing parameters
 SI 32768
 SF 500.3300220 MHz
 WDW EM
 SSB 0
 LB 0.30 Hz
 GB 0
 PC 1.00

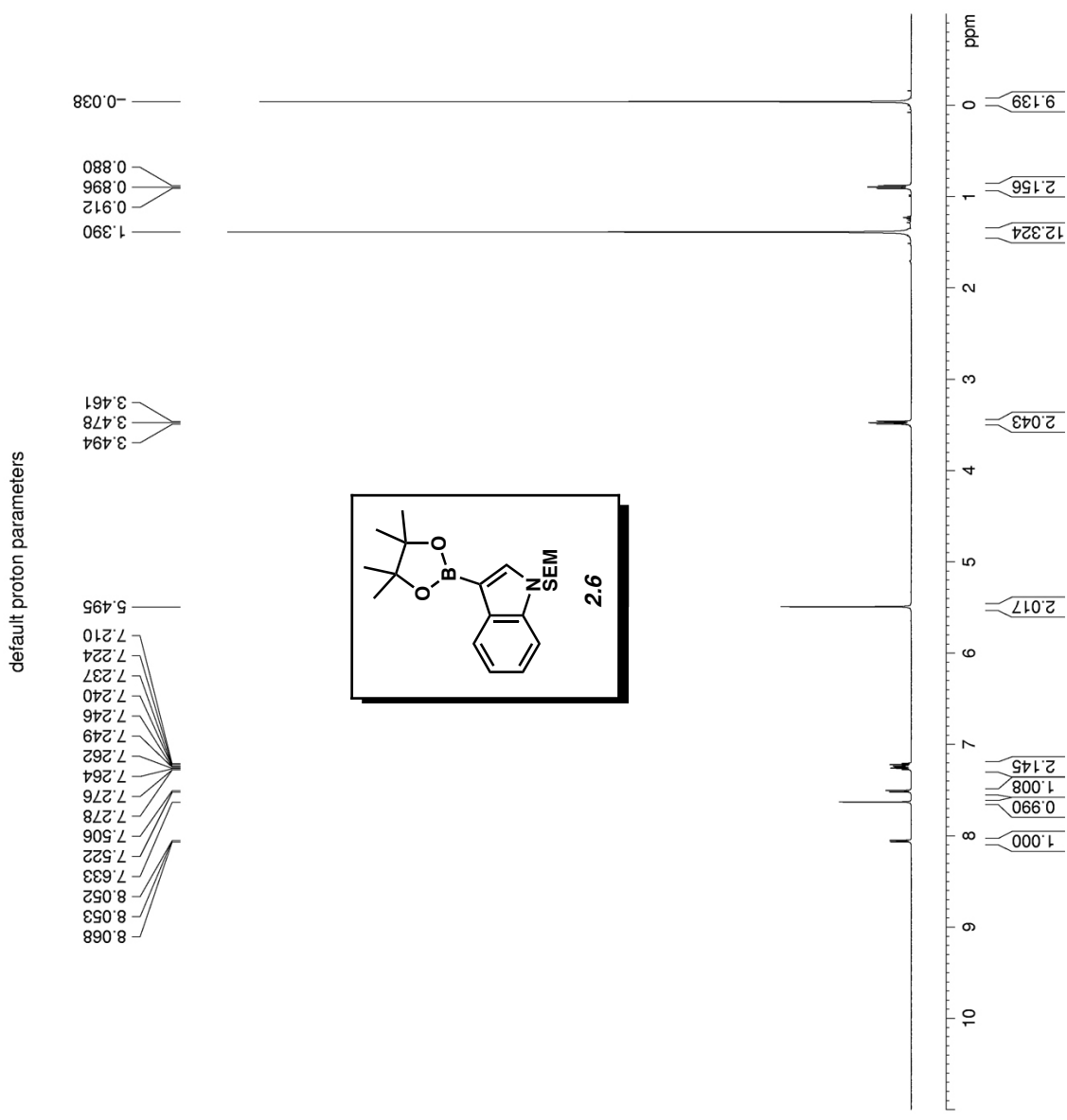


Figure A1.46 ¹H NMR (500 MHz, CDCl₃) of compound 2.6.

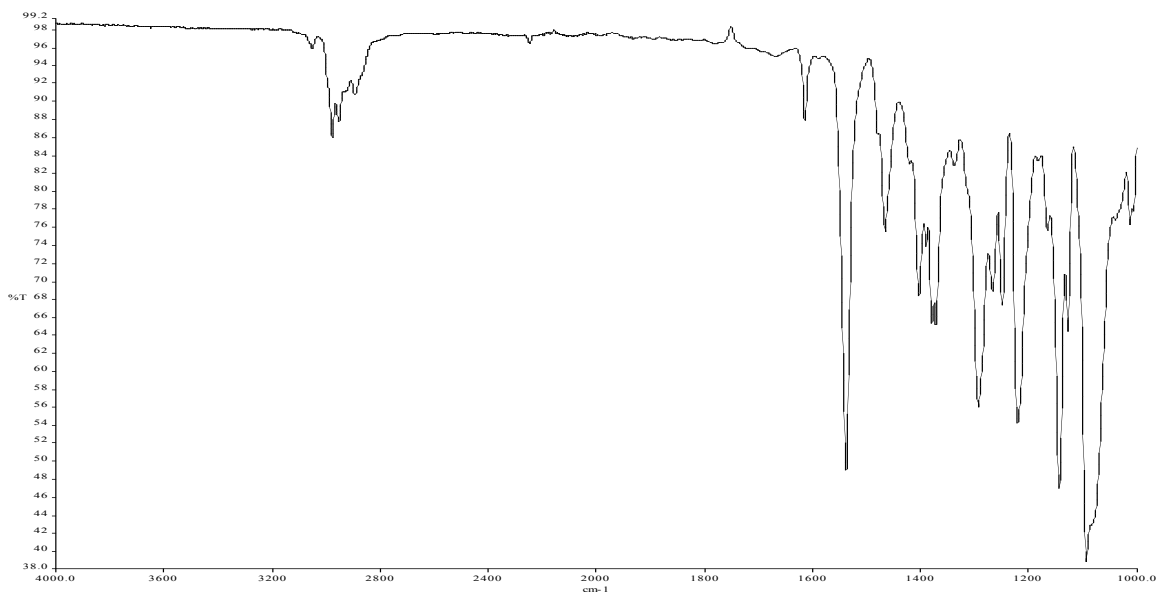


Figure A1.47 Infrared spectrum of compound 2.6.

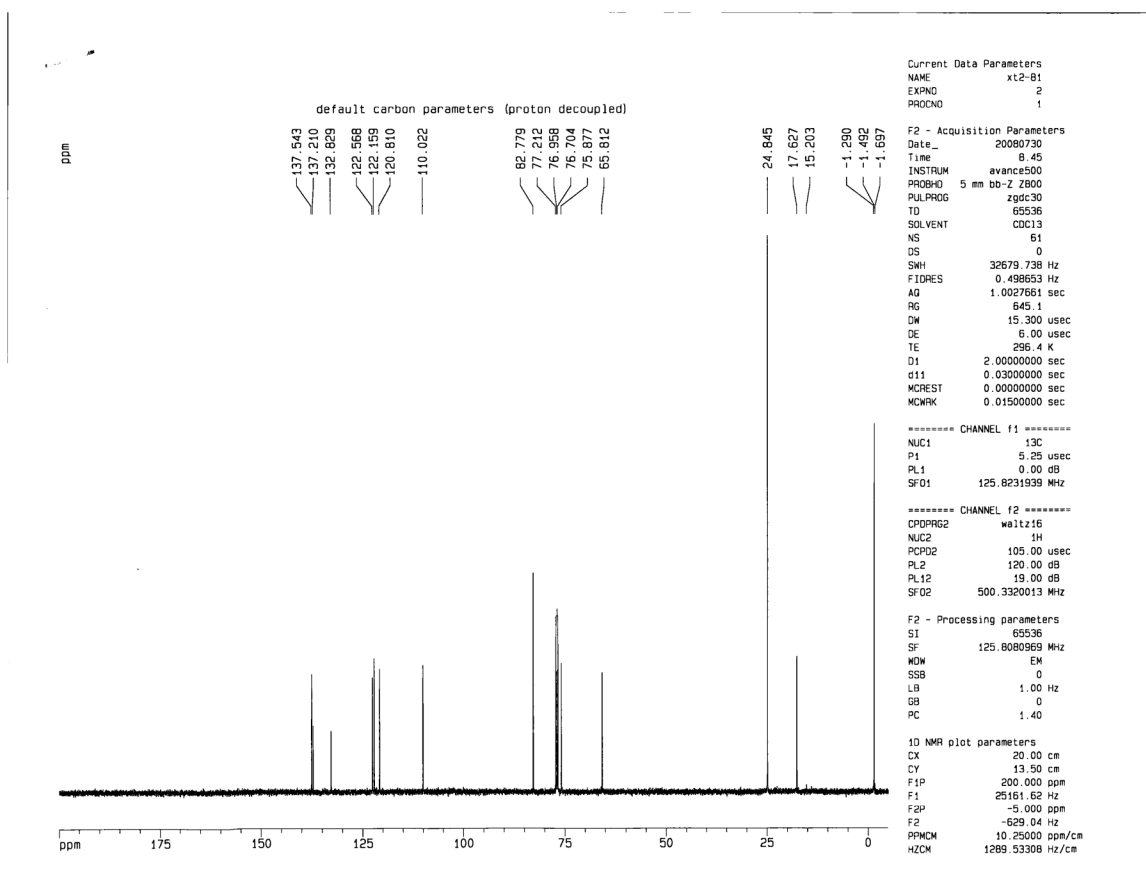


Figure A1.48 ^{13}C NMR (125 MHz, CDCl_3) of compound 2.6.

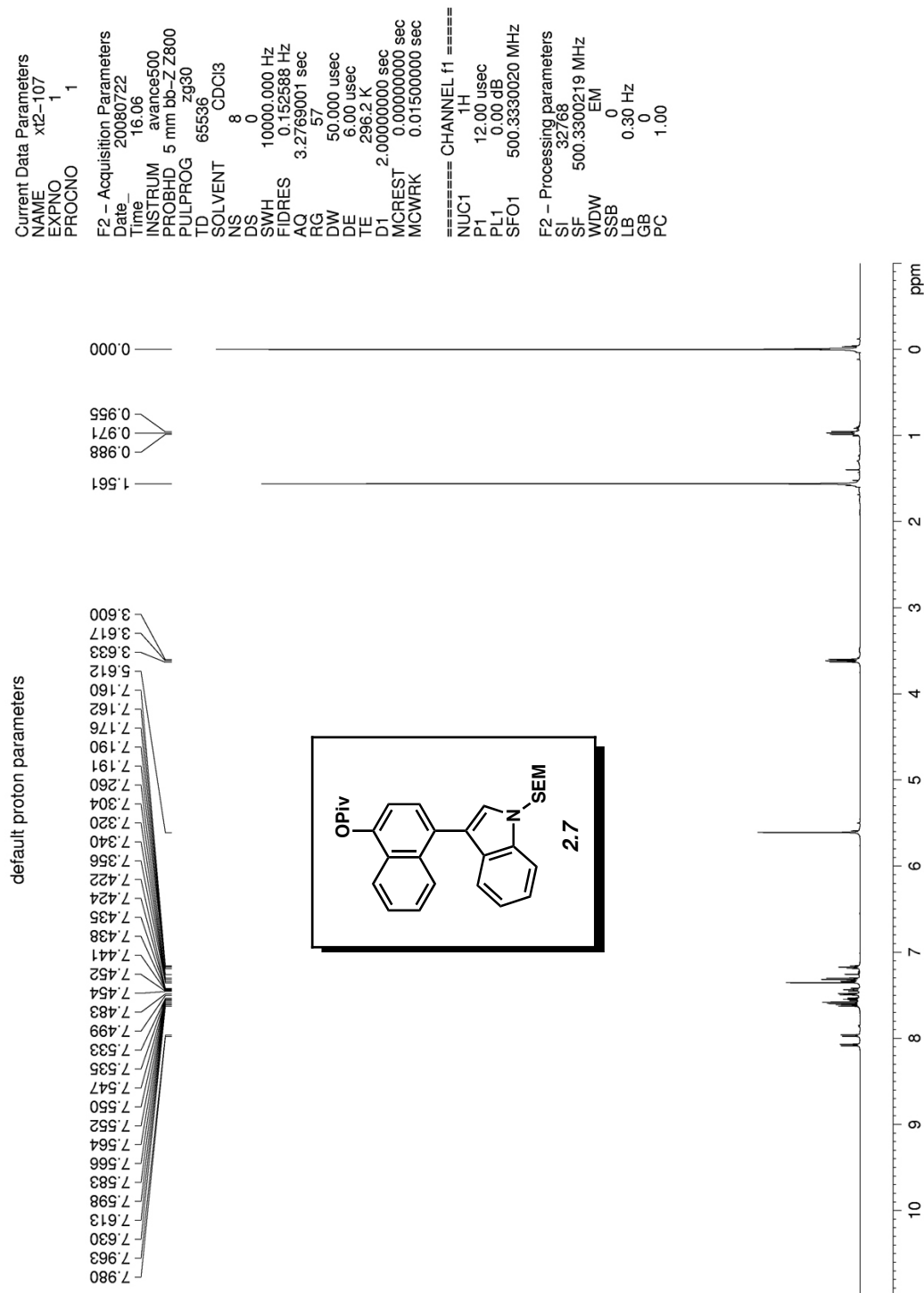


Figure A1.49 ^1H NMR (500 MHz, CDCl_3) of compound 2.7.

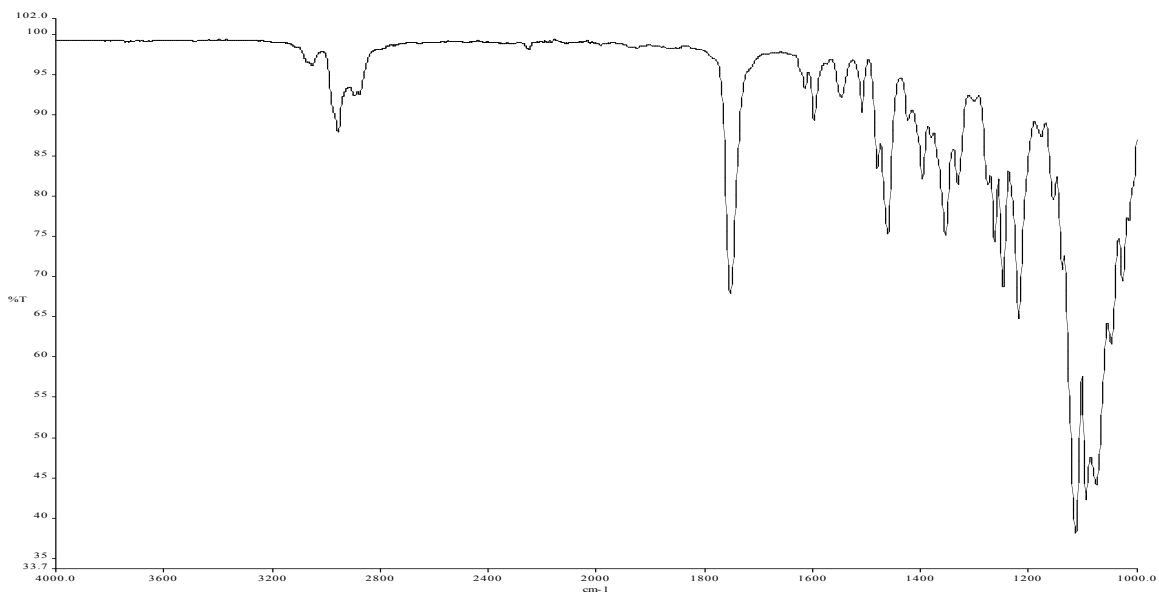


Figure A1.50 Infrared spectrum of compound **2.7**.

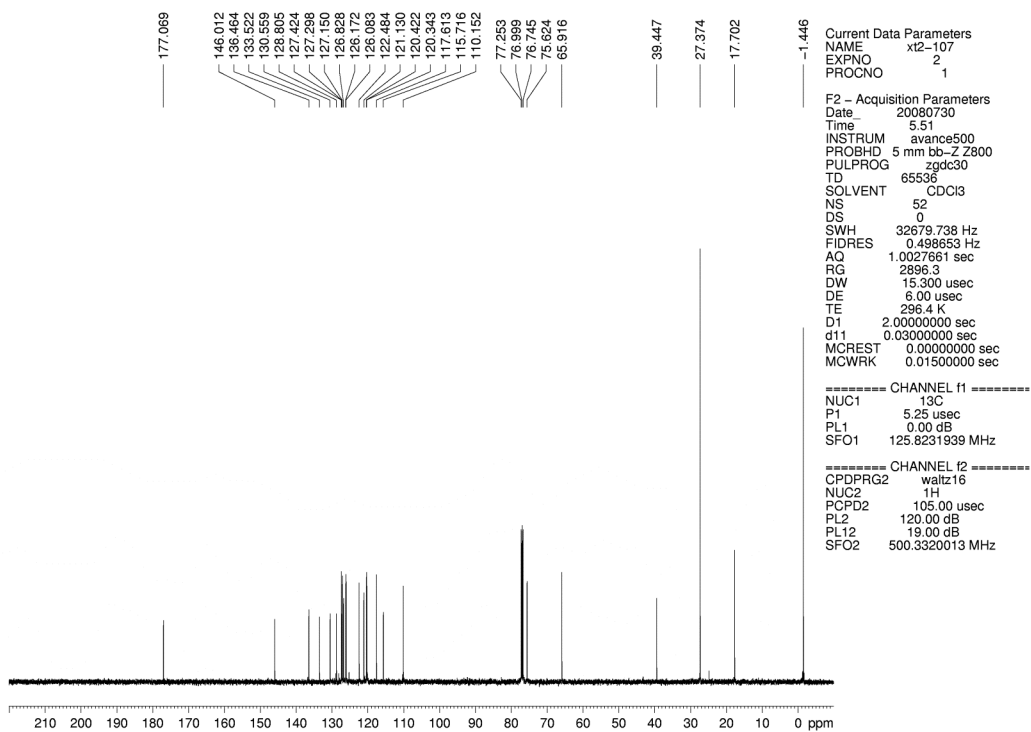


Figure A1.51 ¹³C NMR (125 MHz, CDCl₃) of compound **2.7**.

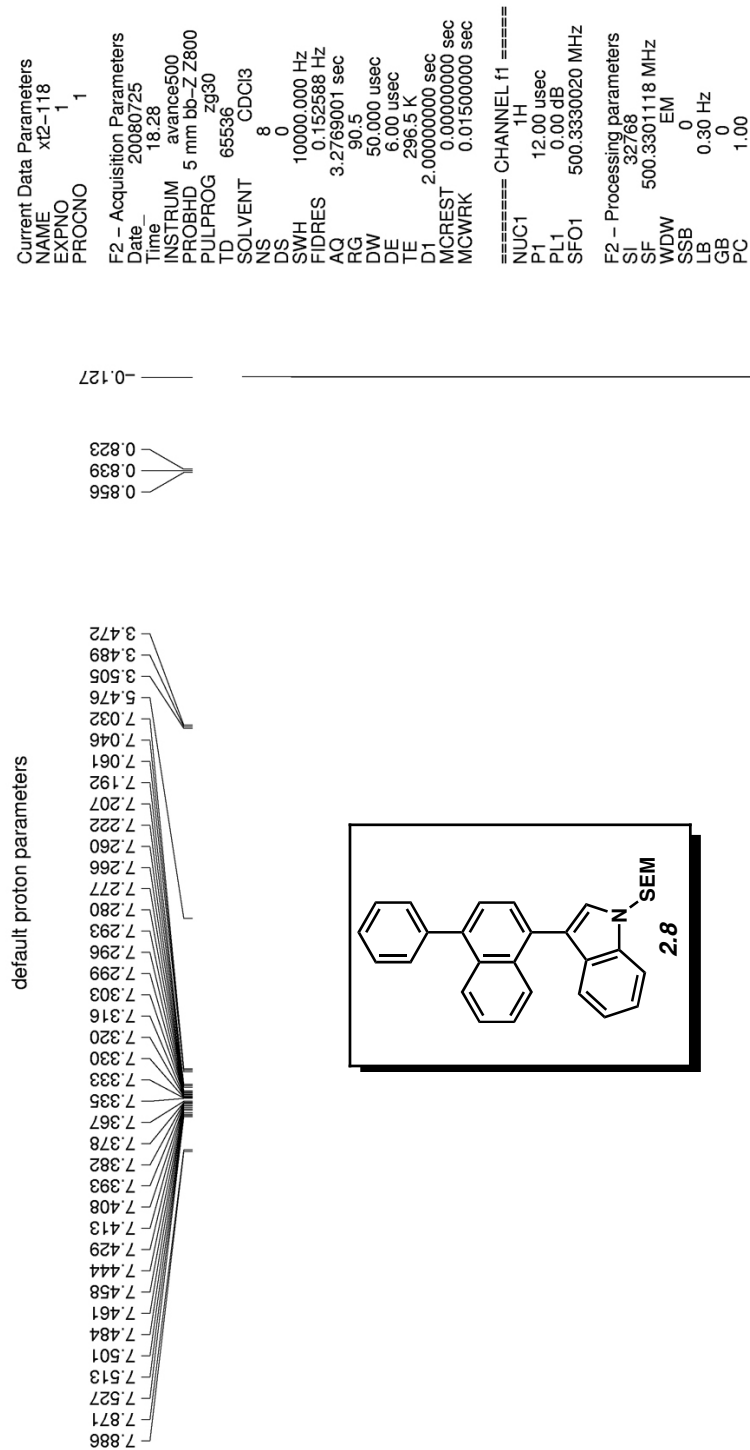


Figure A1.52 ¹H NMR (500 MHz, CDCl₃) of compound 2.8.

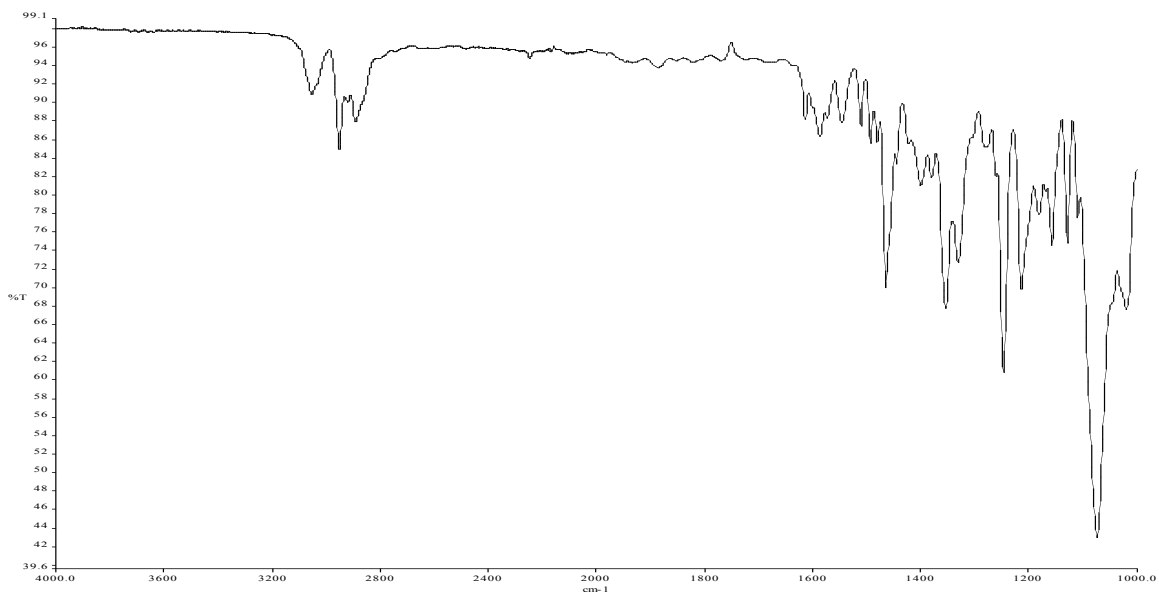


Figure A1.53 Infrared spectrum of compound **2.8**.

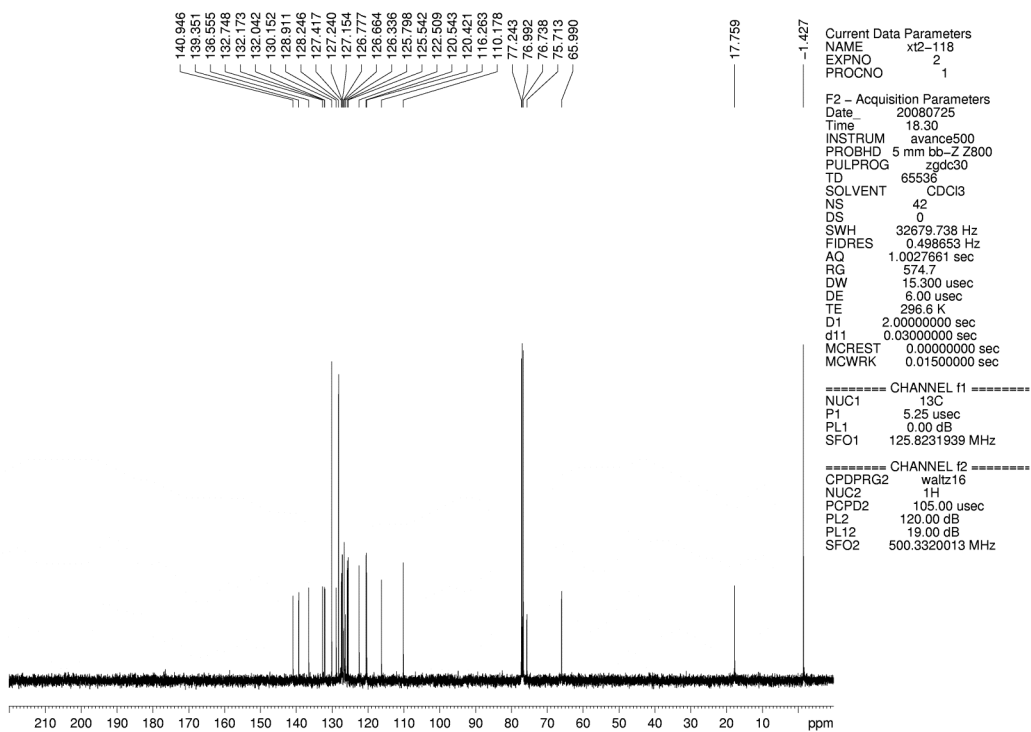


Figure A1.54 ^{13}C NMR (125 MHz, CDCl_3) of compound **2.8**.

CHAPTER THREE

Suzuki–Miyaura Cross-Coupling of Aryl Carbamates and Sulfamates: Experimental and Computational Studies

Kyle W. Quasdorf, Aurora Antoft-Finch, Peng Liu, Amanda L. Silberstein, Anna Komaromi,

Tom Blackburn, Stephen D. Ramgren, K. N. Houk, Victor Snieckus, and Neil K. Garg

J. Am. Chem. Soc. **2011**, *133*, 6352–6363.

3.1 Abstract

The first Suzuki–Miyaura cross-coupling reactions of the synthetically versatile *O*-aryl carbamate and *O*-sulfamate groups is described. The transformations utilize the inexpensive, bench-stable catalyst $\text{NiCl}_2(\text{PCy}_3)_2$ to furnish biaryls in good to excellent yields. A broad scope for this methodology has been demonstrated. Substrates with electron-donating and electron-withdrawing groups (EDGs, EWGs) are tolerated, in addition to those that possess *ortho* substituents. Furthermore, heteroaryl substrates may be employed as coupling partners. A computational study providing the full catalytic cycles for these cross-coupling reactions is described. The oxidative additions with carbamates and sulfamates occur via a five-centered transition state, resulting in the exclusive cleavage of the Ar–O bond. Water is found to stabilize the Ni–carbamate catalyst resting state, and thus provides rationalization of the relative decreased rate of coupling of carbamates. Several synthetic applications are presented to showcase the utility of the methodology in the synthesis of polysubstituted aromatic compounds of natural product and bioactive molecule interest.

3.2 Introduction

Transition metal-catalyzed cross-coupling reactions provide a powerful means to assemble carbon–carbon (C–C) and carbon–heteroatom (C–X) bonds.¹ Although halides are most commonly employed as the electrophilic partner,^{1,2} phenolic derivatives (Figure 3.1), or ‘pseudohalides’, offer a valuable alternative given that phenols are typically inexpensive and readily available materials.³ Cross-couplings of aryl sulfonates have been most widely studied and a range of C–C and C–X bond forming reactions are now established.^{1,4,5} Recent studies have focused on the development of less common phenol-based electrophiles,⁶ such as ethers,⁷ esters,⁸ carbamates,⁹ and sulfamates^{9b,10} since they are commonly more robust, typically unreactive toward Pd-catalysis, and show synthetic advantage for the regioselective construction of aromatics by C–H activation and directed *ortho* metalation (DoM) chemistry.^{11,12,13,14}

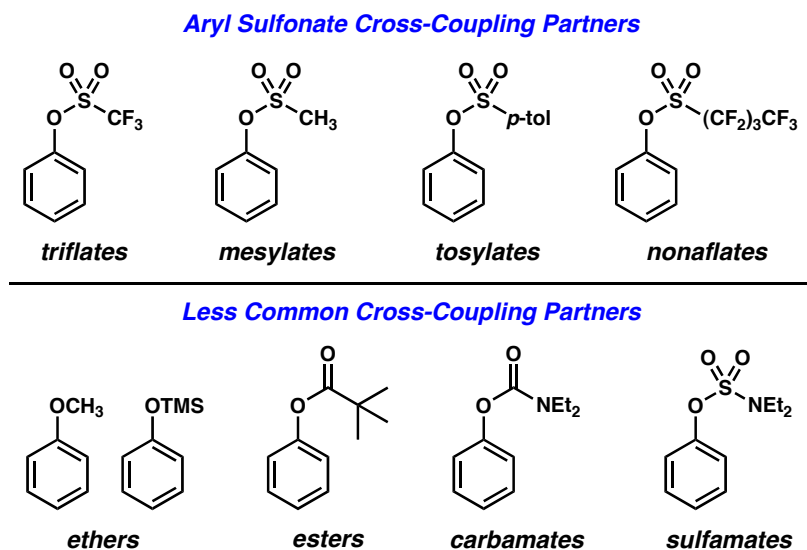
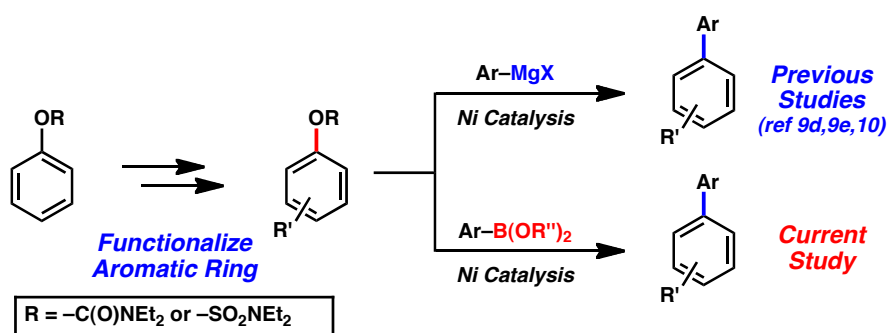


Figure 3.1. Phenol-based cross-coupling partners.

Inspired by the reasons outlined above, our laboratories have pursued the development of cross-coupling reactions involving phenol-derived carbamates and sulfamates (Scheme 3.1). Previous studies have demonstrated the utility of these reaction partners in nickel-catalyzed Kumada couplings.^{9d,9e,10} However, the corresponding Suzuki–Miyaura couplings of these substrates have remained elusive, despite the numerous benefits of organoboronate coupling methodologies. Such advantages include the low toxicity, wide availability, and pronounced stability of organoboronates, in addition to their broad functional group tolerance.^{1,15} In this article, we report a) the development of the Ni-catalyzed Suzuki–Miyaura cross-coupling reactions of aryl *O*-carbamates and *O*-sulfamates, b) the broad scope of these transformations, which includes the cross-coupling of heterocyclic substrates, c) computational studies that elucidate the complete catalytic cycle of these couplings, and d) a variety of synthetic applications, including DoM – linked tactics and a concise synthesis of the anti-inflammatory drug flurbiprofen.¹⁶

Scheme 3.1

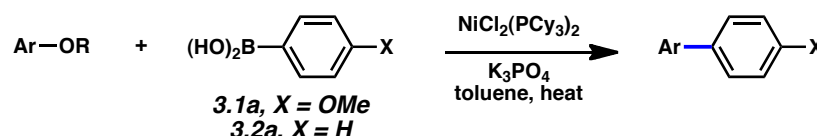


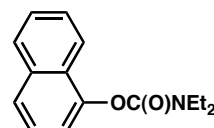
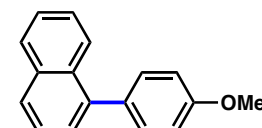
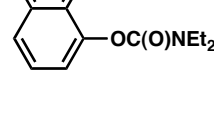
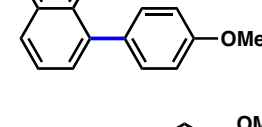
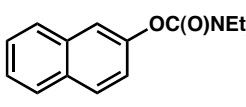
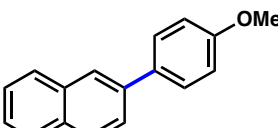
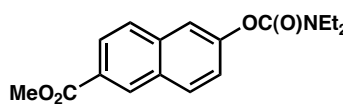
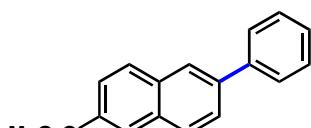
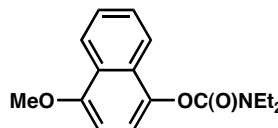
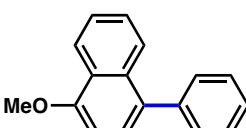
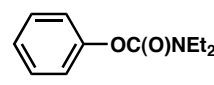
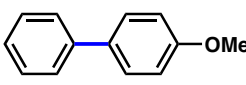
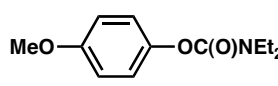
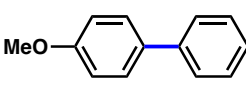
3.3 Suzuki–Miyaura Cross-Coupling Reactions of Aryl *O*-Carbamates

A key challenge in achieving the Suzuki–Miyaura cross-coupling of aryl carbamates lies in activating the fairly inert *aryl* carbon–oxygen bond of these substrates. A similar obstacle had been overcome in our previously reported Suzuki–Miyaura coupling of aryl pivalates.^{8a} Encouraged by our prior success, we explored NiCl₂(PCy₃)₂-promoted conditions to effect the desired Suzuki–Miyaura coupling of aryl carbamates (Table 3.1). Of note, NiCl₂(PCy₃)₂ is readily available, considerably stable to air and water, and can be used on the bench-top rather than in a glovebox.^{17,18,19} Initial studies were directed toward the coupling of fused-aromatic systems, which are typically superior substrates in Ni-catalyzed couplings of phenolic derivatives.^{7,8,9} Unfortunately, applying our optimal conditions for pivalate coupling (i.e., NiCl₂(PCy₃)₂ (5 mol%) and K₃PO₄ (4.5 equiv) in toluene at 80 °C) to a 1-naphthyl carbamate substrate led only to trace amounts of cross-coupled product. By raising the temperature to 110 °C, however, the desired biaryl was obtained in 51% yield (entry 1). Further optimization ultimately established more forcing conditions that delivered the targeted product in 86% yield (entry 2).

Additional carbamate substrates were examined under our Ni-catalyzed reaction conditions (Table 3.1).²⁰ 2-Naphthyl carbamates gave products in lower yields (entries 3 and 4). The reaction proved tolerant of an EWG (–CO₂Me, entry 4) and an EDG (–OMe, entry 5) on the naphthyl ring. The corresponding reactions of aryl carbamates proved more challenging. Nonetheless, carbamates derived from phenol and *p*-methoxyphenol were converted to the corresponding cross-coupled products in 52% and 41% yield, respectively (entries 6 and 7).

Table 3.1. Cross-coupling of aryl carbamates with arylboronic acids^a



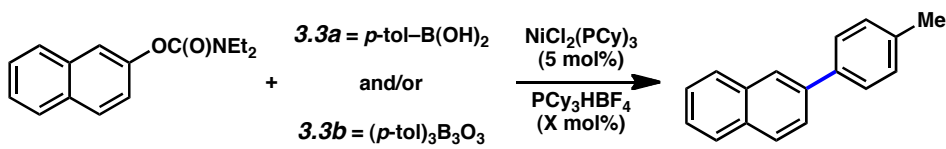
entry	Ar-OR	(HO) ₂ B-Ar	product	yield ^c
1 ^b		3.1a		51%
2		3.1a		86%
3		3.1a		47%
4		3.2a		54%
5		3.2a		77%
6		3.1a		52%
7		3.2a		41%

^a Conditions: NiCl₂(PCy₃)₂ (10 mol%), ArB(OH)₂ (4 equiv), K₃PO₄ (7.2 equiv), toluene (0.3 M), 130 °C for 24 h. ^b Conditions: NiCl₂(PCy₃)₂ (5 mol%), ArB(OH)₂ (2.5 equiv), K₃PO₄ (4.5 equiv), toluene (0.3 M), 110 °C, 24 h. ^c Yields of isolated products.

Further studies were undertaken to uncover higher yielding and more generally useful reaction conditions. The *N,N*-diethyl carbamate of 2-naphthol was subjected to NiCl₂(PCy₃)₂ with variations in temperature, solvent, ligand additive, and organoboron species (Table 3.2). When employing *o*-xylenes at 150 °C, cross-coupling with boroxine **3.3b** proceeded sluggishly but nevertheless furnished the desired biaryl in 61% yield (entry 1). Mixtures of boronic acids and

boroxines were also examined. Using a 1:1 mixture of **3.3a**:**3.3b**, the desired biaryl was obtained in only 26% yield (entry 2). These results, coupled with the observation that **3.3a** liberates excessive water in organic solvents, led us to hypothesize that, although some water is necessary to generate the catalytically active boronate species, excessive water can be detrimental to the carbamate cross-coupling reaction.²¹ Furthermore, Shi had previously reported the critical role of water in the Suzuki–Miyaura coupling of aryl pivalate esters.^{8b} By using a 1:10 ratio of **3.3a**:**3.3b**,²² and thereby minimizing the water content, a quantitative yield of cross-coupled product was obtained (entry 3). Conducting the reaction at 120 °C, with toluene as solvent and 10 mol% Ni catalyst, gave a lower yield of the biaryl adduct (entry 4).²³

Table 3.2. Optimization studies for naphthyl 2-*O*-carbamate coupling



entry ^b	solvent	temp	PCy ₃ HBF ₄	K ₃ PO ₄	ArB(OR) ₂	yield ^a
1	<i>o</i> -xylene	150 °C	10 mol%	5 equiv	3.3b (2.5 equiv)	61%
2	<i>o</i> -xylene	150 °C	10 mol%	5 equiv	3.3a : 3.3b (1:1, 2.5 equiv)	26%
3	<i>o</i> -xylene	150 °C	10 mol%	5 equiv	3.3a : 3.3b (1:10, 2 equiv)	100% (84%)
4 ^c	toluene	120 °C	–	7.2 equiv	3.3a : 3.3b (1:10, 2.5 equiv)	62%

^a Yield by GC/MS analysis (yield of isolated product). ^b All reactions were run for 20 h with the exception of entry 4, which was run for 5 h. ^c 10 mol% NiCl₂(PCy₃)₂.

Having found optimal and reproducible conditions, we turned our attention to defining the scope and functional group tolerance of the carbamate cross-coupling reaction (Table 3.3).²⁰ Substrates derived from 2-naphthol, 1-naphthol, and phenol underwent smooth coupling (entries

1–3). Furthermore, although a substrate bearing the electron-withdrawing fluoro substituent was tolerated (entry 4), coupling in the presence of a cyano derivative was less fruitful (entry 5). The latter result can be explained by competitive cross-coupling at the cyano group, a transformation reported recently by Shi.²⁴ Finally, an electron-rich substrate gave only low yields of product (entry 6).

Table 3.3. Cross-coupling of aryl carbamates under improved conditions^a

$\text{Ar-OC(O)NEt}_2 + (\text{RO})_2\text{B-Ph-X} \xrightarrow[\text{PCy}_3\text{HBF}_4, \text{K}_3\text{PO}_4, \text{o-xylene, 150 }^\circ\text{C, 5-20 h}]{\text{NiCl}_2(\text{PCy}_3)_2} \text{Ar-Ph-X}$

3.1, X = OMe
3.2, X = H
3.3, X = Me

entry	Ar-OC(O)NEt ₂	(RO) ₂ B-Ar	product	yield ^b
1		3.3		100% (84%)
2		3.2		100% (82%)
3		3.1		64% (58%)
4		3.1		80% (69%)
5		3.2		36% (28%)
6		3.2		23% (31%)

^a Conditions: NiCl₂(PCy₃)₂ (5 mol%), PCy₃HBF₄ (10 mol%), ArB(OR)₂ (2.5 equiv), ratio of Ar₃B₃O₃:ArB(OH)₂ = 10:1 (4 equiv), K₃PO₄ (5 equiv). ^b Yield by GC/MS analysis (yield of isolated product).

Several *ortho*-substituted aryl carbamates were tested in the Suzuki–Miyaura coupling (Table 3.4). Substrates of this type can be readily synthesized by DoM¹² or transition metal-catalyzed C–H functionalization.^{14b-e} Substrates with *o*-benzyl, -alkenyl, and -phenyl groups were all tolerated (entries 1–3). Coupling of the *o*-methoxy substrate proceeded in modest yield (entry 4), whereas coupling of a 2,4-dimethylated substrate was unsuccessful (entry 5). In view of the coupling of other *ortho*-substituted systems to afford good to excellent yields of products (entries 1 – 3), rationalization of these results based on steric effects is premature.

Table 3.4. Cross-coupling of *ortho*-substituted aryl *O*-carbamates^a

entry	Ar–OC(O)NEt ₂	product	yield ^b
1			60% (70%)
2			99% (93%)
3			69% (50%)
4			40% (36%)
5			8%

^a Conditions: NiCl₂(PCy₃)₂ (5 mol%), PCy₃HBF₄ (10 mol%), **3.2** (2.5 equiv), ratio of Ph₃B₃O₃:PhB(OH)₂ = 10:1 (4 equiv), K₃PO₄ (5 equiv). ^b Yield by GC/MS analysis (yield of isolated product).

As shown in Table 3.5, the carbamate cross-coupling methodology is also applicable to heterocyclic substrates. Thus, the 3-pyridyl-carbamate was efficiently cross-coupled with a variety of organoboron species (entries 1–5). In addition, a quinoline-derived substrate was tolerated (entry 6) and a carbazole-containing substrate underwent conversion to the desired biaryl under our optimal reaction conditions albeit in modest yield (entry 7).

Table 3.5. Cross-coupling of heterocyclic aryl *O*-carbamates and scope of aryl boronates^a

$\text{HetAr-OC(O)NEt}_2 + (\text{RO})_2\text{B-Ar} \xrightarrow[\text{PCy}_3\text{HBF}_4, \text{K}_3\text{PO}_4, \text{o-xylene, 150 }^\circ\text{C, 5-20 h}]{\text{NiCl}_2(\text{PCy}_3)_2}$ HetAr-Ar

3.1, X = p-OMe; 3.2, X = H;
3.3, X = p-Me; 3.4, X = p-CF₃;
3.5, X = m-OMe

entry	HetAr-OC(O)NEt ₂	(RO) ₂ B-Ar	product	yield ^b
1		3.1		(84%)
2		3.2		100% (85%)
3		3.3		(87%)
4		3.4		(70%)
5		3.5		(65%)
6		3.2		100% (51%)
7		3.2		45% (36%)

^a Conditions: NiCl₂(PCy₃)₂ (5 mol%), PCy₃HBF₄ (10 mol%), ArB(OR)₂ (2.5 equiv), ratio of Ar₃B₃O₃:ArB(OH)₂ = 10:1 (4 equiv), K₃PO₄ (5 equiv). ^b Yield by GC/MS analysis (yield of isolated product).

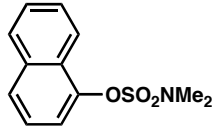
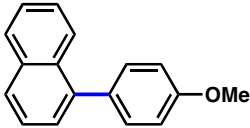
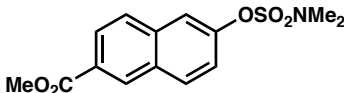
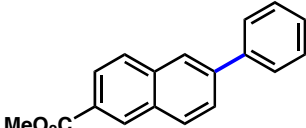
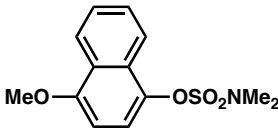
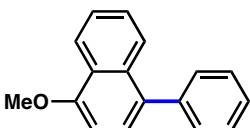
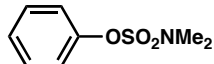
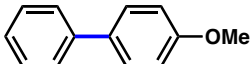
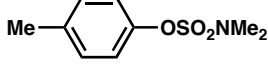
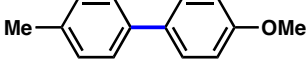
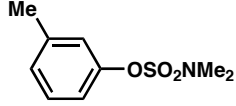
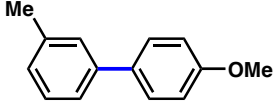
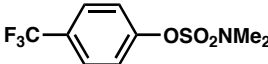
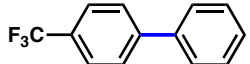
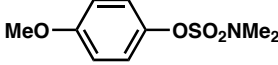
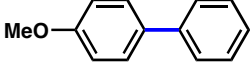
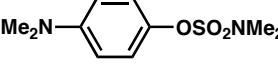
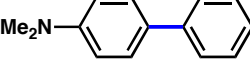
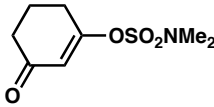
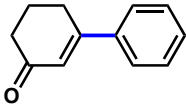
3.4 Suzuki–Miyaura Cross-Coupling Reactions of Aryl *O*-Sulfamates

Concurrent with the above studies on aryl carbamates, aryl sulfamates were targeted as substrates for the Ni-catalyzed Suzuki–Miyaura cross-coupling reactions. Although initial efforts to effect this transformation with dppp as ligand gave initial encouragement,^{10a} employing the tricyclohexylphosphine ligand led to improved results, ultimately rendering aryl sulfamates superior Suzuki–Miyaura coupling partners to the corresponding carbamates (Table 3.6).²⁰ Naphthyl substrates were smoothly converted to biaryl products,²⁵ even in the presence of an EWG or EDG (entries 1–3). Most strikingly, the reaction proceeded comparably well when operating on aryl derivatives (entries 4–9). Methyl and the electron-withdrawing CF₃ substituents are tolerated (entries 5–7). Substrates bearing electron-rich methoxy or amino substituents also afforded very good yields of coupled products (entries 8 and 9). Moreover, an enone sulfamate participated in the Suzuki–Miyaura cross-coupling reaction (entry 10).

Table 3.6. Cross-coupling of aryl sulfamates^a

$$\text{Ar-OSO}_2\text{NMe}_2 + (\text{HO})_2\text{B-C}_6\text{H}_4\text{-X} \xrightarrow[\text{K}_3\text{PO}_4, \text{toluene, 110 }^\circ\text{C}]{\text{NiCl}_2(\text{PCy}_3)_2} \text{Ar-C}_6\text{H}_4\text{-X}$$

3.1a, X = OMe
3.2a, X = H

entry	Ar-OSO ₂ NMe ₂	(HO) ₂ B-Ar	product	yield ^b
1		3.1a		95%
2		3.2a		72%
3		3.2a		92%
4		3.1a		87%
5		3.1a		89%
6		3.1a		91%
7		3.2a		81%
8		3.2a		80%
9		3.2a		76%
10		3.2a		75%

^a Conditions: NiCl₂(PCy₃)₂ (5 mol%), ArB(OH)₂ (2.5 equiv), K₃PO₄ (4.5 equiv), toluene (0.3 M), 110 °C for 24 h. ^b Yields of isolated products.

In view of the availability of many *ortho*-substituted aryl sulfamates by DoM chemistry, such derivatives were also evaluated in the Suzuki–Miyaura cross-coupling reaction (Table 3.7).^{20,26} The transformation was found to be tolerant of an *ortho*-cresol derived substrate, in addition to the sterically burdened sulfamate prepared from 2,6-dimethylphenol (entries 1 and 2). Furthermore, substrates bearing *ortho*-trimethylsilyl, -phenyl, and -methoxy substituents underwent cross-coupling to give the corresponding products in excellent yields (entries 3–5). Interestingly, a substrate possessing a bulky *ortho*-*t*-butylketone substituent could also be utilized in this methodology (entry 6).

Table 3.7. Cross-coupling of *ortho*-substituted aryl sulfamates^a

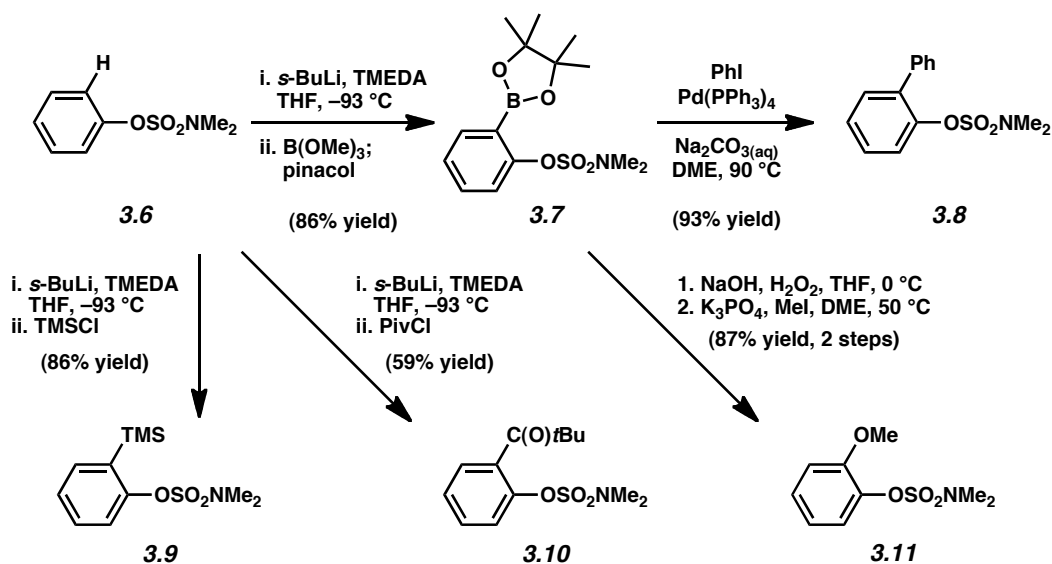
entry	Ar-OSO ₂ NMe ₂	(HO) ₂ B-Ar	product	yield ^b
1		3.1a		92%
2		3.1a		63%
3 ^c		3.1a		92%
4		3.1a		93%
5		3.2a		90%
6 ^c		3.2a		85%

^a Conditions: NiCl₂(PCy₃)₂ (5 mol%), ArB(OH)₂ (2.5 equiv), K₃PO₄ (4.5 equiv), toluene (0.3 M), 110 °C for 24 h. ^b Yields of isolated products. ^c Conditions: NiCl₂(PCy₃)₂ (10 mol%), ArB(OH)₂ (4 equiv), K₃PO₄ (7.2 equiv), toluene (0.3 M), 130 °C for 24 h.

Although the DoM chemistry of aryl sulfamates was initially reported using *N,N*-diethyl substrates,^{10a} the corresponding *N,N*-dimethyl aryl sulfamates were found to undergo metalation under the identical reported reaction conditions. Scheme 3.2 highlights syntheses of substrates **3.8–3.11** beginning from phenyl sulfamate **3.6**, which, in turn, is easily prepared from phenol and commercially available dimethylsulfamoyl chloride²⁷ in quantitative yield. Compounds **3.9** and

3.10 were obtained by lithiation of phenyl sulfamate **3.6**, followed by quenching with TMSCl and PivCl, respectively. Similarly, the boronate **3.7** was derived by quenching the intermediate lithio species with B(OMe)₃, followed by treatment with pinacol.^{10a} Boronate **3.7** served as the common precursor to substituted sulfamates **3.8** and **3.11**. Whereas methoxysulfamate **3.11** was prepared by a straightforward oxidation²⁸/methylation sequence, *ortho*-phenyl sulfamate **3.8** was accessed by a Pd-catalyzed Suzuki–Miyaura cross-coupling. It is notable that the sulfamate remains undisturbed under the Pd-mediated reaction conditions.

Scheme 3.2



The scope of the sulfamate cross-coupling reaction was also found to be broad with respect to the boronic acid component (Table 3.8). A methyl substituent was tolerated at the *para*, *meta*, and *ortho* positions (entries 1–3), as was a 4-methoxymethyl group (entry 4). Cross-coupling of a boronic acid bearing the electron-donating methoxy group proceeded in 95% yield

(entry 5). Finally, electron-withdrawing trifluoromethyl, fluoro, and acetyl substituents were compatible with the sulfamate coupling methodology (entries 6–8).

Table 3.8. Scope of boronic acid in the Suzuki–Miyaura cross-coupling of aryl *O*-sulfamates^a

entry	(HO) ₂ B–Ar	product	yield ^b
1			68%
2			77%
3 ^c			74%
4			80%
5			95%
6 ^d			86%
7			93%
8			62%

^a Conditions: NiCl₂(PCy₃)₂ (5 mol%), ArB(OH)₂ (2.5 equiv), K₃PO₄ (4.5 equiv), toluene (0.3 M), 110 °C for 24 h. ^b Yields of isolated products. ^c Conditions: NiCl₂(PCy₃)₂ (10 mol%), ArB(OH)₂ (4 equiv), K₃PO₄ (7.2 equiv), toluene (0.3 M), 130 °C for 24 h. ^d Conditions: NiCl₂(PCy₃)₂ (5 mol%), ArB(OH)₂ (2.5 equiv), K₃PO₄ (4.5 equiv), toluene (0.3 M), 120 °C for 24 h.

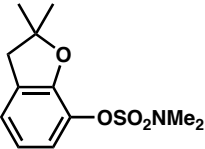
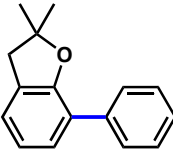
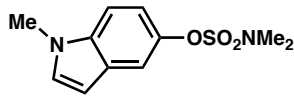
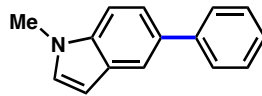
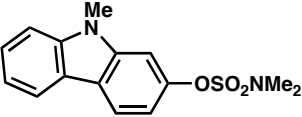
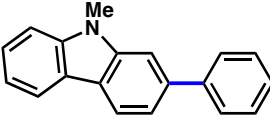
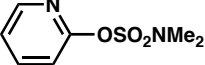
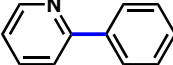
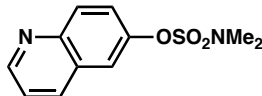
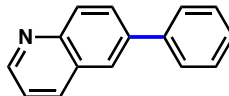
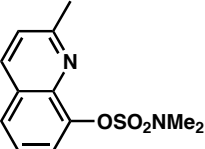
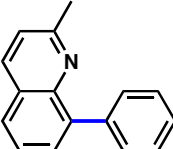
3.5 Suzuki–Miyaura Cross-Coupling Reactions of Heterocyclic *O*-Sulfamates

Given the importance of heterocycles in medicinal agents, we probed the use of heterocyclic partners in the sulfamate Suzuki–Miyaura cross-coupling process.²⁹ As shown in Table 3.9, a variety of heterocyclic aryl sulfamates were suitable for this methodology, although more forcing reaction conditions were often required to achieve synthetically useful yields. Coupling of a dihydrobenzofuran-derived substrate afforded the desired biaryl in 88% yield (entry 1). Similar success was observed in the coupling of nitrogen-containing heteroaryl sulfamates (entries 2–6). In addition to indole and carbazole (entries 2 and 3), the pyridine and quinoline heterocycles, each possessing basic amine functionality, were also tolerated (entries 4–6).

Table 3.9. Cross-coupling of heterocyclic aryl *O*-sulfamates with phenyl boronic acid^a

$\text{HetAr}-\text{OSO}_2\text{NMe}_2 + (\text{HO})_2\text{B}-\text{C}_6\text{H}_5 \xrightarrow[\text{K}_3\text{PO}_4, \text{toluene}]{\text{NiCl}_2(\text{PCy}_3)_2} \text{HetAr}-\text{C}_6\text{H}_5$

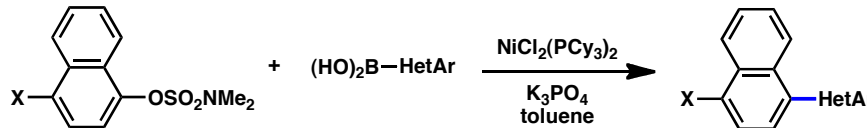
3.2a

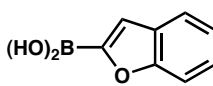
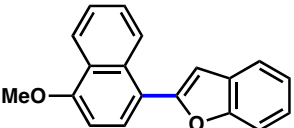
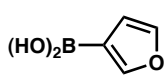
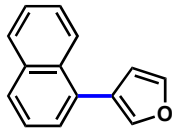
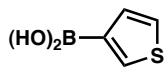
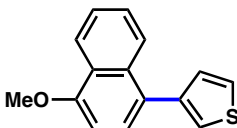
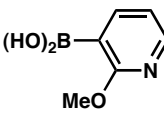
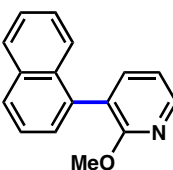
entry	HetAr-OSO ₂ NMe ₂	product	yield ^b
1 ^c			88%
2			75%
3 ^c			89%
4 ^c			72%
5 ^c			89%
6 ^c			74%

^a Conditions: NiCl₂(PCy₃)₂ (5 mol%), **3.2a** (2.5 equiv), K₃PO₄ (4.5 equiv), toluene (0.3 M), 110 °C, 24 h. ^b Yields of isolated products. ^c Conditions: NiCl₂(PCy₃)₂ (10 mol%), **3.2a** (4 equiv), K₃PO₄ (7.2 equiv), toluene (0.3 M), 130 °C for 24 h.

The scope of the sulfamate cross-coupling reaction with respect to heteroaryl boronic acids is summarized in Table 3.10. Benzofuran- and furan-containing substrates underwent smooth cross-coupling under our standard reaction conditions (entries 1 and 2). Furthermore, a sulfur-containing heterocyclic boronic acid could be employed (entry 3). A pyridine 3-boronic acid derivative was also tolerated in our Suzuki–Miyaura coupling methodology (entry 4).

Table 3.10. Cross-coupling of 1-naphthyl-*O*-sulfamates with heterocyclic aryl boronic acids^a

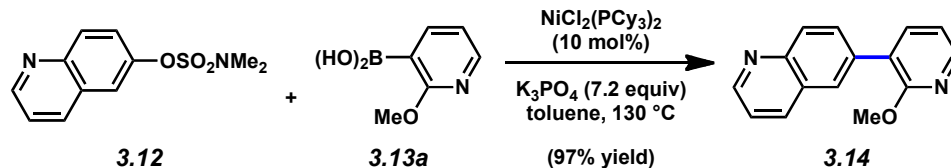


entry	(HO) ₂ B–HetAr	product	yield ^b
1			67%
2			79%
3			80%
4			80%

^a Conditions: NiCl₂(PCy₃)₂ (5 mol%), HetArB(OH)₂ (2.5 equiv), K₃PO₄ (4.5 equiv), toluene (0.3 M), 110 °C, 24 h. ^b Yields of isolated products.

As an additional important test of the sulfamate coupling methodology, we attempted a Suzuki–Miyaura reaction wherein both coupling partners were heterocyclic substrates (Scheme 3.3).²⁹ We were delighted to find that the desired cross-coupling between quinoline-derived sulfamate **3.12** and pyridinyl boronic acid **3.13a** proceeded smoothly to furnish biaryl **3.14** in 97% yield. This result underscores the critical tolerance of the sulfamate cross-coupling process to basic nitrogen substituents.

Scheme 3.3



3.6 Mechanistic Studies

Pd-catalyzed Suzuki–Miyaura cross-couplings have been studied computationally by various groups.^{30,31} The three key steps in the catalytic cycle, oxidative addition,³² transmetallation,³¹ and reductive elimination,³³ have been studied carefully for reactions involving a variety of substrates. The mechanism of Ni-catalyzed Suzuki–Miyaura cross-coupling with aryl acetates has been recently investigated theoretically by Li *et al.*³⁴ Here we report the first theoretical study of the catalytic cycles of the Ni-catalyzed Suzuki–Miyaura cross-coupling with *O*-carbamates and *O*-sulfamates using density functional theory (DFT). The selectivities between couplings with the Ar–O bond and the O–carbonyl/sulfonyl bond and the effects of water on the reactivities are also described.

Figures 3.2 and 3.3 depict the catalytic cycles for the Suzuki–Miyaura cross-coupling of aryl carbamates and sulfamates, respectively, as determined by DFT calculations. The geometries of important transition structures are shown in Figure 3.4 for the coupling of *N,N*-dimethyl phenyl carbamate and *N,N*-dimethyl phenyl sulfamate with phenyl boronic acid. The PCy_3 ligand used in the experiments was also used in the calculations. Geometry optimizations and frequency calculations were performed using B3LYP³⁵ and a mixed basis set employing LANL2DZ for metal and 6-31G(d) for other atoms. Conformational searches of the PCy_3 ligand were performed. The initial geometry of PCy_3 was taken from the crystal structure of

$\text{Ni}(\text{PCy}_3)(\text{C}_2\text{H}_4)_2$.³⁶ Several rotamers of the PCy_3 ligands in the Ni complexes were tested as the initial geometry in the optimizations. Energies reported are Gibbs free energies in solution, which involve zero-point vibrational energy corrections, thermal corrections to Gibbs free energy at 298 K, and solvation free energy corrections computed by singlet point CPCM³⁷ calculations on gas-phase optimized geometries (toluene was used as solvent). The molecular cavities were built up using the United Atom Topological Model (UAHF). Vibrational frequencies were calculated for all optimized structures to confirm the nature of the stationary points. All calculations were performed using Gaussian 03.³⁸

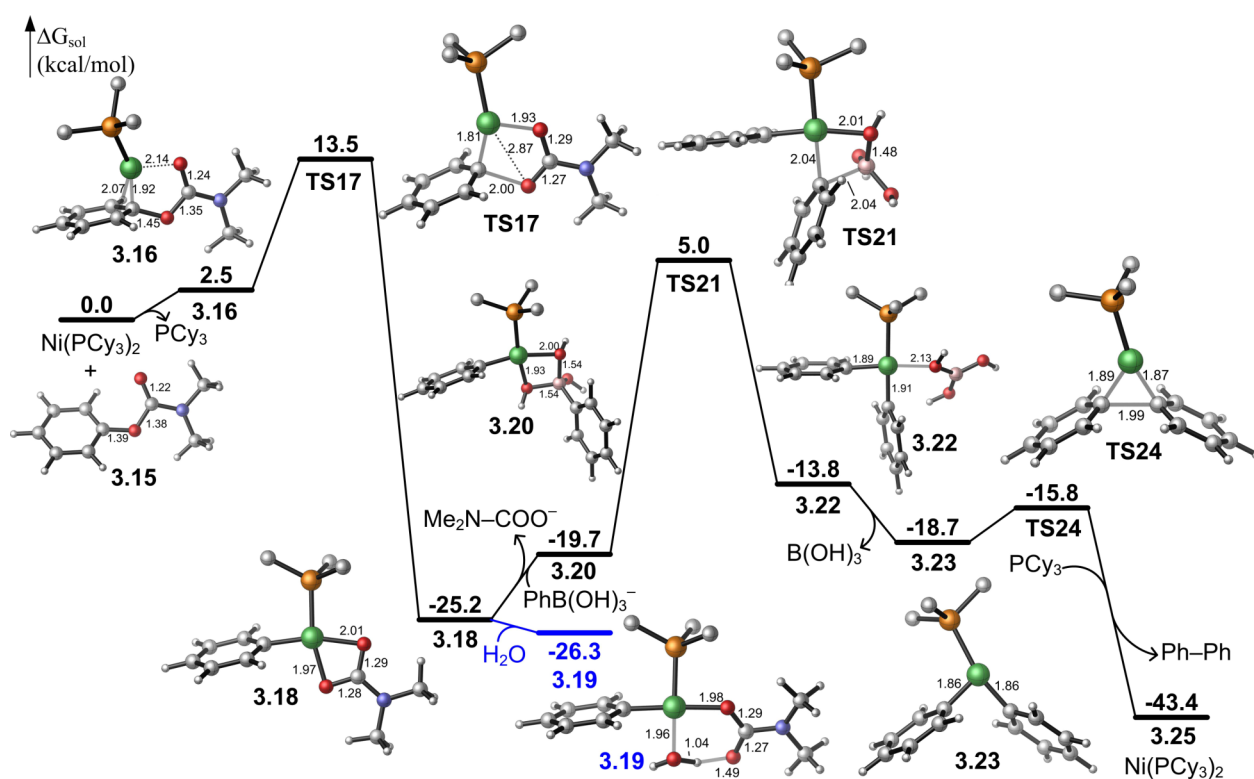


Figure 3.2. Gibbs free energy profile of Ni-catalyzed Suzuki–Miyaura cross-coupling reaction of phenyl *N,N*-dimethyl *O*-carbamate **3.15** with phenylboronic acid. PCy_3 was used as ligand in the calculations. For clarity, the cyclohexyl groups on the ligand are not shown.

The oxidative addition of aryl carbamates may occur via several different pathways: the Ni may be mono- or bis-ligated; the oxidative addition may occur at the Ph–O bond or the O–carbonyl bond of the carbamates. Previous theoretical studies suggested that the oxidative addition of aryl halides to Pd(0) catalysts involves formation of an η^2 LPd(ArX) pre-reaction complex.³² The η^2 LPd(ArX) complex may be generated through ligand dissociation from PdL₂ followed by coordination with aryl halide or through a concerted or stepwise associative displacement pathway.³⁹ Recent density functional calculations by Li *et al.* suggested that the oxidative addition of phenylacetates in Ni-catalyzed Suzuki–Miyaura couplings also involves an η^2 LNi(ArX) pre-reaction complex.^{8c} Upon dissociation of a PCy₃ ligand, the Ni catalyst coordinates with the substrate to generate an η^2 complex **3.16**, which is slightly less stable than Ni(PCy₃)₂.⁴⁰ Li *et al.* suggested that the oxidative addition of phenylacetates occurs via a three-centered transition state, and the weaker PhO–carbonyl bond is more reactive compared to the Ph–O bond.^{8c} We investigated the possible pathways in the oxidative additions with phenyl carbamates (Figures 3.2 and 3.4) and found that the preferred pathway involves oxidative addition at the Ph–O bond via a five-centered transition state (**TS17**, Figures 3.2 and 3.4) in which Ni is mono-ligated and coordinated with the carbonyl oxygen.^{41,42} The corresponding three-centered transition state (**TS30**) that uses a single oxygen of the carboxylate to bridge requires 7.4 kcal/mol higher activation energy. In contrast to previous theoretical studies by Li *et al.*, the Ph–O bond in carbamates is more reactive in oxidative addition than the PhO–carbonyl bond, although the former is a stronger bond in terms of bond dissociation energies.⁴³ Oxidative addition at the O–carbonyl bond can only occur via a three-centered transition state (**TS31**) and requires 3.9 kcal/mol higher energy than the oxidative addition at the Ph–O bond (**TS17**). Thus, the oxidative addition occurs exclusively at the Ph–O bond due to a favorable five-centered

transition state. The carbonyl group is acting as a directing group to activate the Ph–O bond in the oxidative addition. It is conceivable that such activating effects by adjacent oxygenation is also present in oxidative additions with carbonates, sulfonates, and sulfamates, etc.

A stable phenyl Ni(II)-carbamate complex **3.18** is formed after the oxidative addition (Figure 3.2). The carbamate is κ_2 -coordinated with Ni. Subsequent ligand exchange of the carbamate complex **3.18** with phenylboronate leads to phenyl Ni(II) boronate complex **3.20**, which is 5.5 kcal/mol less stable than the Ni-carbamate complex. The detailed mechanism of this ligand exchange step has been suggested to be stepwise.^{15a,44} Previous theoretical studies suggested that the ligand exchange does not have large barrier.^{8c,31b,g} Thus, we assume the transformation from **3.18** to **3.20** is facile.

The following transmetallation (**TS21**) is the rate-determining step of the catalytic cycle, and requires an activation energy of 30.2 kcal/mol from the catalyst resting complex **3.18**. The transmetallation transition state (**TS21**) is consistent with the four-center transition state proposed in previous theoretical studies of Pd- and Ni-catalyzed Suzuki–Miyaura couplings.^{31,8c} The two aryl groups are *cis* to each other in the transmetallation transition state. The *trans* transition state is 3.5 kcal/mol less stable, presumably due to greater steric repulsions between the ligand and the aryl groups. Subsequent reductive elimination of the diphenyl Ni(II) complex (**3.23** → **TS24**) is facile, requiring only a 2.9 kcal/mol activation energy.

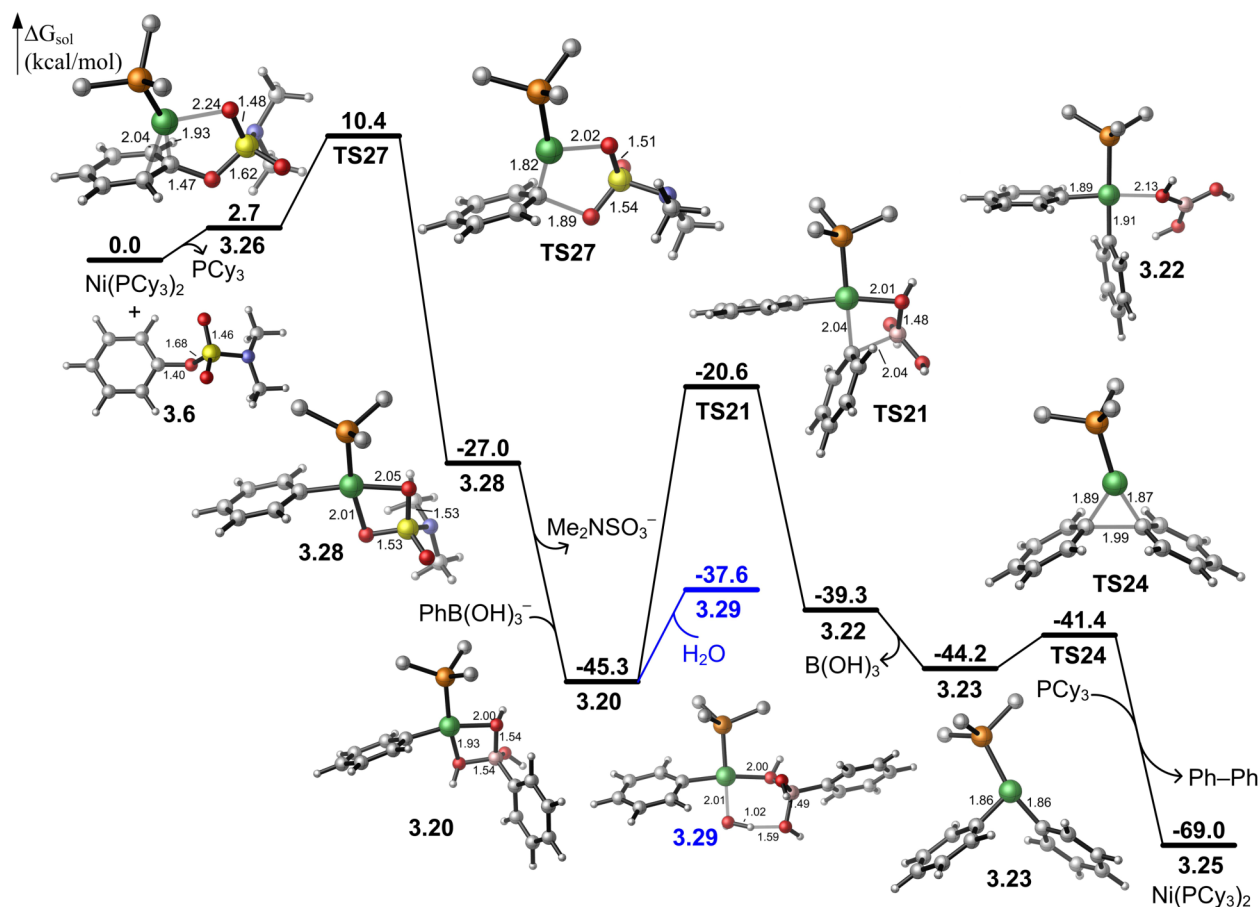


Figure 3.3. Gibbs free energy profile of the Ni-catalyzed Suzuki–Miyaura cross-coupling reaction of *N,N*-dimethyl phenyl *O*-sulfamate with phenylboronic acid. PCy₃ was used as ligand in the calculations. For clarity, the cyclohexyl groups on the ligand are not shown.

Similarly, the oxidative addition of *N,N*-dimethyl phenyl sulfamate occurs via a mono-ligated five-membered transition state (TS27).⁴¹ Three-center transition states TS32 and TS33 are both much higher in energy (Figure 3.4). The activation barrier of oxidative additions of sulfamate **3.6** is 10.4 kcal/mol with respect to the Ni(PCy₃)₂ complex, which is 3.1 kcal/mol lower than that of the oxidative addition of *N,N*-dimethyl phenyl carbamate **3.15**. The higher reactivity of the sulfamate in oxidative addition is due to the weaker Ph–O bond in sulfamate than the corresponding Ph–O bond in the carbamate group. Nonetheless, the oxidative addition with aryl carbamates and aryl sulfamates are both predicted to be very facile. The differences of

their reactivities are attributed to the different activation barriers in the rate-determining transmetalation step. After the oxidative addition of the carbamate, a stable phenyl Ni(II)-carbamate complex **3.18** is formed. Subsequent ligand exchange with phenyl boronate requires 5.5 kcal/mol energy to form the Ni(II) boronate complex **3.20**. In contrast, since sulfamate is a better leaving group, the Ni(II) boronate complex **3.20** is formed spontaneously from the Ni(II)-sulfamate complex **3.28**. The activation barrier of the rate-determining transmetalation step for the cross-coupling with the sulfamate ($\Delta G^\ddagger = 24.7$ kcal/mol) is much lower than that for the corresponding carbamate ($\Delta G^\ddagger = 30.2$ kcal/mol). The subsequent steps after transmetalation are identical for the coupling reactions for carbamates and sulfamates.

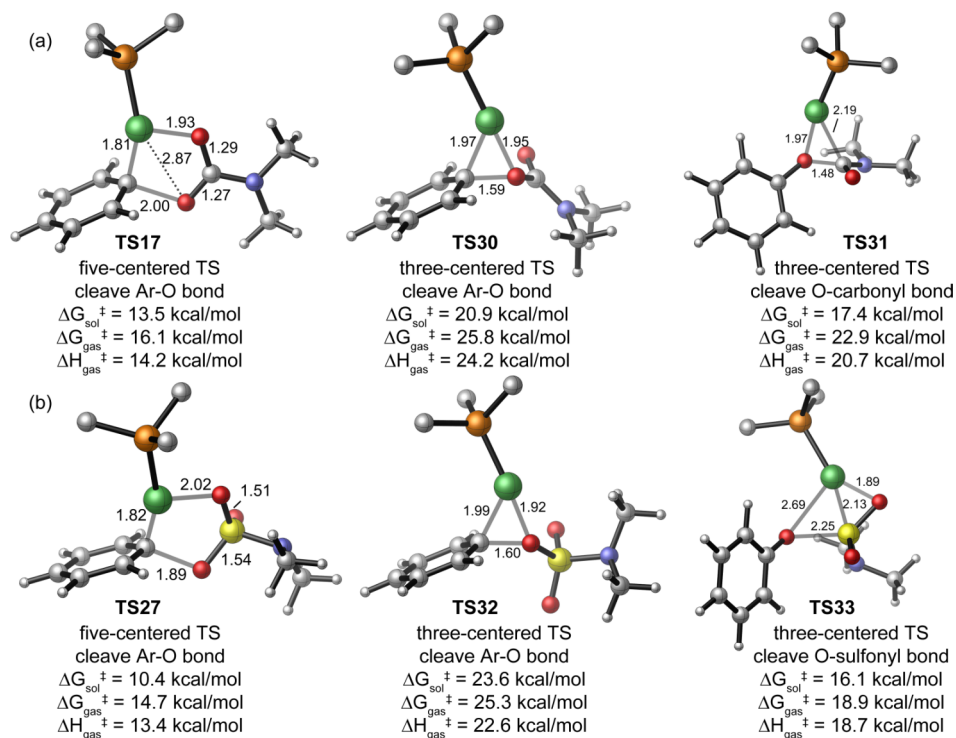


Figure 3.4. Transition state structures of Ni-catalyzed oxidative additions of (a) *N,N*-dimethyl phenyl *O*-carbamate and (b) *N,N*-dimethyl phenyl *O*-sulfamate. PCy₃ was used as ligand in the calculations. For clarity, the cyclohexyl groups on the ligand are not shown.

To support the computational finding that transmetalation is the rate-determining step in the cross-coupling reactions described above, a series of experiments were carried out. Sulfamate **3.34** was independently subjected to reactions with boronic acids **3.1a**, **3.2a**, and **3.4a** in the presence of $\text{NiCl}_2(\text{PCy}_3)_2$ and K_3PO_4 in toluene at $80\text{ }^\circ\text{C}$ (Figure 3.5). In each case, reaction progress was monitored by ^1H NMR analysis using hexamethylbenzene as internal standard. The relative rate of cross-coupling was found to be dependent on the individual boronic acid employed, with a direct correlation between electron-richness of the boronic acid and reaction rate (i.e., relative rate of conversion: **3.1a**>**3.2a**>**3.4a**).⁴⁵ These findings are consistent with a rate-determining transmetalation step for the sulfamate cross-coupling process.⁴⁶

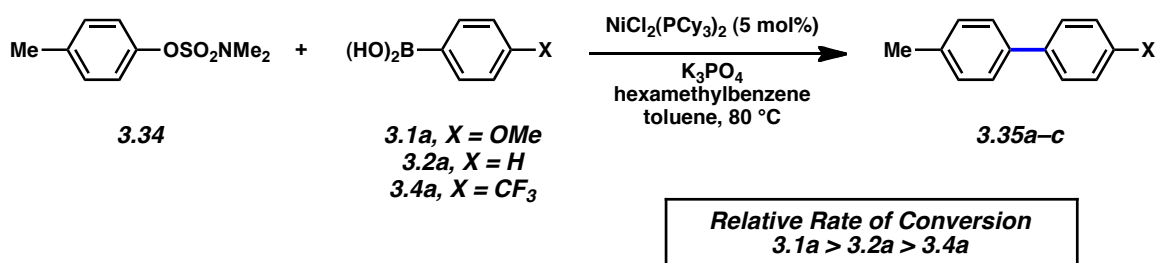


Figure 3.5. Qualitative relative rates of cross-coupling depending on boronic acid.

Similar to the reports by Shi in related Ni-catalyzed Suzuki–Miyaura cross-couplings,^{8b} we have observed that water can play a critical role in the success or failure of a coupling reaction (*vide supra*). To better understand these experimental findings, we examined the role of water computationally. In the coupling with phenyl carbamate, water can coordinate with Ni and stabilize the catalyst resting state, the Ni-carbamate complex **3.18**. A six-membered cyclic Ni(II)-water-carbamate complex **3.19** is formed and is 1.1 kcal/mol more stable than **3.18** (Figure 3.2).⁴⁷ Coordination with water increases the barrier of transmetalation to 31.3 kcal/mol (**3.19** →

TS21), and thus decreases the reactivity of the coupling for the carbamate. In the coupling with phenyl sulfamate, the catalyst resting state is the Ni(II)-boronate complex **3.20**. Upon coordination with a water molecule, a similar six-membered cyclic complex **3.29** is formed in equilibrium. However, **3.29** is 7.7 kcal/mol less stable than **3.20**. This suggests that coordination with water does not affect the barrier of transmetalation in the coupling reaction of the sulfamate. This agrees with the experimental observation that Suzuki–Miyaura cross-couplings of aryl sulfamates are less sensitive to water than couplings of aryl carbamates.

In contrast to the high reactivity of the Ni catalyst in oxidative addition with carbamates and sulfamates, Pd catalysts are much less reactive in the oxidative addition step. Oxidative addition of phenyl *N,N*-dimethylcarbamate with Pd also prefers a five-membered mono-ligated transition state. The activation barrier is 42.2 kcal/mol with respect to the Pd(PCy₃)₂ complex, much higher than that of the corresponding Ni catalyst. Similarly, oxidative addition of phenyl *N,N*-dimethylsulfamate also requires a very high activation barrier of 39.7 kcal/mol. These observations are in agreement with previous mechanistic and theoretical studies that the oxidative addition step to Ni(0) is more facile than that to Pd(0).^{32,40} Therefore, due to the extremely high activation barriers for oxidative addition, Pd catalysts are not effective in couplings with carbamates and sulfamates.

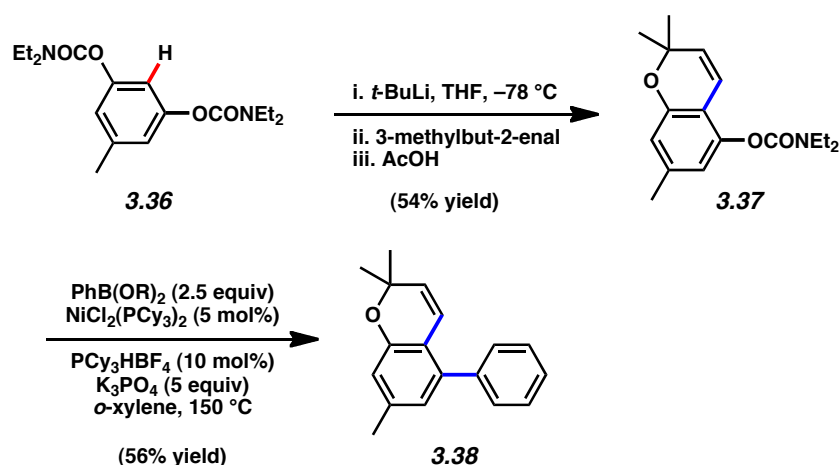
3.7 Synthetic Applications

The scope and limitations of our sulfamate and carbamate coupling methodologies were further examined by way of a variety of synthetic applications. In each of the studies undertaken, the synthetically useful capability of carbamates and sulfamates to function as directed metalation groups (DMGs) and Suzuki–Miyaura coupling partners was exploited. These studies

showcase the utility of our methodology in the synthesis of polysubstituted aromatic compounds, with relevance to natural product and bioactive molecule synthesis.

Scheme 3.4 depicts a concise synthesis of 5-phenyl-2*H*-chromene **3.38** beginning from bis(carbamate) precursor **3.36**. Thus, in a one-pot procedure involving sequential treatment with *t*-BuLi, 3-methylbut-2-enal, and AcOH, compound **3.36** was converted into 2*H*-chromene carbamate **3.37**.^{48,49} Subsequent Suzuki–Miyaura cross-coupling provided biaryl **3.38** in 56% yield. Biaryl **3.38** possesses a heterocyclic framework of bioactivity⁵⁰ and natural product interest.⁵¹

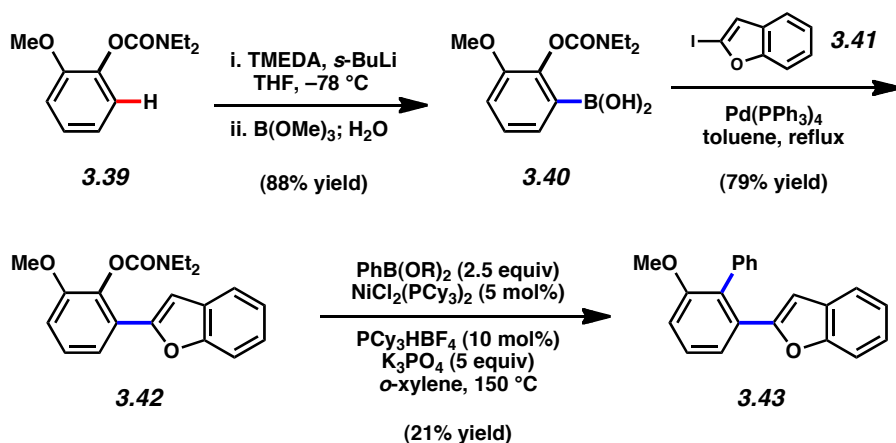
Scheme 3.4



In another application, the unique heterotriaryl **3.43** was constructed using carbamate DoM and cross-coupling methodology (Scheme 3.5). *ortho*-Methoxy carbamate **3.39** was first transformed into boronic acid **3.40** in 88% yield using a standard lithiation/borylation protocol. Subsequent Pd-catalyzed Suzuki–Miyaura cross-coupling with iodobenzofuran **3.41** delivered arylated product **3.42** without disturbance of the aryl carbamate under these conditions.⁵² The

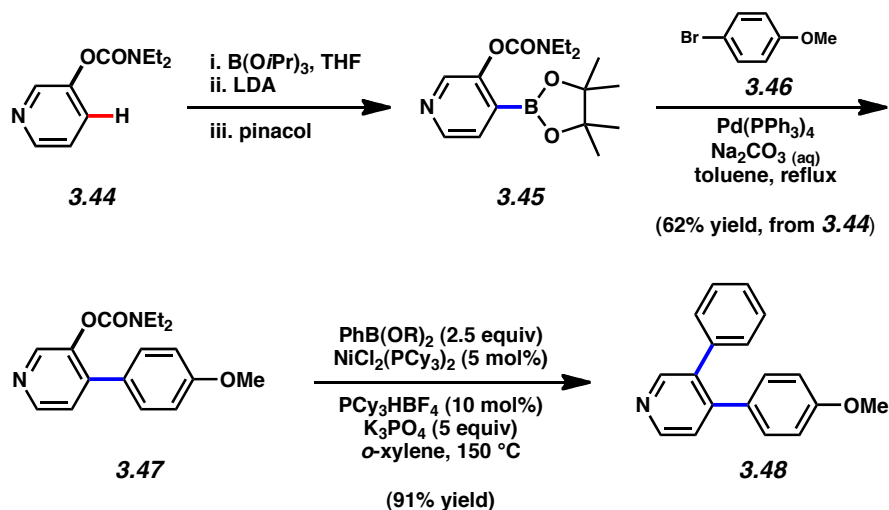
subsequent Ni-catalyzed carbamate cross-coupling with phenyl boronic acid provided the targeted heterotriaryl **3.43**.⁵³

Scheme 3.5



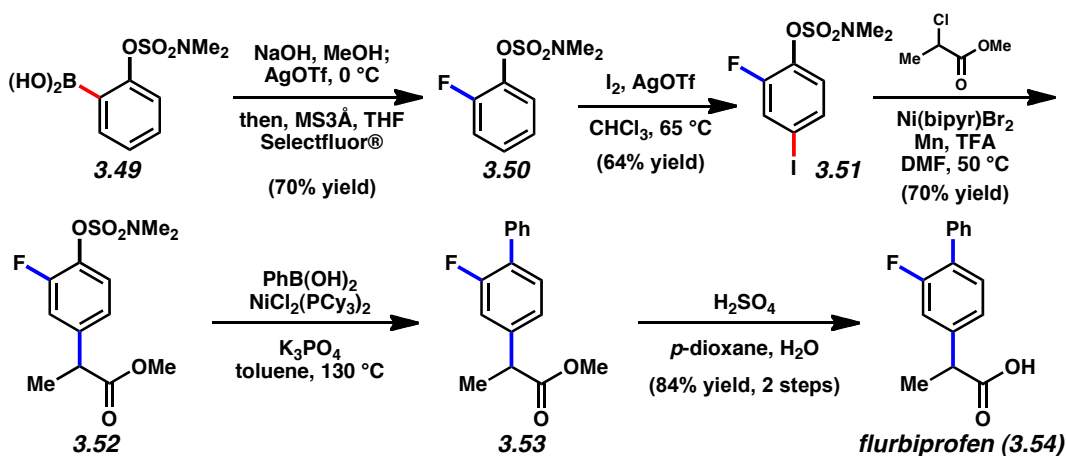
An illustration of the DoM / cross-coupling protocol beginning from a heteroaryl carbamate is presented in Scheme 3.6. Lithiation / borylation of **3.44** afforded the boropinacolate **3.45**, which was subjected to standard Suzuki-Miyaura cross-coupling conditions with bromide **3.46** using Pd catalysis to furnish heterobiaryl **3.47**.⁵⁴ Heteroaryl carbamate **3.47** was found to be an excellent substrate for the Ni-catalyzed cross-coupling using our standard conditions, to afford the heterotriaryl product **3.48** in 91% yield. Compound **3.48** represents a class of pyridines with nonidentical diaryl substitution for which only two synthetic methods are available.⁵⁵

Scheme 3.6



As an application to bioactive molecule synthesis, the anti-inflammatory drug flurbiprofen⁵⁶ was prepared using sulfamate methodology (Scheme 3.7). Boronic acid **3.49**, derived from *o*-lithiation / borylation of *N,N*-dimethyl phenyl sulfamate, was fluorinated using the conditions described by Furuya and Ritter⁵⁷ to provide fluorosulfamate **3.50**. Alternative routes to generate **3.50** by direct lithiation/fluorination of *N,N*-dimethyl phenyl sulfamate were unsuccessful despite numerous attempts.⁵⁸ Nonetheless, *para*-selective electrophilic iodination of **3.50** furnished **3.51** in 64% yield. With the aryl sulfamate being inert to Pd catalysis, we carried out a site-selective enolate coupling to install the necessary propionate side chain. Whereas enolate coupling of aryl iodide **3.51** under Buchwald's Pd-based conditions was feasible,⁵⁹ higher yields of **3.52** were obtained using a Ni-catalyzed variant.⁶⁰ With the sulfamate remaining undisturbed, exposure of **3.52** to our Ni-catalyzed conditions facilitated the key sulfamate cross-coupling and delivered the biaryl **3.53**. Acid-mediated hydrolysis furnished flurbiprofen (**3.54**) in 84% yield over the two steps. It should be emphasized that the aryl fluoride of **3.52** was chemically inert under our Ni-catalyzed cross-coupling conditions.⁶¹

Scheme 3.7



We have observed that aryl carbamates and sulfamates are unreactive toward Pd(0) catalysis (*vide supra*) and related processes.⁶² This feature allows the sequential cross-coupling of an aryl halide, followed by either an aryl sulfamate or carbamate coupling process (see Scheme 3.7). To further probe related issues of orthogonality, we questioned if it would be possible to couple aryl sulfamates in the presence of aryl carbamates. Although aryl sulfamates generally provide higher yields of cross-coupled products compared to aryl carbamates, the relative reactivity of these substrates had not been determined previously. As shown in Figure 3.6, an equimolar mixture of phenyl carbamate **3.55** and phenyl sulfamate **3.6** was treated with an excess of boronic acid **3.3a** under Ni-catalyzed cross-coupling conditions. Although significant selectivity was observed at elevated temperatures, complete selectivity for sulfamate coupling was readily achieved at 50 °C, as determined by ¹H NMR analysis with hexamethylbenzene as internal standard.⁴⁵ The selectivity for sulfamate coupling is attributed to the lower oxidative addition barrier than that in the corresponding step for carbamates (see above computational studies). Analogous experiments were conducted on the naphthyl-based

substrates, carbamate **3.56** and sulfamate **3.57**, and a high selectivity for naphthyl sulfamate over carbamate cross-coupling was observed at 40 °C.⁴⁵ We expect that these observations will be of synthetic value.

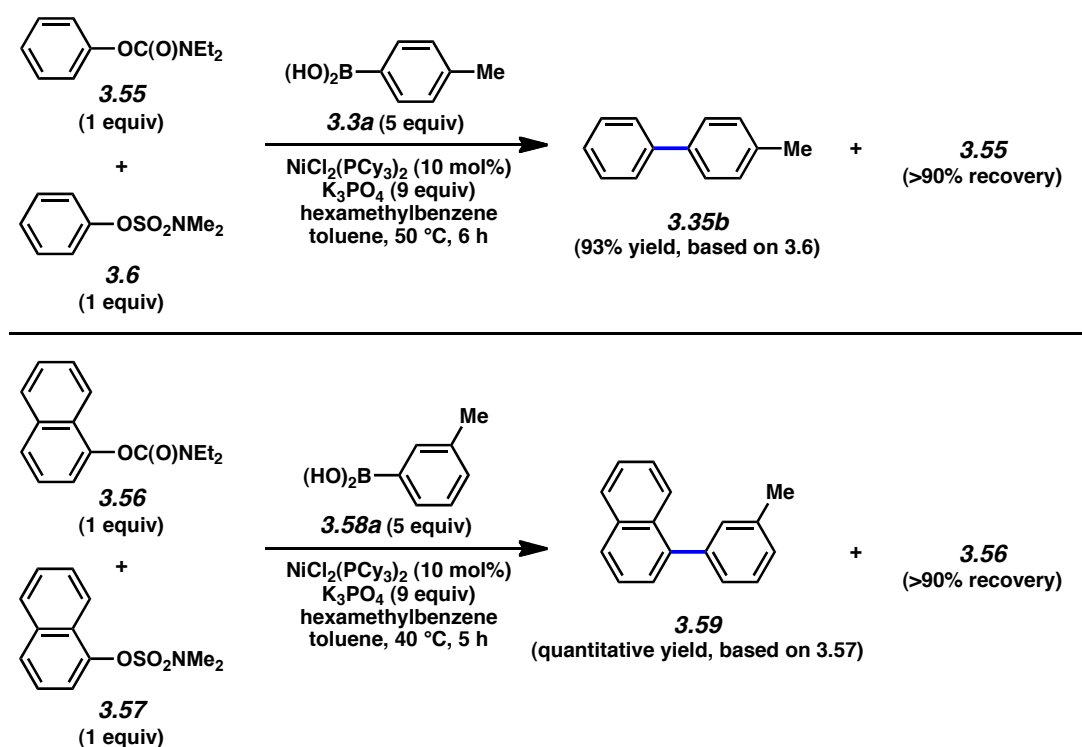


Figure 3.6. Intermolecular competition experiments of aryl sulfamates and aryl carbamates.

3.8 Conclusion

In summary, we have discovered the first Suzuki–Miyaura cross-coupling reactions of the synthetically versatile *O*-aryl carbamate and *O*-sulfamate groups. The transformations utilize the inexpensive, bench-stable catalyst $\text{NiCl}_2(\text{PCy}_3)_2$ to deliver biaryls in good to excellent yields. The methodology is tolerant of substrates bearing electron-donating and electron-withdrawing groups, in addition to those that possess *ortho* substituents and heterocyclic frameworks. Furthermore, a computational study has revealed the full catalytic cycles for these cross-coupling

reactions, thus shedding light on various mechanistic details, rationalizing sulfamate over carbamate higher reactivity, and indicating the role of water in the transition state. As demonstrated by the given synthetic applications, the methodology provides an efficient means to access polysubstituted aromatic compounds, with relevance to both natural product and bioactive molecule synthesis. The orthogonal use of the sulfamate or carbamate reactivities, in combination with directed *ortho* metalation (DoM) and other aryl *O*-based cross-coupling reactions in arene and heteroarene synthesis, may be anticipated.

3.9 Experimental Section

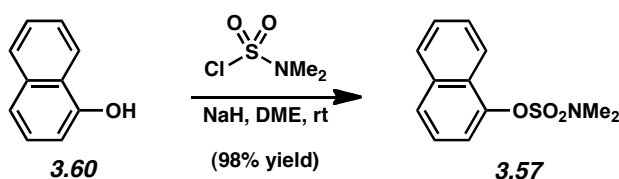
3.9.1 Materials and Methods

Unless stated otherwise, reactions were conducted in flame-dried glassware under an atmosphere of nitrogen using anhydrous solvents (either freshly distilled or passed through activated alumina columns). All commercially obtained reagents were used as received. NiCl_2 (anhydrous) and PCy_3 were obtained from Strem Chemicals. Finely powdered anhydrous K_3PO_4 was obtained from Acros.⁶³ Boronic acids were obtained from Oakwood Products, Inc., Frontier Scientific, Inc. and TCI. Reaction temperatures were controlled using an IKA Mag temperature modulator, and unless stated otherwise, reactions were performed at room temperature (rt, approximately 23 °C). Thin-layer chromatography (TLC) was conducted with EMD gel 60 F254 pre-coated plates (0.25 mm) and visualized using a combination of UV, anisaldehyde, ceric ammonium molybdate, iodine, and potassium permanganate staining. EMD silica gel 60 (particle size 0.040–0.063 mm) was used for flash column chromatography. ^1H NMR spectra were recorded on Bruker spectrometers (at 500 MHz) and are reported relative to deuterated solvent signals. Data for ^1H NMR spectra are reported as follows: chemical shift (δ ppm), multiplicity, coupling constant (Hz) and integration. ^{13}C NMR spectra were recorded on Bruker Spectrometers (at 125 MHz). Data for ^{13}C NMR spectra are reported in terms of chemical shift. IR spectra were recorded on a Perkin-Elmer 100 spectrometer and are reported in terms of frequency of absorption (cm^{-1}). Melting points are uncorrected and were obtained on a Laboratory Devices Mel-Temp II instrument. High resolution mass spectra were obtained from the UC Irvine Mass Spectrometry Facility.

3.9.2 Experimental Procedures

Note: Supporting information for aryl carbamates (synthesis and cross-couplings) and synthetic applications have previously been reported.^{9a,b}

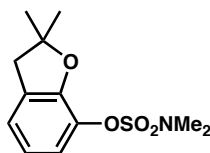
A. Synthesis of Aryl Sulfamate Substrates



Representative Procedure (sulfamate 3.57 is used as an example). A round bottom flask was charged with NaH (0.60 g, 15.12 mmol, 1.2 equiv, 60% dispersion in oil). Then a solution of 1-naphthol (**3.60**) (1.82 g, 12.60 mmol, 1 equiv) in DME (32 mL) was added dropwise via cannula to the NaH. A solution of dimethylsulfamoyl chloride (1.30 mL, 11.97 mmol, 0.95 equiv) in DME (10 mL) was then added dropwise via cannula to the reaction vessel. The reaction was allowed to stir for 17 h, and then quenched with H₂O (2 mL). The volatiles were removed under reduced pressure, and then Et₂O (20 mL) and H₂O (15 mL) were added. The layers were separated, and the organic layer was washed successively with a solution of 1 M KOH (10 mL) and H₂O (20 mL). The combined aqueous layers were extracted with Et₂O (3 x 15 mL). The combined organic layers were then washed with brine (15 mL), dried over MgSO₄, and concentrated under reduced pressure. The crude residue was purified by flash chromatography (4:1 Hexanes:EtOAc) to yield 1-naphthylsulfamate **3.57** as a white solid (2.97 g, 98% yield). *R*_f 0.29 (4:1 Hexanes:EtOAc); ¹H NMR (500 MHz, CDCl₃): δ 8.18 (d, *J* = 8.5, 1H), 7.88 (d, *J* = 7.5, 1H), 7.77 (d, *J* = 8.0, 1H), 7.60-7.53 (m, 3H), 7.46 (t, *J* = 8.0, 1H), 3.07 (s, 6H); ¹³C NMR (125 MHz, CDCl₃): δ 146.0, 134.7, 127.8, 127.0, 126.7, 126.7, 126.6, 125.3, 121.4, 117.7, 38.8;

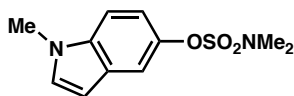
IR (film): 3065, 2944, 195, 1456, 1357 cm^{-1} ; HRMS-ESI (m/z) $[\text{M} + \text{Na}]^+$ calcd for $\text{C}_{12}\text{H}_{13}\text{NO}_3\text{SNa}$, 274.0514; found, 274.0511.

Note: Supporting information for the synthesis of the aryl sulfamates shown in Tables 3.6 and 3.7 have previously been reported.^{9b}



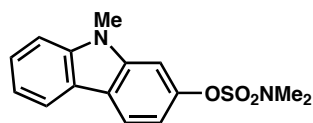
3.61

Sulfamate 3.61 (Table 3.9, entry 1). Purification by flash chromatography (5:1 Benzene:Et₂O) afforded **3.61** as a light yellow oil (66% yield). R_f 0.70 (5:1 Benzene:Et₂O); ¹H NMR (500 MHz, CDCl₃): δ 7.16 (dd, $J = 8.2, 0.7$, 1H), 7.03 (dd, $J = 7.4, 1.1$, 1H), 6.79 (dd, $J = 8.0, 7.5$ 1H), 3.06 (s, 2H), 2.97 (s, 6H), 1.51 (s, 6H); ¹³C NMR (125 MHz, CDCl₃): δ 150.4, 134.3, 130.1, 123.5, 122.7, 120.4, 88.6, 43.2, 38.8, 28.4; IR (film): 2927, 1617, 1478, 1372, 1172, 1009 cm^{-1} ; HRMS-ESI (m/z) $[\text{M} + \text{Na}]^+$ calcd for $\text{C}_{12}\text{H}_{17}\text{NO}_4\text{SNa}$, 294.0776; found, 294.0779.



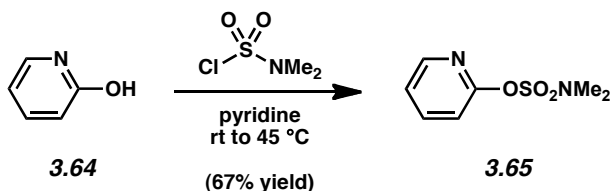
3.62

Sulfamate 3.62 (Table 3.9, entry 2). Supporting information for the synthesis of sulfamate **3.62** has previously been reported.^{9b}



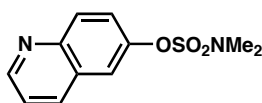
3.63

Sulfamate 3.63 (Table 3.9, entry 3). Purification by flash chromatography (2:1 Hexanes:EtOAc) afforded **3.63** as a white solid (78% yield). R_f 0.70 (1:1 Hexanes:EtOAc); ^1H NMR (500 MHz, CDCl_3): δ 8.07-8.04 (m, 2H), 7.49 (t, $J = 7.5$, 1H), 7.39 (d, $J = 8.0$, 1H), 7.37 (s, 1H), 7.26 (t, $J = 7.5$, 1H), 7.13 (d, $J = 8.0$, 1H), 3.82 (s, 3H), 3.02 (s, 6H); ^{13}C NMR (125 MHz, CDCl_3): δ 148.5, 141.6, 141.2, 125.8, 122.1, 121.3, 210.8, 120.2, 119.4, 112.6, 108.6, 102.1, 38.7, 29.2; IR (film): 2935, 1599, 1452, 1359, 1179 cm^{-1} ; HRMS-ESI (m/z) $[\text{M} + \text{Na}]^+$ calcd for $\text{C}_{15}\text{H}_{16}\text{N}_2\text{O}_3\text{SNa}$, 327.0779; found, 327.0774.



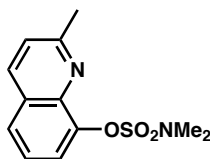
Sulfamate 3.65 (Table 3.9, entry 4). To a solution of 2-hydroxypyridine (**3.64**) (2.00 g, 21.05 mmol, 1 equiv) in pyridine (21.1 mL) was added dimethylsulfamoyl chloride (2.7 mL, 25.26 mmol, 1.2 equiv) dropwise via syringe. The resulting orange solution was heated to 45 °C and allowed to stir for 22 h. After cooling to 23 °C, the solution was diluted with Et_2O (60 mL) and 1 M KOH (15 mL), and the layers were separated. The aqueous layer was extracted with Et_2O (2 x 60 mL), followed by EtOAc (1 x 60 mL). The combined organic layers were then washed with brine (10 mL), dried over MgSO_4 , and concentrated under reduced pressure. The crude residue was purified by flash chromatography (3:2 Hexanes:EtOAc) to yield **3.65** as a yellow oil (67% yield). R_f 0.29 (2:1 Hexanes: EtOAc); ^1H NMR (500 MHz, CDCl_3): δ 8.26-8.24 (m, 1H), 7.72-

7.69 (m, 1H), 7.16 (m, 1H), 7.06 (d, $J = 2.0$, 1H), 2.92 (s, 6H); ^{13}C NMR (125 MHz, CDCl_3): δ 157.1, 147.9, 140.0, 122.1, 115.0, 38.3; IR (film): 2941, 1591, 1430, 1375, 1162 cm^{-1} ; HRMS-ESI (m/z) [$\text{M} + \text{Na}$] $^+$ calcd for $\text{C}_7\text{H}_{10}\text{N}_2\text{O}_3\text{SNa}$, 225.0310; found, 225.0305.



3.12

Sulfamate 3.66 (Table 3.9, entry 5). Purification by flash chromatography (100% Et_2O) afforded **3.12** as a white solid (84% yield). R_f 0.50 (4:1 Hexanes:EtOAc); ^1H NMR (500 MHz, CDCl_3): δ 8.91 (dd, $J = 4.5, 2.0$, 1H), 8.16-8.10 (m, 2H), 7.75 (d, $J = 2.5$, 1H), 7.60 (dd, $J = 9.0, 2.5$, 1H), 7.42-7.38 (m, 1H), 3.02 (s, 6H); ^{13}C NMR (125 MHz, CDCl_3): δ 150.7, 147.9, 146.5, 135.9, 131.6, 128.4, 124.2, 121.8, 118.7, 38.7; IR (film): 2979, 1498, 1174, 1113, 791 cm^{-1} ; HRMS-ESI (m/z) [$\text{M} + \text{Na}$] $^+$ calcd for $\text{C}_{11}\text{H}_{12}\text{N}_2\text{O}_3\text{SNa}$, 275.0446; found, 275.0470.

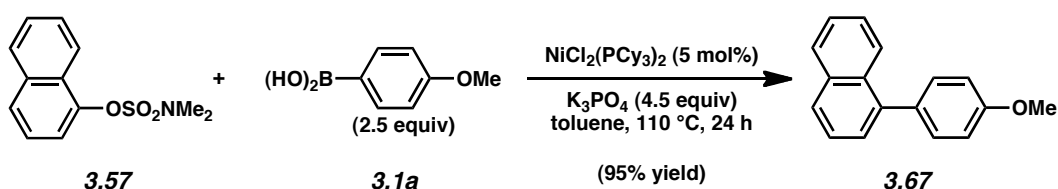


3.66

Sulfamate (Table 3.9, entry 6). Purification by flash chromatography (2:1 Hexanes:EtOAc) afforded **3.66** as a white solid (78% yield). R_f 0.44 (2:1 Hexanes:EtOAc); ^1H NMR (500 MHz, CDCl_3): δ 8.05 (d, $J = 8.5$, 1H), 7.74 (d, $J = 8.0$, 1H), 7.69 (d, $J = 8.0$, 1H), 7.46 (t, $J = 8.0$, 1H), 7.33 (d, $J = 8.5$, 1H), 3.04 (s, 6H), 2.76 (s, 3H); ^{13}C NMR (125 MHz, CDCl_3): δ 159.6, 145.7, 136.0, 127.8, 126.1, 125.3, 122.7, 122.6, 38.9, 25.4; IR (film): 2922, 1426, 1369, 1167, 1069 cm^{-1} ; HRMS-ESI (m/z) [$\text{M} + \text{Na}$] $^+$ calcd for $\text{C}_{12}\text{H}_{14}\text{N}_2\text{O}_3\text{SNa}$, 289.0623; found, 289.0624.

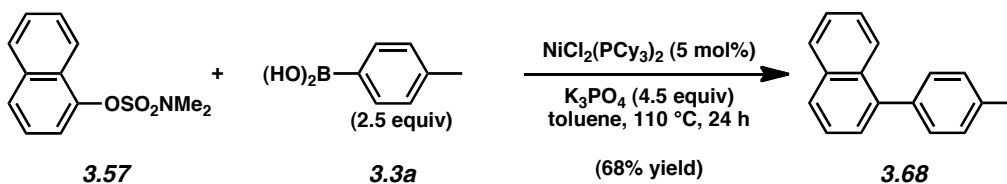
B. Cross-Coupling Reactions of Aryl Sulfamates

Note: Supporting information for the cross-coupling of the aryl sulfamates shown in Tables 3.6 and 3.7 have previously been reported.^{9b}

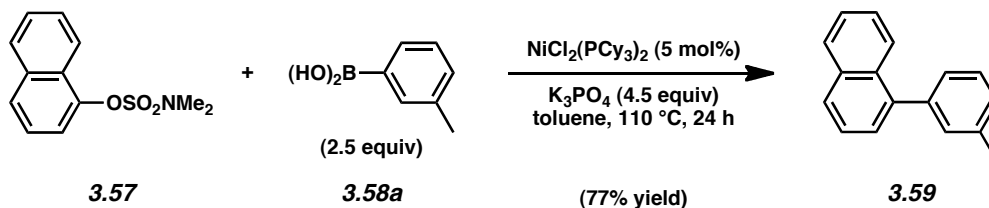


Representative Procedure (coupling of naphthyl sulfamate 3.57, Table 3.6, entry 1) is used as an example). Biaryl 3.67. A 1-dram vial was charged with anhydrous powdered K_3PO_4 (382 mg, 1.80 mmol, 4.5 equiv, *obtained from Acros*) and a magnetic stir bar. The vial and contents were flame-dried under reduced pressure, then allowed to cool under N_2 . Boronic acid **3.1a** (152 mg, 1.00 mmol, 2.5 equiv), $\text{NiCl}_2(\text{PCy}_3)_2$ (13.7 mg, 0.02 mmol, 5 mol%), and sulfamate substrate **3.57** (100 mg, 0.40 mmol, 1 equiv) were added. The vial was then evacuated and backfilled with N_2 . Toluene (1.5 mL) was added and the vial was sealed with a Teflon-lined screw cap. The heterogeneous mixture was allowed to stir at 23 °C for 1 h, then heated to 110 °C for 24 h. The reaction vessel was cooled to 23 °C and then transferred to a round bottom flask containing CH_2Cl_2 (20 mL). Silica gel (3 mL) was added and the solvent was removed under reduced pressure to afford a free-flowing powder. This powder was then dry-loaded onto a silica gel column (4.5 x 5 cm) and purified by flash chromatography (2:1 Hexanes: Benzene) to yield biaryl product **3.67** (89 mg, 95% yield) as a colorless solid. R_f 0.35 (2:1 Hexanes: Benzene); ^1H NMR (500 MHz, CDCl_3): δ 7.95 (d, $J = 8.5$, 1H), 7.92 (d, $J = 8.5$, 1H), 7.86 (d, $J = 8.5$, 1H), 7.57-7.48 (m, 2H), 7.48-7.39 (m, 4H), 7.06 (d, $J = 8.5$, 2H), 3.92 (s, 3H). All spectral data are consistent with those previously reported.⁶⁴

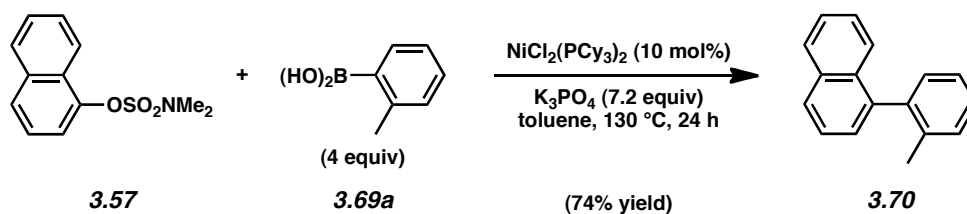
Any modifications of the conditions shown in this representative procedure are specified in the following schemes, which depict all of the results shown in Table 3.8–3.10 and Scheme 3.3.



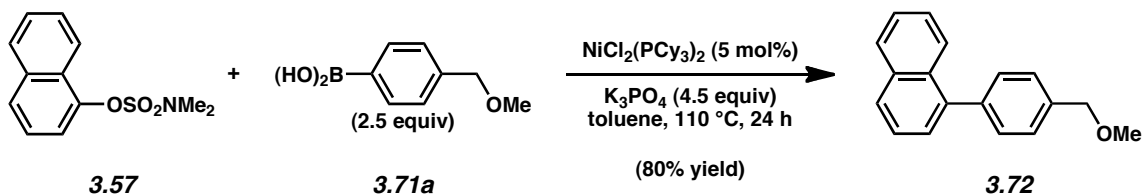
Biaryl 3.68 (Table 3.8, entry 1). Purification by flash chromatography (100% Hexanes) afforded a mixture (30.8 to 1) of biaryl product **3.68** (68% yield) and 4,4'-dimethylbiphenyl. R_f 0.74 (9:1 Hexanes:EtOAc). All spectral data are consistent with those previously reported.⁶⁵



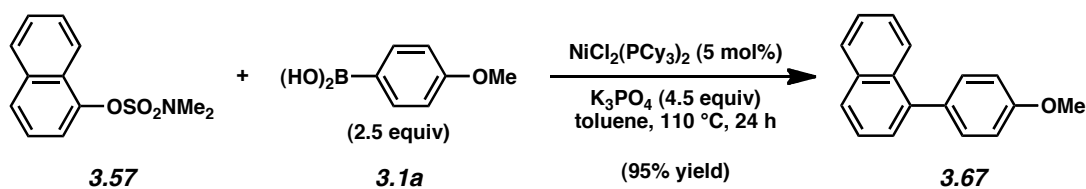
Biaryl 3.59 (Table 3.8, entry 2). Purification by flash chromatography (100% Hexanes) afforded a mixture (15.8 to 1) of biaryl product **3.59** (77% yield) and 3,3'-dimethylbiphenyl. R_f 0.66 (9:1 Hexanes:EtOAc). All spectral data are consistent with those previously reported.⁶⁶



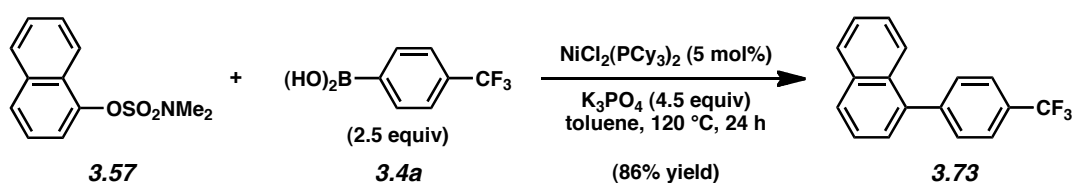
Biaryl 3.70 (Table 3.8, entry 3). Purification by flash chromatography (100% Hexanes) afforded a mixture (51.8 to 1) of biaryl product **3.70** (74% yield) and 2,2'-dimethylbiphenyl. R_f 0.66 (9:1 Hexanes:EtOAc). All spectral data are consistent with those previously reported.⁶⁷



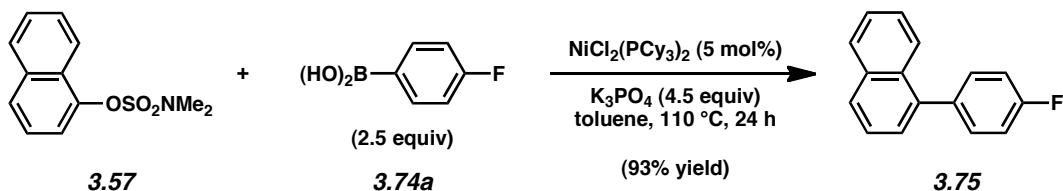
Biaryl 3.72 (Table 3.8, entry 4). Purification by flash chromatography (9:1 Hexanes:EtOAc) afforded **3.72** as a clear oil (80% yield). R_f 0.58 (9:1 Hexanes:EtOAc); ^1H NMR (500 MHz, C_6D_6): δ 8.02 (d, $J = 8.4$, 1H), 7.70 (d, $J = 8.1$, 1H), 7.65 (d, $J = 7.9$, 1H), 7.38 (d, $J = 7.9$, 2H), 7.35-7.25 (m, 5H), 7.22 (m, 1H) 4.31 (s, 2H), 3.18 (s, 3H); ^{13}C NMR (125 MHz, C_6D_6): δ 140.0, 139.8, 137.5, 133.8, 131.7, 129.7, 127.6, 127.4, 127.4, 127.2, 127.2, 126.7, 125.9, 125.7, 125.4, 125.1, 73.8, 57.3; IR (film): 2923, 1592, 1504, 1395, 1096 cm^{-1} ; HRMS-ESI (m/z) [$\text{M} + \text{NH}_4$]⁺ calcd for $\text{C}_{18}\text{H}_{16}\text{ONH}_4$, 266.1545; found, 266.1550.



Biaryl 3.67 (Table 3.8, entry 5). Purification by flash chromatography (2:1 Hexanes:Benzenes) afforded **3.67** as a white solid (95% yield). R_f 0.35 (2:1 Hexanes:Benzenes). Spectral data match those reported above.

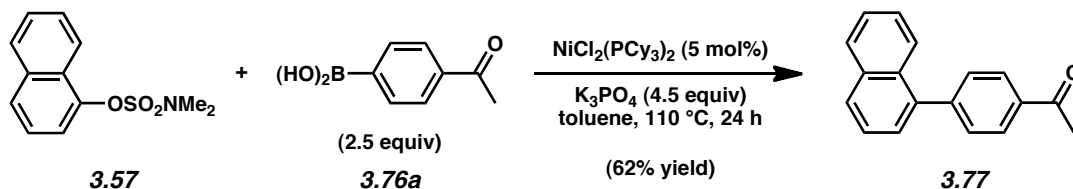


Biaryl 3.73 (Table 3.8, entry 6). Purification by flash chromatography (2:1 Hexanes:Benzenes) afforded a mixture (25.0 to 1) of biaryl product **3.73** (86% yield) and 4,4'-bis(trifluoromethyl)biphenyl. R_f 0.76 (2:1 Hexanes:Benzenes). All spectral data are consistent with those previously reported.⁶⁸

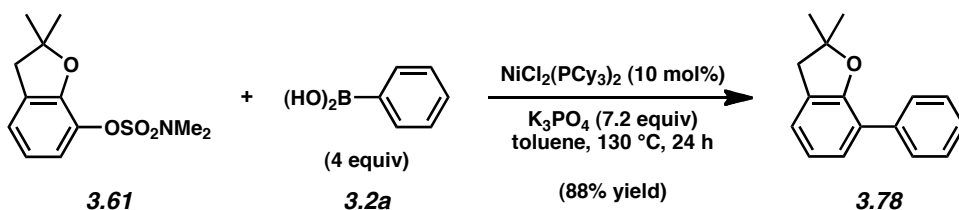


Biaryl 3.75 (Table 3.8, entry 7). Purification by flash chromatography (20:1 Hexanes:EtOAc) afforded **3.75** as a white solid (93% yield). R_f 0.61 (9:1 Hexanes:EtOAc); ^1H NMR (500 MHz, CDCl_3): δ 7.91 (d, $J = 7.6$, 1H), 7.87 (d, $J = 8.4$, 1H), 7.85 (d, $J = 8.4$, 1H), 7.55-7.48 (m, 2H), 7.48-7.42 (m, 3H), 7.40 (d, $J = 7.0$, 1H), 7.19 (t, $J = 8.6$, 2H); ^{13}C NMR (125 MHz, CDCl_3) δ 139.3, 136.8 (d), 134.0, 131.8, 131.8, 131.7, 128.5, 128.0, 127.2, 126.3, 126.0, 125.9, 125.5, 115.4, 115.3; IR (film): 3043, 1604, 1503, 1395, 1219, 1157 cm^{-1} ; HRMS-ESI (m/z) [$\text{M} + \text{NH}_4$] $^+$

calcd for C₁₆H₁₁FNH₄, 240.1189; found, 240.1198. All spectral data are consistent with those previously reported.⁶⁹

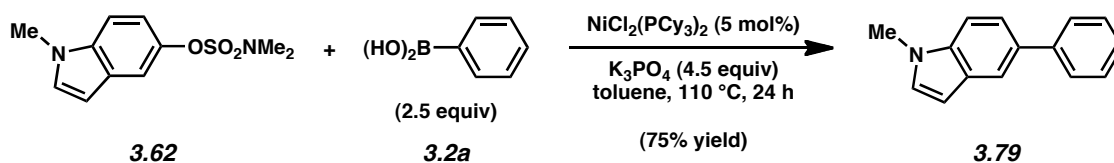


Biaryl 3.77 (Table 3.8, entry 8). Purification by flash chromatography (9:1 Hexanes:EtOAc) afforded **3.77** as a white solid (62% yield). R_f 0.52 (4:1 Hexanes:EtOAc); ¹HNMR (500 MHz, CDCl₃): δ 8.10 (d, *J* = 8.3, 2H), 7.92 (dd, *J* = 13.0, 8.2, 2H), 7.86 (d, *J* = 8.4, 1H), 7.61 (d, *J* = 8.3, 2H), 7.57-7.50 (m, 2H), 7.49-7.41 (m, 2H), 2.69 (s, 3H); ¹³CNMR (125 MHz, CDCl₃) δ 197.7, 145.7, 138.9, 135.9, 133.7, 131.1, 130.2, 128.3, 128.3, 128.3, 126.8, 126.3, 125.9, 125.5, 125.2, 26.6; IR (film): 3054, 1682, 1605, 1503, 1403, 1268 cm⁻¹; HRMS-ESI (*m/z*) [M + NH₄]⁺ calcd for C₁₈H₁₄ONH₄, 264.1388; found, 264.1394. All spectral data are consistent with those previously reported.⁷⁰

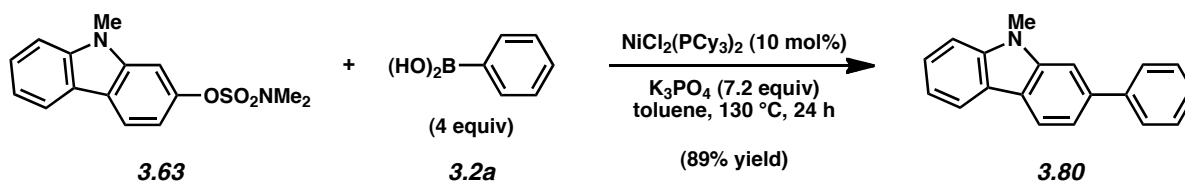


Biaryl 3.78 (Table 3.9, entry 1). Purification by flash chromatography (1:1 Benzene:Hexanes) afforded **3.78** as a light yellow oil (88% yield). R_f 0.52 (1:1 Benzene:Hexanes); ¹H NMR (500 MHz, CDCl₃): δ 7.77 (d, *J* = 7.7, 2H), 7.45 (t, *J* = 7.7, 2H), 7.34-7.31 (m, 2H), 7.14 (dd *J* = 7.2, 0.9, 1H), 6.93 (t, *J* = 7.5, 1H), 3.09 (s, 2H), 1.54 (s, 6H); ¹³C NMR (125 MHz, CDCl₃): δ 156.3, 137.7, 128.4, 128.4, 128.2, 127.9, 127.0, 124.3, 123.4, 120.0, 86.5, 43.0, 28.4; IR (film): 2972,

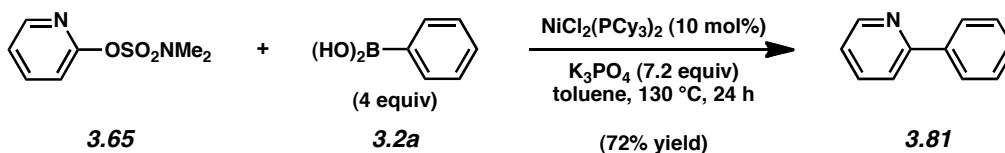
1597, 1459, 1425, 1139 cm^{-1} ; HRMS-ESI (m/z) $[\text{M} + \text{H}]^+$ calcd for $\text{C}_{16}\text{H}_{17}\text{O}$, 225.1279; found, 225.1274.



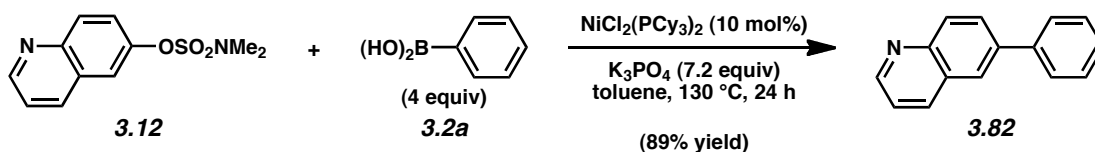
Biaryl 3.79 (Table 3.9, entry 2). Purification by flash chromatography (2:1 Hexanes:Benzene) afforded **3.79** as a white solid (75% yield). R_f 0.42 (2:1 Hexanes:Benzene). All spectral data are consistent with those previously reported.⁷¹



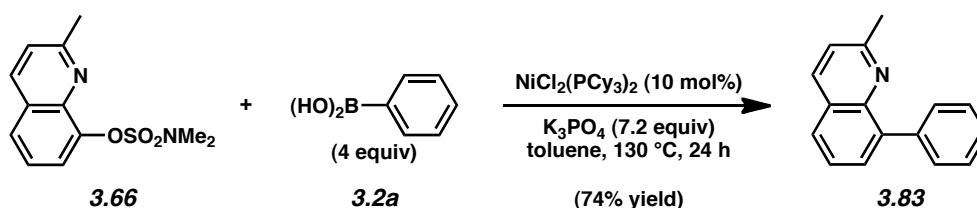
Biaryl 3.80 (Table 3.9, entry 3). Purification by flash chromatography (4:1 Hexanes:EtOAc) afforded **3.80** as a white solid (89% yield). R_f 0.74 (4:1 Hexanes:EtOAc). All spectral data are consistent with those previously reported.⁷²



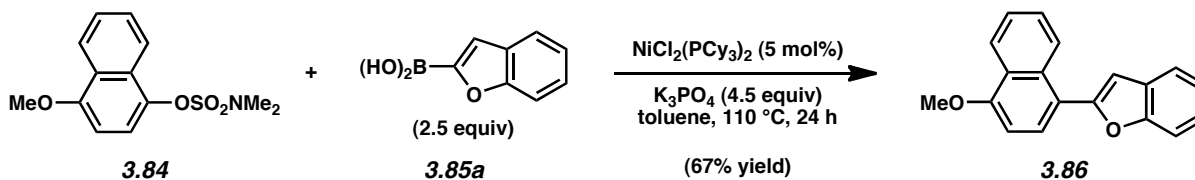
Biaryl 3.81 (Table 3.9, entry 4). Purification by flash chromatography (4:1 Hexanes:EtOAc) afforded **3.81** as a white solid (72% yield). R_f 0.52 (2:1 Hexanes:EtOAc). All spectral data are consistent with those previously reported.⁷³



Biaryl 3.82 (Table 3.9, entry 5). Purification by flash chromatography (1:1 Hexanes:Benzene) afforded **3.82** as a white solid (89% yield). R_f 0.35 (1:1 Hexanes:EtOAc). All spectral data are consistent with those previously reported.⁷⁴

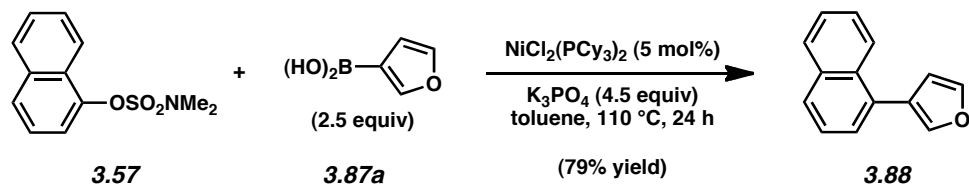


Biaryl 3.83 (Table 3.9, entry 6). Purification by flash chromatography (4:1 Hexanes:EtOAc) afforded **3.83** as a white solid (74% yield). R_f 0.62 (4:1 Hexanes:EtOAc); ^1H NMR (500 MHz, CDCl_3): δ 8.09 (d, $J = 8.0$, 1H), 7.87-7.84 (m, 2H), 7.82-7.76 (m, 2H), 7.58-7.52 (m, 3H), 7.48-7.43 (m, 1H), 7.31 (d, $J = 8.0$, 1H), 2.79 (s, 3H); ^{13}C NMR (125MHz, CDCl_3): δ 158.5, 145.3, 139.7, 139.5, 136.0, 130.9, 130.1, 127.6, 127.1, 126.9, 126.7, 125.2, 121.6, 25.5; IR (film): 3050, 1612, 1600, 1496, 1326, 1238 cm^{-1} ; HRMS-ESI (m/z) $[\text{M} + \text{Na}]^+$ calcd for $\text{C}_{16}\text{H}_{14}\text{N}$, 220.1126; found, 220.1126.

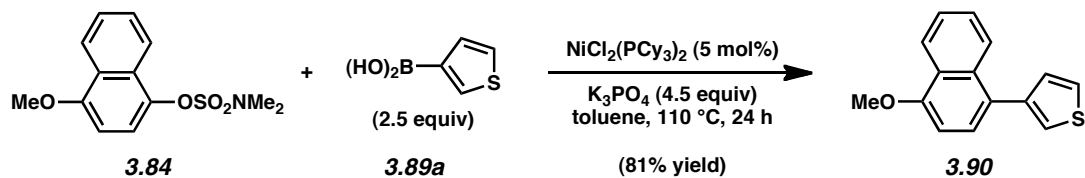


Biaryl 3.86 (Table 3.10, entry 1). Purification by flash chromatography (4:1 Hexanes:EtOAc) afforded **3.86** as a yellow oil (67% yield). R_f 0.58 (4:1 Hexanes:EtOAc); ^1H NMR (400 MHz, CDCl_3): δ 8.42 (d, $J = 8.5$, 1H), 8.38 (d, $J = 8.3$, 1H), 7.82 (d, $J = 8.1$, 1H), 7.66 (d, $J = 7.5$, 1H),

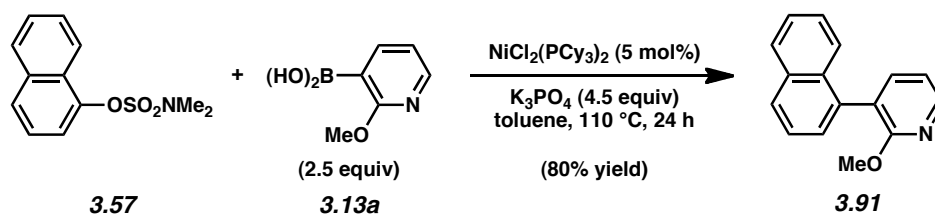
7.61-7.53 (m, 3H), 7.35-7.25 (m, 2H), 7.00 (s, 3H), 6.91 (d, $J = 8.1$, 1H), 4.07 (s, 3H); ^{13}C NMR (125MHz, CDCl_3): δ 156.3, 156.0, 154.8, 131.7, 129.2, 127.9, 127.3, 125.7, 125.4, 125.2, 123.9, 122.8, 122.4, 120.8, 120.7, 111.1, 104.7, 103.4, 55.6; IR (film): 2934, 1584, 1448, 1246, 1080 cm^{-1} ; HRMS-ESI (m/z) $[\text{M} + \text{H}]^+$ calcd for $\text{C}_{19}\text{H}_{15}\text{O}_2$, 275.1072; found, 275.1078.



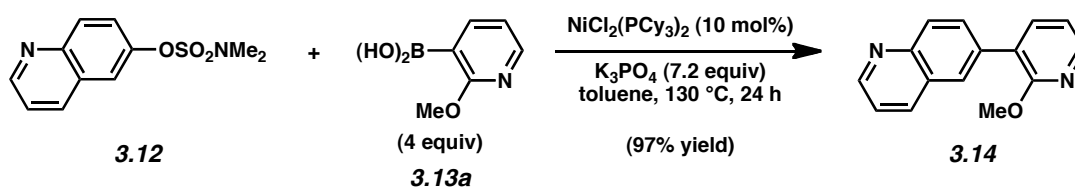
Biaryl 3.88 (Table 3.10, entry 2). Purification by flash chromatography (100% Hexanes) afforded **3.88** as a white solid (79% yield). R_f 0.62 (100% Hexanes). All spectral data are consistent with those previously reported.⁷⁵



Biaryl 3.90 (Table 3.10, entry 3). Purification by flash chromatography (2:1 Hexanes:EtOAc) afforded **3.90** as a yellow oil (81% yield). R_f 0.55 (1:1 Hexanes:EtOAc); ^1H NMR (400 MHz, CDCl_3): δ 8.35-8.33 (m, 1H), 8.00-7.97 (m, 1H), 7.52-7.43 (m, 3H), 7.40 (d, $J = 7.9$, 1H), 7.34 (dd, $J = 3.0$, $J = 1.3$, 1H), 7.28 (dd, $J = 4.9$, 1.3, 1H), 6.85, (d, $J = 8.7$, 1H), 4.05 (s, 3H); ^{13}C NMR (125MHz, CDCl_3): δ 155.0, 141.2, 132.6, 129.7, 127.3, 126.8, 126.6, 125.6, 125.5, 125.1, 125.0, 122.9, 122.2, 103.3, 55.5; IR (film): 2933, 1578, 1458, 1232, 1101 cm^{-1} ; HRMS-ESI (m/z) $[\text{M} + \text{H}]^+$ calcd for $\text{C}_{15}\text{H}_{12}\text{OS}$, 241.0687; found, 241.0693.

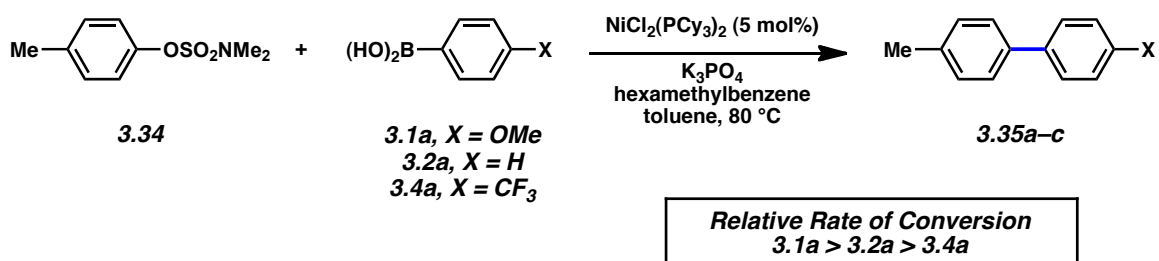


Biaryl 3.91 (Table 3.10, entry 4). Purification by flash chromatography (10:1 Hexanes:EtOAc) afforded **3.91** as a white solid (80% yield). R_f 0.70 (10:1 Hexanes:EtOAc); $^1\text{H NMR}$ (500 MHz, CDCl_3): δ 8.32 (d, $J = 5.0, 1.9$, 1H), 7.93-7.90 (m, 2H), 7.61-7.42 (m, 6H), 7.06-7.03 (m, 1H), 3.98 (s, 3H); $^{13}\text{C NMR}$ (125 MHz, CDCl_3): δ 161.6, 146.3, 140.1, 134.9, 133.5, 131.7, 128.2, 128.2, 127.4, 125.9, 125.8, 125.7, 125.3, 123.5, 116.6, 53.4; IR (film): 2945, 1578, 1459, 1362, 1174 cm^{-1} ; HRMS-ESI (m/z) [$\text{M} + \text{H}$] $^+$ calcd for $\text{C}_{16}\text{H}_{13}\text{NO}$, 236.1075; found, 236.1082.

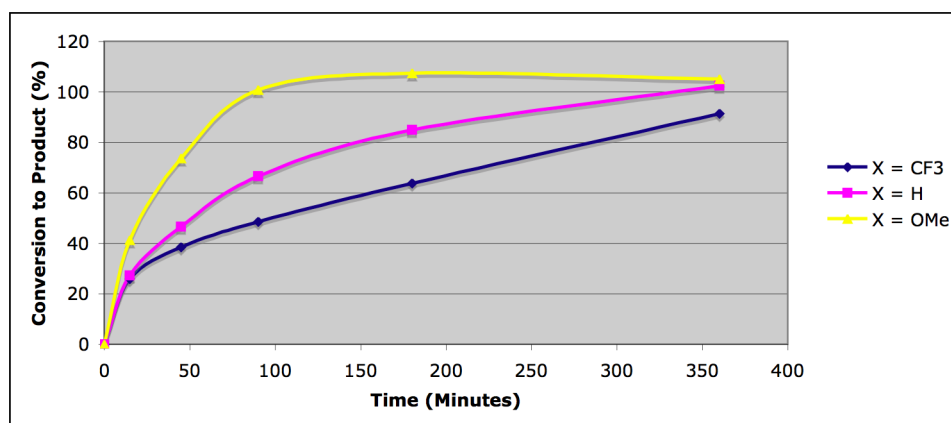


Biaryl 3.14. Purification by flash chromatography (10:1 Hexanes:EtOAc) afforded **3.14** as a white solid (97% yield). R_f 0.70 (10:1 Hexanes:EtOAc); $^1\text{H NMR}$ (500 MHz, CDCl_3): δ 8.85 (dd, $J = 4.0, 1.4$, 1H), 8.15 (dd, $J = 5.0, 1.8$, 1H), 8.11-8.07 (m, 2H), 7.88-7.86 (m, 2H), 7.62 (dd, $J = 7.3, 1.8$, 1H), 7.31 (q, $J = 4.2$, 1H), 6.95-6.92 (dd, $J = 7.3, 5.0$, 1H), 3.95 (s, 3H); $^{13}\text{C NMR}$ (125 MHz, CDCl_3): δ 160.8, 150.4, 147.5, 146.1, 138.7, 136.0, 135.0, 130.8, 128.9, 128.0, 127.7, 123.6, 121.2, 117.1, 53.5; IR (film): 3046, 2945, 1578, 1461, 1403, 1018 cm^{-1} ; HRMS-ESI (m/z) [$\text{M} + \text{H}$] $^+$ calcd for $\text{C}_{15}\text{H}_{13}\text{NO}$, 237.1028; found, 237.1025.

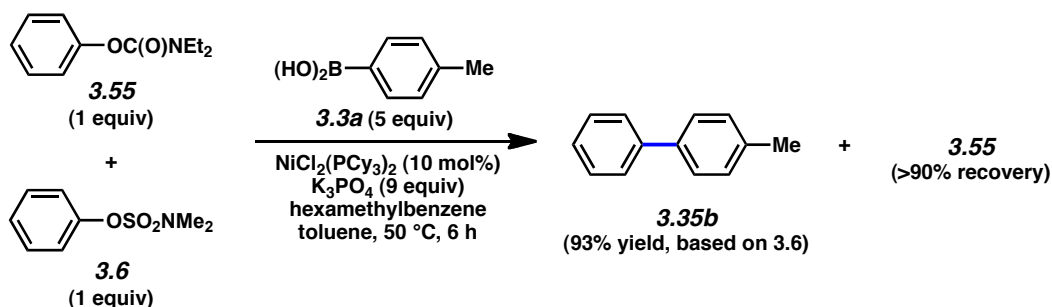
C. Mechanistic and Competition Experiments



Influence of boronic acid on the reaction rate. To determine the influence of boronic acid identity on reaction rate, sulfamate **3.34** was allowed to react independently with boronic acids **3.1a**, **3.2a**, and **3.4a**. To monitor progress over time, in each case, five reactions were setup simultaneously under identical reaction conditions. These reactions were removed from heat at varying time points (15 min, 45 min, 90 min, 3 h, 6 h) and the percentage conversions were determined by ¹H NMR analysis with hexamethylbenzene as internal standard. The results shown below indicate that the relative rate of cross-coupling is dependent on the identity of the boronic acid, with a direct correlation between electron-richness of the boronic acid and reaction rate (i.e., rate of conversion: **3.1a**>**3.2a**>**3.4a**).

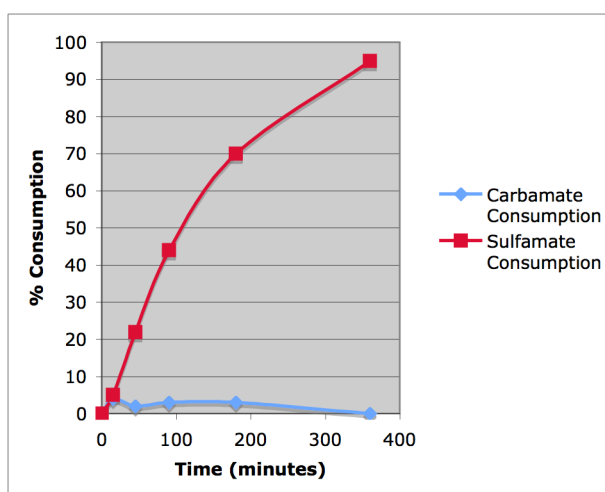


Representative procedure (coupling of sulfamate 3.34 with boronic acid 3.2a is used as an example). A 1-dram vial was charged with anhydrous powdered K_3PO_4 (419 mg, 1.98 mmol, 4.5 equiv, *obtained from Acros*) and a magnetic stir bar. The vial and contents were flame-dried under reduced pressure, and then allowed to cool under N_2 . Boronic acid **3.2a** (134 mg, 1.10 mmol, 2.5 equiv), $NiCl_2(PCy_3)_2$ (15 mg, 0.0219 mmol, 5 mol%), and the sulfamate substrate **3.34** (94 mg, 0.439 mmol, 1 equiv) were added. The vial was then evacuated and backfilled with N_2 . 1.5 mL of a 4.6 mg/mL solution of hexamethylbenzene in toluene was added and the vial was sealed with a Teflon-lined screw cap. The heterogeneous mixture was allowed to stir at 23 °C for 1 h, and then heated to 80 °C for the desired time indicated above. The reaction vessel was then immediately opened and the contents transferred to a test tube containing 1 M HCl (5 mL) and Et_2O (5 mL). Et_2O (1 mL) and H_2O (1 mL) were used to dissolve and transfer residual solids to the test tube. The layers were separated and the aqueous layer was extracted with Et_2O (3x5 mL). The combined organic layers were dried over $MgSO_4$. A sample (1.5 mL) was taken, and the solvent was removed under reduced pressure. The residue was dissolved in $CDCl_3$; the resulting solution was subjected to filtration through a cotton plug and analyzed by 1H NMR.



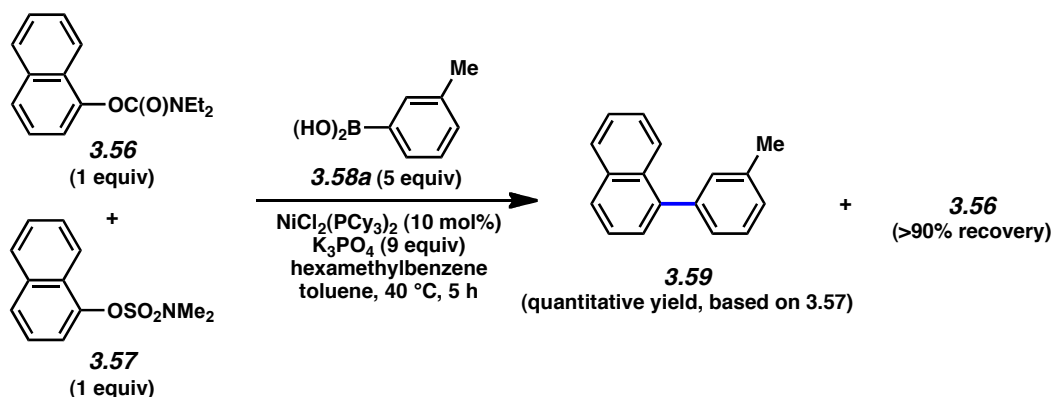
Sulfamate-selective coupling using aryl substrates. Experiments were carried out to effect the selective cross-coupling of aryl sulfamate **3.6** without effecting reaction of aryl carbamate **3.55**. To monitor progress over time, five reactions were setup simultaneously under identical reaction

conditions. These reactions were removed from heat at varying time points (15 min, 45 min, 90 min, 3 h, 6 h) and the percentage conversions were determined by ^1H NMR analysis with hexamethylbenzene internal standard. The results shown below indicate that selective sulfamate coupling was readily achieved at 50 °C reaction temperature.

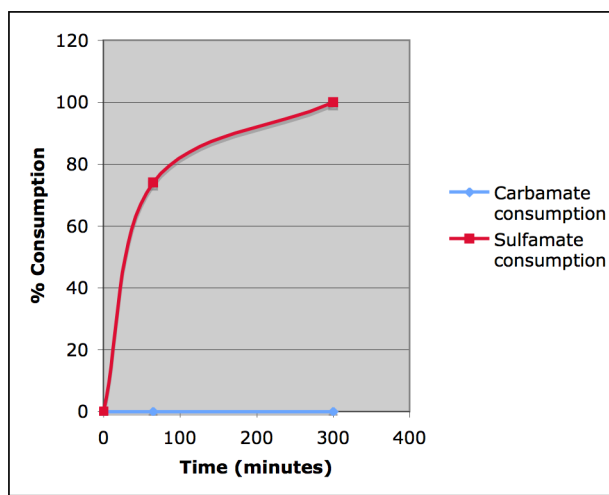


Procedure: A 1-dram vial was charged with anhydrous powdered K_3PO_4 (380 mg, 1.79 mmol, 9 equiv, obtained from Acros) and a magnetic stir bar. The vial and contents were flame-dried under reduced pressure, then allowed to cool under N_2 . Boronic acid **3.3a** (135 mg, 1.00 mmol, 5 equiv), $\text{NiCl}_2(\text{PCy}_3)_2$ (13.8 mg, 0.02 mmol, 10 mol%) were added. The vial was then evacuated and backfilled with N_2 . A solution containing sulfamate **3.6** (40 mg, 0.20 mmol, 1 equiv), carbamate **3.55** (38 mg, 0.20 mmol, 1 equiv) and hexamethylbenzene (4.9 mg, 0.03 mmol, 15 mol%) in toluene (1.5 mL) was added and the vial was sealed with a Teflon-lined screw cap. The heterogeneous mixture was stirred at 23 °C for 1 h, then heated to 50 °C for the desired time indicated above. The reaction vessel was then immediately opened and the contents transferred to a test tube containing 1 M HCl (5 mL) and ethyl acetate (5 mL). Ethyl acetate (1 mL) and H_2O (1 mL) were used to dissolve and transfer residual solids to the test tube. The layers were separated and the aqueous layer was extracted with ethyl acetate (3x5 mL). The combined

organic layers were dried over MgSO_4 . A sample (1.5 mL) was evaporated to dryness under reduced pressure. The residue was dissolved in CDCl_3 and analyzed by ^1H NMR.



Sulfamate-selective coupling using fused aromatic substrates. Experiments were carried out to effect the selective cross-coupling of aryl sulfamate **3.57** without disturbing aryl carbamate **3.56**. To monitor progress over time, two reactions were setup simultaneously under identical reaction conditions. These reactions were stopped at varying time points (65 min and 5 h) and the percentage conversions were determined by ^1H NMR analysis with hexamethylbenzene internal standard. The results shown below indicate that selective sulfamate coupling was readily achieved at 40 °C reaction temperature.



Procedure: A 1-dram vial was charged with anhydrous powdered K_3PO_4 (119 mg, 0.90 mmol, 9 equiv, *obtained from Acros*) and a magnetic stir bar. The vial and contents were flame-dried under reduced pressure, then allowed to cool under N_2 . Boronic acid **3.58a** (68 mg, 0.50 mmol, 0.5 equiv), $NiCl_2(PCy_3)_2$ (6.9 mg, 0.01 mmol, 10 mol%) were added. The vial was then evacuated and backfilled with N_2 . A solution containing sulfamate **3.57** (25 mg, 0.10 mmol, 1 equiv), carbamate **3.56** (24 mg, 0.10 mmol, 1 equiv), and hexamethylbenzene (2.4 mg, 0.02 mmol, 15 mol%) in toluene (0.7 mL) was added and the vial was sealed with a Teflon-lined screw cap. The heterogeneous mixture was allowed to stir at 23 °C for 1 h, then heated to 40 °C for the desired time indicated above. The reaction vessel was then cooled, immediately opened and the contents transferred to a test tube containing 1 M HCl (5 mL) and ethyl acetate (5 mL). Ethyl acetate (1 mL) and H_2O (1 mL) were used to dissolve and transfer residual solids to the test tube. The layers were separated and the aqueous layer was extracted with ethyl acetate (3x5 mL). The combined organic layers were dried over $MgSO_4$. A sample (1.5 mL) was evaporated to dryness under reduced pressure. The residue was dissolved in $CDCl_3$ and analyzed by 1H NMR.

3.10 Notes and References

- (1) (a) *Metal-Catalyzed Cross-Coupling Reactions*; Diederich, F., Meijere, A., Eds.; Wiley-VCH: Weinheim, 2004. (b) Hassan, J.; Sévignon, M.; Gozzi, C.; Schulz, E.; Lemaire, M. *Chem. Rev.* **2002**, *102*, 1359–1469. (c) *Topics in Current Chemistry*; Miyaura, N., Ed.; Vol. 219; Springer-Verlag: New York, 2002. (d) Corbet, J.; Mignani, G. *Chem. Rev.* **2006**, *106*, 2651–2710. (e) Negishi, E. *Bull. Chem. Soc. Jpn.* **2007**, *80*, 233–257.
- (2) For a pertinent review, see: Littke, A. F.; Fu, G. C. *Angew. Chem. Int. Ed.* **2002**, *41*, 4176–4211.
- (3) *The Chemistry of Phenols*; Rappoport, Z., Ed.; John Wiley & Sons Ltd: Chichester, 2003.
- (4) For recent examples of C–C bond formation involving aryl sulfonates, see: (a) Naber, J. R.; Fors, B. P.; Wu, X.; Gunn, J. T.; Buchwald, S. L. *Heterocycles* **2010**, *80*, 1215–1226. (b) Chow, W. K.; So, C. M.; Lau, C. P.; Kwong, F. Y. *J. Org. Chem.* **2010**, *75*, 5109–5112. (c) Bhayana, B.; Fors, B. P.; Buchwald, S. L. *Org. Lett.* **2009**, *11*, 3954–3957. (d) Munday, R. H.; Martinelli, J. R.; Buchwald, S. L. *J. Am. Chem. Soc.* **2008**, *130*, 2754–2755. (e) So, C. M.; Lau, C. P.; Chan, A. S. C.; Kwong, F. Y. *J. Org. Chem.* **2008**, *73*, 7731–7734. (f) Zhang, L.; Meng, T.; Wu, J. *J. Org. Chem.* **2007**, *72*, 9346–9349. (g) Limmert, M. E.; Roy, A. H.; Hartwig, J. F. *J. Org. Chem.* **2005**, *70*, 9364–9370. (h) Tang, Z.-Y.; Hu, Q.-S. *J. Am. Chem. Soc.* **2004**, *126*, 3058–3059.
- (5) For recent examples of C–X bond formation involving aryl sulfonates, see: (a) Dooleweerd, K.; Fors, B. P.; Buchwald, S. L. *Org. Lett.* **2010**, *12*, 2350–2353. (b) Vo, G. D.; Hartwig, J. F. *J. Am. Chem. Soc.* **2009**, *131*, 11049–11061. (c) So, C. M.; Zhou, Z.; Lau, C. P.; Kwong, F. Y. *Angew. Chem. Int. Ed.* **2008**, *47*, 6402–6406. (d) Ogata, T.; Hartwig, J. F. *J. Am. Chem.*

- Soc.* **2008**, *130*, 13848–13849. (e) Fors, B. P.; Watson, D. A.; Biscoe, M. R.; Buchwald, S. L. *J. Am. Chem. Soc.* **2008**, *130*, 13552–13554. (f) Gao, C. Y.; Yang, L. M. *J. Org. Chem.* **2008**, *73*, 1624–1627.
- (6) For pertinent reviews and highlights, see: (a) Rosen, B. M.; Quasdorf, K. W.; Wilson, D. A.; Zhang, N.; Resmerita, A.-M.; Garg, N. K.; Percec, V. *Chem. Rev.* **2011**, *111*, 1396–1416. (b) Yu, D.-G.; Li, B.-J.; Shi, Z.-J. *Acc. Chem. Res.* **2010**, *43*, 1486–1495. (c) Knappke, C. E. I.; Jacobi von Wangelin, A. *Angew. Chem. Int. Ed.* **2010**, *49*, 3568–3570. (d) Gooben, L. J.; Gooben, K.; Stanciu, C. *Angew. Chem. Int. Ed.* **2009**, *48*, 3569–3571.
- (7) (a) Tobisu, M.; Shimasaki, T.; Chatani, N. *Chem. Lett.* **2009**, *38*, 710–711. (b) Tobisu, M.; Shimasaki, T.; Chatani, N. *Angew. Chem. Int. Ed.* **2008**, *47*, 4866–4869. (c) Guan, B.-T.; Xiang, S.-K.; Wu, T.; Sun, Z.-P.; Wang, B.-Q.; Zhao, K.-Q.; Shi, Z.-J. *Chem. Commun.* **2008**, 1437–1439. (d) Dankwardt, J. W. *Angew. Chem. Int. Ed.* **2004**, *43*, 2428–2432. (e) Wenkert, E.; Michelotti, E. L.; Swindell, C. S. *J. Am. Chem. Soc.* **1979**, *101*, 2246–2247.
- (8) (a) Quasdorf, K. W.; Tian, X.; Garg, N. K. *J. Am. Chem. Soc.* **2008**, *130*, 14422–14423. (b) Guan, B.-T.; Wang, Y.; Li, B.-J.; Yu, D.-G.; Shi, Z.-J. *J. Am. Chem. Soc.* **2008**, *130*, 14468–14470. (c) Li, Z.; Zhang, S.-L.; Fu, Y.; Guo Q.-X.; Liu, L. *J. Am. Chem. Soc.* **2009**, *131*, 8815–8823. (d) Li, B.-J.; Li, Y.-Z.; Lu, X.-Y.; Liu, J.; Guan, B.-T.; Shi, Z.-J. *Angew. Chem. Int. Ed.* **2008**, *47*, 10124–10127. (e) Shimasaki, T.; Tobisu, M.; Chatani, N. *Angew. Chem. Int. Ed.* **2010**, *49*, 2929–2932. (f) Molander, G. A.; Beaumard, F. *Org. Lett.* **2010**, *12*, 4022–4025.
- (9) (a) Antoft-Finch, A.; Blackburn, T.; Snieckus, V. *J. Am. Chem. Soc.* **2009**, *131*, 17750–17752. (b) Quasdorf, K. W.; Riener, M.; Petrova, K. V.; Garg, N. K. *J. Am. Chem. Soc.* **2009**,

- 131, 17748–17749. (c) Xi, L.; Li, B.-J.; Wu, Z.-H.; Lu, X.-Y.; Guan, B.-T.; Wang, B.-Q.; Zhao, K.-Q.; Shi, Z.-J. *Org. Lett.* **2010**, *12*, 884–887. (d) Dallaire, C.; Kolber, I.; Gingras, M. *Org. Synth.* **2002**, *78*, 42. (e) Sengupta, S.; Leite, M.; Raslan, D. S.; Quesnelle, C.; Snieckus, V. *J. Org. Chem.* **1992**, *57*, 4066–4068.
- (10) (a) Macklin, T. K.; Snieckus, V. *Org. Lett.* **2005**, *7*, 2519–2522. (b) Wehn, P. M.; Du Bois, J. *Org. Lett.* **2005**, *7*, 4685–4688. (c) Ramgren, S. D.; Silberstein, A. L.; Yang, Y.; Garg, N. K. *Angew. Chem. Int. Ed.* **2011**, *50*, 2171–2173.
- (11) For functionalization by electrophilic aromatic substitution, which favors *para* substitution, see: Smith, M. B.; March, J. *March's Advanced Organic Chemistry*; 6th ed.; John Wiley & Sons, Inc.: New Jersey, 2007; p 670.
- (12) For functionalization by directed *ortho* metalation, see: (a) Snieckus, V. *Chem. Rev.* **1990**, *90*, 879–933. (b) Hartung, C. G.; Snieckus, V. In *Modern Arene Chemistry*; Astruc, D., Ed.; Wiley-VCH: New York, 2002; pp 330–367. (c) Macklin, T.; Snieckus, V. In *Handbook of C-H Transformations*; Dyker, G., Ed.; Wiley-VCH: New York, 2005; pp 106–119.
- (13) For functionalization using directed *ortho* metalation / *ipso*-desilylation, see: (a) Zhao, Z.; Snieckus, V. *Org. Lett.* **2005**, *7*, 2523–2526. (b) Bracegirdle, S.; Anderson, E. A. *Chem. Commun.* **2010**, *46*, 3454–3456.
- (14) For Pd-catalyzed *ortho* functionalization of aryl pivalates, see: (a) Xiao, B.; Fu, Y.; Xu, J.; Gong, T.-J.; Dai, J.-J.; Yi, J.; Liu, L. *J. Am. Chem. Soc.* **2010**, *132*, 468–469. For Pd-catalyzed *ortho* functionalization of aryl carbamates, see: (b) Bedford, R. B.; Webster, R. L.; Mitchell, C. J. *Org. Biomol. Chem.* **2009**, *7*, 4853–4857. (c) Zhao, X.; Yeung, C. S.; Dong, V. M. *J. Am. Chem. Soc.* **2010**, *132*, 5837–5844. (d) Nishikata, T.; Abela, A. R.; Huang, S.;

- Lipshutz, B. H. *J. Am. Chem. Soc.* **2010**, *132*, 4978–4979. For a recent Ir-catalyzed process, see: (e) Yamazaki, K.; Kawamorita, S.; Ohmiya, H.; Sawamura, M. *Org. Lett.* **2010**, *12*, 3978–3981.
- (15) (a) Miyaura, N.; Suzuki, A. *Chem. Rev.* **1995**, *95*, 2457–2483. (b) Suzuki, A. *Chem. Commun.* **2005**, 4759–4763. (c) Doucet, H. *Eur. J. Org. Chem.* **2008**, 2013–2030.
- (16) (a) For preliminary communications involving this work, see references 9a and 9b. (b) Following these publications, Shi and coworkers reported an alternate protocol for the Suzuki–Miyaura coupling of aryl carbamates (see ref 9c). (c) For Suzuki–Miyaura couplings of aryl carbamates and sulfamates under microwave conditions, see: Baghbanzadeh, M.; Pilger, C.; Kappe, C. O. *J. Org. Chem.* **2011**, *76*, 1507–1510.
- (17) $\text{NiCl}_2(\text{PCy}_3)_2$ (CAS# 19999-87-2) is commercially available from Strem Chemicals, Inc. (catalog #28-0091) and Aldrich Chemical Co., Inc. (catalog #708526). Alternatively, it can be prepared in multigram quantities following a simple one-step protocol, see reference 8a and: (a) Stone, P. J.; Dori, Z. *Inorg. Chim. Acta* **1970**, *5*, 434–438. (b) Barnett, K. W. *J. Chem. Educ.* **1974**, *51*, 422–423.
- (18) Quasdorf, K. W.; Garg, N. K. *Encyclopedia of Reagents for Organic Synthesis*, DOI: 10.1002/047084289X.rn01201.
- (19) In the presence of excess arylboronic acid, $\text{NiCl}_2(\text{PCy}_3)_2$ likely undergoes reduction to an active Ni(0) catalyst; see: Zim, D.; Monteiro, A. L. *Org. Lett.* **2001**, *3*, 3049.
- (20) The selection of boronic acid coupling partner was made in order to facilitate product purification.

- (21) Control experiments show that a large excess of water significantly reduces catalytic activity, likely by forming inactive nickel hydroxides/oxides, see: Inada, K.; Miyaura, N. *Tetrahedron* **2000**, *56*, 8657–8660.
- (22) (a) Since the addition of water to the boroxine is inaccurate on small-scale operation, the boronic acids were heated under vacuum for 1–12 h using Kugelrohr apparatus to achieve a 1:10 ratio of boronic acid:boroxine. The ratio was determined by ¹H NMR analysis immediately prior to use. (b) For comment on similar observations, see: Storgaard, M.; Ellman, J. A. *Org. Synth.* **2009**, *86*, 360–373. (c) For the crucial role of water in aryl acetate cross-couplings, see ref 8b.
- (23) Comparable yields were obtained from reactions containing 10 or 20 mol% of the PCy₃HBF₄ additive.
- (24) Yu, D.-G.; Yu, M.; Guan, B.-T.; Li, B.-J.; Zheng, Y.; Wu, Z.-H.; Shi, Z.-J. *Org. Lett.* **2009**, *11*, 3374–3377.
- (25) Comparable results were obtained when *N,N*-diethyl sulfamates were used in place of *N,N*-dimethyl sulfamates. The *N,N*-dimethyl derivatives were pursued because the *N,N*-dimethyl sulfamoylating reagent is commercially available, see reference 27.
- (26) Aryl sulfamates have been shown to be less effective, but still synthetically useful, substrates in DoM reactions compared to aryl carbamates; see reference 10a.
- (27) *N,N*-Dimethylsulfamoyl chloride from Aldrich Chemical Co., Inc. costs approximately \$0.80 per gram (CAS# 13360-57-1).
- (28) de Silva, S. O.; Reed, J. N.; Billedeau, R. J.; Wang, X.; Norris, D. J.; Snieckus, V. *Tetrahedron* **1992**, *48*, 4863–4878.

- (29) For examples of Pd-catalyzed Suzuki–Miyaura couplings that are tolerant of heterocycles, see: (a) Billingsley, K.; Buchwald, S. L. *J. Am. Chem. Soc.* **2007**, *129*, 3358–3366. (b) Guram, A. S.; Wang, X.; Bunel, E.; Faul, M. M.; Larsen, R. D.; Martinelli, M. J. *J. Org. Chem.* **2007**, *72*, 5104–5112. (c) For a pertinent review, see: Slagt, V. F.; de Vries, A. H. M.; de Vries, J. G.; Kellogg, R. M. *Org. Proc. Res. Dev.* **2010**, *14*, 30–47.
- (30) For reviews of theoretical studies, see: (a) Braga, A. A. C.; Ujaque G.; Maseras, F. In *Computational Modeling for Homogeneous and Enzymatic Catalysis. A Knowledge-Base for Designing Efficient Catalysis*, ed. Morokuma, K.; Musaev, D. G. WILEY-VCH GmbH & Co. KGaA, Weinheim, 2008, pp. 109–130. (b) Xue, L. Q.; Lin, Z. Y. *Chem. Soc. Rev.* **2010**, *39*, 1692–1705.
- (31) For theoretical studies of Pd-catalyzed Suzuki–Miyaura couplings, see: (a) Sumimoto, M.; Iwane, N.; Takahama, T.; Sakaki, S. *J. Am. Chem. Soc.* **2004**, *126*, 10457–10471. (b) Braga, A. A. C.; Morgon, N. H.; Ujaque, G.; Maseras, F. *J. Am. Chem. Soc.* **2005**, *127*, 9298–9307. (c) Goossen, L. J.; Koley, D.; Hermann, H. L.; Thiel, W. *J. Am. Chem. Soc.* **2005**, *127*, 11102–11114. (d) Goossen, L. J.; Koley, D.; Hermann, H. L.; Thiel, W. *Organometallics* **2006**, *25*, 54–67. (e) Braga, A. A. C.; Ujaque, G.; Maseras, F. *Organometallics* **2006**, *25*, 3647–3658. (f) Braga, A. A. C.; Morgon, N. H.; Ujaque, G.; Lledos, A.; Maseras, F. *J. Organomet. Chem.* **2006**, *691*, 4459–4466. (g) Sicre, C.; Braga, A. A. C.; Maseras, F.; Cid, M. M. *Tetrahedron* **2008**, *64*, 7437–7443. (h) Huang, Y. L.; Weng, C. M.; Hong, F. E. *Chem.-Eur. J.* **2008**, *14*, 4426–4434. (i) Gourlaouen, C.; Ujaque, G.; Lledós, A.; Medio-Simon, M.; Asensio, G.; Maseras, F. *J. Org. Chem.* **2009**, *74*, 4049–4054. (j) Jover, J.; Fey, N.; Purdie, M.; Lloyd-Jones, G. C.; Harvey, J. N. *J. Mol. Catal. A: Chem.* **2010**, *324*, 39–47.

- (32) (a) Ahlquist, M.; Fristrup, P.; Tanner, D.; Norrby, P. O. *Organometallics* **2006**, *25*, 2066–2073. (b) Ahlquist, M.; Norrby, P. O. *Organometallics* **2007**, *26*, 550–553. (c) Li, Z.; Fu, Y.; Guo, Q. X.; Liu, L. *Organometallics* **2008**, *27*, 4043–4049. (d) McMullin, C. L.; Jover, J.; Harvey, J. N.; Fey, N. *Dalton Trans.* **2010**, *39*, 10833–10836.
- (33) (a) Ananikov, V. P.; Musaev, D. G.; Morokuma, K. *J. Am. Chem. Soc.* **2002**, *124*, 2839–2852. (b) Ananikov, V. P.; Musaev, D. G.; Morokuma, K. *Organometallics* **2005**, *24*, 715–723. (c) Zuidema, E.; van Leeuwen, P. W. N. M.; Bo, C. *Organometallics* **2005**, *24*, 3703–3710. (d) Ananikov, V. P.; Musaev, D. G.; Morokuma, K. *Eur. J. Inorg. Chem.* **2007**, 5390–5399. (e) Koizumi, T.; Yamazaki, A.; Yamamoto, T. *Dalton Trans.* **2008**, 3949–3952. (f) Ariafard, A.; Yates, B. F. *J. Organomet. Chem.* **2009**, *694*, 2075–2084.
- (34) For a theoretical study of Ni-catalyzed Suzuki–Miyaura cross-couplings of aryl acetates, see ref 8c.
- (35) (a) Becke, A. D. *J. Chem. Phys.* **1993**, *98*, 5648–5652. (b) Lee, C.; Yang, W.; Parr, R. G. *Phys. Rev. B* **1988**, *37*, 785–789.
- (36) Kruger, C.; Tsay, Y.-H. *J. Organomet. Chem.* **1972**, *34*, 387–395.
- (37) (a) Barone V.; Cossi, M. *J. Phys. Chem. A* **1998**, *102*, 1995–2001. (b) Cossi, M.; Rega, N.; Scalmani, G.; Barone, V. *J. Comp. Chem.* **2003**, *24*, 669–681.
- (38) Gaussian 03, Revision D.01: Frisch, M. J. *et al.* Gaussian, Inc., Wallingford CT, **2004**.
- (39) The exact mechanism of the formation of the η^2 LPd(ArX) complex is controlled by the size of the ligand, see ref. 31j for a recent theoretical study on the details of this process.
- (40) For a mechanistic study on the formation of Ni η^2 complexes with aryl halides, see: Yoshikai, N.; Matsuda, H.; Nakamura, E. *J. Am. Chem. Soc.* **2008**, *130*, 15258–15259.

- (41) Oxidative addition of *O*-aryl thiocarbamates using Pd catalyst also occurs via a similar five-membered transition state: Harvey, J. N.; Jover, J.; Lloyd-Jones, G. C.; Moseley, J. D.; Murray, P.; Renny, J. S., *Angew. Chem., Int. Ed.* **2009**, *48*, 7612–7615.
- (42) See Supporting Information for details of calculations of bis-ligated species.
- (43) The gas phase bond dissociation enthalpy of the Ph–O bond in phenyl *N,N*-dimethyl carbamate is 22.4 higher than that of the O–carbonyl bond according to B3LYP/6-31G(d) calculations.
- (44) Miyaura, N. *J. Organomet. Chem.* **2002**, *653*, 54–57.
- (45) See page 48 for details.
- (46) Reductive elimination to form the biaryl product is considered to be a facile step in the catalytic cycle, see ref 8c and references therein.
- (47) In gas phase calculations, **3.19** is 3.2 kcal/mol more stable than **3.18**.
- (48) Chauder, B. A.; Kalinin, A. V.; Snickus, V. *Synthesis* **2001**, 140–144.
- (49) Chauder, B. A.; Kalinin, A. V.; Taylor, N. J.; Snickus, V. *Angew. Chem. Int. Ed.* **1999**, *38*, 1435–1438.
- (50) (a) Petasis, N. A.; Butkevich, A. N. *J. Organomet. Chem.* **2009**, *694*, 1747–1753. (b) Nicolaou, K. C.; Pfefferkorn, J. A.; Roecker, A. J.; Cao, G. Q.; Barleunga, S.; Mitchell, H. J. *J. Am. Chem. Soc.* **2000**, *122*, 9939–9953.
- (51) Veitch, N. C.; Grayer, R. J. *Nat. Prod. Rep.* **2008**, *25*, 555–611.
- (52) For the general DoM – directed remote metalation (DreM) – Suzuki cross-coupling approach to this and related systems, see: James, C. A.; Coelho, A. L.; Gevaert, M.; Forgione, P.; Snieckus, V. *J. Org. Chem.* **2009**, *74*, 4094–4103.

- (53) The low yield of **3.43** is a result of reductive cleavage and arylation of benzofuran, rather than low conversion of **3.42** owing to steric hindrance effects.
- (54) Alessi, M.; Larkin, A. L.; Ogilvie, K. A.; Green, L. A.; Lai, S.; Lopez, S.; Snieckus, V. *J. Org. Chem.* **2007**, *72*, 1588–1594.
- (55) (a) Chang, M.-Y.; Lin, C.-Y.; Hung, C.-Y. *Tetrahedron* **2007**, *63*, 3312–3320. (b) Karig, G.; Thasana, N.; Gallagher, T. *Synlett* **2002**, 808–810.
- (56) For pertinent reviews, see: (a) Richy, F.; Rabehnda, V.; Mawet, A.; Reginster, J.-Y. *Int. J. Clin. Pract.* **2007**, *61*, 1396–1406. (b) Kumar, P.; Pathak, P. K.; Gupta, V. K.; Srivastava, B. K.; Kushwaha, B. S. *Asian J. Chem.* **2004**, *16*, 558–562.
- (57) Furuya, T.; Ritter, T. *Org. Lett.* **2009**, *11*, 2860–2863.
- (58) For the DoM approach to ortho-fluorination, see: Snieckus, V.; Beaulieu, F.; Morhi, K.; Han, W.; Murphy, C. K.; Davis, F. A. *Tetrahedron Lett.* **1994**, *35*, 3465–3468.
- (59) Moradi, W. A.; Buchwald, S. L. *J. Am. Chem. Soc.* **2001**, *123*, 7996–8002.
- (60) Durandetti, M.; Gosmini, C.; Périchon, J. *Tetrahedron* **2007**, *63*, 1146–1153.
- (61) For Ni-catalyzed Kumada and Suzuki–Miyaura cross-coupling reactions of aryl fluorides, see: (a) Yoshikai, N.; Mashima, H.; Nakamura, E. *J. Am. Chem. Soc.* **2005**, *127*, 17978–17979. (b) Dankwardt, J. W. *J. Organomet. Chem.* **2005**, *690*, 932–938. (c) Schaub, T.; Backes, M.; Radius, U. *J. Am. Chem. Soc.* **2006**, *128*, 15964–15965.
- (62) The iodide of **3.51** could also be used in copper-catalyzed C–N bond forming reactions without disturbing the aryl sulfamate; Ramgren, S. D.; Silberstein, A. L.; Garg, N. K. University of California, Los Angeles, CA. Unpublished work, 2010.

- (63) Powdered potassium phosphate was found to be essential for reproducibility and high yields. Granular or pellet material from Sigma-Aldrich, Strem Chemicals, or Pfaltz & Bauer gave poor results, even after grinding with mortar and pestle.
- (64) Denmark, S. E.; Ober, M. H. *Org. Lett.* **2003**, *5*, 1357–1360.
- (65) Mino, T.; Shirae, Y.; Sakamoto, M.; Fujita, T. *J. Org. Chem.* **2005**, *70*, 2191–2194.
- (66) Zhang, L.; Cheng, J.; Zhang, W.; Lin, B.; Pan, C.; Chen, J. *Synth. Commun.* **2007**, *37*, 3809–3814.
- (67) Dalpozzo R.; Nino, A.; Maiuolo, L.; Oliverio, M.; Porcopio, A.; Russo, B.; Tocci, A. *Australian J. Chem.* **2007**, *60*, 75–79.
- (68) Song, C.; Ma, Y.; Chai, Q.; Ma, C.; Jiang, W.; Andrus, M. B. *Tetrahedron* **2005**, *61*, 7438–7446.
- (69) Okamoto, H.; Satake, K.; Kimura, M. *Bull. Chem. Soc. Jpn.* **1995**, *68*, 3557–3562.
- (70) Adjabeng, G.; Brenstrum, T.; Frampton, C. S.; Robertson, A. J.; Hillhouse, J.; McNulty, J.; Capretta, A. *J. Org. Chem.* **2004**, *69*, 5082–5086.
- (71) Quasdorf, K. W.; Riener, M.; Petrova, K. V.; Garg, N. K. *J. Am. Chem. Soc.* **2009**, *131*, 17748–17749.
- (72) Kong, W.; Fu, C.; Ma, S. *Chem. Commun.* **2009**, 4572–4574.
- (73) Sprouse, S.; King, K. A.; Spellane, P. J.; Watts, R. J. *J. Am. Chem. Soc.* **1984**, *106*, 6647–6653.
- (74) So, C. M.; Lau, C. P.; Kwong, F. Y. *Angew. Chem. Int. Ed.* **2008**, *47*, 8059–8063.
- (75) Molander, G. A.; Biolatto, B. *J. Org. Chem.* **2003**, *68*, 4302–4314.

APPENDIX TWO

Spectra Relevant to Chapter Three:

Suzuki–Miyaura Cross-Coupling of Aryl Carbamates and Sulfamates:

Experimental and Computational Studies

Kyle W. Quasdorf, Aurora Antoft-Finch, Peng Liu, Amanda L. Silberstein, Anna Komaromi,

Tom Blackburn, Stephen D. Ramgren, K. N. Houk, Victor Snieckus, and Neil K. Garg

J. Am. Chem. Soc. **2011**, *133*, 6352–6363.

Current Data Parameters
 NAME AS-1-62_R
 EXPNO 1
 PROCNO 1

F2 - Acquisition Parameters
 Date_ 20100502
 Time 17.03
 INSTRUM arx500
 PROBHD 5 mm broadband
 PULPROG zg30
 TD 65536
 SOLVENT CDCl3
 NS 16
 DS 0
 SWH 10000.000 Hz
 FIDRES 0.152588 Hz
 AQ 3.2768500 sec
 RG 2860
 DW 50.000 usec
 DE 71.43 usec
 TE 300.0 K
 D1 2.0000000 sec
 P1 11.00 usec
 SFO1 500.1330008 MHz
 NUCLEUS 1H

F2 - Processing parameters
 SI 32768
 SF 500.1300237 MHz
 WDW EM
 SSB 0
 LB 0.30 Hz
 GB 0
 PC 1.00

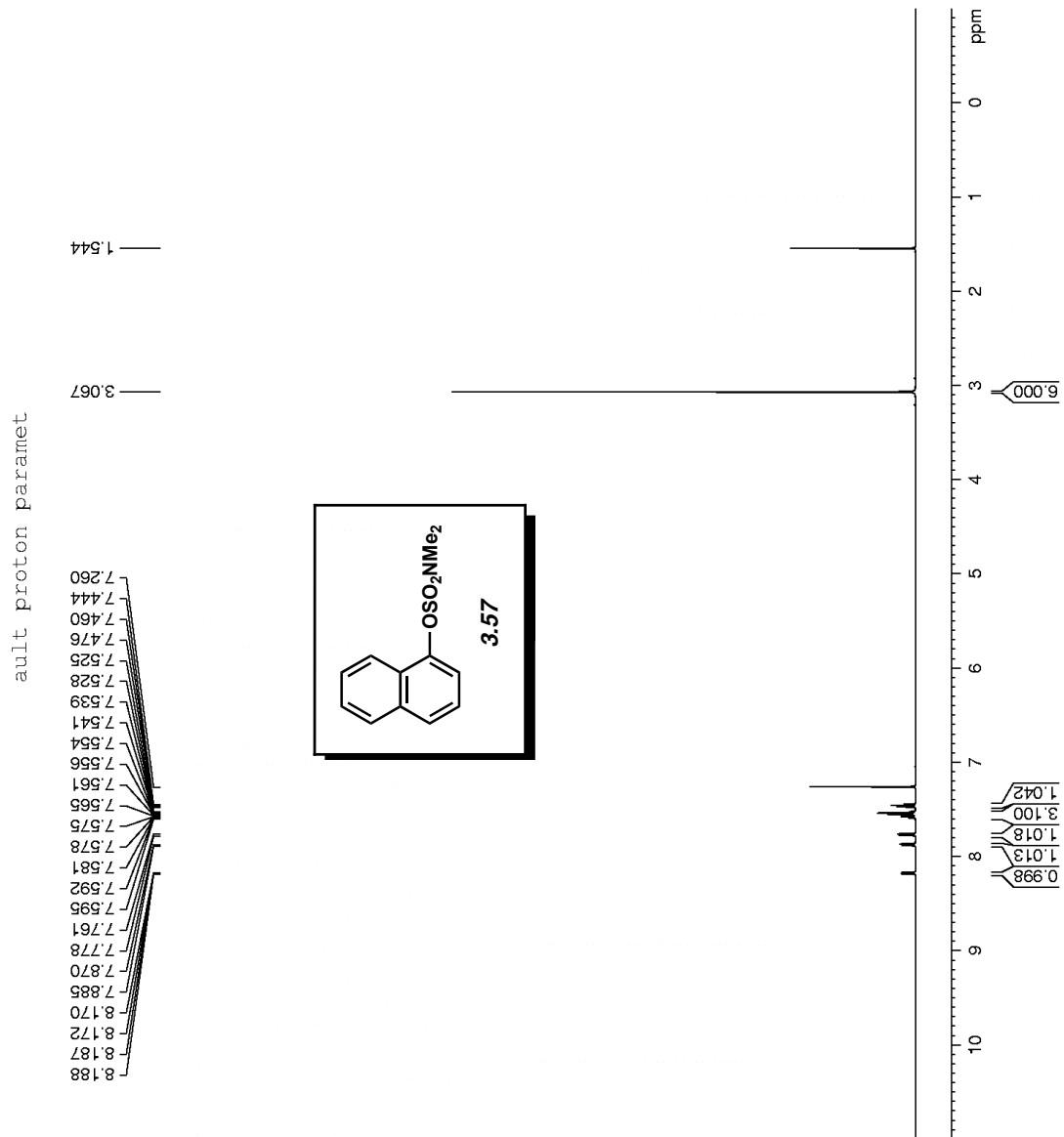


Figure A2.1 ¹H NMR (500 MHz, CDCl₃) of compound 3.57.

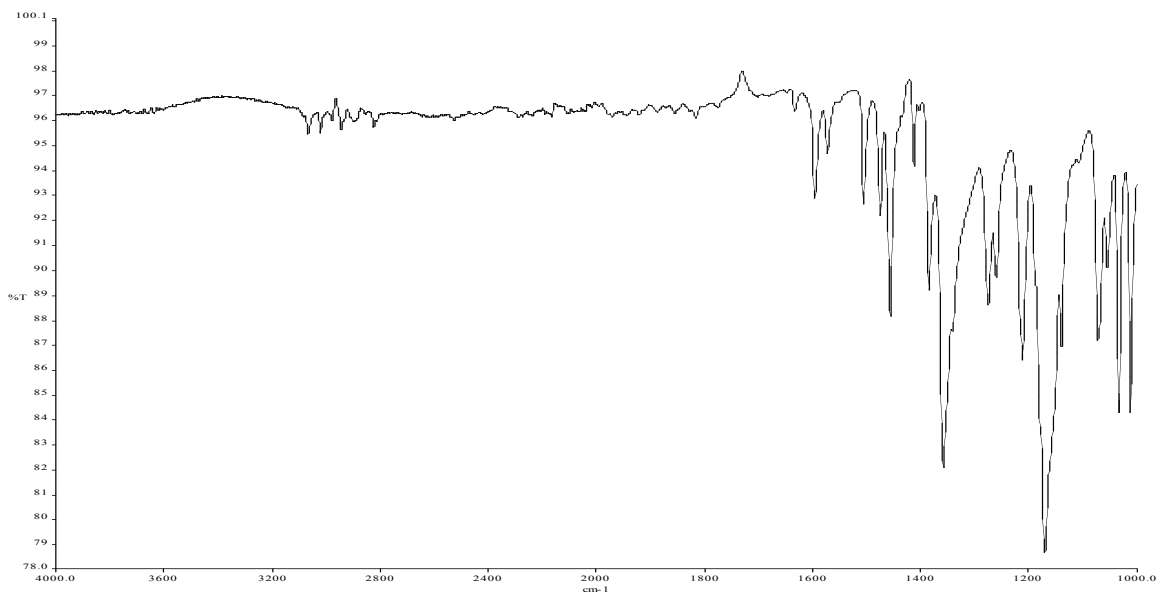


Figure A2.2 Infrared spectrum of compound **3.57**.

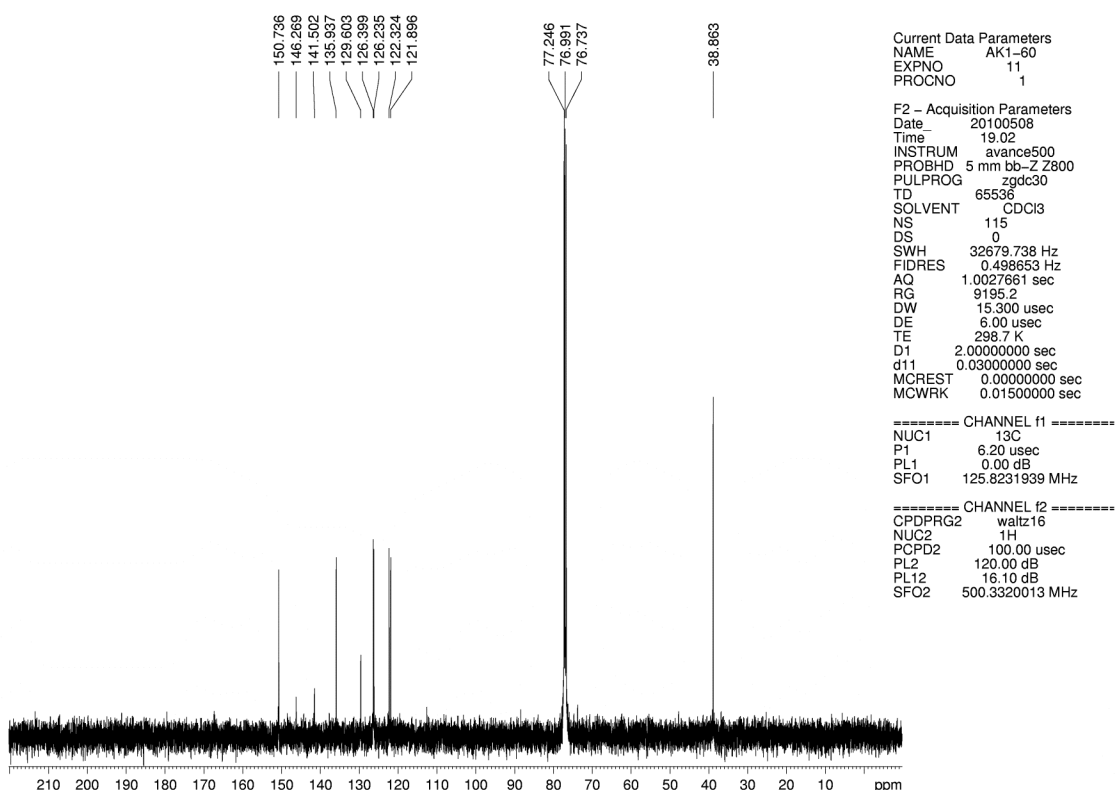


Figure A2.3 ^{13}C NMR (125 MHz, CDCl_3) of compound **3.57**.

Current Data Parameters
 NAME SDR1-188
 EXPNO 15
 PROCNO 1

F2 - Acquisition Parameters
 Date_ 20100509
 Time_ 19.42
 INSTRUM arx500
 PROBHD 5 mm broadband
 PULPROG zg30
 TD 65536
 SOLVENT CDCl3
 NS 8
 DS 0
 SWH 10000.000 Hz
 FIDRES 0.152588 Hz
 AQ 3.2768500 sec
 RG 1024
 DW 50.000 usec
 DE 71.43 usec
 TE 300.0 K
 D1 2.0000000 sec
 P1 11.00 usec
 SFO1 500.1330008 MHz
 NUCLEUS 1H

F2 - Processing parameters
 SI 32768
 SF 500.1300240 MHz
 WDW EM
 SSB 0
 LB 0.30 Hz
 GB 0
 PC 1.00

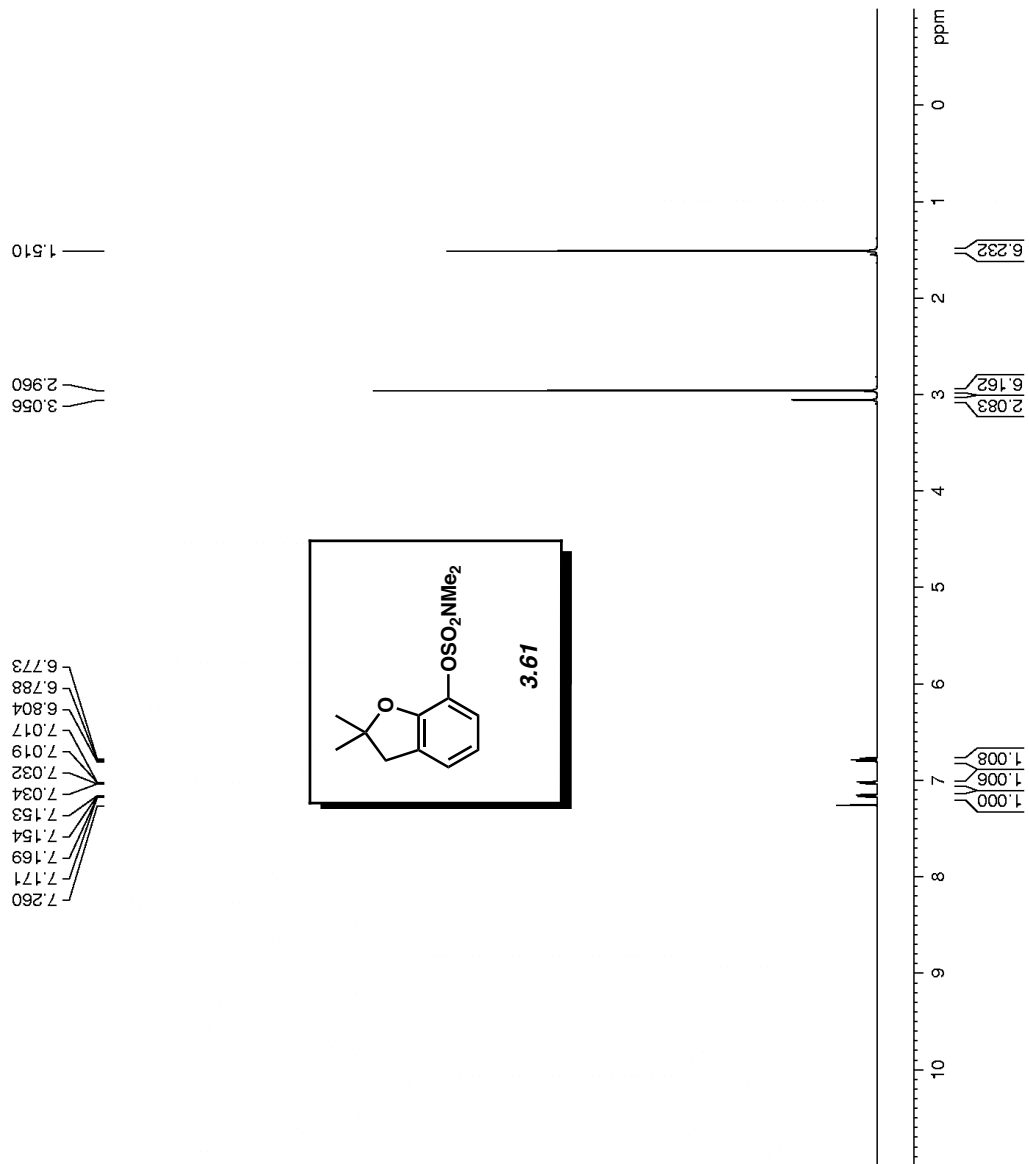


Figure A2.4 ¹H NMR (500 MHz, CDCl₃) of compound 3.61.

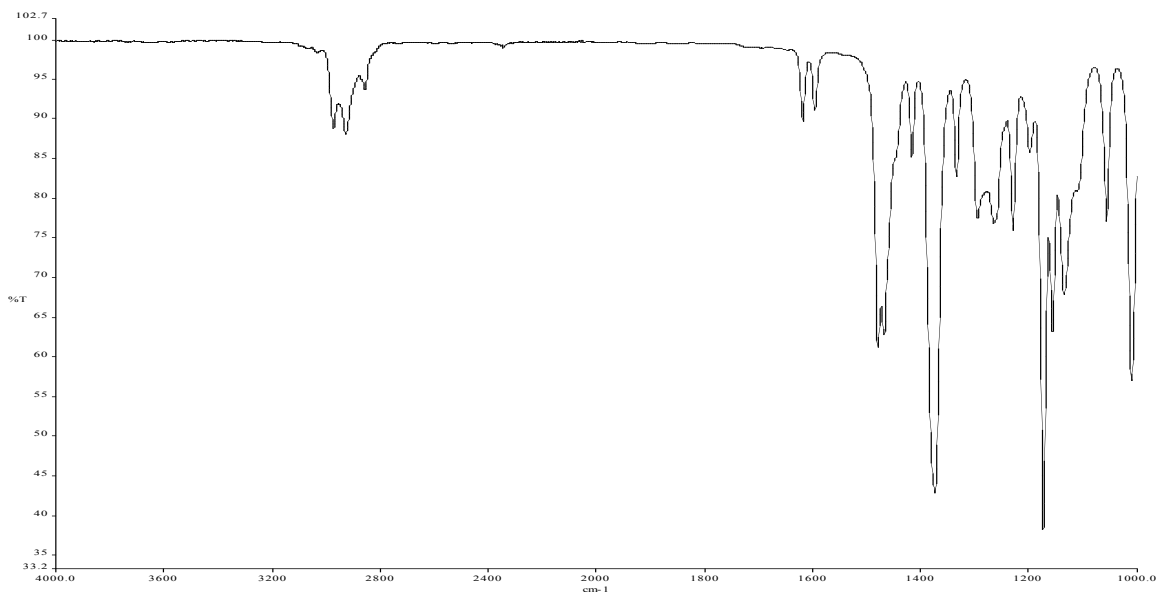


Figure A2.5 Infrared spectrum of compound **3.61**.

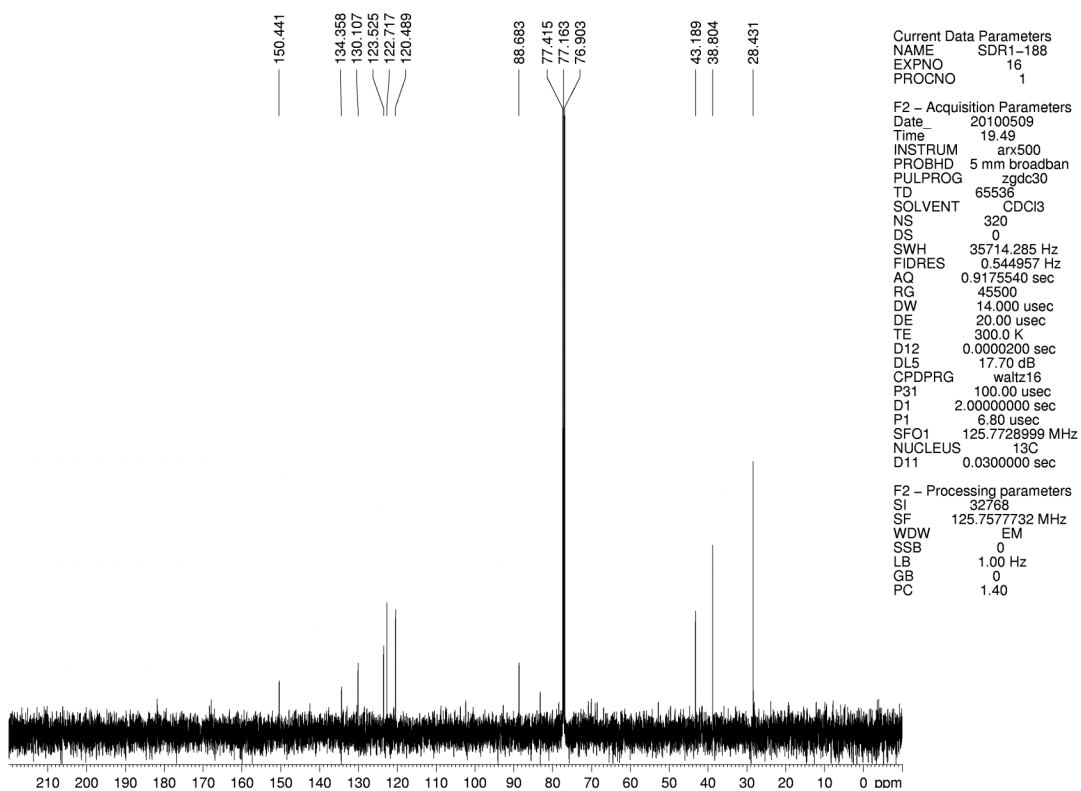


Figure A2.6 ^{13}C NMR (125 MHz, CDCl_3) of compound **3.61**.

Current Data Parameters
 NAME KQ3-50
 EXPNO 3
 PROCNO 1

F2 - Acquisition Parameters
 Date_ 20090220
 Time 17.35
 INSTRUM arx500
 PROBHD 5 mm broadband
 PULPROG zg30
 TD 65536
 SOLVENT CDCl3
 NS 9
 DS 0
 SWH 10000.000 Hz
 FIDRES 0.152588 Hz
 AQ 3.2768500 sec
 RG 2860
 DW 50.000 usec
 DE 71.43 usec
 TE 300.0 K
 D1 2.0000000 sec
 P1 11.00 usec
 SFO1 500.1330008 MHz
 NUCLEUS 1H

F2 - Processing parameters
 SI 32768
 SF 500.1300187 MHz
 WDW EM
 SSB 0
 LB 0.30 Hz
 GB 0
 PC 1.00

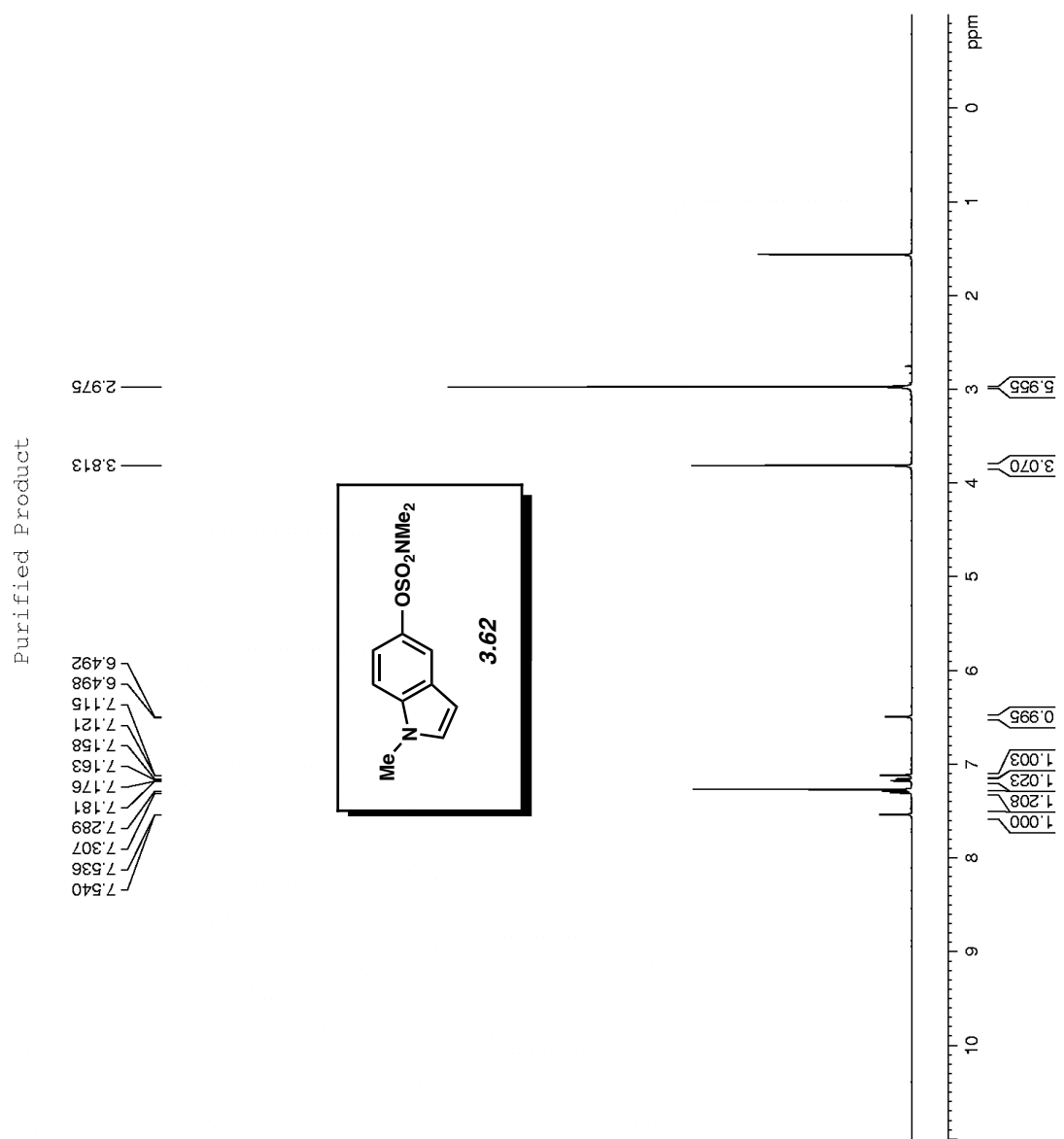


Figure A2.7 ¹H NMR (500 MHz, CDCl₃) of compound 3.62.

```

Current Data Parameters
NAME      ak-1-34
EXPNO    1
PROCNO   1

F2 - Acquisition Parameters
Date_    20100414
Time     0.22
INSTRUM  avance500
PROBHD   5 mm bb-Z800
PULPROG  zg30
TD        65536
SOLVENT  CDCI3
NS        8
DS        0
SWH       10000.000 Hz
FIDRES    0.152588 Hz
AQ         3.2769001 sec
RG         90.5
DW         50.000 usec
DE         6.00 usec
TE         298.3 K
D1         2.0000000 sec
MCREST    0.0000000 sec
MCWRK     0.01500000 sec

===== CHANNEL f1 =====
NUC1      1H
P1         12.00 usec
PL1        0.00 dB
SFO1      500.3330020 MHz

F2 - Processing parameters
SI         32768
SF         500.3300220 MHz
WDW        EIM
SSB        0
LB         0.30 Hz
GB         0
PC         1.00

```

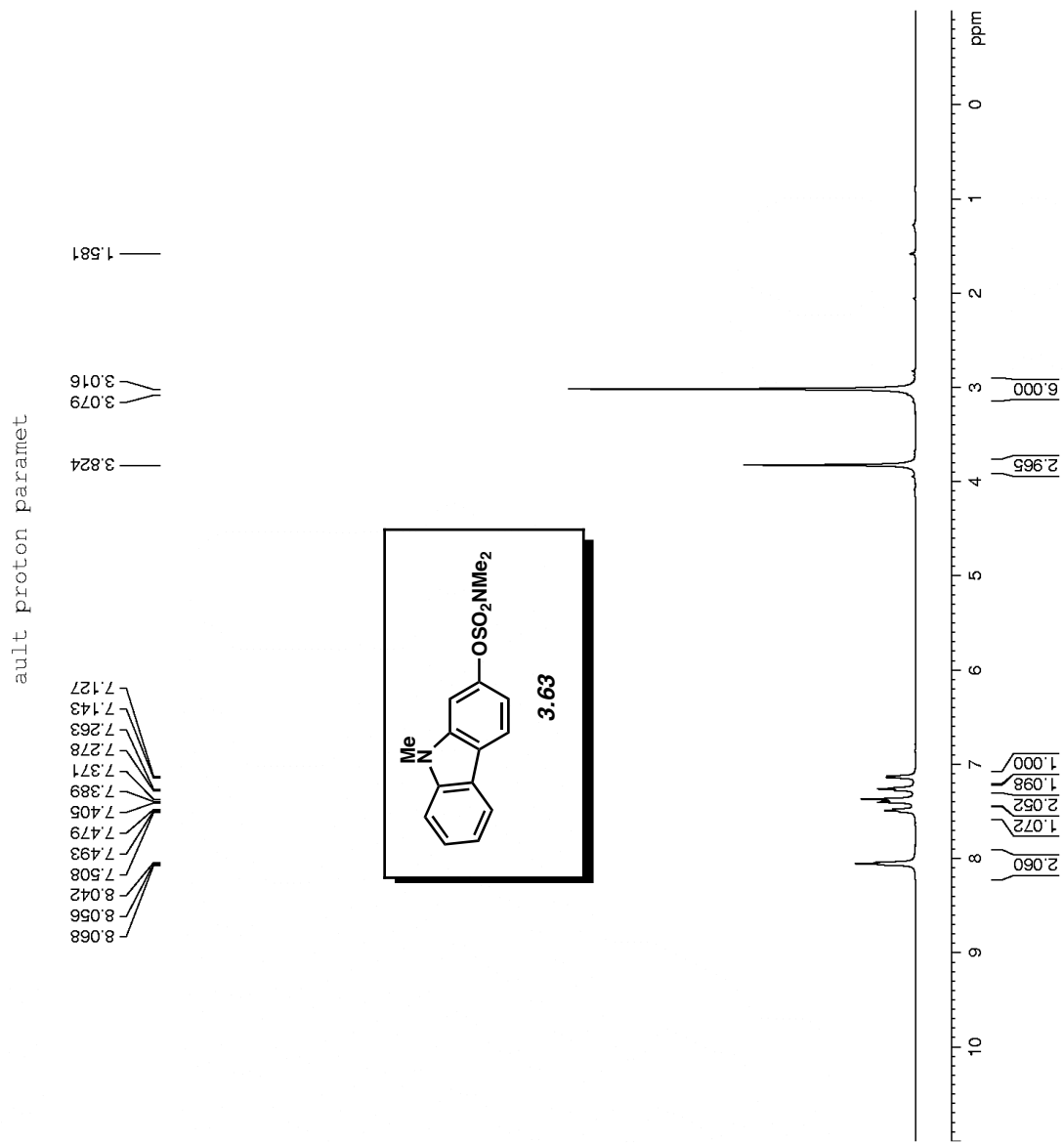


Figure A2.8 ¹H NMR (500 MHz, CDCl₃) of compound **3.63**.

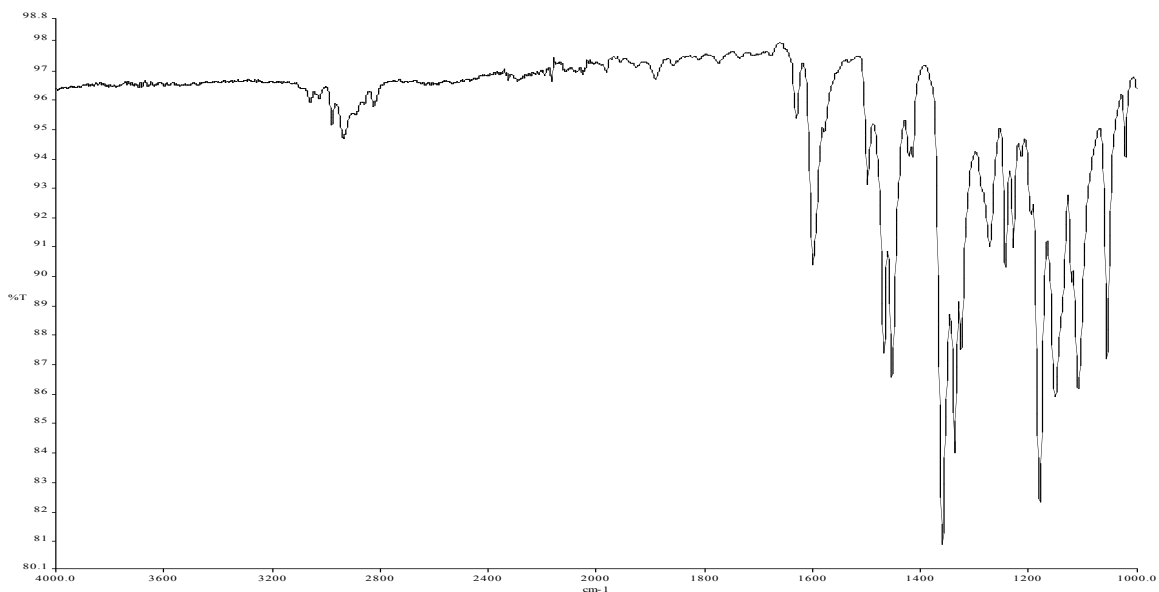


Figure A2.9 Infrared spectrum of compound **3.63**.

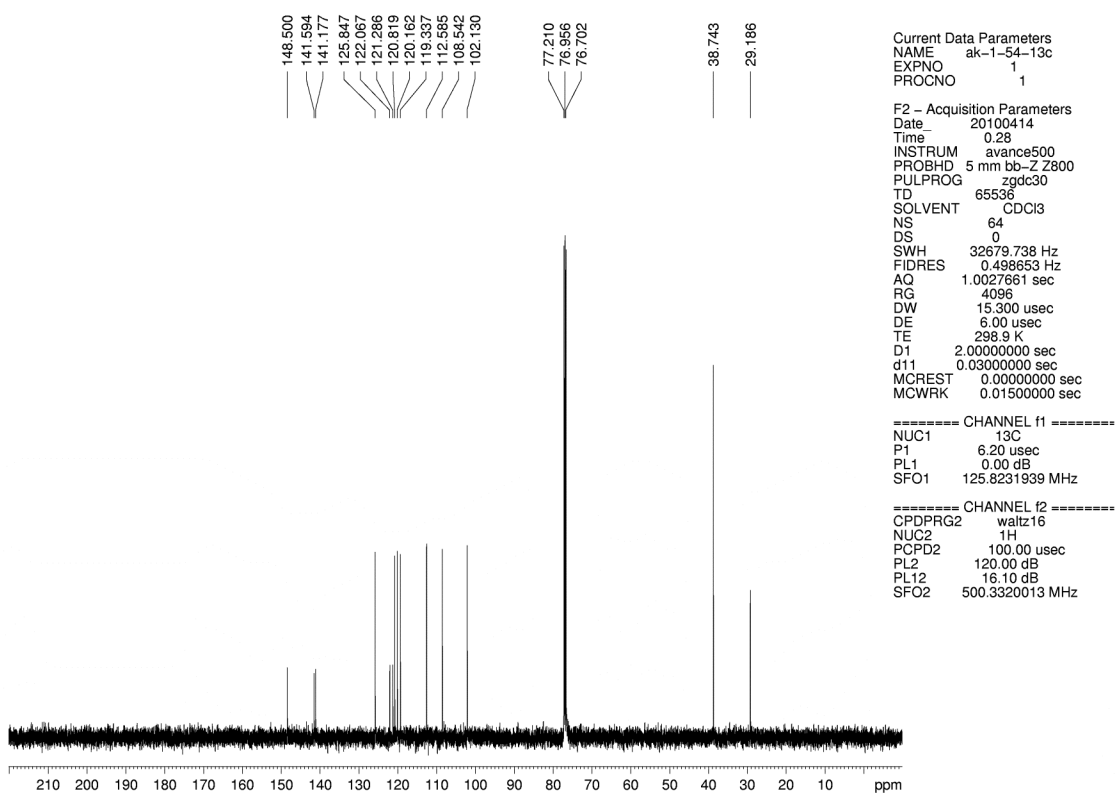


Figure A2.10 ^{13}C NMR (125 MHz, CDCl_3) of compound **3.63**.

```

Current Data Parameters
NAME      AST-27
EXPNO    10
PROCNO   1

F2 - Acquisition Parameters
Date_    20100508
Time     19.55
INSTRUM  avance500
PROBHD   5 mm bb-Z Z800
PULPROG  zg30
TD       65536
SOLVENT  CDCl3
NS       8
DS       0
SWH      10000.000 Hz
FIDRES   0.152588 Hz
AQ       3.2769001 sec
RG       45.3
DW       50.000 usec
DE       6.00 usec
TE       298.7 K
D1       2.00000000 sec
MCREST   0.00000000 sec
MCWRK    0.01500000 sec

===== CHANNEL f1 =====
NUC1     1H
P1       12.00 usec
PL1      0.00 dB
SFO1     500.3330020 MHz

F2 - Processing parameters
SI       32768
SF       500.3300220 MHz
WDW      EM
SSB      0
LB       0.30 Hz
GB       0
PC       1.00

```

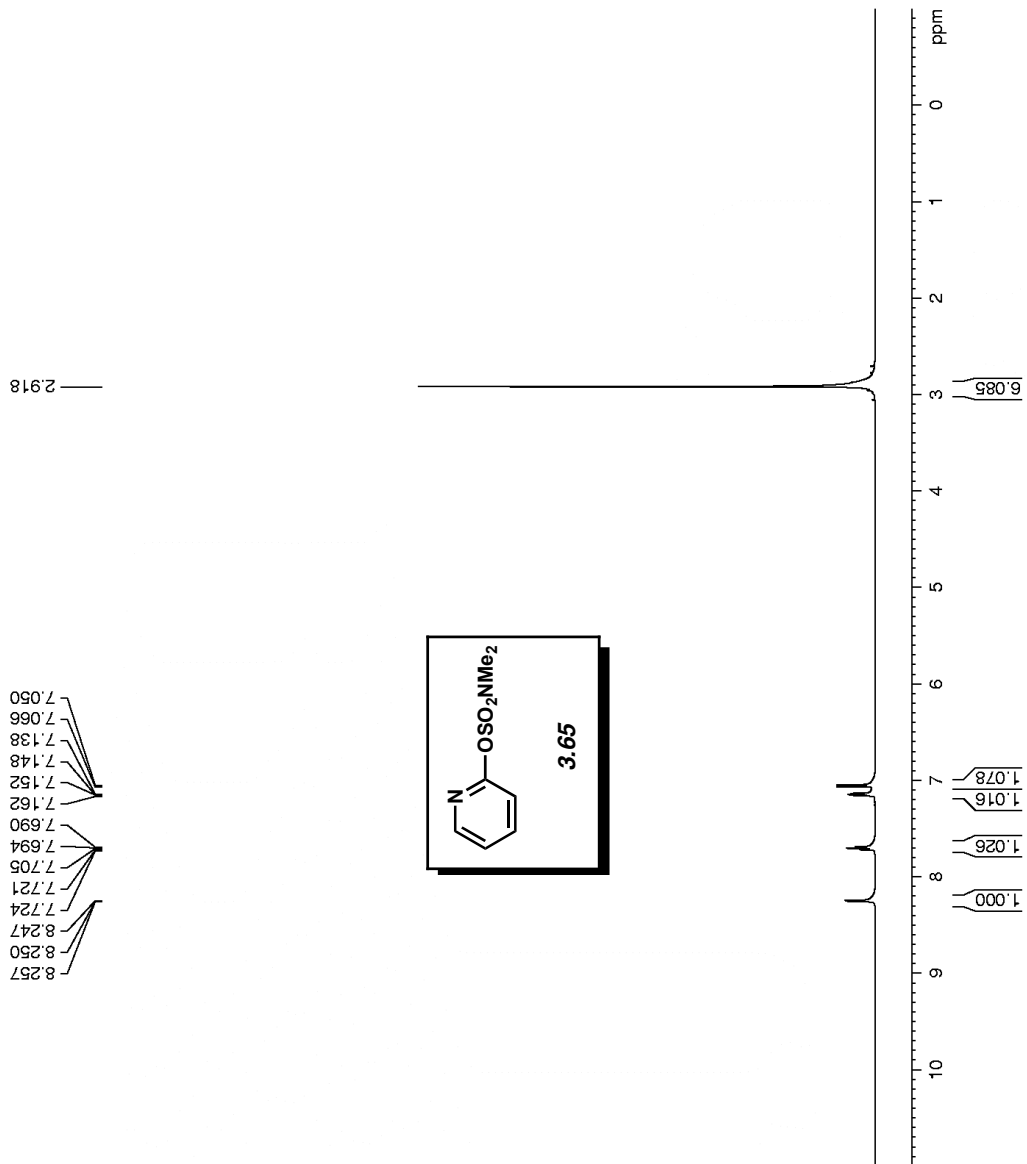


Figure A2.11 ¹H NMR (500 MHz, CDCl₃) of compound 3.65.

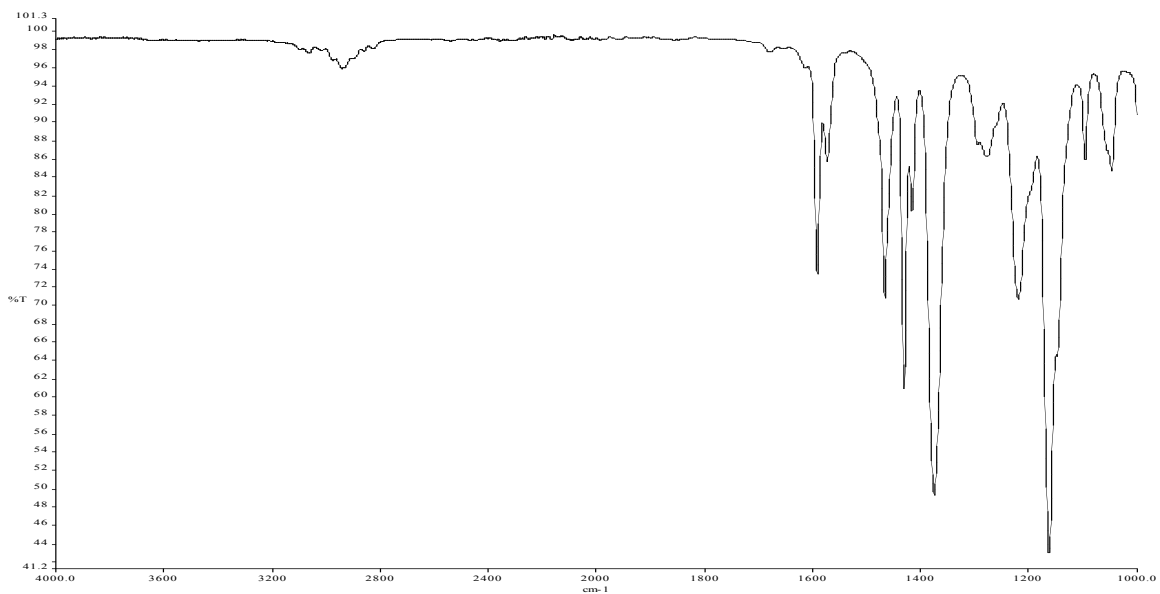


Figure A2.12 Infrared spectrum of compound **3.65**.

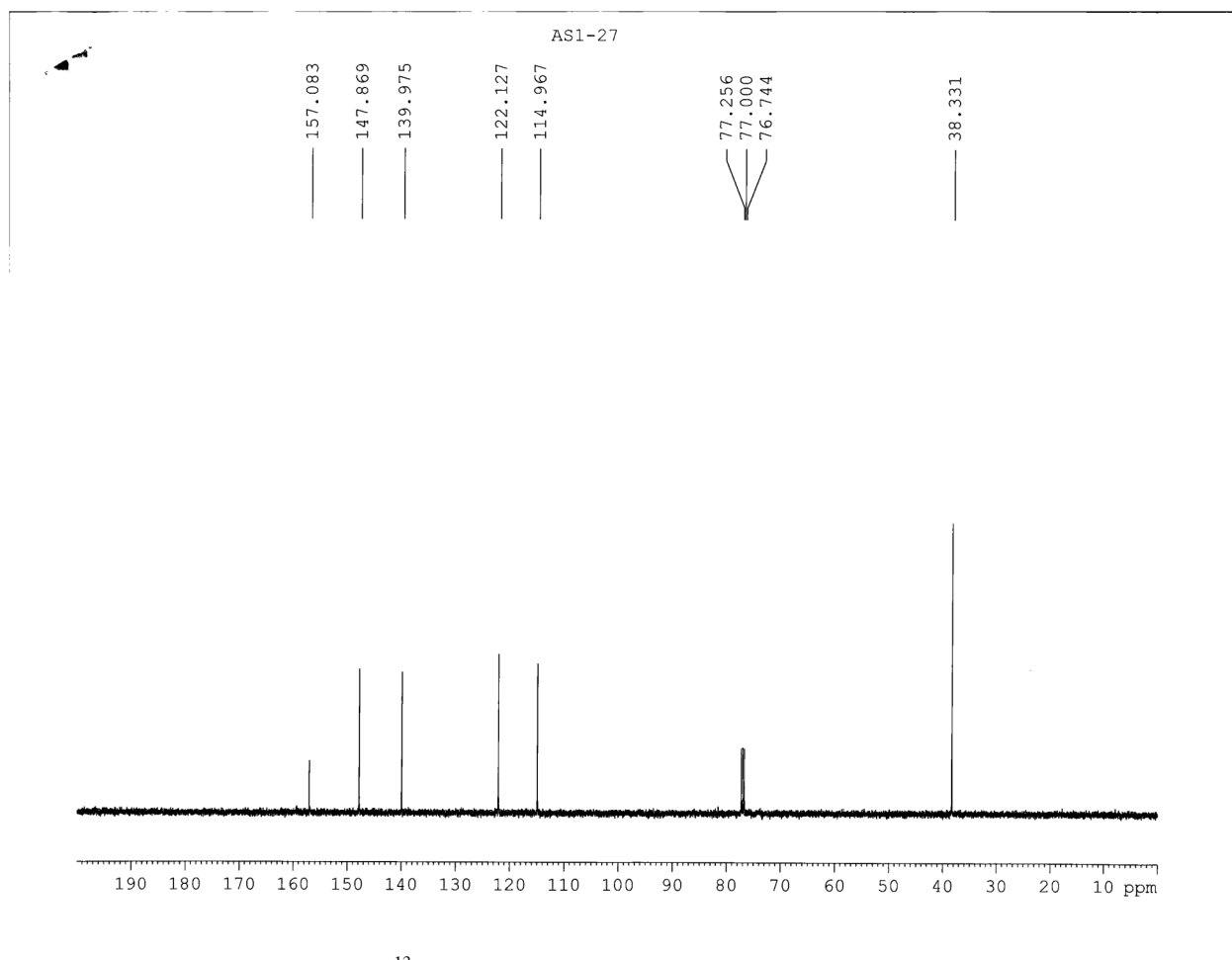


Figure A2.13 ¹³C NMR (125 MHz, CDCl₃) of compound **3.65**.

Current Data Parameters
 NAME ak1-69
 EXPNO 10
 PROCNO 1

F2 - Acquisition Parameters
 Date_ 20100508
 Time_ 19.30
 INSTRUM avance500
 PROBHD 5 mm bb-Z Z800
 PULPROG zg30
 TD 65536
 SOLVENT CDCI3
 NS 8
 DS 0
 SWH 10000.000 Hz
 FIDRES 0.152588 Hz
 AQ 3.2769001 sec
 RG 90.5
 DW 50.000 usec
 DE 6.00 usec
 TE 298.6 K
 D1 2.0000000 sec
 MCREST 0.0000000 sec
 MCWRK 0.01500000 sec

===== CHANNEL f1 =====
 NUC1 1H
 P1 12.00 usec
 PL1 0.00 dB
 SFO1 500.3330020 MHz

F2 - Processing parameters
 SI 32768
 SF 500.3300220 MHz
 WDW EM
 SSB 0
 LB 0.30 Hz
 GB 0
 PC 1.00

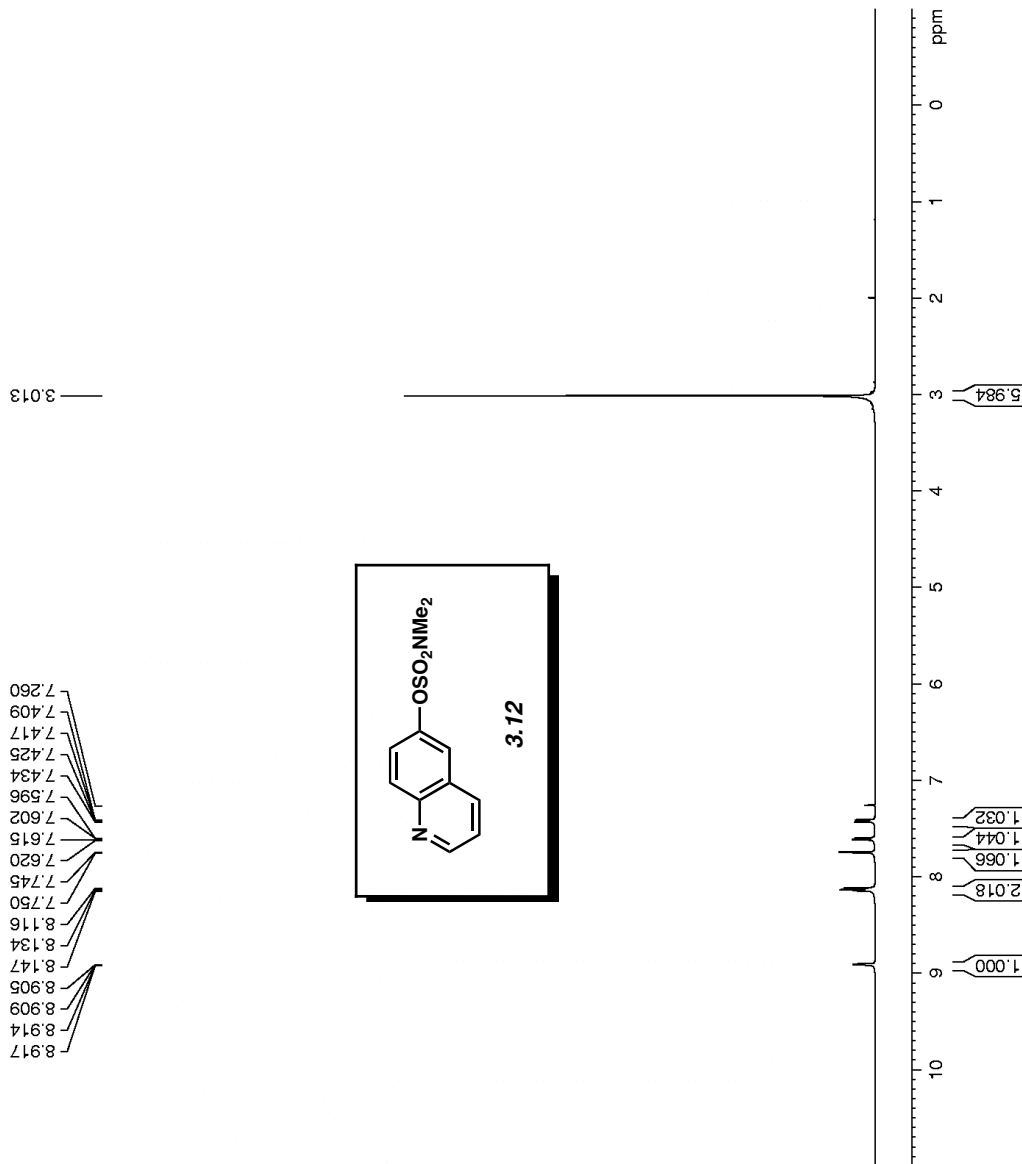


Figure A2.14 ¹H NMR (500 MHz, CDCl₃) of compound 3.12.

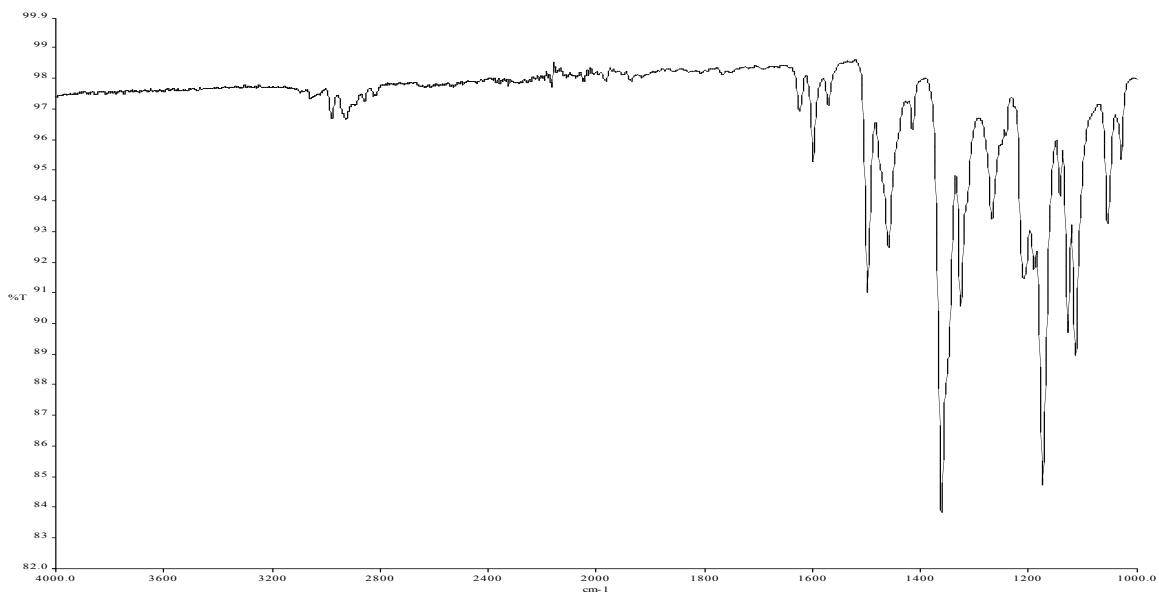


Figure A2.15 Infrared spectrum of compound 3.12.

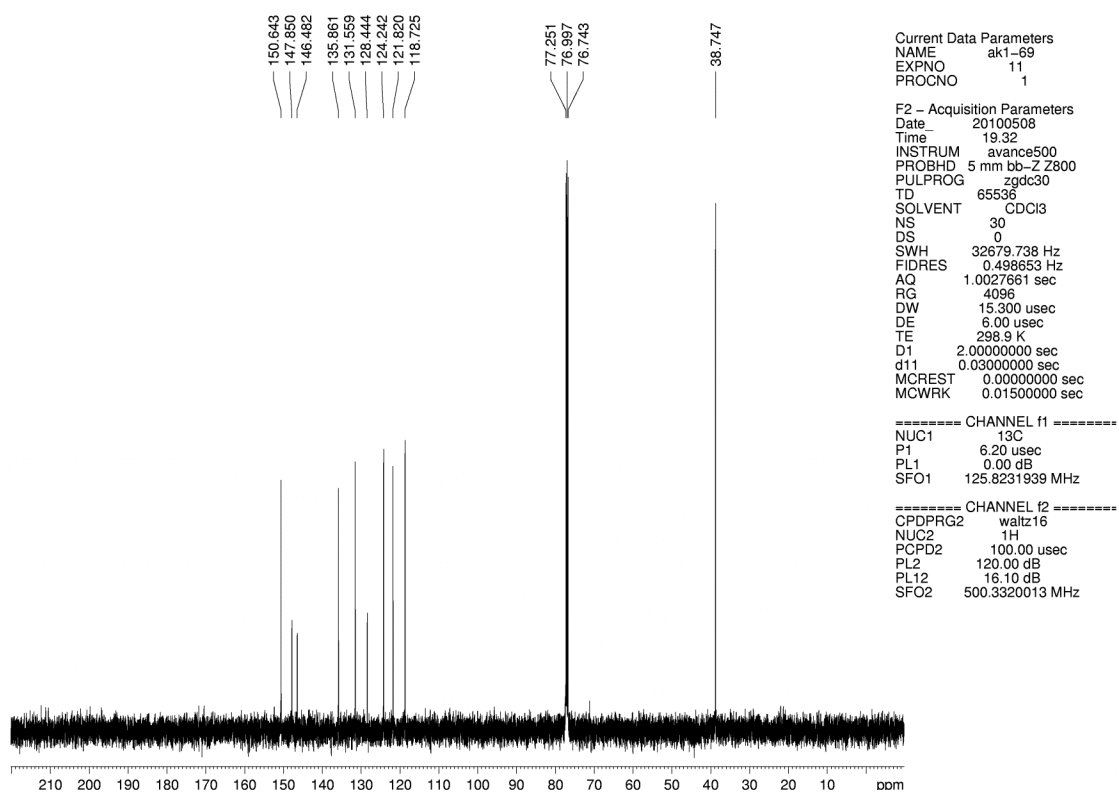


Figure A2.16 ¹³C NMR (125 MHz, CDCl₃) of compound 3.12.

Current Data Parameters
 NAME AK1-59
 EXPNO 10
 PROCNO 1

F2 - Acquisition Parameters
 Date_ 20100508
 Time_ 18.52
 INSTRUM avance500
 PROBHD 5 mm bb-Z Z800
 PULPROG zg30
 TD 65536
 SOLVENT CDCl3
 NS 8
 DS 0
 SWH 10000.000 Hz
 FIDRES 0.152588 Hz
 AQ 3.2769001 sec
 RG 128
 DW 50.000 usec
 DE 6.00 usec
 TE 298.5 K
 D1 2.0000000 sec
 MCREST 0.0000000 sec
 MCWRK 0.01500000 sec

==== CHANNEL f1 =====
 NUC1 1H
 P1 12.00 usec
 PL1 0.00 dB
 SFO1 500.3330020 MHz

F2 - Processing parameters
 SI 32768
 SF 500.3300220 MHz
 WDW EM
 SSB 0
 LB 0.30 Hz
 GB 0
 PC 1.00

3.040
 2.764

8.064
 8.047
 7.749
 7.733
 7.702
 7.686
 7.478
 7.462
 7.446
 7.346
 7.329
 7.259

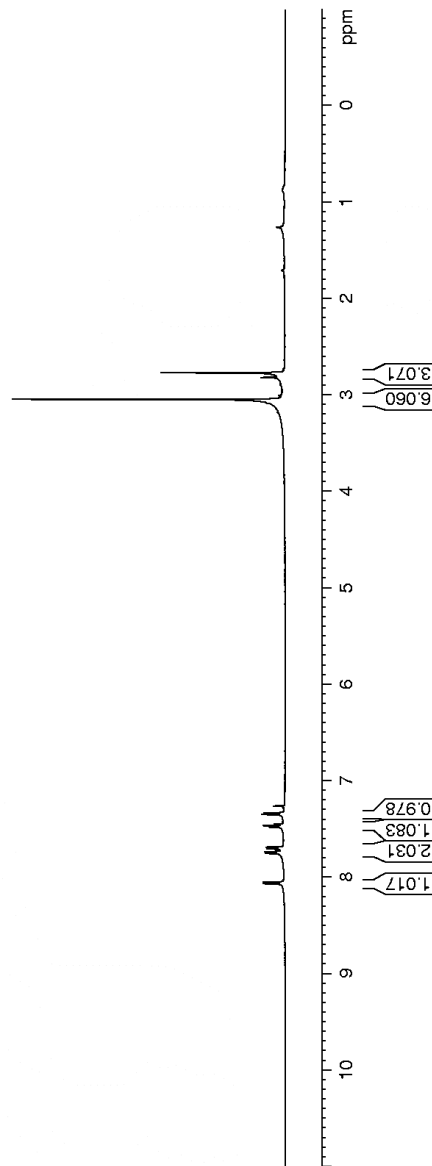
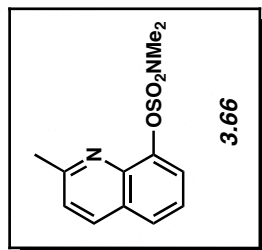


Figure A2.17 ¹H NMR (500 MHz, CDCl₃) of compound **3.66**.

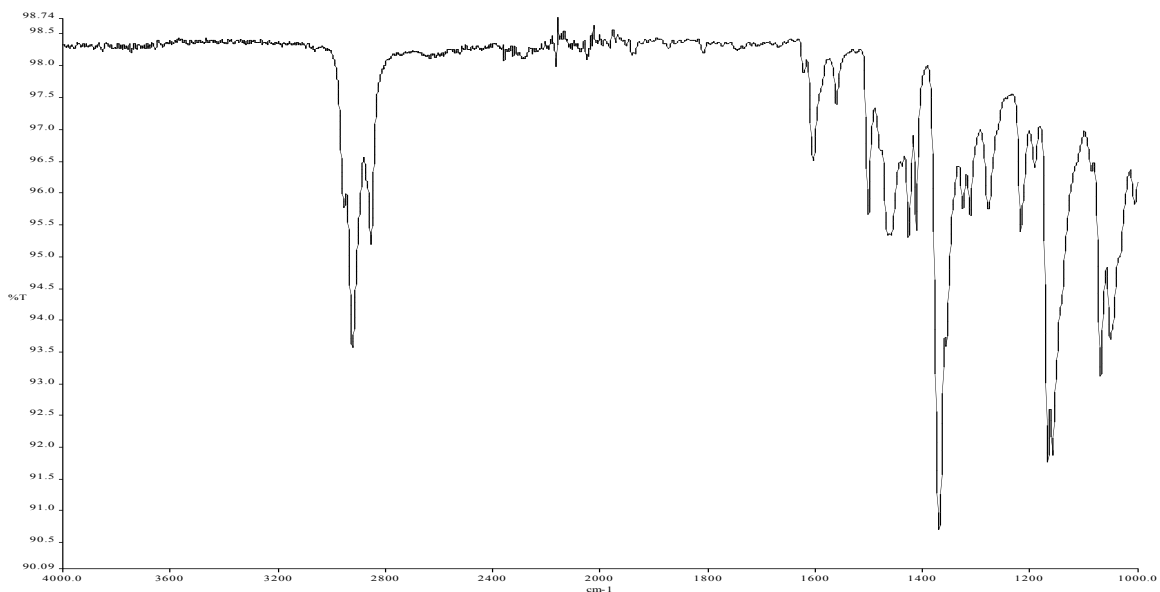


Figure A2.18 Infrared spectrum of compound **3.66**.

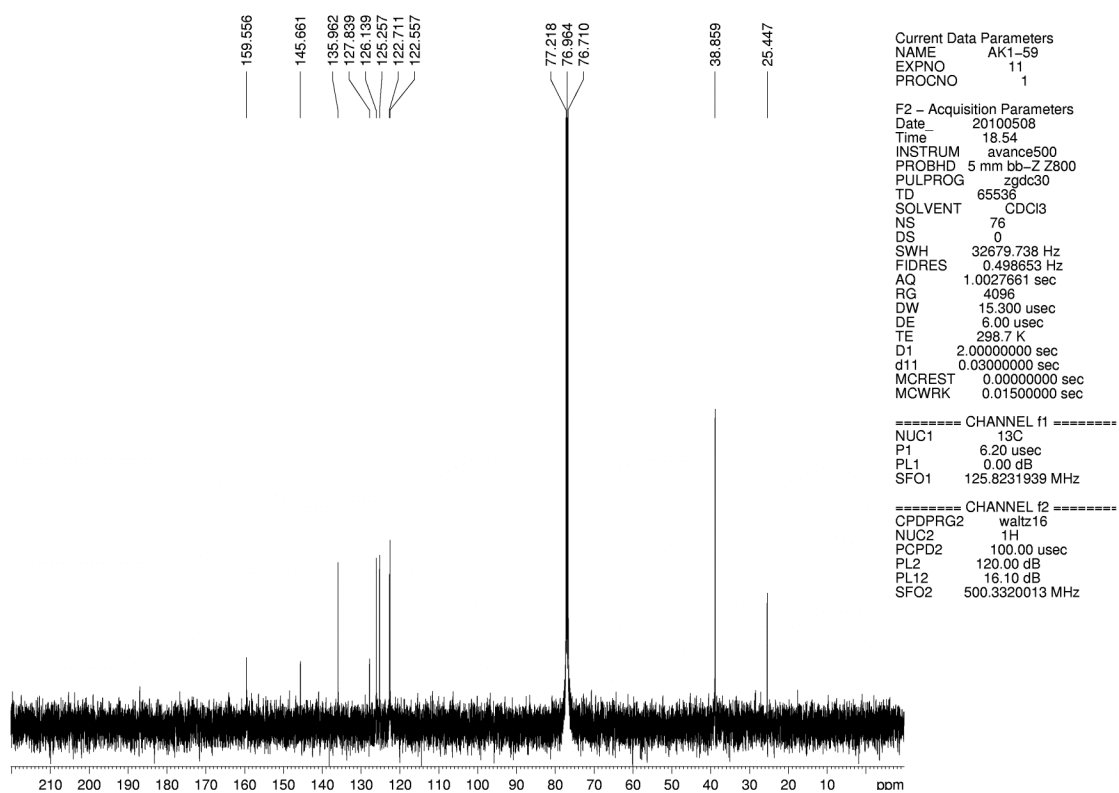


Figure A2.19 ^{13}C NMR (125 MHz, CDCl_3) of compound **3.66**.

Current Data Parameters
 NAME AS-1-86
 EXPNO 1
 PROCNO 1

F2 - Acquisition Parameters
 Date_ 20100325
 Time 3.45
 INSTRUM avance500
 PROBHD 5 mm bb-Z Z800
 PULPROG zg30
 TD 65536
 SOLVENT CDCl3
 NS 16
 DS 0
 SWH 10000.000 Hz
 FIDRES 0.152588 Hz
 AQ 3.2769001 sec
 RG 287.4
 DW 50.000 usec
 DE 6.00 usec
 TE 296.0 K
 D1 2.0000000 sec
 MCREST 0.0000000 sec
 MCWRK 0.01500000 sec

===== CHANNEL f1 =====
 NUC1 1H
 P1 12.00 usec
 PL1 0.00 dB
 SFO1 500.3330020 MHz

F2 - Processing parameters
 SI 32768
 SF 500.3300225 MHz
 WDW EM
 SSB 0
 LB 0.30 Hz
 GB 0
 PC 1.00

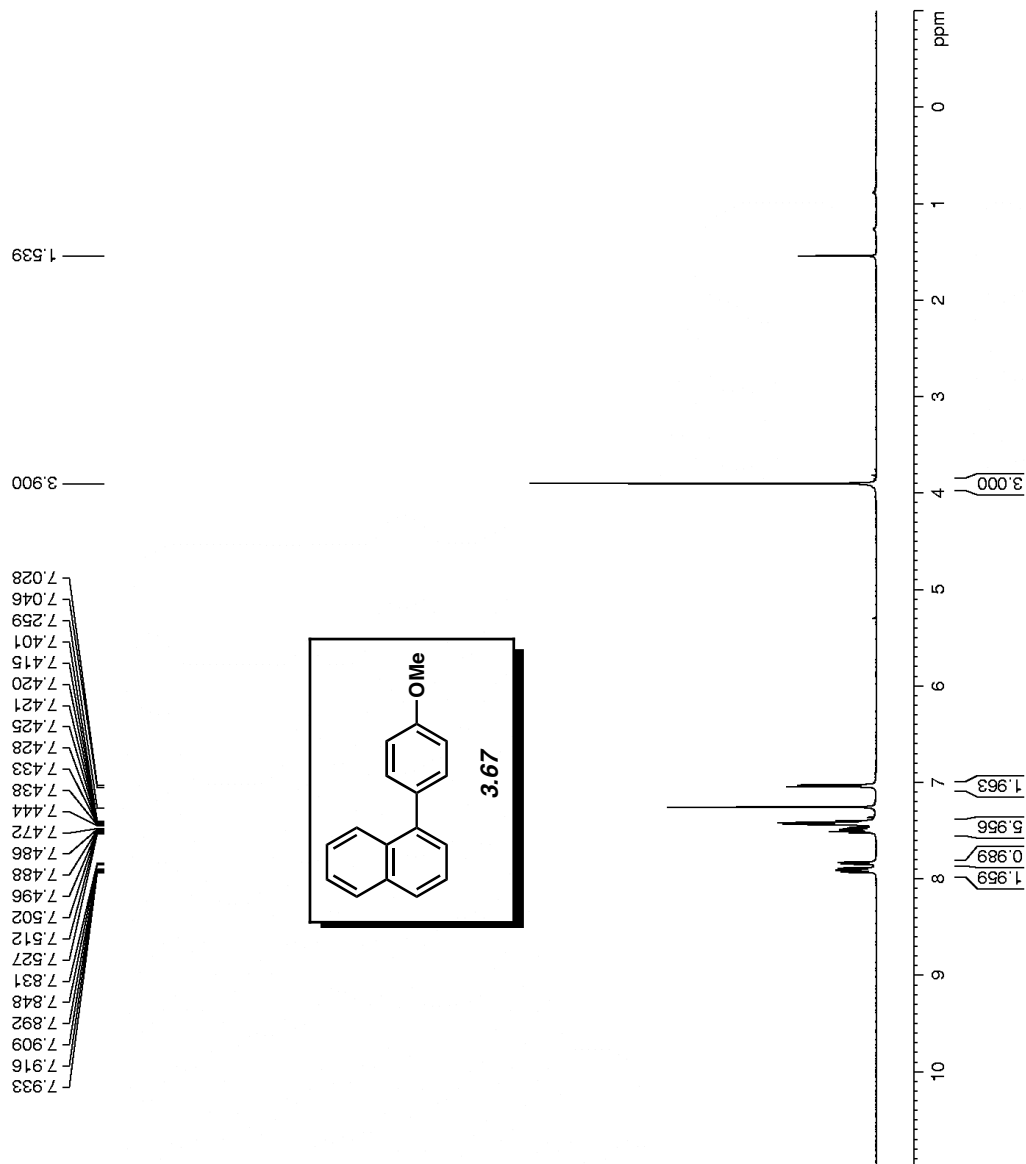


Figure A2.20 ¹H NMR (500 MHz, CDCl₃) of compound 3.67.

Current Data Parameters
 NAME AS-1-76
 EXPNO 1
 PROCNO 1

F2 - Acquisition Parameters
 Date_ 20100401
 Time 17.38
 INSTRUM avance500
 PROBHD 5 mm bb-Z Z800
 PULPROG zg30
 TD 65536
 SOLVENT CDCl3
 NS 16
 DS 0
 SWH 10000.000 Hz
 FIDRES 0.152588 Hz
 AQ 3.2769001 sec
 RG 71.8
 DW 50.000 usec
 DE 6.00 usec
 TE 295.6 K
 D1 2.00000000 sec
 MCREST 0.00000000 sec
 MCWRK 0.01500000 sec

==== CHANNEL f1 =====
 NUJC1 1H
 P1 12.00 usec
 PL1 0.00 dB
 SFO1 500.3330020 MHz

F2 - Processing parameters
 SI 32768
 SF 500.3300221 MHz
 WDW EM
 SSB 0
 LB 0.30 Hz
 GB 0
 PC 1.00

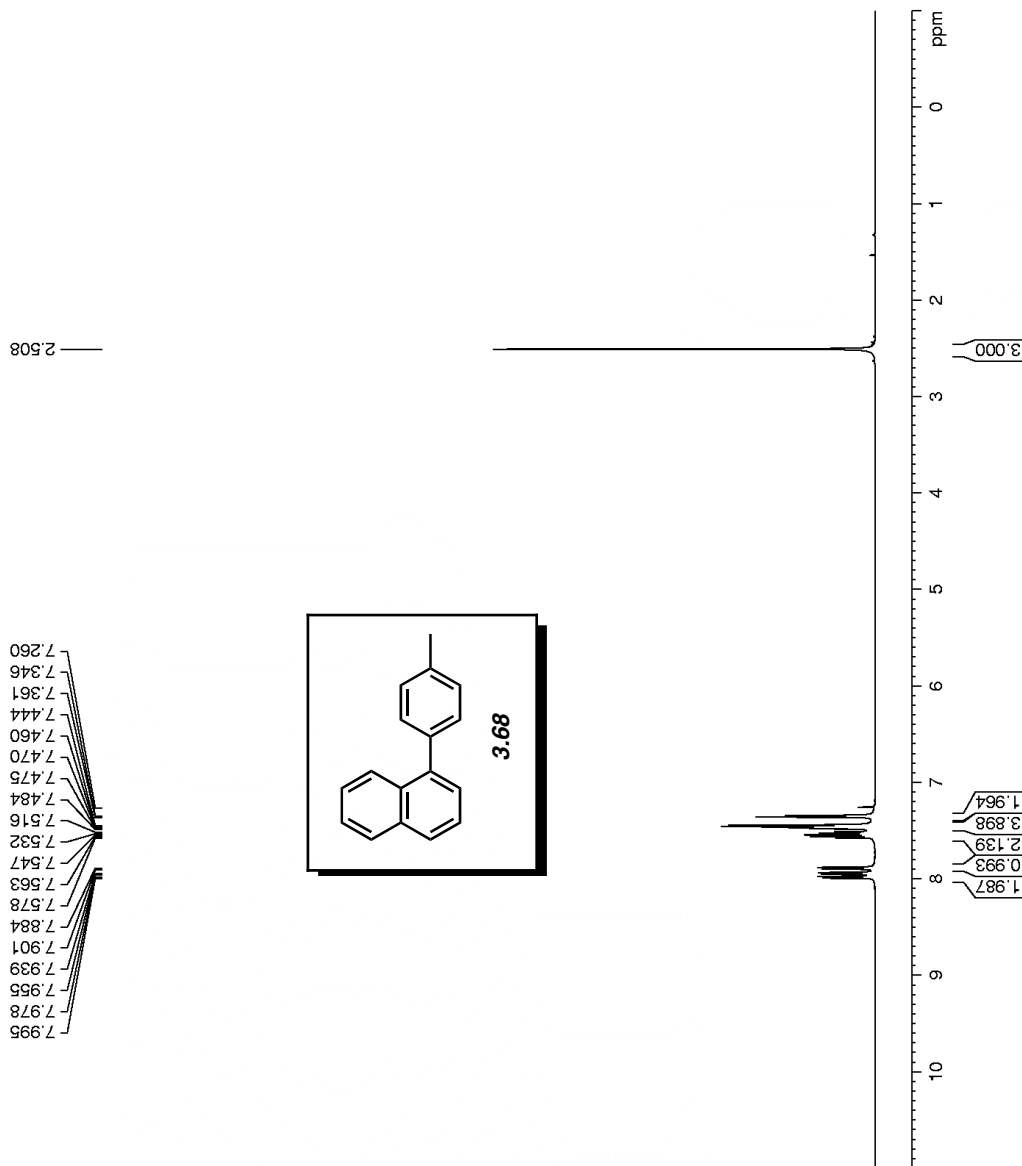


Figure A2.21 ¹H NMR (500 MHz, CDCl₃) of compound 3.68.

```

Current Data Parameters
NAME      AS-1-74
EXPNO    1
PROCNO   1

F2 - Acquisition Parameters
Date_    20100401
Time     17.34
INSTRUM  avance500
PROBHD   5 mm bb-Z Z800
PULPROG  zg30
TD       65536
SOLVENT  CDCl3
NS       16
DS       0
SWH      10000.000 Hz
FIDRES   0.152588 Hz
AQ       3.2769001 sec
RG       57
DW       50.000 usec
DE       6.00 usec
TE       295.6 K
D1       2.0000000 sec
MCREST   0.0000000 sec
MCWRK    0.01500000 sec

===== CHANNEL f1 =====
NUC1     1H
P1       12.25 usec
PL1      0.00 dB
SFO1     500.3330020 MHz

F2 - Processing parameters
SI       32768
SF       500.3300223 MHz
WDW      EM
SSB      0
LB       0.30 Hz
GB       0
PC       1.00

```

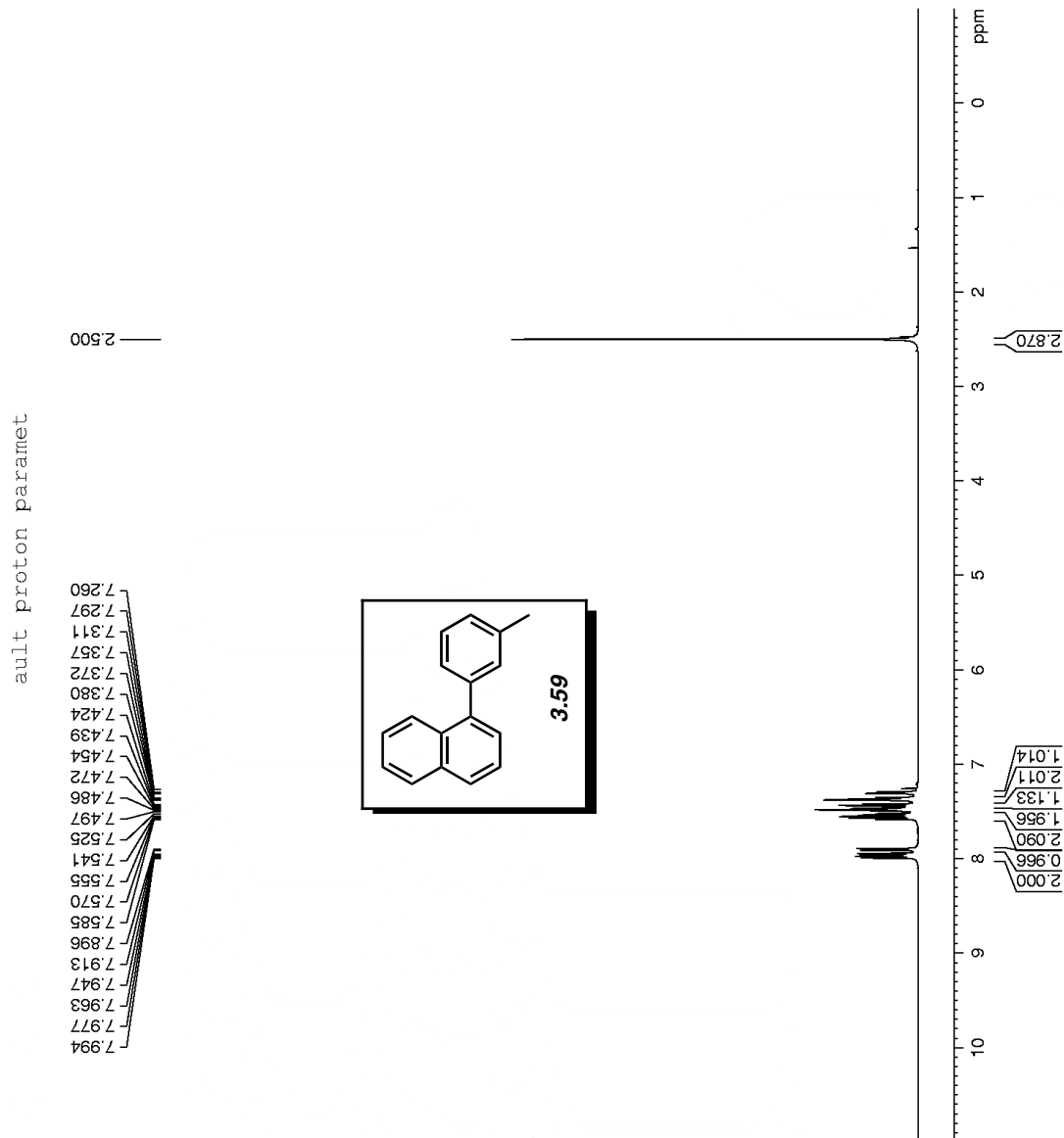


Figure A2.22 ¹H NMR (500 MHz, CDCl₃) of compound 3.59.

Current Data Parameters
 NAME AS-1-79
 EXPNO 1
 PROCNO 1

F2 - Acquisition Parameters
 Date_ 20100406
 Time 5.05
 INSTRUM avance500
 PROBHD 5 mm bb-Z Z800
 PULPROG zg30
 TD 65536
 SOLVENT CDCl3
 NS 16
 DS 0
 SWH 10000.000 Hz
 FIDRES 0.152588 Hz
 AQ 3.2769001 sec
 RG 128
 DW 50.000 usec
 DE 6.00 usec
 TE 301.2 K
 D1 2.00000000 sec
 MCREST 0.00000000 sec
 MCWRK 0.01500000 sec

===== CHANNEL f1 =====
 NUC1 1H
 P1 12.00 usec
 PL1 0.00 dB
 SFO1 500.3330020 MHz

F2 - Processing parameters
 SI 32768
 SF 500.3300220 MHz
 WDW EM
 SSB 0
 LB 0.30 Hz
 GB 0
 PC 1.00

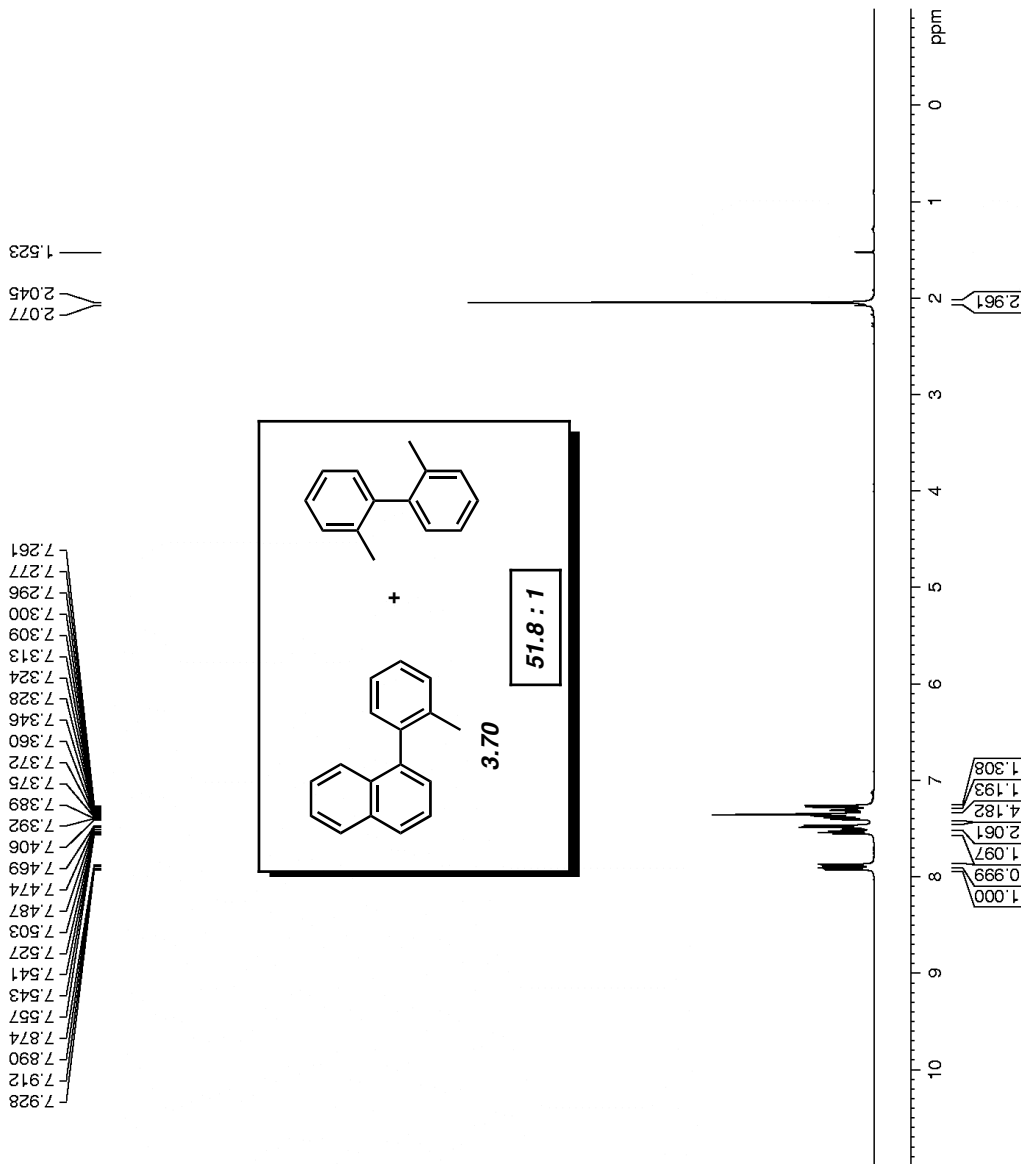


Figure A2.23 ¹H NMR (500 MHz, CDCl₃) of compound **3.70**.

```

Current Data Parameters
NAME      AS-1-97B
EXPNO    1
PROCNO   1

F2 - Acquisition Parameters
Date_    20100421
Time     20.22
INSTRUM  avance500
PROBHD   5 mm bb-Z Z800
PULPROG  zg30
TD       65536
SOLVENT  C6D6
NS       8
DS       0
SWH      10000.000 Hz
FIDRES   0.152588 Hz
AQ       3.2769001 sec
RG       80.6
DW       50.000 usec
DE       6.00 usec
TE       298.2 K
D1       2.00000000 sec
MCREST   0.00000000 sec
MCWRK    0.01500000 sec

===== CHANNEL f1 =====
NUC1     1H
P1       12.25 usec
PL1      0.00 dB
SFO1     500.3330020 MHz

F2 - Processing parameters
SI       32768
SF       500.3300110 MHz
WDW      EM
SSB      0
LB       0.30 Hz
GB       0
PC       1.00

```

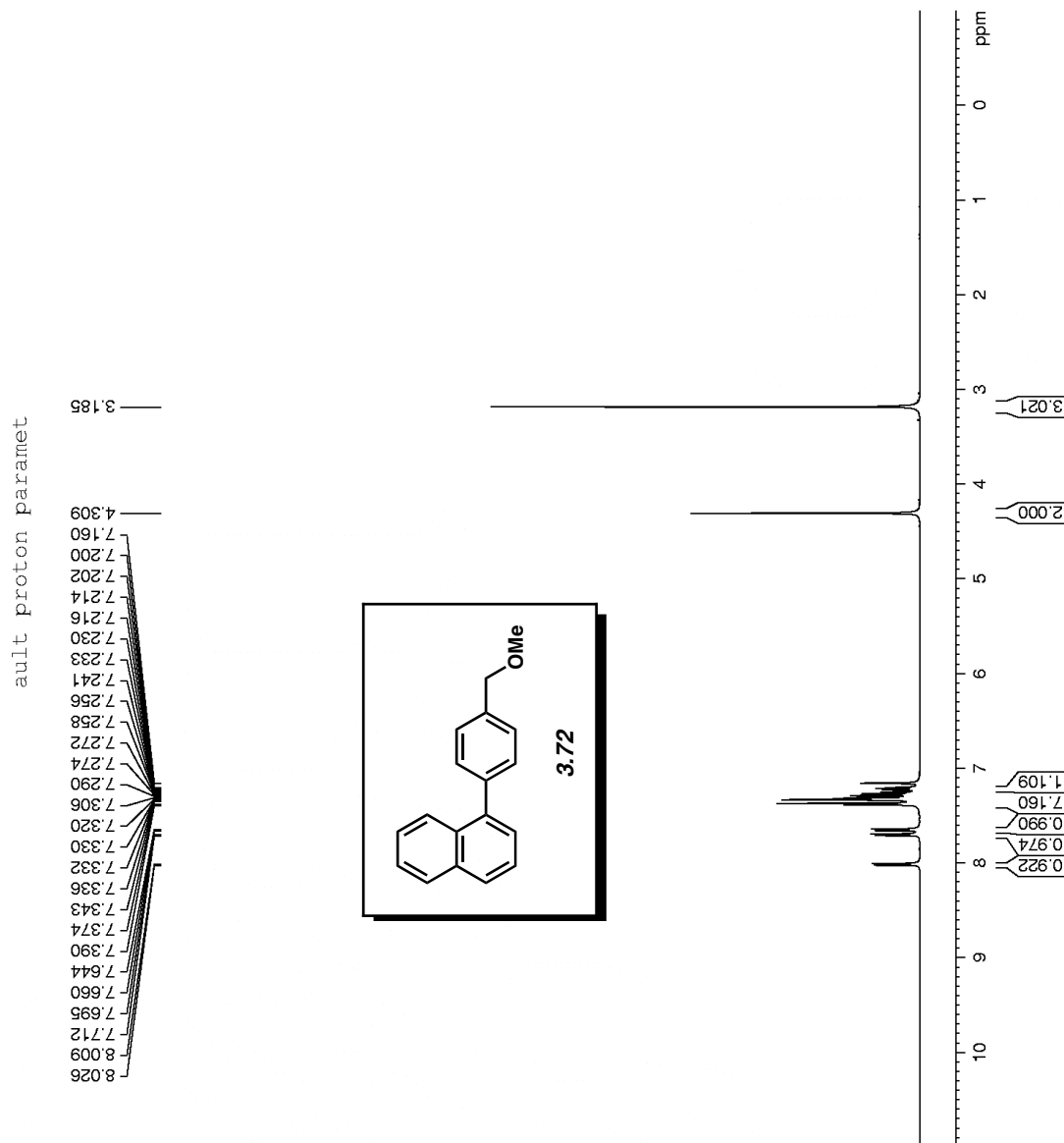


Figure A2.24 ¹H NMR (500 MHz, C₆D₆) of compound 3.72.

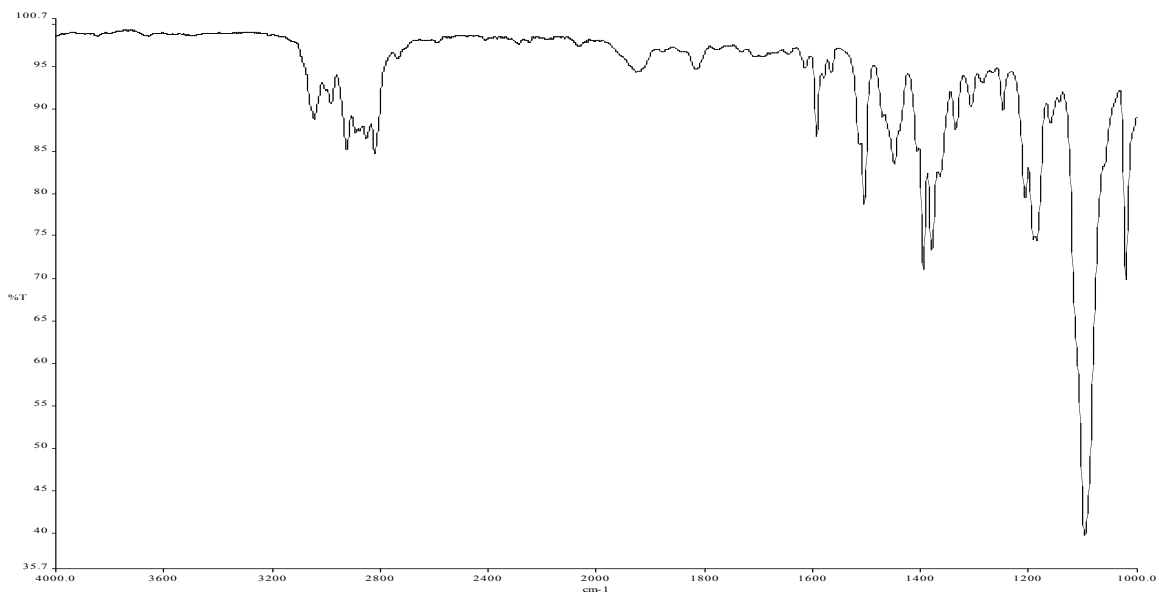


Figure A2.25 Infrared spectrum of compound 3.72.

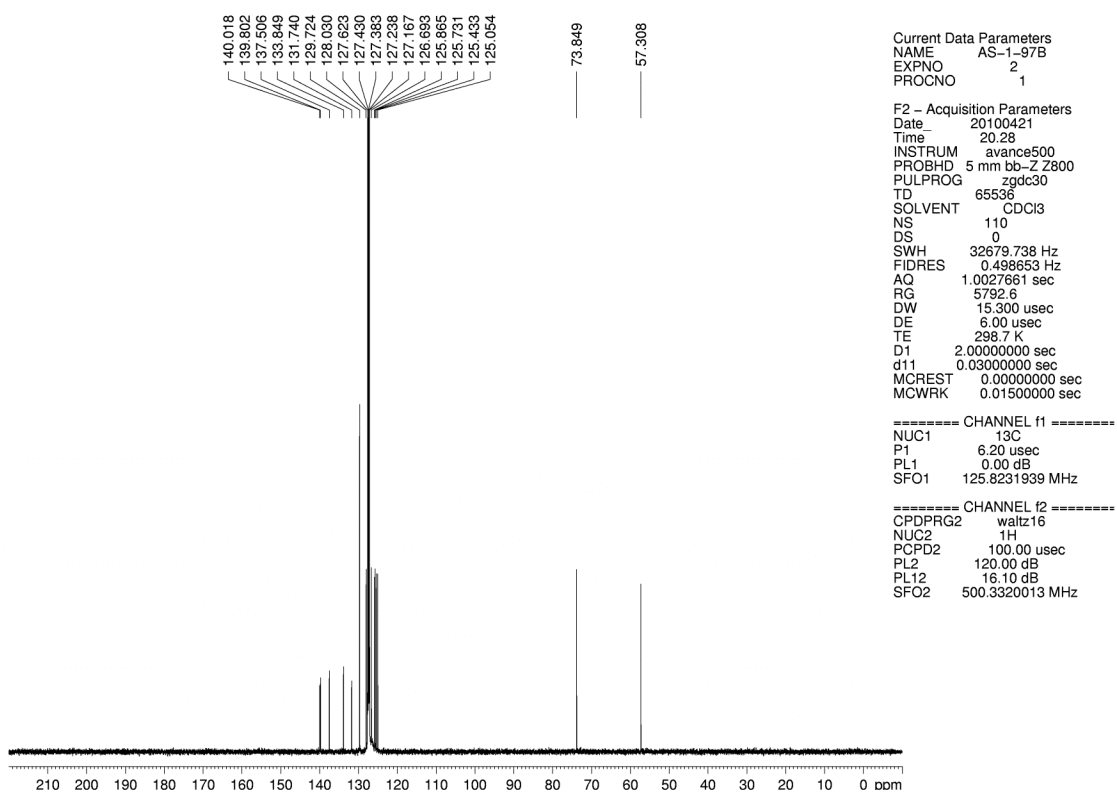


Figure A2.26 ¹³C NMR (125 MHz, C₆D₆) of compound 3.72.

Account no. nkg338
AS-1-78

Current Data Parameters
NAME AS-1-78
EXPNO 390
PROCNO 1

F2 - Acquisition Parameters
Date_ 20100402
Time 22.03
INSTRUM arx400
PROBHD 5 mm QNP 1H
PULPROG zg30
TD 65536
SOLVENT CDCl3
NS 32
DS 0
SWH 8064.516 Hz
FIDRES 0.123055 Hz
AQ 4.0632820 sec
RG 256
DW 62.000 usec
DE 88.57 usec
TE 300.0 K
D1 2.0000000 sec
P1 7.50 usec
SFO1 400.1324008 MHz
NUCLEUS 1H

F2 - Processing parameters
SI 65536
SF 400.1300179 MHz
WDW EM
SSB 0
LB 0.30 Hz
GB 0
PC 1.00

Account no. nkg338
AS-1-78

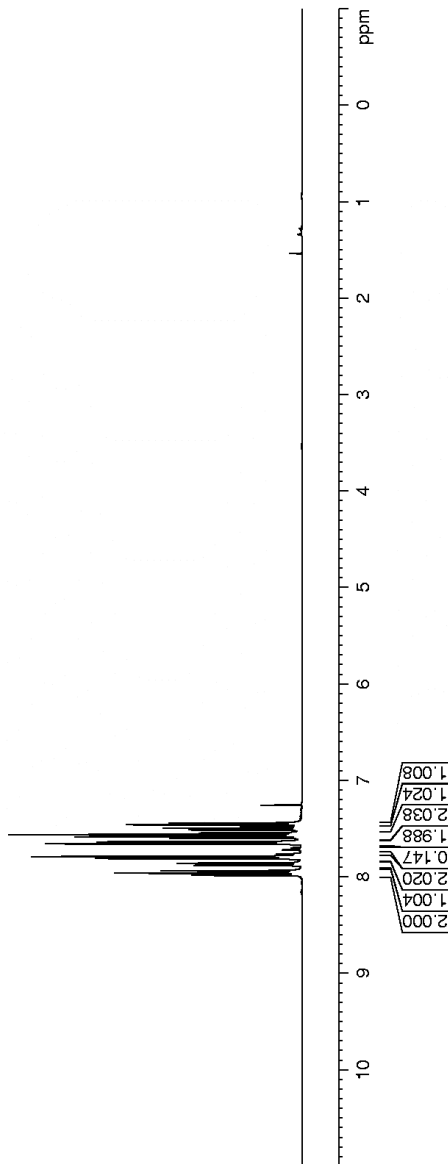
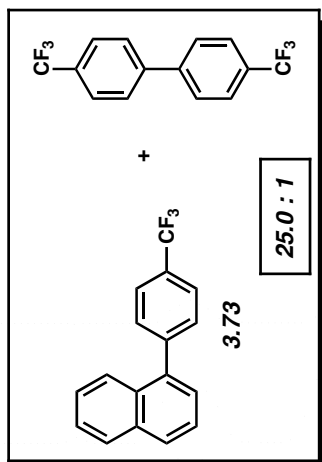
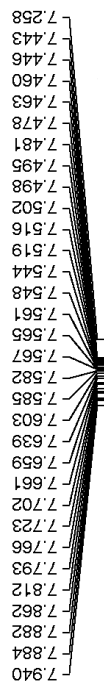


Figure A2.27 ^1H NMR (400 MHz, CDCl_3) of compound **3.73**.

Current Data Parameters
 NAME AS-1-129A
 EXPNO 3
 PROCNO 1

F2 - Acquisition Parameters
 Date_ 20100606
 Time_ 14.49
 INSTRUM avance500
 PROBHD 5 mm bb-Z Z800
 PULPROG zg30
 TD 65536
 SOLVENT CDCl3
 NS 8
 DS 0
 SWH 10000.000 Hz
 FIDRES 0.152588 Hz
 AQ 3.2769001 sec
 RG 181
 DW 50.000 usec
 DE 6.00 usec
 TE 298.3 K
 D1 2.00000000 sec
 MCREST 0.00000000 sec
 MCWRK 0.01500000 sec

==== CHANNEL f1 =====
 NUC1 1H
 P1 12.25 usec
 PL1 0.00 dB
 SFO1 500.3330020 MHz

F2 - Processing parameters
 SI 32768
 SF 500.3300222 MHz
 EM
 WDW 0
 SSB 0
 LB 0.30 Hz
 GB 0
 PC 1.00

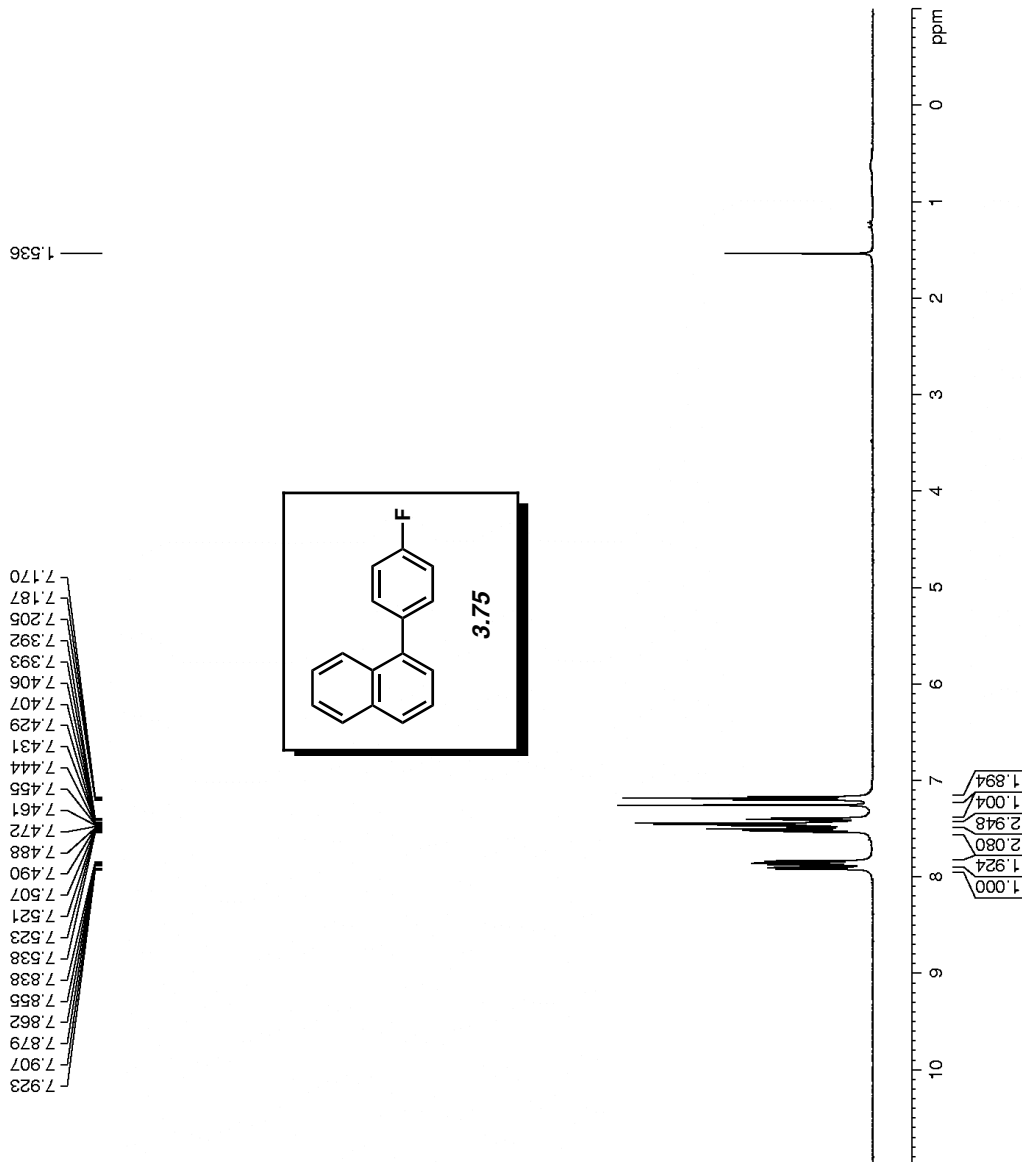


Figure A2.28 ¹H NMR (500 MHz, CDCl₃) of compound 3.75.

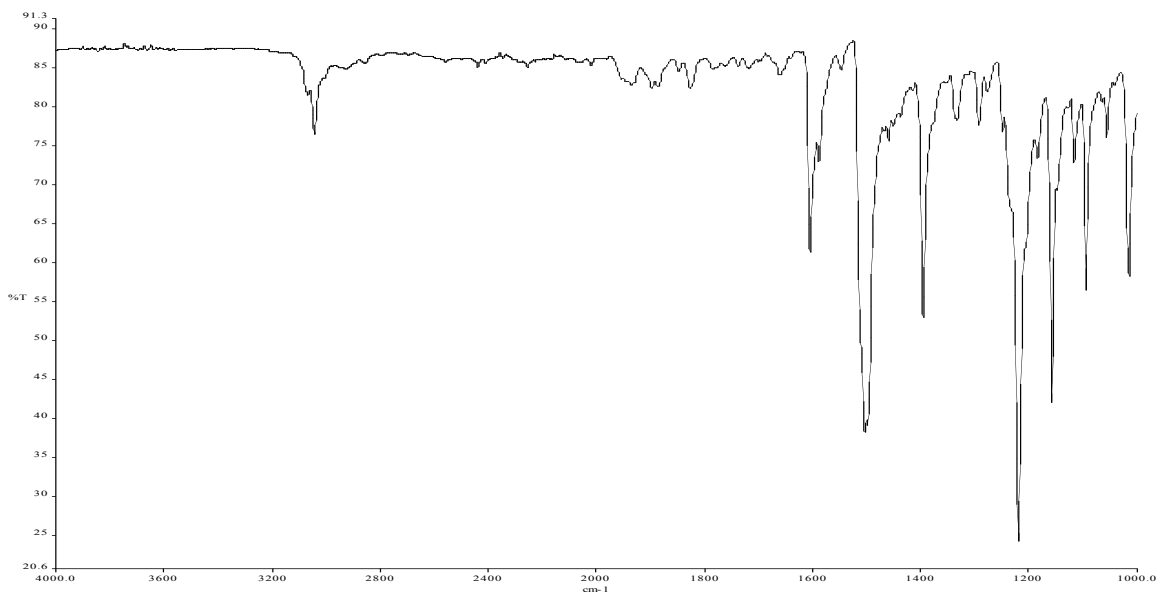


Figure A2.29 Infrared spectrum of compound **3.75**.

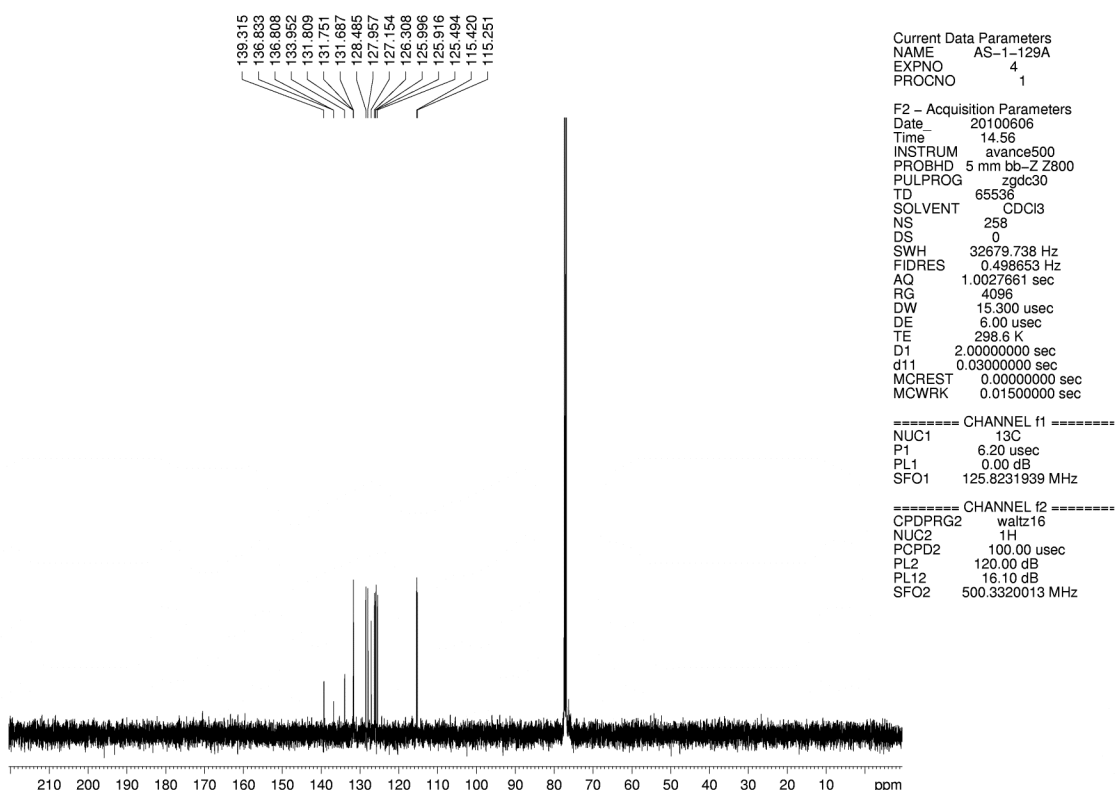


Figure A2.30 ^{13}C NMR (125 MHz, CDCl_3) of compound **3.75**.

```

Current Data Parameters
NAME      AS-1-127
EXPNO     1
PROCNO    1

F2 - Acquisition Parameters
Date_     20100512
Time      19.46
INSTRUM   avance500
PROBHD    5 mm bb-Z Z800
PULPROG   zg30
TD         65536
SOLVENT   CDCl3
NS         16
DS         0
SWH        10000.000 Hz
FIDRES     0.152588 Hz
AQ         3.2769001 sec
RG         90.5
DW         50.000 usec
DE         6.00 usec
TE         297.8 K
D1         2.00000000 sec
MCREST     0.00000000 sec
MCWRK     0.01500000 sec

===== CHANNEL f1 =====
NUC1       1H
P1         12.25 usec
PL1        0.00 dB
SFO1       500.3330020 MHz

F2 - Processing parameters
SI         32768
SF         500.3300220 MHz
WDW        EM
SSB        0
LB         0.30 Hz
GB         0
PC         1.00

```

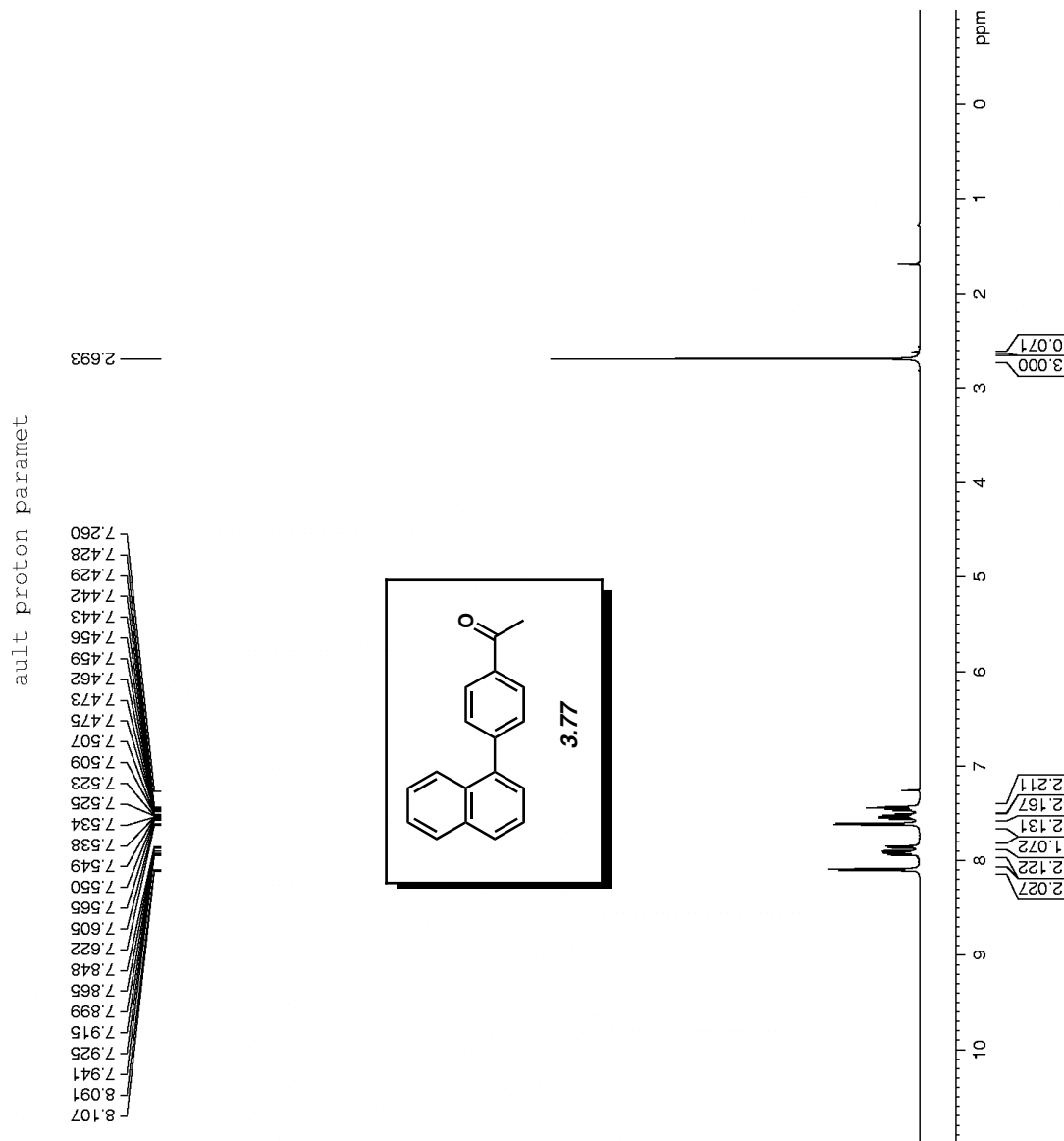


Figure A2.31 ¹H NMR (500 MHz, CDCl₃) of compound **3.77**.

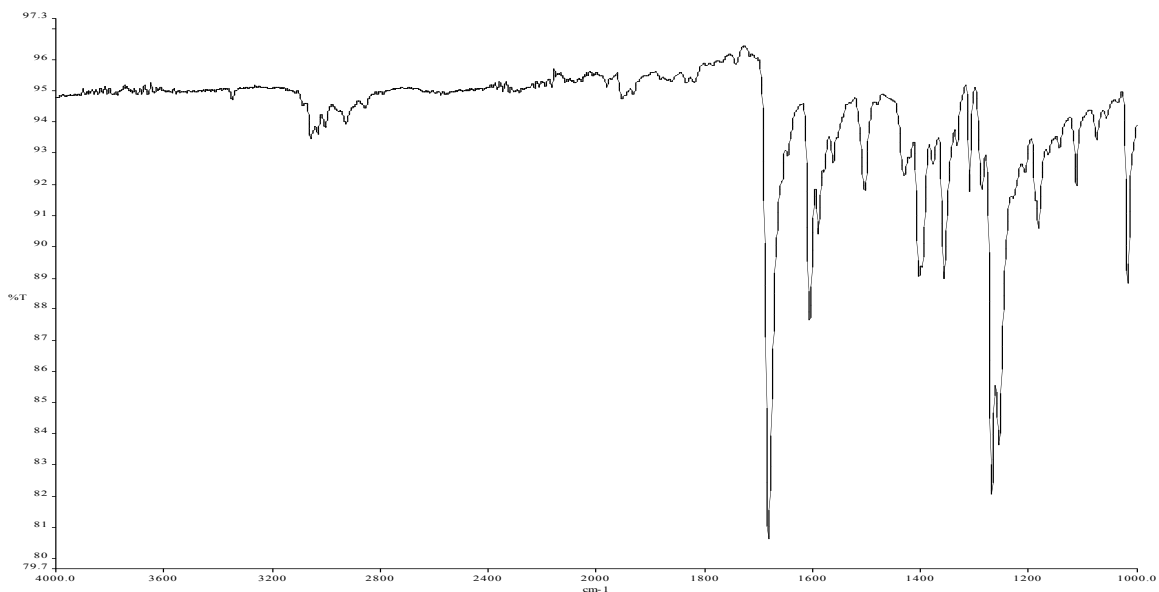


Figure A2.32 Infrared spectrum of compound 3.77.

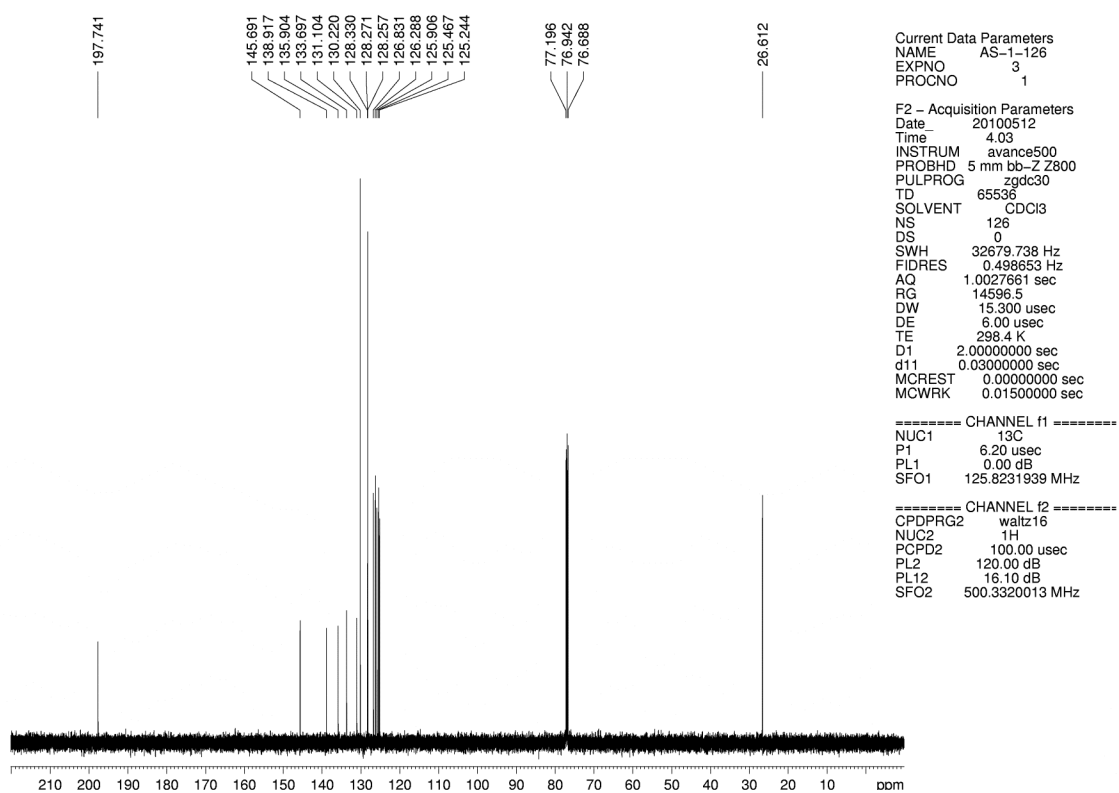


Figure A2.33 ^{13}C NMR (125 MHz, CDCl_3) of compound 3.77.

Current Data Parameters
 NAME SDR1-164
 EXPNO 1
 PROCNO 1

F2 - Acquisition Parameters
 Date_ 20100412
 Time_ 17.09
 INSTRUM avance500
 PROBHD 5 mm bb-Z Z800
 PULPROG zg30
 TD 65536
 SOLVENT CDCl3
 NS 8
 DS 0
 SWH 10000.000 Hz
 FIDRES 0.152588 Hz
 AQ 3.2769001 sec
 RG 71.8
 DW 50.000 usec
 DE 6.00 usec
 TE 298.2 K
 D1 2.0000000 sec
 MCREST 0.0000000 sec
 MCWRK 0.01500000 sec

===== CHANNEL f1 =====
 NUC1 1H
 P1 12.00 usec
 PL1 0.00 dB
 SFO1 500.3330020 MHz

F2 - Processing parameters
 SI 32768
 SF 500.3300216 MHz
 WDW EM
 SSB 0
 LB 0.30 Hz
 GB 0
 PC 1.00

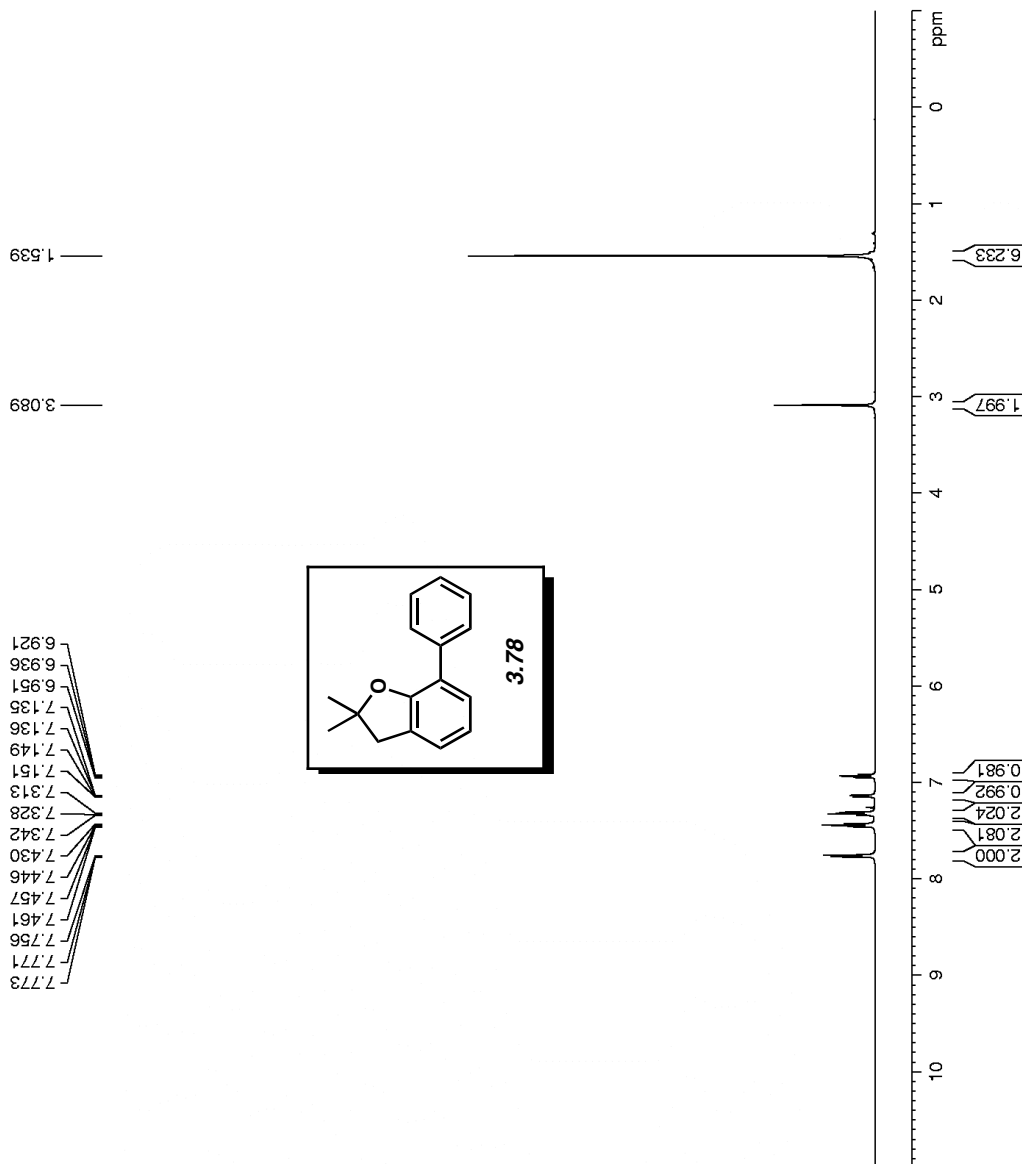


Figure A2.34 ¹H NMR (500 MHz, CDCl₃) of compound 3.78.

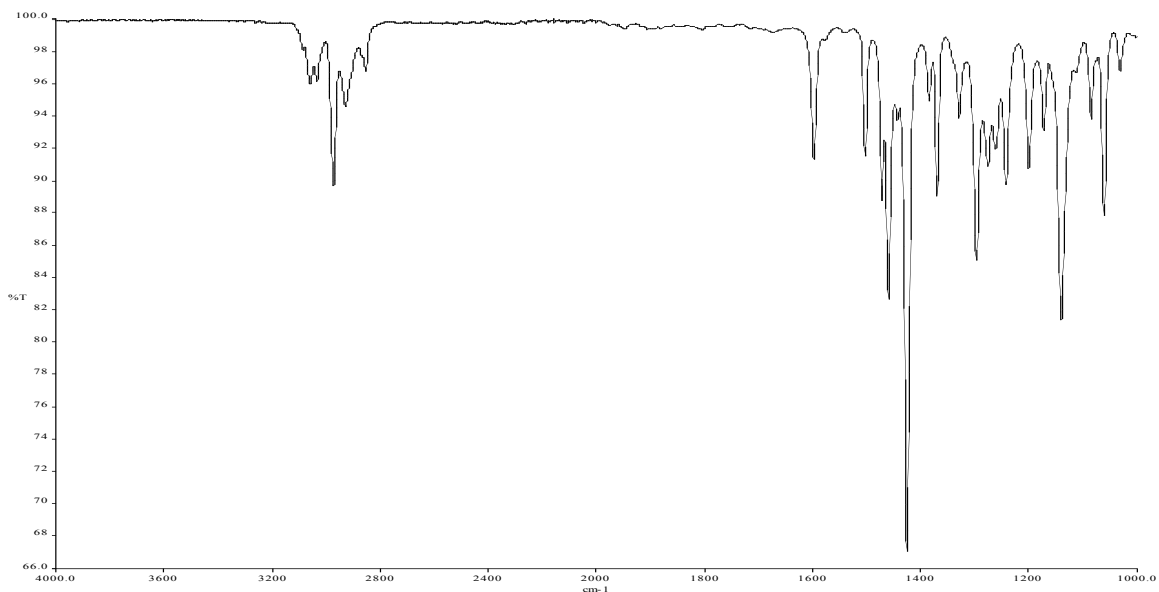


Figure A2.35 Infrared spectrum of compound **3.78**.

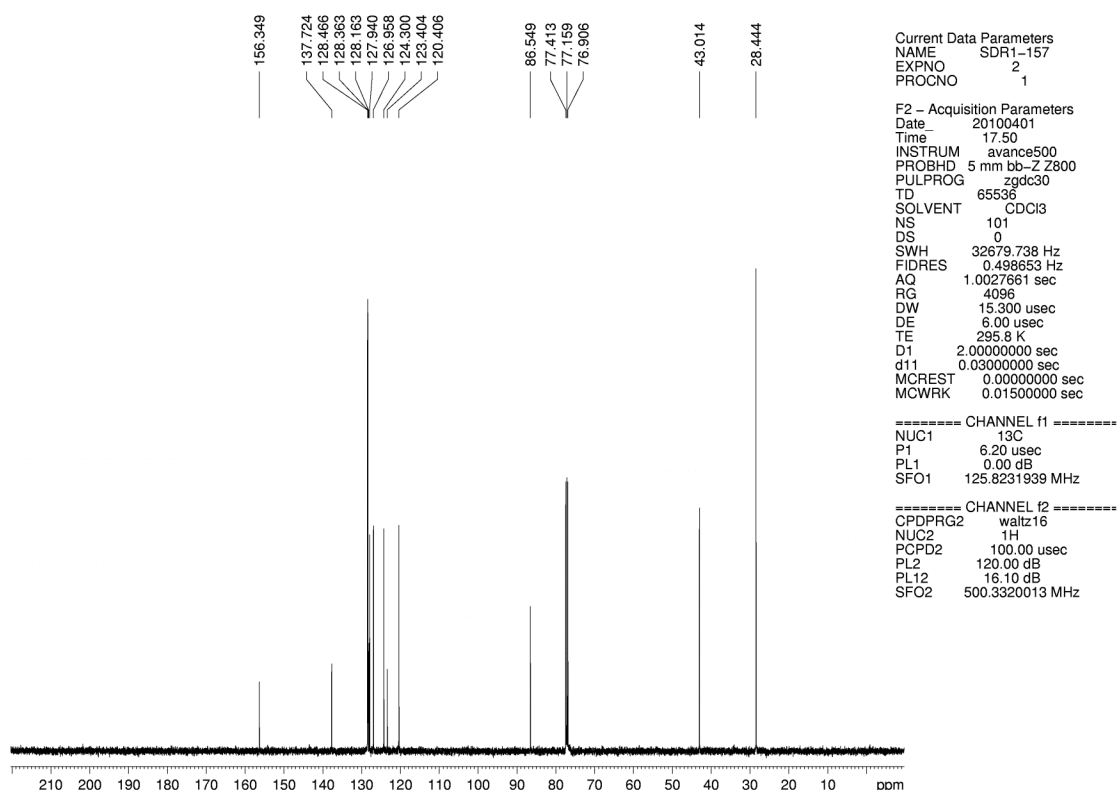


Figure A2.36 ^{13}C NMR (125 MHz, CDCl_3) of compound **3.78**.

```

Current Data Parameters
NAME      KVP-1-186
EXPNO    1
PROCNO   1

F2 - Acquisition Parameters
Date_    20090309
Time     9.47
INSTRUM  avance500
PROBHD   5 mm bb-Z Z800
PULPROG  zg30
TD        65536
SOLVENT  CDCl3
NS        16
DS        0
SWH       10000.000 Hz
FIDRES    0.152588 Hz
AQ        3.2769001 sec
RG        256
DW        50.000 usec
DE        6.00 usec
TE        292.6 K
D1        2.0000000 sec
MCREST    0.0000000 sec
MCWRK    0.01500000 sec

===== CHANNEL f1 =====
NUC1      1H
P1        12.00 usec
PL1       0.00 dB
SFO1      500.3330020 MHz

F2 - Processing parameters
SI        32768
SF        500.3300234 MHz
WDW       EM
SSB       0
LB        0.30 Hz
GB        0
PC        1.00

```

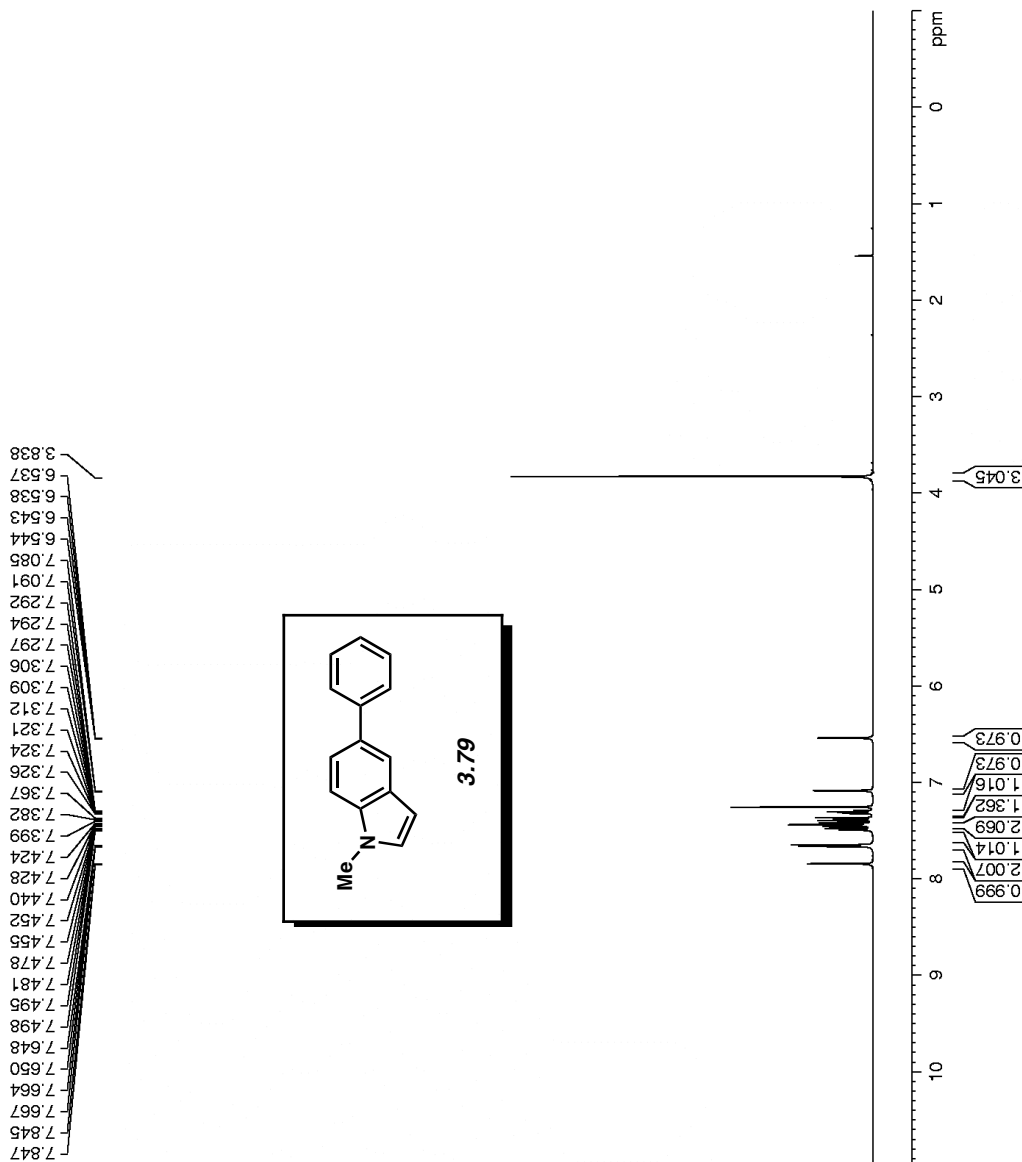


Figure A2.37 ¹H NMR (500 MHz, CDCl₃) of compound 3.79.

Account no. nkg339
AK1-75

Current Data Parameters
NAME AK1-75
EXPNO 380
PROCNO 1

F2 - Acquisition Parameters
Date_ 20100428
Time 15:57
INSTRUM arx400
PROBHD 5 mm QNP 1H
PULPROG zg30
TD 65536
SOLVENT CDCl3
NS 8
DS 0
SWH 8064.516 Hz
FIDRES 0.123055 Hz
AQ 4.0632820 sec
RG 2048
DW 62.000 usec
DE 88.57 usec
TE 300.0 K
D1 2.0000000 sec
P1 7.50 usec
SFO1 400.1324008 MHz
NUCLEUS 1H

F2 - Processing parameters
SI 65536
SF 400.1300173 MHz
WDW EM
SSB 0
LB 0.30 Hz
GB 0
PC 1.00

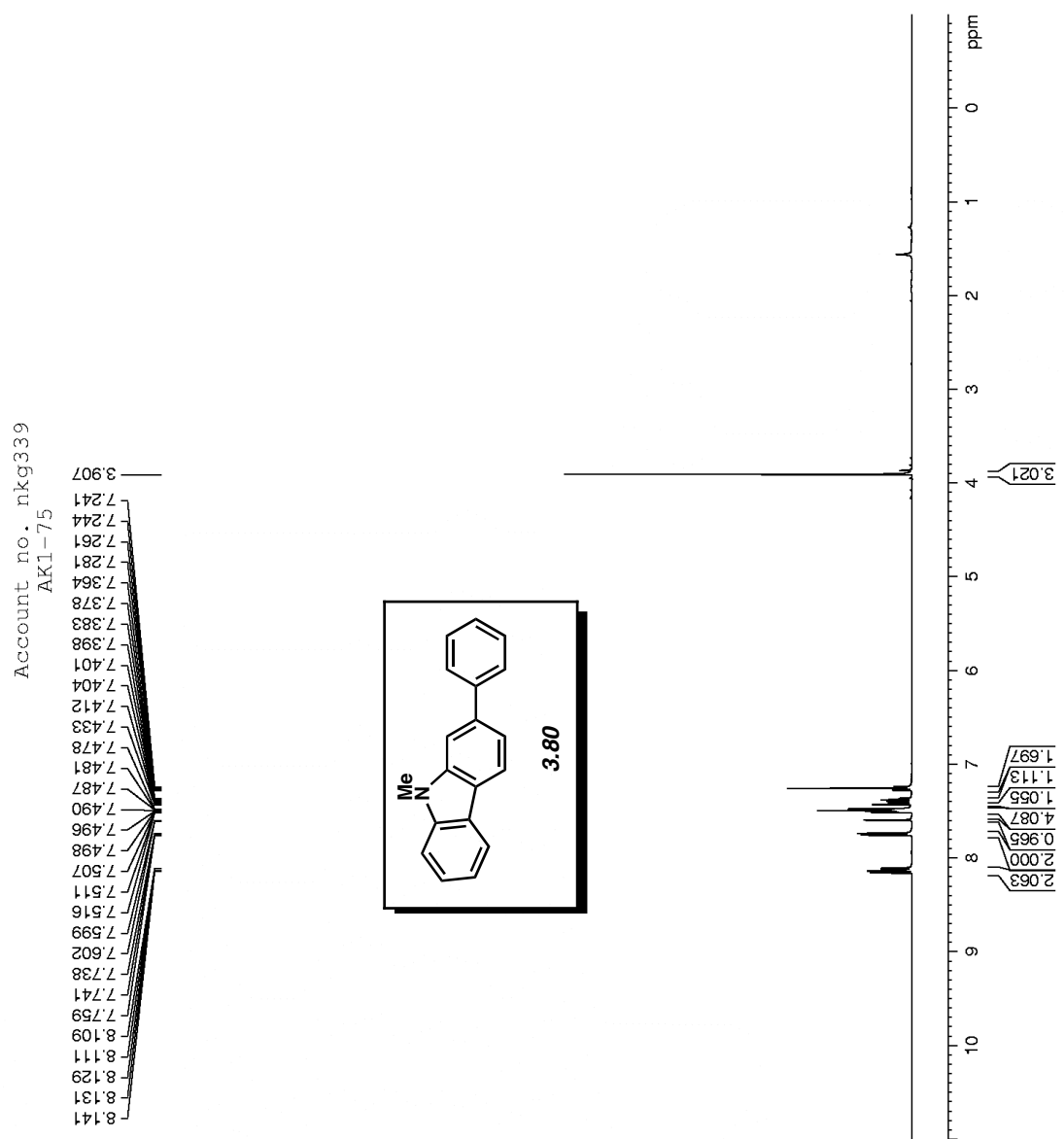


Figure A2.38 ¹H NMR (400 MHz, CDCl₃) of compound 3.80.

Current Data Parameters
 NAME AK1-078
 EXPNO 10
 PROCNO 1

F2 - Acquisition Parameters
 Date_ 20100929
 Time_ 13.07
 INSTRUM avance500
 PROBHD 5 mm bb-Z Z800
 PULPROG zg30
 TD 65536
 SOLVENT CDCl3
 NS 8
 DS 0
 SWH 10000.000 Hz
 FIDRES 0.152588 Hz
 AQ 3.2769001 sec
 RG 181
 DW 50.000 usec
 DE 6.00 usec
 TE 296.3 K
 D1 2.00000000 sec
 MCREST 0.00000000 sec
 MCWRK 0.01500000 sec

==== CHANNEL f1 =====
 NUC1 1H
 P1 12.25 usec
 PL1 0.00 dB
 SFO1 500.3330020 MHz

F2 - Processing parameters
 SI 32768
 SF 500.3300220 MHz
 WDW EM
 SSB 0
 LB 0.30 Hz
 GB 0
 PC 1.00

8.705
8.696
8.000
7.985
7.757
7.754
7.724
7.497
7.494
7.482
7.466
7.433
7.419
7.415
7.404
7.247
7.244
7.237
7.234
7.230
7.224
7.221

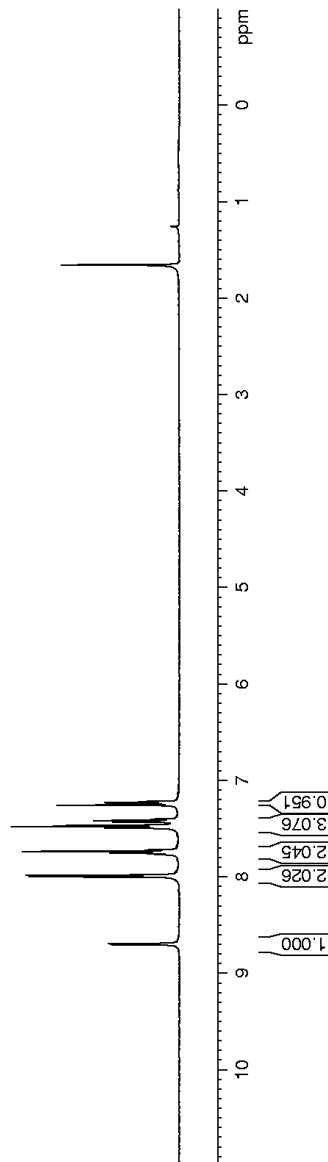
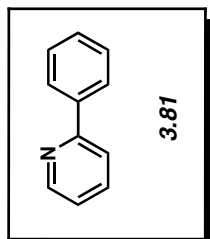
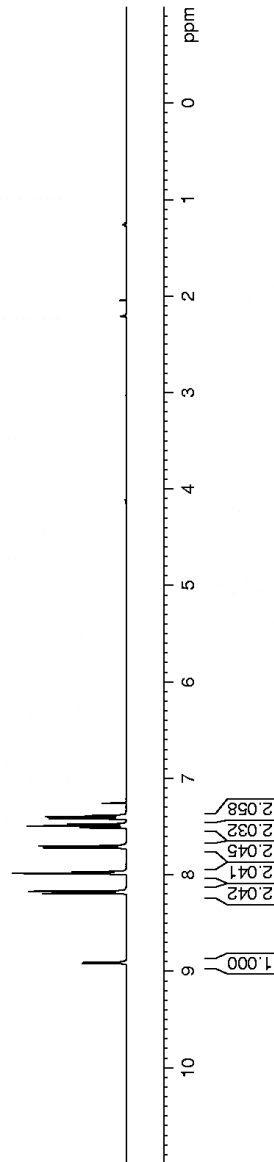
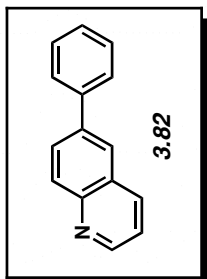
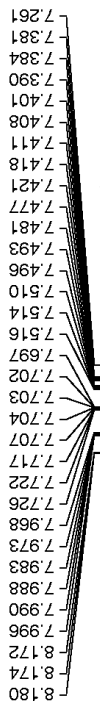


Figure A2.39 ¹H NMR (500 MHz, CDCl₃) of compound **3.81**.

Account no. nkg339
AK1-77



Current Data Parameters
NAME AK1-77
EXPNO 550
PROCNO 1

F2 - Acquisition Parameters
Date_ 20100428
Time 20.26
INSTRUM aix400
PROBHD 5 mm QNP 1H
PULPROG zg30
TD 65536
SOLVENT CDCl3
NS 8
DS 0
SWH 8064.516 Hz
FIDRES 0.123055 Hz
AQ 4.0632820 sec
RG 360
DW 62.000 usec
DE 88.57 usec
TE 300.0 K
D1 2.0000000 sec
P1 7.50 usec
SFO1 400.1324008 MHz
NUCLEUS 1H

F2 - Processing parameters
SI 65536
SF 400.1300173 MHz
WDW EM
SSB 0
LB 0.30 Hz
GB 0
PC 1.00

Figure A2.40 ^1H NMR (400 MHz, CDCl_3) of compound **3.82**.

Current Data Parameters
 NAME AK1-79
 EXPNO 500
 PROCNO 1

F2 - Acquisition Parameters
 Date_ 20100429
 Time 19.49
 INSTRUM arx400
 PROBHD 5 mm QNP 1H
 PULPROG zg30
 TD 65536
 SOLVENT CDCl3
 NS 8
 DS 0
 SWH 8064.516 Hz
 FIDRES 0.123055 Hz
 AQ 4.0632820 sec
 RG 180
 DW 62.000 usec
 DE 88.57 usec
 TE 300.0 K
 D1 2.00000000 sec
 P1 7.50 usec
 SFO1 400.1324008 MHz
 NUCLEUS 1H

F2 - Processing parameters
 SI 65536
 SF 400.1300173 MHz
 WDW EM
 SSB 0
 LB 0.30 Hz
 GB 0
 PC 1.00

Account no. NKG339
 AK1-79

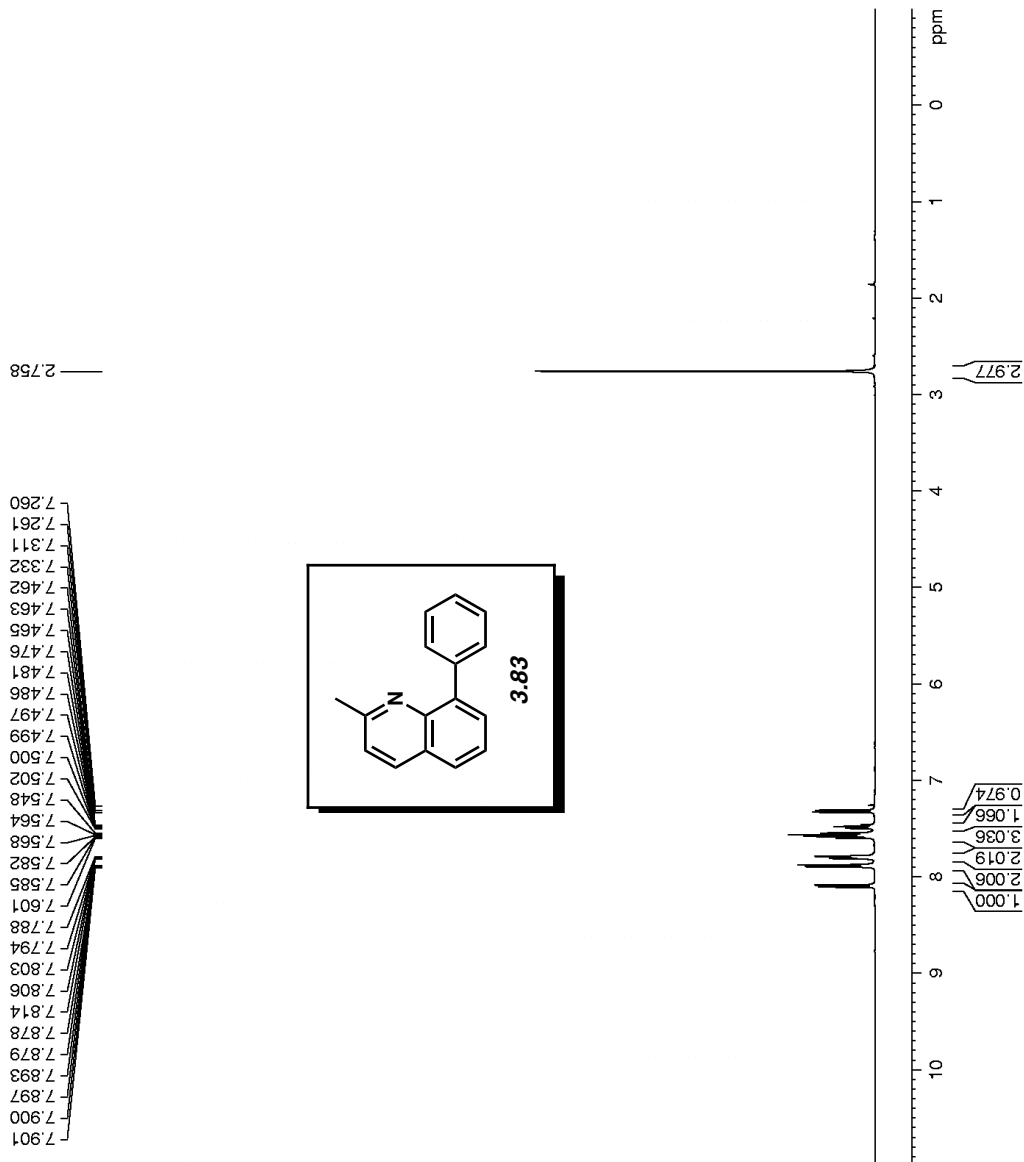


Figure A2.41 ¹H NMR (400 MHz, CDCl₃) of compound **3.83**.

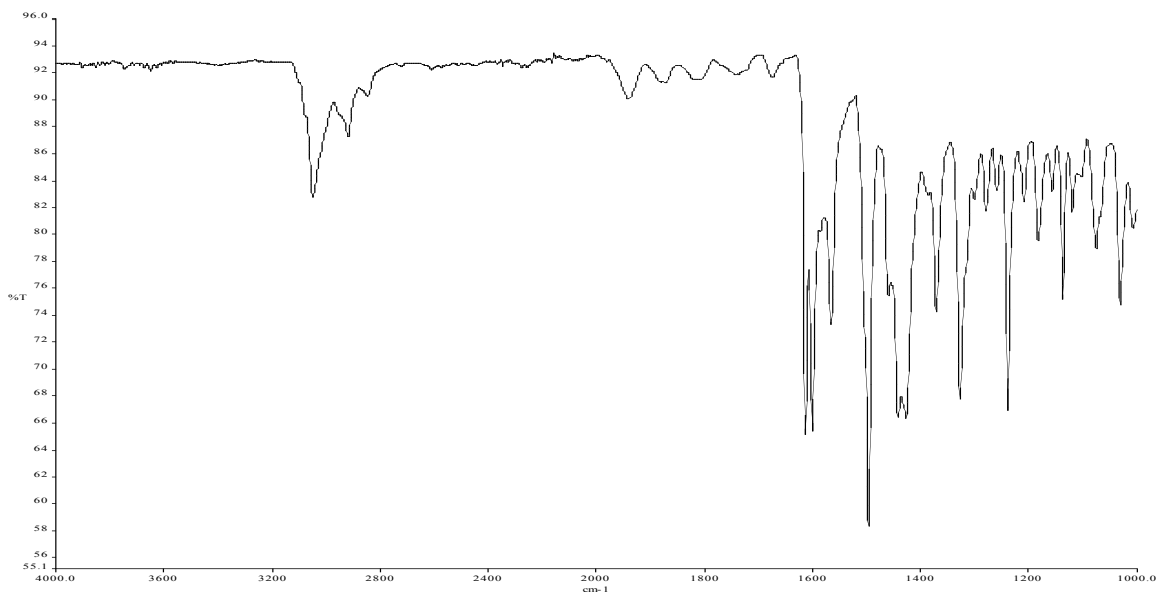


Figure A2.42 Infrared spectrum of compound **3.83**.

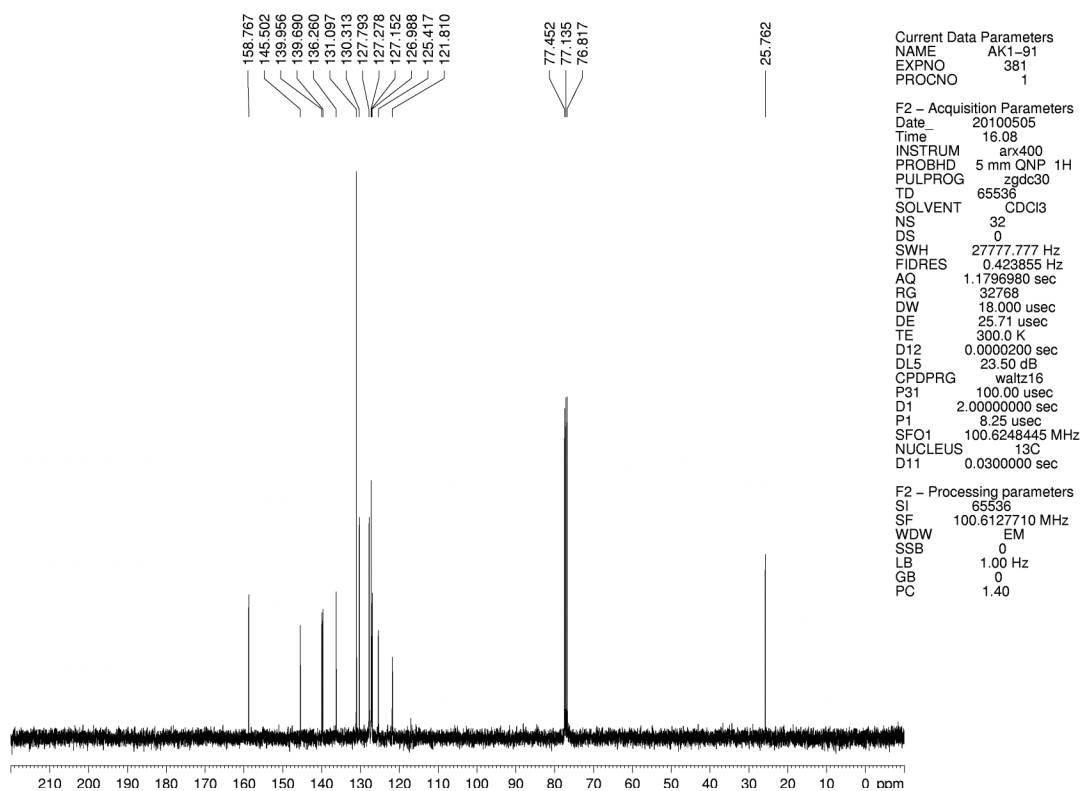


Figure A2.43 ^{13}C NMR (100 MHz, CDCl_3) of compound **3.83**.

Current Data Parameters
 NAME AK1-42
 EXPNO 350
 PROCNO 1

F2 - Acquisition Parameters
 Date_ 20100407
 Time 17.16
 INSTRUM arx400
 PROBHD 5 mm QNP 1H
 PULPROG zg30
 TD 65536
 SOLVENT CDCl3
 NS 8
 DS 0
 SWH 8064.516 Hz
 FIDRES 0.123055 Hz
 AQ 4.0632820 sec
 RG 1024
 DW 62.000 usec
 DE 88.57 usec
 TE 300.0 K
 D1 2.00000000 sec
 P1 7.50 usec
 SFO1 400.1324008 MHz
 NUCLEUS 1H

F2 - Processing parameters
 SI 65536
 SF 400.1300173 MHz
 WDW EM
 SSB 0
 LB 0.30 Hz
 GB 0
 PC 1.00

Account no. nkg339
 AK1-42

7.832
7.812
7.670
7.669
7.667
7.665
7.651
7.648
7.619
7.616
7.603
7.595
7.583
7.578
7.571
7.568
7.550
7.533
7.530
7.352
7.348
7.334
7.330
7.315
7.310
7.307
7.304
7.289
7.285
7.270
7.267
7.260
7.174
6.996
6.922
6.902
4.070

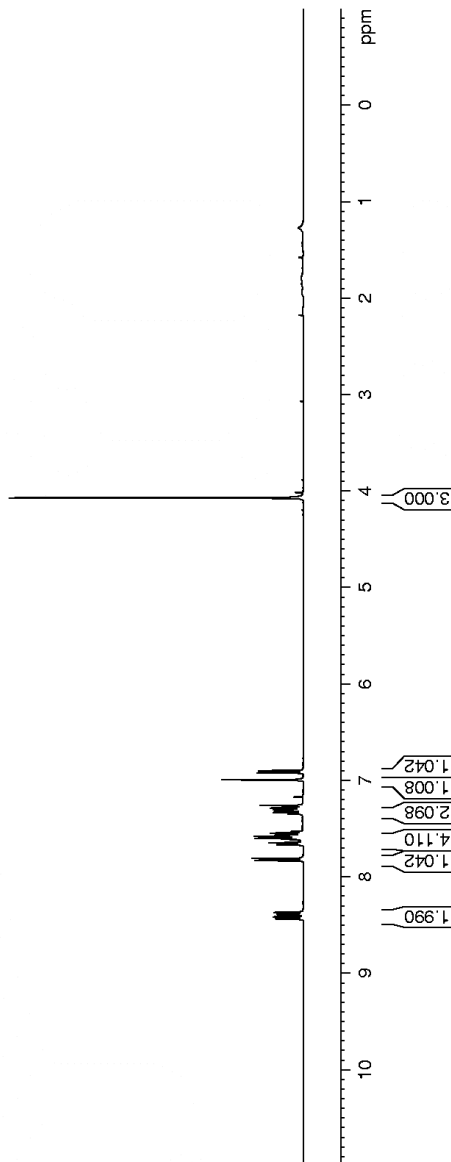
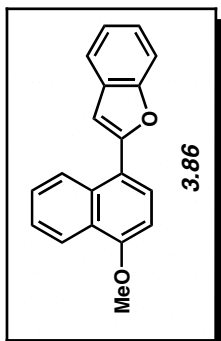


Figure A2.44 ¹H NMR (400 MHz, CDCl₃) of compound **3.86**.

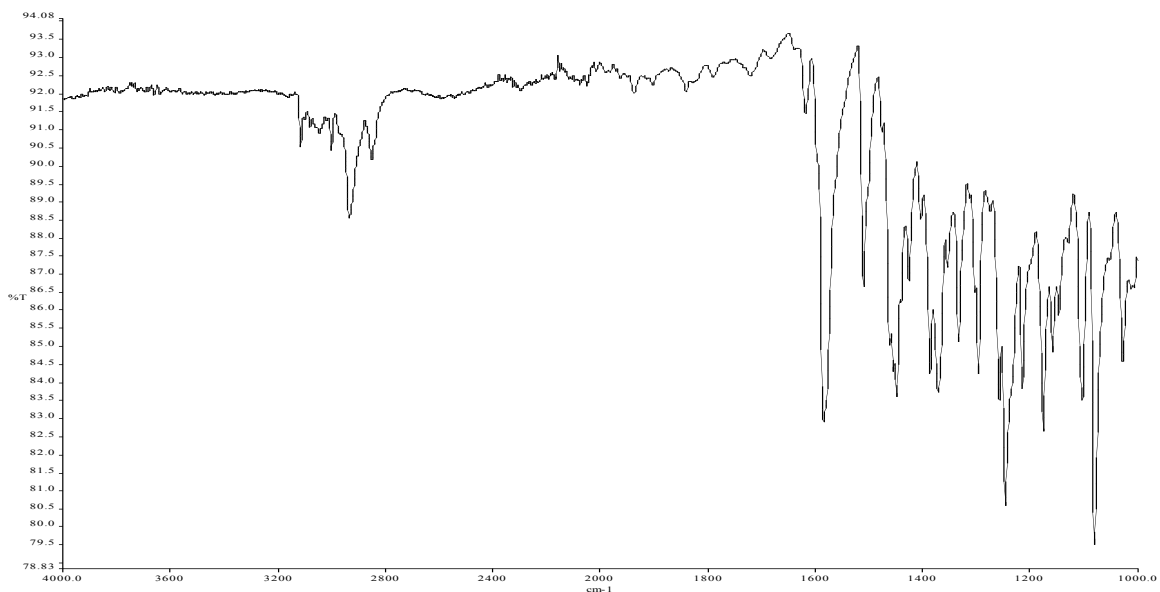


Figure A2.45 Infrared spectrum of compound **3.86**.

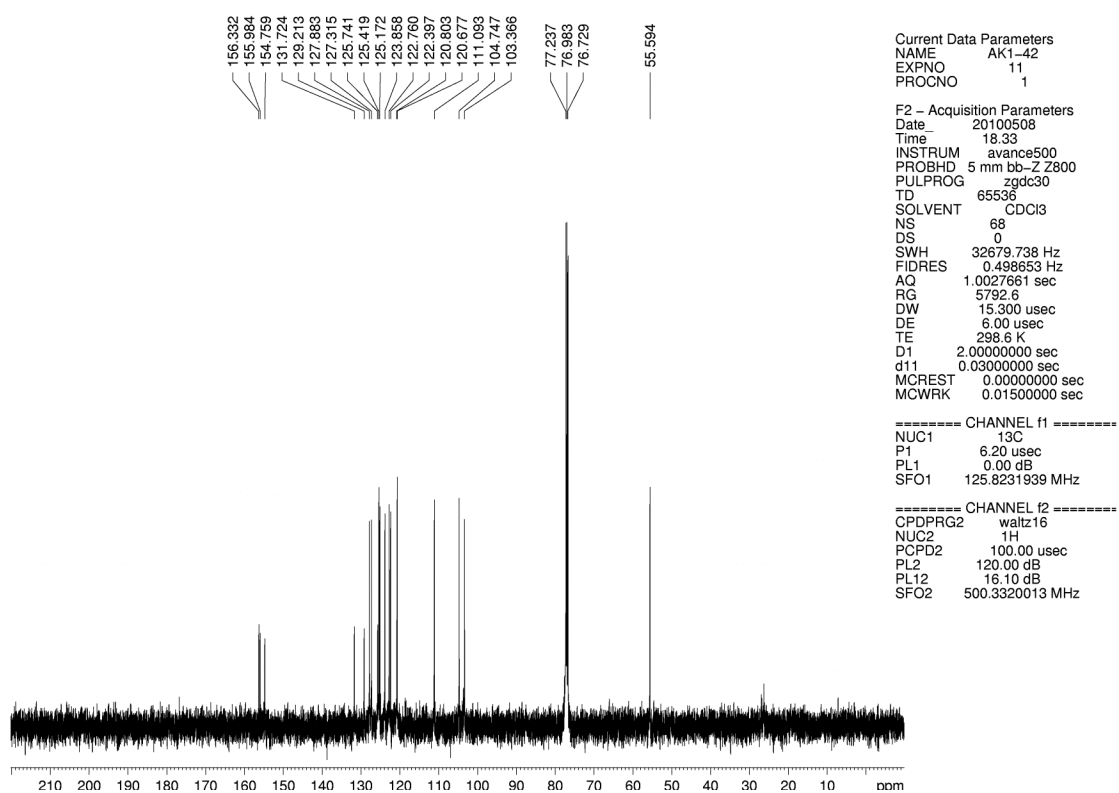


Figure A2.46 ^{13}C NMR (125 MHz, CDCl_3) of compound **3.86**.

Current Data Parameters
 NAME AK1-25
 EXPNO 90
 PROCNO 1

F2 - Acquisition Parameters
 Date_ 20100330
 Time_ 11.30
 INSTRUM arx400
 PROBHD 5 mm QNP 1H
 PULPROG zg30
 TD 65536
 SOLVENT CDCl3
 NS 8
 DS 0
 SWH 8064.516 Hz
 FIDRES 0.123055 Hz
 AQ 4.0632820 sec
 RG 512
 DW 62.000 usec
 DE 88.57 usec
 TE 300.0 K
 D1 2.0000000 sec
 P1 7.50 usec
 SFO1 400.1324008 MHz
 NUCLEUS 1H

F2 - Processing parameters
 SI 65536
 SF 400.1300198 MHz
 WDW EM
 SSB 0
 LB 0.30 Hz
 GB 0
 PC 1.00

Account no. nkg339
 AK1-25

8.148
8.140
7.927
7.918
7.912
7.905
7.898
7.895
7.888
7.867
7.857
7.850
7.840
7.834
7.824
7.685
7.683
7.681
7.602
7.598
7.593
7.543
7.538
7.526
7.521
7.512
7.503
7.494
7.487
7.477
7.253
6.730
6.728
6.726
6.724

1.540

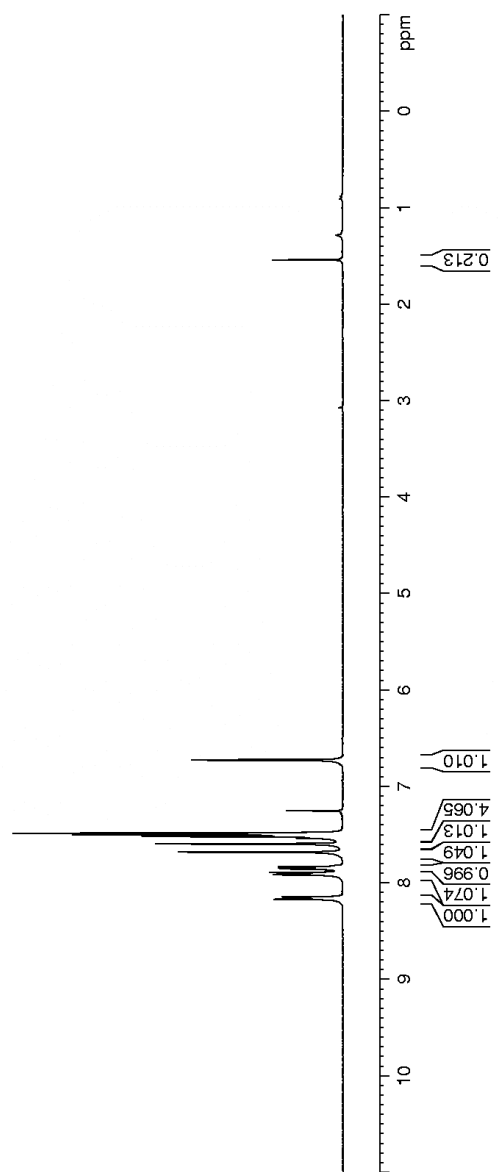
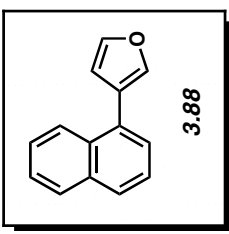


Figure A2.47 ¹H NMR (400 MHz, CDCl₃) of compound **3.88**.

Current Data Parameters
 NAME AK1-29
 EXPNO 240
 PROCNO 1

F2 - Acquisition Parameters
 Date_ 20100402
 Time_ 17.51
 INSTRUM arx400
 PROBHD 5 mm QNP 1H
 PULPROG zg30
 TD 65536
 SOLVENT CDCl3
 NS 8
 DS 0
 SWH 8064.516 Hz
 FIDRES 0.123055 Hz
 AQ 4.0632820 sec
 RG 2048
 DW 62.000 usec
 DE 88.57 usec
 TE 300.0 K
 D1 2.0000000 sec
 P1 7.50 usec
 SFO1 400.1324008 MHz
 NUCLEUS 1H

F2 - Processing parameters
 SI 65536
 SF 400.1300169 MHz
 WDW EM
 SSB 0
 LB 0.30 Hz
 GB 0
 PC 1.00

Account no. nkg339
 AK1-29

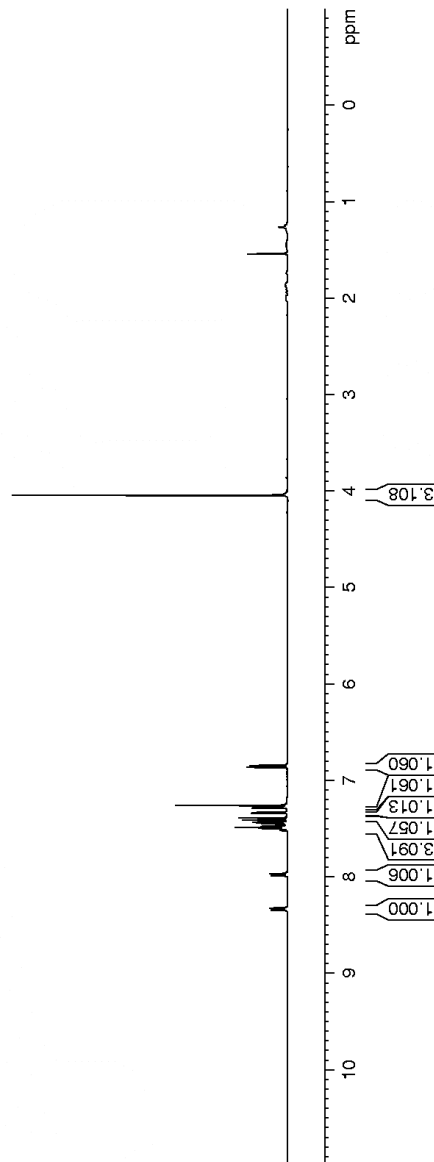
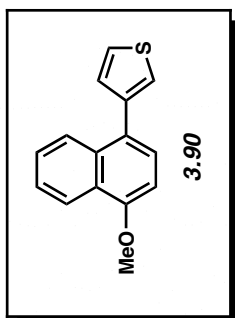
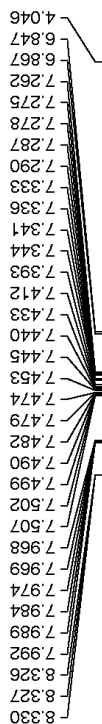


Figure A2.48 ¹H NMR (400 MHz, CDCl₃) of compound **3.90**.

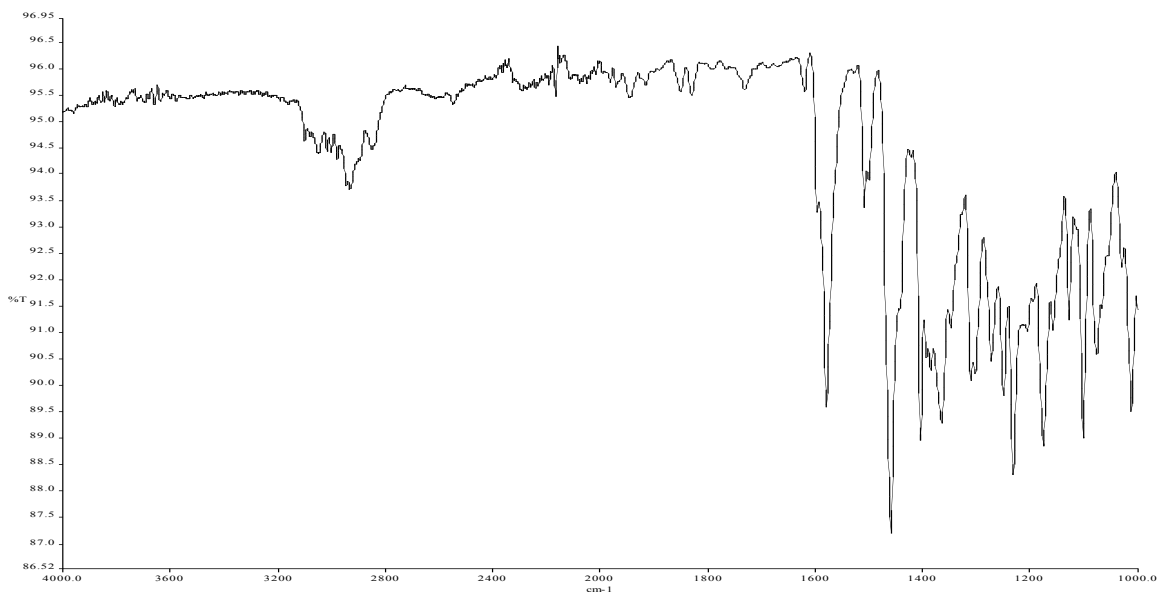


Figure A2.49 Infrared spectrum of compound **3.90**.

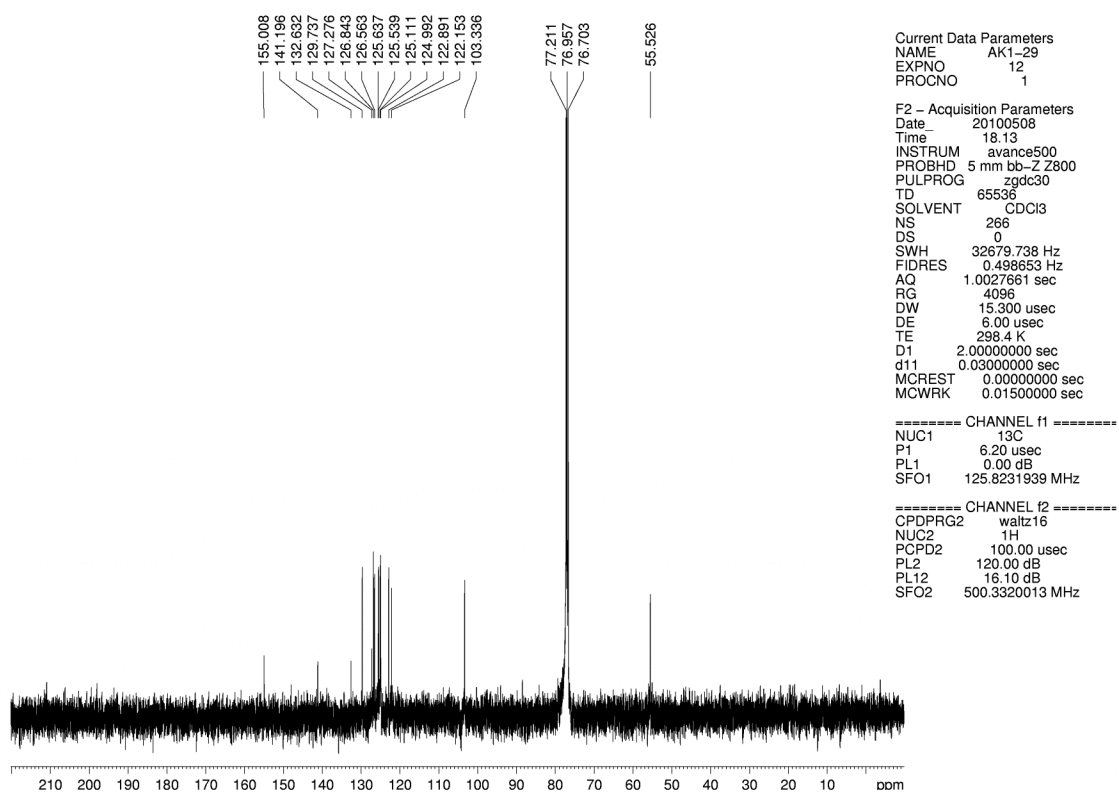


Figure A2.50 ^{13}C NMR (125 MHz, CDCl_3) of compound **3.90**.

Current Data Parameters
 NAME AK1-43
 EXPNO 10
 PROCNO 1

F2 - Acquisition Parameters
 Date_ 20100508
 Time_ 18.41
 INSTRUM avance500
 PROBHD 5 mm bb-Z Z800
 PULPROG zg30
 TD 65536
 SOLVENT CDCl3
 NS 8
 DS 0
 SWH 10000.000 Hz
 FIDRES 0.152588 Hz
 AQ 3.2769001 sec
 RG 64
 DW 50.000 usec
 DE 6.00 usec
 TE 298.5 K
 D1 2.00000000 sec
 MCREST 0.00000000 sec
 MCWRK 0.01500000 sec

===== CHANNEL f1 =====
 NUC1 1H
 P1 12.00 usec
 PL1 0.00 dB
 SFO1 500.3330020 MHz

F2 - Processing parameters
 SI 32768
 SF 500.3300220 MHz
 WDW EM
 SSB 0
 LB 0.00 Hz
 GB 0
 PC 1.00

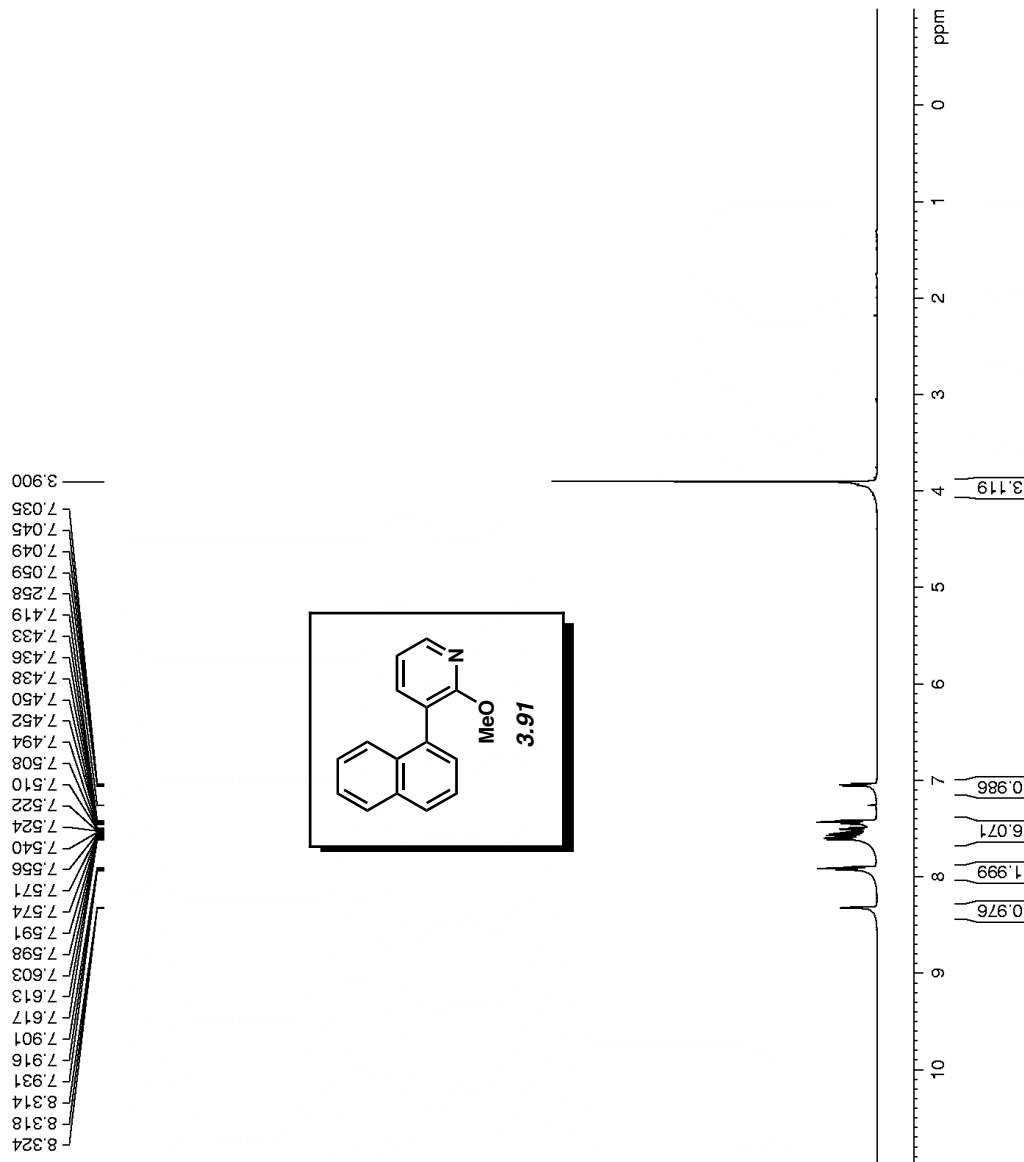


Figure A2.51 ¹H NMR (500 MHz, CDCl₃) of compound 3.91.

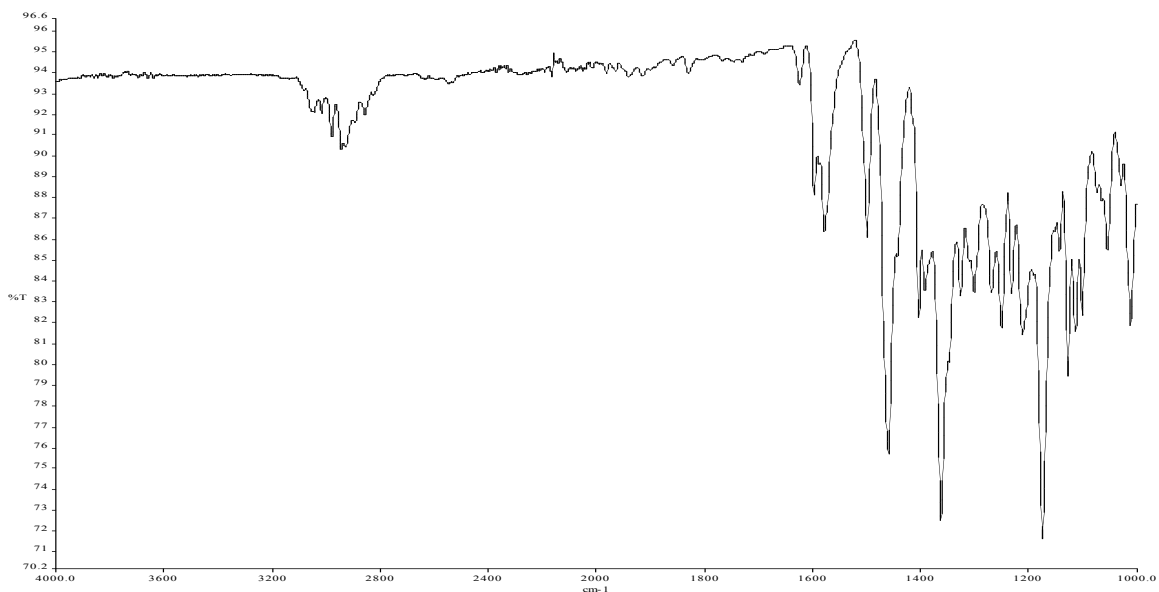


Figure A2.52 Infrared spectrum of compound **3.91**.

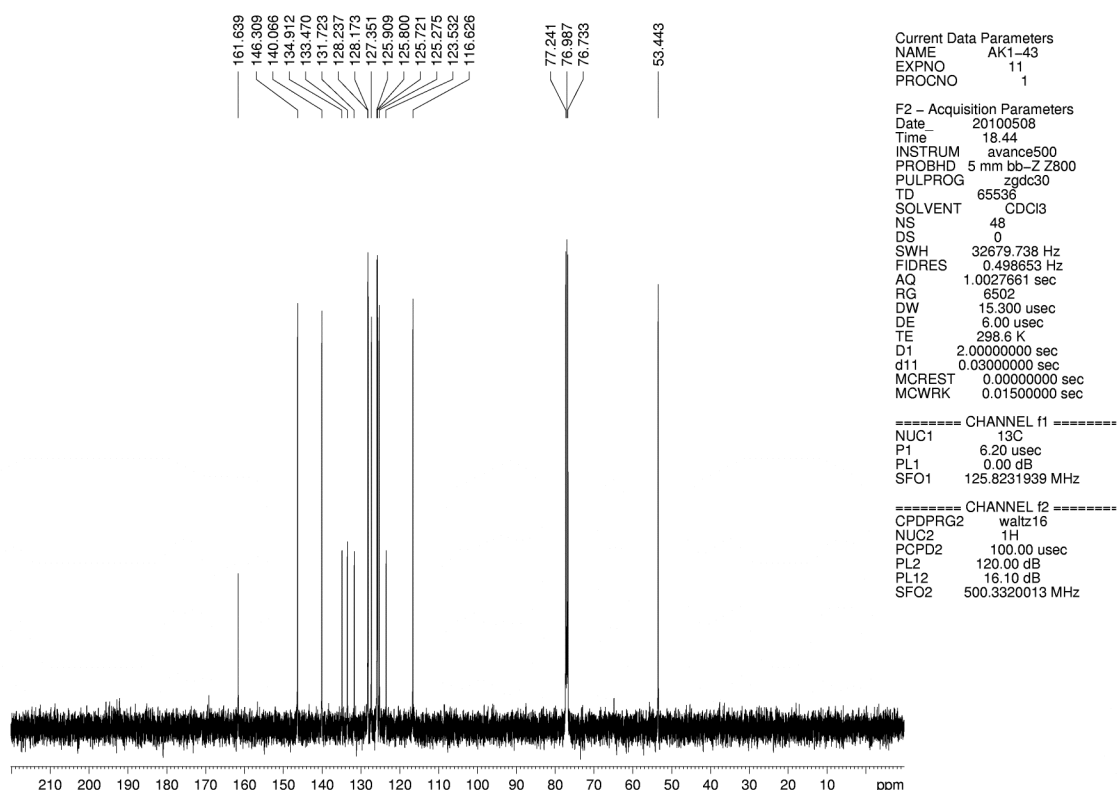


Figure A2.53 ^{13}C NMR (125 MHz, CDCl_3) of compound **3.91**.

Current Data Parameters
 NAME AK1-93
 EXPNO 10
 PROCNO 1

F2 - Acquisition Parameters
 Date_ 20100508
 Time_ 19.48
 INSTRUM avance500
 PROBHD 5 mm bb-Z Z800
 PULPROG zg30
 TD 65536
 SOLVENT CDCl3
 NS 8
 DS 0
 SWH 10000.000 Hz
 FIDRES 0.152588 Hz
 AQ 3.2769001 sec
 RG 64
 DW 50.000 usec
 DE 6.00 usec
 TE 298.7 K
 D1 2.00000000 sec
 MCREST 0.00000000 sec
 MCWRK 0.01500000 sec

===== CHANNEL f1 =====
 NUC1 1H
 P1 12.00 usec
 PL1 0.00 dB
 SFO1 500.3330020 MHz

F2 - Processing parameters
 SI 32768
 SF 500.3300220 MHz
 WDW EM
 SSB 0
 LB 0.30 Hz
 GB 0
 PC 1.00

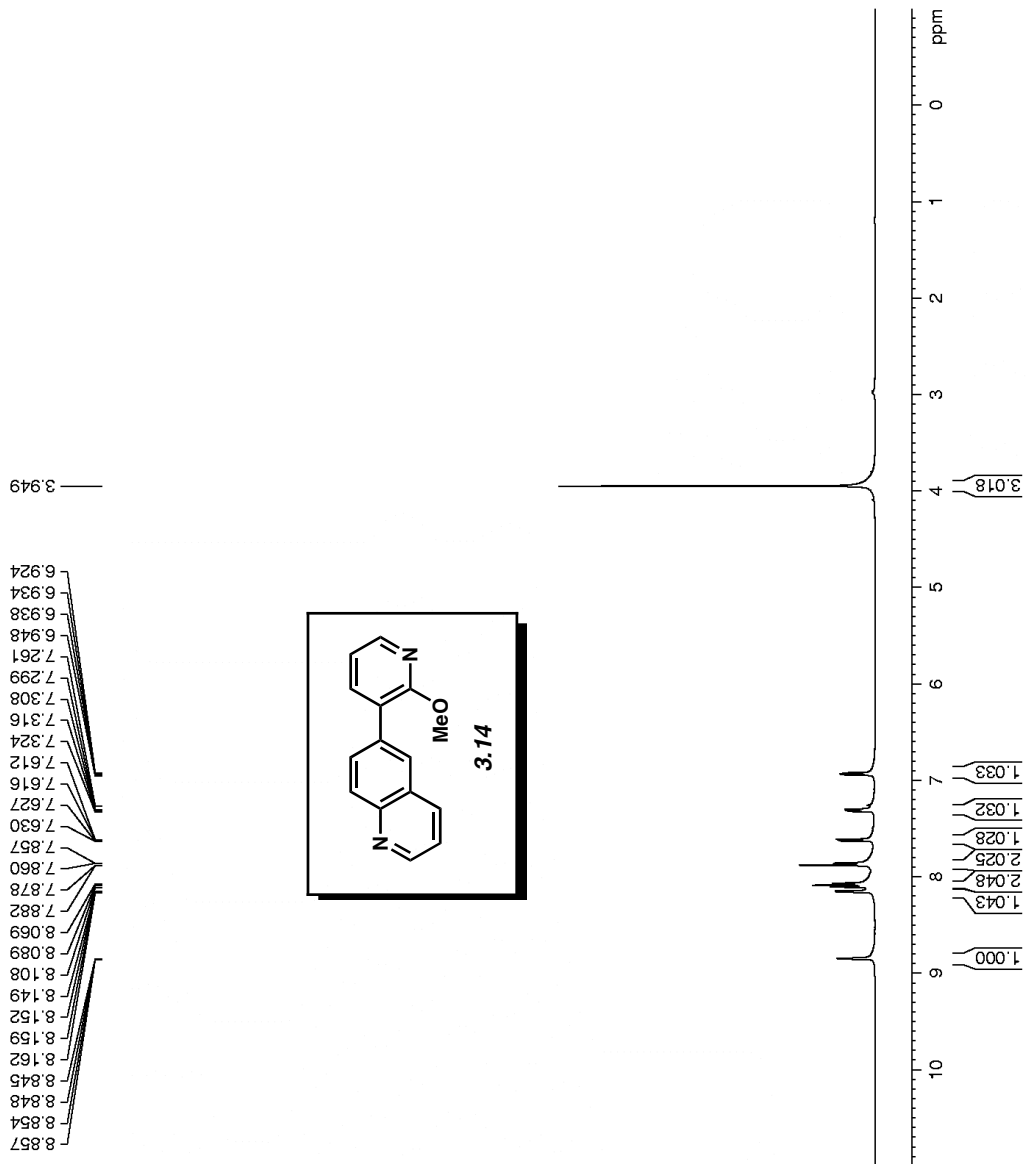


Figure A2.54 ¹H NMR (500 MHz, CDCl₃) of compound 3.14.

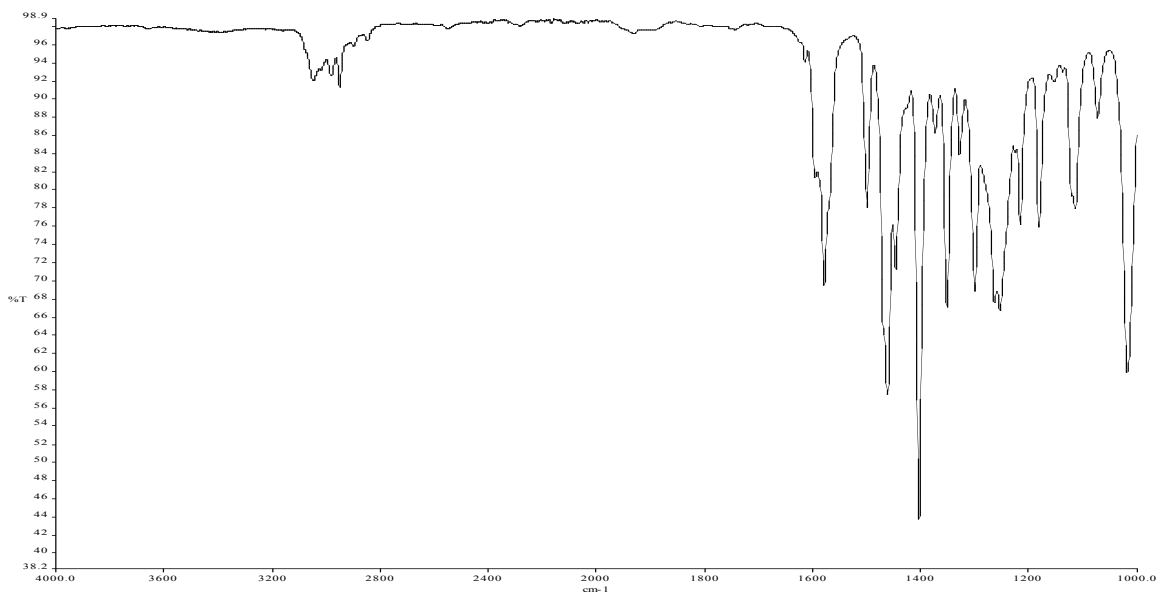


Figure A2.55 Infrared spectrum of compound **3.14**.

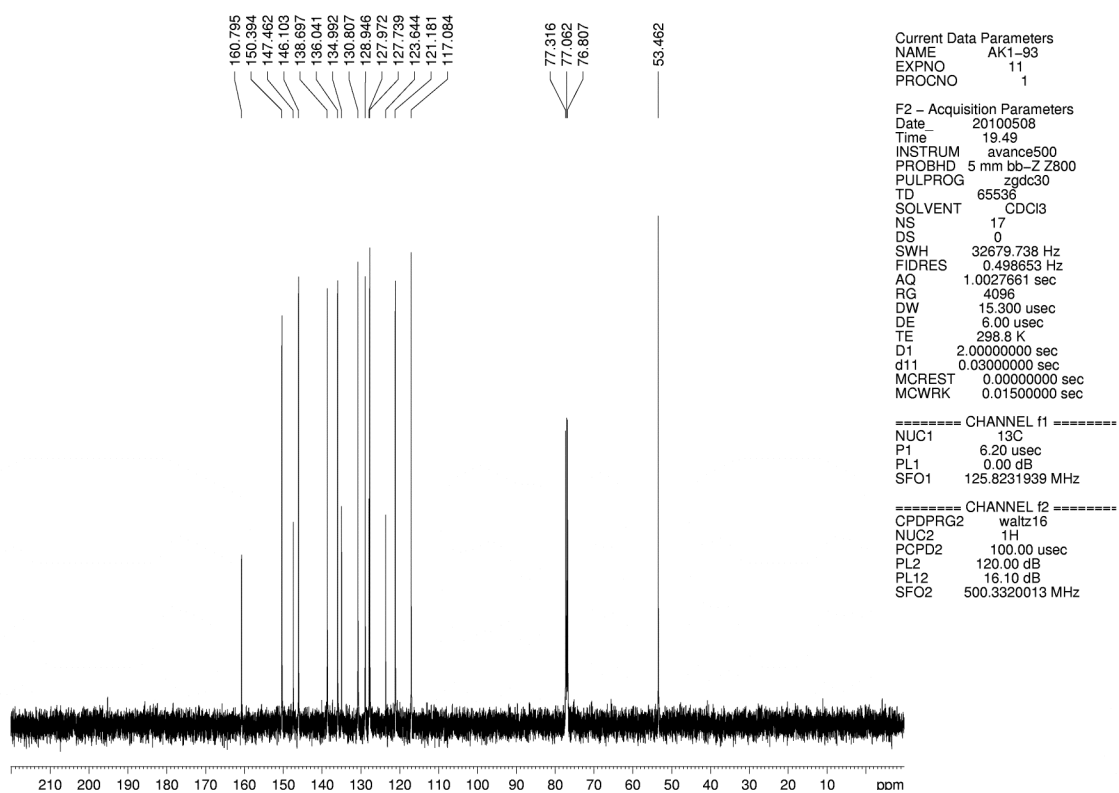


Figure A2.56 ^{13}C NMR (125 MHz, CDCl_3) of compound **3.14**.

CHAPTER FOUR

Total Synthesis of (–)-*N*-Methylwelwitindolinone C Isothiocyanate

Alexander D. Hutters, Kyle W. Quasdorf, Evan D. Styduhar, and Neil K. Garg.

J. Am. Chem. Soc. **2011**, *133*, 15797–15799.

4.1 Abstract

We report the first total synthesis of (–)-*N*-methylwelwitindolinone C isothiocyanate. Our route features a number of key transformations, including an indolyne cyclization to assemble the [4.3.1]-bicyclic scaffold, as well as a late-stage intramolecular nitrene insertion to functionalize the C11 bridgehead carbon en route to the natural product.

4.2 Introduction

The welwitindolinones are a unique class of natural products isolated from the blue-green algae *Hapalosiphon welwitschii* and *Westiella intricata*.¹ Ten welwitindolinones have been identified to date, nine of which possess [4.3.1]-bicyclic cores (e.g., **4.1–4.3**, Figure 4.1).² Although compact in size, each of these natural products contains a dense array of functionality that has plagued synthetic efforts for nearly two decades. To date, more than ten laboratories have reported progress toward the bicyclic welwitindolinones.^{3,4} Whereas these exhaustive efforts have resulted in several elegant methods for bicycle generation, completion of these targets has remained a formidable challenge. In fact, the only total synthesis of a [4.3.1]-bicyclic welwitindolinone was recently achieved by Rawal and co-workers, with their breakthrough synthesis of (±)-**4.3** in 2011.⁵

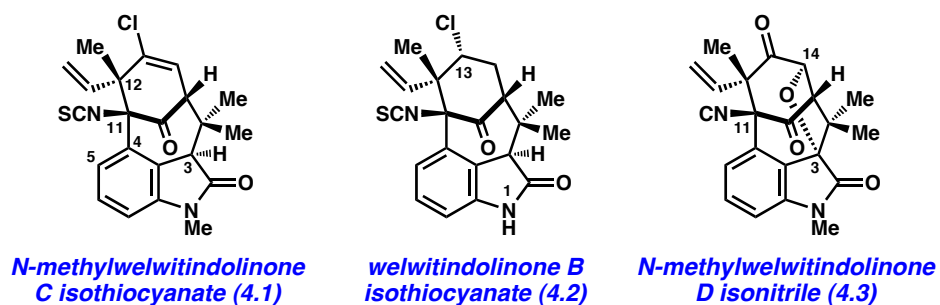


Figure 4.1. [4.3.1]-Bicyclic welwitindolinones **4.1–4.3**.

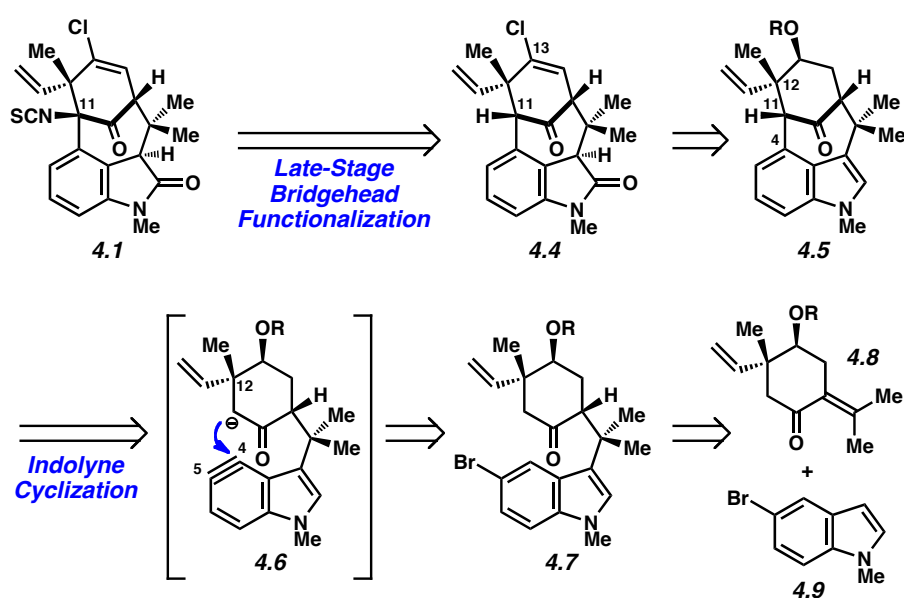
With the aim of synthesizing alkaloids **4.1–4.3** and other family members, we selected **4.1** as our initial synthetic target. Of note, welwitindolinone **4.1** was uniquely found to reverse P-glycoprotein-mediated multiple drug resistance (MDR) to a variety of anti-cancer drugs in human cancer cell lines, and is therefore a promising lead for the treatment of drug resistant tumors.⁶ The densely functionalized bicyclic framework of **4.1** presents numerous synthetic challenges, including a 3,4-disubstituted oxindole, a heavily substituted cyclohexyl ring, and a bridgehead isothiocyanate substituent at C11. In this communication, we report the first total synthesis of (–)-*N*-methylwelwitindolinone C isothiocyanate (**4.1**).

4.3 Retrosynthetic Analysis of (–)-*N*-Methylwelwitindolinone C Isothiocyanate

Retrosynthetically, it was envisioned that **4.1** would be derived from bicycle **4.4** through late-stage functionalization of the C11 bridgehead position (Scheme 4.1). In turn, intermediate **4.4** would arise from indole precursor **4.5** by introduction of the vinyl chloride and oxindole moieties. In the key complexity generating step, the [4.3.1]-bicycle would be fashioned through intramolecular addition of an enolate onto an in situ-generated “indolyne” species (see transition structure **4.6**).⁷ The use of an indolyne intermediate^{8,9} was considered advantageous as the high reactivity of the aryne would permit the assembly of the congested C4–C11 bond linkage, where

a tertiary center would be introduced adjacent to the C12 quaternary stereocenter. Of note, the indolyne would be inherently electrophilic, representing an uncommon umpolung of the indole's typical reactivity. Bromoindole **4.7** was thought to be a suitable precursor to the desired indolyne via the classic dehydrohalogenation method for aryne generation. Finally, cyclohexyl derivative **4.8** and indole **4.9** were identified as suitable starting fragments.

Scheme 4.1

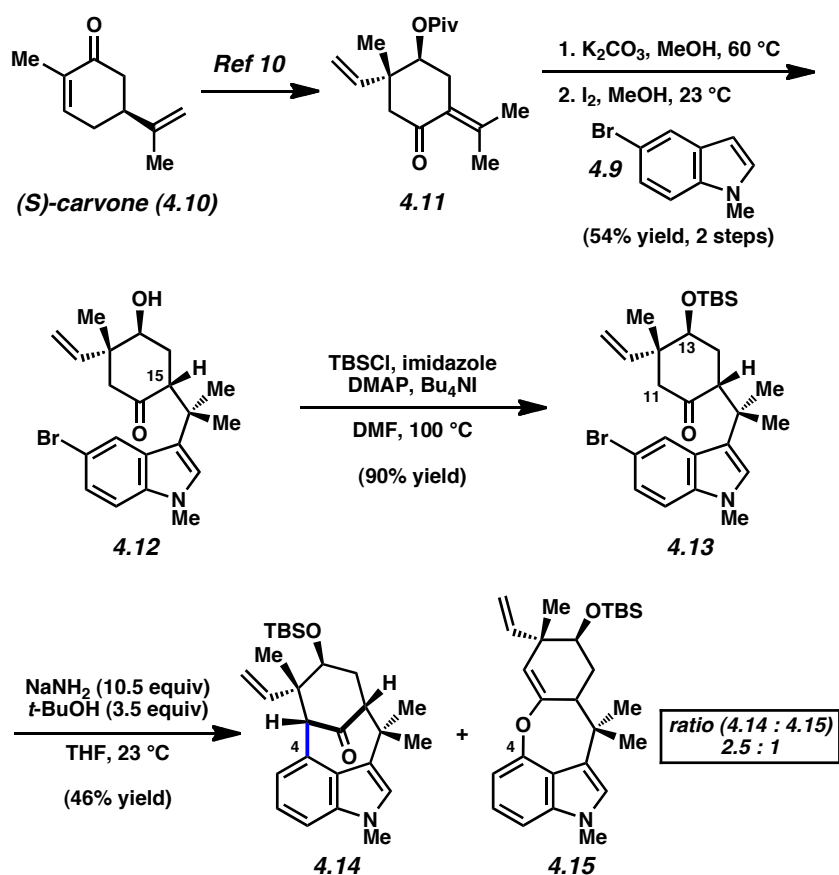


4.4 Construction of the [4.3.1]-Bicyclic Framework

Our synthesis commenced with the concise preparation of the key [4.3.1]-bicycle (Scheme 4.2). (*S*)-Carvone (**4.10**) was elaborated to enone **4.11** using the robust five step procedure reported by Natsume in the enantiomeric series.¹⁰ Subsequent pivalate cleavage, followed by I₂-promoted addition of bromoindole **4.9**,¹¹ furnished adduct **4.12** in 54% yield over two steps.¹² TBS-protection of **4.12** provided silylether **4.13**, which in turn was employed in the critical indolyne cyclization. To our delight, treatment of **4.13** with NaNH₂ and *t*-BuOH in THF

at ambient temperatures^{3p,13} led to indolyne adducts **4.14** and **4.15** in a combined 46% yield (2.5 : 1 ratio).^{14,15} Although *O*-arylated product **4.15** was observed,¹⁶ the major product **4.14** possesses the desired [4.3.1]-bicyclic framework of the natural product and is available in gram quantities.¹⁷ Moreover, it was believed that bicycle **4.14** was suitably functionalized to allow for the ultimate completion of the natural product synthesis.

Scheme 4.2

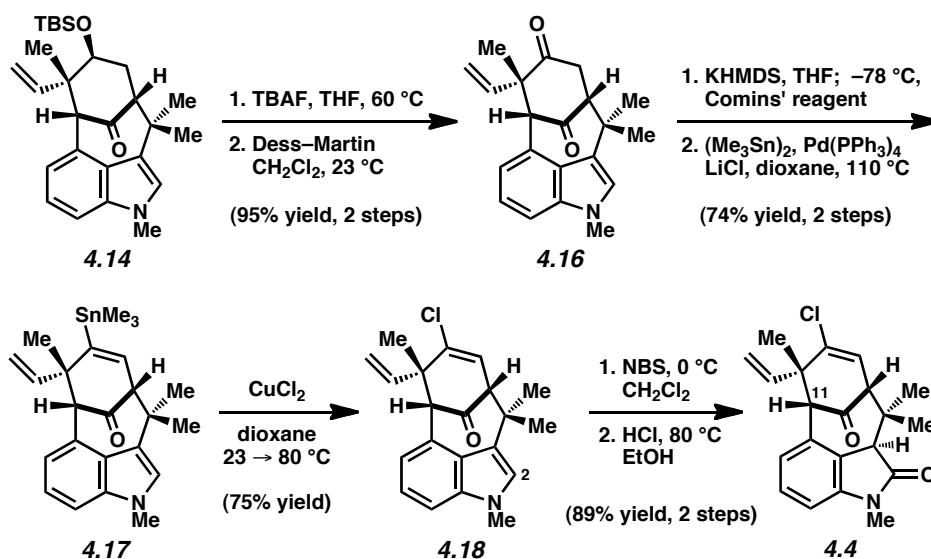


4.5 Introduction of the Vinyl Chloride and Oxindole Moieties

Having assembled the bicyclic framework of the natural product, we focused efforts on introduction of the vinyl chloride and oxindole moieties (Scheme 4.3). Desilylation of **4.14**,

followed by Dess–Martin oxidation, smoothly furnished diketone **4.16**. Subsequently, a sequence involving triflation and Pd-catalyzed stannylation provided vinyl stannane **4.17**.¹⁸ Exposure of **4.17** to CuCl_2 in dioxane afforded vinyl chloride **4.18**.¹⁹ To arrive at the necessary oxindole, a two-step procedure involving sequential C2 bromination and hydrolysis was employed to deliver late-stage intermediate **4.4**.⁷

Scheme 4.3

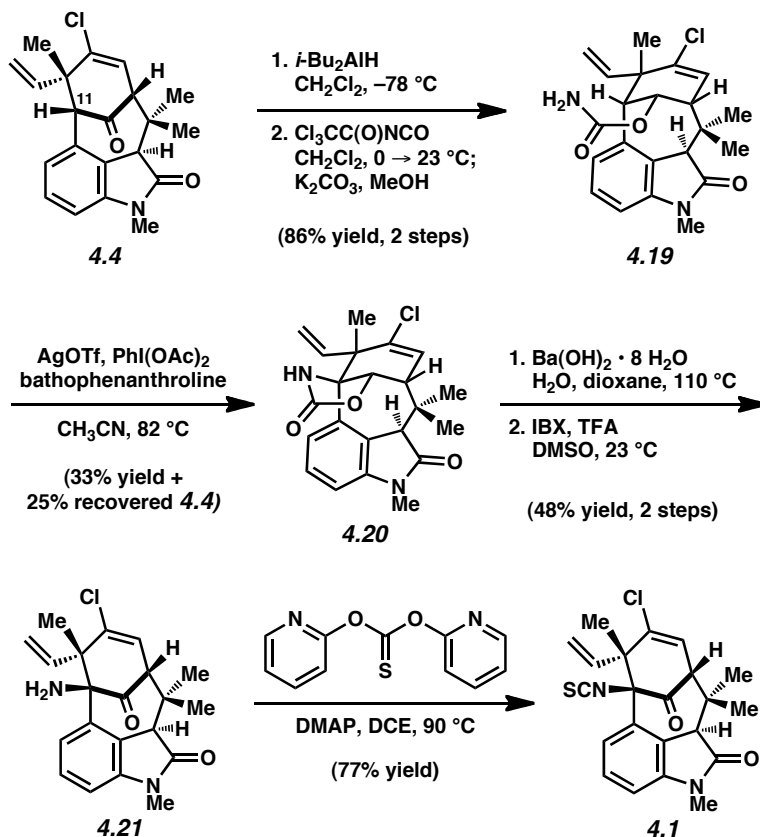


4.6 Completion of (–)-*N*-Methylwelwitindolinone C Isothiocyanate

With intermediate **4.4** lacking only the isothiocyanate substituent, we turned our attention to functionalization of the sterically congested C11 bridgehead position.²⁰ Unfortunately, attempts to substitute C11 through intermolecular processes were unsuccessful.²¹ As a workaround, we postulated that an intramolecular nitrene C–H insertion might be more fruitful.^{22,23} Ketone reduction of **4.4** proceeded efficiently using *i*- Bu_2AlH to furnish a secondary alcohol intermediate as a single diastereomer (Scheme 4.4). Subsequent carbamoylation

furnished **4.19**,²³ the key substrate for the critical C–H insertion reaction. The cyclization of carbamate **4.19** was attempted using a variety of reaction conditions that had previously been used to construct 5-membered oxazolidinones fused to cyclohexyl rings.²⁴ Although use of Rh catalysis furnished ketone **4.4** rather than the desired product **4.20**,²⁵ Ag catalysis^{24b,c} was found to be more effective. Upon treatment of **4.19** with AgOTf, bathophenanthroline, and PhI(OAc)₂ in CH₃CN at elevated temperatures, the desired nitrene insertion took place to deliver oxazolidinone **4.20** as the major product. Ketone **4.4** was also recovered, and could be recycled through our synthetic route. Nonetheless, hydrolysis of **4.20** followed by IBX oxidation generated the penultimate intermediate **4.21**. With aminoketone **4.21** in hand, final introduction of the isothiocyanate^{3m,26} furnished **4.1**. Spectral data for synthetic **4.1** was identical in all respects to that reported for the natural product.^{1a,27}

Scheme 4.4



4.7 Conclusion

In summary, we have achieved the first total synthesis of (-)-*N*-methylwelwitindolinone C isothiocyanate (**4.1**). Our enantiospecific route proceeds in 17 steps from known carvone derivative **4.11** and features a number of key transformations, including: (a) an indolyne cyclization to assemble the [4.3.1]-bicycle, (b) late-stage introduction of the vinyl chloride and oxindole moieties, and (c) a nitrene insertion reaction to functionalize the sterically congested C11 bridgehead position. Our synthesis of (-)-(**4.1**) validates the use of indolynes as intermediates in complex molecule synthesis and provides a promising entryway to the other [4.3.1]-bicyclic welwitindolinones.

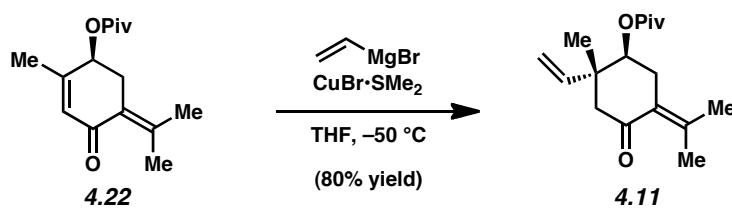
4.8 Experimental Section

4.8.1 Materials and Methods

Unless stated otherwise, reactions were conducted in flame-dried glassware under an atmosphere of nitrogen using anhydrous solvents (either freshly distilled or passed through activated alumina columns). All commercially available reagents were used as received unless otherwise specified. (*S*)-Carvone was obtained from Aldrich. 5-bromoindole was obtained from Biosynth. NaNH₂ was obtained from Alfa Aesar. Comins' reagent was obtained from Aldrich. Hexamethylditin was obtained from Aldrich. Tetrakis(triphenylphosphine) palladium(0) was obtained from Strem. Anhydrous CuCl₂ was obtained from Aldrich. Trichloroacetyl isocyanate was obtained from Aldrich. AgOTf was obtained from Strem. Bathophenanthroline was obtained from Alfa Aesar. *O,O*-di(2-pyridinyl) thiocarbonate was obtained from Aldrich. 2-Iodoxybenzoic acid (IBX) and Dess–Martin periodinane were prepared from known literature procedures.^{28,29} *t*-BuOH was distilled from CaH₂ and stored in a Schlenk tube prior to use. 1,4-dioxane was distilled from Na/benzophenone prior to use. 1,2-dichloroethane was distilled from P₂O₅ and stored in a Schlenk tube over 4Å molecular sieves prior to use. Unless stated otherwise, reactions were performed at room temperature (rt, approximately 23 °C). Thin-layer chromatography (TLC) was conducted with EMD gel 60 F254 pre-coated plates (0.25 mm) and visualized using a combination of UV, anisaldehyde, iodine, and potassium permanganate staining. Silicycle silica gel 60 (particle size 0.040–0.063 mm) was used for flash column chromatography. ¹H NMR spectra were recorded on Bruker spectrometers (500 MHz). Data for ¹H NMR spectra are reported as follows: chemical shift (δ ppm), multiplicity, coupling constant (Hz), integration and are referenced to the residual solvent peak 7.26 ppm³⁰ for CDCl₃ and 5.32 ppm for CD₂Cl₂. ¹³C NMR spectra are reported in terms of chemical shift (at 125 MHz) and are referenced to the

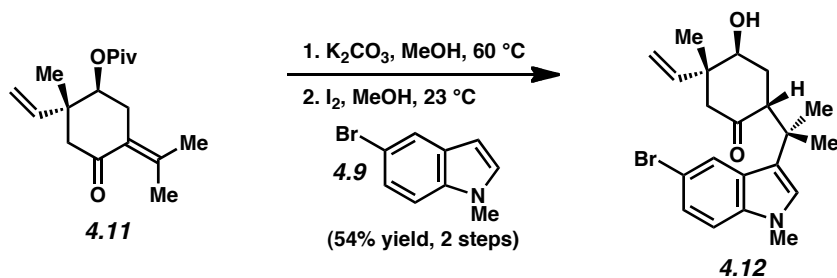
residual solvent peak 77.16 ppm³⁰ for CDCl₃ and 53.84 for CD₂Cl₂. IR spectra were recorded on a Perkin-Elmer 100 spectrometer and are reported in terms of frequency absorption (cm⁻¹). Optical rotations were measured with a Rudolf Autopol IV Automatic Polarimeter. Uncorrected melting points were measured with a Mel-Temp II melting point apparatus and a Fluke 50S thermocouple. High resolution mass spectra were obtained from the UC Irvine Mass Spectrometry Facility.

4.8.2 Experimental Procedures



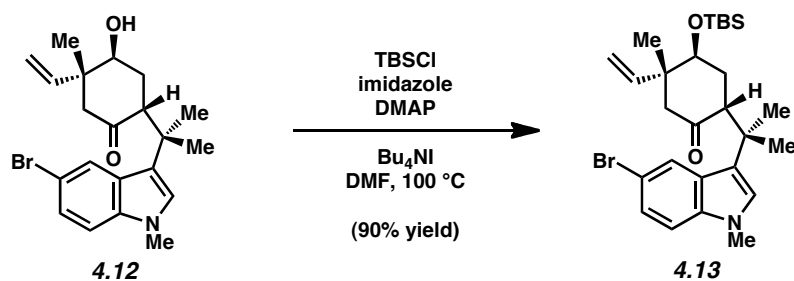
Enone 4.11. Enone **4.11** was prepared using Natsume's procedure (originally performed in the enantiomeric series).³¹ A flask was charged with CuBr·SMe₂ (196 mg, 0.956 mmol, 0.1 equiv) followed by the addition of THF (90 mL). The resulting suspension was cooled to -50 °C and the vinyl magnesium bromide solution (1.0 M in THF, 28.7 mL, 28.7 mmol, 3.0 equiv) was added via syringe pump at a rate of 44.2 mL/hr. Once the addition was complete, a solution of **4.22**³¹ (2.39 g, 9.56 mmol, 1.0 equiv) in THF (90 mL) was added via syringe pump at a rate of 86.0 mL/hr. After the addition of **4.22** was complete, the reaction was allowed to stir for 10 minutes and then quenched with a solution of saturated aqueous NH₄Cl (25 mL). The reaction vessel was then removed from the -50 °C bath, diluted with Et₂O (100 mL) and a solution of 1 M aqueous HCl (30 mL), and then allowed to warm to room temperature. The resulting mixture was vigorously stirred until all solids had dissolved. The resulting biphasic mixture was

transferred to a separatory funnel and extracted with Et₂O (3 x 75 mL). The organic layers were combined, dried over MgSO₄, and evaporated under reduced pressure. The resulting residue was purified by flash chromatography (3:1 hexanes:Et₂O) to afford enone **4.11** (2.58 g, 80% yield) as a light yellow oil. Enone **4.11**: R_f 0.48 (3:1 hexanes:Et₂O); ¹H NMR (500 MHz, CDCl₃): δ 5.76 (dd, *J* = 17.6, 10.7, 1H), 5.09 (d, *J* = 17.6, 1H), 5.09 (d, *J* = 10.7, 1H), 4.95 (t, *J* = 4.9, 1H), 2.70–2.66 (m, 2H), 2.54 (d, *J* = 15.8, 1H), 2.50 (d, *J* = 15.8, 1H), 2.02 (t, *J* = 1.6, 3H), 1.75 (s, 3H), 1.19 (s, 9H), 1.08 (s, 3H); ¹³C NMR (125 MHz, CDCl₃): δ 201.3, 177.9, 146.0, 142.8, 127.4, 114.7, 74.1, 49.2, 43.0, 39.2, 31.1, 27.2, 23.3, 22.6, 22.3; IR (film): 2975, 1720, 1679, 1480, 1280, 1215, 1157 cm⁻¹; HRMS-ESI (*m/z*) [M + Na]⁺ calcd for C₁₇H₂₆O₃Na, 301.1780; found 301.1776; [α]_D^{24.5} +41.4° (*c* = 1.000, CHCl₃).



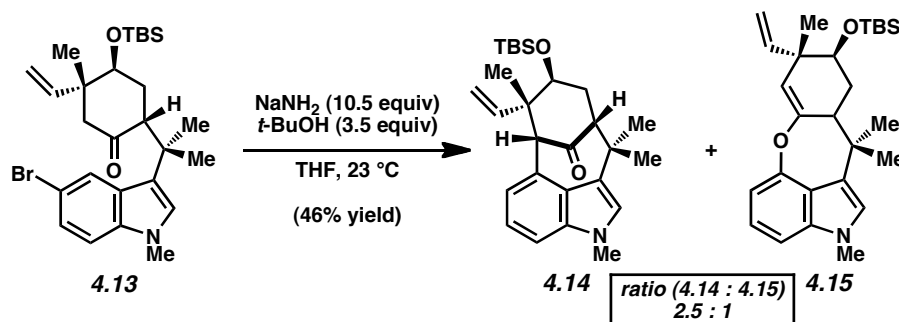
Indole 4.12. To a flask containing a solution of enone **4.11** (1.05 g, 3.79 mmol, 1.0 equiv) in MeOH (77.4 mL) was added K₂CO₃ (1.31 g, 9.47 mmol, 2.5 equiv) in one portion. The flask was fitted with a reflux condenser, flushed with N₂, and then allowed to stir at 60 °C. After 24 h, the reaction was cooled to room temperature and transferred to a separatory funnel with Et₂O (40 mL), H₂O (20 mL), and a solution of saturated aqueous NH₄Cl (20 mL). The resulting biphasic mixture was extracted with Et₂O (3 x 40 mL). The organic layers were combined, dried over MgSO₄, and evaporated under reduced pressure. The resulting crude residue was used in the subsequent reaction without further purification.

To a flask containing the crude residue from the previous step was added 5-bromo-*N*-methylindole³² (1.23 g, 5.89 mmol, 1.5 equiv), followed by MeOH (7.82 mL). The resulting suspension was stirred at room temperature until the mixture became homogeneous, and then iodine (198 mg, 0.78 mmol, 0.2 equiv) was added in one portion. The flask was flushed the N₂ and allowed to stir at room temperature. After 19 h, the reaction was quenched with a solution of saturated aqueous Na₂S₂O₃ (15 mL) and transferred to a separatory funnel with Et₂O (50 mL) and H₂O (15 mL). The resulting biphasic mixture was extracted with Et₂O (3 x 30 mL). The organic layers were combined, dried over MgSO₄, and evaporated under reduced pressure. The resulting residue was purified by flash chromatography (2:1:1 hexanes:CH₂Cl₂:Et₂O) to afford indole **4.12** (823 mg, 54% yield, over two steps) as a white solid. Indole **4.12**: mp: 71 °C; R_f 0.43 (2:1:1 hexanes:CH₂Cl₂:Et₂O); ¹H NMR (500 MHz, CD₂Cl₂): δ 7.85, (d, *J* = 1.7, 1H), 7.26 (dd, *J* = 8.7, 1.7, 1H), 7.18 (d, *J* = 8.7, 1H), 6.82 (s, 1H), 5.64 (dd, *J* = 17.7, 10.9, 1H), 5.07 (d, *J* = 17.7, 1H), 5.05 (d, *J* = 10.9, 1H), 3.70 (s, 3H), 3.61 (br. s, 1H), 3.37 (dd, *J* = 12.7, 5.5, 1H), 2.71 (d, *J* = 13.7, 1H), 2.23 (dd, *J* = 13.7, 1.1, 1H), 1.82 (dt, *J* = 12.9, 2.4, 1H), 1.58 (s, 3H), 1.57–1.51 (m, 1H), 1.41 (s, 3H), 1.08 (s, 3H); ¹³C NMR (125 MHz, CD₂Cl₂): δ 210.5, 144.1, 136.9, 127.9, 127.7, 124.1, 123.8, 123.6, 114.7, 112.0, 111.4, 72.8, 50.2, 48.7, 47.3, 36.6, 33.10, 33.08, 27.7, 24.6, 22.9; IR (film): 3463, 2966, 1703, 1479, 1214 cm⁻¹; HRMS-ESI (*m/z*) [M + Na]⁺ calcd for C₂₁H₂₆NO₂BrNa, 426.1045; found 426.1044; [α]^{24.8}_D +76.2° (*c* = 1.000, CHCl₃).



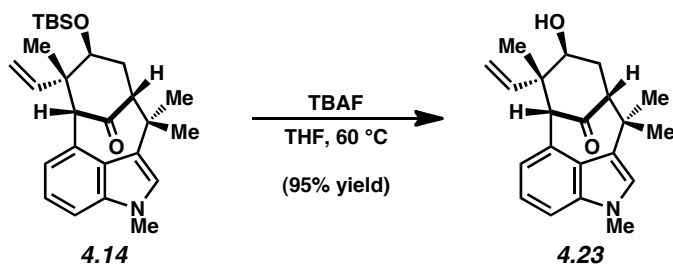
Silyl Ether 4.13. To a solution of indole **4.12** (3.84 g, 9.50 mmol, 1.0 equiv) in DMF (47.5 mL) was added imidazole (3.23 g, 47.5 mmol, 5 equiv), DMAP (1.17 g, 9.50 mmol, 1.0 equiv), tetrabutylammonium iodide (3.51 g, 9.50 mmol, 1.0 equiv), and TBSCl (4.30 g, 28.5 mmol, 3.0 equiv), all as solids in one portion. The flask was fitted with a reflux condenser, flushed with N_2 , and then allowed to stir at $100\text{ }^\circ\text{C}$. After 12 h, the reaction was cooled to room temperature and transferred to a separatory funnel with EtOAc (75 mL), H_2O (30 mL), and a solution of saturated aqueous NH_4Cl (100 mL). The resulting biphasic mixture was extracted with EtOAc (4 x 75 mL). The organic layers were combined, washed with H_2O (1 x 20 mL), washed with brine (2 x 20 mL), dried over MgSO_4 , and evaporated under reduced pressure. The resulting residue was purified by flash chromatography (1:1 hexanes:Et₂O) to afford silyl ether **4.13** (4.43 g, 90% yield) as a white solid. Silyl ether **4.13**: mp: $117\text{ }^\circ\text{C}$; R_f 0.68 (1:1 hexanes:Et₂O); ^1H NMR (500 MHz, CDCl_3): δ 7.79 (d, $J = 1.8$, 1H), 7.24 (dd, $J = 8.7, 1.8$, 1H), 7.12 (d, $J = 8.7$, 1H), 6.78 (s, 1H), 5.61 (dd, $J = 17.6, 11.0$, 1H), 5.07 (d, $J = 17.6$, 1H), 5.04 (d, $J = 11.0$, 1H), 3.70 (s, 3H), 3.56 (br. s, 1H), 3.27 (dd, $J = 13.0, 5.4$, 1H), 2.67 (d, $J = 13.4$, 1H), 2.16 (dd, $J = 13.4, 0.9$, 1H), 1.81 (dt, $J = 13.4, 2.0$, 1H), 1.63 (s, 3H), 1.61–1.59 (m, 1H), 1.38 (s, 3H), 1.00 (s, 3H), 0.86 (s, 9H), -0.04 (s, 3H), -0.42 (s, 3H); ^{13}C NMR (125 MHz, CDCl_3): δ 211.0, 143.7, 136.5, 127.7, 127.3, 124.0, 123.71, 123.66, 114.7, 112.1, 110.9, 73.3, 50.4, 48.4, 48.1, 36.0, 33.3, 32.9, 26.5, 26.1, 25.6, 24.1, 18.2, -4.7 , -5.1 ; IR (film): 2953, 2926, 2858, 1708, 1477, 1361, 1256, 1218,

1073 cm^{-1} ; HRMS-ESI (m/z) [$M + \text{Na}$] $^+$ calcd for $\text{C}_{27}\text{H}_{40}\text{NO}_2\text{BrSiNa}$, 540.1909; found 540.1903; $[\alpha]_D^{22.7} +72.4^\circ$ ($c = 1.000, \text{CHCl}_3$).

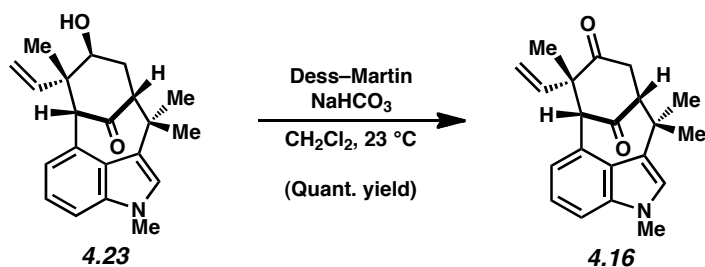


Bicycle 4.14. Inside of the glovebox, a flask was charged with NaNH_2 (2.13 g, 54.50 mmol, 10.5 equiv). The flask was then sealed and removed from the glovebox. THF (30.0 mL) was then added, followed by $t\text{-BuOH}$ (1.75 mL, 18.20 mmol, 3.5 equiv). The resulting suspension was heated to 40°C and stirred vigorously for 1 h. The reaction was cooled to room temperature and a solution of silyl ether **4.13** (2.68 g, 5.20 mmol, 1.0 equiv) in THF (22.0 mL) was added. After stirring at room temperature, the reaction was quenched via the dropwise addition of H_2O until no more gas evolution was observed. The reaction was then transferred to a separatory funnel with EtOAc (40 mL) and a solution of saturated aqueous NH_4Cl (40 mL). The resulting biphasic mixture was extracted with EtOAc (3 x 100 mL) and the organic layers were combined, dried over MgSO_4 , and evaporated under reduced pressure. The resulting residue was purified by flash chromatography (100% benzene) to afford bicycle **4.14** (749 mg, 33% yield) as a light yellow oil and *O*-arylated product **4.15** (288 mg, 13% yield) as a clear oil. Bicycle **4.14**: R_f 0.56 (100% benzene); $^1\text{H NMR}$ (500 MHz, CDCl_3): δ 7.19 (d, $J = 8.1$, 1H), 7.13 (dd, $J = 8.1, 7.3$, 1H), 6.95 (s, 1H), 6.71 (d, $J = 7.3$, 1H), 4.96 (dd, $J = 14.6, 4.6$, 1H), 4.91–4.84 (m, 2H), 3.77 (s, 3H), 3.72 (dd, $J = 11.0, 5.0$, 1H), 3.60 (d, $J = 1.5$, 1H), 2.63 (d, $J = 8.3$, 1H), 2.21 (ddd, $J = 14.5, 5.0, 1.8$,

1H), 2.00 (ddd, $J = 14.5, 8.3, 2.8$), 1.57 (s, 3H), 1.18 (s, 3H), 1.07 (s, 3H), 0.72 (s, 9H), -0.21 (s, 3H), -0.38 (s, 3H); ^{13}C NMR (125 MHz, CDCl_3): δ 212.4, 145.0, 137.4, 126.3, 126.2, 125.2, 122.6, 122.5, 121.1, 113.0, 108.1, 69.1, 69.0, 60.0, 49.8, 35.8, 35.7, 33.0, 32.1, 28.2, 25.9, 18.0, 16.8, -4.3 , -4.8 ; IR (film): 2956, 2926, 1705, 1472, 1256, 1092 cm^{-1} ; HRMS-ESI (m/z) [$\text{M} + \text{Na}$] $^+$ calcd for $\text{C}_{27}\text{H}_{39}\text{NO}_2\text{SiNa}$, 460.2648; found 460.2650; $[\alpha]_D^{24.9} +101.8^\circ$ ($c = 1.000$, CHCl_3).

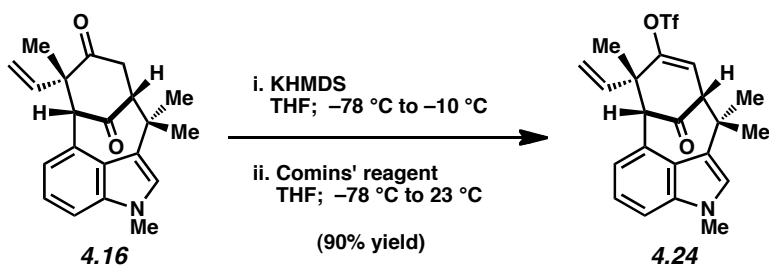


Alcohol 4.23. A flask was charged with bicycle **4.14** (848 mg, 1.94 mmol, 1.0 equiv) followed by the addition of THF (20 mL). A solution of TBAF (1.0 M in THF, 5.82 mL, 5.82 mmol, 3.0 equiv) was then added and the flask was fitted with a reflux condenser, flushed with N_2 , and allowed to stir at 60°C . After 12 h, the reaction was cooled to room temperature and transferred to a separatory funnel with EtOAc (30 mL) and a solution of 1 M aqueous NaHSO_4 (15 mL). The resulting biphasic mixture was extracted with EtOAc (3 x 30 mL). The combined organic layers were dried over MgSO_4 and evaporated under reduced pressure. The resulting residue was purified by flash chromatography (2:1 hexanes:EtOAc) to afford **4.23** (605 mg, 96% yield) as a white solid. **4.23**: R_f 0.25 (2:1 hexanes:EtOAc); ^1H NMR (500 MHz, CDCl_3): δ 7.20 (d, $J = 8.2$, 1H), 7.15 (dd, $J = 8.2, 7.2$, 1H), 6.96 (s, 1H), 6.72 (d, $J = 7.2$, 1H), 5.18–5.02 (m, 3H), 3.77 (s, 3H), 3.74 (ddd, $J = 5.6, 3.0, 2.5$, 1H), 3.67 (d, $J = 1.5$, 1H), 2.70 (d, $J = 8.5$, 1H), 2.42 (dd, $J = 14.2, 5.6$, 1H), 1.97 (ddd, $J = 14.2, 8.5, 2.5$, 1H), 1.61 (s, 3H), 1.18 (s, 3H), 1.08 (s, 3H).

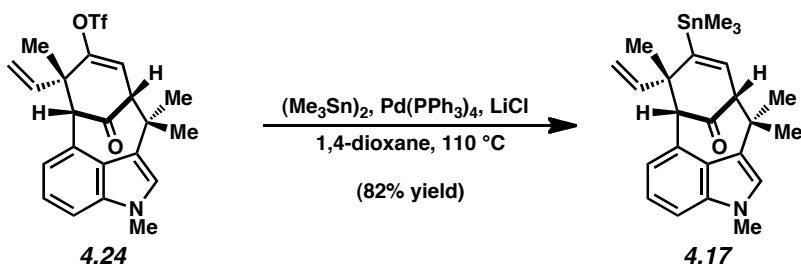


Diketone 4.16. A flask was charged with **4.23** (601 mg, 1.86 mmol, 1.0 equiv), NaHCO₃ (781 mg, 9.30 mmol, 5.0 equiv), and CH₂Cl₂ (37 mL). To the resulting suspension was added the Dess–Martin periodinane reagent (1.02 g, 2.42 mmol, 1.3 equiv) in one portion. The flask was flushed with N₂, and the reaction mixture was allowed to stir at room temperature. After 90 min, the reaction mixture was diluted with a solution of NaHCO₃ (1 g) and Na₂S₂O₃ (1 g) in H₂O (20 mL). The resulting biphasic mixture was vigorously stirred until both layers were no longer cloudy. The mixture was then transferred to a separatory funnel with EtOAc (50 mL) then extracted with EtOAc (3 x 50 mL). The organic layers were combined, dried over MgSO₄, and evaporated under reduced pressure. The resulting residue was purified by flash chromatography (2:1:1 hexanes:CH₂Cl₂:Et₂O) to afford diketone **4.16** (600 mg, quant. yield) as a white solid.

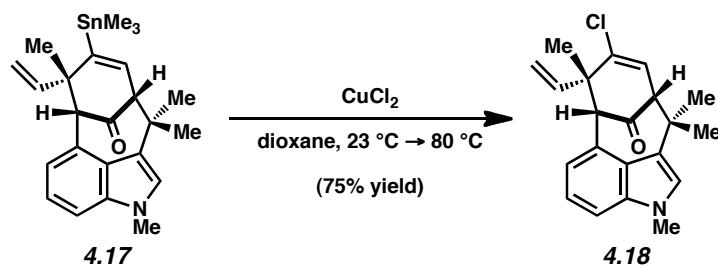
Diketone 4.16: mp: 194 °C; R_f 0.48 (2:1:1 hexanes:CH₂Cl₂:Et₂O); ¹H NMR (500 MHz, CDCl₃): δ 7.20 (d, *J* = 8.4, 1H), 7.15 (dd, *J* = 8.4, 7.7, 1H), 6.94 (s, 1H), 6.80 (d, *J* = 7.7, 1H), 5.64 (dd, *J* = 17.4, 10.8, 1H), 5.21 (d, *J* = 10.8, 1H), 5.16 (d, *J* = 17.4, 1H), 3.90 (s, 1H), 3.75 (s, 3H), 3.00–2.87 (m, 3H), 1.51 (s, 3H), 1.47 (s, 3H), 1.17 (s, 3H); ¹³C NMR (125 MHz, CDCl₃): δ 209.9, 209.4, 139.3, 137.8, 127.1, 123.8, 123.5, 122.8, 121.1, 120.2, 114.8, 108.9, 68.9, 58.5, 56.3, 40.2, 37.4, 33.6, 33.1, 28.2, 22.2; IR (film): 2976, 2922, 1714, 1706, 1541, 1418, 1234 cm⁻¹; HRMS-ESI (*m/z*) [M + Na]⁺ calcd for C₂₁H₂₃NO₂Na, 344.1627; found 344.1624; [α]^{25.1}_D +165.8° (*c* = 1.000, CHCl₃).



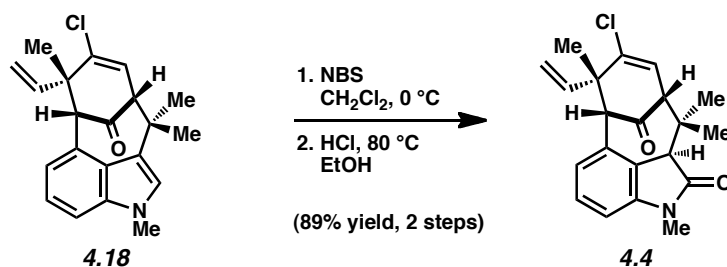
Vinyl Triflate 4.24. Inside of the glovebox, a flask was charged with solid KHMDS (327 mg, 1.65 mmol, 1.2 equiv). The flask was then sealed and removed from the glovebox. THF (7.0 mL) was added and the resulting solution was cooled to $-78\text{ }^{\circ}\text{C}$. A solution of diketone **4.16** (440 mg, 1.37 mmol, 1.0 equiv) in THF (7.0 mL) was then added dropwise. Upon completion of the addition, the reaction was allowed to stir at $-78\text{ }^{\circ}\text{C}$ for 15 min, and was then warmed to $-10\text{ }^{\circ}\text{C}$ for 1 additional hour. The reaction vessel was then cooled to $-78\text{ }^{\circ}\text{C}$ and a solution of Comins' reagent (590 mg, 1.51 mmol, 1.1 equiv) in THF (3 mL) was added dropwise. After stirring at $-78\text{ }^{\circ}\text{C}$ for 45 min, the reaction mixture was warmed to room temperature and allowed to stir for an additional 15 min. The reaction was then quenched by the addition of a solution of saturated aqueous NH_4Cl (5 mL) and transferred to a separatory funnel with EtOAc (30 mL) and H_2O (20 mL). The resulting biphasic mixture was extracted with EtOAc (3 x 30 mL). The organic layers were combined, dried over MgSO_4 , and evaporated under reduced pressure. The resulting residue was purified by flash chromatography (2:1:1 hexanes: CH_2Cl_2 : Et_2O) to afford vinyl triflate **4.24** (555 mg, 90% yield) as a light yellow oil. Vinyl triflate **4.24**: R_f 0.64 (2:1:1 hexanes: CH_2Cl_2 : Et_2O); ^1H NMR (500 MHz, CDCl_3): δ 7.23 (d, $J = 8.2$, 1H), 7.15 (dd, $J = 8.2$, 7.3, 1H), 6.92 (s, 1H), 6.75 (d, $J = 7.3$, 1H), 5.93 (d, $J = 3.8$, 1H), 5.24–5.17 (m, 3H), 3.80 (s, 1H), 3.76 (s, 3H), 3.15 (d, $J = 3.8$, 1H), 1.63 (s, 3H), 1.49 (s, 3H), 1.22 (s, 3H).



Vinyl Stannane 4.17. In the glovebox, a 20 mL scintillation vial was charged with Pd(PPh₃)₄ (59 mg, 0.051 mmol, 0.2 equiv), LiCl (258 mg, 6.51 mmol, 24 equiv), and hexamethylditin (254 μ L, 1.23 mmol, 4.8 equiv). A separate 20 mL scintillation vial was charged with **4.24** (116 mg, 0.256 mmol, 1.0 equiv), followed by the addition of 1,4-dioxane (3.8 mL) which had been taken through three freeze-pump-thaw cycles prior to use. The resulting solution was then added to the vial containing the palladium catalyst, sealed, taken outside of the glovebox, and allowed to stir at 110 °C. After 20 h, the reaction was cooled to room temperature and filtered through a plug of silica gel topped with Celite. The filter cake was then washed with CH₂Cl₂ (15 mL), and the filtrate was evaporated under reduced pressure. The resulting residue was purified by flash chromatography (5:1 hexanes:Et₂O) to afford vinyl stannane **4.17** (97 mg, 82% yield) as a white solid. Vinyl stannane **4.17**: mp: 158 °C; R_f 0.34 (5:1 hexanes:Et₂O); ¹H NMR (500 MHz, CDCl₃): δ 7.15 (d, J = 8.0, 1H), 7.10 (dd, J = 8.0, 7.0, 1H), 6.84 (s, 1H), 6.72 (d, J = 7.0, 1H), 5.93 (d, J = 3.2, $J_{\text{H-Sn}}$ = 72.0, 1H), 5.42 (dd, J = 17.7, 10.7, 1H), 5.07 (dd, J = 17.7, 1.1, 1H), 5.05 (dd, J = 10.7, 1.1, 1H), 3.73 (app. s, 4H), 2.93 (d, J = 3.2, 1H), 1.65 (s, 3H), 1.24 (s, 3H), 1.21 (s, 3H), –0.10 (s, $J_{\text{H-Sn}}$ = 52.7, 9H); ¹³C NMR (125 MHz, CDCl₃): δ 211.9, 149.9, 145.4, 137.6, 135.5, 125.6, 125.5, 124.5, 122.9, 122.0, 120.5, 112.2, 107.8, 68.6, 61.8, 53.2, 37.1, 34.4, 33.0, 28.5, 25.7, –7.5; IR (film): 2973, 2919, 2875, 1703, 1454, 1420, 1371, 1255 cm⁻¹; HRMS-ESI (m/z) [M + Na]⁺ calcd for C₂₄H₃₁NOSnNa, 492.1330; found 492.1327; [α]_D^{25.2} +46.6° (c = 1.000, CHCl₃).



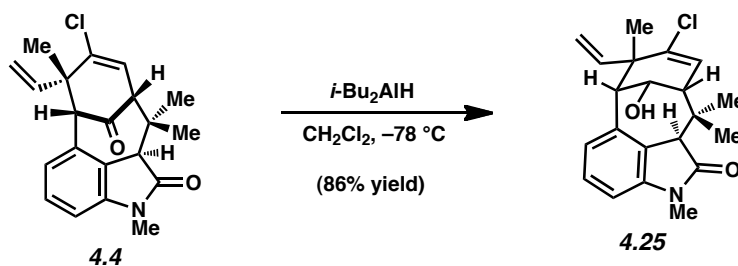
Vinyl Chloride 4.18. A 20 mL scintillation vial was charged with vinyl stannane **4.17** (100 mg, 0.214 mmol, 1.0 equiv), and then transferred to the glovebox. Dioxane (4.27 mL) was added and to the resulting solution was added CuCl_2 (63 mg, 0.470 mmol, 2.2 equiv) in one portion. The vial was sealed and removed from the glovebox. The reaction mixture was allowed to stir at 23 °C for 30 min, and was then warmed to 80 °C. After 24 h, the reaction was diluted with brine (5 mL) and the resulting mixture was transferred to a separatory funnel with EtOAc (10 mL) and H_2O (5 mL). The resulting biphasic mixture was extracted with EtOAc (3 x 20 mL). The organic layers were combined, dried over MgSO_4 , and evaporated under reduced pressure. The resulting residue was purified by preparative thin layer chromatography (benzene eluent) to afford vinyl chloride **4.18** (54 mg, 75% yield) as a white solid. Vinyl chloride **4.18**: mp: 83 °C; R_f 0.27 (5:1 hexanes:Et₂O); ¹H NMR (500 MHz, CDCl_3): δ 7.20 (d, $J = 8.4$, 1H), 7.13 (dd, $J = 8.4$, 7.2, 1H), 6.89 (s, 1H), 6.76 (d, $J = 7.2$, 1H), 6.01 (d, $J = 3.9$, 1H), 5.27–5.12 (m, 3H), 3.82 (s, 1H), 3.75 (s, 3H), 3.02 (d, $J = 3.9$, 1H), 1.63 (s, 3H), 1.45 (s, 3H), 1.19 (s, 3H); ¹³C NMR (125 MHz, CDCl_3): δ 208.8, 142.2, 138.8, 137.7, 125.9, 124.31, 124.29, 124.2, 123.7, 121.4, 120.8, 113.8, 108.5, 68.6, 61.6, 51.9, 37.1, 34.0, 33.0, 28.3, 23.9; IR (film): 2970, 1716, 1450, 1418, 1368, 1255, 1152 cm^{-1} ; HRMS-ESI (m/z) [$\text{M} + \text{Na}$]⁺ calcd for $\text{C}_{21}\text{H}_{22}\text{NOClNa}$, 362.1288; found 362.1283; $[\alpha]_D^{22.8} +62.8^\circ$ ($c = 1.000$, CHCl_3).



Oxindole 4.4. To a solution of vinyl chloride **4.18** (46 mg, 0.136 mmol, 1.0 equiv) in CH_2Cl_2 (2.75 mL) at 0 °C was added NBS (24.3 mg, 0.136 mmol, 1.0 equiv) in one portion. The reaction vial was flushed with N_2 , and allowed to stir at 0 °C. After 25 min, solid NaHCO_3 (46 mg) was added in one portion. The reaction was removed from the 0 °C bath, and allowed to stir at room temperature for 5 min. The resulting suspension was filtered through a plug of silica gel (CH_2Cl_2 eluent, 10 mL). Evaporation under reduced pressure provided the crude brominated product, which was used in the subsequent step without further purification.

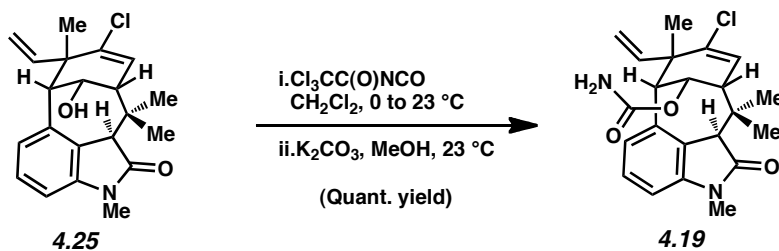
To the crude product was added absolute ethanol (1.5 mL) and concentrated aqueous HCl (1.5 mL). After heating to 80 °C for 14 h, the the reaction was cooled to room temperature and transferred to a separatory funnel with H_2O (10 mL) and EtOAc (20 mL). To the funnel was added solid NaHCO_3 until no more gas evolution was observed. The resulting biphasic mixture was extracted with EtOAc (3 x 20 mL) and the organic layers were combined, dried over MgSO_4 , and evaporated under reduced pressure. The resulting residue was purified by flash chromatography (2:1:1 hexanes: CH_2Cl_2 :Et₂O) to afford oxindole **4.4** (42.8 mg, 89% yield) as a white solid. Oxindole **4.4**: mp: 193 °C; R_f 0.40 (2:1:1 hexanes: CH_2Cl_2 :Et₂O); ^1H NMR (500 MHz, CDCl_3): δ 7.19 (dd, $J = 7.9, 7.9$, 1H), 6.71 (d, $J = 7.9$, 1H), 6.60 (d, $J = 7.9$, 1H), 6.16 (d, $J = 5.1$, 1H), 5.37 (dd, $J = 17.4, 10.6$, 1H), 5.13 (d, $J = 17.4$, 1H), 5.09 (d, $J = 10.6$, 1H), 3.81 (s, 1H), 3.52 (d, $J = 1.4$, 1H), 3.18 (s, 3H), 2.93 (dd, $J = 5.1, 1.4$, 1H), 1.62 (s, 3H), 1.47 (s, 3H), 0.73 (s, 3H); ^{13}C NMR (125 MHz, CDCl_3): δ 204.7, 175.4, 144.7, 141.4, 140.3, 130.5, 128.6,

127.1, 124.6, 123.9, 115.4, 107.3, 68.8, 63.8, 52.0, 51.9, 41.7, 26.4, 25.8, 25.6, 21.4; IR (film): 2966, 2922, 1700, 1609, 1595, 1465 cm^{-1} ; HRMS-ESI (m/z) $[\text{M} + \text{Na}]^+$ calcd for $\text{C}_{21}\text{H}_{22}\text{NO}_2\text{ClNa}$, 378.1237; found 378.1248; $[\alpha]^{23.4}_{\text{D}} -132.8^\circ$ ($c = 1.000$, CHCl_3).



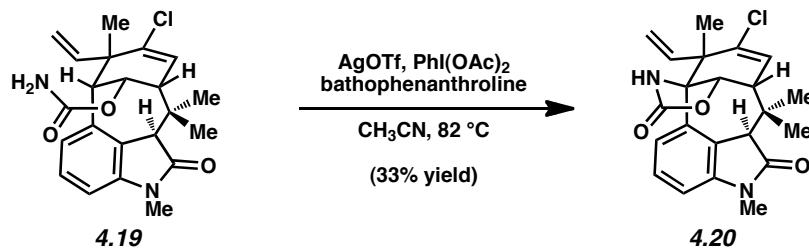
Alcohol 4.25. To a solution of oxindole **4.4** (43.0 mg, 0.121 mmol, 1.0 equiv) in CH_2Cl_2 (4.00 mL) at -78°C was added a solution of $i\text{-Bu}_2\text{AlH}$ (1.0 M in hexanes, 145 μL , 0.145 mmol, 1.2 equiv) dropwise. After stirring at -78°C for 1 h, an additional portion of $i\text{-Bu}_2\text{AlH}$ (1.0 M in hexanes, 24 μL , 0.024 mmol, 0.2 equiv) was added. After stirring at -78°C for 1 h, a third portion of $i\text{-Bu}_2\text{AlH}$ (1.0 M in hexanes, 24 μL , 0.024 mmol, 0.2 equiv) was added and the mixture was allowed to stir at -78°C for 1 h. At this time, a final portion of $i\text{-Bu}_2\text{AlH}$ (1.0 M in hexanes, 48 μL , 0.048 mmol, 0.4 equiv) was added. After 30 min, the reaction was quenched at -78°C with a solution of saturated aqueous NH_4Cl (1 mL) and Rochelle's salt (1 mL). The mixture was stirred at room temperature for 1 h, transferred to a separatory with EtOAc (20 mL) and a solution of saturated aqueous NH_4Cl (20 mL), and extracted with EtOAc (3 x 20 mL). The organic layers were combined, dried over MgSO_4 , and evaporated under reduced pressure. The resulting residue was purified by flash chromatography (1:1:1 hexanes: CH_2Cl_2 : Et_2O) to afford alcohol **4.25** (37.2 mg, 86% yield) as a white solid. Alcohol **4.25**: R_f 0.12 (2:1:1 hexanes: CH_2Cl_2 : Et_2O); ^1H NMR (500 MHz, CDCl_3): δ 7.17 (dd, $J = 7.8, 7.7$, 1H), 6.70 (d, $J = 7.8$, 1H), 6.68 (d, $J = 7.7$, 1H), 6.19 (d, $J = 6.7$, 1H), 5.23 (dd, $J = 17.4, 10.7$, 1H), 5.03 (dd, $J =$

17.4, 0.7, 1H), 4.89 (dd, $J = 10.7, 0.7$, 1H), 4.59–4.55 (app. t, $J = 4.9$, 1H), 3.62 (s, 1H), 3.18 (s, 3H), 3.14 (dd, $J = 4.9, 1.0$, 1H), 2.58 (ddd, $J = 6.7, 5.4, 1.0$, 1H), 1.57 (s, 3H), 1.53 (s, 3H), 0.95 (s, 3H).



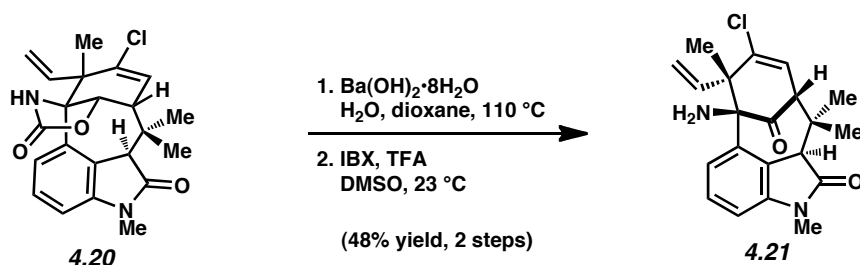
Carbamate 4.19. To a solution of **4.25** (78 mg, 0.218 mmol, 1.0 equiv) in CH_2Cl_2 (2.2 mL) at 0 °C was added trichloroacetyl isocyanate (27 μL , 0.229 mmol, 1.05 equiv) in a dropwise manner. The resulting mixture was allowed to stir at 0 °C for 5 min, and then at room temperature for 20 min. The solvent was evaporated under reduced pressure. To the resulting residue was added MeOH (4.4 mL) and solid K_2CO_3 (165 mg, 1.19 mmol, 5.5 equiv) in one portion. The reaction was flushed with N_2 and left to stir at room temperature for 90 min. The reaction was diluted with EtOAc (3 mL) and H_2O (1 mL) and the resulting biphasic mixture was transferred to a test tube with EtOAc (2 mL) and brine (2 mL). After extracting with EtOAc (3 x 3 mL), the organic layers were combined, dried over MgSO_4 , and evaporated under reduced pressure. The resulting residue was purified by flash chromatography (1:1 hexanes:EtOAc) to afford carbamate **4.19** (90 mg, quant. yield) as a white solid. Carbamate **4.19**: mp: 135 °C; R_f 0.41 (1:1 hexanes:EtOAc); ^1H NMR (500 MHz, CDCl_3): δ 7.13 (dd, $J = 7.8, 7.7$, 1H), 6.68 (d, $J = 7.7$, 1H), 6.61 (d, $J = 7.8$, 1H), 6.18 (d, $J = 6.8$, 1H), 5.47 (dd, $J = 5.3, 4.8$, 1H), 5.19 (dd, $J = 17.3, 10.6$, 1H), 5.04 (dd, $J = 17.3, 0.8$, 1H), 4.91 (dd, $J = 10.6, 0.8$, 1H), 4.41 (br. s, 2H), 3.62 (s, 3H), 3.18 (s, 3H), 3.15 (d, $J = 4.8$, 1H), 2.78 (dd, $J = 6.8, 5.3$, 1H), 1.61 (s, 3H), 1.52 (s, 3H), 0.87 (s, 3H); ^{13}C NMR (125

MHz, CDCl₃): δ 176.3, 155.9, 144.3, 141.2, 141.0, 136.9, 127.7, 127.3, 126.4, 125.7, 114.7, 106.6, 72.7, 55.9, 52.6, 50.6, 49.0, 38.7, 28.0, 26.3, 26.2, 22.7; IR (film): 3497, 3341, 2936, 1730, 1698, 1609, 1470, 1341, 1066 cm⁻¹; HRMS-ESI (*m/z*) [M + Na]⁺ calcd for C₂₂H₂₅N₂O₃ClNa, 423.1451; found 423.1459; [α]_D^{23.0} -166.4° (*c* = 1.000, CHCl₃).



Oxazolidinone 4.20. A 20 mL scintillation vial containing CH₃CN and a separate 20 mL scintillation vial charged with bathophenanthroline (24.1 mg, 0.0750 mmol, 0.5 equiv) were transferred into the glovebox. AgOTf (19.2 mg, 0.0750 mmol, 0.5 equiv) and CH₃CN (4.30 mL) were added to the vial containing the bathophenanthroline, and the resulting suspension was allowed to stir at room temperature for 20 min. Next, a third 20 mL scintillation vial containing carbamate **4.19** (55 mg, 0.150 mmol, 1.0 equiv) and PhI(OAc)₂ (96.4 mg, 0.300 mmol, 2.0 equiv) was transferred into the glovebox and the AgOTf/bathophenanthroline suspension was added to this vial. The vial was then sealed, removed from the glovebox, and the resulting mixture was allowed to stir at 82 °C. After 24 h, the reaction was cooled to room temperature and filtered through a plug of silica gel (EtOAc eluent, 50 mL). The filtrate was evaporated under reduced pressure, and the resulting residue was purified by preparative thin layer chromatography (2:1 benzene:EtOAc) to afford oxazolidinone **4.20** (18 mg, 33% yield) as a white solid and recovered oxindole **4.4** (12 mg, 25% yield) as a white solid. Oxazolidinone **4.20**: mp: 329 °C; R_f 0.35 (2:1 benzene:EtOAc); ¹H NMR (500 MHz, CDCl₃): δ 7.55 (br. s, 1H), 7.15

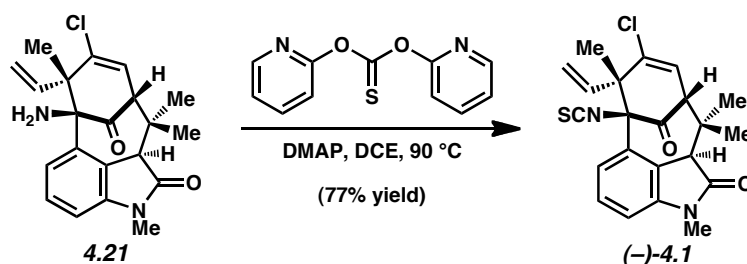
(dd, $J = 8.3, 7.6$, 1H), 6.72 (d, $J = 8.3$, 1H), 6.71 (d, $J = 7.6$, 1H), 6.29 (d, $J = 5.8$, 1H), 5.19–5.05 (m, 3H), 5.02 (d, $J = 6.5$, 1H), 3.62 (s, 1H), 3.19 (s, 3H), 2.98 (dd, $J = 6.5, 5.8$, 1H), 1.65 (s, 3H), 1.56 (s, 3H), 1.04 (s, 3H); ^{13}C NMR (125 MHz, CDCl_3): δ 174.9, 159.2, 144.2, 141.2, 140.6, 136.8, 128.2, 126.0, 125.5, 124.0, 116.4, 107.4, 81.3, 69.9, 54.2, 52.1, 49.6, 38.7, 27.4, 26.4, 22.0, 20.2; IR (film): 3270, 1755, 1686, 1612, 1460, 1202, 1152 cm^{-1} ; HRMS-ESI (m/z) [$\text{M} + \text{Na}$] $^+$ calcd for $\text{C}_{22}\text{H}_{23}\text{N}_2\text{O}_3\text{ClNa}$, 421.1295; found 421.1289; $[\alpha]_D^{25.5} -109.4^\circ$ ($c = 1.000$, CHCl_3).



Aminoketone 4.21. A Schlenk tube was charged with oxazolidinone **4.20** (15 mg, 0.0376 mmol, 1.0 equiv) and $\text{Ba}(\text{OH})_2 \cdot 8\text{H}_2\text{O}$ (59 mg, 0.188 mmol, 5.0 equiv). The reaction vessel was then evacuated and backfilled with N_2 five times. A 2:1 mixture of 1,4-dioxane: H_2O (1.4 mL) that had been taken through seven freeze-pump-thaw cycles prior to use was then added and the Schlenk tube. The vessel was sealed, and then transferred to the glovebox where the reaction was allowed to stir at 110°C . After 16 h, the Schlenk tube was removed from the glovebox and the contents were transferred to a test tube with EtOAc (6 mL), H_2O (1 mL), and brine (1 mL). The resulting biphasic mixture was extracted with EtOAc (3 x 4 mL). The organic layers were combined, dried over MgSO_4 , and evaporated under reduced pressure to afford the crude product, which was used directly in the subsequent reaction.

To the crude residue was added DMSO (1.4 mL) and TFA (3 μL , 0.0413 mmol, 1.1 equiv). The resulting solution was allowed to stir at room temperature for 2 min. IBX (53 mg,

0.188 mmol, 5 equiv) was then added in one portion, and the vial was flushed with N₂. After stirring at room temperature for 20 h, the reaction mixture transferred with EtOAc (3 mL) to a test tube containing a solution of aqueous K₂CO₃ (1 mL, concentration of 50 mg/mL). The resulting biphasic mixture was extracted with EtOAc (5 x 3 mL) and the organic layers were combined, dried over MgSO₄, and evaporated under reduced pressure. The resulting residue was purified by preparative thin layer chromatography (1:1 hexanes:EtOAc) to afford aminoketone **4.21** (6.7 mg, 48% yield, over two steps) as an amorphous solid. Aminoketone **4.21**: R_f 0.42 (1:1 hexanes:EtOAc); ¹H NMR (500 MHz, CDCl₃): δ 7.34 (d, *J* = 8.4, 1H), 7.27 (dd, *J* = 8.4, 7.6, 1H), 6.75 (d, *J* = 7.6, 1H), 6.18 (d, *J* = 4.2, 1H), 5.44 (dd, *J* = 17.3, 10.9, 1H), 5.22 (d, *J* = 10.9, 1H), 5.17 (d, *J* = 17.3, 1H), 3.82 (s, 1H), 3.18 (s, 3H), 3.15 (d, *J* = 4.2, 1H), 1.71 (br. s, 2H), 1.69 (s, 3H), 1.31 (s, 3H), 0.78 (s, 3H); ¹³C NMR (125 MHz, CDCl₃): δ 207.4, 174.7, 144.1, 140.6, 138.9, 135.2, 128.2, 124.2, 123.8, 123.7, 116.2, 107.7, 71.8, 62.8, 56.7, 53.8, 40.0, 26.4, 25.9, 21.6, 20.6; IR (film): 2973, 1709, 1698, 1609, 1583, 1457 cm⁻¹; HRMS-ESI (*m/z*) [M + H]⁺ calcd for C₂₁H₂₄N₂O₂Cl, 371.1526; found 371.1516; [α]_D^{23.8} -70.2° (*c* = 1.000, CHCl₃).



(-)-*N*-Methylwelwitindolinone C Isothiocyanate (**4.1**). To solution of aminoketone **4.21** (5.0 mg, 0.0135 mmol, 1.0 equiv) in 1,2-dichloroethane (540 μL) was added DMAP (0.8 mg, 0.0067 mmol, 0.5 equiv) and *O,O*-di(2-pyridinyl) thiocarbonate (15.7 mg, 0.067 mmol, 5 equiv) in one portion. The reaction vial was flushed with N₂ and then allowed to stir at 90 °C. After 14 h, the

reaction was cooled to room temperature and then passed over a plug of silica gel (EtOAc eluent, 20 mL). The filtrate was evaporated under reduced pressure. The resulting residue was purified by preparative thin layer chromatography (9:1 benzene:EtOAc) to afford (–)-**4.1** (4.3 mg, 77% yield) as an amorphous solid. (–)-*N*-methylwelwitindolinone C isothiocyanate (**4.1**): R_f 0.81 (1:1 hexanes:EtOAc); ^1H NMR (500 MHz, CDCl_3): δ 7.30 (dd, $J = 8.4, 7.8$, 1H), 7.18 (dd, $J = 8.4, 0.9$, 1H), 6.79 (dd, $J = 8.4, 0.9$, 1H), 6.17 (d, $J = 4.4$, 1H), 5.35 (dd, $J = 16.8, 10.6$, 1H), 5.29–5.17 (m, 2H), 3.73 (s, 1H), 3.24 (d, $J = 4.4$, 1H), 3.17 (s, 3H) 1.68 (s, 3H), 1.47 (s, 3H), 0.80 (s, 3H); ^{13}C NMR (125 MHz, CDCl_3): δ 196.3, 174.1, 144.5, 140.7, 138.7, 137.2, 130.1, 128.6, 124.7, 123.3, 122.5, 117.7, 108.5, 83.8, 61.7, 57.0, 53.1, 40.8, 26.4, 25.7, 22.2, 21.4; IR (film): 2970, 2932, 2041, 1712, 1609, 1460, 1341 cm^{-1} ; HRMS-ESI (m/z) $[\text{M} + \text{Na}]^+$ calcd for $\text{C}_{22}\text{H}_{21}\text{N}_2\text{O}_2\text{SCINa}$, 435.0910; found 435.0899; $[\alpha]_D^{23.6} -223.9^\circ$ ($c = 0.77, \text{CH}_2\text{Cl}_2$).³³

4.9 Notes and References

- (1) (a) Stramann, K.; Moore, R. E.; Bonjouklian, R.; Deeter, J. B.; Patterson, G. M. L.; Shaffer, S.; Smith, C. D.; Smitka, T. A. *J. Am. Chem. Soc.* **1994**, *116*, 9935–9942. (b) Jimenez, J. L.; Huber, U.; Smith, C. D.; Patterson, G. M. L. *J. Nat. Prod.* **1999**, *62*, 569–572.
- (2) Welwitindolinone A isonitrile, a unique welwitindolinone that possesses a C3 spirooxindoline core, has been synthesized independently by the Baran and Wood groups; see: (a) Baran, P. S.; Richter, J. M. *J. Am. Chem. Soc.* **2005**, *127*, 15394–15396. (b) Reisman, S. E.; Ready, J. M.; Hasuoka, A.; Smith, C. J.; Wood, J. L. *J. Am. Chem. Soc.* **2006**, *128*, 1448–1449.
- (3) (a) Konopelski, J. P.; Deng, H.; Schiemann, K.; Keane, J. M.; Olmstead, M. M. *Synlett* **1998**, 1105–1107. (b) Wood, J. L.; Holubec, A. A.; Stoltz, B. M.; Weiss, M. M.; Dixon, J. A.; Doan, B. D.; Shamji, M. F.; Chen, J. M.; Heffron, T. P. *J. Am. Chem. Soc.* **1999**, *121*, 6326–6327. (c) Kaoudi, T.; Ouiclet-Sire, B.; Seguin, S.; Zard, S. Z. *Angew. Chem., Int. Ed.* **2000**, *39*, 731–733. (d) Deng, H.; Konopelski, J. P. *Org. Lett.* **2001**, *3*, 3001–3004. (e) Jung, M. E.; Slowinski, F. *Tetrahedron Lett.* **2001**, *42*, 6835–6838. (f) López-Alvarado, P.; García-Granda, S.; Ivarez-Rúa, C.; Avendaño, C. *Eur. J. Org. Chem.* **2002**, 1702–1707. (g) MacKay, J. A.; Bishop, R. L.; Rawal, V. H. *Org. Lett.* **2005**, *7*, 3421–3424. (h) Baudoux, J.; Blake, A. J.; Simpkins, N. S. *Org. Lett.* **2005**, *7*, 4087–4089. (i) Greshock, T. J.; Funk, R. L. *Org. Lett.* **2006**, *8*, 2643–2645. (j) Lauchli, R.; Shea, K. J. *Org. Lett.* **2006**, *8*, 5287–5289. (k) Guthikonda, K.; Caliendo, B. J.; Du Bois, J. Abstracts of Papers, 232nd ACS National Meeting, September, 2006, abstr ORGN-002. (l) Xia, J. Brown, L. E.; Konopelski, J. P. *J. Org. Chem.* **2007**, *72*, 6885–6890. (m) Richter, J. M.; Ishihara, Y.; Masuda, T.; Whitefield,

- B. W.; Llamas, T.; Pohjakallio, A.; Baran, P. S. *J. Am. Chem. Soc.* **2008**, *130*, 17938–17945.
- (n) Boissel, V.; Simpkins, N. S.; Bhalay, G.; Blake, A. J.; Lewis, W. *Chem. Commun.* **2009**, 1398–1400. (o) Boissel, V.; Simpkins, N. S.; Bhalay, G. *Tetrahedron Lett.* **2009**, *50*, 3283–3286. (p) Tian, X.; Hutters, A. D.; Douglas, C. J.; Garg, N. K. *Org. Lett.* **2009**, *11*, 2349–2351. (q) Trost, B. M.; McDougall, P. J. *Org. Lett.* **2009**, *11*, 3782–3785. (r) Brailsford, J. A.; Lauchli, R.; Shea, K. J. *Org. Lett.* **2009**, *11*, 5330–5333. (s) Freeman, D. B. et al. *Tetrahedron* **2010**, *66*, 6647–6655. (t) Heidebrecht, R. W., Jr.; Gullledge, B.; Martin, S. F. *Org. Lett.* **2010**, *12*, 2492–2495. (u) Ruiz, M.; López-Alvarado, P.; Menéndez, J. C. *Org. Biomol. Chem.* **2010**, *8*, 4521–4523.
- (4) For pertinent reviews, see: (a) Brown, L. E.; Konopelski, J. P. *Org. Prep. Proc. Intl.* **2008**, *40*, 411–445. (b) Avendaño, C.; Menéndez, J. C. *Curr. Org. Synth.* **2004**, *1*, 65–82.
- (5) Bhat, V.; Allan, K. M.; Rawal, V. H. *J. Am. Chem. Soc.* **2011**, *133*, 5798–5801.
- (6) (a) Smith, C. D.; Zilfou, J. T.; Stratmann, K.; Patterson, G. M. L.; Moore, R. E. *Mol. Pharmacol.* **1995**, *47*, 241–247. (b) Zhang, X.; Smith, C. D. *Mol. Pharmacol.* **1996**, *49*, 288–294.
- (7) For a model system study of this transformation, see ref 3p.
- (8) For seminal indolyne studies, see: (a) Julia, M.; Huang, Y.; Igolen, J. *C. R. Acad. Sci., Ser. C* **1967**, *265*, 110–112. (b) Igolen, J.; Kolb, A. *C. R. Acad. Sci., Ser. C* **1969**, *269*, 54–56. (c) Julia, M.; Le Goffic, F.; Igolen, J.; Baillarge, M. *Tetrahedron Lett.* **1969**, *10*, 1569–1571. For related studies, see: (d) Julia, M.; Goffic, F. L.; Igolen, J.; Baillarge, M. *C. R. Acad. Sci., Ser. C* **1967**, *264*, 118–120. (e) Julia, M.; Igolen, J.; Kolb, M. *C. R. Acad. Sci., Ser. C* **1971**, *273*, 1776–1777.

- (9) For recent indolyne studies, see: (a) Bronner, S. M.; Bahnck, K. B.; Garg, N. K. *Org. Lett.* **2009**, *11*, 1007–1010. (b) Cheong, P. H.-Y.; Paton, R. S.; Bronner, S. M.; Im, G.-Y.; Garg, N. K.; Houk, K. N. *J. Am. Chem. Soc.* **2010**, *132*, 1267–1269. (c) Im, G.-Y.; Bronner, S. M.; Goetz, A. E.; Paton, R. S.; Cheong, P. H.-Y.; Houk, K. N.; Garg, N. K. *J. Am. Chem. Soc.* **2010**, *132*, 17933–17944. (d) Bronner, S. M.; Goetz, A. E.; Garg, N. K. *J. Am. Chem. Soc.* **2011**, *133*, 3832–3835. (e) Buszek, K. R.; Luo, D.; Kondrashov, M.; Brown, N.; VanderVelde, D. *Org. Lett.* **2007**, *9*, 4135–4137. (f) Brown, N.; Luo, D.; VanderVelde, D.; Yang, S.; Brassfield, A.; Buszek, K. R. *Tetrahedron Lett.* **2009**, *50*, 63–65. (g) Buszek, K. R.; Brown, N.; Luo, D. *Org. Lett.* **2009**, *11*, 201–204. (h) Brown, N.; Luo, D.; Decapo, J. A.; Buszek, K. R. *Tetrahedron Lett.* **2009**, *50*, 7113–7115. (i) Garr, A. N.; Luo, D.; Brown, N.; Cramer, C. J.; Buszek, K. R.; VanderVelde, D. *Org. Lett.* **2010**, *12*, 96–99. (j) Thornton, P. D.; Brown, N.; Hill, D.; Neunswander, B.; Lushington, G. H.; Santini, C.; Buszek, K. R. *ACS Comb. Sci.* **2011**, *13*, 443–448. (k) Nguyen, T. D.; Webster, R.; Lautens, M. *Org. Lett.* **2011**, *13*, 1370–1373.
- (10) Sakagami, M.; Muratake, H.; Natsume, M. *Chem. Pharm. Bull.* **1994**, *42*, 1393–1398.
- (11) Wang, S.-Y.; Ji, S.-J.; Loh, T.-P. *Synlett* **2003**, *15*, 2377–2379.
- (12) The C15 epimer of **4.12** was also obtained in 22% yield. Upon treatment of this compound with DBU in heated toluene, a separable mixture of **4.12** and epi-**4.12** is readily obtained.
- (13) Caubere, P. *Acc. Chem. Res.* **1974**, *7*, 301–308.
- (14) Variations in reaction conditions (e.g., temperature, stoichiometry, counterion, etc.) did not lead to improvements in the conversion of **4.13** to **4.14**.

- (15) The remaining balance of mass in the indolyne cyclization is largely attributed to aminoindole products, which presumably form by intermolecular addition of NH_2^- to the indolyne intermediate. Attempts to suppress this undesired reaction pathway have been unsuccessful.
- (16) *O*-arylated product **4.15** is often isolated with small amounts of the isomeric tetrasubstituted olefin.
- (17) Interestingly, the C13 epimer of substrate **4.13** does not undergo conversion to the corresponding [4.3.1]-bicycle.
- (18) Wulff, W. D.; Peterson, G. A.; Bauta, W. E.; Chan, K.-S.; Faron, K. L.; Gilbertson, S. R.; Kaesler, R. W.; Yang, D. C.; Murray, C. K. *J. Org. Chem.* **1986**, *51*, 277–279.
- (19) Simpkins, S. M. E.; Kariuki, B. M.; Aricó, C. S.; Cox, L. R. *Org. Lett.* **2003**, *5*, 3971–3974.
- (20) Exhaustive efforts to effect indolyne cyclization of substrates bearing *N*- or *C*-substituents at C11 were unsuccessful, thus preventing earlier installation of the C11 bridgehead functionality.
- (21) Intermolecular functionalization methods that were tested include bridgehead enolate chemistry, nitrene insertion reactions, and radical halogenations.
- (22) (a) Davies, H. M. L.; Manning, J. R. *Nature* **2008**, *451*, 417–424. (b) Collet, F.; Lescot, C.; Liang, C.; Dauban, P. *Dalton Trans.* **2010**, *39*, 10401–10413.
- (23) For an elegant late-stage nitrene insertion in natural product total synthesis, see: Hinman, A.; Du Bois, J. *J. Am. Chem. Soc.* **2003**, *125*, 11510–11511.
- (24) For intramolecular nitrene C–H insertion reactions using carbamate substrates, see: a) Espino, C. G.; Du Bois, J. *Angew. Chem., Int. Ed.* **2001**, *40*, 598–600. b) Li, Z.; Capretto, D.

- A.; Rahaman, R.; He, C. *Angew. Chem., Int. Ed.* **2007**, *46*, 5184–5186. c) Cui, Y.; He, C. *Angew. Chem., Int. Ed.* **2004**, *43*, 4210–4212.
- (25) Ketone **4.4** likely forms by a pathway involving initial insertion into the α C–H bond; for related observations, see: Hinman, A. W. Ph.D. Dissertation, Stanford University, Stanford, CA, 2004.
- (26) Kim, S.; Yi, K. Y. *J. Org. Chem.* **1986**, *51*, 2613–2615.
- (27) A sample of natural **4.1** was not available for direct comparison.
- (28) Frigerio, M.; Santagostino, M.; Sputore, S. *J. Org. Chem.* **1999**, *64*, 4537–4538.
- (29) Niu, C.; Pettersson, T.; Miller, M. J. *J. Org. Chem.* **1996**, *61*, 1014–1022.
- (30) For compound **4.1** the ^1H NMR residual solvent peak is set to 7.24 ppm and the ^{13}C NMR residual solvent peak is set to 77.0 ppm to match the reference values set in the isolation paper.
- (31) Sakagami, M.; Muratake, H.; Natsume, M. *Chem. Pharm. Bull.* **1994**, *42*, 1393–1398.
- (32) **4.9** is commercially available, or can be easily prepared in one step from 5-bromoindole on multigram scale; see: Jiang, X.; Tiwari, A.; Thompson, M.; Chen, Z.; Cleary, T. P.; Lee, T. B. K. *Org. Proc. Res. Dev.* **2001**, *5*, 604–608.
- (33) Reported values for specific rotations can be highly variable; for a pertinent discussion, see: Gawley, R. E. *J. Org. Chem.* **2006**, *71*, 2411–2416.

APPENDIX THREE

Spectra Relevant to Chapter Four:

Total Synthesis of (-)-*N*-Methylwelwitindolinone C Isothiocyanate

Alexander D. Hutters, Kyle W. Quasdorf, Evan D. Styduhar, and Neil K. Garg.

J. Am. Chem. Soc. **2011**, *133*, 15797–15799.

Current Data Parameters
 NAME KCB-192
 EXPNO 3
 PROCNO 1

F2 - Acquisition Parameters
 Date_ 20110515
 Time 14.33
 INSTRUM arx500
 PROBHD 5 mm broadband
 PULPROG zg30
 TD 65536
 SOLVENT CDCl3
 NS 13
 DS 0
 SWH 10000.000 Hz
 FIDRES 0.152588 Hz
 AQ 3.2768500 sec
 RG 2860
 DW 50.000 usec
 DE 71.43 usec
 TE 300.0 K
 D1 2.00000000 sec
 P1 11.00 usec
 SFO1 500.1330008 MHz
 NUCLEUS 1H

F2 - Processing parameters
 SI 32768
 SF 500.1300237 MHz
 WDW EM
 SSB 0
 LB 0.00 Hz
 GB 0
 PC 1.00

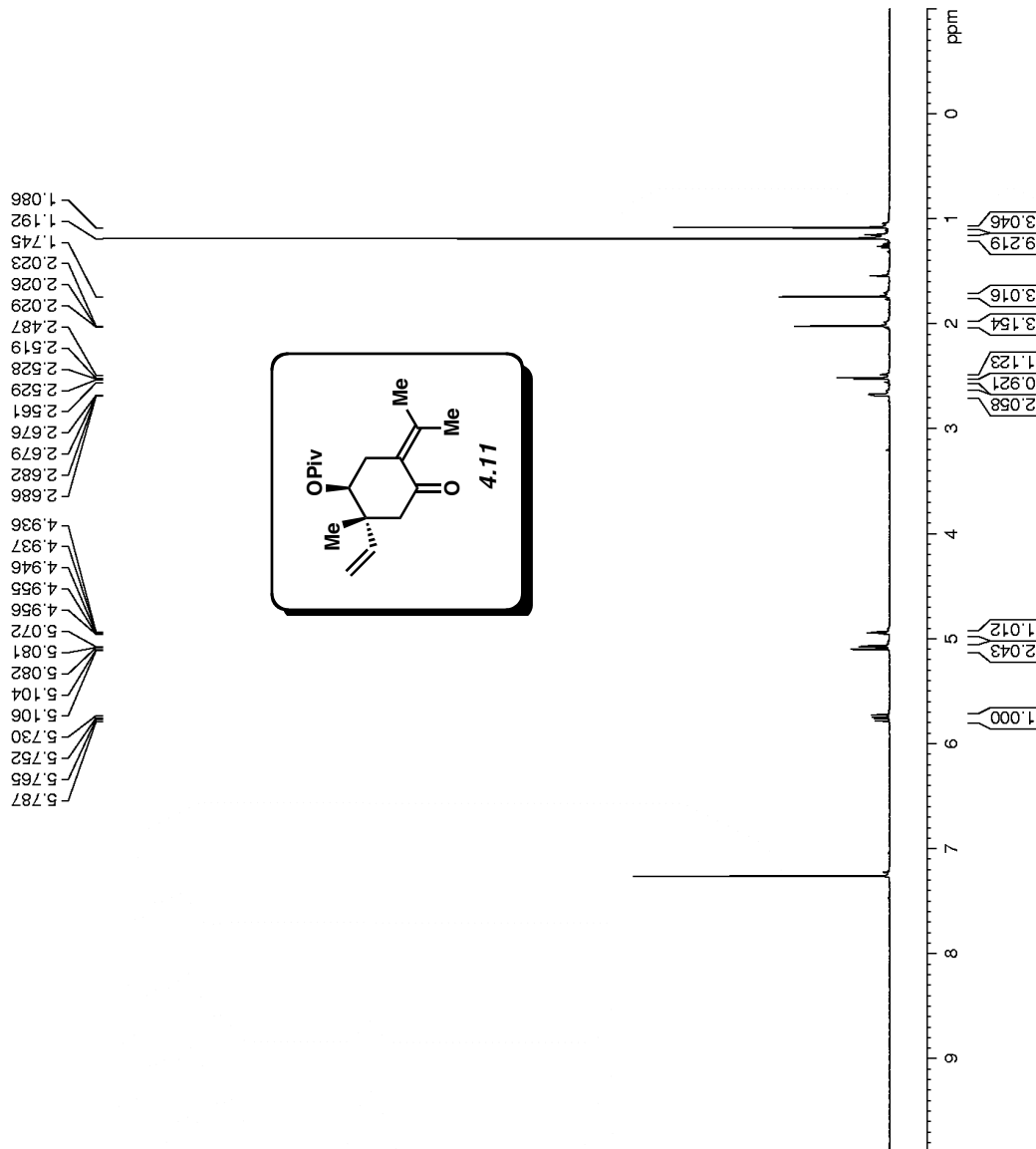


Figure A3.1 ¹H NMR (500 MHz, CDCl₃) of compound 4.11.

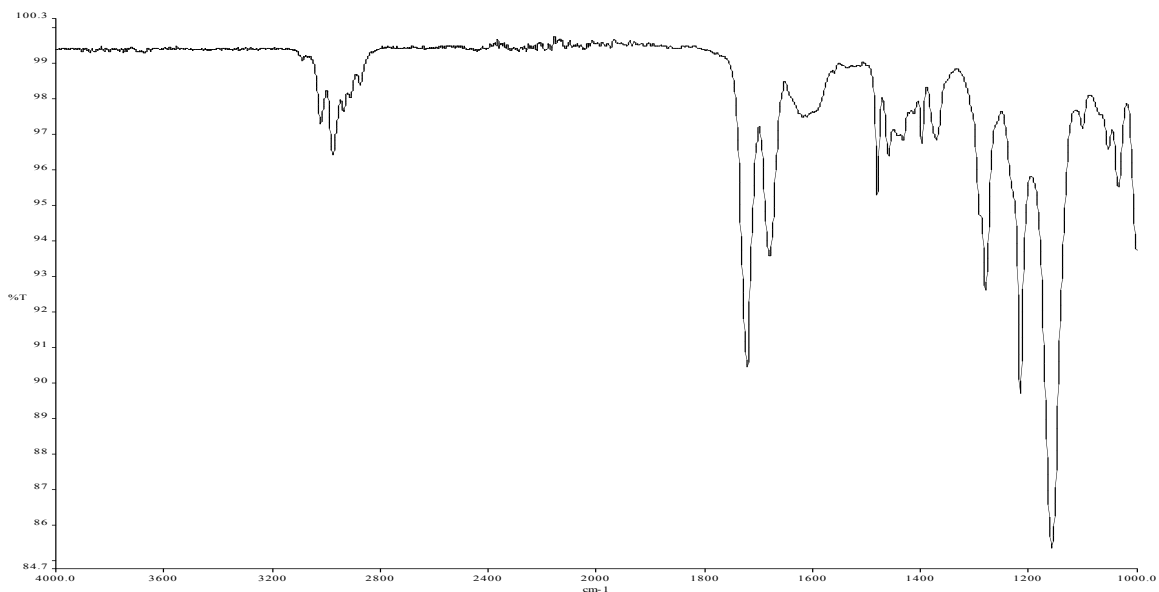


Figure A3.2 Infrared spectrum of compound 4.11.

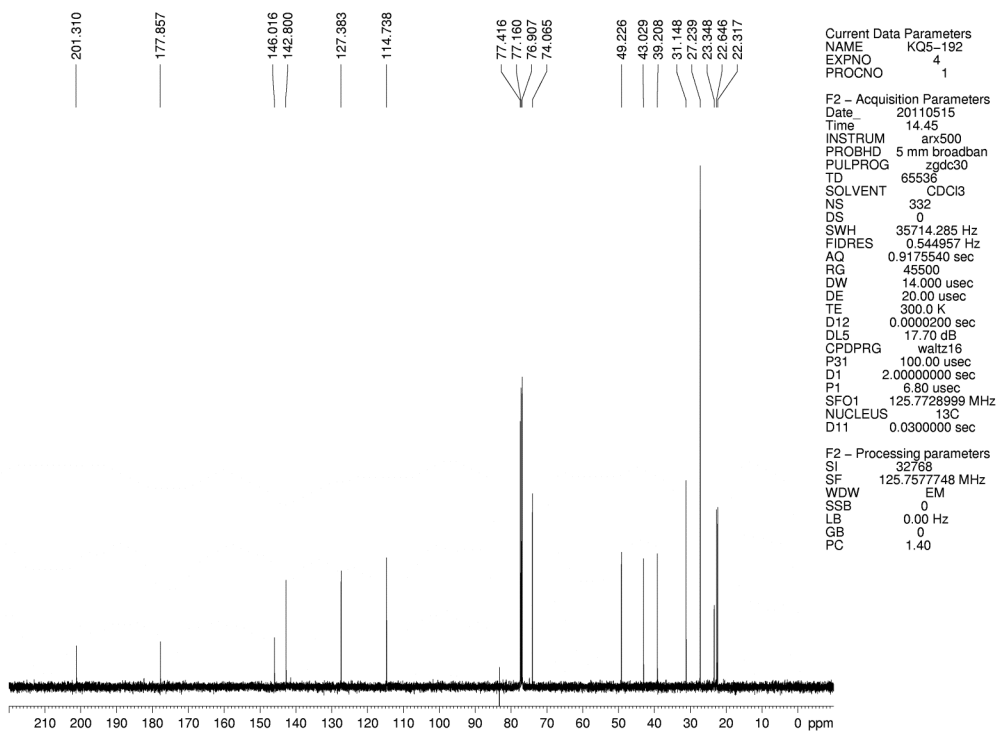


Figure A3.3 ^{13}C NMR (125 MHz, CDCl_3) of compound 4.11.

Current Data Parameters
 NAME ESI-188
 EXPNO 4
 PROCNO 1

F2 - Acquisition Parameters
 Date_ 20110527
 Time 12:57
 INSTRUM advance600
 PROBHD 5 mm bb-Z Z800
 PULPROG zg30
 TD 65536
 SOLVENT CDCl3
 NS 44
 DS 0
 SWH 10000.000 Hz
 FIDRES 0.152588 Hz
 AQ 3.2769001 sec
 RG 512
 DW 50.000 usec
 DE 6.00 usec
 TE 296.7 K
 D1 2.00000000 sec
 MCREST 0.00000000 sec
 MCWRK 0.01500000 sec

==== CHANNEL f1 =====
 NUC1 1H
 P1 12.25 usec
 PL1 0.00 dB
 SFO1 500.3330020 MHz

F2 - Processing parameters
 SI 32768
 SF 500.3310001 MHz
 WDW EM
 SSB 0
 LB 0.30 Hz
 GB 0
 PC 1.00

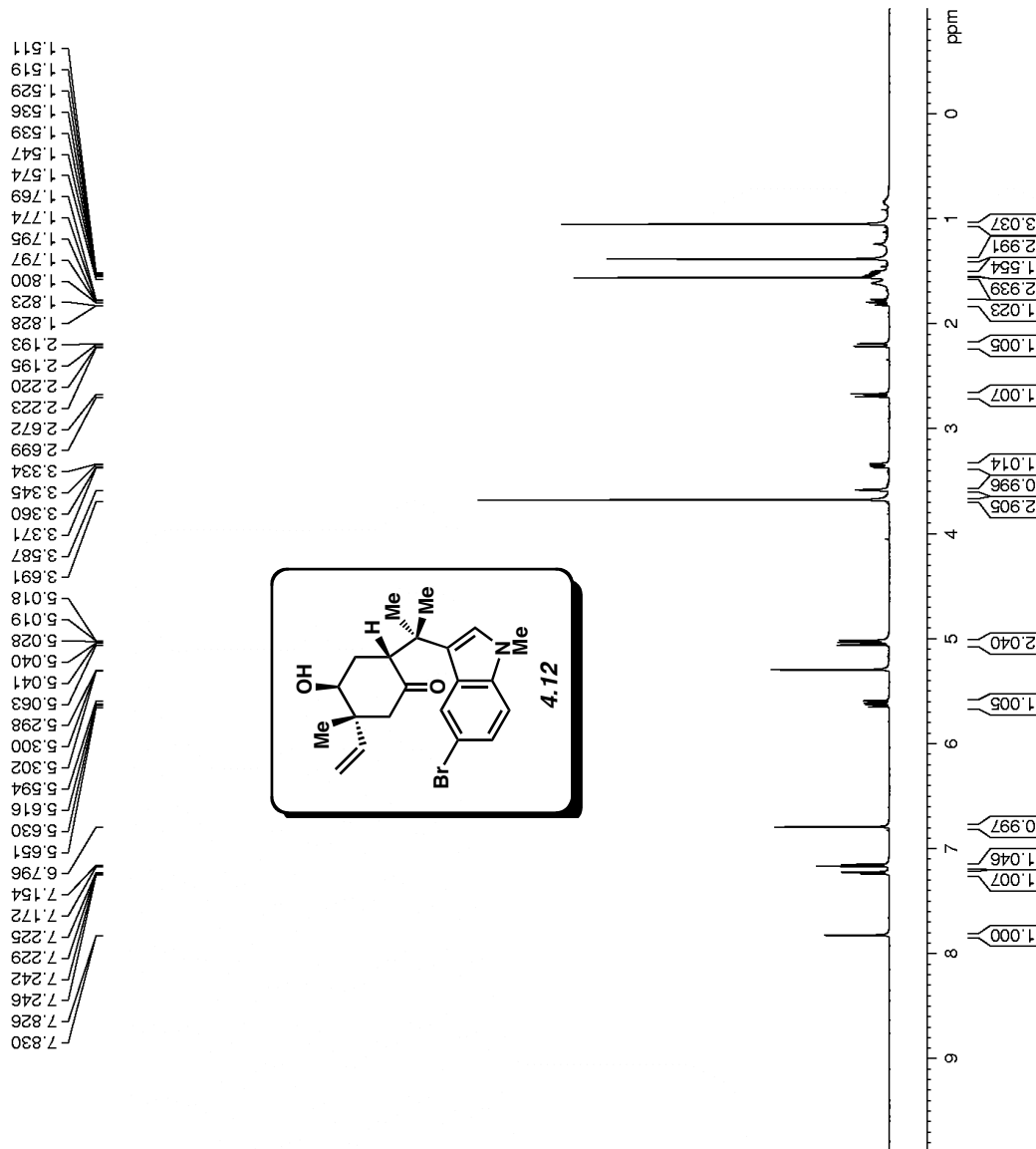


Figure A3.4 ¹H NMR (500 MHz, CDCl₃) of compound 4.12.

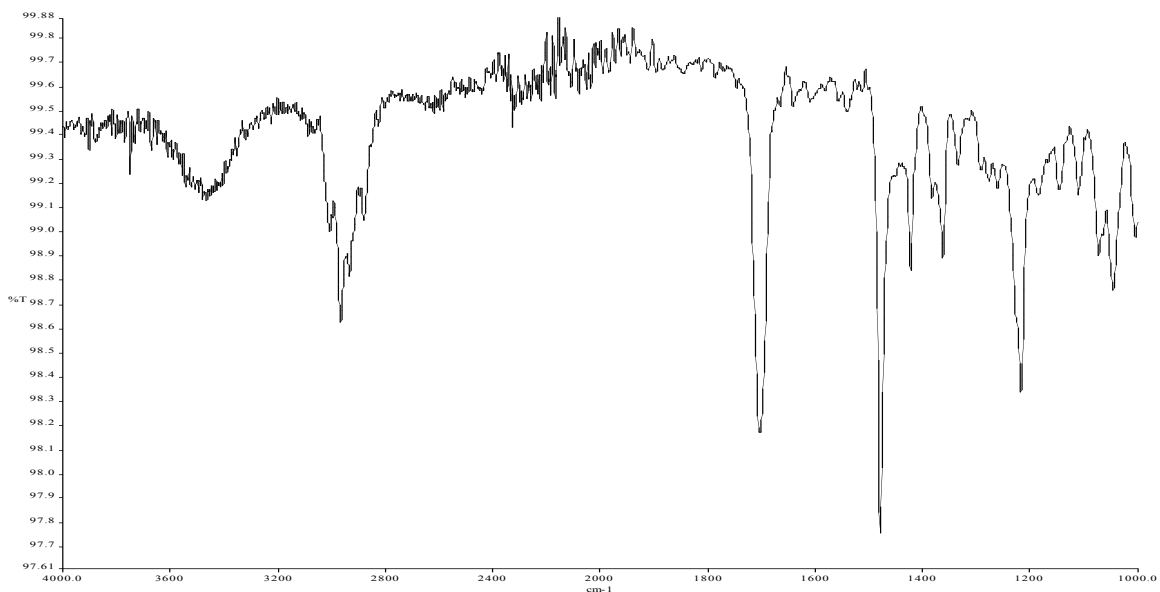


Figure A3.5 Infrared spectrum of compound **4.12**.

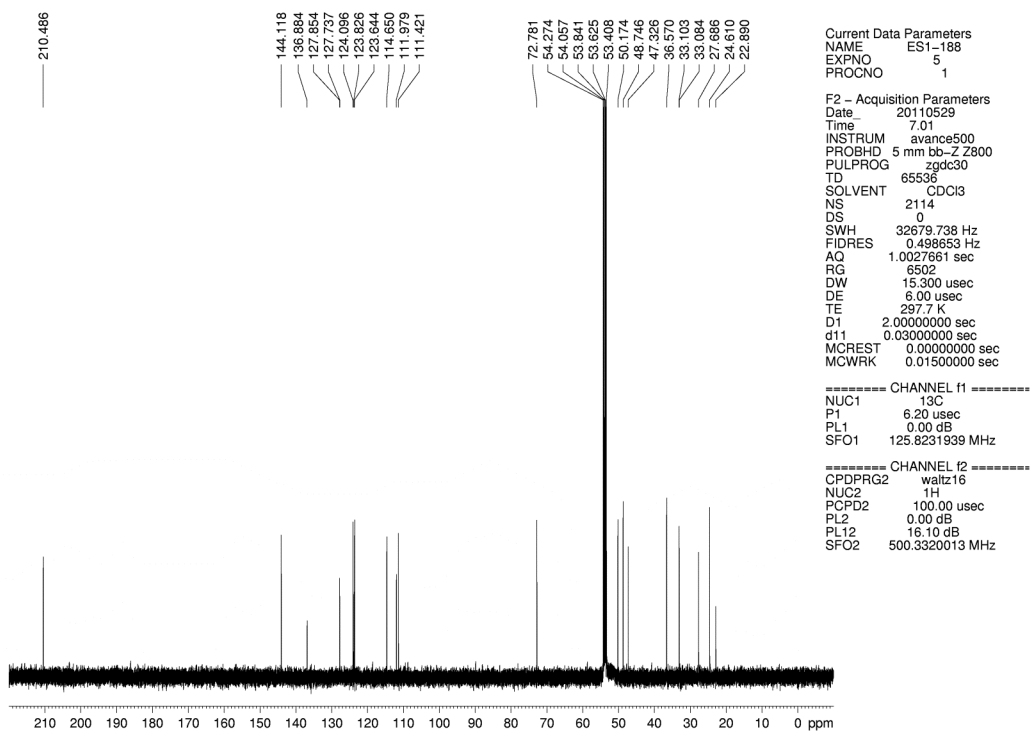


Figure A3.6 ^{13}C NMR (125 MHz, CDCl_3) of compound **4.12**.

Current Data Parameters
 NAME ADH-3-81-p
 EXPNO 1
 PROCNO 1

F2 - Acquisition Parameters
 Date_ 20110612
 Time_ 13.31
 INSTRUM avance600
 PROBHD 5 mm bb-Z Z800
 PULPROG zg30
 TD 65536
 SOLVENT CDCl3
 NS 8
 DS 0
 SWH 10000.000 Hz
 FIDRES 0.152588 Hz
 AQ 3.2769001 sec
 RG 181
 DW 50.000 usec
 DE 6.00 usec
 TE 296.6 K
 D1 2.0000000 sec
 MCREST 0.0000000 sec
 MCWFRK 0.01500000 sec

===== CHANNEL f1 =====
 NUC1 1H
 P1 12.00 usec
 PL1 0.00 dB
 SFO1 500.3330020 MHz

F2 - Processing parameters
 SI 32768
 SF 500.33300222 MHz
 WDW EM
 SSB 0
 LB 0.30 Hz
 GB 0
 PC 1.00

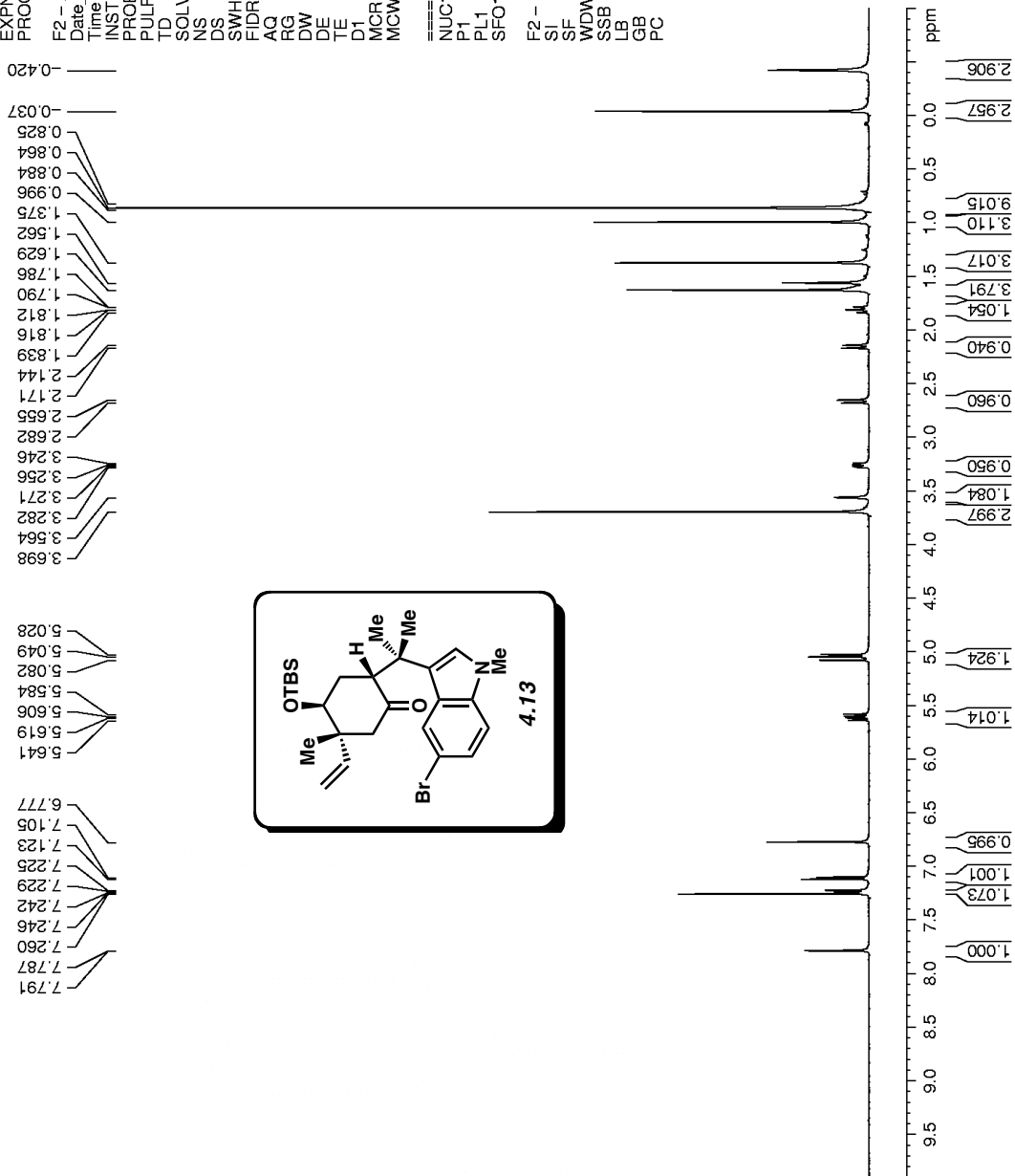


Figure A3.7 ¹H NMR (500 MHz, CDCl₃) of compound 4.13.

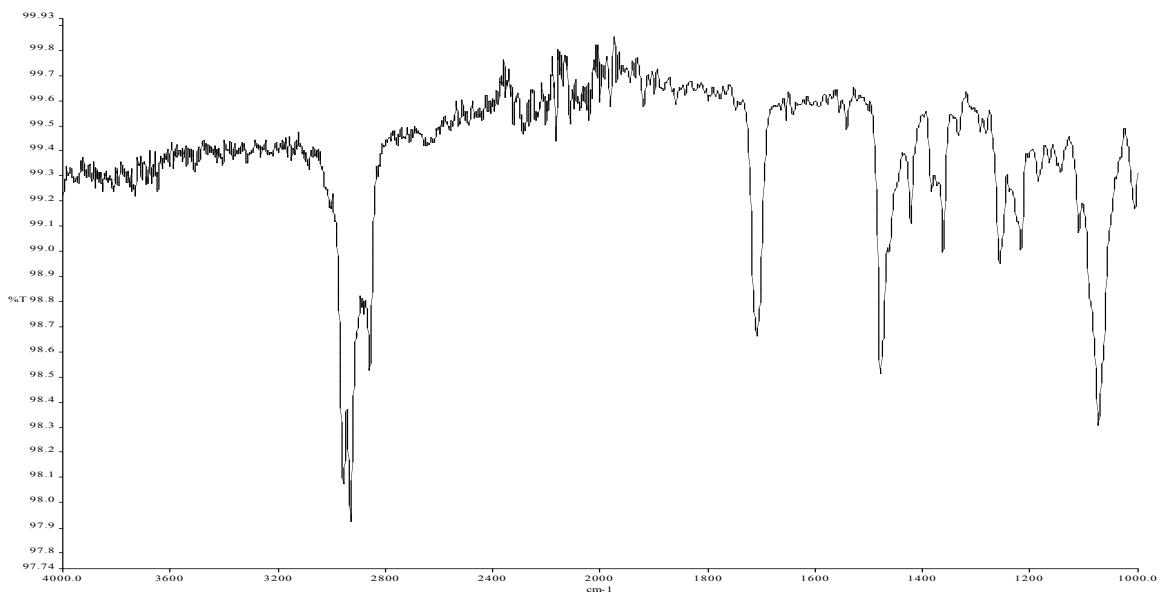


Figure A3.8 Infrared spectrum of compound **4.13**.

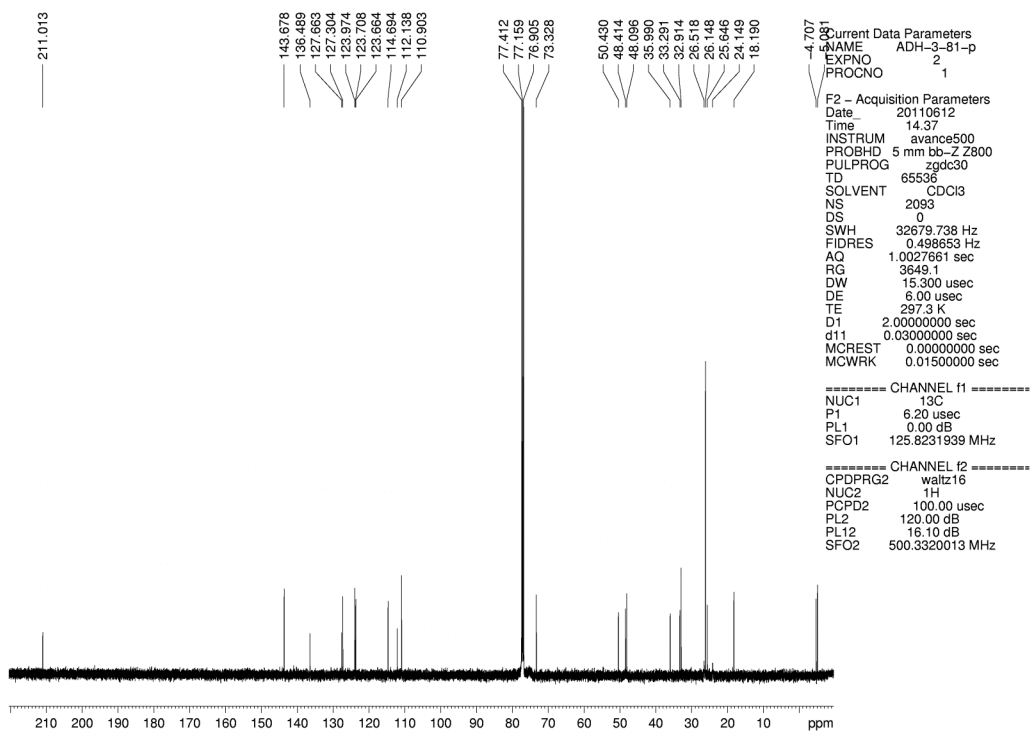


Figure A3.9 ^{13}C NMR (125 MHz, CDCl_3) of compound **4.13**.

Current Data Parameters
 NAME ADH-3-79-p
 EXPNO 5
 PROCNO 1

F2 - Acquisition Parameters
 Date_ 20110529
 Time_ 15.41
 INSTRUM avance600
 PROBHD 5 mm bb-Z Z800
 PULPROG zg30
 TD 65536
 SOLVENT CDCl3
 NS 8
 DS 0
 SWH 10000.000 Hz
 FIDRES 0.152588 Hz
 AQ 3.2769001 sec
 RG 181
 DW 50.000 usec
 DE 6.00 usec
 TE 296.6 K
 D1 2.0000000 sec
 MCREST 0.0000000 sec
 MCWFRK 0.01500000 sec

===== CHANNEL f1 =====
 NUC1 1H
 P1 12.00 usec
 PL1 0.00 dB
 SFO1 500.3330020 MHz

F2 - Processing parameters
 SI 32768
 SF 500.3330222 MHz
 WDW EM
 SSB 0
 LB 0.30 Hz
 GB 0
 PC 1.00

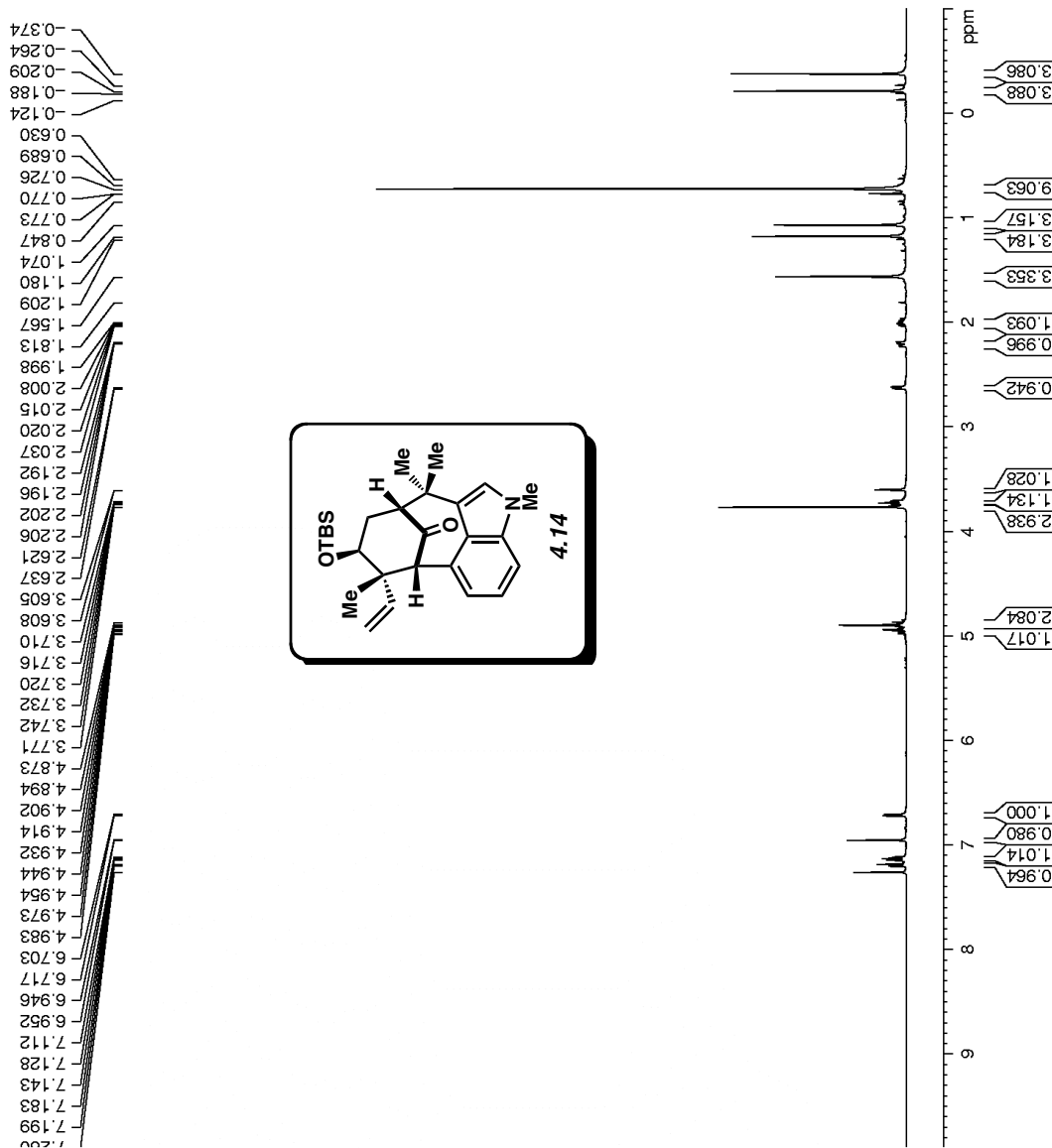


Figure A3.10 ^1H NMR (500 MHz, CDCl_3) of compound 4.14.

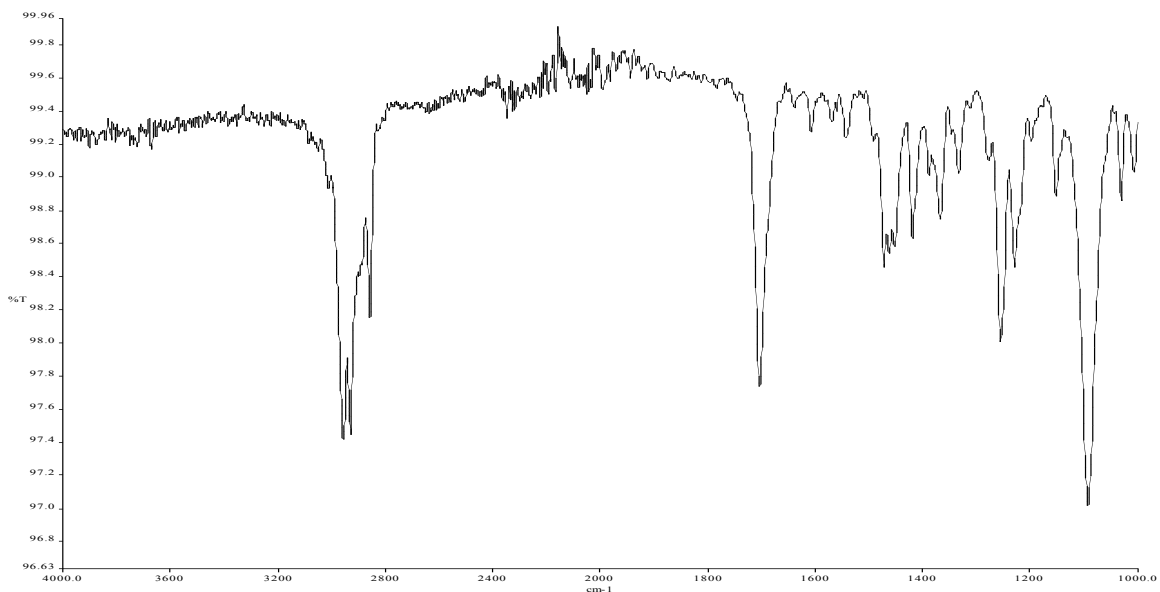


Figure A3.11 Infrared spectrum of compound **4.14**.

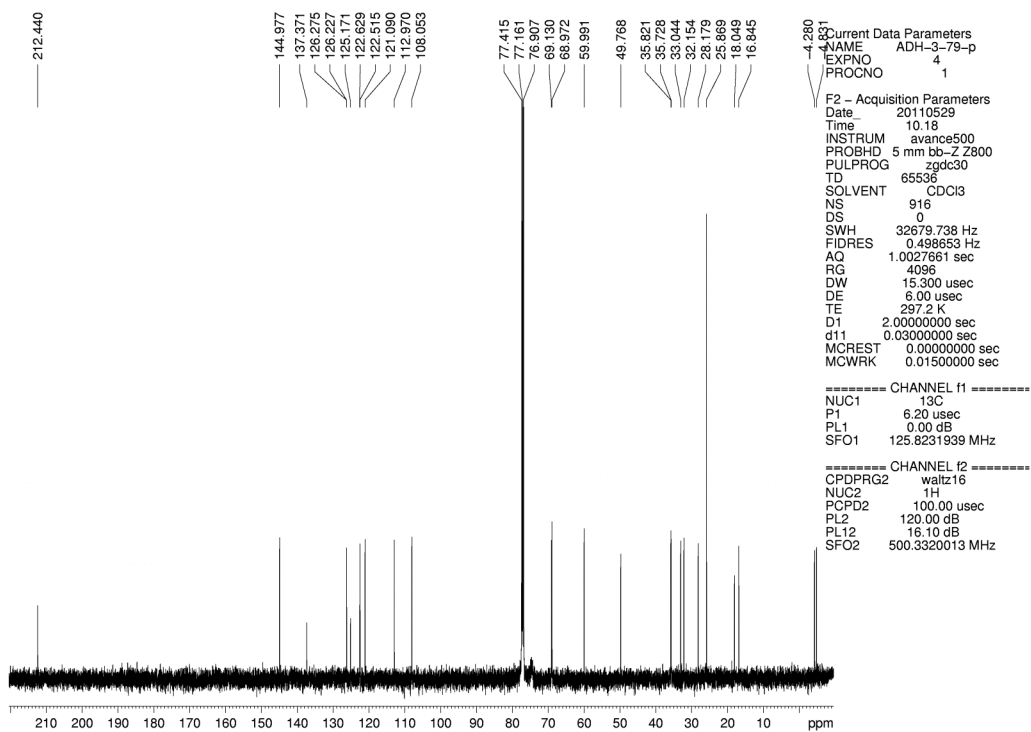


Figure A3.12 ¹³C NMR (125 MHz, CDCl₃) of compound **4.14**.

Current Data Parameters
 NAME ADH-2-263-p
 EXPNO 1
 PROCNO 1
 F2 - Acquisition Parameters
 Date_ 20110128
 Time_ 15:26
 INSTRUM arx500
 PROBHD 5 mm broadband
 PULPROG zg30
 TD 65536
 SOLVENT CDCl3
 NS 8
 DS 0
 SWH 10000.000 Hz
 FIDRES 0.152588 Hz
 AQ 3.2768500 sec
 RG 4096
 DW 50.000 usec
 DE 71.43 usec
 TE 300.0 K
 D1 2.00000000 sec
 P1 11.00 usec
 SFO1 500.1330008 MHz
 NUCLEUS 1H
 F2 - Processing parameters
 SI 32768
 SF 500.1300237 MHz
 WDW EM
 SSB 0
 LB 0.30 Hz
 GB 0
 PC 1.00

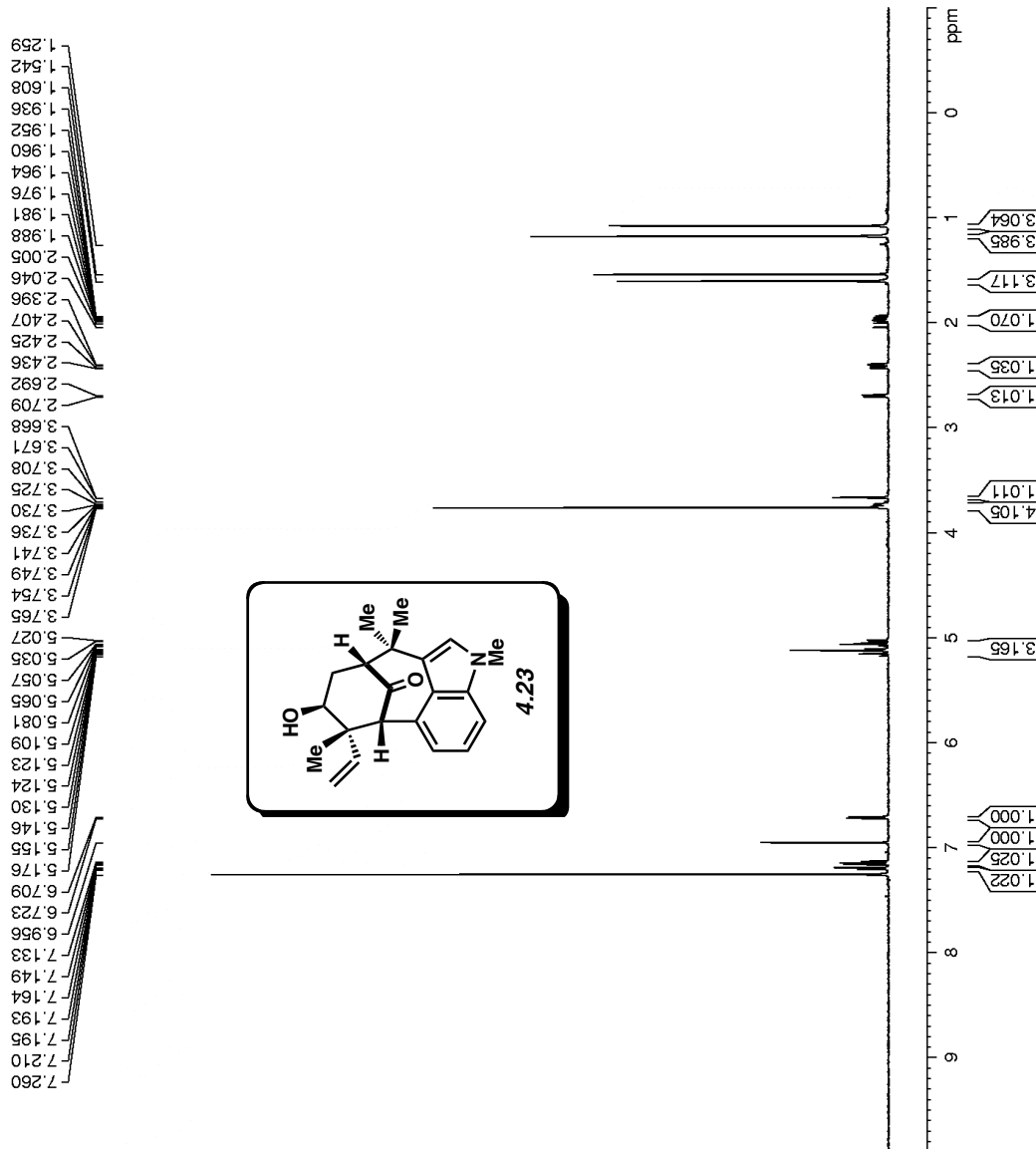


Figure A3.13 ^1H NMR (500 MHz, CDCl_3) of compound 4.23.

Current Data Parameters
 NAME ADH-3-83-p
 EXPNO 2
 PROCNO 1

F2 - Acquisition Parameters
 Date_ 20110531
 Time_ 13.54
 INSTRUM avance600
 PROBHD 5 mm bb-Z Z800
 PULPROG zg30
 TD 65536
 SOLVENT CDCl3
 NS 8
 DS 0
 SWH 10000.000 Hz
 FIDRES 0.152588 Hz
 AQ 3.2769001 sec
 RG 181
 DW 50.000 usec
 DE 6.00 usec
 TE 296.6 K
 D1 2.0000000 sec
 MCREST 0.0000000 sec
 MCWRK 0.01500000 sec

===== CHANNEL f1 =====
 NUC1 1H
 P1 12.00 usec
 PL1 0.00 dB
 SFO1 500.3330020 MHz

F2 - Processing parameters
 SI 32768
 SF 500.33300222 MHz
 WDW EM
 SSB 0
 LB 0.00 Hz
 GB 0
 PC 1.00

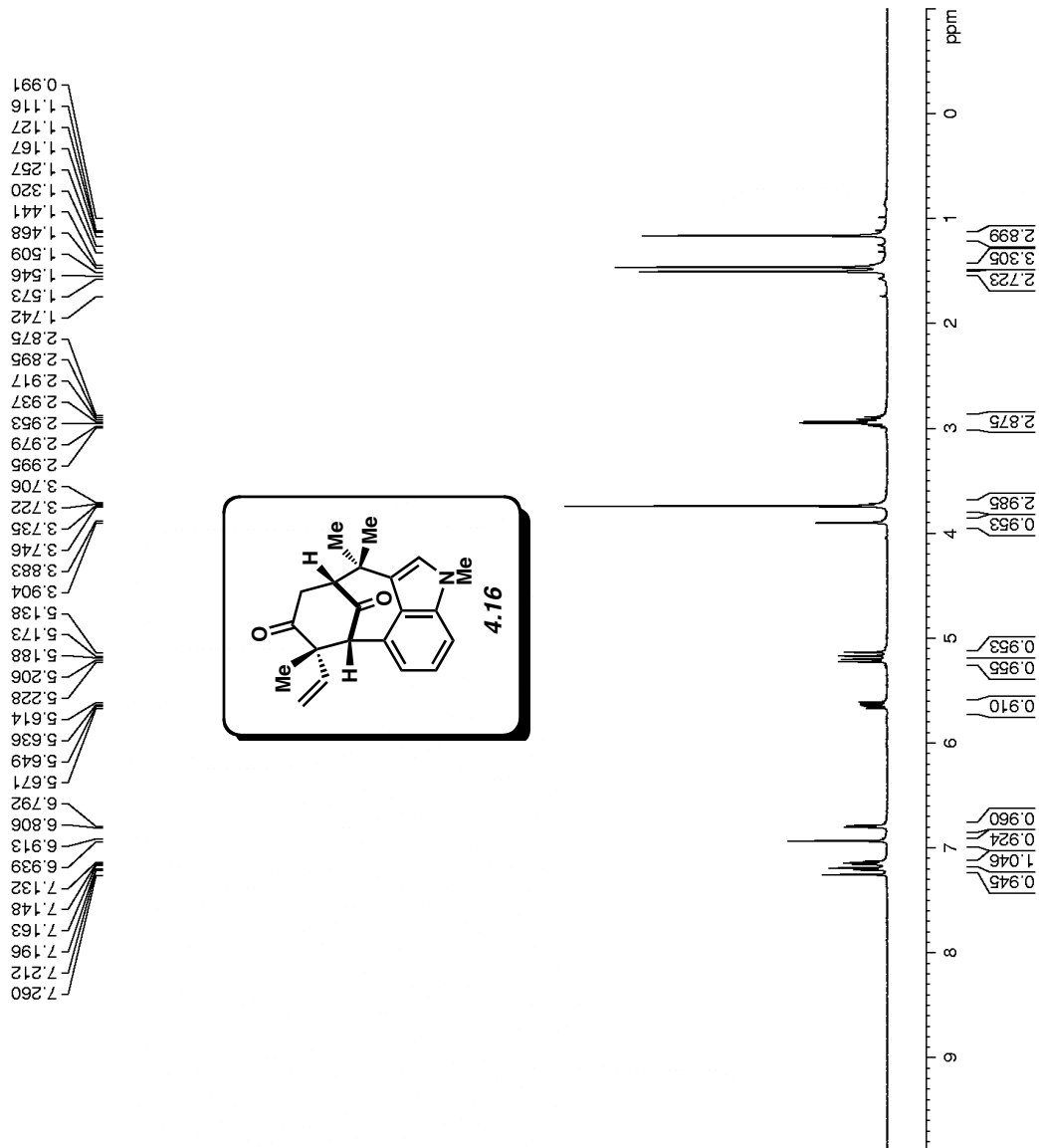


Figure A3.14 ¹H NMR (500 MHz, CDCl₃) of compound 4.16.

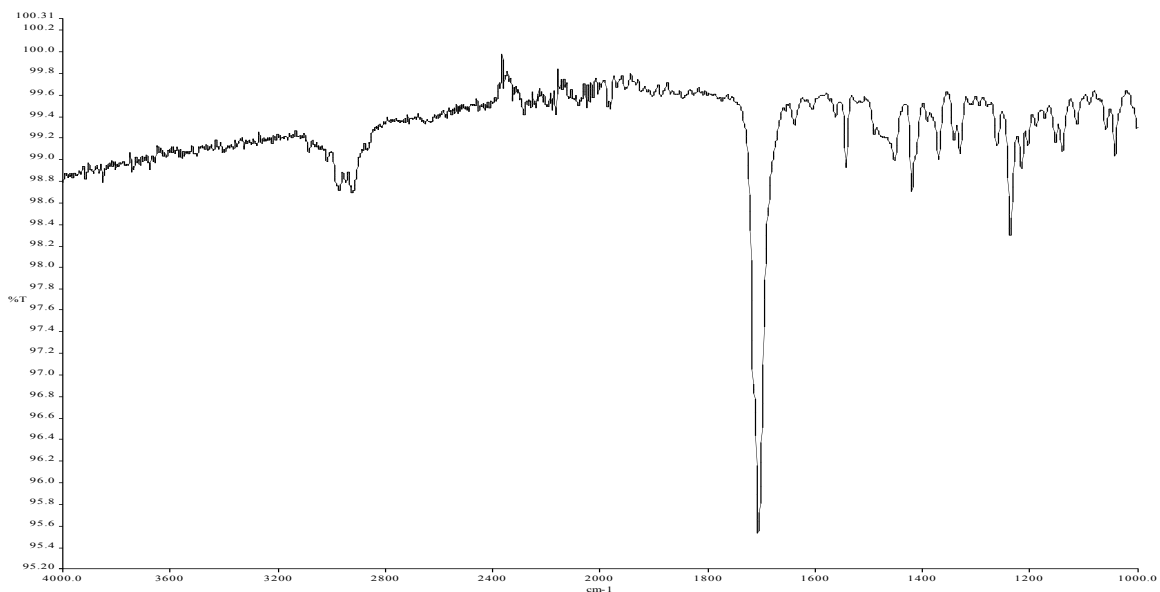


Figure A3.15 Infrared spectrum of compound **4.16**.

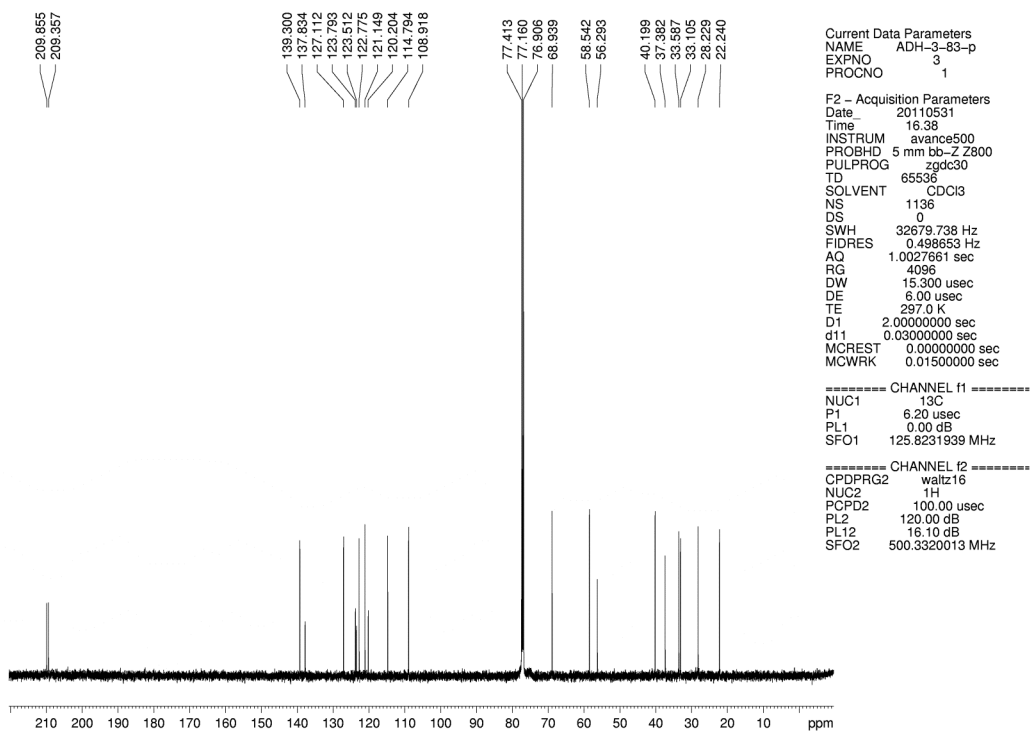


Figure A3.16 ^{13}C NMR (125 MHz, CDCl_3) of compound **4.16**.

```

Current Data Parameters
NAME      KCB-214
EXPNO    1
PROCNO   1

F2 - Acquisition Parameters
Date_    20110531
Time     13.16
INSTRUM  avance500
PROBHD   5 mm bb-Z Z800
PULPROG  zg30
TD        65536
SOLVENT  CDCl3
NS        20
DS        0
SWH      10000.000 Hz
FIDRES   0.152588 Hz
AQ        3.2769001 sec
RG        362
DW        50.000 usec
DE        6.00 usec
TE        296.6 K
D1        2.0000000 sec
MCREST   0.0000000 sec
MCWRK    0.01500000 sec

===== CHANNEL f1 =====
NUC1      1H
P1        12.00 usec
PL1       0.00 dB
SFO1     500.3330020 MHz

F2 - Processing parameters
SI        32768
SF        500.3300219 MHz
WDW       EM
SSB       0
LB        0.30 Hz
GB        0
PC        1.00

```

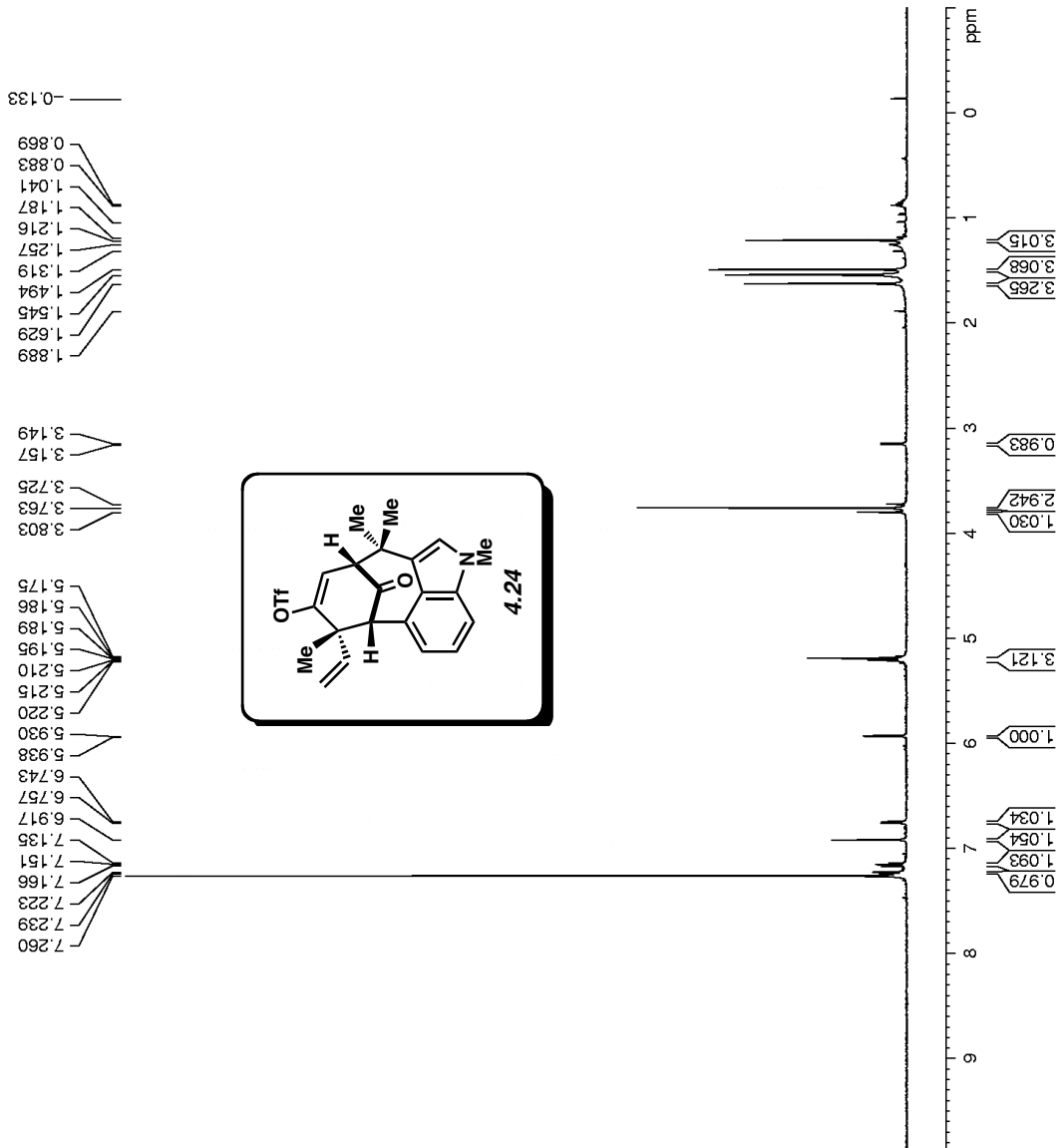
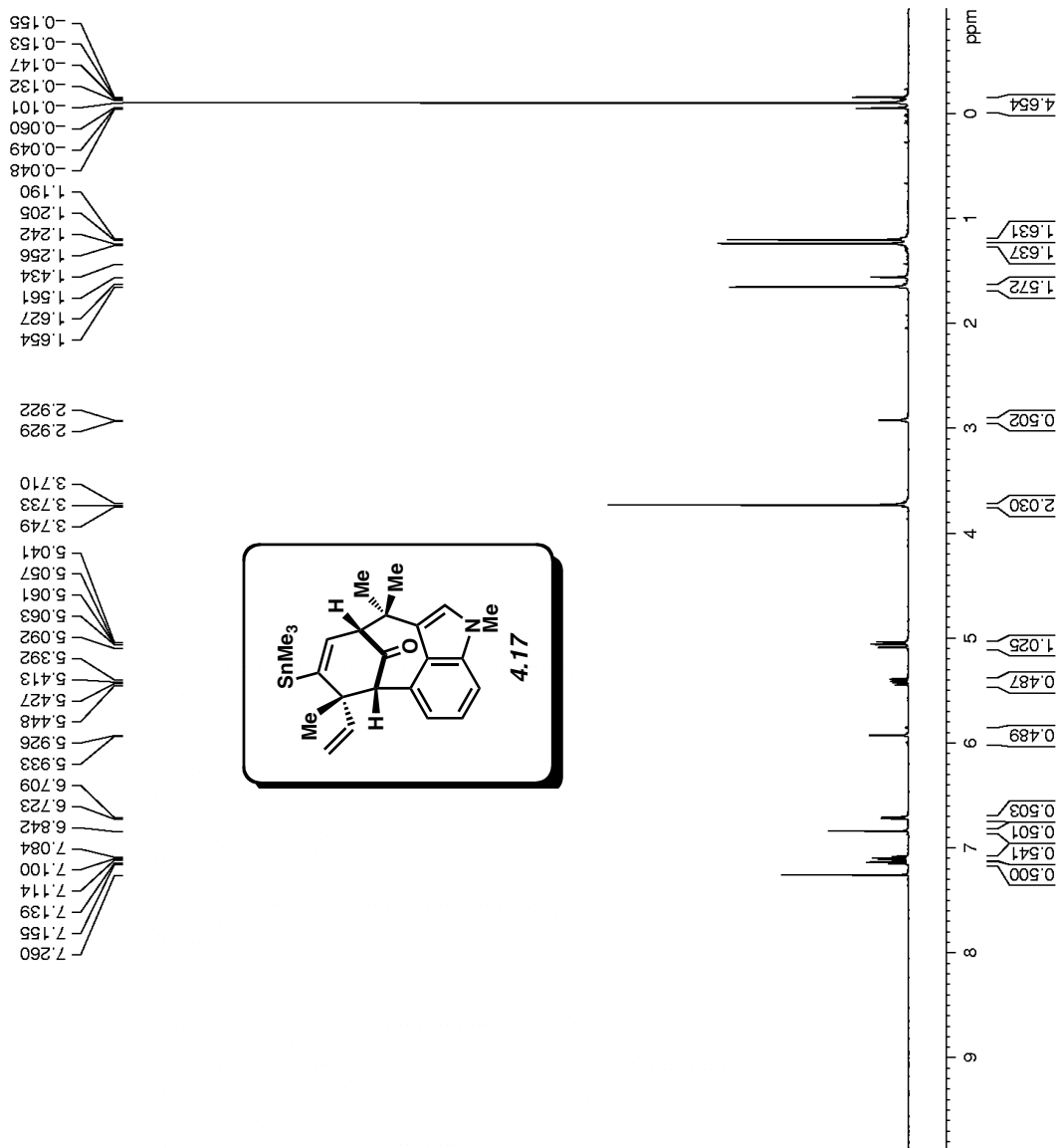


Figure A3.17 ¹H NMR (500 MHz, CDCl₃) of compound 4.24.

Current Data Parameters
 NAME ADH-3-87-p
 EXPNO 1
 PROCNO 1

F2 - Acquisition Parameters
 Date_ 20110603
 Time_ 15:38
 INSTRUM arx500
 PROBHD 5 mm broadband
 PULPROG zg30
 TD 65536
 SOLVENT CDCl3
 NS 8
 DS 0
 SWH 10000.000 Hz
 FIDRES 0.152588 Hz
 AQ 3.2768500 sec
 RG 2048
 DW 50.000 usec
 DE 71.43 usec
 TE 300.0 K
 D1 2.00000000 sec
 P1 11.00 usec
 SFO1 500.1330008 MHz
 NUCLEUS 1H

F2 - Processing parameters
 SI 32768
 SF 500.1300231 MHz
 WDW EM
 SSB 0
 LB 0.00 Hz
 GB 0
 PC 1.00



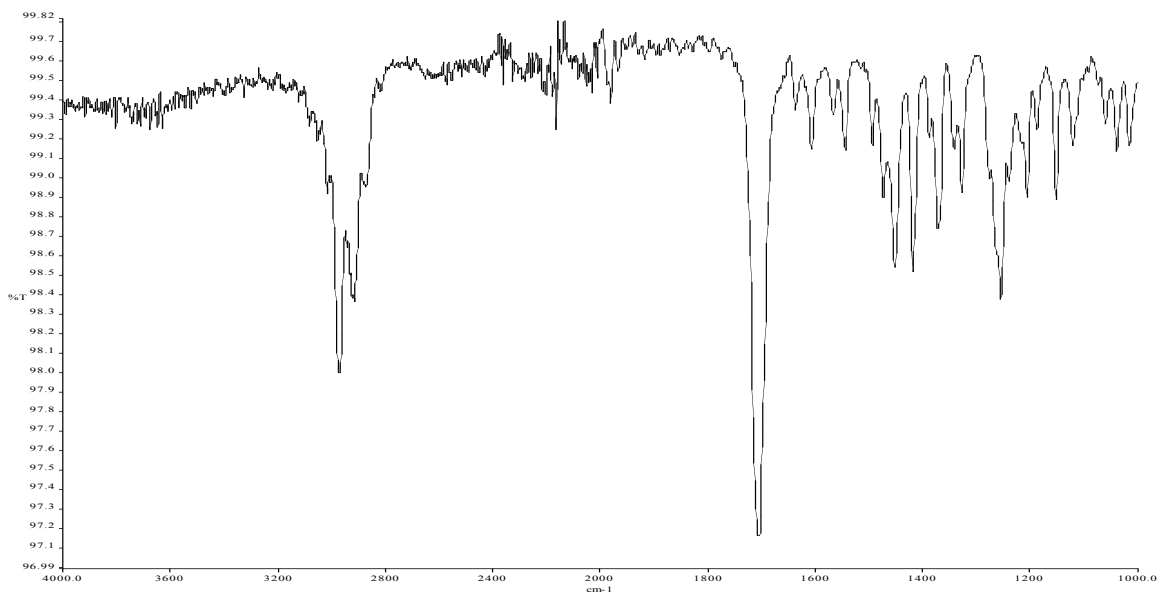


Figure A3.19 Infrared spectrum of compound **4.17**.

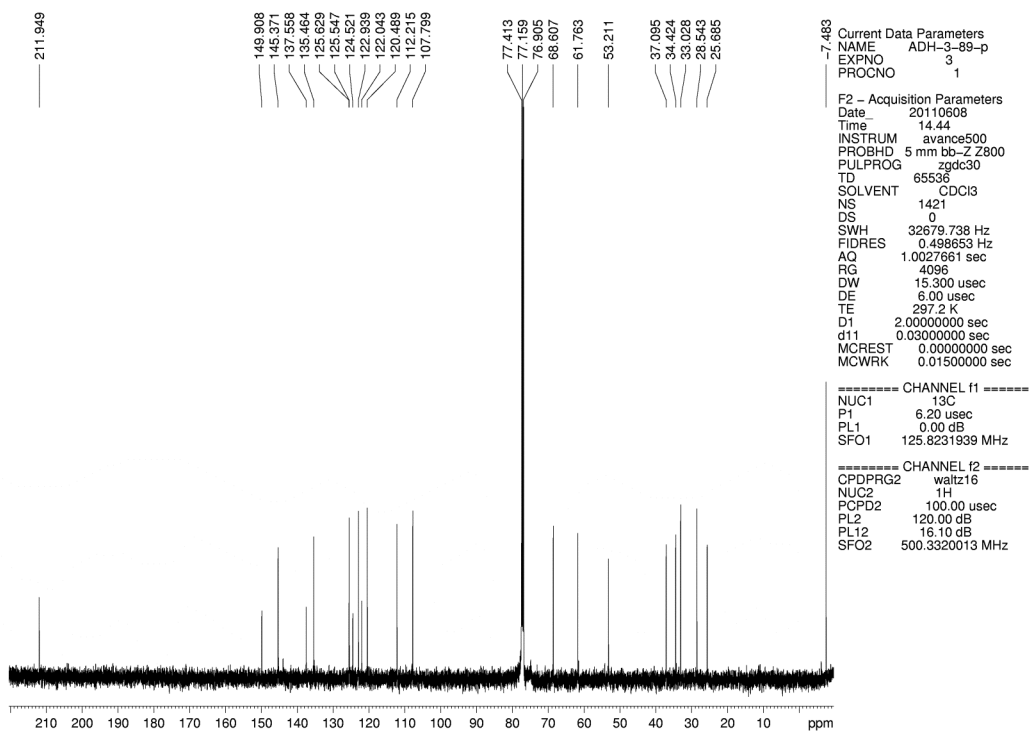


Figure A3.20 ^{13}C NMR (125 MHz, CDCl_3) of compound **4.17**.

Current Data Parameters
 NAME ESI-206
 EXPNO 4
 PROCNO 1

F2 - Acquisition Parameters
 Date_ 20110619
 Time 16.09
 INSTRUM advance600
 PROBHD 5 mm bb-Z Z800
 PULPROG zg30
 TD 65536
 SOLVENT CDCl3
 NS 32
 DS 0
 SWH 10000.000 Hz
 FIDRES 0.152588 Hz
 AQ 3.2769001 sec
 RG 143.7
 DW 50.000 usec
 DE 6.00 usec
 TE 296.8 K
 D1 2.0000000 sec
 MCREST 0.0000000 sec
 MCWFRK 0.01500000 sec

===== CHANNEL f1 =====
 NUC1 1H
 P1 12.25 usec
 PL1 0.00 dB
 SFO1 500.3330020 MHz

F2 - Processing parameters
 SI 32768
 SF 500.330219 MHz
 WDW EM
 SSB 0
 LB 0.30 Hz
 GB 0
 PC 1.00

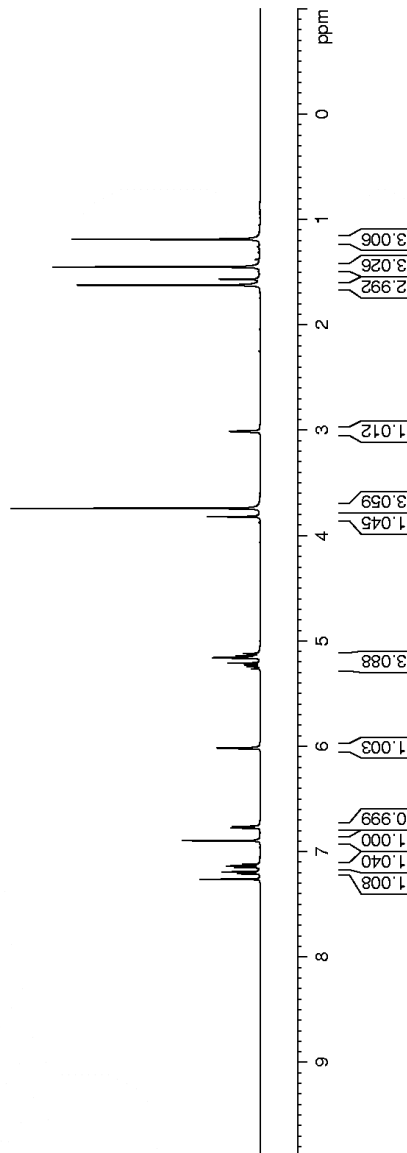
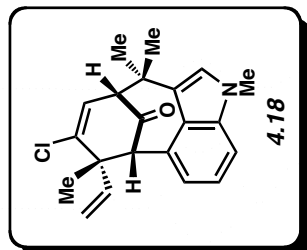
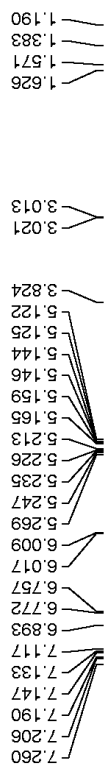


Figure A3.21 ¹H NMR (500 MHz, CDCl₃) of compound 4.18.

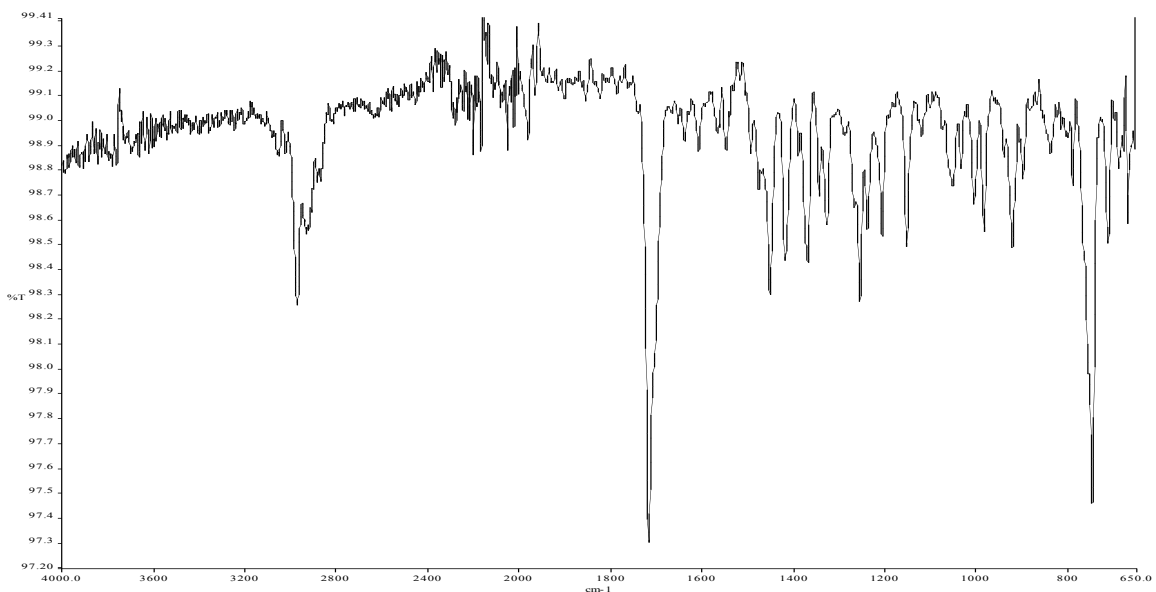


Figure A3.22 Infrared spectrum of compound **4.18**.

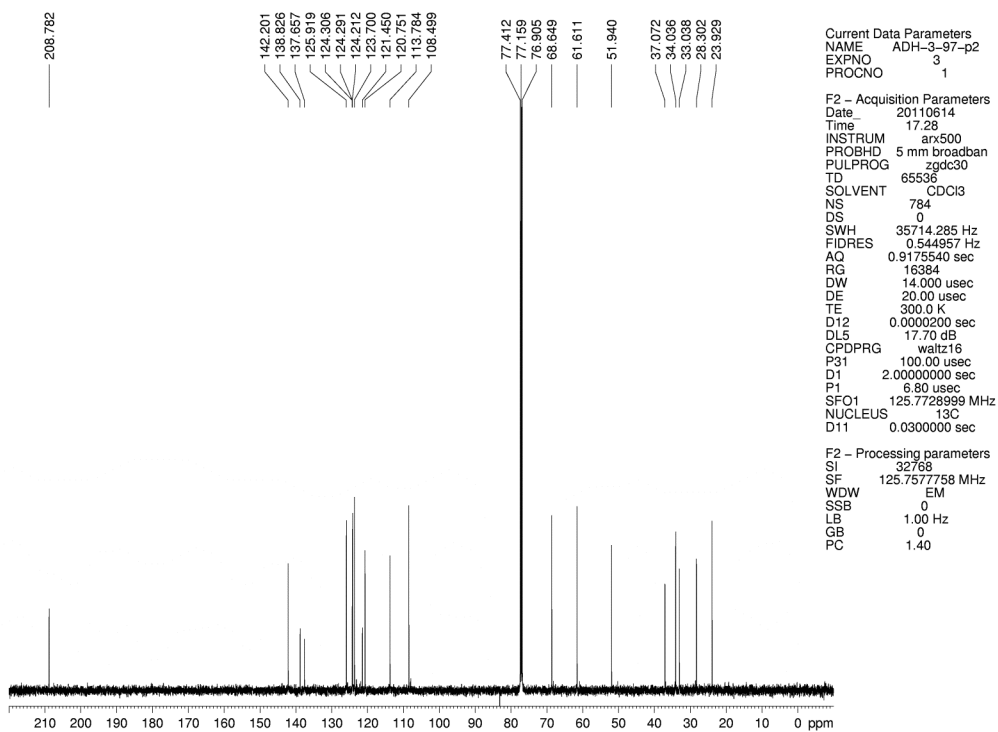


Figure A3.23 ^{13}C NMR (125 MHz, CDCl_3) of compound **4.18**.

Current Data Parameters
 NAME ADH-3-115-p
 EXPNO 1
 PROCNO 1

F2 - Acquisition Parameters
 Date_ 20110702
 Time_ 12.52
 INSTRUM arx500
 PROBHD 5 mm broadband
 PULPROG zg30
 TD 65536
 SOLVENT CDCl3
 NS 8
 DS 0
 SWH 10000.000 Hz
 FIDRES 0.152588 Hz
 AQ 3.2768500 sec
 RG 2860
 DW 50.000 usec
 DE 71.43 usec
 TE 300.0 K
 D1 2.00000000 sec
 P1 11.00 usec
 SFO1 500.1330008 MHz
 NUCLEUS 1H

F2 - Processing parameters
 SI 32768
 SF 500.1300237 MHz
 WDW EM
 SSB 0
 LB 0.30 Hz
 GB 0
 PC 1.00

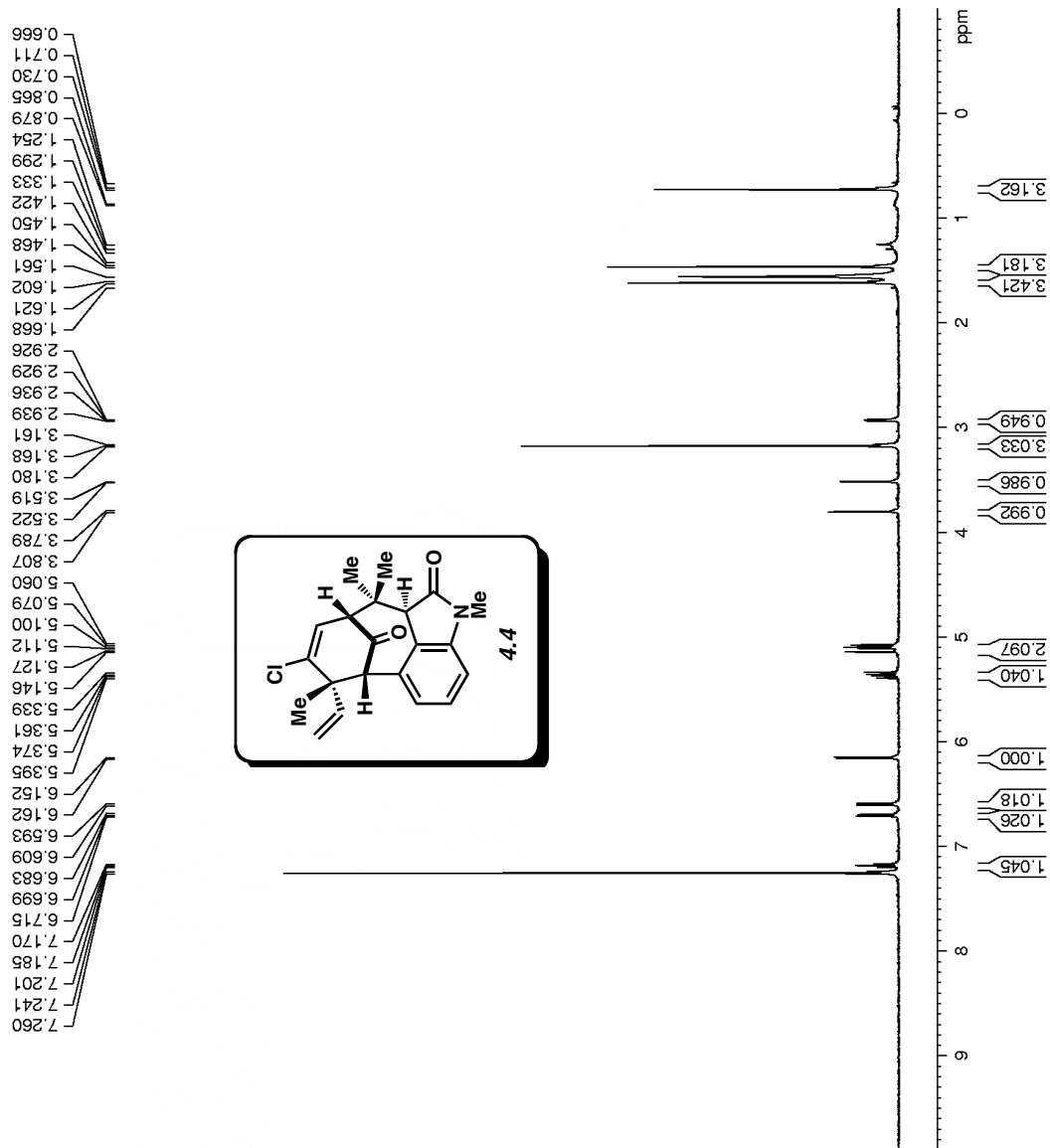


Figure A3.24 ¹H NMR (500 MHz, CDCl₃) of compound 4.4.

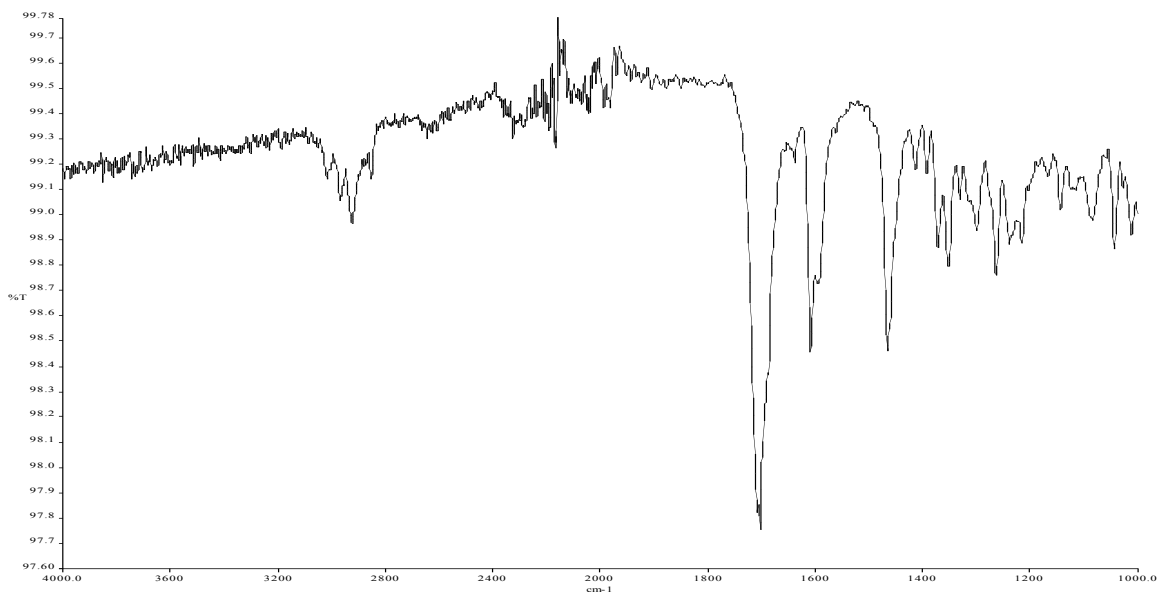


Figure A3.25 Infrared spectrum of compound 4.4.

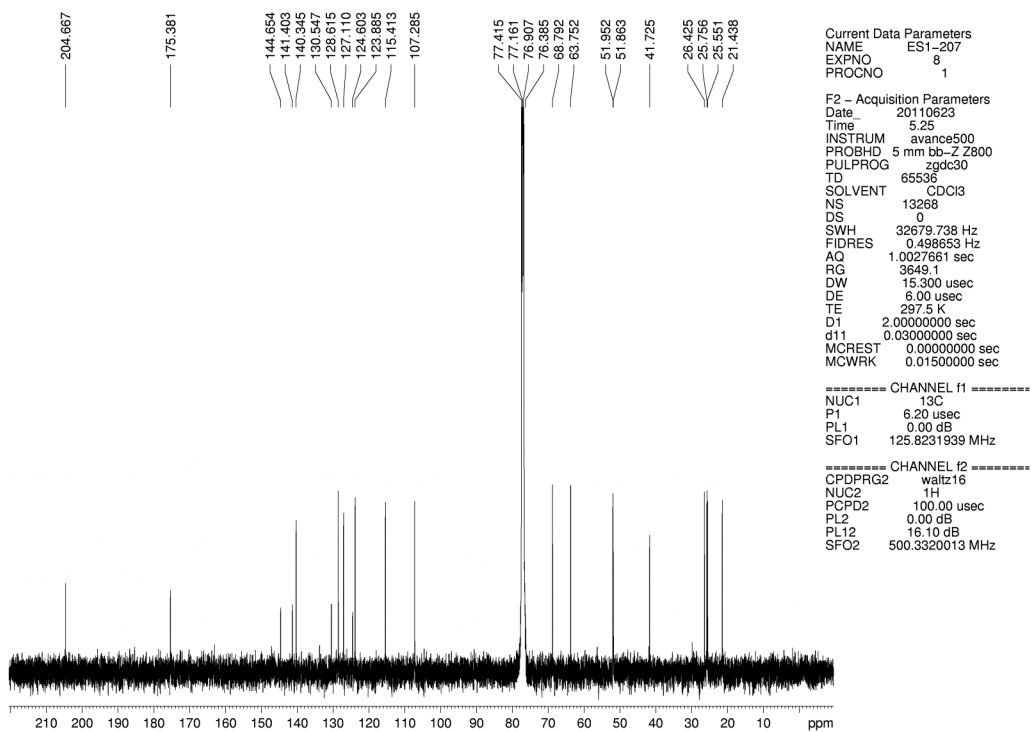


Figure A3.26 ^{13}C NMR (125 MHz, CDCl_3) of compound 4.4.

```

Current Data Parameters
NAME      ADH-3-116-p
EXPNO    1
PROCNO   1
F2 - Acquisition Parameters
Date_    20110702
Time    16.02
INSTRUM  avance500
PROBHD   5 mm bb-Z Z800
PULPROG  zg30
TD       65536
SOLVENT  CDCl3
NS       8
DS       0
SWH      10000.000 Hz
FIDRES   0.152588 Hz
AQ       3.2769001 sec
RG       256
DW       50.000 usec
DE       6.00 usec
TE       296.7 K
D1       2.00000000 sec
MCREST   0.00000000 sec
MCWRK   0.01500000 sec
===== CHANNEL f1 =====
NUC1     1H
P1       12.00 usec
PL1      0.00 dB
SFO1    500.3330020 MHz
F2 - Processing parameters
SI       32768
SF       500.3300222 MHz
WDW      EM
SSB      0
LB       0.30 Hz
GB       0
PC       1.00

```

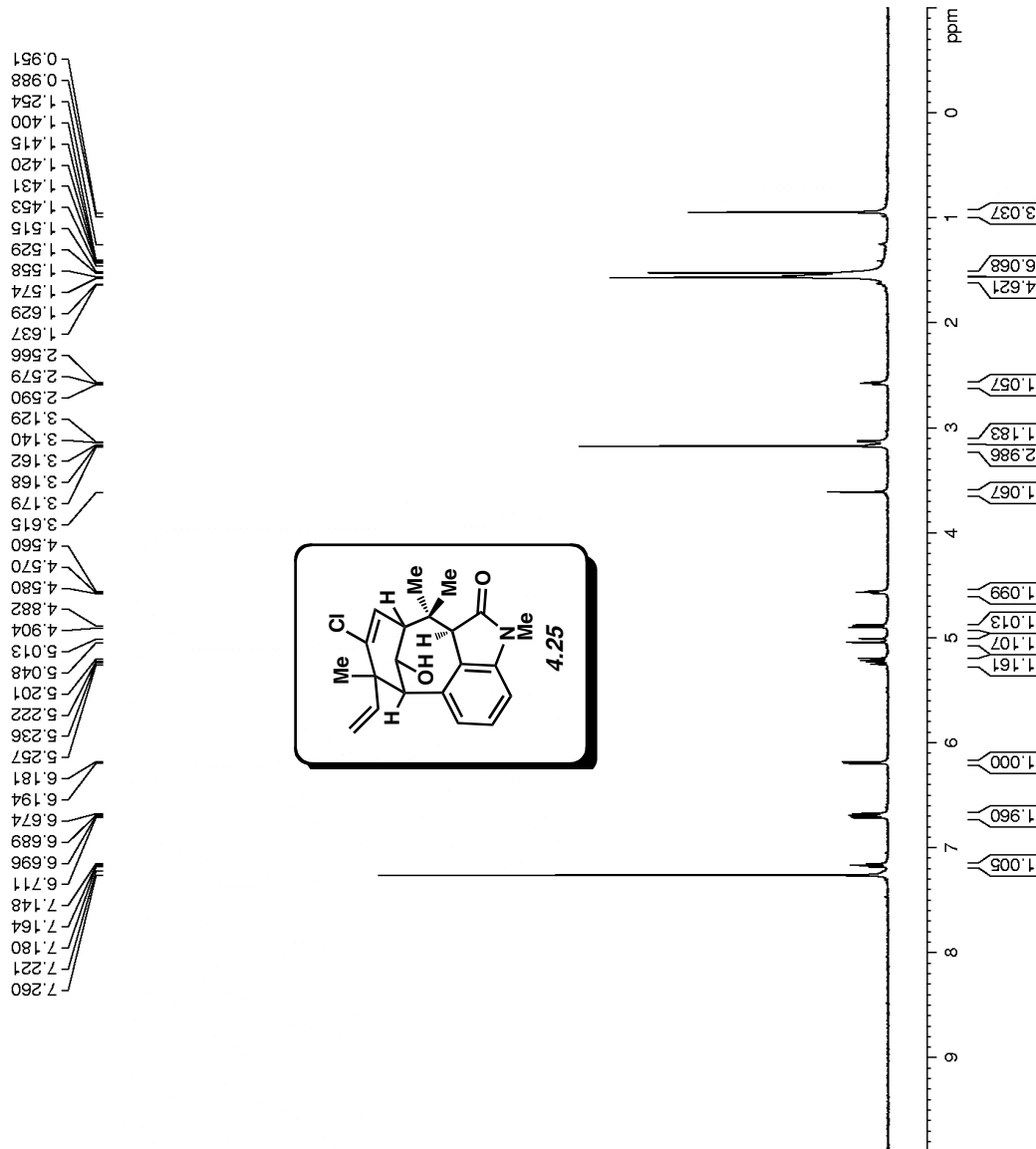


Figure A3.27 ¹H NMR (500 MHz, CDCl₃) of compound 4.25.

Current Data Parameters
 NAME KQ6-239-clar
 EXPNO 1
 PROCNO 1

F2 - Acquisition Parameters
 Date_ 20110705
 Time_ 8.01
 INSTRUM avance600
 PROBHD 5 mm bb-Z Z800
 PULPROG zg30
 TD 65536
 SOLVENT CDCl3
 NS 8
 DS 0
 SWH 10000.000 Hz
 FIDRES 0.152588 Hz
 AQ 3.2769001 sec
 RG 181
 DW 50.000 usec
 DE 6.00 usec
 TE 296.7 K
 D1 2.00000000 sec
 MCREST 0.00000000 sec
 MCWRK 0.01500000 sec

===== CHANNEL f1 =====
 NUC1 1H
 P1 12.00 usec
 PL1 0.00 dB
 SFO1 500.3330020 MHz

F2 - Processing parameters
 SI 32768
 SF 500.3300222 MHz
 EM
 WDW EM
 SSB 0
 LB 0.00 Hz
 GB 0
 PC 1.00

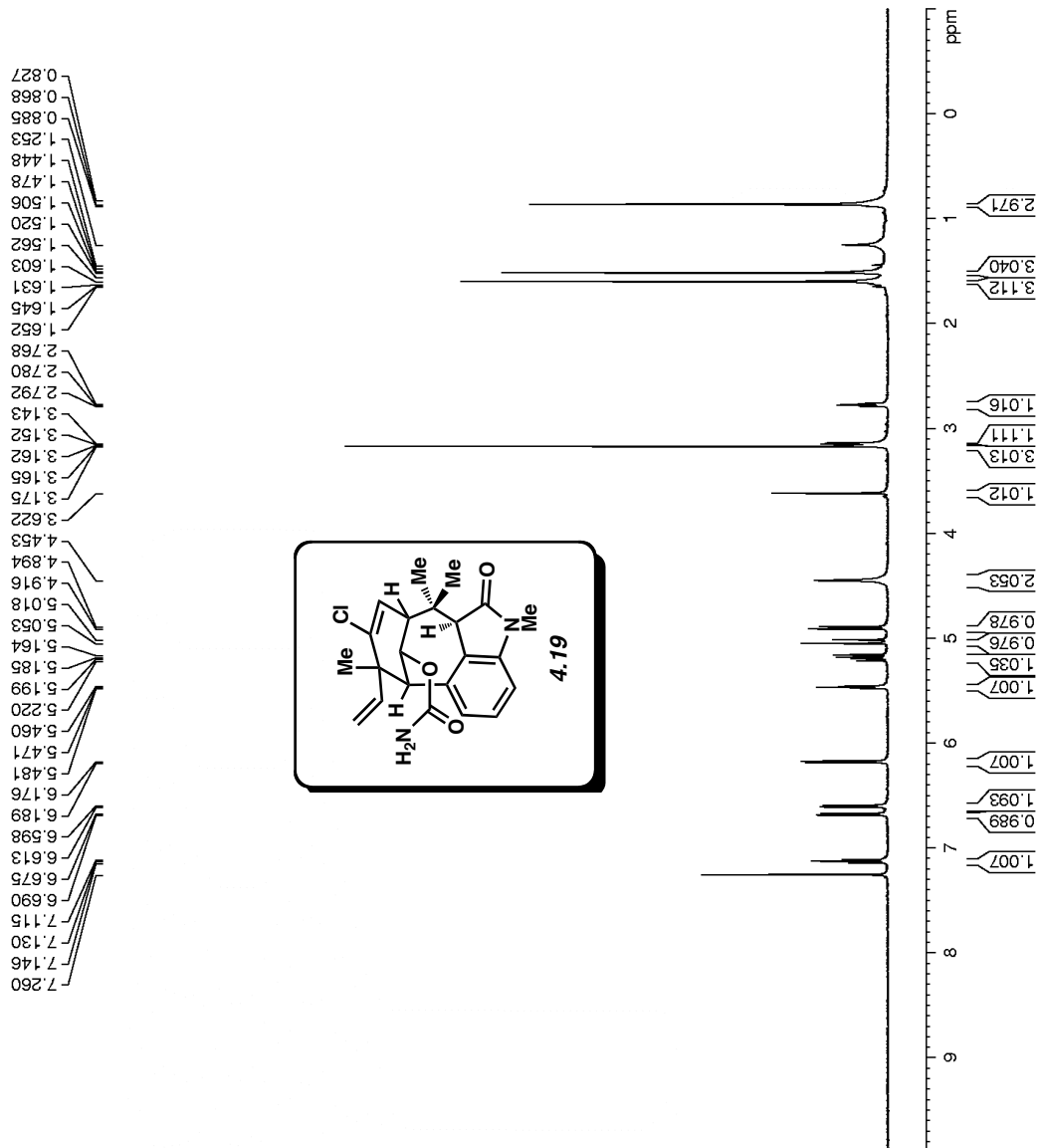


Figure A3.28 ¹H NMR (500 MHz, CDCl₃) of compound 4.19.

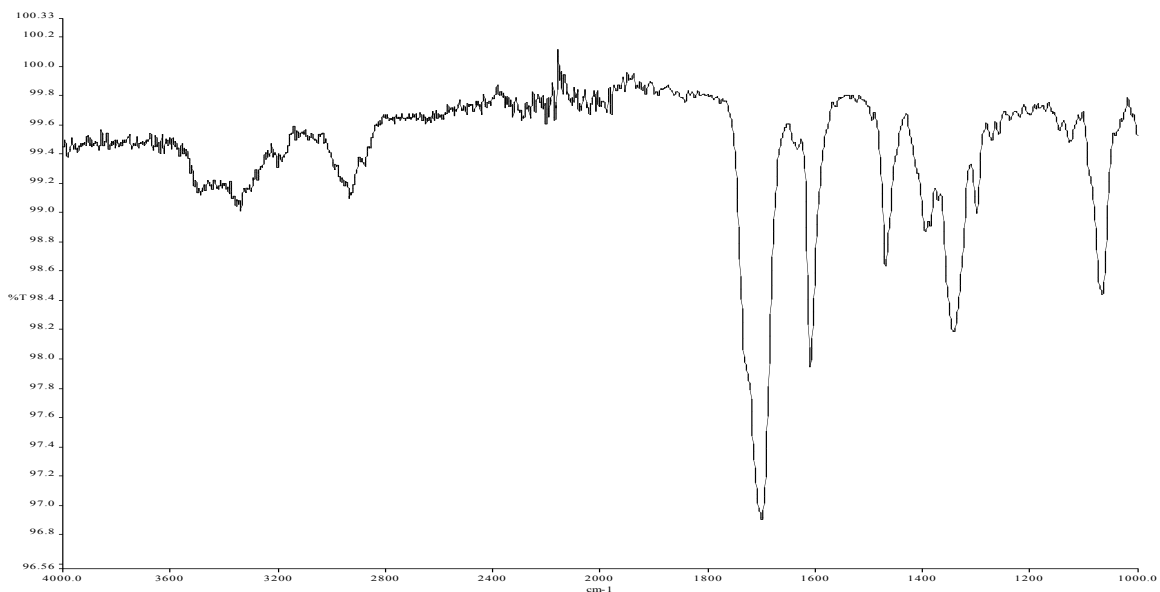


Figure A3.29 Infrared spectrum of compound 4.19.

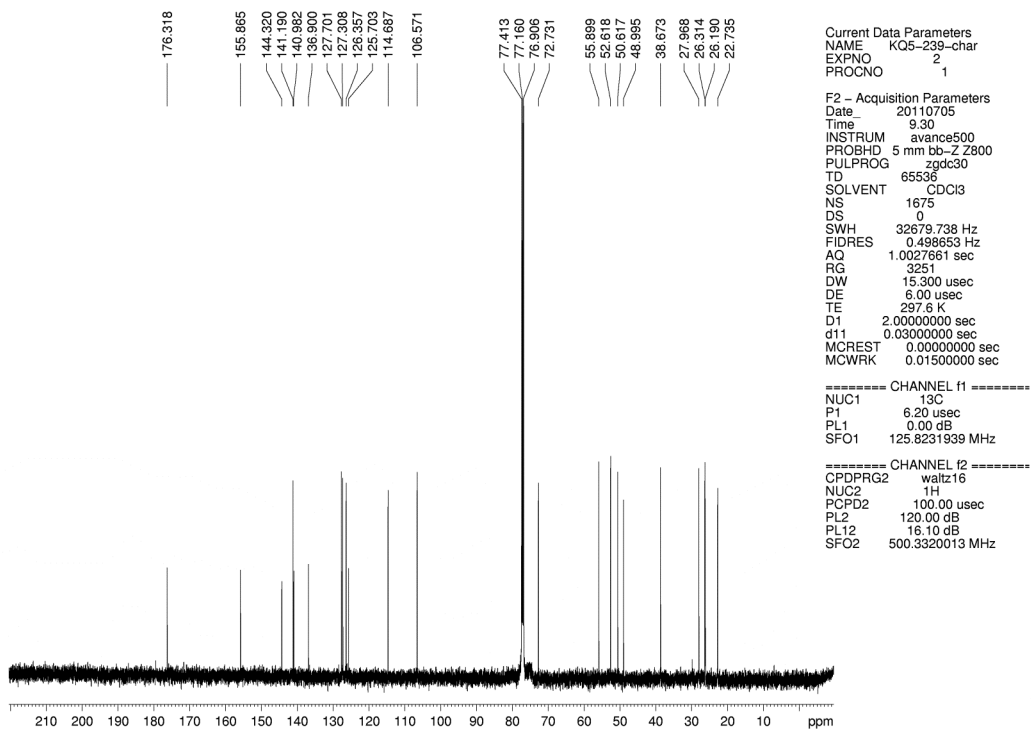


Figure A3.30 ¹³C NMR (125 MHz, CDCl₃) of compound 4.19.

Current Data Parameters
 NAME ADH-3-117-p
 EXPNO 1
 PROCNO 1
 F2 - Acquisition Parameters
 Date_ 20110707
 Time_ 8.03
 INSTRUM avance600
 PROBHD 5 mm bb-Z 2800
 PULPROG zg30
 TD 65536
 SOLVENT CDCl3
 NS 8
 DS 0
 SWH 10000.000 Hz
 FIDRES 0.152588 Hz
 AQ 3.2769001 sec
 RG 256
 DW 50.000 usec
 DE 6.00 usec
 TE 296.7 K
 D1 2.0000000 sec
 MCREST 0.0000000 sec
 MCWRK 0.01500000 sec
 ===== CHANNEL f1 =====
 NUC1 1H
 P1 12.00 usec
 PL1 0.00 dB
 SFO1 500.3330020 MHz
 F2 - Processing parameters
 SI 32768
 SF 500.3300225 MHz
 WDW EM
 SSB 0
 LB 0.30 Hz
 GB 0
 PC 1.00

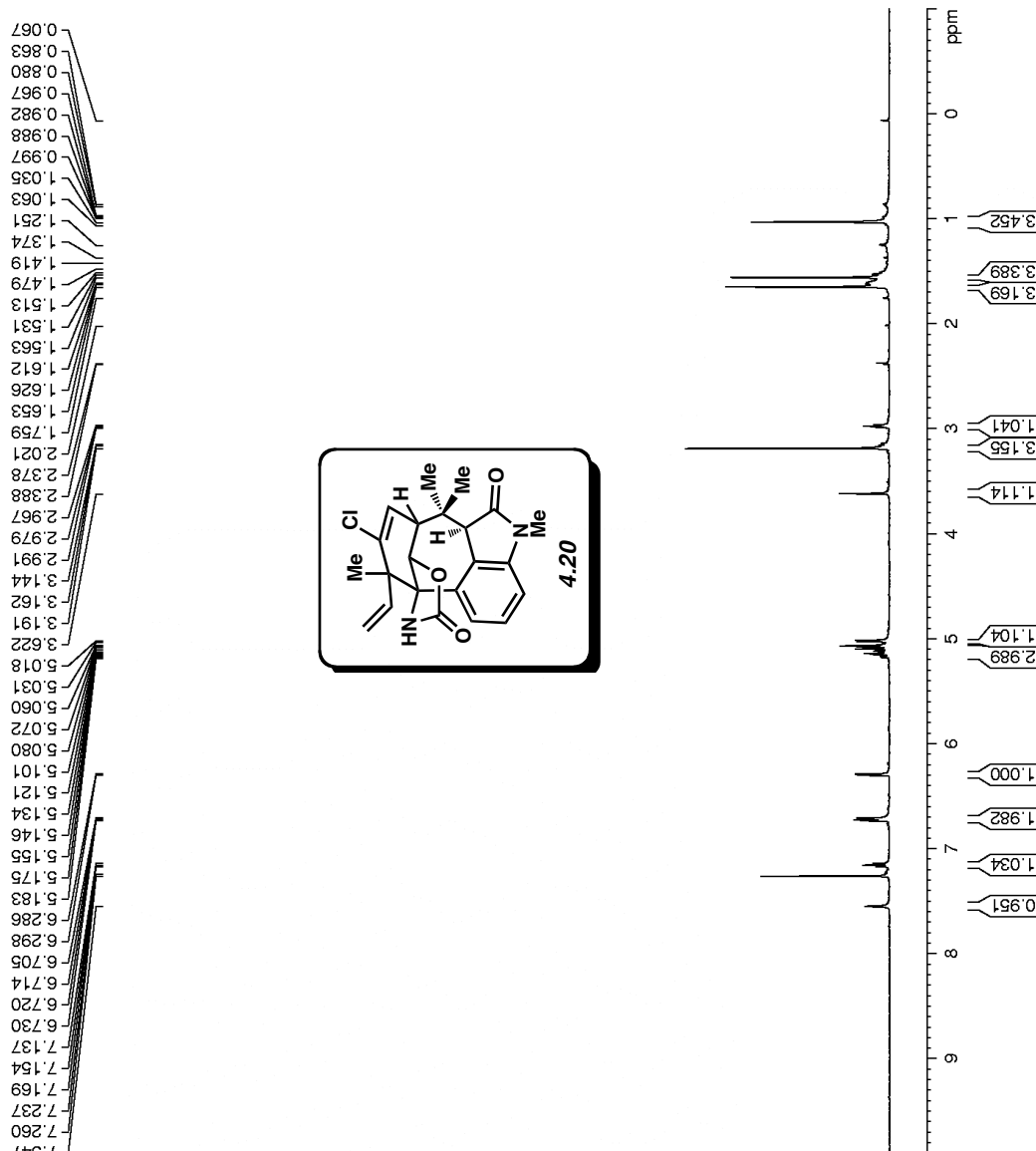


Figure A3.31 ¹H NMR (500 MHz, CDCl₃) of compound 4.20.

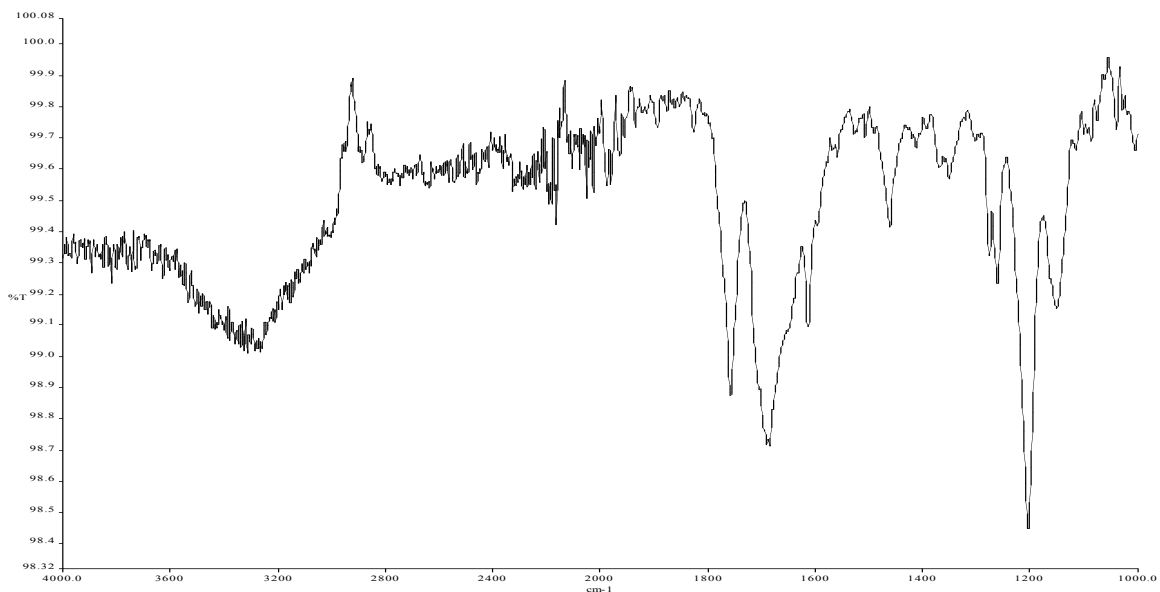


Figure A3.32 Infrared spectrum of compound 4.20.

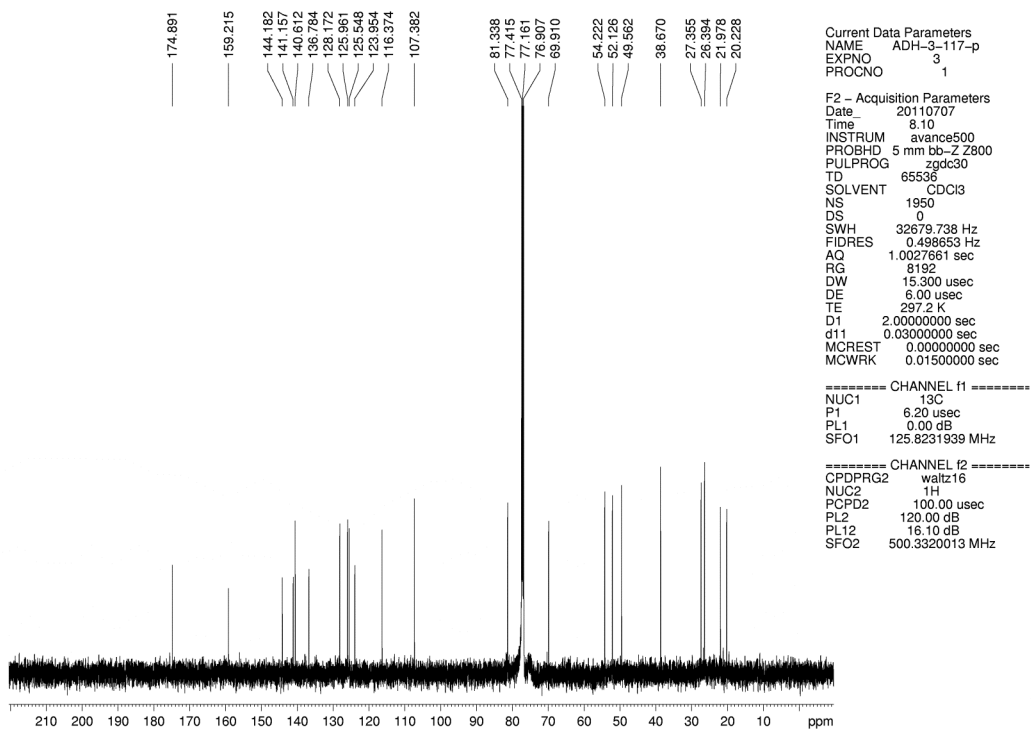


Figure A3.33 ^{13}C NMR (125 MHz, CDCl_3) of compound 4.20.

Current Data Parameters
 NAME KCB-241
 EXPNO 4
 PROCNO 1

F2 - Acquisition Parameters
 Date_ 20110707
 Time_ 15.36
 INSTRUM avance600
 PROBHD 5 mm bb-Z Z800
 PULPROG zg30
 TD 65536
 SOLVENT CDCl3
 NS 20
 DS 0
 SWH 10000.000 Hz
 FIDRES 0.152588 Hz
 AQ 3.2769001 sec
 RG 256
 DW 50.000 usec
 DE 6.00 usec
 TE 296.7 K
 D1 2.00000000 sec
 MCREST 0.00000000 sec
 MCWFRK 0.01500000 sec

===== CHANNEL f1 =====
 NUC1 1H
 P1 12.00 usec
 PL1 0.00 dB
 SFO1 500.3330020 MHz

F2 - Processing parameters
 SI 32768
 SF 500.33300220 MHz
 WDW EM
 SSB 0
 LB 0.00 Hz
 GB 0
 PC 1.00

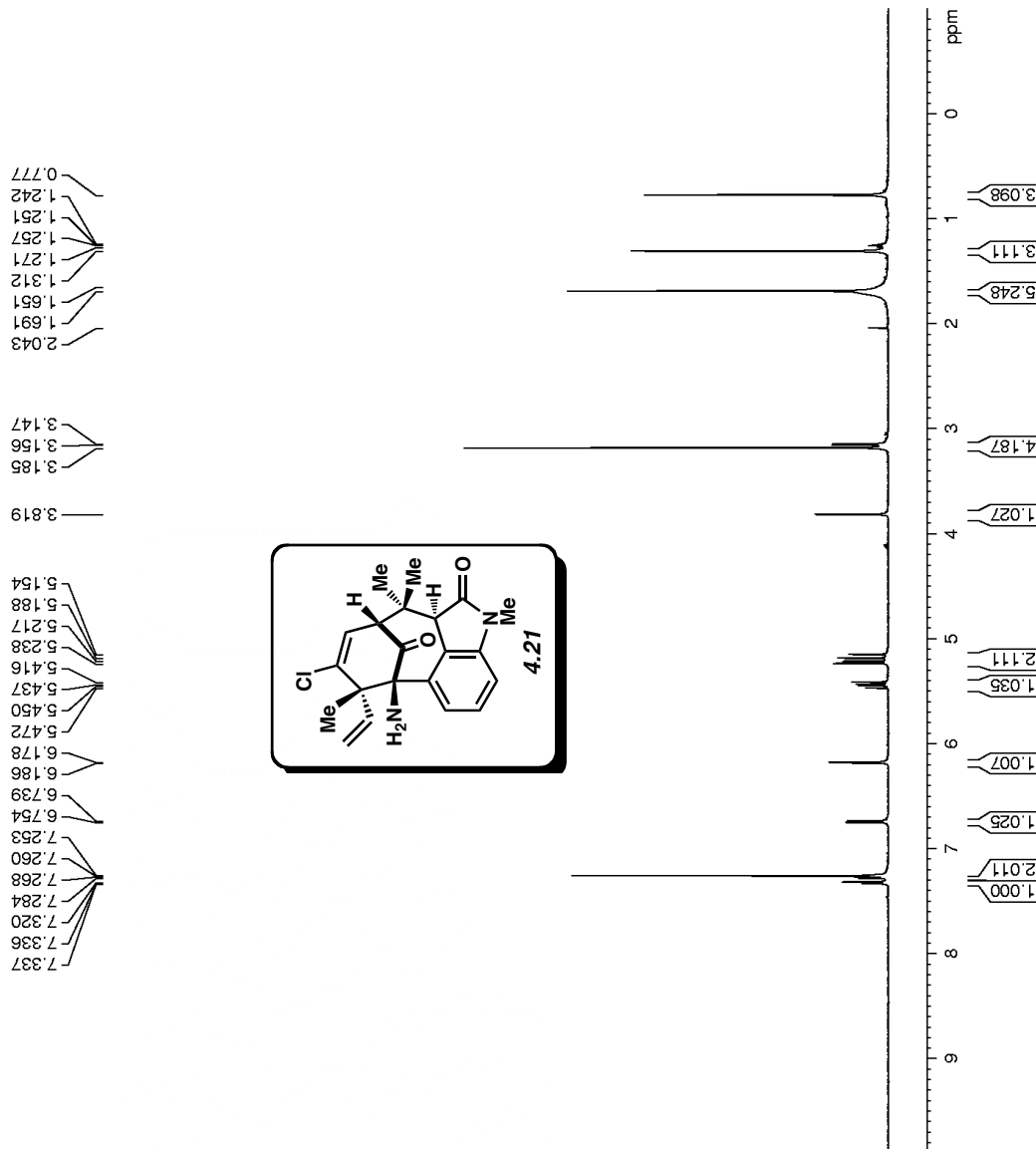


Figure A3.34 ^1H NMR (500 MHz, CDCl_3) of compound 4.21.

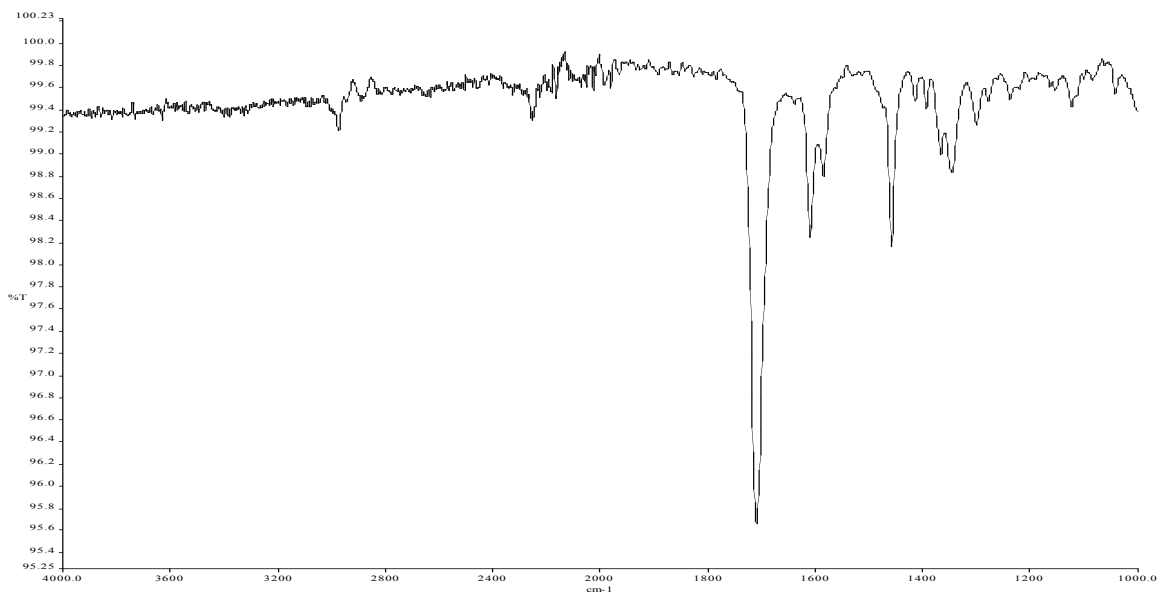


Figure A3.35 Infrared spectrum of compound 4.21.

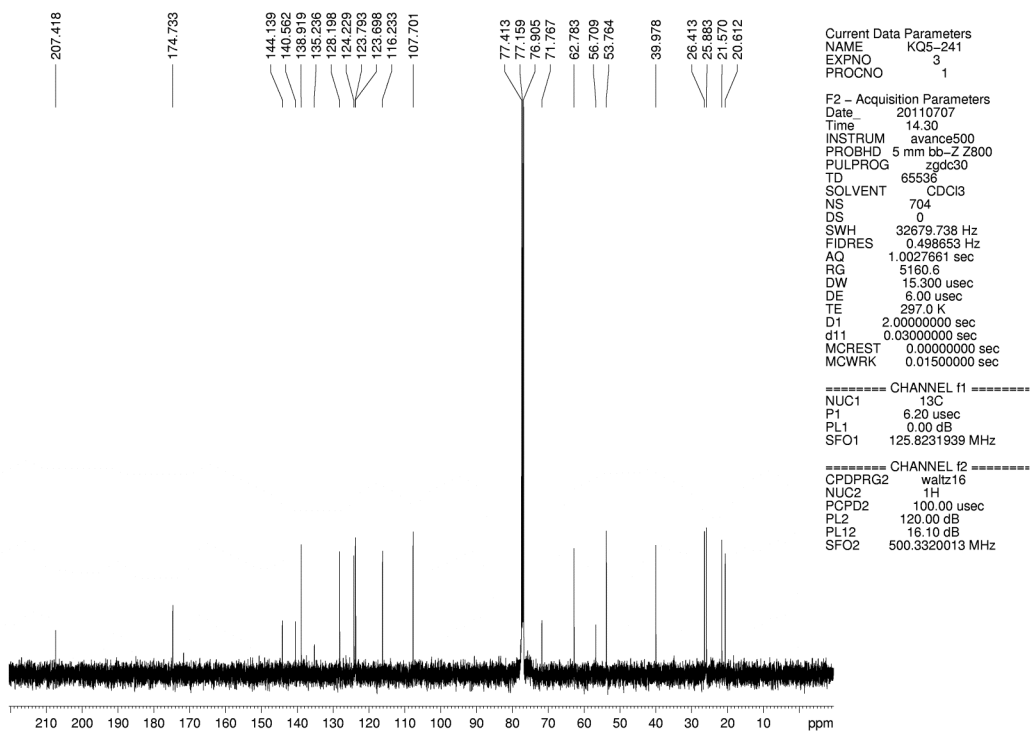


Figure A3.36 ^{13}C NMR (125 MHz, CDCl_3) of compound 4.21.

Current Data Parameters
 NAME KCB-243
 EXPNO 6
 PROCNO 1

F2 - Acquisition Parameters
 Date_ 20110710
 Time 13.06
 INSTRUM avance600
 PROBHD 5 mm bb-Z Z800
 PULPROG zg30
 TD 65536
 SOLVENT CDCl3
 NS 12
 DS 0
 SWH 10000.000 Hz
 FIDRES 0.152588 Hz
 AQ 3.2769001 sec
 RG 322.5
 DW 50.000 usec
 DE 6.00 usec
 TE 296.6 K
 D1 2.0000000 sec
 MCREST 0.0000000 sec
 MCWRK 0.01500000 sec

===== CHANNEL f1 =====
 NUC1 1H
 P1 12.00 usec
 PL1 0.00 dB
 SFO1 500.3330020 MHz

F2 - Processing parameters
 SI 32768
 SF 500.3330319 MHz
 WDW EM
 SSB 0
 LB 0.00 Hz
 GB 0
 PC 1.00

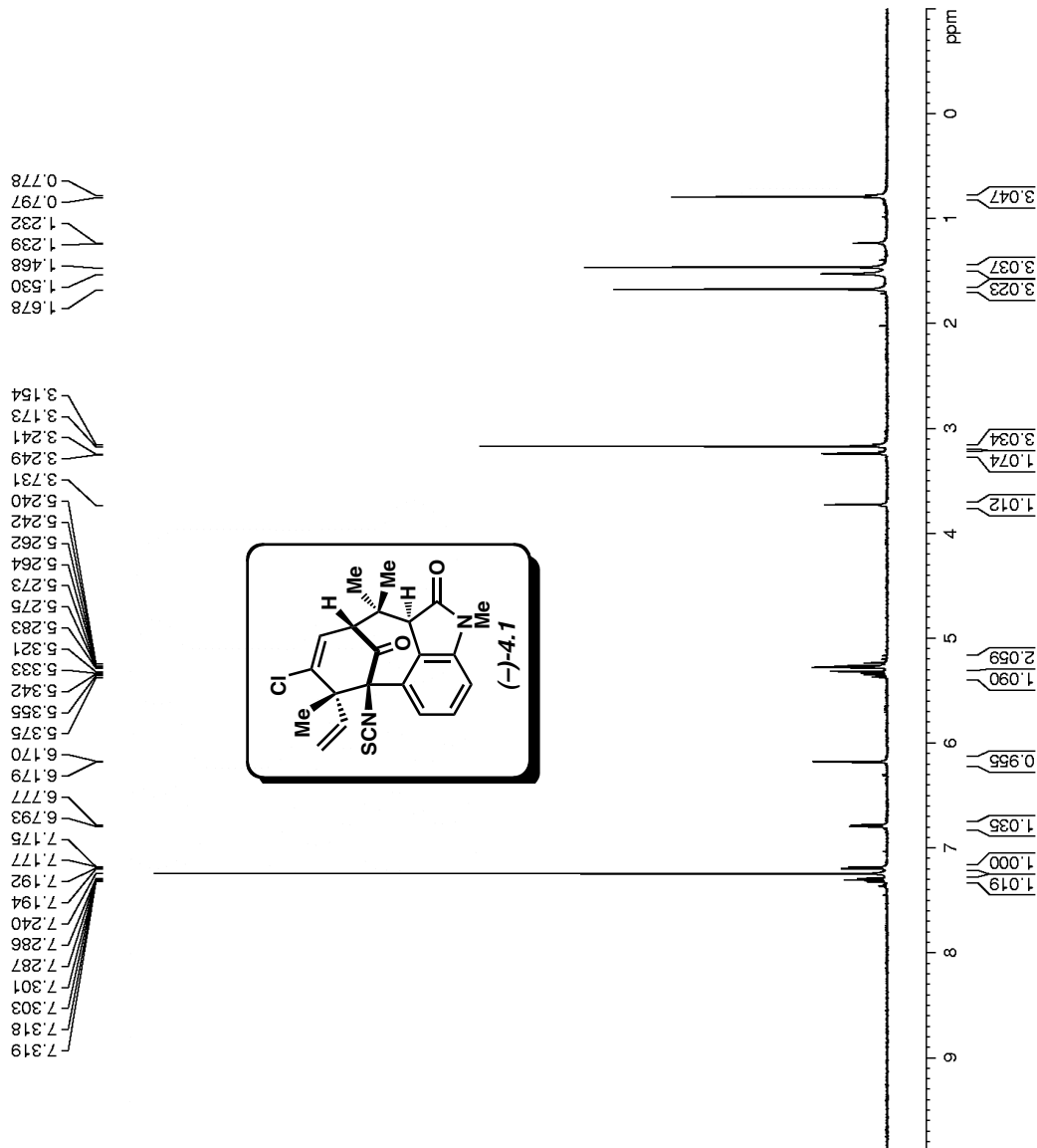


Figure A3.37 ¹H NMR (500 MHz, CDCl₃) of compound 4.1.

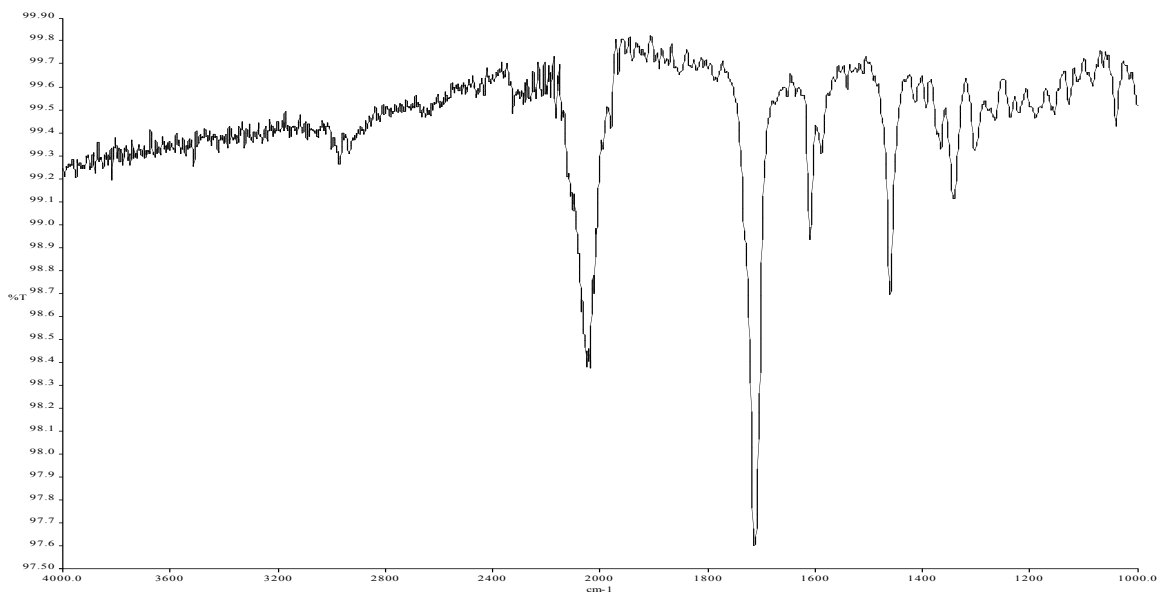


Figure A3.38 Infrared spectrum of compound 4.1.

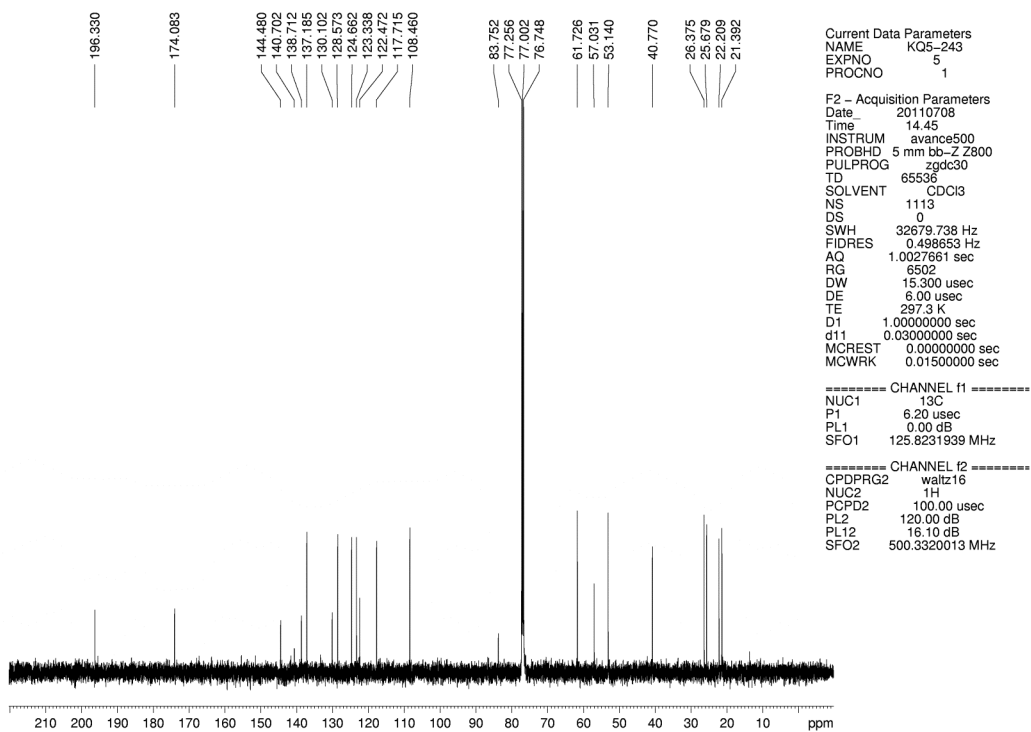


Figure A3.39 ¹³C NMR (125 MHz, CDCl₃) of compound 4.1.

CHAPTER FIVE

Total Synthesis of Oxidized Welwitindolinones and (-)-*N*-Methylwelwitindolinone C Isonitrile

Kyle W. Quasdorf, Alexander D. Hutters, Michael W. Lodewyk, Dean J. Tantillo, and Neil K. Garg.

J. Am. Chem. Soc. **2012**, *134*, 1396–1399.

5.1 Abstract

We report the total synthesis of (-)-*N*-methylwelwitindolinone C isonitrile, in addition to the total syntheses of the 3-hydroxylated welwitindolinones. Our routes to these elusive natural products feature the strategic use of a deuterium kinetic isotope effect to improve the efficiency of a late-stage nitrene insertion reaction. We also provide a computational prediction for the stereochemical configuration at C3 of the hydroxylated welwitindolinones, which was confirmed by experimental studies.

5.2 Introduction

Since their isolation reports in 1994 and 1999,¹ the welwitindolinone natural products have captivated synthetic chemists worldwide.² To date, nine welwitindolinones with [4.3.1]-bicyclic frameworks have been discovered (e.g., **5.1–5.5**, Figure 5.1), some of which show promising activity for the treatment of drug resistant cancer cells.³ The dense array of functional groups that decorate the compact structure of these targets has taunted chemists for nearly two decades. More than fifteen laboratories have reported progress toward these intriguing natural products, resulting in many elegant approaches to the bicyclic core.^{4,5} The strategies used by our laboratory and Rawal's, respectively, have recently facilitated the first two syntheses of these

elusive natural products.^{6,7} However, syntheses of several challenging members of the welwitindolinone family of natural products have not been reported.⁸

In this communication, we report the total syntheses of three natural products in the welwitindolinone C series: (-)-**5.2**, (-)-**5.3** and (-)-**5.4**. The latter two of these targets represent the so-called "oxidized welwitindolinones", whose configuration at C3 had not been unambiguously defined. We also describe the strategic manipulation of a kinetic isotope effect to improve the efficiency of a challenging C–H activation / nitrene-insertion reaction, which takes place late-stage in the total syntheses to forge a critical C–N bond.

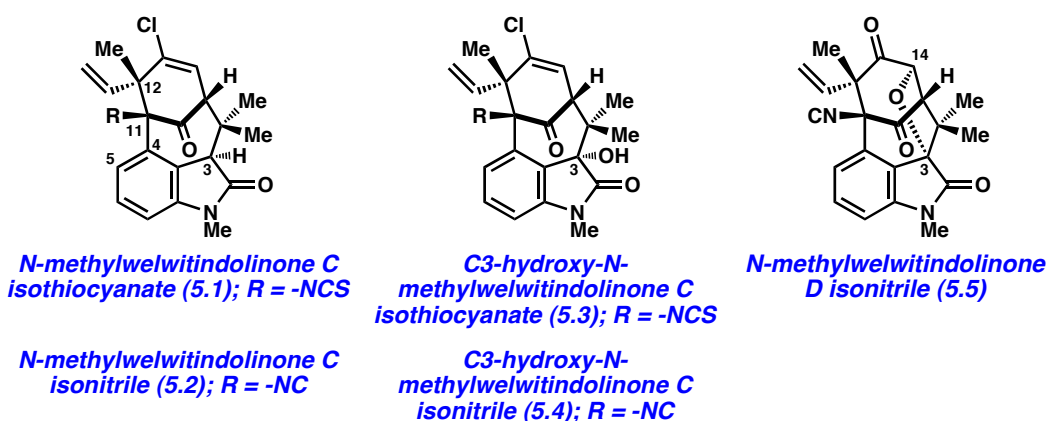


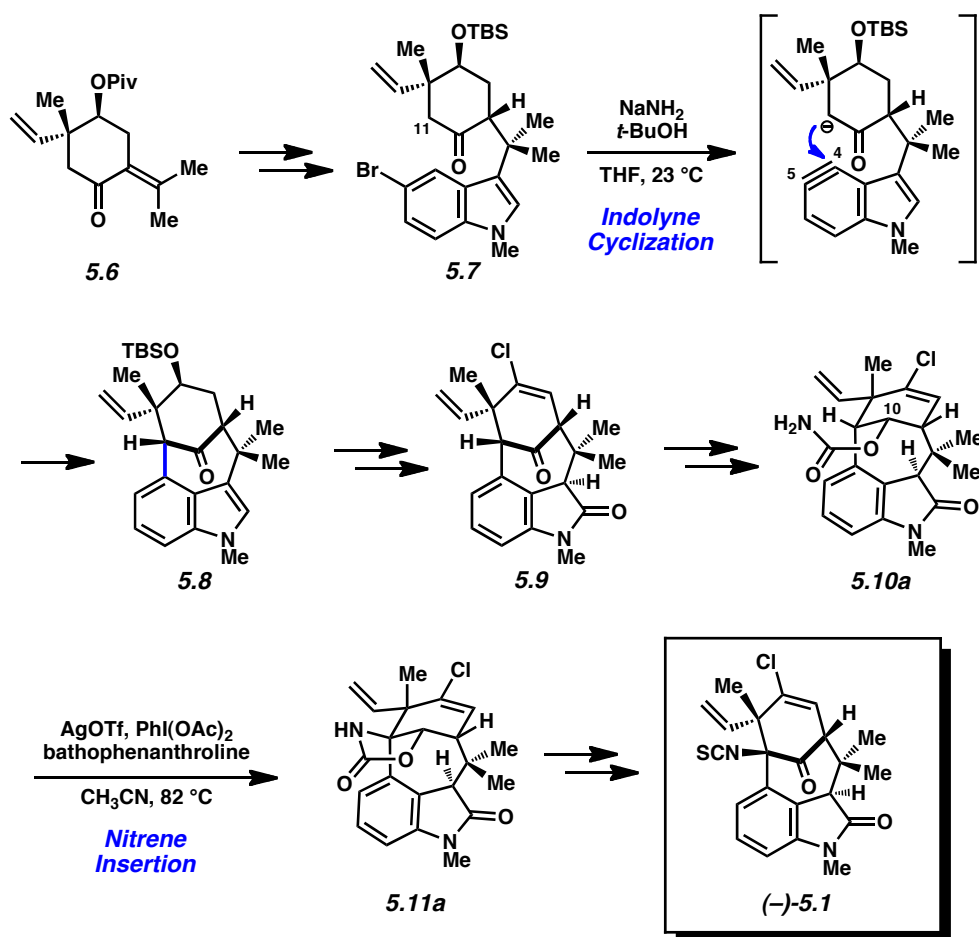
Figure 5.1. Welwitindolinones **5.1–5.5**.

5.3 Previous Total Synthesis of (-)-*N*-Methylwelwitindolinone C Isothiocyanate

A summary of our recent total synthesis of (-)-**5.1**⁷ is shown in Scheme 5.1. Known carvone derivative **5.6** was elaborated to bromoindole **5.7** over three synthetic steps. Subsequent treatment of **5.7** with NaNH₂ and *t*-BuOH in THF facilitated an indolyne cyclization to afford **5.8**, which possesses the desired [4.3.1]-bicycle. Bicycle **5.8** was elaborated to ketone **5.9**, which lacked only the isothiocyanate functional group. Thus, ketone **5.9** was readily converted to

carbamate **5.10a** the substrate for a critical nitrene C–H insertion reaction.^{9,10,11} We were delighted to find that the desired C–H functionalization took place to afford **5.11a** upon exposure of substrate **5.10a** to the Ag-promoted conditions described by He.^{11b,c} Insertion product **5.11a** could be elaborated to the elusive natural product (–)-**5.1** over three additional transformations.

Scheme 5.1



5.4 Optimization of Nitrene Insertion

In order to facilitate syntheses of the remaining natural products in the welwitindolinone C series, we sought to first improve the efficiency of the late-stage nitrene insertion reaction (i.e.,

5.10a→**5.11a**, Scheme 5.1), which had proceeded in a modest 33% yield. It was noted that a major byproduct of the insertion step was ketone **5.9**, which presumably formed through the undesired insertion of the intermediate nitrene species into the C10 C–H bond.¹² We hypothesized that replacing the problematic hydrogen with deuterium would subdue the undesired insertion process, thereby favoring the desired functionalization event.¹³ The deuterated substrate **5.10b** was readily prepared by a sequence involving reduction of ketone **5.9** with super deuteride, followed by carbamoylation (Figure 5.2). We were delighted to find that exposure of this substrate to our optimal reaction conditions for nitrene insertion furnished the desired product **5.11b** in 60% yield, while the formation of ketone **5.9** was diminished. The strategic use of a deuterium kinetic isotope effect in total synthesis is rare,¹⁴ and the present study marks the first use of this approach to facilitate a C–H functionalization event en route to natural products.

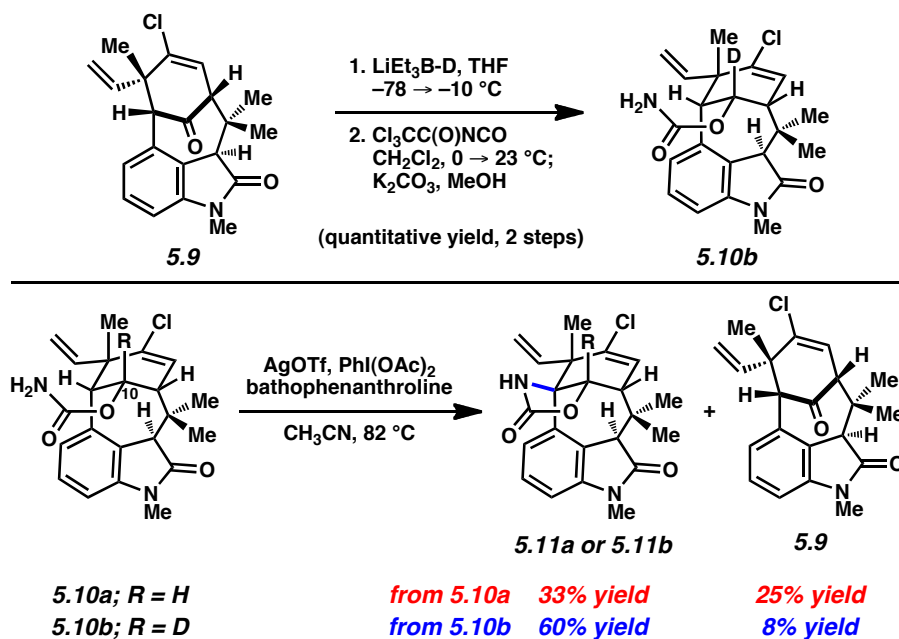
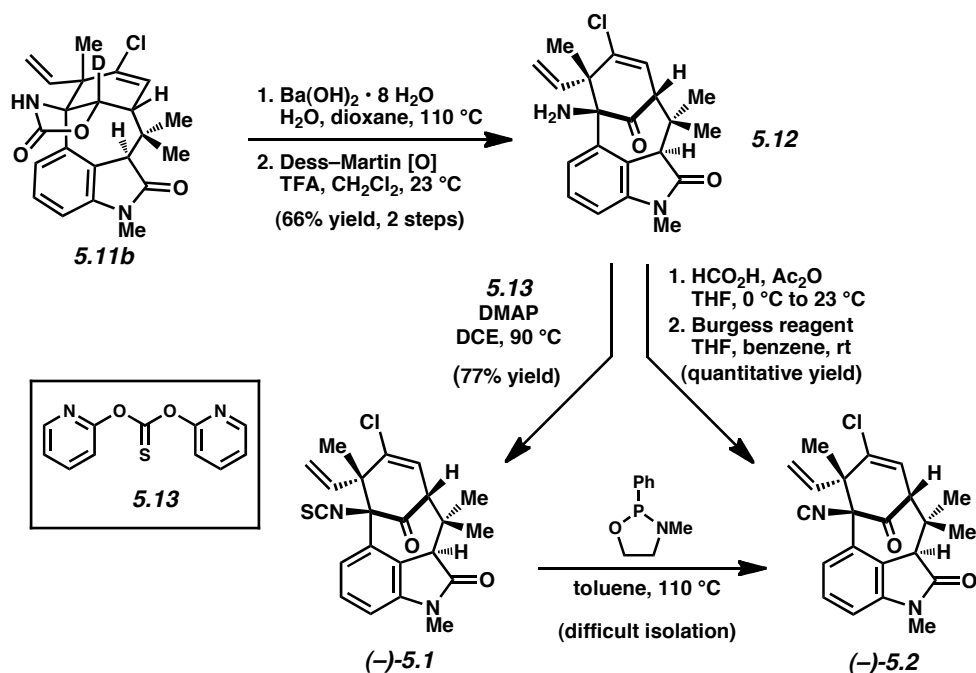


Figure 5.2. Nitrene insertion of substrates **5.10a** and **5.10b**.

5.5 Syntheses of *N*-Methylwelwitindolinone C Isothiocyanate and *N*-Methylwelwitindolinone Isonitrile

With improved access to a C11 *N*-functionalized product, we explored elaboration of **5.11b** to several welwitindolinone natural products. Hydrolysis of the carbamate, followed by Dess–Martin oxidation, proceeded smoothly to furnish aminoketone **5.12** (Scheme 5.2). Subsequent elaboration of **5.12** delivered *N*-methylwelwitindolinone C isothiocyanate (–)-**5.1** as we have shown previously.⁶ Subsequently, exposure of this natural product to Rawal’s desulfurization conditions provided (–)-*N*-methylwelwitindolinone isonitrile (**5.2**) as the major product.⁶ Unfortunately, purification of the crude natural product proved difficult.¹⁵ As a workaround, aminoketone **5.12** was subjected to sequential formylation^{4s} and dehydration^{4m} to afford the desired natural product (–)-**5.2** in 88% yield.¹⁶ Spectral data for synthetic (–)-**5.2** was in accord with that provided for natural (–)-**5.2** in the isolation report.^{1a}

Scheme 5.2



5.6 Syntheses of the C3-hydroxylated Welwitindolinones

We next pursued total syntheses of the C3-hydroxylated welwitindolinones, the two oxidized welwitindolinones that had not been synthesized previously. Furthermore, the stereochemical configuration of these natural products at C3 had not been rigorously established spectroscopically, but rather, had been assigned based on analogy to the non-hydroxylated welwitindolinone natural products.¹⁷ In our first attempts toward these natural products, aminoketone **5.12** was treated with various bases, with the reaction vessels being under standard atmospheric conditions to allow for air-oxidation. Although the corresponding C3 oxidized product was formed and could be manipulated further, low yields and irreproducibility hampered our efforts. However, direct oxidation of the non-hydroxylated natural products was found to be a more fruitful strategy (Figure 5.3). It should be noted that related aerobic oxidations of oxindoles have been reported,¹⁸ including an impressive example in the context of the welwitindolinones.¹⁹ Treatment of (–)-*N*-methylwelwitindolinone C isonitrile (**5.2**) with NaH in the presence of air, provided (–)-3-hydroxy-*N*-methylwelwitindolinone C isonitrile (**5.4**). Similarly, oxidation of (–)-*N*-methylwelwitindolinone C isothiocyanate (**5.1**) delivered (–)-3-hydroxy-*N*-methylwelwitindolinone C isonitrile (**5.3**). Both oxidations occurred selectively to furnish single diastereomers of hydroxylated products, while leaving the sensitive C11 functional groups undisturbed.

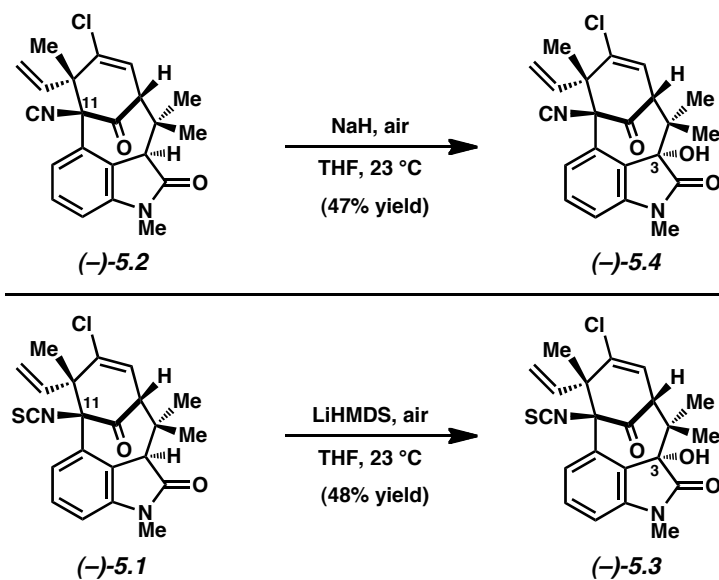
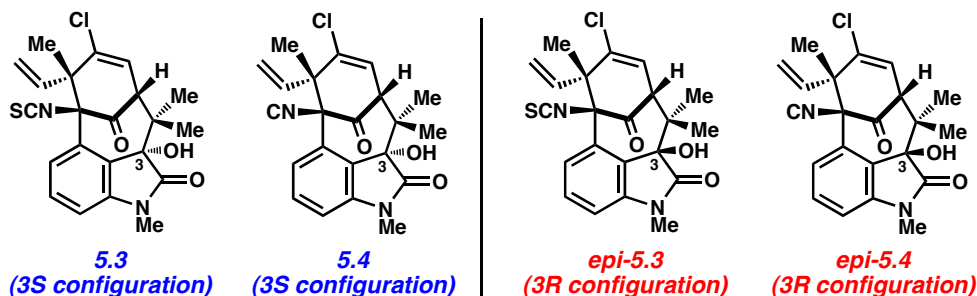


Figure 5.3. Total synthesis of oxidized welwitindolinones **5.3** and **5.4**.

5.7 Computational and Experimental Studies to Establish the Stereochemistry of the C3-hydroxylated Welwitindolinones

For each of the natural products synthesized, our synthetic samples matched the natural materials by spectroscopic means.^{1b,20} However, for the hydroxylated welwitindolinones, the C3 stereochemistry remained to be unambiguously established. Since computational predictions for ¹H and ¹³C NMR chemical shifts have proven valuable in elucidating stereochemical configurations of natural products,^{21,22} we calculated the ¹H and ¹³C NMR chemical shifts for the C3 epimers of welwitindolinones **5.3** and **5.4** (Figure 5.4).²³ In both cases, the computed chemical shifts for the C3(*S*) diastereomer matched the experimental data better than did the computed shifts for the C3(*R*) diastereomer. For example, although computed ¹³C shifts for **5.4** and *epi*-**5.4** deviated from the experimental shifts by similar amounts (mean absolute deviations (MADs) of 2.13 and 2.69 ppm, with largest outliers off by 5.59 and 5.34 ppm for **5.4** and *epi*-**5.4**, respectively), computed ¹H shifts for **5.4** matched the experimental values much more closely than did computed shifts for *epi*-**5.4** (MADs of 0.08 (0.05 without the OH proton included) and

0.36 ppm (0.34 without the OH proton included), with largest C–H outliers off by 0.13 and 0.79 ppm for **5.4** and *epi-5.4*, respectively). Similar results were obtained for **5.3**.²³ We therefore propose that the stereochemical configuration at C3 is *S* in **5.3** and **5.4**, in accord with the hypothesis made by the isolation chemists.¹

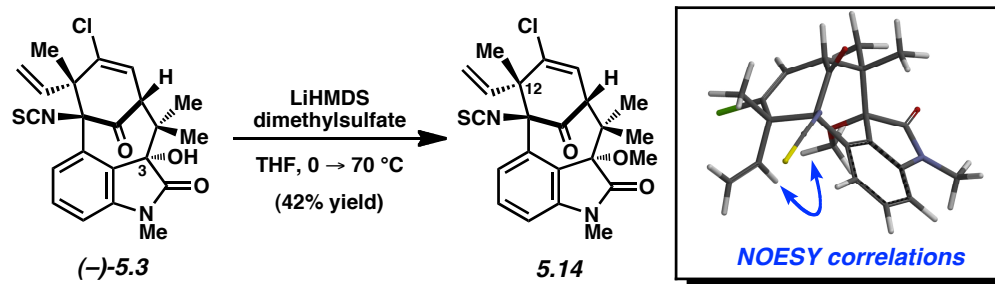


computational predictions for ¹HNMR and ¹³CNMR shifts
match experimental data for *3S* configuration

Figure 5.4. Structures of **5.3** and **5.4**, in addition to C3 epimers, and summary of computational findings.

To provide evidence for this stereochemical assignment, (–)-3-hydroxy-*N*-methylwelwitindolinone C isothiocyanate (**5.3**) was treated with LiHMDS and dimethylsulfate (Scheme 5.3). Despite the severely hindered nature of the tertiary alcohol, methylation proceeded to provide ether **5.14**. 2D-NOESY experiments of **5.14** showed correlations between the methoxy protons and the protons of the vinyl group at C12, thus supporting the proposed C3(*S*) configuration.²⁴ This result further validates the promising use of computational chemistry to establish stereochemical assignments on complex molecules.^{21,22}

Scheme 5.3



5.8 Conclusion

In summary, we have completed the total syntheses of several elusive welwitindolinone natural products. Our routes to these natural products feature the strategic use of a deuterium kinetic isotope effect to improve the efficiency of a late-stage nitrene insertion reaction. We also provide a computational prediction for the stereochemical configuration at C3 of the hydroxylated welwitindolinones **3** and **4**. This prediction was confirmed by experimental studies. Our findings are expected to facilitate the total syntheses of other welwitindolinone natural products, while demonstrating the utility of computational chemistry in elucidating stereochemical assignments and the strategic manipulation of kinetic isotope effects in total synthesis.

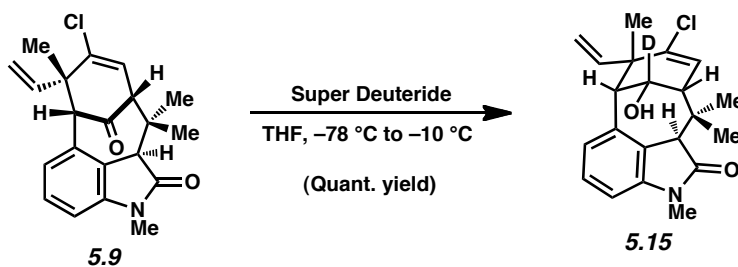
5.9 Experimental Section

5.9.1 Materials and Methods

Unless stated otherwise, reactions were conducted in flame-dried glassware under an atmosphere of nitrogen using anhydrous solvents (either freshly distilled or passed through activated alumina columns). All commercially available reagents were used as received unless otherwise specified. (*S*)-carvone was obtained from Aldrich. 5-bromoindole was obtained from Biosynth. NaNH₂ was obtained from Alfa Aesar. Comins' reagent was obtained from Aldrich. Hexamethylditin was obtained from Aldrich. Tetrakis(triphenylphosphine)palladium(0) was obtained from Strem. Anhydrous CuCl₂ was obtained from Aldrich. Trichloroacetyl isocyanate was obtained from Aldrich. LiEt₃BD ("super deuteride") was obtained from Aldrich. AgOTf was obtained from Strem. Bathophenanthroline was obtained from Alfa Aesar. *O,O*-di(2-pyridinyl) thiocarbonate was obtained from Aldrich. 2-Iodoxybenzoic acid (IBX) and Dess–Martin periodinane were prepared from known literature procedures.^{25,26} *t*-BuOH was distilled from CaH₂ and stored in a Schlenk tube prior to use. 1,4-dioxane was distilled from Na/benzophenone prior to use. 1,2-dichloroethane was distilled from P₂O₅ and stored in a Schlenk tube over 4Å molecular sieves prior to use. Unless stated otherwise, reactions were performed at room temperature (rt, approximately 23 °C). Thin-layer chromatography (TLC) was conducted with EMD gel 60 F254 pre-coated plates (0.25 mm) and visualized using a combination of UV, anisaldehyde, iodine, and potassium permanganate staining. Silicycle silica gel 60 (particle size 0.040–0.063 mm) was used for flash column chromatography. ¹H NMR spectra were recorded on Bruker spectrometers (500 MHz). Data for ¹H spectra are reported as follows: chemical shift (δ ppm), multiplicity, coupling constant (Hz), integration and are referenced to the residual solvent peak 7.26 ppm for CDCl₃ and 5.32 ppm for CD₂Cl₂. Data for ²H NMR spectra are

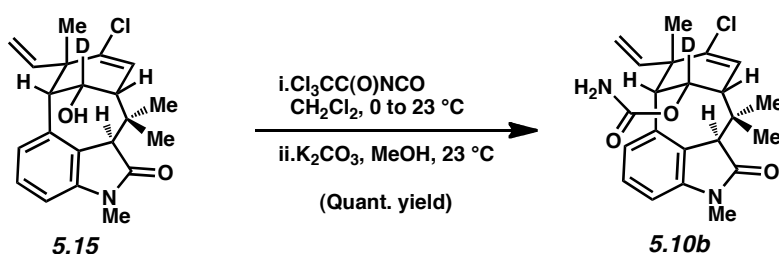
reported as follow: chemical shift (δ ppm, at 77 MHz), multiplicity, coupling constant, integration and are referenced to the residual solvent peak 7.26 ppm for CDCl_3 . ^{13}C NMR spectra are reported in terms of chemical shift (at 125 MHz) and are referenced to the residual solvent peak 77.16 ppm for CDCl_3 , 53.84 for CD_2Cl_2 , and 128.06 for C_6D_6 . IR spectra were recorded on a Perkin-Elmer 100 spectrometer and are reported in terms of frequency absorption (cm^{-1}). Optical rotations were measured with a Rudolf Autopol IV Automatic Polarimeter. Uncorrected melting points were measured with a Mel-Temp II melting point apparatus and a Fluke 50S thermocouple. High resolution mass spectra were obtained from the UC Irvine Mass Spectrometry Facility.

5.9.2 Experimental Procedures



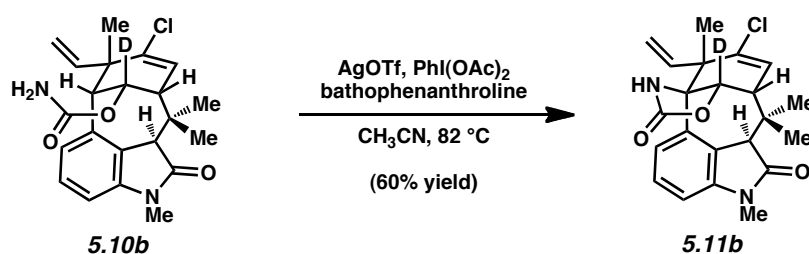
Alcohol 5.15. To a solution of ketone **5.9**⁷ (367 mg, 1.03 mmol, 1.0 equiv) in THF (34.0 mL) at $-78\text{ }^\circ\text{C}$ was added a solution of LiEt_3BD (“super deuteride”, 1.0 M in THF, 1.13 mL, 1.13 mmol, 1.1 equiv) in a dropwise manner. After stirring at $-78\text{ }^\circ\text{C}$ for 10 min the reaction was warmed to $-10\text{ }^\circ\text{C}$ and stirred for an additional 1 h. The reaction was then quenched with the addition of MeOH (5 mL) and warmed to room temperature. The resulting mixture was transferred to a separatory funnel with EtOAc (50 mL), H_2O (15 mL), and brine (25 mL). The resulting biphasic mixture was extracted with EtOAc (3 x 50 mL), the organic layers were combined, dried over

MgSO₄, and evaporated under reduced pressure. The resulting residue was purified by flash chromatography (1:1:1 hexanes:CH₂Cl₂:Et₂O) to afford alcohol **5.15** (370 mg, quant. yield) as a white solid. Alcohol **5.15**: R_f 0.12 (2:1:1 hexanes:CH₂Cl₂:Et₂O); ¹H NMR (500 MHz, CDCl₃): δ 7.17 (ddd, *J* = 7.8, 7.7, 0.9, 1H), 6.70 (d, *J* = 7.8, 0.9 1H), 6.68 (d, *J* = 7.7, 1H), 6.19 (d, *J* = 6.7, 1H), 5.23 (dd, *J* = 17.4, 10.7, 1H), 5.03 (dd, *J* = 17.4, 0.7, 1H), 4.89 (dd, *J* = 10.7, 0.7, 1H), 3.62 (s, 1H), 3.18 (s, 3H), 3.13 (d, *J* = 0.9, 1H), 2.57 (dd, *J* = 6.7, 0.9, 1H), 1.57 (s, 3H), 1.53 (s, 3H), 0.95 (s, 3H).



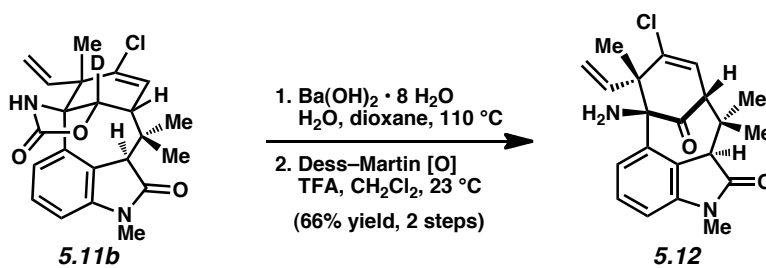
Carbamate 5.10b. To a solution of **5.15** (370 mg, 1.03 mmol, 1.0 equiv) in CH₂Cl₂ (21.0 mL) at 0 °C was added trichloroacetyl isocyanate (129 μL, 1.08 mmol, 1.05 equiv) in a dropwise manner. The resulting mixture was stirred at 0 °C for 5 min, and then at room temperature for an additional 20 min. The solvent was evaporated under reduced pressure. To the resulting residue was added MeOH (21.0 mL) and solid K₂CO₃ (784 mg, 5.67 mmol, 5.5 equiv) in one portion. The reaction was flushed with N₂ and left to stir at room temperature for 3.5 h. The reaction was quenched with a saturated aqueous NH₄Cl solution (50 mL) and the resulting biphasic mixture was transferred to a separatory funnel with EtOAc (50 mL) and H₂O (25 mL). After extracting with EtOAc (3 x 50 mL), the organic layers were combined, dried over MgSO₄, and evaporated under reduced pressure. The resulting residue was purified by flash chromatography (1:1 hexanes:EtOAc) to afford carbamate **5.10b** (416 mg, quant. yield) as a white solid. Carbamate

5.10b: mp: 135 °C; R_f 0.41 (1:1 hexanes:EtOAc); ^1H NMR (500 MHz, CDCl_3): δ 7.13 (dd, $J = 7.8, 7.7$, 1H), 6.68 (d, $J = 7.7$, 1H), 6.61 (d, $J = 7.8$, 1H), 6.18 (d, $J = 6.7$, 1H), 5.19 (dd, $J = 17.3, 10.6$, 1H), 5.04 (dd, $J = 17.3, 0.8$, 1H), 4.91 (dd, $J = 10.6, 0.8$, 1H), 4.46 (br. s, 2H), 3.62 (s, 3H), 3.17 (s, 3H), 3.14 (s, 1H), 2.77 (dd, $J = 6.7, 0.9$, 1H), 1.60 (s, 3H), 1.52 (s, 3H), 0.87 (s, 3H); ^2H NMR (77 MHz, CDCl_3) δ 5.48 (br. s, 1D); ^{13}C NMR (21 of 22 observed, 125 MHz, CDCl_3): δ 176.3, 155.9, 144.3, 141.2, 141.0, 136.9, 127.7, 127.3, 126.4, 125.7, 114.7, 106.6, 55.8, 52.6, 50.6, 49.0, 38.7, 28.0, 26.3, 26.2, 22.7; IR (film): 3493, 3351, 2929, 2875, 1723, 1698, 1609, 1469, 1375, 1084 cm^{-1} ; HRMS-ESI (m/z) $[\text{M} + \text{Na}]^+$ calcd for $\text{C}_{22}\text{H}_{24}\text{DN}_2\text{O}_3\text{ClNa}$, 424.1514; found 424.1504; $[\alpha]_D^{24.2} -151.0^\circ$ ($c = 1.000$, CH_2Cl_2).



Oxazolidinone 5.11b. A 20 mL scintillation vial containing CH_3CN and two separate 20 mL scintillation vials each charged with bathophenanthroline (40.1 mg, 0.124 mmol, 0.5 equiv) were transferred into the glovebox. AgOTf (32.0 mg, 0.124 mmol, 0.5 equiv) and CH_3CN (7.00 mL) were added to each vial containing the bathophenanthroline, and the resulting suspensions were stirred at room temperature for 20 min. Next, two additional 20 mL scintillation vials each containing carbamate **5.10b** (100 mg, 0.249 mmol, 1.0 equiv) and PhI(OAc)_2 (160 mg, 0.498 mmol, 2.0 equiv) were transferred into the glovebox and a AgOTf /bathophenanthroline suspension was added to each of these vials. The vials were then sealed, removed from the glovebox, and the resulting mixtures were allowed to stir at 82 °C. After 24 h, the reactions were

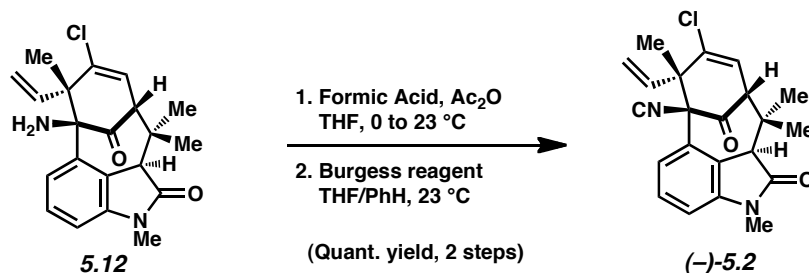
cooled to room temperature and combined then filtered through a plug of silica gel (EtOAc eluent, 50 mL). The filtrate was evaporated under reduced pressure, and the resulting residue was purified by flash chromatography (4:1 benzene:EtOAc) to afford oxazolidinone **5.11b** (59.3 mg, 60% yield) as a white solid and recovered ketone **5.9** (7.0 mg, 8% yield) as a white solid. Oxazolidinone **5.11b**: mp: 329 °C; R_f 0.35 (2:1 benzene:EtOAc); $^1\text{H NMR}$ (500 MHz, CDCl_3): δ 7.53 (br. s, 1H), 7.15 (ddd, $J = 8.3, 7.6, 0.7$ 1H), 6.72 (d, $J = 8.3$, 1H), 6.71 (d, $J = 7.6$, 1H), 6.29 (d, $J = 5.9$, 1H), 5.19–5.05 (m, 3H), 3.62 (s, 1H), 3.19 (s, 3H), 2.97 (d, $J = 5.9$, 1H), 1.65 (s, 3H), 1.56 (s, 3H), 1.04 (s, 3H); $^2\text{H NMR}$ (77 MHz, CDCl_3) δ 5.02 (br. s, 1D); $^{13}\text{C NMR}$ (125 MHz, CDCl_3): δ 174.9, 159.2, 144.2, 141.1, 140.6, 136.8, 128.2, 125.9, 125.5, 123.9, 116.4, 107.4, 80.9 (t, $J_{\text{C-D}} = 21.9$), 69.8, 54.2, 52.1, 49.4, 38.6, 27.3, 26.4, 22.0, 20.2; IR (film): 3280, 2997, 1757, 1707, 1610, 1460, 1346 cm^{-1} ; HRMS-ESI (m/z) $[\text{M} + \text{Na}]^+$ calcd for $\text{C}_{22}\text{H}_{22}\text{DN}_2\text{O}_3\text{ClNa}$, 422.1358; found 422.1357; $[\alpha]_{\text{D}}^{25.2} -147.6^\circ$ ($c = 1.000$, CH_2Cl_2).



Aminoketone 5.12. A Schlenk tube was charged with oxazolidinone **5.11b** (20 mg, 0.050 mmol, 1.0 equiv) and $\text{Ba(OH)}_2 \cdot 8 \text{H}_2\text{O}$ (79 mg, 0.250 mmol, 5.0 equiv). The reaction vessel was then evacuated and backfilled with N_2 five times. A 2:1 mixture of 1,4-dioxane: H_2O (1.9 mL) that had been taken through seven freeze-pump-thaw cycles prior to use was then added to the Schlenk tube. The vessel was sealed, and the reaction vessel was heated to 110 °C. After 14 h, the reaction was cooled to room temperature, and the contents were transferred to a test tube with

EtOAc (6 mL), H₂O (3 mL), and brine (3 mL). The resulting biphasic mixture was extracted with EtOAc (5 x 5 mL). The organic layers were combined, dried over MgSO₄, and evaporated under reduced pressure to afford the crude product, which was used directly in the subsequent reaction.

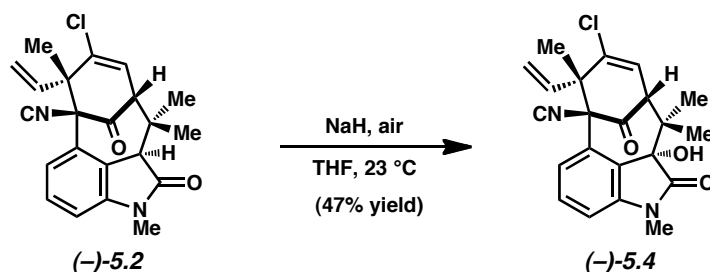
To the crude residue was added CH₂Cl₂ (1.1 mL) and TFA (4.2 μL, 0.0413 mmol, 1.1 equiv). The resulting solution was stirred at room temperature for 2 min. Dess–Martin periodinane (28 mg, 0.065 mmol, 1.3 equiv) was then added in one portion, and the vial was flushed with N₂. After stirring at room temperature for 17 h, the reaction was diluted with a 1:1 mixture of saturated aqueous solutions of NaHCO₃ and Na₂S₂O₃ (2 mL). The resulting biphasic mixture was vigorously stirred until both layers were no longer cloudy. The resulting mixture was transferred to a test tube with EtOAc (2 mL). After extracting with EtOAc (4 x 2 mL), the organic layers were combined, dried over MgSO₄, and evaporated under reduced pressure. The resulting residue was purified by flash chromatography (4:1 hexanes:EtOAc) to afford aminoketone **5.12** (12.3 mg, 66% yield, over two steps) as an amorphous solid. Aminoketone **5.12**: R_f 0.42 (1:1 hexanes:EtOAc); ¹H NMR (500 MHz, CDCl₃): δ 7.34 (d, *J* = 8.4, 1H), 7.27 (dd, *J* = 8.4, 7.6, 1H), 6.75 (d, *J* = 7.6, 1H), 6.18 (d, *J* = 4.2, 1H), 5.44 (dd, *J* = 17.3, 10.9, 1H), 5.22 (d, *J* = 10.9, 1H), 5.17 (d, *J* = 17.3, 1H), 3.82 (s, 1H), 3.18 (s, 3H), 3.15 (d, *J* = 4.2, 1H), 1.71 (br. s, 2H), 1.69 (s, 3H), 1.31 (s, 3H), 0.78 (s, 3H); ¹³C NMR (125 MHz, CDCl₃): δ 207.4, 174.7, 144.1, 140.6, 138.9, 135.2, 128.2, 124.2, 123.8, 123.7, 116.2, 107.7, 71.8, 62.8, 56.7, 53.8, 40.0, 26.4, 25.9, 21.6, 20.6; IR (film): 2973, 1709, 1698, 1609, 1583, 1457 cm⁻¹; HRMS-ESI (*m/z*) [M + H]⁺ calcd for C₂₁H₂₄N₂O₂Cl, 371.1526; found 371.1516; [α]_D^{23.8} -70.2° (*c* = 1.000, CHCl₃).



(-)-*N*-Methylwelwitindolinone Isonitrile (**5.2**). A 1-dram vial was charged with 96% formic acid (0.100 mL) and acetic anhydride (0.100 mL), and then stirred at 60 °C for 1 h. The reaction vessel was cooled to room temperature and 68 μ L of the 96% formic acid/acetic anhydride mixture was added to a solution of aminoketone **5.12** (7.5 mg, 0.0203 mmol, 1 equiv) in THF (450 μ L) at 0 °C. The reaction was stirred at 0 °C for 5 minutes, and then warmed to room temperature. After stirring for an additional 30 minutes, the reaction mixture was then transferred to a test tube containing EtOAc (1 mL) and a saturated solution of aqueous NaHCO₃ (1 mL). The resulting biphasic mixture was extracted with EtOAc (3 x 3 mL). The organic layers were combined, dried over MgSO₄, and evaporated under reduced pressure to afford the crude product, which was used directly in the subsequent reaction.

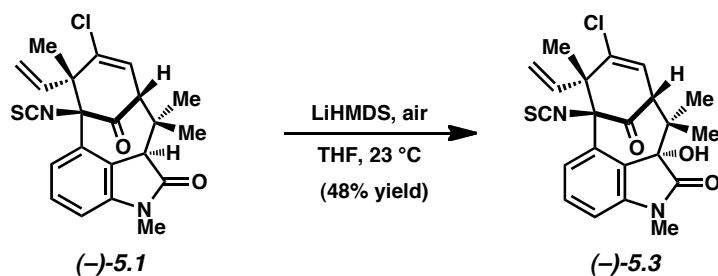
To the crude residue was added THF (1 mL) and benzene (1 mL), followed by the addition of Burgess reagent (12 mg, 0.0406 mmol, 2 equiv). The vial was flushed with N₂ and allowed to stir at room temperature for 1 h. The reaction was then filtered through a plug of silica gel (EtOAc eluent, 20 mL). The filtrate was evaporated under reduced pressure, and the resulting residue was purified by prep TLC (1:1 hexanes:EtOAc) to afford (-)-**5.2** (7.8 mg, quant. yield) as an amorphous solid. (-)-*N*-Methylwelwitindolinone C isonitrile (**5.2**). Spectral data for synthetic **5.2** was consistent with literature reports^{1b}: R_f 0.60 (1:1 hexanes:EtOAc); ¹H NMR (500 MHz, CDCl₃): δ 7.33 (ddd, *J* = 8.5, 7.7, 0.9, 1H), 7.27 (dd, *J* = 8.5, 0.9, 1H), 6.81 (dd, *J* = 7.7, 0.9, 1H), 6.18 (d, *J* = 4.4, 1H), 5.37–5.30 (m, 3H), 3.73 (s, 1H), 3.23 (d, *J* = 4.4, 1H), 3.18 (s, 3H), 1.68 (s,

3H), 1.53 (s, 3H), 0.79 (s, 3H); ^{13}C NMR (125 MHz, CDCl_3): δ 193.4, 173.9, 163.5, 144.5, 138.3, 136.2, 128.7, 127.7, 124.6, 123.3, 122.8, 118.3, 108.8, 81.9, 61.6, 55.6, 53.2, 40.7, 26.4, 25.6, 22.6, 21.3; IR (film): 2969, 2141, 1735, 1711, 1609, 1587, 1460, 1341 cm^{-1} ; HRMS-ESI (m/z) $[\text{M} + \text{Na}]^+$ calcd for $\text{C}_{22}\text{H}_{21}\text{N}_2\text{O}_2\text{ClNa}$, 403.1189; found 403.1178; $[\alpha]_D^{24.2} -90.4^\circ$ ($c = 0.25$, CH_2Cl_2).²⁷



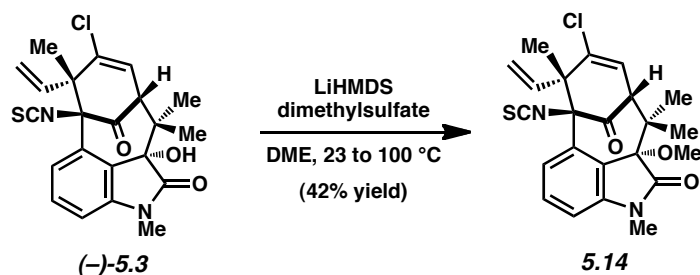
(-)-3-Hydroxy-*N*-Methylwelwitindolinone C Isonitrile (5.4). To a solution of (-)-**5.2** (7.8 mg, 0.0205 mmol, 1.0 equiv) in THF (1.1 mL) was added NaH (60% dispersion in mineral oil, 4.0 mg, 0.103 mmol, 5 equiv) in one portion. The vial was sealed under ambient atmospheric conditions and allowed to stir at room temperature. After 2.5 h, the reaction was filtered through a plug of silica gel (EtOAc eluent, 20 mL). The filtrate was evaporated under reduced pressure and the resulting residue was purified by prep TLC (1:1 hexanes:EtOAc) to afford (-)-**5.4** (3.8 mg, 47% yield) as an amorphous solid. (-)-3-Hydroxy-*N*-methylwelwitindolinone C isonitrile (**5.4**). Spectral data for synthetic **5.4** was consistent with literature reports^{1b}: R_f 0.46 (1:1 hexanes:EtOAc); ^1H NMR (500 MHz, CD_2Cl_2): δ 7.44 (dd, $J = 8.2, 7.6$, 1H), 7.33 (dd, $J = 8.2, 0.9$, 1H), 6.89 (dd, $J = 7.6, 0.9$, 1H), 6.40 (d, $J = 4.6$, 1H), 5.50 (dd, $J = 17.2, 10.4$, 1H), 5.40 (dd, $J = 17.2, 0.8$, 1H), 5.37 (dd, $J = 10.4, 0.8$, 1H), 3.18 (d, $J = 4.6$, 1H), 3.15 (s, 3H), 1.71 (s, 3H), 1.56 (s, 3H), 0.81 (s, 3H); ^{13}C NMR (125 MHz, C_6D_6): δ 192.6, 173.2, 166.5, 145.1, 137.4, 132.8, 130.3, 128.8, 126.4, 126.00, 125.98, 117.8, 109.2, 82.3, 80.2, 60.6, 55.4, 42.3, 25.6, 22.6,

22.0, 20.8; IR (film): 3395, 2973, 2922, 2142, 1723, 1610, 1587, 1459 cm^{-1} ; HRMS-ESI (m/z) $[\text{M} + \text{Na}]^+$ calcd for $\text{C}_{22}\text{H}_{21}\text{N}_2\text{O}_3\text{ClNa}$, 419.1138; found 419.1137; $[\alpha]^{23.1}_{\text{D}}$ -90.0° ($c = 0.4$, CH_2Cl_2).²⁷



(-)-3-Hydroxy-*N*-Methylwelwitindolinone C Isothiocyanate (5.3). A 1-dram vial was charged with (-)-**5.1** (2.4 mg, 0.0058 mmol, 1.0 equiv) and then sealed under ambient atmospheric conditions. THF (300 μL) was then added, followed by the dropwise addition of 100 μL of an 11 mg/mL solution of LiHMDS in THF. The reaction was stirred at room temperature for 6 h, and then another 50 μL of the LiHMDS solution was added. After an additional 90 minutes, another 50 μL of the LiHMDS solution was added and the reaction was stirred for an additional 14 h. The reaction was then filtered through a plug of silica gel (EtOAc eluent, 20 mL). The filtrate was evaporated under reduced pressure and the resulting residue was purified by prep TLC (1:1 hexanes:EtOAc) to afford (-)-**5.3** (1.2 mg, 48% yield) as an amorphous solid. (-)-3-hydroxy-*N*-methylwelwitindolinone C isothiocyanate (**5.3**)²⁰: R_f 0.46 (1:1 hexanes:EtOAc); ^1H NMR (500 MHz, CD_2Cl_2): δ 7.41 (dd, $J = 8.4, 7.6$, 1H), 7.25 (dd, $J = 8.4, 0.9$, 1H), 6.87 (dd, $J = 7.6, 0.9$, 1H), 6.40 (d, $J = 4.5$, 1H), 5.48 (dd, $J = 17.5, 10.2$, 1H), 5.33–5.29 (m, 2H), 3.21 (d, $J = 4.5$, 1H), 3.14 (s, 3H), 1.71 (s, 3H), 1.50 (s, 3H), 0.81 (s, 3H); ^{13}C NMR (125 MHz, CD_2Cl_2): δ 196.3, 173.7, 145.5, 140.7, 138.0, 133.8, 130.7, 130.6, 126.2, 126.1, 125.9, 117.9, 109.7, 84.5, 80.6, 61.1, 57.1, 42.9, 26.6, 22.9, 21.7, 21.2; IR (film): 3399, 2966, 2929, 2044, 1721, 1610, 1585,

1457 cm^{-1} ; HRMS-ESI (m/z) [$M + \text{Na}$] $^+$ calcd for $\text{C}_{22}\text{H}_{21}\text{N}_2\text{O}_3\text{SClNa}$, 451.0859; found 451.0860; $[\alpha]_{\text{D}}^{25.2} -206.0^\circ$ ($c = 1.00, \text{CH}_2\text{Cl}_2$).²⁷



Methyl Ether 5.14. To a stirred solution of (-)-**5.3** (2.3 mg, 0.0054 mmol, 1.0 equiv) in DME (200 μL) was added 100 μL of a 10 mg/mL solution of LiHMDS in DME. The reaction was stirred at room temperature for 1 h. Dimethylsulfate (10.2 μL , 0.107 mmol, 20 equiv) was added and the reaction was heated to 100 $^\circ\text{C}$. After 24 h, the reaction was cooled to room temperature and filtered through a plug of silica gel (EtOAc eluent, 20 mL). The filtrate was evaporated under reduced pressure and the resulting residue was purified by prep TLC (2:1:1 hexanes: CH_2Cl_2 : Et_2O) to afford **5.14** (1.0 mg, 42% yield) as an amorphous solid. Methyl Ether **5.14**: R_f 0.58 (1:1 hexanes:EtOAc); ^1H NMR (500 MHz, CDCl_3): δ 7.41 (dd, $J = 8.5, 7.9, 1\text{H}$), 7.32 (dd, $J = 8.5, 0.9, 1\text{H}$), 6.82 (dd, $J = 7.9, 0.9, 1\text{H}$), 6.31 (d, $J = 4.4, 1\text{H}$), 5.46 (dd, $J = 17.5, 10.1, 1\text{H}$), 5.34 (d, $J = 17.5, 1\text{H}$), 5.34 (d, $J = 10.1, 1\text{H}$), 3.19 (s, 3H), 3.16 (d, $J = 4.4, 1\text{H}$), 1.70 (s, 3H), 1.49 (s, 3H), 0.81 (s, 3H); ^{13}C NMR (125 MHz, CDCl_3): δ 196.3, 172.0, 145.7, 140.7, 137.9, 132.3, 131.1, 130.7, 126.7, 126.1, 122.1, 117.7, 108.6, 85.2, 84.4, 61.1, 56.6, 51.3, 43.7, 26.1, 22.9, 21.62, 21.55; IR (film): 2916, 2050, 1725, 1607, 1583, 1455 cm^{-1} ; HRMS-ESI (m/z) [$M + \text{Na}$] $^+$ calcd for $\text{C}_{23}\text{H}_{23}\text{N}_2\text{O}_3\text{SClNa}$, 465.1016; found 465.1028; $[\alpha]_{\text{D}}^{25.2} -118.7^\circ$ ($c = 0.15, \text{CH}_2\text{Cl}_2$).

5.9.3 Computational Data

Computed NMR Chemical Shift Data

Table 5.1. Comparison of Experimental and Computed NMR Chemical Shifts for Structure **5.4**.

¹³ C NMR Chemical Shifts (ppm)				¹ H NMR Chemical Shifts (ppm)			
Nucleus # ^a	Expt. ^b	Computed ^c Original	Computed ^c C3 epimer	Nucleus # ^a	Expt. ^b	Computed ^c Original	Computed ^c C3 epimer
N CH ₃	26.60	24.75	24.68	N CH ₃	3.15	3.02	3.00
2	173.60	171.48	172.62	OH	2.65	2.20	1.96
3	80.60	80.47	80.08	5	7.33	7.20	7.37
4	128.40	129.46	132.98	6	7.44	7.39	7.36
5	126.20	124.05	123.51	7	6.89	6.82	6.78
6	130.80	128.65	128.49	14	6.40	6.40	5.83
7	110.00	108.52	108.75	15	3.18	3.22	3.09
8	145.50	144.64	143.77	17	1.71	1.66	0.94
9	126.40	126.15	127.18	18	0.81	0.77	1.60
10	193.60	196.02	198.73	19	1.55	1.55	1.36
11	82.00	82.13	77.56	20	5.49	5.48	6.25
12	55.50	60.92	60.84	21 <i>E</i>	5.34	5.36	5.65
13	133.30	140.06	142.36	21 <i>Z</i>	5.40	5.40	5.58
14	126.00	128.32	127.63				
15	61.00	61.60	59.56				
16	42.80	48.39	47.55				
17	22.80	19.42	21.41				
18	21.20	21.49	21.51				
19	22.10	20.56	20.48				
20	137.10	139.50	140.61				
21	118.40	118.25	120.00				
23	164.30	168.17	166.42				
	CMAD^d	2.13	2.69		CMAD^d	0.08	0.36

^aSee page 316. ^bData taken from isolation report; see reference 1b. ^cConformationally averaged values – see page 317. Largest outliers are indicated in red. Note that higher than average errors are expected for the carbon atom bearing a chlorine atom (C13) – due to heavy-atom effects, and for the hydroxyl proton – due to concentration-dependent hydrogen bonding.²⁰ ^dCMAD = corrected mean absolute deviation and is computed as $\frac{1}{n} \sum_i |\delta_{\text{comp}} - \delta_{\text{exp}}|$ where δ_{comp} refers to the scaled computed chemical shifts.

Note: For the C3 epimer structure, a modest improvement in the match to experimental data is found if the C17 and C18 methyl protons are switched in their experimental assignments

(CMAD = 0.26 ppm). This amount of improvement is not sufficient to change our overall conclusion.

Table 5.2. Comparison of Experimental and Computed NMR Chemical Shifts for Structure **5.3**.

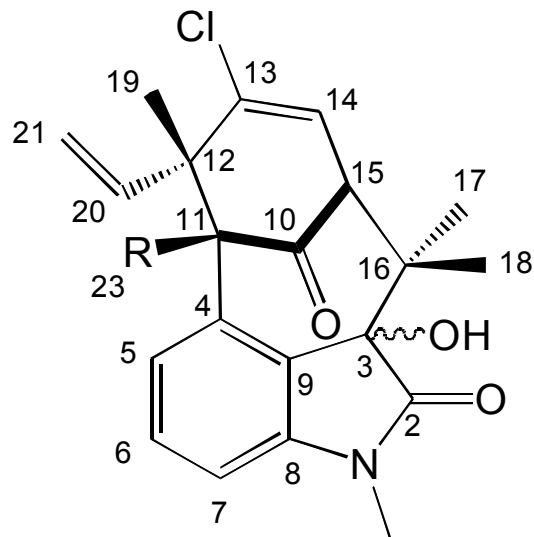
¹³ C NMR Chemical Shifts (ppm)				¹ H NMR Chemical Shifts (ppm)			
Nucleus # ^a	Expt. ^b	Computed ^c Original	Computed ^c C3 epimer	Nucleus # ^a	Expt. ^b	Computed ^c Original	Computed ^c C3 epimer
N CH ₃	26.60	24.89	24.57	N CH ₃	3.14	3.02	3.01
2	173.70	172.44	173.12	OH	<i>not obsv.</i>		
3	80.60	80.37	79.50	5	7.25	7.14	7.38
4	130.60	132.41	132.88	6	7.41	7.30	7.26
5	126.20	124.24	123.93	7	6.87	6.83	6.73
6	130.70	128.78	127.83	14	6.40	6.34	5.87
7	109.70	108.20	108.22	15	3.21	3.20	3.29
8	145.50	144.63	144.49	17	1.71	1.62	0.96
9	125.90	125.36	126.44	18	0.81	0.79	1.61
10	196.30	198.52	201.21	19	1.50	1.49	1.38
11	84.50	86.70	82.20	20	5.48	5.42	6.30
12				21 <i>E</i>	5.33–	5.25	5.56
	57.10	61.87	60.36		5.29		
13				21 <i>Z</i>	5.33–	5.30	5.42
	133.80	140.56	143.45		5.29		
14	126.10	126.98	127.83				
15	61.10	60.63	59.72				
16	42.90	48.15	47.78				
17	22.90	19.33	21.88				
18	21.70	21.38	21.69				
19	21.70	19.95	20.29				
20	138.00	141.57	142.17				
21	117.90	116.31	118.28				
23	140.60	144.85	146.31				
	CMAD^d	2.25	2.50		CMAD^d	0.06	0.33

^a See page 316). ^b Data obtained from Prof Philip Williams (University of Hawaii); see ref 20.

^cLowest energy conformation – see page 317). Largest outliers are indicated in red. Note that higher than average errors are expected for the carbon atom bearing a chlorine atom (C13) – due to heavy-atom effects, and for the hydroxyl proton – due to concentration-dependent hydrogen bonding.²⁰ ^dCMAD = corrected mean absolute deviation and is computed as $\frac{1}{n} \sum |\delta_{\text{comp}} - \delta_{\text{exp}}|$ where δ_{comp}

refers to the scaled computed chemical shifts. Where the experimental value is a range, the mean value is used.

Atom #'s used in Tables 5.1 & 5.2, taken from reference **1b**.



Methods

General

Calculations (geometry optimization, frequency, and NMR chemical shift) were performed on C3-hydroxyl-N-methylwelwitindolinone C isonitrile (structure **5.4**) and its C3 epimer, as well as C3-hydroxyl-N-methylwelwitindolinone C isothiocyanate (structure **5.3**) and its C3 epimer.

Calculations were performed with GAUSSIAN09.²⁸ Geometries were optimized in the gas-phase using the B3LYP/6-31+G(d,p)²⁹ level of theory. Frequency calculations (at 298.15 K) at the same level of theory were used to confirm the nature of all stationary points as minima and also provided values for computed free energies. NMR single point calculations (GIAO)³⁰ were performed on these geometries at the mPW1PW91/6-311+G(d,p)³¹ level of theory in an implicit chloroform solvent continuum (SMD³² method).

Conformational Analysis

For structure **5.4** and its C3 epimer, nine candidate conformers (three conformations of the vinyl group and three conformations of the hydroxyl group) for each epimer were subjected to geometry optimization. This resulted in four unique conformers for structure **5.4** and six unique conformers of its C3 epimer. For both epimers, Boltzmann-weighted averaging of the computed chemical shifts based on the relative computed free energies at 298.15 K of each conformer was performed, using the equation below to determine relative populations.

$$\frac{P_i}{P_j} = e^{\frac{-(E_i - E_j)}{RT}}$$

P_i = population of conformer i relative to lowest energy conformer j
 E_i, E_j = computed free energies (in J/mol)
 R = molar gas constant (8.314510 J mol⁻¹ K⁻¹)
 T = 298.15 K

The relative populations were then converted to Boltzmann-weighting factors by means of a set of linear equations.

Although only one conformer of the ring system seemed to be likely, both epimers of structure **5.4** were subjected to a conformational search (in Spartan'10).³³ As expected, only a single conformation of the ring system was found in each case.

For the isothiocyanate structure **5.3**, the major contributing (lowest energy) conformer of isonitrile structure **5.4** was converted into the corresponding isothiocyanate, and subjected to geometry optimization, followed by frequency and NMR chemical shift calculations (for both epimers).

Empirical Scaling of Computed NMR Chemical Shifts

Computed chemical shifts are commonly scaled empirically in order to remove systematic error that results from a variety of sources. The scaling factors themselves are generally determined by comparison of computed NMR data with known experimental chemical shifts for large databases of molecules. These factors (slope and intercept from a best fit line) are specific for each level of theory used computationally. We have generated numerous such scaling factors for ^1H and ^{13}C chemical shifts utilizing a database originally compiled by Rablen and co-workers and have made them available on our web site at <http://cheshirenmr.info>.

One of our preferred methods for obtaining high quality computed chemical shifts at reasonable costs is to use mPW1PW91/6-311+G(2d,p) NMR calculations (with the SMD chloroform continuum model) on B3LYP/6-31+G(d,p) geometries. After scaling, this method produces average errors (CMAD's) of 0.11-0.15 ppm for ^1H and 1.8-2.5 ppm for ^{13}C on diverse sets of small organic molecules. Details and numerous references on linear regression methods applied to computed chemical shifts can be found in our review paper.²²

The specific scaling factors used in this study are given below and are applied to the computed NMR isotropic shielding constants by way of the equation shown.

$$\begin{array}{l} \delta = \text{computed chemical shift relative to TMS} \\ \sigma = \text{computed isotropic shielding constant} \\ m = \text{slope, } b = \text{intercept} \end{array} \quad \delta = \frac{b - \sigma}{-m}$$

DP4 Probability Analysis

For further support of our assignment to the C3(*S*) diastereomer for isonitrile structure **5.4**, we utilized the DP4 probability analysis of Smith and Goodman.³⁴ When both possible epimers were compared to the experimental data, the analysis suggested a 67.5% probability of C3(*S*) being correct based on the ¹³C data, a 100% probability based on the ¹H data, and a 100% probability based on both sets of data.

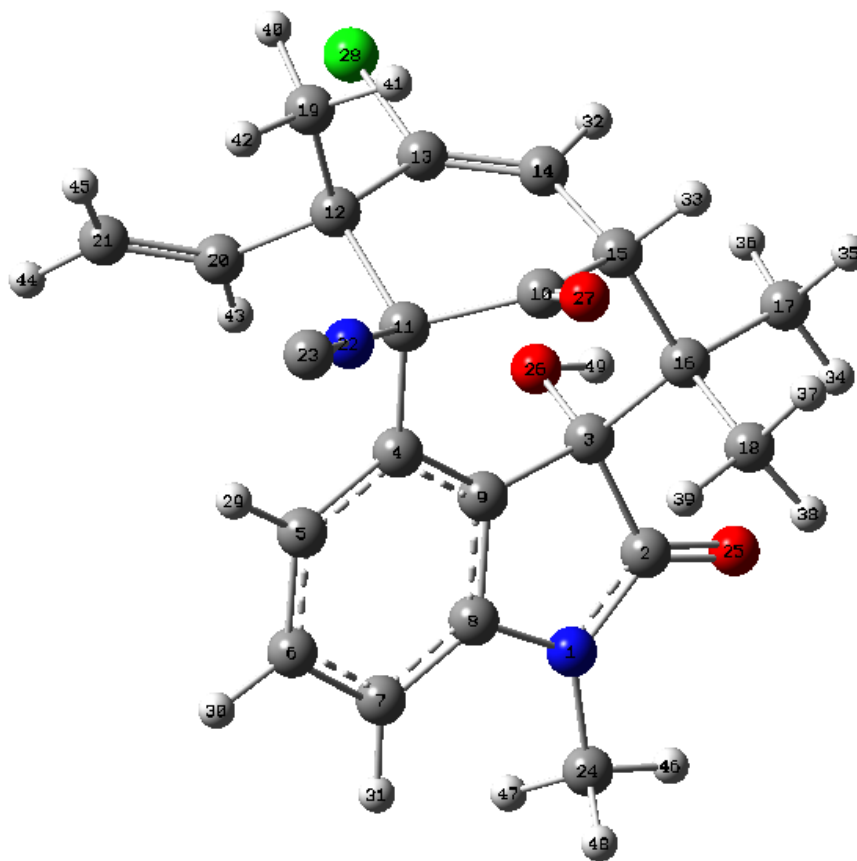
Energies, coordinates, and NMR isotropic shielding constants

Structure 5.4, conformer 1

Sum of electronic and thermal free energies = -1645.99519 H

Center Number	Atomic Number	Coordinates (Angstroms)		
		X	Y	Z
1	7	-3.380511	0.751109	-0.617354
2	6	-3.108729	-0.579788	-0.477610
3	6	-1.576958	-0.739243	-0.229973
4	6	0.100593	1.342374	0.224316
5	6	0.166355	2.747156	0.083118
6	6	-0.926998	3.509133	-0.308650
7	6	-2.164939	2.908981	-0.547955
8	6	-2.224961	1.528726	-0.433403
9	6	-1.115549	0.717867	-0.099250
10	6	0.911574	-0.488942	1.794213
11	6	1.361546	0.651230	0.832091
12	6	2.441035	0.080430	-0.232322
13	6	1.991257	-1.302366	-0.688458
14	6	1.114541	-2.103441	-0.085843
15	6	0.340831	-1.738622	1.154370
16	6	-1.226129	-1.694004	0.949197
17	6	-1.694972	-3.141817	0.675179
18	6	-1.918249	-1.203489	2.239070
19	6	3.813867	-0.103077	0.460532
20	6	2.502368	1.034876	-1.415368
21	6	3.497088	1.873522	-1.710270
22	7	2.033204	1.616907	1.637432
23	6	2.586836	2.357422	2.363512
24	6	-4.681175	1.269742	-0.999762
25	8	-3.902935	-1.495419	-0.652588
26	8	-1.090993	-1.225047	-1.496027
27	8	1.040237	-0.387499	2.994192
28	17	2.810643	-1.908346	-2.135113
29	1	1.094865	3.254364	0.304017
30	1	-0.819288	4.585337	-0.400957
31	1	-3.037307	3.497044	-0.810138
32	1	0.936332	-3.087914	-0.503238
33	1	0.500607	-2.520825	1.907413
34	1	-2.776929	-3.181623	0.543748
35	1	-1.426114	-3.773261	1.528812
36	1	-1.231478	-3.576643	-0.214547
37	1	-1.578758	-1.786674	3.099890
38	1	-3.002030	-1.330487	2.154846
39	1	-1.711653	-0.151953	2.456298
40	1	4.498705	-0.599373	-0.230537
41	1	3.714525	-0.727653	1.352535
42	1	4.252712	0.847527	0.762572
43	1	1.626966	1.010046	-2.060573
44	1	3.429437	2.518753	-2.581112
45	1	4.403556	1.951460	-1.119072
46	1	-5.361472	0.421841	-1.084425
47	1	-4.622074	1.785227	-1.964582
48	1	-5.056951	1.965669	-0.242570
49	1	-1.689279	-1.931402	-1.787016

2	C	Isotropic =	5.3824	29	H	Isotropic =	23.9179
3	C	Isotropic =	101.9705	30	H	Isotropic =	23.7070
4	C	Isotropic =	49.7929	31	H	Isotropic =	24.3199
5	C	Isotropic =	55.7165	32	H	Isotropic =	24.8577
6	C	Isotropic =	51.0288	33	H	Isotropic =	28.2880
7	C	Isotropic =	72.1794	34	H	Isotropic =	29.1701
8	C	Isotropic =	34.1558	35	H	Isotropic =	30.8685
9	C	Isotropic =	53.9450	36	H	Isotropic =	30.0279
10	C	Isotropic =	-20.0573	37	H	Isotropic =	30.5775
11	C	Isotropic =	100.0258	38	H	Isotropic =	30.8627
12	C	Isotropic =	122.5598	39	H	Isotropic =	31.4457
13	C	Isotropic =	39.6653	40	H	Isotropic =	30.0039
14	C	Isotropic =	51.8523	41	H	Isotropic =	30.6930
15	C	Isotropic =	121.7132	42	H	Isotropic =	29.6167
16	C	Isotropic =	135.6107	43	H	Isotropic =	25.8003
17	C	Isotropic =	166.2994	44	H	Isotropic =	25.9664
18	C	Isotropic =	164.0007	45	H	Isotropic =	25.8850
19	C	Isotropic =	165.0069	46	H	Isotropic =	27.5588
20	C	Isotropic =	39.3145	47	H	Isotropic =	28.9537
21	C	Isotropic =	62.5941	48	H	Isotropic =	28.9597
23	C	Isotropic =	9.4942	49	H	Isotropic =	29.4283
24	C	Isotropic =	160.3779				

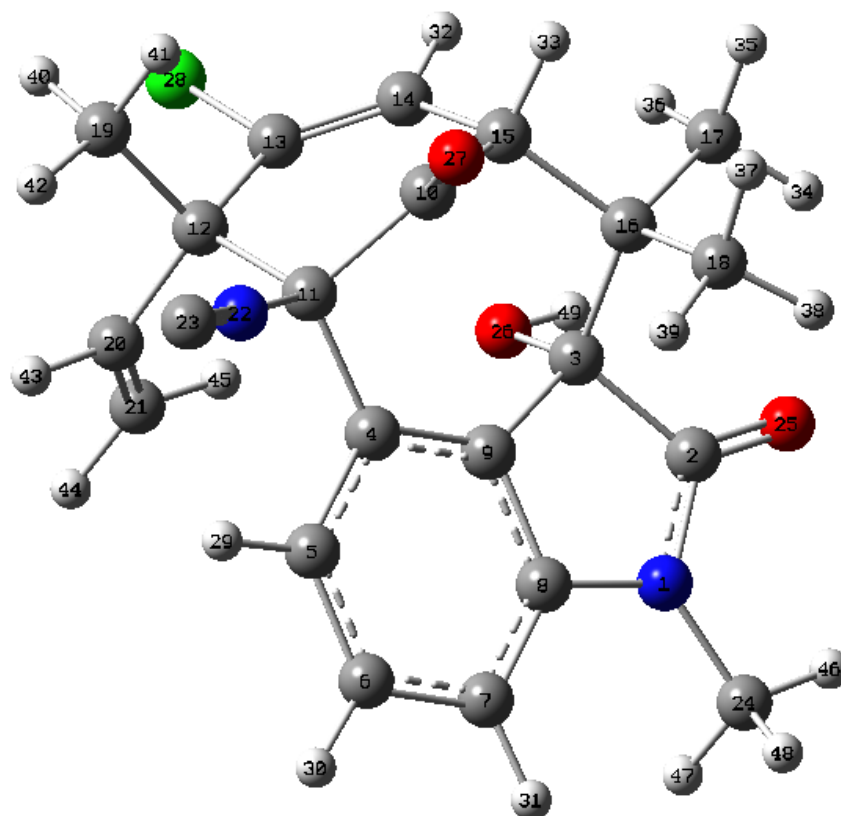


Structure 5.4, conformer 2

Sum of electronic and thermal free energies = -1645.992378 H

Center Number	Atomic Number	Coordinates (Angstroms)		
		X	Y	Z
1	7	-3.389910	0.411641	-0.584188
2	6	-2.965521	-0.872239	-0.398840
3	6	-1.427194	-0.846062	-0.141642
4	6	0.012876	1.426251	0.172806
5	6	-0.088399	2.823398	-0.011922
6	6	-1.268385	3.441804	-0.404375
7	6	-2.431329	2.695800	-0.605917
8	6	-2.329062	1.322773	-0.445527
9	6	-1.129801	0.657371	-0.101630
10	6	1.030557	-0.187507	1.832779
11	6	1.356655	0.894958	0.758969
12	6	2.436090	0.330558	-0.322514
13	6	2.169786	-1.147259	-0.573941
14	6	1.396904	-1.962253	0.142545
15	6	0.567402	-1.538793	1.325806
16	6	-0.991904	-1.665159	1.111119
17	6	-1.311230	-3.169442	0.949863
18	6	-1.738553	-1.147243	2.358981
19	6	3.869594	0.421973	0.274214
20	6	2.371154	1.204721	-1.566937
21	6	1.672684	0.966313	-2.677686
22	7	1.980856	1.972917	1.454311
23	6	2.499432	2.806413	2.101395
24	6	-4.742986	0.763434	-0.974618
25	8	-3.645808	-1.880969	-0.539796
26	8	-0.879667	-1.372703	-1.364425
27	8	1.169300	0.037695	3.014619
28	17	3.113201	-1.882915	-1.883336
29	1	0.776650	3.444181	0.173272
30	1	-1.286911	4.519781	-0.530763
31	1	-3.369095	3.170462	-0.871934
32	1	1.366618	-3.013474	-0.122288
33	1	0.786676	-2.220689	2.157072
34	1	-2.383033	-3.328798	0.826617
35	1	-0.982069	-3.705397	1.846601
36	1	-0.803240	-3.618029	0.092046
37	1	-1.359121	-1.638557	3.259701
38	1	-2.806525	-1.374337	2.280869
39	1	-1.625833	-0.069313	2.502672
40	1	4.565784	-0.076892	-0.403155
41	1	3.926828	-0.068257	1.250262
42	1	4.188723	1.458815	0.387579
43	1	2.951041	2.123283	-1.491520
44	1	1.689639	1.674541	-3.500899
45	1	1.066322	0.074939	-2.805571
46	1	-5.322154	-0.159042	-1.024872
47	1	-4.746801	1.248298	-1.956963
48	1	-5.193416	1.438110	-0.239220
49	1	-1.404343	-2.153019	-1.604425

2	C	Isotropic =	4.9313	29	H	Isotropic =	23.8898
3	C	Isotropic =	101.8846	30	H	Isotropic =	23.7819
4	C	Isotropic =	47.7504	31	H	Isotropic =	24.3539
5	C	Isotropic =	56.1850	32	H	Isotropic =	24.8360
6	C	Isotropic =	50.5833	33	H	Isotropic =	28.3687
7	C	Isotropic =	72.3931	34	H	Isotropic =	29.2774
8	C	Isotropic =	34.0780	35	H	Isotropic =	30.8967
9	C	Isotropic =	54.5485	36	H	Isotropic =	29.9107
10	C	Isotropic =	-19.4205	37	H	Isotropic =	30.6386
11	C	Isotropic =	98.4760	38	H	Isotropic =	30.9444
12	C	Isotropic =	120.3660	39	H	Isotropic =	31.4424
13	C	Isotropic =	39.7763	40	H	Isotropic =	29.7032
14	C	Isotropic =	48.9210	41	H	Isotropic =	30.6575
15	C	Isotropic =	121.5678	42	H	Isotropic =	29.9034
16	C	Isotropic =	135.6714	43	H	Isotropic =	25.7159
17	C	Isotropic =	166.5375	44	H	Isotropic =	26.1295
18	C	Isotropic =	164.1755	45	H	Isotropic =	26.4239
19	C	Isotropic =	158.0736	46	H	Isotropic =	27.5589
20	C	Isotropic =	40.9847	47	H	Isotropic =	28.9945
21	C	Isotropic =	54.8881	48	H	Isotropic =	28.9520
23	C	Isotropic =	7.6178	49	H	Isotropic =	29.4036
24	C	Isotropic =	160.4337				

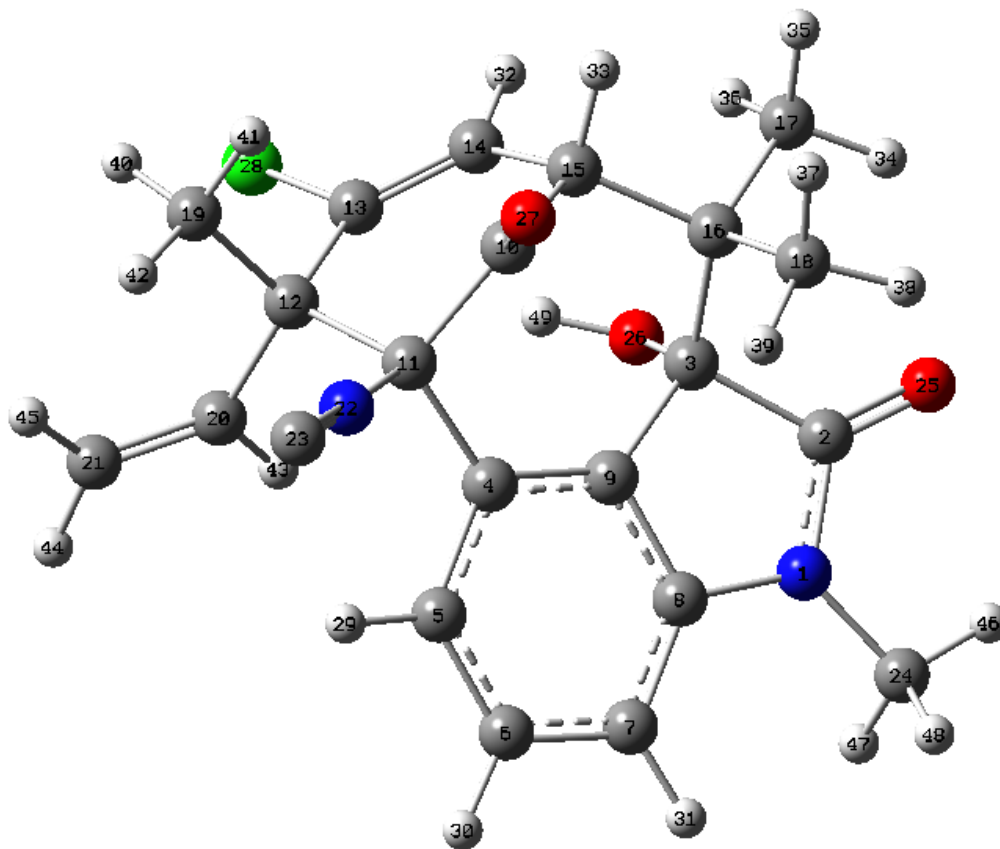


Structure 5.4, conformer 3

Sum of electronic and thermal free energies = -1645.993819 H

Center Number	Atomic Number	Coordinates (Angstroms)		
		X	Y	Z
1	7	-3.368932	0.825648	-0.629677
2	6	-3.157544	-0.516396	-0.430269
3	6	-1.615809	-0.722439	-0.255060
4	6	0.110041	1.315147	0.269538
5	6	0.216937	2.720030	0.145044
6	6	-0.846054	3.511664	-0.269219
7	6	-2.092278	2.944669	-0.546407
8	6	-2.196843	1.566140	-0.436883
9	6	-1.116419	0.723442	-0.077750
10	6	0.893998	-0.610775	1.760484
11	6	1.349943	0.587841	0.876648
12	6	2.449760	0.069134	-0.194197
13	6	1.964466	-1.253081	-0.780820
14	6	1.076899	-2.090895	-0.235152
15	6	0.318438	-1.813115	1.038195
16	6	-1.251673	-1.752414	0.852265
17	6	-1.730562	-3.171703	0.473467
18	6	-1.918724	-1.347152	2.184506
19	6	3.784465	-0.234372	0.531732
20	6	2.603352	1.114144	-1.288207
21	6	3.654511	1.911392	-1.484484
22	7	2.010776	1.505779	1.742841
23	6	2.556233	2.206743	2.513309
24	6	-4.666021	1.390904	-0.949739
25	8	-4.017924	-1.377950	-0.464930
26	8	-1.278846	-1.185915	-1.578005
27	8	1.025223	-0.591597	2.963826
28	17	2.785009	-1.759528	-2.265224
29	1	1.151272	3.201081	0.398496
30	1	-0.709502	4.585596	-0.349512
31	1	-2.941161	3.557803	-0.827679
32	1	0.888501	-3.043511	-0.719605
33	1	0.487428	-2.651677	1.725197
34	1	-2.816004	-3.189593	0.373942
35	1	-1.437135	-3.875270	1.260605
36	1	-1.313172	-3.510827	-0.476299
37	1	-1.562267	-1.983655	2.999523
38	1	-3.002208	-1.472190	2.108315
39	1	-1.710453	-0.310705	2.465781
40	1	4.481365	-0.696440	-0.171052
41	1	3.625627	-0.926805	1.362777
42	1	4.242145	0.670104	0.931887
43	1	1.750170	1.203559	-1.957080
44	1	3.652028	2.630787	-2.297749
45	1	4.544204	1.883991	-0.864411
46	1	-5.377827	0.566846	-1.006027
47	1	-4.632832	1.908513	-1.914460
48	1	-4.985630	2.095613	-0.174126
49	1	-0.322909	-1.100994	-1.701002

2	C	Isotropic =	8.2332	29	H	Isotropic =	23.9698
3	C	Isotropic =	100.9151	30	H	Isotropic =	23.7605
4	C	Isotropic =	52.2624	31	H	Isotropic =	24.4222
5	C	Isotropic =	56.4224	32	H	Isotropic =	24.6004
6	C	Isotropic =	51.0441	33	H	Isotropic =	28.2420
7	C	Isotropic =	72.3600	34	H	Isotropic =	28.9353
8	C	Isotropic =	34.2295	35	H	Isotropic =	30.8612
9	C	Isotropic =	52.2202	36	H	Isotropic =	29.6794
10	C	Isotropic =	-19.6241	37	H	Isotropic =	30.4989
11	C	Isotropic =	100.3225	38	H	Isotropic =	30.7159
12	C	Isotropic =	122.0071	39	H	Isotropic =	31.5247
13	C	Isotropic =	36.0314	40	H	Isotropic =	30.1151
14	C	Isotropic =	50.0042	41	H	Isotropic =	30.6694
15	C	Isotropic =	121.3573	42	H	Isotropic =	29.6456
16	C	Isotropic =	135.2910	43	H	Isotropic =	25.8986
17	C	Isotropic =	165.0367	44	H	Isotropic =	25.7683
18	C	Isotropic =	163.3592	45	H	Isotropic =	25.7723
19	C	Isotropic =	166.0095	46	H	Isotropic =	27.5553
20	C	Isotropic =	40.3261	47	H	Isotropic =	28.9550
21	C	Isotropic =	61.0648	48	H	Isotropic =	29.0701
23	C	Isotropic =	9.3674	49	H	Isotropic =	29.2466
24	C	Isotropic =	160.7578				

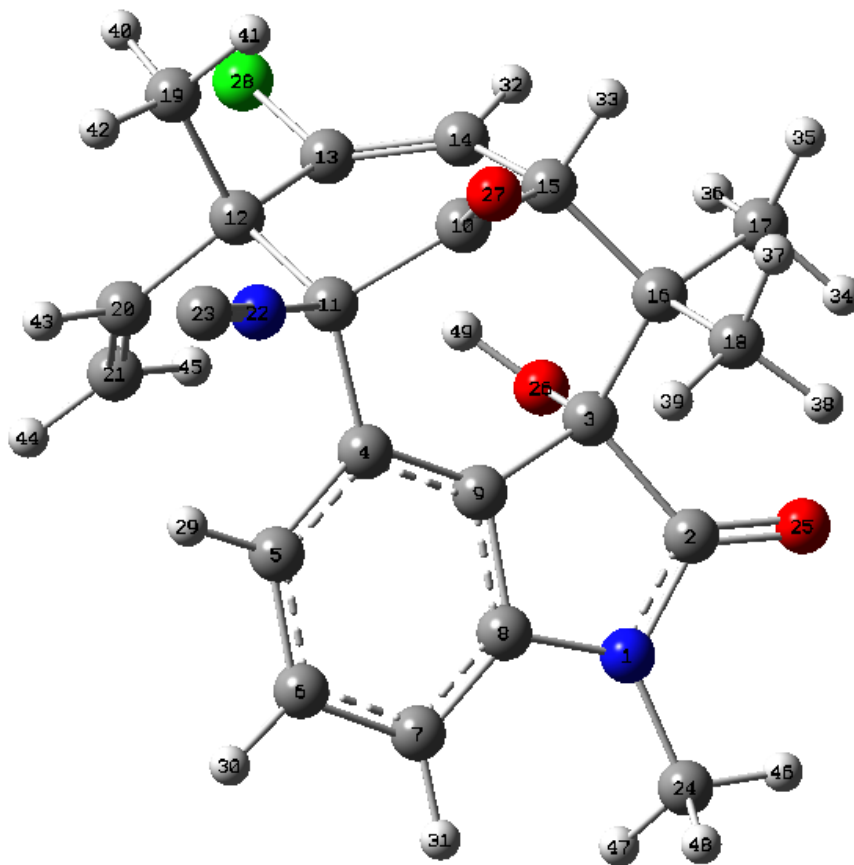


Structure 5.4, conformer 4

Sum of electronic and thermal free energies = -1645.990807 H

Center Number	Atomic Number	Coordinates (Angstroms)		
		X	Y	Z
1	7	-3.383740	0.566778	-0.610315
2	6	-3.053866	-0.749632	-0.404647
3	6	-1.502026	-0.816780	-0.214802
4	6	0.041698	1.369611	0.272369
5	6	0.019676	2.777398	0.141515
6	6	-1.111888	3.469606	-0.267287
7	6	-2.302822	2.791942	-0.538165
8	6	-2.281883	1.410361	-0.422782
9	6	-1.130076	0.669650	-0.061469
10	6	0.985067	-0.440706	1.799880
11	6	1.344407	0.756735	0.872524
12	6	2.471665	0.293020	-0.205474
13	6	2.119896	-1.097394	-0.718871
14	6	1.302069	-1.977261	-0.128904
15	6	0.502608	-1.706429	1.120501
16	6	-1.064392	-1.781722	0.924539
17	6	-1.419350	-3.245934	0.582480
18	6	-1.770669	-1.396033	2.241871
19	6	3.848229	0.151181	0.507979
20	6	2.589793	1.375056	-1.266159
21	6	2.063455	1.389910	-2.491065
22	7	1.949458	1.746286	1.702698
23	6	2.450688	2.501879	2.451465
24	6	-4.725876	1.012629	-0.932908
25	8	-3.833050	-1.685569	-0.439157
26	8	-1.108252	-1.282675	-1.518983
27	8	1.118726	-0.370258	3.001027
28	17	3.064853	-1.681170	-2.100933
29	1	0.906429	3.344477	0.387287
30	1	-1.072432	4.551192	-0.351229
31	1	-3.204506	3.324865	-0.818126
32	1	1.228235	-2.977031	-0.544828
33	1	0.731191	-2.503770	1.838738
34	1	-2.499142	-3.360044	0.484947
35	1	-1.066253	-3.902404	1.385728
36	1	-0.973398	-3.569377	-0.359684
37	1	-1.371713	-1.981726	3.075163
38	1	-2.840486	-1.607855	2.163737
39	1	-1.645868	-0.339626	2.496583
40	1	4.568505	-0.279372	-0.191013
41	1	3.779438	-0.504005	1.381016
42	1	4.225967	1.121416	0.832729
43	1	3.160923	2.240385	-0.934546
44	1	2.211380	2.246374	-3.141755
45	1	1.480996	0.570431	-2.899529
46	1	-5.360630	0.127838	-0.989069
47	1	-4.738278	1.530177	-1.898183
48	1	-5.108798	1.686745	-0.158694
49	1	-0.151893	-1.164749	-1.608721

2	C	Isotropic =	8.2386	29	H	Isotropic =	23.9665
3	C	Isotropic =	100.8098	30	H	Isotropic =	23.7824
4	C	Isotropic =	50.6591	31	H	Isotropic =	24.4111
5	C	Isotropic =	55.8937	32	H	Isotropic =	24.4481
6	C	Isotropic =	51.4584	33	H	Isotropic =	28.2770
7	C	Isotropic =	72.3683	34	H	Isotropic =	28.9619
8	C	Isotropic =	34.4162	35	H	Isotropic =	30.8492
9	C	Isotropic =	52.3402	36	H	Isotropic =	29.6213
10	C	Isotropic =	-19.4601	37	H	Isotropic =	30.5030
11	C	Isotropic =	99.3093	38	H	Isotropic =	30.7587
12	C	Isotropic =	119.5882	39	H	Isotropic =	31.5047
13	C	Isotropic =	36.6404	40	H	Isotropic =	29.7433
14	C	Isotropic =	46.8267	41	H	Isotropic =	30.5658
15	C	Isotropic =	121.3607	42	H	Isotropic =	29.8611
16	C	Isotropic =	135.3283	43	H	Isotropic =	25.4891
17	C	Isotropic =	165.1747	44	H	Isotropic =	26.0009
18	C	Isotropic =	163.5269	45	H	Isotropic =	26.6548
19	C	Isotropic =	159.0525	46	H	Isotropic =	27.5470
20	C	Isotropic =	42.1685	47	H	Isotropic =	28.9975
21	C	Isotropic =	56.4925	48	H	Isotropic =	29.0701
23	C	Isotropic =	8.0406	49	H	Isotropic =	29.0085
24	C	Isotropic =	160.7613				

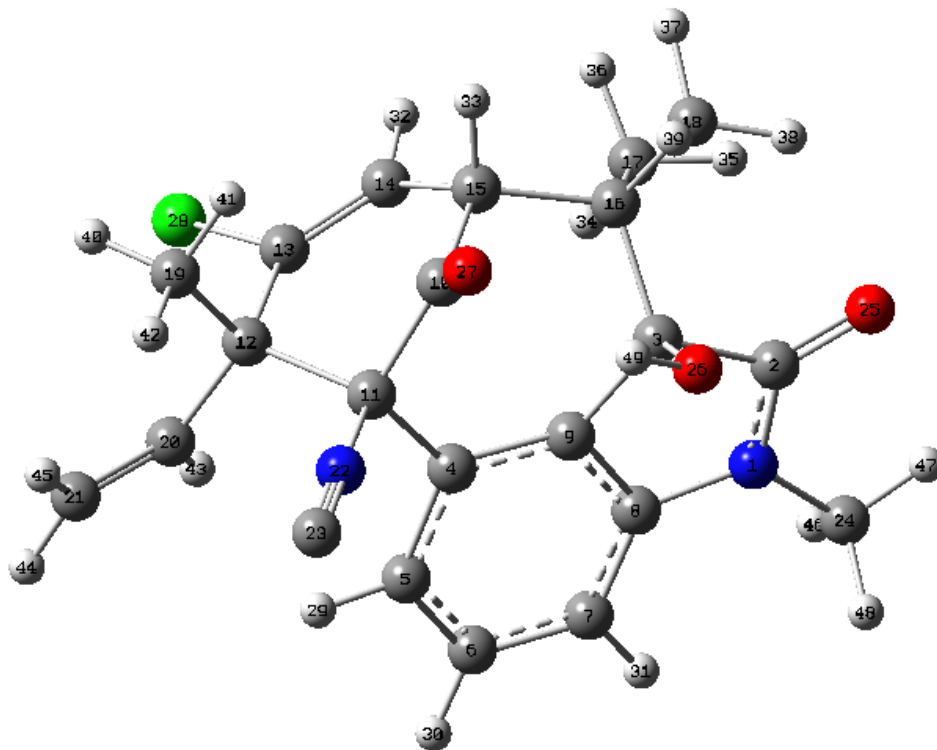


Structure 5.4, C3 epimer, conformer 1

Sum of electronic and thermal free energies = -1645.990153 H

Center Number	Atomic Number	Coordinates (Angstroms)		
		X	Y	Z
1	7	-3.288099	1.175668	-0.492135
2	6	-3.342285	-0.126122	-0.051393
3	6	-1.919172	-0.517146	0.467896
4	6	0.216887	1.116132	0.417828
5	6	0.574596	2.469902	0.244971
6	6	-0.328608	3.404260	-0.250180
7	6	-1.640543	3.038434	-0.570087
8	6	-2.007208	1.721176	-0.330716
9	6	-1.109312	0.751089	0.163076
10	6	0.677127	-1.267257	1.184698
11	6	1.289584	0.140867	0.966776
12	6	2.575046	-0.092689	0.000328
13	6	2.049458	-0.793428	-1.248061
14	6	0.990422	-1.602758	-1.280469
15	6	0.181495	-1.977392	-0.064002
16	6	-1.406789	-1.847788	-0.199949
17	6	-1.804230	-1.873909	-1.691333
18	6	-2.052391	-3.058982	0.505371
19	6	3.567136	-1.054323	0.705381
20	6	3.251073	1.220955	-0.359613
21	6	4.341876	1.730577	0.216459
22	7	1.754250	0.642592	2.213633
23	6	2.123883	1.053143	3.252223
24	6	-4.450401	1.908166	-0.958184
25	8	-4.337098	-0.828475	-0.041046
26	8	-2.162345	-0.633914	1.873909
27	8	0.582003	-1.758320	2.292595
28	17	3.012929	-0.604441	-2.717114
29	1	1.565825	2.796251	0.528119
30	1	-0.012579	4.435246	-0.376291
31	1	-2.349097	3.766197	-0.949937
32	1	0.745583	-2.103865	-2.209250
33	1	0.362853	-3.043980	0.123176
34	1	-1.454774	-0.989199	-2.233915
35	1	-2.890367	-1.935564	-1.783427
36	1	-1.388636	-2.758513	-2.183704
37	1	-1.801792	-3.972569	-0.046034
38	1	-3.138164	-2.948786	0.529867
39	1	-1.696158	-3.173178	1.531216
40	1	4.421744	-1.229297	0.047779
41	1	3.103579	-2.019656	0.922715
42	1	3.929574	-0.637874	1.646851
43	1	2.788680	1.770696	-1.173443
44	1	4.746011	2.680106	-0.121828
45	1	4.868284	1.245979	1.031658
46	1	-4.286205	2.289523	-1.971632
47	1	-5.294088	1.217278	-0.961382
48	1	-4.673133	2.747444	-0.289889
49	1	-1.356329	-0.880342	2.350000

2	C	Isotropic =	8.1779	29	H	Isotropic =	23.7702
3	C	Isotropic =	101.0505	30	H	Isotropic =	23.7763
4	C	Isotropic =	47.8541	31	H	Isotropic =	24.4329
5	C	Isotropic =	57.3462	32	H	Isotropic =	25.3772
6	C	Isotropic =	51.2848	33	H	Isotropic =	28.2214
7	C	Isotropic =	71.9486	34	H	Isotropic =	31.0741
8	C	Isotropic =	35.1191	35	H	Isotropic =	30.3962
9	C	Isotropic =	50.6689	36	H	Isotropic =	30.6682
10	C	Isotropic =	-31.7935	37	H	Isotropic =	30.6696
11	C	Isotropic =	103.2573	38	H	Isotropic =	29.3534
12	C	Isotropic =	123.3461	39	H	Isotropic =	29.7256
13	C	Isotropic =	36.3752	40	H	Isotropic =	30.2138
14	C	Isotropic =	53.0628	41	H	Isotropic =	30.9754
15	C	Isotropic =	124.3429	42	H	Isotropic =	29.6424
16	C	Isotropic =	136.0421	43	H	Isotropic =	24.9394
17	C	Isotropic =	162.8294	44	H	Isotropic =	25.6098
18	C	Isotropic =	161.6207	45	H	Isotropic =	25.7081
19	C	Isotropic =	164.8084	46	H	Isotropic =	29.0151
20	C	Isotropic =	39.1842	47	H	Isotropic =	27.6030
21	C	Isotropic =	59.8987	48	H	Isotropic =	29.0021
23	C	Isotropic =	10.1194	49	H	Isotropic =	29.7586
24	C	Isotropic =	160.7944				

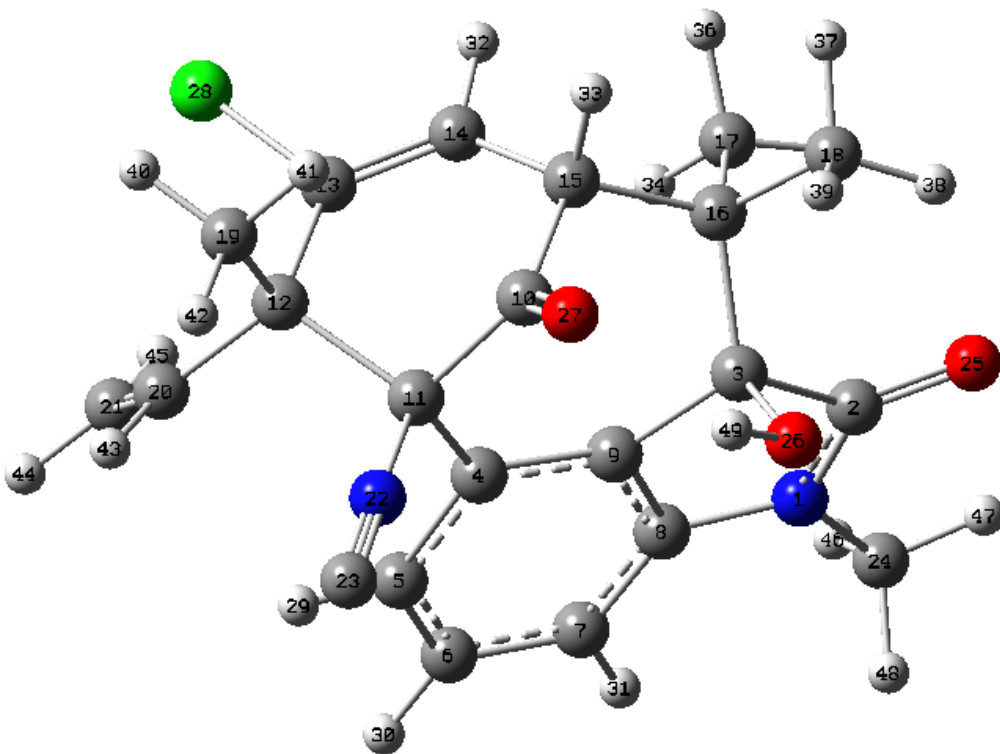


Structure 5.4, C3 epimer, conformer 2

Sum of electronic and thermal free energies = -1645.984941 H

Center Number	Atomic Number	Coordinates (Angstroms)		
		X	Y	Z
1	7	-3.278393	1.117972	-0.533461
2	6	-3.310383	-0.209469	-0.178852
3	6	-1.902906	-0.587507	0.389296
4	6	0.185832	1.105916	0.535168
5	6	0.498441	2.480029	0.471956
6	6	-0.414085	3.416622	-0.001700
7	6	-1.694216	3.031209	-0.411083
8	6	-2.023780	1.689516	-0.276956
9	6	-1.117140	0.717749	0.196082
10	6	0.678948	-1.295351	1.201769
11	6	1.266480	0.132206	1.075058
12	6	2.607114	-0.025916	0.162271
13	6	2.176542	-0.689437	-1.139566
14	6	1.130719	-1.511176	-1.253244
15	6	0.261511	-1.951592	-0.102602
16	6	-1.317902	-1.862164	-0.319460
17	6	-1.631250	-1.813554	-1.830465
18	6	-1.963050	-3.129295	0.280033
19	6	3.588562	-1.007686	0.872083
20	6	3.341014	1.300907	0.055371
21	6	3.389177	2.161408	-0.962656
22	7	1.668367	0.584181	2.365535
23	6	1.977950	0.945099	3.441586
24	6	-4.440003	1.843416	-1.011636
25	8	-4.279727	-0.942319	-0.263731
26	8	-2.211929	-0.787911	1.773533
27	8	0.548325	-1.842008	2.279464
28	17	3.272230	-0.583978	-2.525662
29	1	1.463443	2.821562	0.813100
30	1	-0.129282	4.463551	-0.041017
31	1	-2.410581	3.759099	-0.775830
32	1	0.969213	-2.010491	-2.201256
33	1	0.466678	-3.020853	0.041535
34	1	-1.277141	-0.890238	-2.301119
35	1	-2.708330	-1.897056	-1.988036
36	1	-1.163913	-2.657356	-2.347271
37	1	-1.653516	-4.002908	-0.305300
38	1	-3.051393	-3.051544	0.248445
39	1	-1.661113	-3.290452	1.316941
40	1	4.477093	-1.126810	0.246868
41	1	3.145988	-1.995540	1.023409
42	1	3.899830	-0.615425	1.842892
43	1	3.899484	1.542858	0.957834
44	1	3.981398	3.068289	-0.877126
45	1	2.857633	2.015263	-1.895536
46	1	-4.242538	2.286829	-1.993526
47	1	-5.261236	1.130562	-1.092827
48	1	-4.718029	2.636531	-0.308601
49	1	-1.420214	-1.020993	2.279312

2	C	Isotropic =	8.5407	29	H	Isotropic =	23.7140
3	C	Isotropic =	100.7337	30	H	Isotropic =	23.8762
4	C	Isotropic =	48.2975	31	H	Isotropic =	24.4155
5	C	Isotropic =	56.1226	32	H	Isotropic =	25.3406
6	C	Isotropic =	52.0942	33	H	Isotropic =	28.1967
7	C	Isotropic =	72.0936	34	H	Isotropic =	31.0889
8	C	Isotropic =	35.5088	35	H	Isotropic =	30.4055
9	C	Isotropic =	50.9200	36	H	Isotropic =	30.6679
10	C	Isotropic =	-31.9216	37	H	Isotropic =	30.7191
11	C	Isotropic =	103.7739	38	H	Isotropic =	29.3263
12	C	Isotropic =	120.9632	39	H	Isotropic =	29.6950
13	C	Isotropic =	38.4030	40	H	Isotropic =	29.8207
14	C	Isotropic =	50.6647	41	H	Isotropic =	30.8758
15	C	Isotropic =	123.5190	42	H	Isotropic =	29.8531
16	C	Isotropic =	137.1848	43	H	Isotropic =	25.2441
17	C	Isotropic =	162.7858	44	H	Isotropic =	25.4090
18	C	Isotropic =	161.7333	45	H	Isotropic =	26.1240
19	C	Isotropic =	159.8194	46	H	Isotropic =	29.0313
20	C	Isotropic =	43.5803	47	H	Isotropic =	27.5970
21	C	Isotropic =	52.4288	48	H	Isotropic =	29.0234
23	C	Isotropic =	9.4675	49	H	Isotropic =	29.7756
24	C	Isotropic =	160.9283				

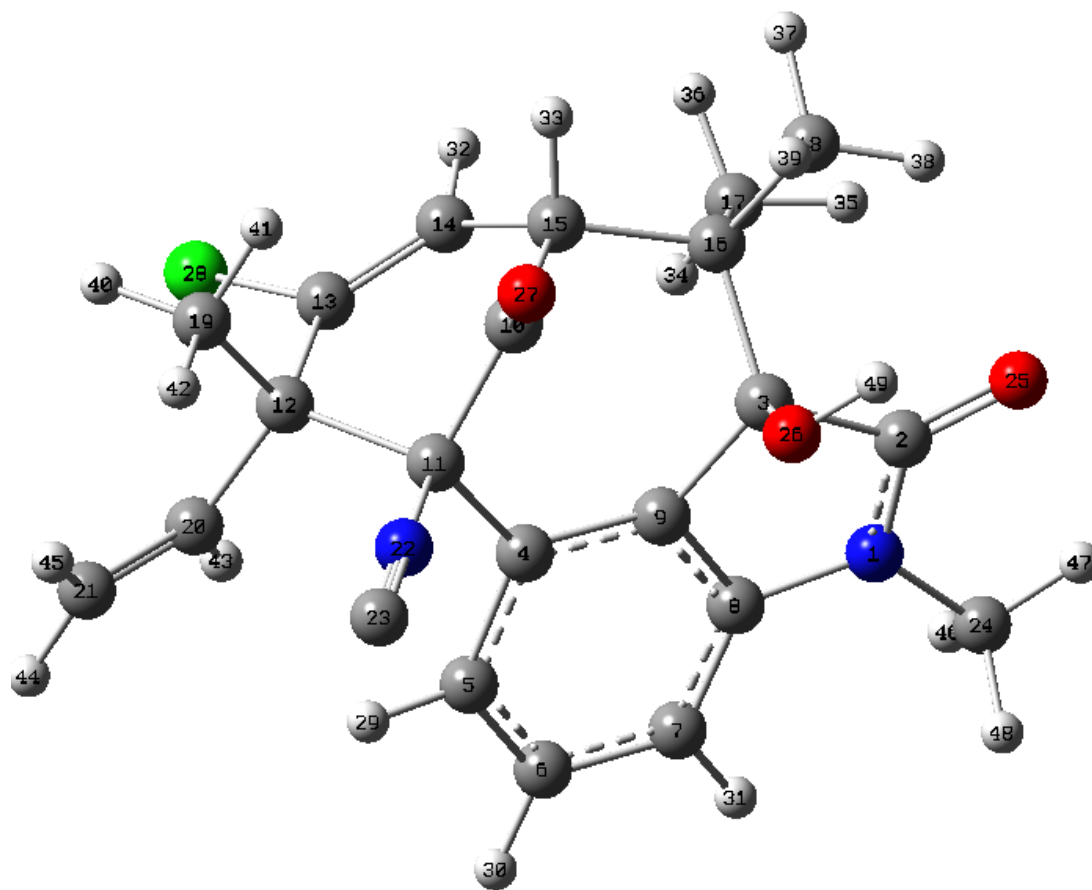


Structure 5.4, C3 epimer, conformer 3

Sum of electronic and thermal free energies = -1645.993218 H

Center Number	Atomic Number	Coordinates (Angstroms)		
		X	Y	Z
1	7	-3.304913	1.158080	-0.473247
2	6	-3.343767	-0.124220	0.012860
3	6	-1.900808	-0.526113	0.438143
4	6	0.202583	1.098414	0.441505
5	6	0.549857	2.458531	0.300853
6	6	-0.349169	3.394542	-0.201661
7	6	-1.654658	3.030875	-0.552499
8	6	-2.016782	1.709150	-0.335573
9	6	-1.114512	0.741754	0.146499
10	6	0.712752	-1.342329	1.145440
11	6	1.262646	0.108362	0.982553
12	6	2.560517	-0.074405	0.005008
13	6	2.038092	-0.733226	-1.267192
14	6	0.977493	-1.539015	-1.335178
15	6	0.165346	-1.970739	-0.137086
16	6	-1.410666	-1.832481	-0.278582
17	6	-1.827944	-1.804664	-1.763284
18	6	-2.052035	-3.069296	0.389982
19	6	3.578225	-1.040036	0.666839
20	6	3.217110	1.261431	-0.309193
21	6	4.289669	1.774829	0.297376
22	7	1.719682	0.579075	2.241375
23	6	2.085755	0.958664	3.292619
24	6	-4.488163	1.905444	-0.858646
25	8	-4.346060	-0.811932	0.151027
26	8	-1.913560	-0.658144	1.862321
27	8	0.831333	-1.960728	2.176980
28	17	3.004922	-0.490953	-2.728440
29	1	1.529805	2.790146	0.614743
30	1	-0.036243	4.429139	-0.304160
31	1	-2.360881	3.764169	-0.926083
32	1	0.737318	-2.002744	-2.285010
33	1	0.350153	-3.045699	-0.012173
34	1	-1.474030	-0.906708	-2.279741
35	1	-2.916945	-1.848538	-1.846404
36	1	-1.430496	-2.676692	-2.291910
37	1	-1.805258	-3.964359	-0.191192
38	1	-3.141320	-2.978058	0.419119
39	1	-1.671232	-3.222910	1.403675
40	1	4.445008	-1.142476	0.009787
41	1	3.150534	-2.030982	0.826388
42	1	3.914830	-0.662151	1.634015
43	1	2.757918	1.825543	-1.114875
44	1	4.680780	2.740848	-0.008234
45	1	4.811897	1.277404	1.107423
46	1	-4.380090	2.298264	-1.874694
47	1	-5.337383	1.222389	-0.820208
48	1	-4.662884	2.738110	-0.167863
49	1	-2.611489	-1.284980	2.106659

2	C	Isotropic =	4.5082	29	H	Isotropic =	23.7408
3	C	Isotropic =	102.2206	30	H	Isotropic =	23.7433
4	C	Isotropic =	46.4347	31	H	Isotropic =	24.3823
5	C	Isotropic =	56.3911	32	H	Isotropic =	25.4292
6	C	Isotropic =	51.1940	33	H	Isotropic =	28.4365
7	C	Isotropic =	71.9627	34	H	Isotropic =	31.0058
8	C	Isotropic =	35.0494	35	H	Isotropic =	30.6109
9	C	Isotropic =	52.6692	36	H	Isotropic =	30.6921
10	C	Isotropic =	-22.5454	37	H	Isotropic =	30.6963
11	C	Isotropic =	104.8751	38	H	Isotropic =	29.5775
12	C	Isotropic =	122.4370	39	H	Isotropic =	29.9092
13	C	Isotropic =	36.5446	40	H	Isotropic =	30.3197
14	C	Isotropic =	52.0920	41	H	Isotropic =	30.9179
15	C	Isotropic =	123.7915	42	H	Isotropic =	29.7019
16	C	Isotropic =	136.4725	43	H	Isotropic =	24.9580
17	C	Isotropic =	164.0214	44	H	Isotropic =	25.6285
18	C	Isotropic =	164.0273	45	H	Isotropic =	25.6935
19	C	Isotropic =	164.9704	46	H	Isotropic =	28.9284
20	C	Isotropic =	38.3761	47	H	Isotropic =	27.6248
21	C	Isotropic =	60.1109	48	H	Isotropic =	29.0147
23	C	Isotropic =	11.2619	49	H	Isotropic =	29.5616
24	C	Isotropic =	160.4922				

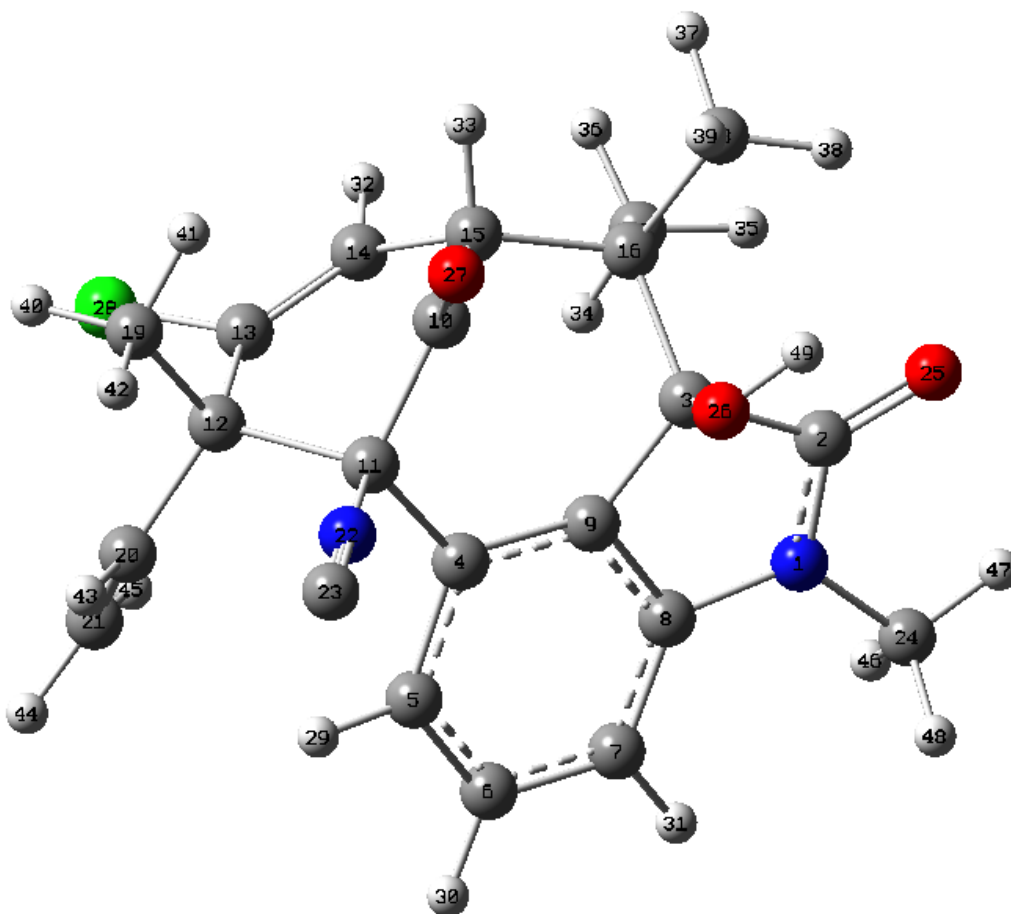


Structure 5.4, C3 epimer, conformer 4

Sum of electronic and thermal free energies = -1645.987825 H

Center Number	Atomic Number	Coordinates (Angstroms)		
		X	Y	Z
1	7	-3.296992	1.098062	-0.519742
2	6	-3.317437	-0.210481	-0.111600
3	6	-1.884018	-0.593435	0.359311
4	6	0.167951	1.087122	0.557247
5	6	0.468669	2.464755	0.525766
6	6	-0.438472	3.403086	0.042077
7	6	-1.709896	3.021859	-0.399926
8	6	-2.034115	1.677458	-0.287498
9	6	-1.123219	0.709965	0.176459
10	6	0.714456	-1.368430	1.162040
11	6	1.234122	0.098595	1.090693
12	6	2.587794	-0.006527	0.172366
13	6	2.166070	-0.632158	-1.150719
14	6	1.121171	-1.449679	-1.302106
15	6	0.245808	-1.942975	-0.174963
16	6	-1.320668	-1.840181	-0.402156
17	6	-1.650628	-1.730027	-1.905135
18	6	-1.963149	-3.132190	0.150963
19	6	3.600765	-0.983010	0.844450
20	6	3.295345	1.337588	0.109250
21	6	3.360863	2.218882	-0.890052
22	7	1.625594	0.519045	2.392415
23	6	1.929422	0.848788	3.479734
24	6	-4.483964	1.831598	-0.919345
25	8	-4.301992	-0.935598	-0.063345
26	8	-1.957268	-0.806376	1.772259
27	8	0.808081	-2.034886	2.165788
28	17	3.272247	-0.483221	-2.526924
29	1	1.419198	2.810462	0.901120
30	1	-0.157996	4.451844	0.025838
31	1	-2.423665	3.754808	-0.759696
32	1	0.969832	-1.914653	-2.269756
33	1	0.455063	-3.017670	-0.091631
34	1	-1.288388	-0.794356	-2.343013
35	1	-2.731464	-1.790928	-2.056824
36	1	-1.202105	-2.559204	-2.460985
37	1	-1.657828	-3.982723	-0.468039
38	1	-3.054361	-3.070632	0.122706
39	1	-1.636281	-3.339575	1.173934
40	1	4.498186	-1.032525	0.222334
41	1	3.198684	-1.992566	0.946629
42	1	3.887046	-0.623190	1.835406
43	1	3.824146	1.570334	1.031876
44	1	3.936363	3.132432	-0.768057
45	1	2.859783	2.084733	-1.841219
46	1	-4.339782	2.288596	-1.903624
47	1	-5.310886	1.122067	-0.964380
48	1	-4.720173	2.615082	-0.190315
49	1	-2.645567	-1.466065	1.947961

2	C	Isotropic =	4.8033	29	H	Isotropic =	23.7027
3	C	Isotropic =	101.9481	30	H	Isotropic =	23.8476
4	C	Isotropic =	47.3036	31	H	Isotropic =	24.3863
5	C	Isotropic =	54.9469	32	H	Isotropic =	25.4145
6	C	Isotropic =	52.1010	33	H	Isotropic =	28.4066
7	C	Isotropic =	72.2651	34	H	Isotropic =	31.0133
8	C	Isotropic =	35.5006	35	H	Isotropic =	30.6263
9	C	Isotropic =	52.9277	36	H	Isotropic =	30.6721
10	C	Isotropic =	-22.4746	37	H	Isotropic =	30.6941
11	C	Isotropic =	105.2378	38	H	Isotropic =	29.5224
12	C	Isotropic =	119.2896	39	H	Isotropic =	29.8903
13	C	Isotropic =	38.7276	40	H	Isotropic =	29.9140
14	C	Isotropic =	49.9270	41	H	Isotropic =	30.7893
15	C	Isotropic =	122.8680	42	H	Isotropic =	29.8884
16	C	Isotropic =	137.0406	43	H	Isotropic =	25.2216
17	C	Isotropic =	163.9270	44	H	Isotropic =	25.4410
18	C	Isotropic =	164.2834	45	H	Isotropic =	26.1526
19	C	Isotropic =	160.3357	46	H	Isotropic =	28.9489
20	C	Isotropic =	42.8063	47	H	Isotropic =	27.6230
21	C	Isotropic =	53.4203	48	H	Isotropic =	29.0286
23	C	Isotropic =	10.6569	49	H	Isotropic =	29.5085
24	C	Isotropic =	160.6551				

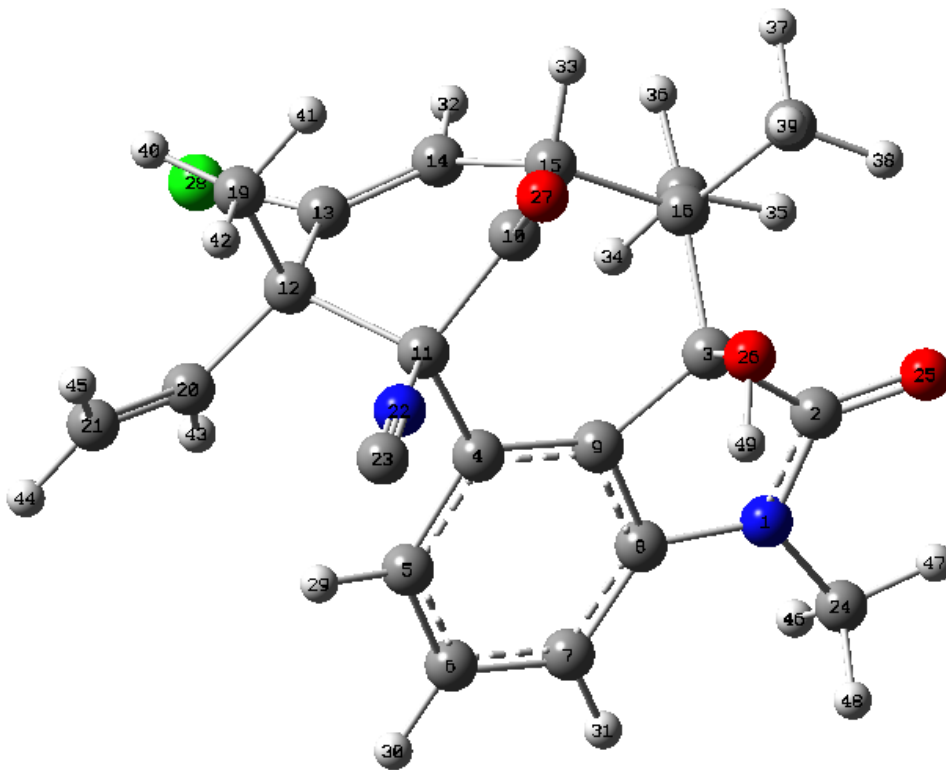


Structure 5.4, C3 epimer, conformer 5

Sum of electronic and thermal free energies = -1645.991068 H

Center Number	Atomic Number	Coordinates (Angstroms)		
		X	Y	Z
1	7	-3.316210	1.144844	-0.470852
2	6	-3.353000	-0.145626	0.016414
3	6	-1.900274	-0.530040	0.456442
4	6	0.195691	1.110009	0.426253
5	6	0.535916	2.470473	0.269947
6	6	-0.371177	3.397256	-0.235857
7	6	-1.677562	3.024701	-0.573098
8	6	-2.033824	1.702602	-0.342798
9	6	-1.122774	0.741996	0.142090
10	6	0.725498	-1.322317	1.175416
11	6	1.263098	0.131843	0.975234
12	6	2.556738	-0.062327	-0.003870
13	6	2.036001	-0.767570	-1.251864
14	6	0.981869	-1.583705	-1.293192
15	6	0.165831	-1.980456	-0.085158
16	6	-1.411863	-1.842012	-0.237032
17	6	-1.816382	-1.832304	-1.725165
18	6	-2.065012	-3.064028	0.447132
19	6	3.592983	-0.991378	0.680623
20	6	3.190944	1.272471	-0.365900
21	6	4.266338	1.816945	0.207755
22	7	1.721041	0.632824	2.223792
23	6	2.081051	1.038479	3.267421
24	6	-4.496318	1.870426	-0.902808
25	8	-4.354671	-0.833775	0.108351
26	8	-1.897460	-0.778516	1.865497
27	8	0.880065	-1.916681	2.215989
28	17	3.001830	-0.566105	-2.720418
29	1	1.517588	2.808976	0.570713
30	1	-0.063227	4.431928	-0.351967
31	1	-2.388990	3.750671	-0.951099
32	1	0.747195	-2.079790	-2.227923
33	1	0.342733	-3.052577	0.068531
34	1	-1.453253	-0.945486	-2.255049
35	1	-2.904431	-1.874170	-1.816303
36	1	-1.419353	-2.715718	-2.234178
37	1	-1.807241	-3.967991	-0.116408
38	1	-3.151829	-2.961174	0.463288
39	1	-1.713413	-3.182768	1.473244
40	1	4.452775	-1.107859	0.016800
41	1	3.178446	-1.980092	0.881730
42	1	3.937337	-0.574397	1.628771
43	1	2.712322	1.806697	-1.180794
44	1	4.640389	2.777977	-0.133001
45	1	4.808607	1.349899	1.022736
46	1	-4.369044	2.238269	-1.926233
47	1	-5.338560	1.178550	-0.866659
48	1	-4.697542	2.719456	-0.239400
49	1	-1.981566	0.058863	2.343130

2	C	Isotropic =	5.1952	29	H	Isotropic =	23.6966
3	C	Isotropic =	102.1608	30	H	Isotropic =	23.7777
4	C	Isotropic =	46.0600	31	H	Isotropic =	24.4347
5	C	Isotropic =	56.4614	32	H	Isotropic =	25.3922
6	C	Isotropic =	50.9654	33	H	Isotropic =	28.3243
7	C	Isotropic =	72.0633	34	H	Isotropic =	31.0289
8	C	Isotropic =	35.4876	35	H	Isotropic =	30.5817
9	C	Isotropic =	52.2471	36	H	Isotropic =	30.7290
10	C	Isotropic =	-21.8691	37	H	Isotropic =	30.7986
11	C	Isotropic =	105.0030	38	H	Isotropic =	29.4384
12	C	Isotropic =	122.2357	39	H	Isotropic =	29.6777
13	C	Isotropic =	36.8419	40	H	Isotropic =	30.2849
14	C	Isotropic =	51.7461	41	H	Isotropic =	30.8969
15	C	Isotropic =	123.6310	42	H	Isotropic =	29.7062
16	C	Isotropic =	136.1821	43	H	Isotropic =	24.9935
17	C	Isotropic =	163.9169	44	H	Isotropic =	25.6372
18	C	Isotropic =	163.1060	45	H	Isotropic =	25.7188
19	C	Isotropic =	165.0023	46	H	Isotropic =	28.9835
20	C	Isotropic =	38.3576	47	H	Isotropic =	27.5879
21	C	Isotropic =	60.6279	48	H	Isotropic =	29.0337
23	C	Isotropic =	11.3981	49	H	Isotropic =	30.5600
24	C	Isotropic =	160.7619				

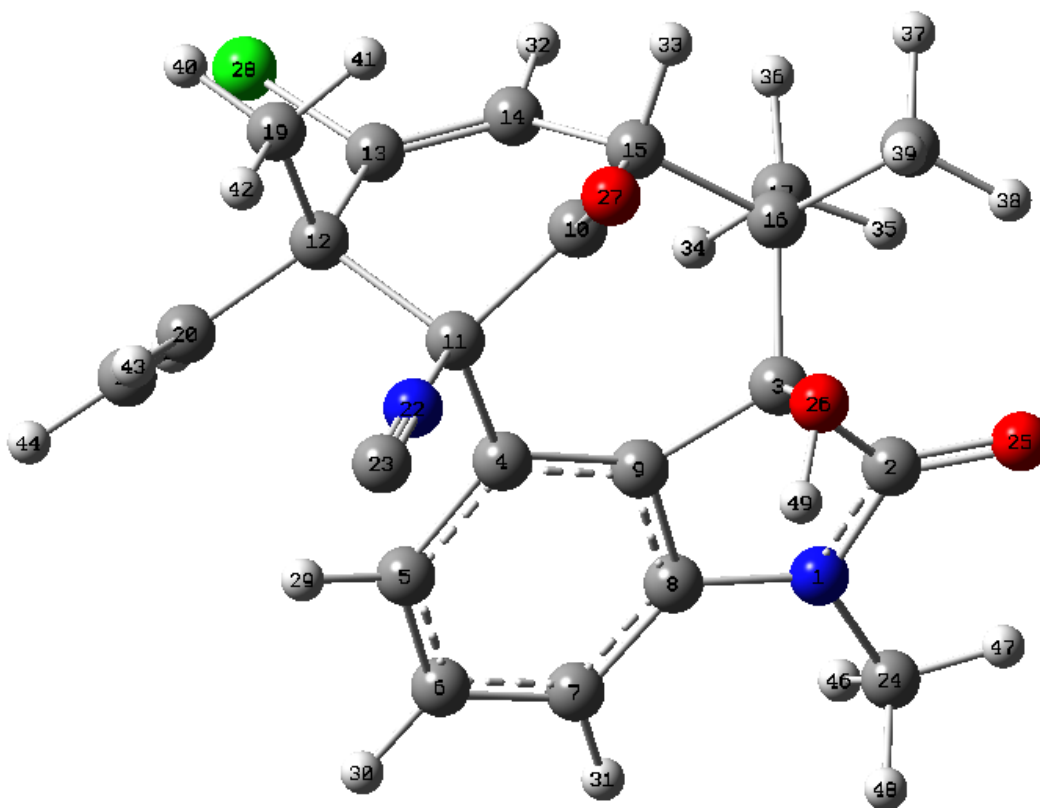


Structure 5.4, C3 epimer, conformer 6

Sum of electronic and thermal free energies = -1645.986160 H

Center Number	Atomic Number	Coordinates (Angstroms)		
		X	Y	Z
1	7	-3.312624	1.070087	-0.517719
2	6	-3.323492	-0.246966	-0.110163
3	6	-1.880062	-0.604648	0.379318
4	6	0.156962	1.103937	0.542283
5	6	0.443307	2.484536	0.495961
6	6	-0.476925	3.408969	0.009569
7	6	-1.747298	3.010784	-0.419833
8	6	-2.058333	1.663388	-0.294924
9	6	-1.133600	0.707541	0.171626
10	6	0.735897	-1.340861	1.196557
11	6	1.236535	0.133516	1.082426
12	6	2.584691	0.023322	0.157121
13	6	2.167810	-0.661675	-1.137978
14	6	1.133465	-1.497661	-1.257865
15	6	0.255063	-1.954172	-0.117195
16	6	-1.312905	-1.858185	-0.354434
17	6	-1.630140	-1.772956	-1.861439
18	6	-1.962419	-3.137148	0.220416
19	6	3.624972	-0.902505	0.857785
20	6	3.258600	1.380226	0.032286
21	6	3.287376	2.220559	-1.003236
22	7	1.631285	0.589556	2.372781
23	6	1.930996	0.948564	3.451996
24	6	-4.497128	1.778340	-0.965471
25	8	-4.301112	-0.975325	-0.109797
26	8	-1.933180	-0.927604	1.772579
27	8	0.869596	-1.978865	2.213930
28	17	3.274935	-0.554405	-2.518122
29	1	1.393378	2.843624	0.859876
30	1	-0.206985	4.460228	-0.019166
31	1	-2.470221	3.732707	-0.783612
32	1	0.991383	-2.002287	-2.206844
33	1	0.458766	-3.026367	-0.000361
34	1	-1.261198	-0.847576	-2.316215
35	1	-2.709337	-1.836217	-2.020688
36	1	-1.179506	-2.614846	-2.395392
37	1	-1.640594	-3.999269	-0.374910
38	1	-3.051135	-3.069846	0.176867
39	1	-1.667942	-3.302582	1.258096
40	1	4.515211	-0.960810	0.226305
41	1	3.244144	-1.914013	1.008749
42	1	3.916936	-0.494254	1.828047
43	1	3.794607	1.662499	0.936979
44	1	3.840698	3.152754	-0.929232
45	1	2.777150	2.032186	-1.940362
46	1	-4.335374	2.210442	-1.958528
47	1	-5.313299	1.056398	-1.011084
48	1	-4.762161	2.579062	-0.265378
49	1	-2.081707	-0.121526	2.286962

2	C	Isotropic =	5.6260	29	H	Isotropic =	23.7169
3	C	Isotropic =	101.7692	30	H	Isotropic =	23.8617
4	C	Isotropic =	46.8953	31	H	Isotropic =	24.4447
5	C	Isotropic =	54.4966	32	H	Isotropic =	25.3600
6	C	Isotropic =	51.9572	33	H	Isotropic =	28.2891
7	C	Isotropic =	72.3771	34	H	Isotropic =	31.0062
8	C	Isotropic =	36.0630	35	H	Isotropic =	30.6048
9	C	Isotropic =	52.3668	36	H	Isotropic =	30.7046
10	C	Isotropic =	-21.6655	37	H	Isotropic =	30.8278
11	C	Isotropic =	105.1827	38	H	Isotropic =	29.3924
12	C	Isotropic =	119.2166	39	H	Isotropic =	29.6543
13	C	Isotropic =	39.0046	40	H	Isotropic =	29.9060
14	C	Isotropic =	49.4286	41	H	Isotropic =	30.7720
15	C	Isotropic =	122.6971	42	H	Isotropic =	29.9302
16	C	Isotropic =	136.9722	43	H	Isotropic =	25.2462
17	C	Isotropic =	163.8095	44	H	Isotropic =	25.4644
18	C	Isotropic =	163.3482	45	H	Isotropic =	26.2006
19	C	Isotropic =	160.5311	46	H	Isotropic =	28.9944
20	C	Isotropic =	43.0063	47	H	Isotropic =	27.5786
21	C	Isotropic =	53.1354	48	H	Isotropic =	29.0435
23	C	Isotropic =	10.8252	49	H	Isotropic =	30.5209
24	C	Isotropic =	160.9110				

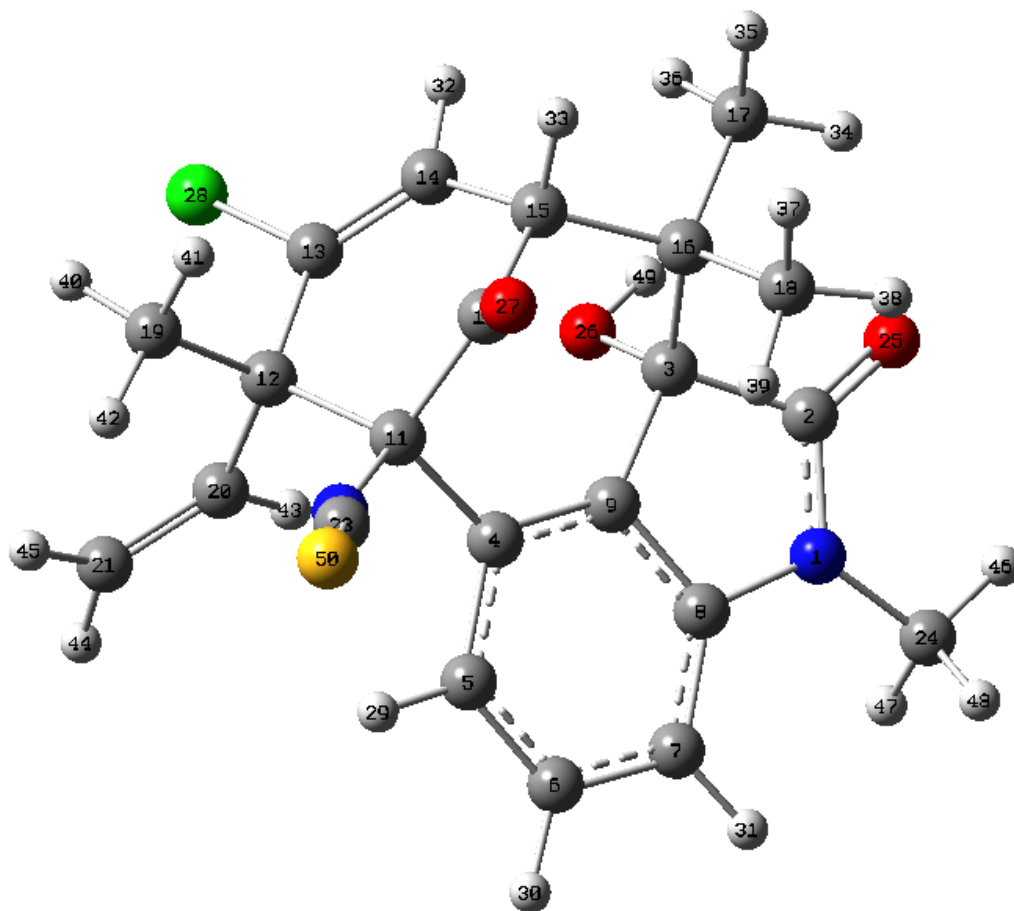


Structure 5.3

Sum of electronic and thermal free energies = -2044.228627 H

Center Number	Atomic Number	Coordinates (Angstroms)		
		X	Y	Z
1	7	3.491312	-1.137705	-0.667141
2	6	3.468337	-0.007255	0.098748
3	6	1.986878	0.464263	0.228362
4	6	-0.133580	-0.961406	-0.663930
5	6	-0.448307	-2.047557	-1.512488
6	6	0.528610	-2.836392	-2.106567
7	6	1.883265	-2.602645	-1.856977
8	6	2.193617	-1.523155	-1.044414
9	6	1.225434	-0.665468	-0.473704
10	6	-0.926198	0.041919	1.521845
11	6	-1.341403	-0.285430	0.058195
12	6	-1.939853	1.036289	-0.661648
13	6	-1.153515	2.259394	-0.206882
14	6	-0.324087	2.348248	0.831109
15	6	0.033732	1.196340	1.733996
16	6	1.559826	0.785272	1.692658
17	6	2.368264	1.966387	2.277266
18	6	1.797448	-0.449467	2.587994
19	6	-3.404688	1.245858	-0.205723
20	6	-1.813324	0.867272	-2.169007
21	6	-2.805218	0.640241	-3.031626
22	7	-2.400780	-1.249285	0.099800
23	6	-3.026178	-1.987924	0.812450
24	6	4.713110	-1.784422	-1.109825
25	8	4.449019	0.604419	0.503796
26	8	1.928088	1.619649	-0.628398
27	8	-1.377734	-0.588383	2.453942
28	17	-1.455073	3.726927	-1.150965
29	1	-1.488757	-2.280390	-1.692551
30	1	0.230614	-3.658003	-2.750493
31	1	2.653856	-3.237184	-2.280203
32	1	0.129295	3.307096	1.055940
33	1	-0.141596	1.501619	2.773437
34	1	3.432782	1.731081	2.308767
35	1	2.026890	2.166259	3.298657
36	1	2.244315	2.887411	1.701496
37	1	1.399713	-0.274079	3.591868
38	1	2.870180	-0.644828	2.683311
39	1	1.317164	-1.351718	2.199932
40	1	-3.775657	2.193237	-0.602938
41	1	-3.467205	1.285730	0.885515
42	1	-4.056144	0.443475	-0.552501
43	1	-0.795340	0.940058	-2.545759
44	1	-2.595628	0.529276	-4.091361
45	1	-3.845373	0.563052	-2.732652
46	1	5.550706	-1.247887	-0.663214
47	1	4.797453	-1.744513	-2.201407
48	1	4.734444	-2.830131	-0.786015
49	1	2.712081	2.160658	-0.443242
50	16	-3.967455	-3.023543	1.559218

2	C	Isotropic =	4.8855	29	H	Isotropic =	23.9984
3	C	Isotropic =	101.8740	30	H	Isotropic =	23.8156
4	C	Isotropic =	47.0518	31	H	Isotropic =	24.3353
5	C	Isotropic =	55.6586	32	H	Isotropic =	24.8723
6	C	Isotropic =	50.8762	33	H	Isotropic =	28.3058
7	C	Isotropic =	72.5542	34	H	Isotropic =	29.2384
8	C	Isotropic =	34.1863	35	H	Isotropic =	30.8878
9	C	Isotropic =	54.4800	36	H	Isotropic =	29.9737
10	C	Isotropic =	-22.5835	37	H	Isotropic =	30.5709
11	C	Isotropic =	95.1988	38	H	Isotropic =	30.8818
12	C	Isotropic =	121.3605	39	H	Isotropic =	31.3575
13	C	Isotropic =	38.4718	40	H	Isotropic =	30.0976
14	C	Isotropic =	52.7774	41	H	Isotropic =	30.6923
15	C	Isotropic =	122.6604	42	H	Isotropic =	29.7414
16	C	Isotropic =	135.8042	43	H	Isotropic =	25.8781
17	C	Isotropic =	166.1601	44	H	Isotropic =	26.0590
18	C	Isotropic =	164.0081	45	H	Isotropic =	26.0025
19	C	Isotropic =	165.5144	46	H	Isotropic =	27.5723
20	C	Isotropic =	37.4105	47	H	Isotropic =	28.9626
21	C	Isotropic =	64.0130	48	H	Isotropic =	28.9522
23	C	Isotropic =	33.9484	49	H	Isotropic =	29.4462
24	C	Isotropic =	160.3097				

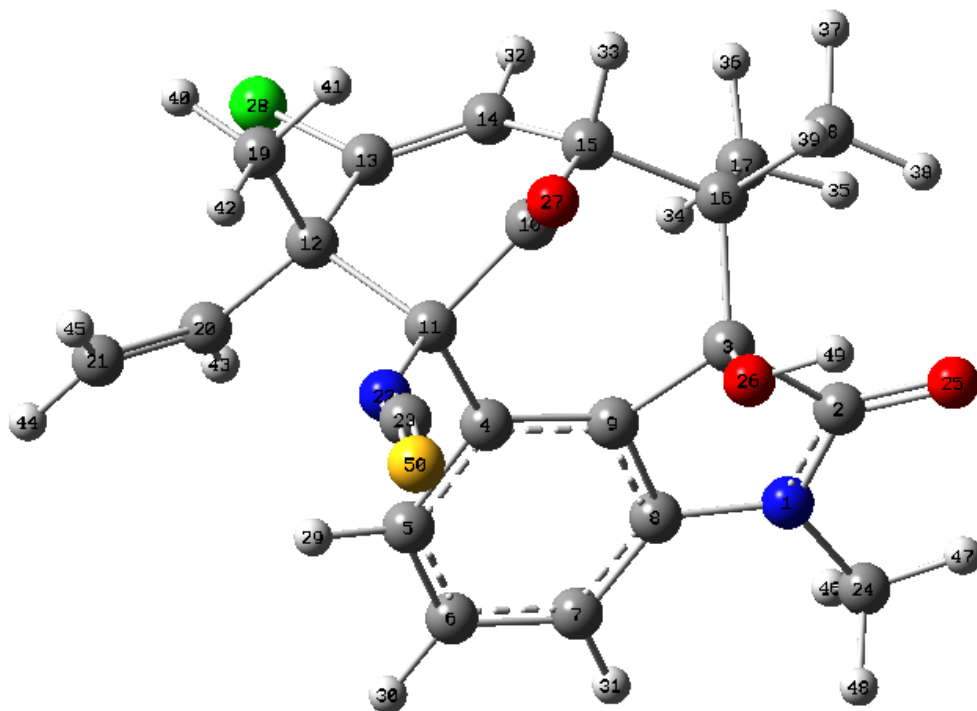


Structure 5.3, C3 epimer

Sum of electronic and thermal free energies = -2044.226582 H

Center Number	Atomic Number	Coordinates (Angstroms)		
		X	Y	Z
1	7	3.508897	0.034700	1.185185
2	6	3.461453	0.331733	-0.153051
3	6	1.966000	0.401803	-0.582116
4	6	-0.111304	0.205516	1.063527
5	6	-0.435091	0.191248	2.437306
6	6	0.537608	0.016818	3.417095
7	6	1.890944	-0.110910	3.081768
8	6	2.214182	-0.013667	1.736157
9	6	1.242227	0.135284	0.728037
10	6	-0.725084	0.459204	-1.433944
11	6	-1.250533	0.387511	0.031499
12	6	-2.314605	-0.848701	0.005622
13	6	-1.550717	-2.067344	-0.500202
14	6	-0.494633	-2.028799	-1.313731
15	6	0.069515	-0.759401	-1.906174
16	6	1.641233	-0.566342	-1.772568
17	6	2.342801	-1.921963	-1.550555
18	6	2.151556	0.042890	-3.098071
19	6	-3.443991	-0.532057	-1.008790
20	6	-2.897771	-1.117065	1.385510
21	6	-4.077035	-0.690080	1.842611
22	7	-1.968062	1.577656	0.363280
23	6	-2.174575	2.717022	0.037974
24	6	4.738606	0.001779	1.955649
25	8	4.422504	0.567687	-0.872661
26	8	1.697331	1.770336	-0.903737
27	8	-1.030153	1.365191	-2.175190
28	17	-2.213061	-3.648178	-0.059791
29	1	-1.461894	0.344490	2.738410
30	1	0.241807	-0.000457	4.461714
31	1	2.651105	-0.228044	3.846218
32	1	-0.072017	-2.964162	-1.662136
33	1	-0.123922	-0.810457	-2.985629
34	1	2.085865	-2.370219	-0.585513
35	1	3.427262	-1.794094	-1.598822
36	1	2.068332	-2.632093	-2.336814
37	1	2.038672	-0.692049	-3.902375
38	1	3.211259	0.303132	-3.027751
39	1	1.576691	0.928942	-3.382477
40	1	-4.158028	-1.358859	-1.016138
41	1	-3.055202	-0.406748	-2.020645
42	1	-3.973162	0.383702	-0.737975
43	1	-2.282292	-1.729326	2.037431
44	1	-4.399704	-0.946336	2.847548
45	1	-4.757634	-0.080157	1.258455
46	1	4.831705	-0.949218	2.489822
47	1	5.568994	0.110459	1.257192
48	1	4.765071	0.824457	2.679261
49	1	2.335551	2.059062	-1.573813
50	16	-2.567777	4.231745	-0.213587

2	C	Isotropic =	4.1786	29	H	Isotropic =	23.7346
3	C	Isotropic =	102.7844	30	H	Isotropic =	23.8586
4	C	Isotropic =	46.5561	31	H	Isotropic =	24.4441
5	C	Isotropic =	55.9890	32	H	Isotropic =	25.3803
6	C	Isotropic =	51.8771	33	H	Isotropic =	28.1997
7	C	Isotropic =	72.5350	34	H	Isotropic =	30.9148
8	C	Isotropic =	34.3350	35	H	Isotropic =	30.6643
9	C	Isotropic =	53.3429	36	H	Isotropic =	30.6711
10	C	Isotropic =	-25.4087	37	H	Isotropic =	30.7396
11	C	Isotropic =	99.9395	38	H	Isotropic =	29.5377
12	C	Isotropic =	122.9421	39	H	Isotropic =	29.8480
13	C	Isotropic =	35.4253	40	H	Isotropic =	30.2733
14	C	Isotropic =	51.8841	41	H	Isotropic =	30.9084
15	C	Isotropic =	123.6216	42	H	Isotropic =	29.6995
16	C	Isotropic =	136.1963	43	H	Isotropic =	24.9076
17	C	Isotropic =	163.4768	44	H	Isotropic =	25.7231
18	C	Isotropic =	163.6791	45	H	Isotropic =	25.8722
19	C	Isotropic =	165.1487	46	H	Isotropic =	28.9125
20	C	Isotropic =	36.7707	47	H	Isotropic =	27.5861
21	C	Isotropic =	61.9335	48	H	Isotropic =	29.0421
23	C	Isotropic =	32.4181	49	H	Isotropic =	29.5902
24	C	Isotropic =	160.6404				



5.10 Notes and References

- (1) (a) Stratmann, K.; Moore, R. E.; Bonjouklian, R.; Deeter, J. B.; Patterson, G. M. L.; Shaffer, S.; Smith, C. D.; Smitka, T. A. *J. Am. Chem. Soc.* **1994**, *116*, 9935–9942. (b) Jimenez, J. L.; Huber, U.; Moore, R. E.; Patterson, G. M. L. *J. Nat. Prod.* **1999**, *62*, 569–572.
- (2) Welwitindolinone A isonitrile, a unique welwitindolinone that possesses a C3 spirooxindoline core, has been synthesized independently by the Baran and Wood groups; see: (a) Baran, P. S.; Richter, J. M. *J. Am. Chem. Soc.* **2005**, *127*, 15394–15396. (b) Reisman, S. E.; Ready, J. M.; Hasuoka, A.; Smith, C. J.; Wood, J. L. *J. Am. Chem. Soc.* **2006**, *128*, 1448–1449.
- (3) (a) Smith, C. D.; Zilfou, J. T.; Stratmann, K.; Patterson, G. M. L.; Moore, R. E. *Mol. Pharmacol.* **1995**, *47*, 241–247. (b) Zhang, X.; Smith, C. D. *Mol. Pharmacol.* **1996**, *49*, 288–294.
- (4) (a) Konopelski, J. P.; Deng, H.; Schiemann, K.; Keane, J. M.; Olmstead, M. M. *Synlett* **1998**, 1105–1107. (b) Wood, J. L.; Holubec, A. A.; Stoltz, B. M.; Weiss, M. M.; Dixon, J. A.; Doan, B. D.; Shamji, M. F.; Chen, J. M.; Heffron, T. P. *J. Am. Chem. Soc.* **1999**, *121*, 6326–6327. (c) Kaoudi, T.; Ouiclet-Sire, B.; Seguin, S.; Zard, S. Z. *Angew. Chem., Int. Ed.* **2000**, *39*, 731–733. (d) Deng, H.; Konopelski, J. P. *Org. Lett.* **2001**, *3*, 3001–3004. (e) Jung, M. E.; Slowinski, F. *Tetrahedron Lett.* **2001**, *42*, 6835–6838. (f) López-Alvarado, P.; García-Granda, S.; Ivarez-Rúa, C.; Avendaño, C. *Eur. J. Org. Chem.* **2002**, 1702–1707. (g) MacKay, J. A.; Bishop, R. L.; Rawal, V. H. *Org. Lett.* **2005**, *7*, 3421–3424. (h) Baudoux, J.; Blake, A. J.; Simpkins, N. S. *Org. Lett.* **2005**, *7*, 4087–4089. (i) Greshock, T. J.; Funk, R. L. *Org. Lett.* **2006**, *8*, 2643–2645. (j) Lauchli, R.; Shea, K. J. *Org. Lett.* **2006**, *8*, 5287–5289. (k)

- Guthikonda, K.; Caliando, B. J.; Du Bois, J. Abstracts of Papers, 232nd ACS National Meeting, September, 2006, abstr ORGN-002. (l) Xia, J. Brown, L. E.; Konopelski, J. P. *J. Org. Chem.* **2007**, *72*, 6885–6890. (m) Richter, J. M.; Ishihara, Y.; Masuda, T.; Whitefield, B. W.; Llamas, T.; Pohjakallio, A.; Baran, P. S. *J. Am. Chem. Soc.* **2008**, *130*, 17938–17945. (n) Boissel, V.; Simpkins, N. S.; Bhalay, G.; Blake, A. J.; Lewis, W. *Chem. Commun.* **2009**, 1398–1400. (o) Boissel, V.; Simpkins, N. S.; Bhalay, G. *Tetrahedron Lett.* **2009**, *50*, 3283–3286. (p) Tian, X.; Hutters, A. D.; Douglas, C. J.; Garg, N. K. *Org. Lett.* **2009**, *11*, 2349–2351. (q) Trost, B. M.; McDougall, P. J. *Org. Lett.* **2009**, *11*, 3782–3785. (r) Brailsford, J. A.; Lauchli, R.; Shea, K. J. *Org. Lett.* **2009**, *11*, 5330–5333. (s) Freeman, D. B. et. al. *Tetrahedron* **2010**, *66*, 6647–6655. (t) Heidebrecht, R. W., Jr.; Gullledge, B.; Martin, S. F. *Org. Lett.* **2010**, *12*, 2492–2495. (u) Ruiz, M.; López-Alvarado, P.; Menéndez, J. C. *Org. Biomol. Chem.* **2010**, *8*, 4521–4523. (v) Bhat, V.; Rawal, V. H. *Chem. Comm.* **2011**, *47*, 9705–9707. (w) Bhat, V.; MacKay, J. A.; Rawal, V. H. *Org. Lett.* **2011**, *13*, 3214–3217. (x) Bhat, V.; MacKay, J. A.; Rawal, V. H. *Tetrahedron* **2011**, *67*, 10097–10104.
- (5) For pertinent reviews, see: (a) Brown, L. E.; Konopelski, J. P. *Org. Prep. Proc. Intl.* **2008**, *40*, 411–445. (b) Avendaño, C.; Menéndez, J. C. *Curr. Org. Synth.* **2004**, *1*, 65–82.
- (6) For Rawal’s breakthrough total synthesis of (±)-**5.5**, see: Bhat, V.; Allan, K. M.; Rawal, V. H. *J. Am. Chem. Soc.* **2011**, *133*, 5798–5801.
- (7) For the total synthesis of (–)-**5.1**, see: Hutters, A. D.; Quasdorf, K. W.; Styduhar, E. D.; Garg, N. K. *J. Am. Chem. Soc.* **2011**, *133*, 15797–15799.
- (8) For Rawal and coworkers asymmetric total syntheses of **5.1–5.3**, see: Allan, K. M.; Kobayashi, K.; Rawal, V. H. *J. Am. Chem. Soc.* **2012**, *134*, 1392–1395.

- (9) (a) Davies, H. M. L.; Manning, J. R. *Nature* **2008**, *451*, 417–424. (b) Collet, F.; Lescot, C.; Liang, C.; Dauban, P. *Dalton Trans.* **2010**, *39*, 10401–10413.
- (10) For an elegant late-stage nitrene insertion in natural product total synthesis, see: Hinman, A.; Du Bois, J. *J. Am. Chem. Soc.* **2003**, *125*, 11510–11511.
- (11) For intramolecular nitrene C–H insertion reactions using carbamate substrates, see: (a) Espino, C. G.; Du Bois, J. *Angew. Chem., Int. Ed.* **2001**, *40*, 598–600. (b) Li, Z.; Capretto, D. A.; Rahaman, R.; He, C. *Angew. Chem., Int. Ed.* **2007**, *46*, 5184–5186. (c) Cui, Y.; He, C. *Angew. Chem., Int. Ed.* **2004**, *43*, 4210–4212.
- (12) Related oxidation processes have previously been observed; see: Hinman, A. W. Ph.D. Dissertation, Stanford University, Stanford, CA, 2004.
- (13) For a study of the kinetic isotope effect in Rh-catalyzed nitrene insertion reactions, see: Fiori, K. W.; Espino, C. G.; Brodsky, B. H.; Du Bois, J. *Tetrahedron* **2009**, *65*, 3042–3051.
- (14) For elegant examples involving the strategic use of deuterium in total synthesis, see: (a) Clive, D. L. J.; Cantin, M.; Khodabocus, A.; Kong, X.; Tao, Y. *Tetrahedron* **1993**, *49*, 7917–7930. (b) Vedejs, E.; Little, J. *J. Am. Chem. Soc.* **2002**, *124*, 748–749. (c) Miyashita, M.; Sasaki, M.; Hattori, I.; Sakai, M.; Tanino, K. *Science* **2004**, *305*, 495–499.
- (15) Rawal and coworkers have recently achieved this transformation; see reference 8.
- (16) Moore and coworkers have shown that (–)-**5.2** can be converted to (–)-**5.4** and (–)-**5.5**, albeit in low yield (5% and 3% yield, respectively) using a photooxidation procedure. Thus, the synthesis of (–)-**5.2** also constitutes formal total syntheses of (–)-**5.4** and (–)-**5.5**.
- (17) The C3 stereochemical configuration of **5.4** was assigned based on this compound having similar ¹HNMR and CD spectra in comparison to **5.2**. Further support was obtained by the

experiment described in reference 16. The C3 configuration of **5.3** was assigned by analogy to **5.4**. See reference 1b.

- (18) For recent examples of the aerobic oxidation of oxindoles to C3-hydroxy oxindoles, see: (a) Shen, H. C.; Ding, F.-X.; Colletti, S. L. *Org. Lett.* **2006**, *8*, 1447–1450. (b) Durbin, M. J.; Willis, M. C. *Org. Lett.* **2008**, *10*, 1413–1415. (c) Sano, D.; Nagata, K.; Itoh, T. *Org. Lett.* **2008**, *10*, 1593–1595.
- (19) Holubec, A. A. Ph.D. Dissertation, Yale University, New Haven, CT, 2000.
- (20) NMR data for synthetic **5.3** did not match the tabulated data provided in the original isolation report (see reference 1b). However, an authentic sample of **5.3** was recently located at the University of Hawaii, and subsequent NMR analysis revealed that the NMR data for **5.3** reported upon isolation was mis-tabulated. Indeed, synthetic **5.3** matched natural **5.3** by all spectroscopic means. We thank Philip Williams and Wesley Yoshida (University of Hawaii) for resolving this discrepancy. Of note, Rawal and coworkers have arrived at the same conclusion regarding the spectral data for **5.3**; see reference 8.
- (21) Recent examples: (a) Saielli, G.; Nicolaou, K. C.; Ortiz, A.; Zhang, H.; Bagnò, A. *J. Am. Chem. Soc.* **2011**, *133*, 6072–6077. (b) Smith, S. G.; Goodman, J. M. *J. Am. Chem. Soc.* **2010**, *132*, 12946–12959. (c) Lodewyk, M. W.; Tantillo, D. J. *J. Nat. Prod.* **2011**, *74*, 1339–1343. (d) Schwartz, B. D.; White, L. V.; Banwell, M. G.; Willis, A. C. *J. Org. Chem.* **2011**, *76*, 8560–8563.
- (22) For a review on chemical shift calculations, see: Lodewyk, M. W.; Siebert, M. R.; Tantillo, D. J. *Chem. Rev.* ASAP, DOI: 10.1021/cr200106v.

- (23) Calculated at the SMD(chloroform)-mPW1PW91/6-311+G(2d,p)//B3LYP/6-31+G(d,p) level with linear scaling (see <http://cheshireNMR.info> and Jain, R. J.; Bally, T.; Rablen, P. R. *J. Org. Chem.* **2009**, *74*, 4017–4023). A thorough conformational search was performed on **5.4** and computed shifts were averaged based on a Boltzman distribution.
- (24) The 3-dimensional structure shown in Scheme 5.3 was obtained by geometry optimization calculations (MMFF) using MacSpartan '10 (Wavefunction, Inc. Irvine, CA).
- (25) Frigerio, M.; Santagostino, M.; Sputore, S. *J. Org. Chem.* **1999**, *64*, 4537–4538.
- (26) Niu, C.; Pettersson, T.; Miller, M. J. *J. Org. Chem.* **1996**, *61*, 1014–1022.
- (27) Reported values for specific rotations can be highly variable; for a pertinent discussion, see: Gawley, R. E. *J. Org. Chem.* **2006**, *71*, 2411–2416.
- (28) G09: Gaussian 09, Revision B.01, Frisch, M. J.; Trucks, G. W.; Schlegel, H. B.; Scuseria, G. E.; Robb, M. A.; Cheeseman, J. R.; Scalmani, G.; Barone, V.; Mennucci, B.; Petersson, G. A.; Nakatsuji, H.; Caricato, M.; Li, X.; Hratchian, H. P.; Izmaylov, A. F.; Bloino, J.; Zheng, G.; Sonnenberg, J. L.; Hada, M.; Ehara, M.; Toyota, K.; Fukuda, R.; Hasegawa, J.; Ishida, M.; Nakajima, T.; Honda, Y.; Kitao, O.; Nakai, H.; Vreven, T.; Montgomery, Jr., J. A.; Peralta, J. E.; Ogliaro, F.; Bearpark, M.; Heyd, J. J.; Brothers, E.; Kudin, K. N.; Staroverov, V. N.; Kobayashi, R.; Normand, J.; Raghavachari, K.; Rendell, A.; Burant, J. C.; Iyengar, S. S.; Tomasi, J.; Cossi, M.; Rega, N.; Millam, N. J.; Klene, M.; Knox, J. E.; Cross, J. B.; Bakken, V.; Adamo, C.; Jaramillo, J.; Gomperts, R.; Stratmann, R. E.; Yazyev, O.; Austin, A. J.; Cammi, R.; Pomelli, C.; Ochterski, J. W.; Martin, R. L.; Morokuma, K.; Zakrzewski, V. G.; Voth, G. A.; Salvador, P.; Dannenberg, J. J.; Dapprich, S.; Daniels, A. D.; Farkas, Ö.; Foresman, J. B.; Ortiz, J. V.; Cioslowski, J.; Fox, D. J. Gaussian, Inc., Wallingford CT, **2009**.

- (29) (a) Becke, A. D. *J. Chem. Phys.* **1993**, *98*, 1372–1377. (b) Becke, A. D. *J. Chem. Phys.* **1993**, *98*, 5648–5652. (c) Lee, C.; Yang, W.; Parr, R. G. *Phys. Rev. B* **1988**, *37*, 785–789. (d) Stephens, P. J.; Devlin, F. J.; Chabalowski, C. F.; Frisch, M. J. *J. Phys. Chem.* **1994**, *98*, 11623–11627. (e) Tirado-Rives, J.; Jorgensen, W. L. *J. Chem. Theory Comput.* **2008**, *4*, 297–306.
- (30) (a) London, F. *J. Phys. Radium* **1937**, *8*, 397–409. (b) McWeeny, R. *Phys. Rev.* **1962**, *126*, 1028–1034. (c) Ditchfield, R. *Mol. Phys.* **1974**, *27*, 789–807. (d) Wolinski, K.; Hilton, J. F.; Pulay, P. *J. Am. Chem. Soc.* **1990**, *112*, 8251–8260. (e) Cheeseman, J. R.; Trucks, G. W.; Keith, T. A.; Frisch, M. J. *J. Chem. Phys.* **1996**, *104*, 5497–5509.
- (31) Adamo, C.; Barone, V. *J. Chem. Phys.* **1998**, *108*, 664–675.
- (32) Marenich, A. V.; Cramer, C. J.; Truhlar, D. G. *J. Phys. Chem.* **2009**, *113*, 6378–6396.
- (33) *Spartan'10*; Wavefunction, Inc., Irvine, CA.
- (34) Smith, S. G.; Goodman, J. M. *J. Am. Chem. Soc.* **2010**, *132*, 12946–12959. Use of the DP4 analysis is quite practical, owing to a versatile Java applet that the Goodman group has made available online. The current URL is: <http://www-jmg.ch.cam.ac.uk/tools/nmr/nmrParameters.html>

APPENDIX FOUR

Spectra Relevant to Chapter Five:

Total Synthesis of Oxidized Welwitindolinones and

(-)-*N*-Methylwelwitindolinone C Isonitrile

Kyle W. Quasdorf, Alexander D. Hutters, Michael W. Lodewyk, Dean J. Tantillo, and Neil K. Garg.

J. Am. Chem. Soc. **2012**, *134*, 1396–1399.

Current Data Parameters
 NAME ADH-3-115-p
 EXPNO 1
 PROCNO 1
 F2 - Acquisition Parameters
 Date_ 20110702
 Time 12:52
 INSTRUM arx500
 PROBHD 5 mm broadband
 PULPROG zg30
 TD 65536
 SOLVENT CDCl3
 NS 8
 DS 0
 SWH 10000.000 Hz
 FIDRES 0.152588 Hz
 AQ 3.2768500 sec
 RG 2860
 DW 50.000 usec
 DE 71.43 usec
 TE 300.0 K
 D1 2.00000000 sec
 P1 11.00 usec
 SFO1 500.1330008 MHz
 NUCLEUS 1H
 F2 - Processing parameters
 SI 32768
 SF 500.1300237 MHz
 WDW EM
 SSB 0
 LB 0.30 Hz
 GB 0
 PC 1.00

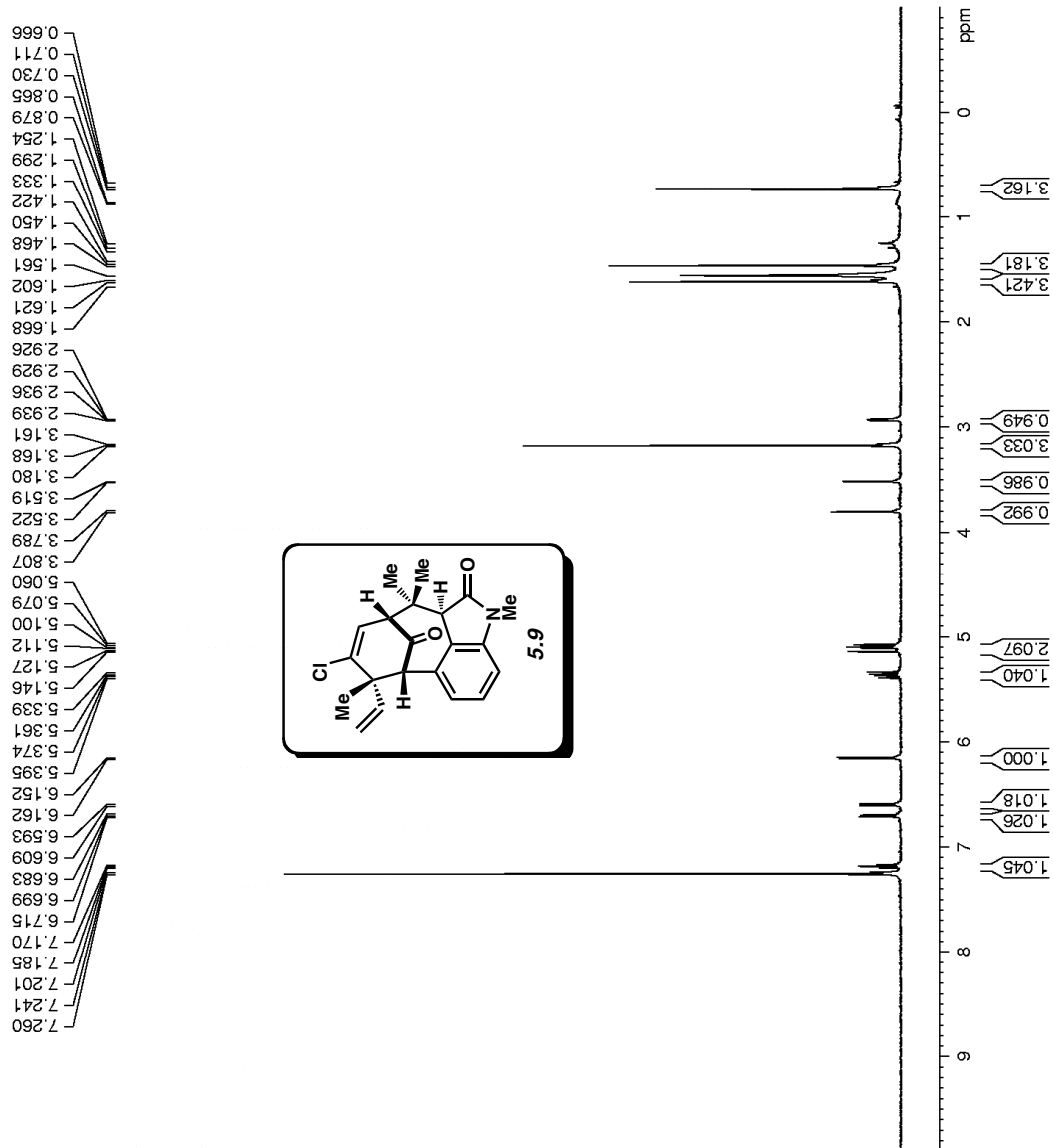


Figure A4.1 ¹H NMR (500 MHz, CDCl₃) of compound 5.9.

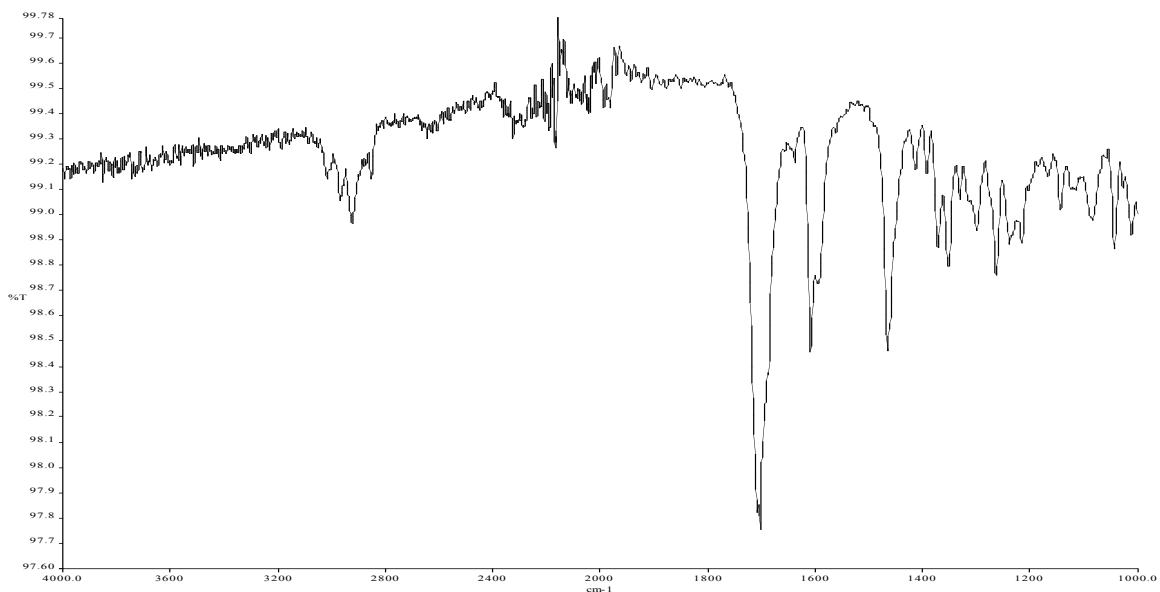


Figure A4.2 Infrared spectrum of compound **5.9**.

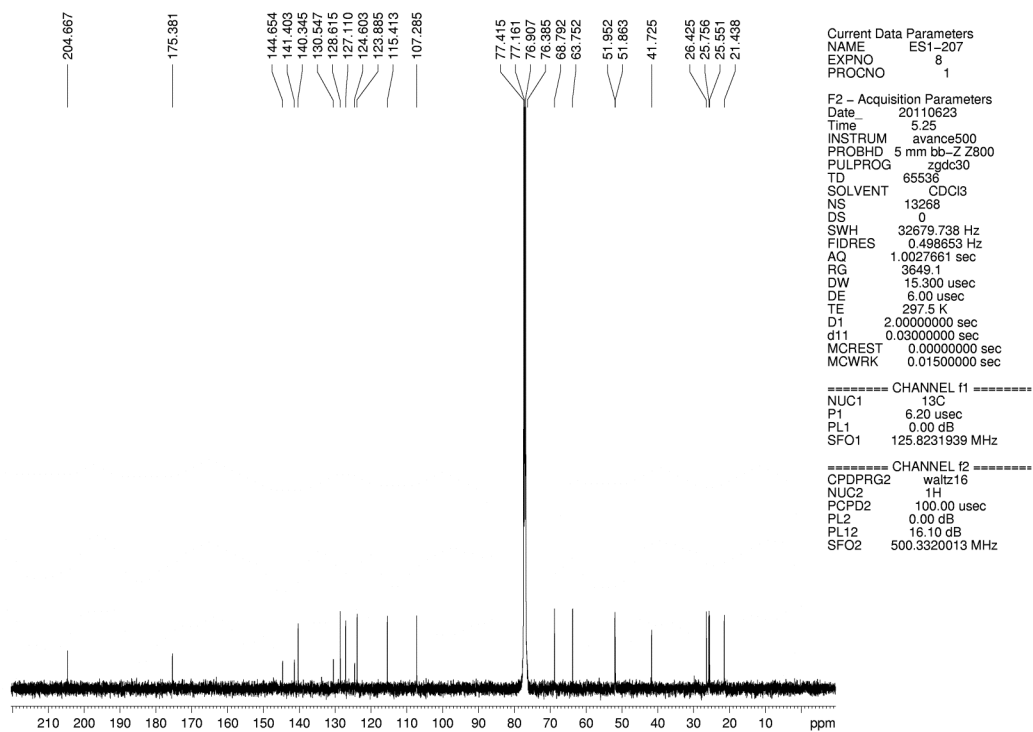


Figure A4.3 ^{13}C NMR (125 MHz, CDCl_3) of compound **5.9**.

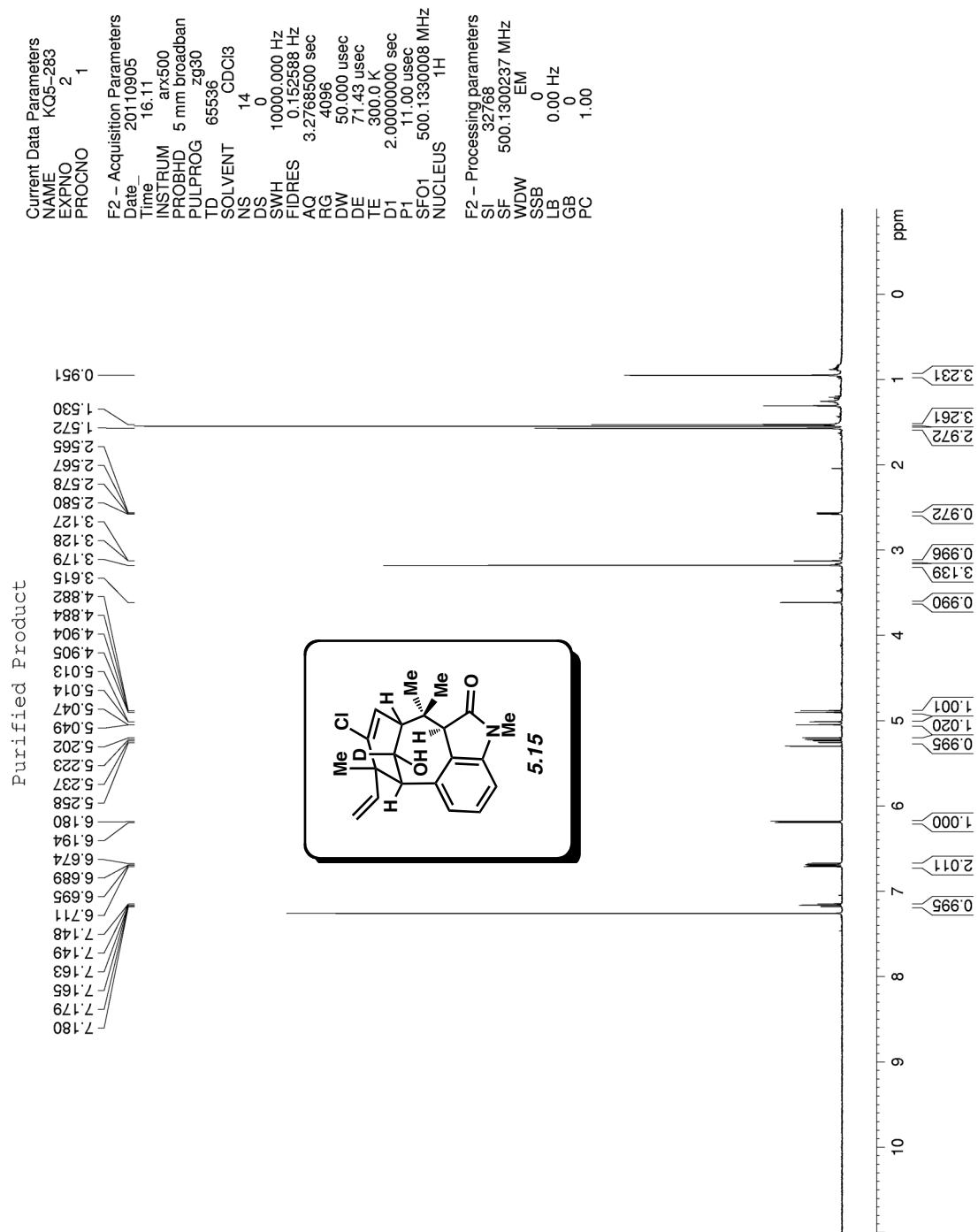


Figure A4.4 ¹H NMR (500 MHz, CDCl₃) of compound 5.15.

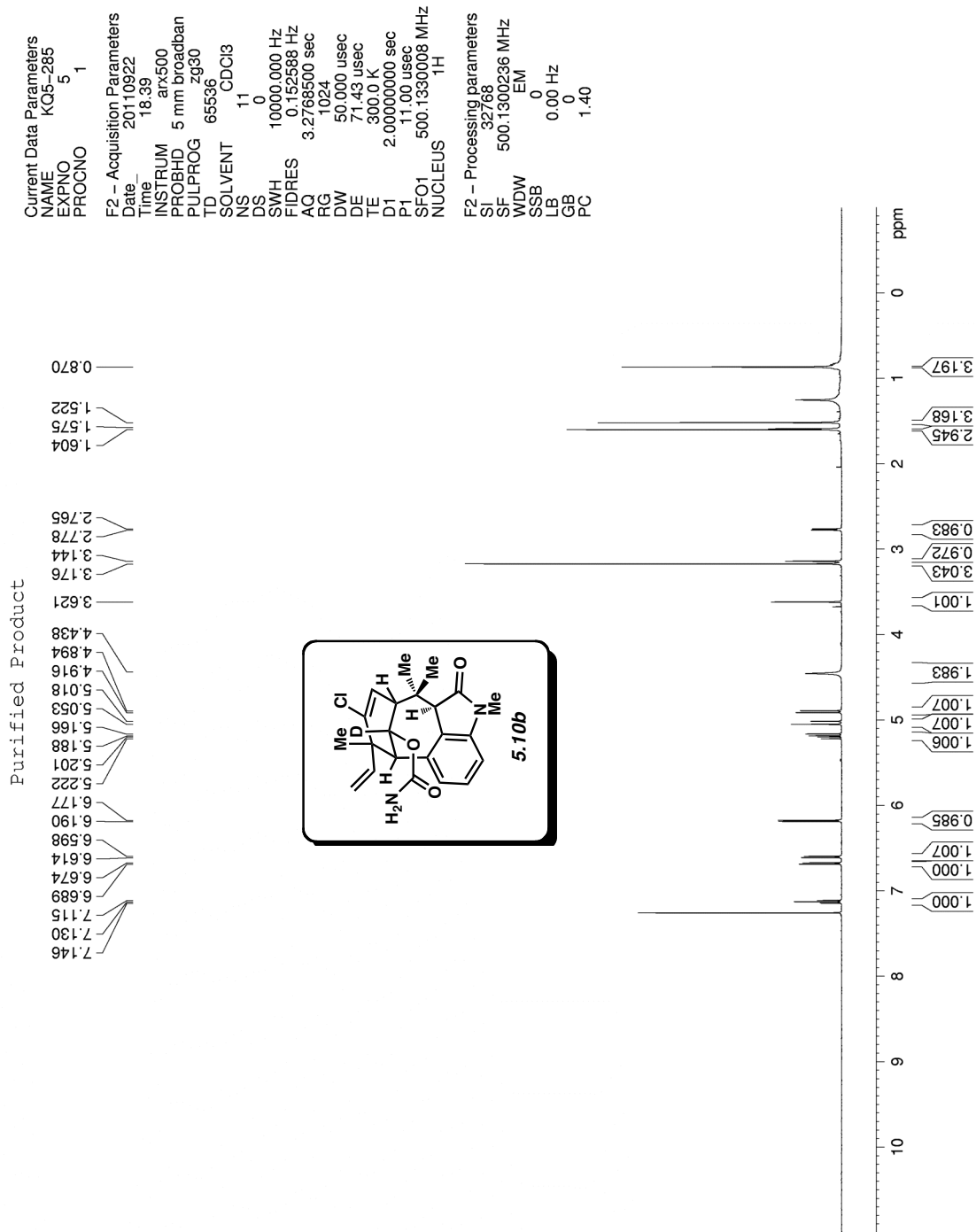


Figure A4.5 ¹H NMR (500 MHz, CDCl₃) of compound 5.10b.

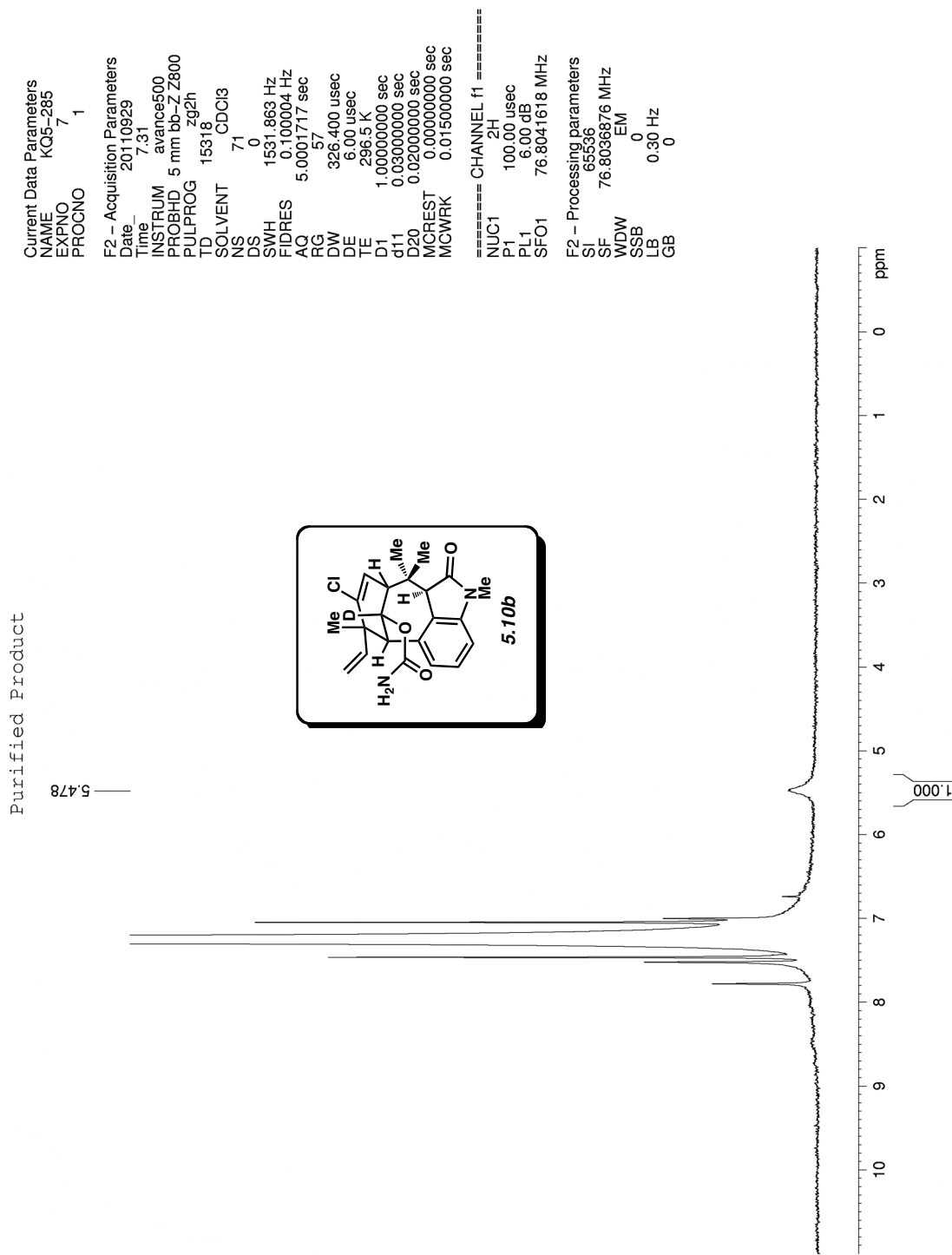


Figure A4.6 ^1H NMR (77 MHz, CDCl_3) of compound **5.10b**.

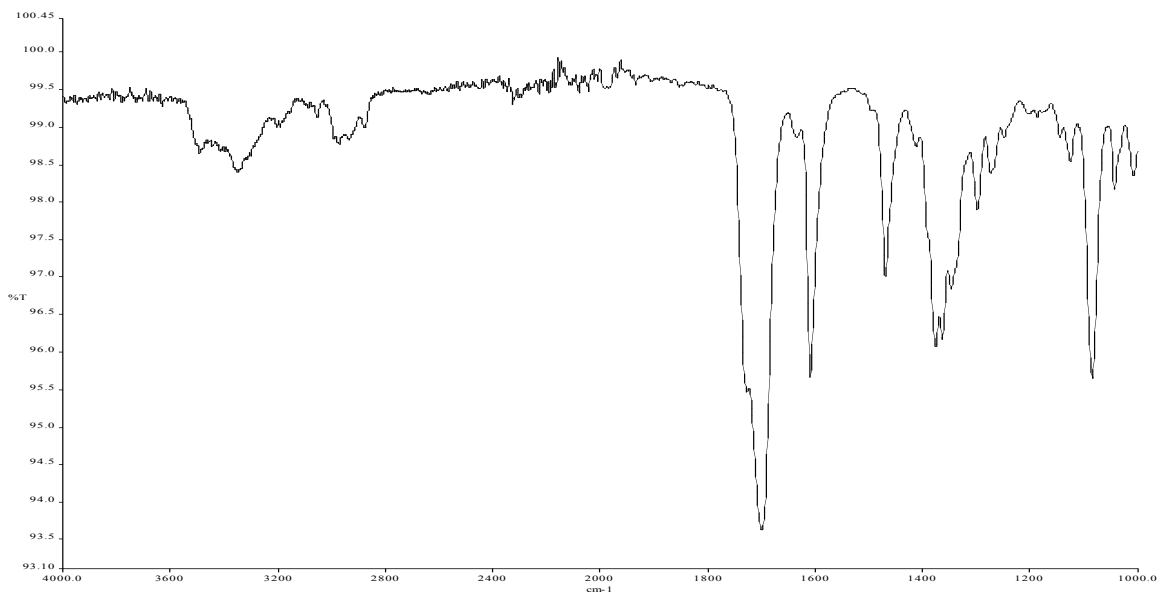


Figure A4.7 Infrared spectrum of compound **5.10b**.

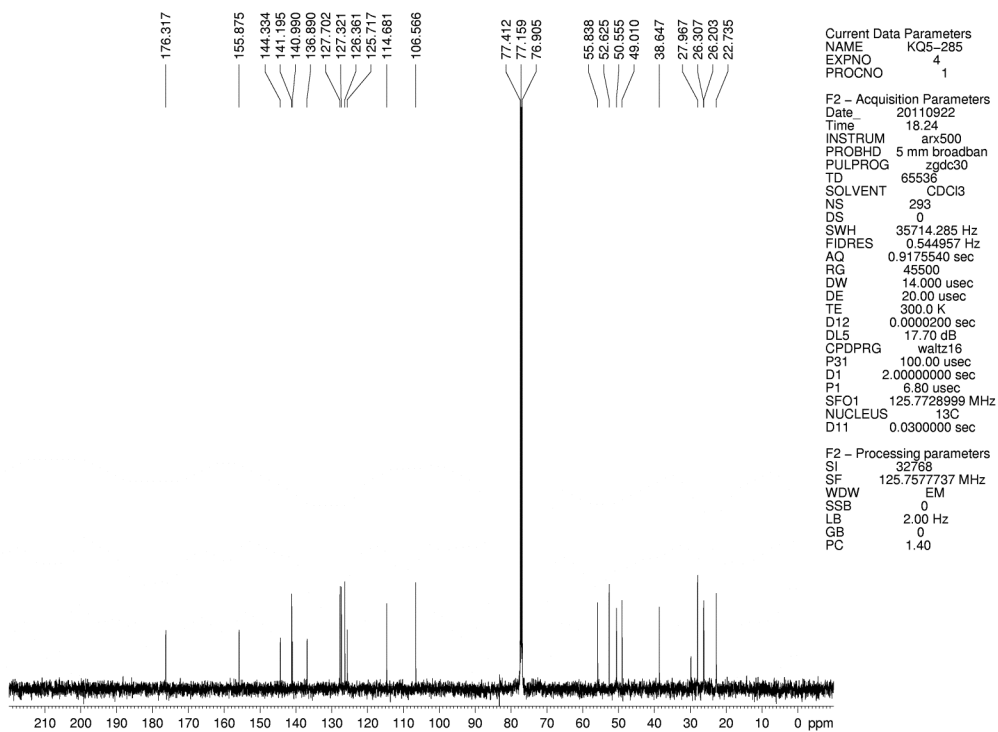


Figure A4.8 ¹³C NMR (125 MHz, CDCl₃) of compound **5.10b**.

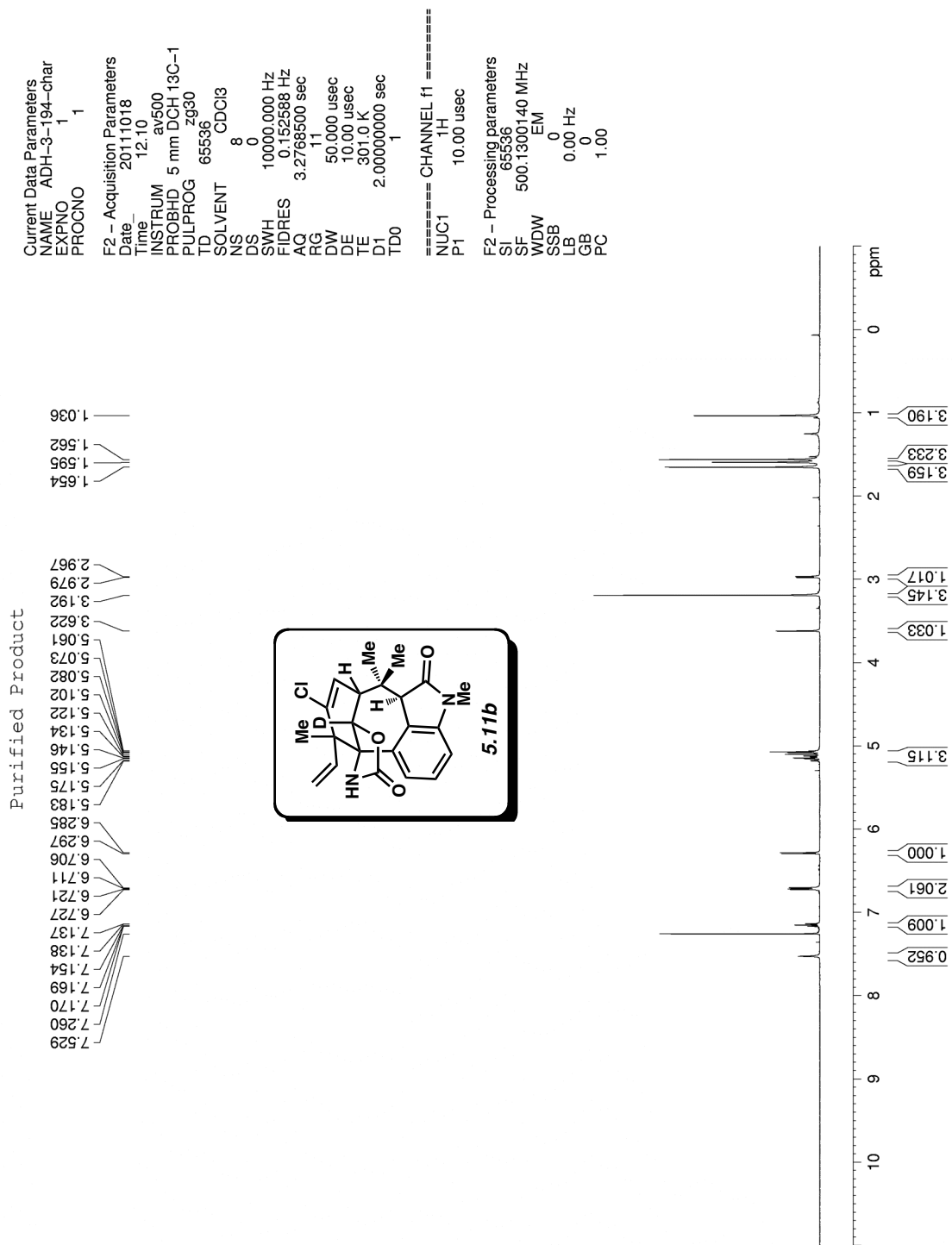


Figure A4.9 ¹H NMR (500 MHz, CDCl₃) of compounds **5.11b**.

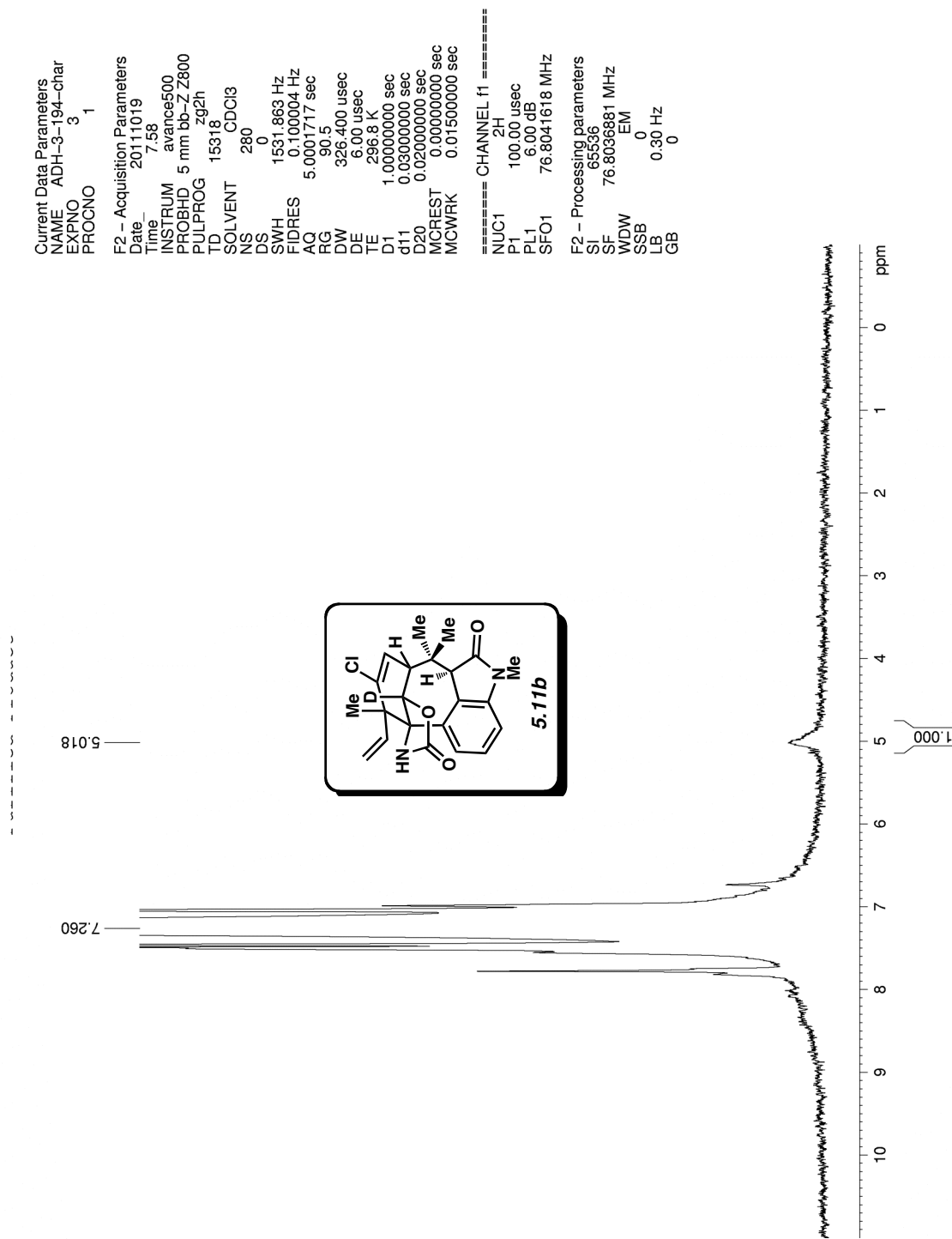


Figure A4.10 ^1H NMR (77 MHz, CDCl_3) of compound 5.11b.

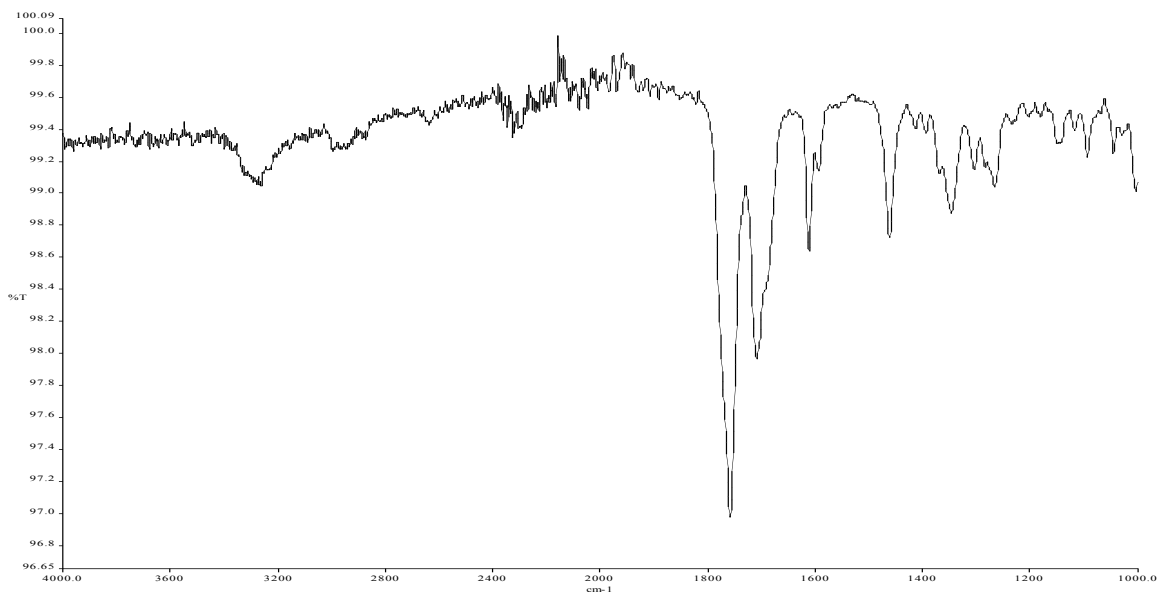


Figure A4.11 Infrared spectrum of compound **5.11b**.

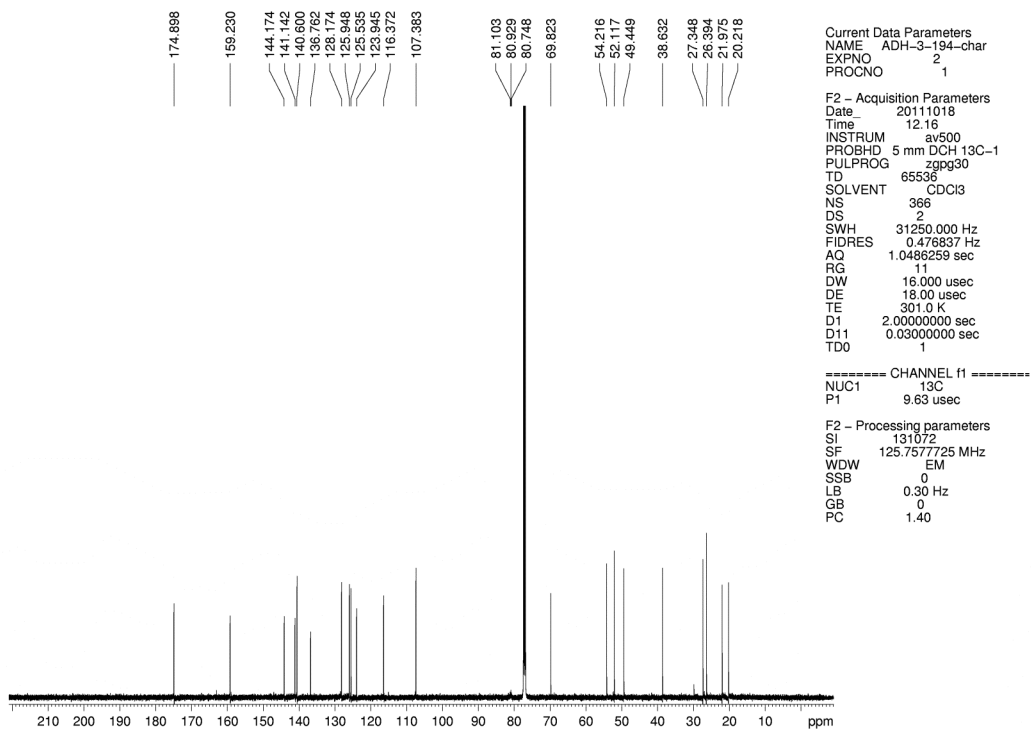


Figure A4.12 ^{13}C NMR (125 MHz, CDCl_3) of compound **5.11b**.

Current Data Parameters
 NAME KC8-241
 EXPNO 4
 PROCNO 1

F2 - Acquisition Parameters
 Date_ 20110707
 Time_ 15.36
 INSTRUM avance600
 PROBHD 5 mm bb-Z Z800
 PULPROG zg30
 TD 65536
 SOLVENT CDCl3
 NS 20
 DS 0
 SWH 10000.000 Hz
 FIDRES 0.152588 Hz
 AQ 3.2769001 sec
 RG 256
 DW 50.000 usec
 DE 6.00 usec
 TE 296.7 K
 D1 2.0000000 sec
 MCREST 0.0000000 sec
 MCWFRK 0.01500000 sec

===== CHANNEL f1 =====
 NUC1 1H
 P1 12.00 usec
 PL1 0.00 dB
 SFO1 500.3330020 MHz

F2 - Processing parameters
 SI 32768
 SF 500.3300220 MHz
 WDW EM
 SSB 0
 LB 0.00 Hz
 GB 0
 PC 1.00

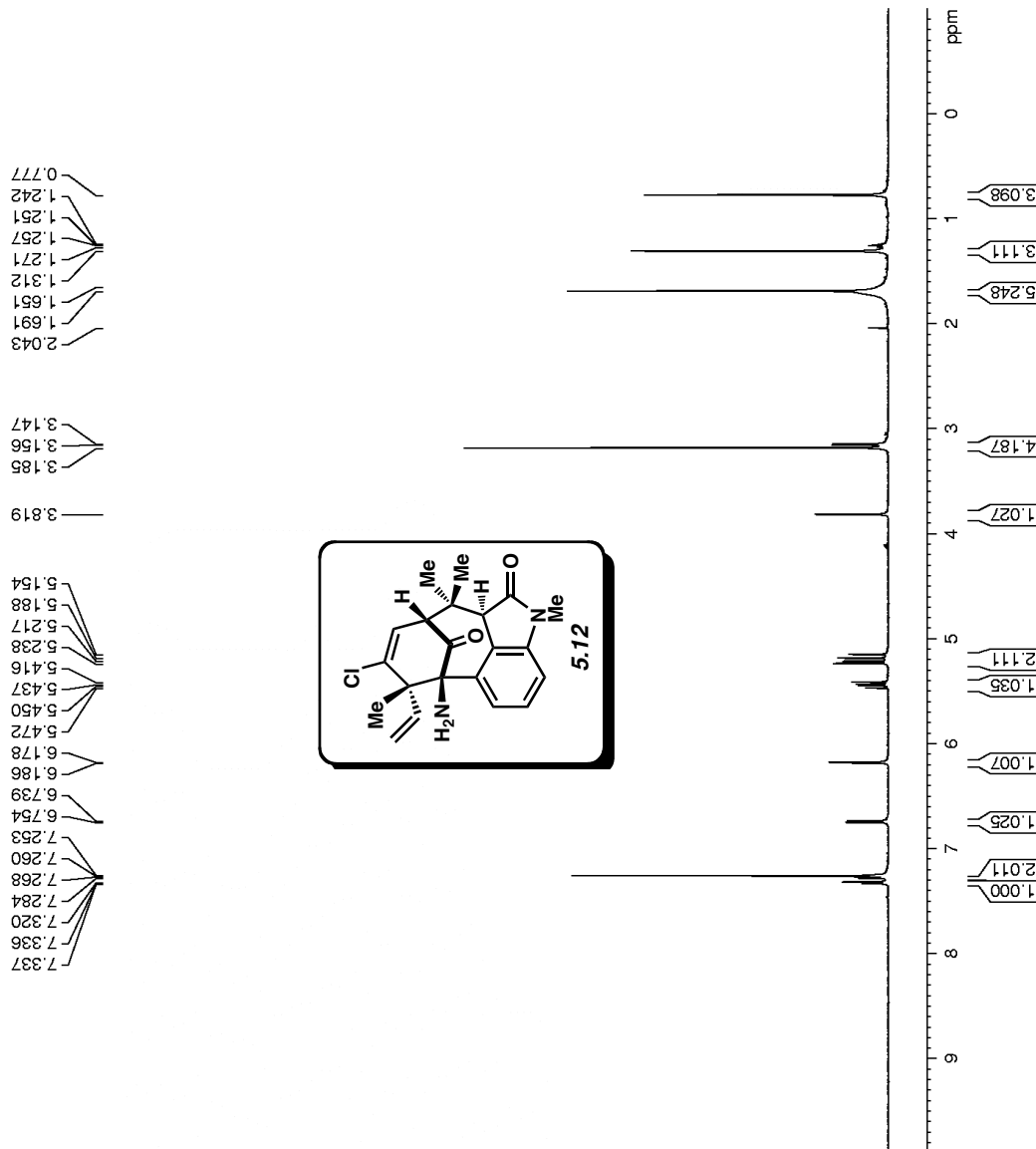


Figure A4.13 ^1H NMR (500 MHz, CDCl_3) of compound 5.12.

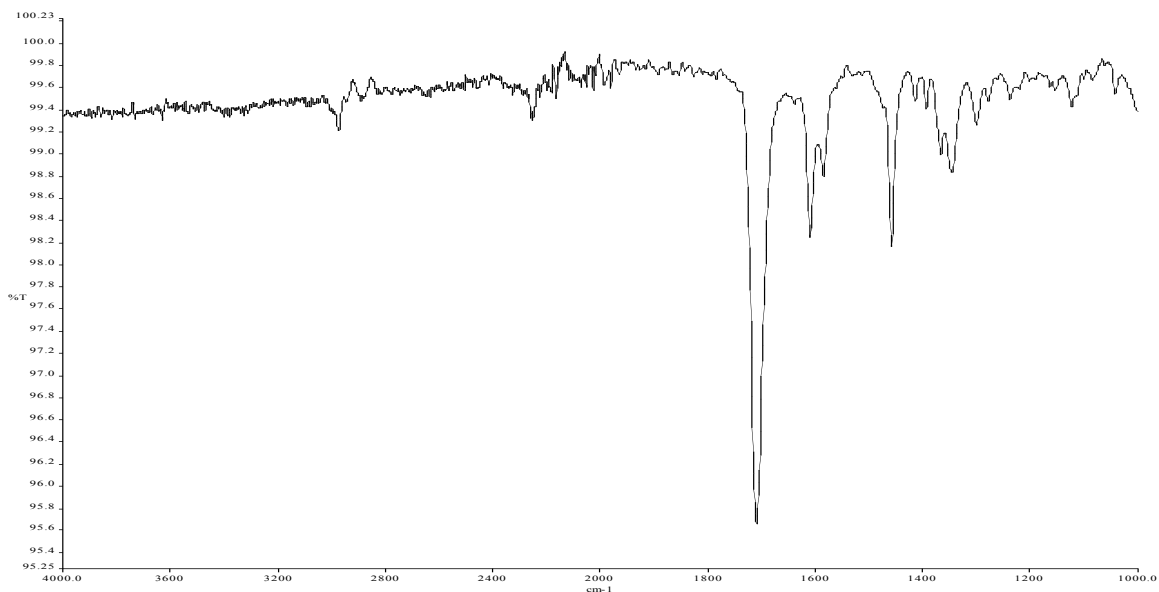


Figure A4.14 Infrared spectrum of compound **5.12**.

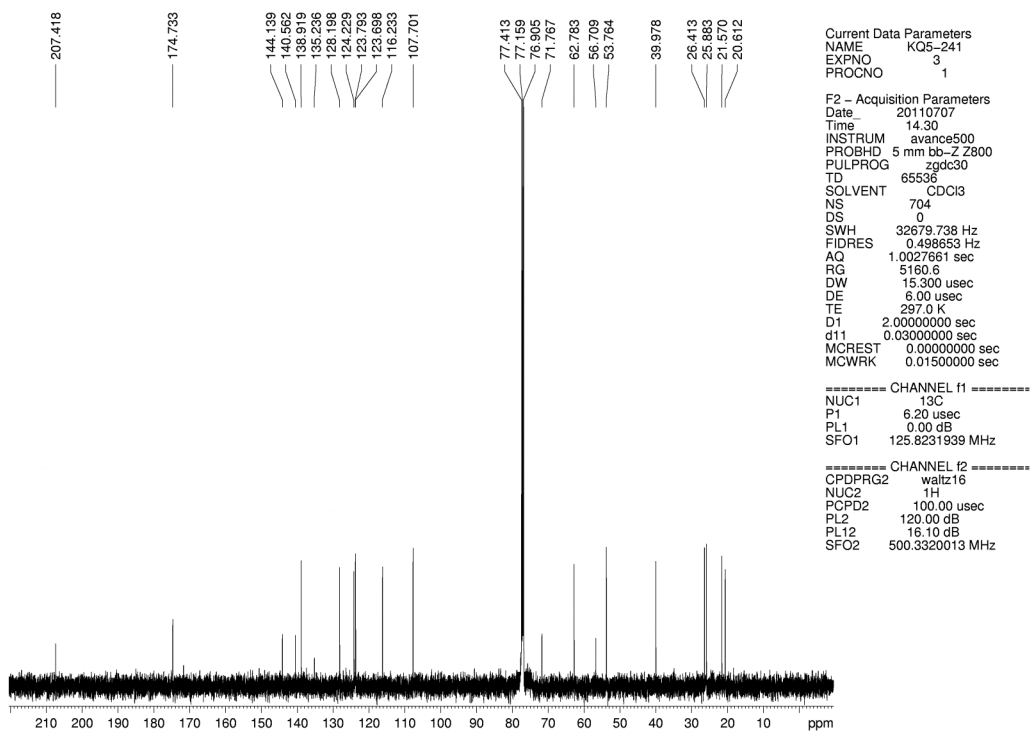


Figure A4.15 ^{13}C NMR (125 MHz, CDCl_3) of compound **5.12**.

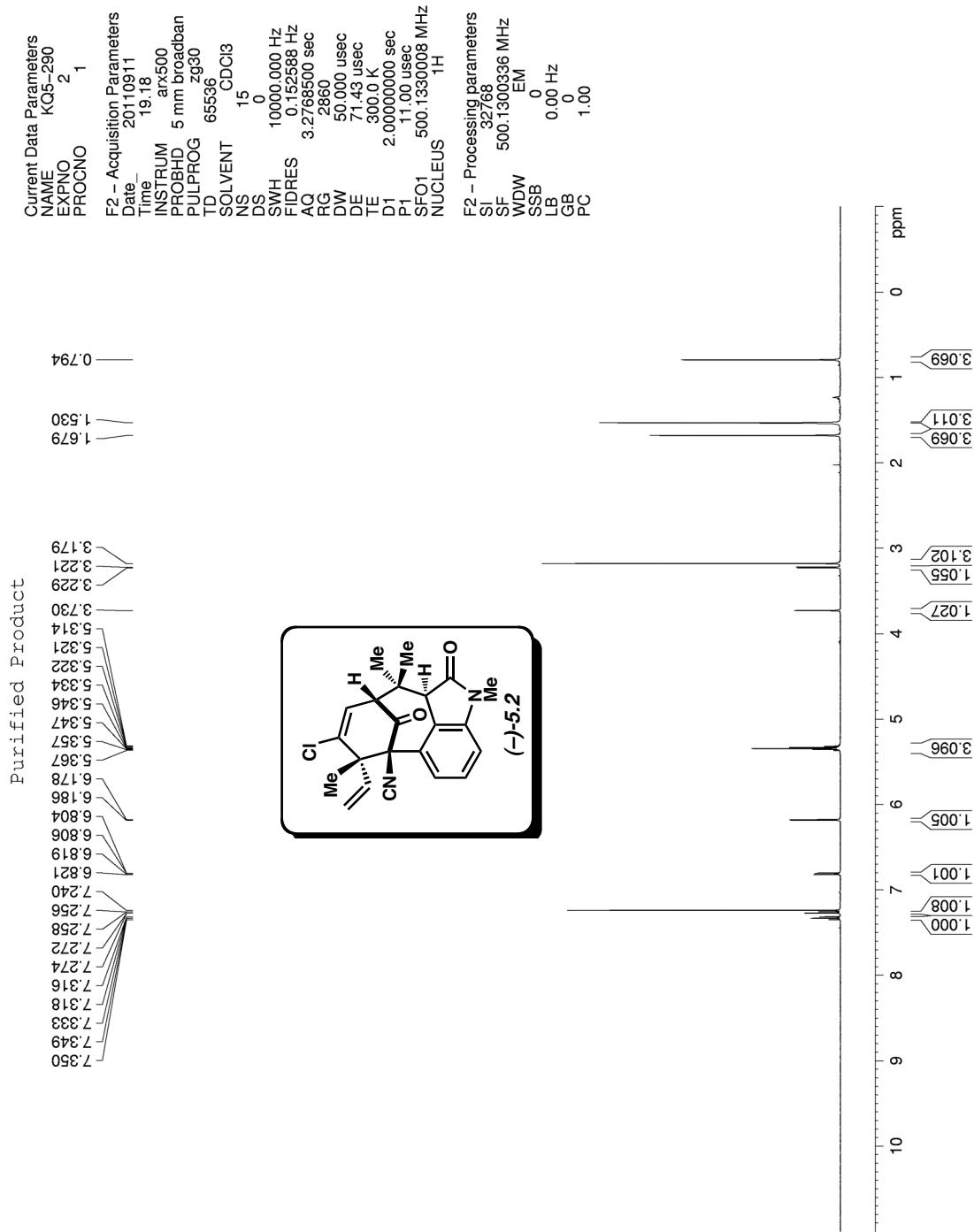


Figure A4.16 ¹H NMR (500 MHz, CDCl₃) of compound 5.2.

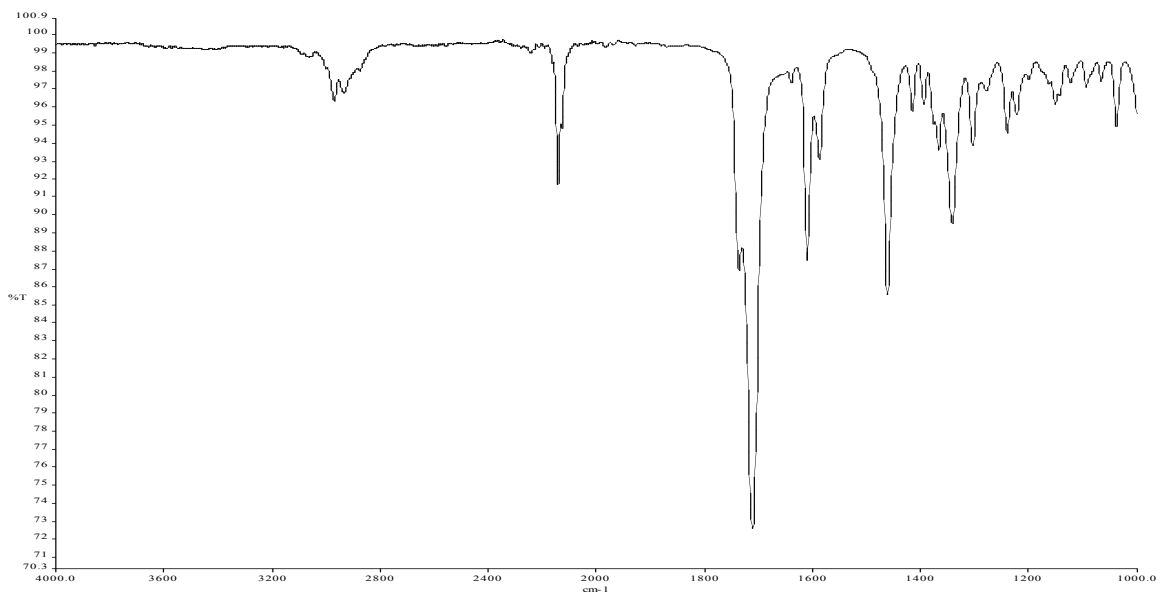


Figure A4.17 Infrared spectrum of compound 5.2.

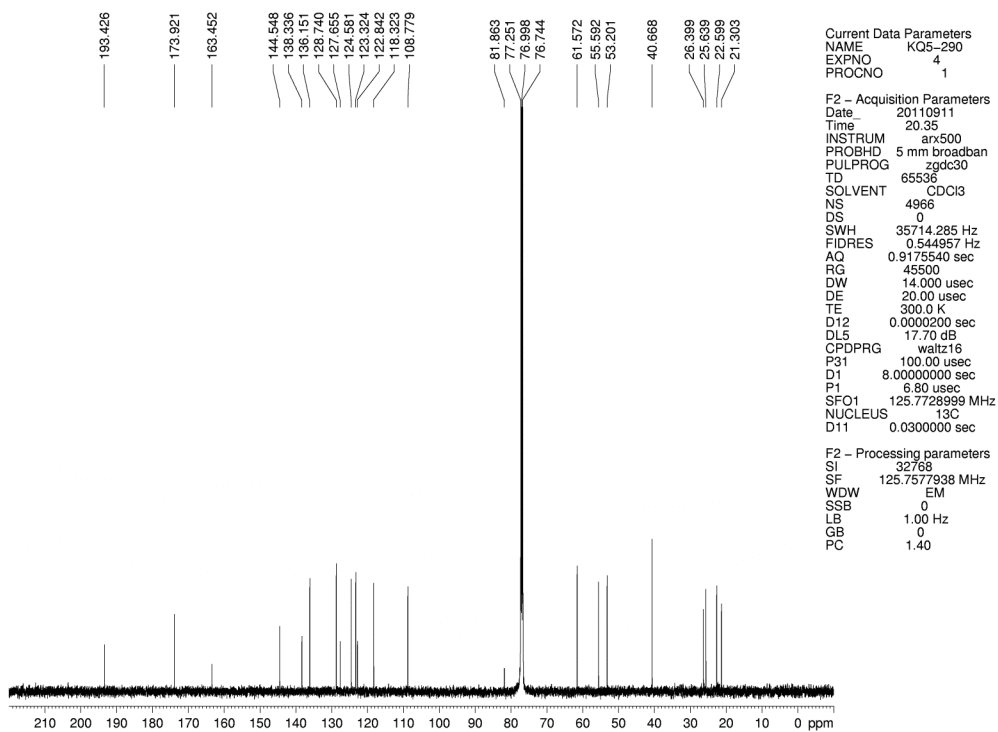


Figure A4.18 ^{13}C NMR (125 MHz, CDCl_3) of compound 5.2.

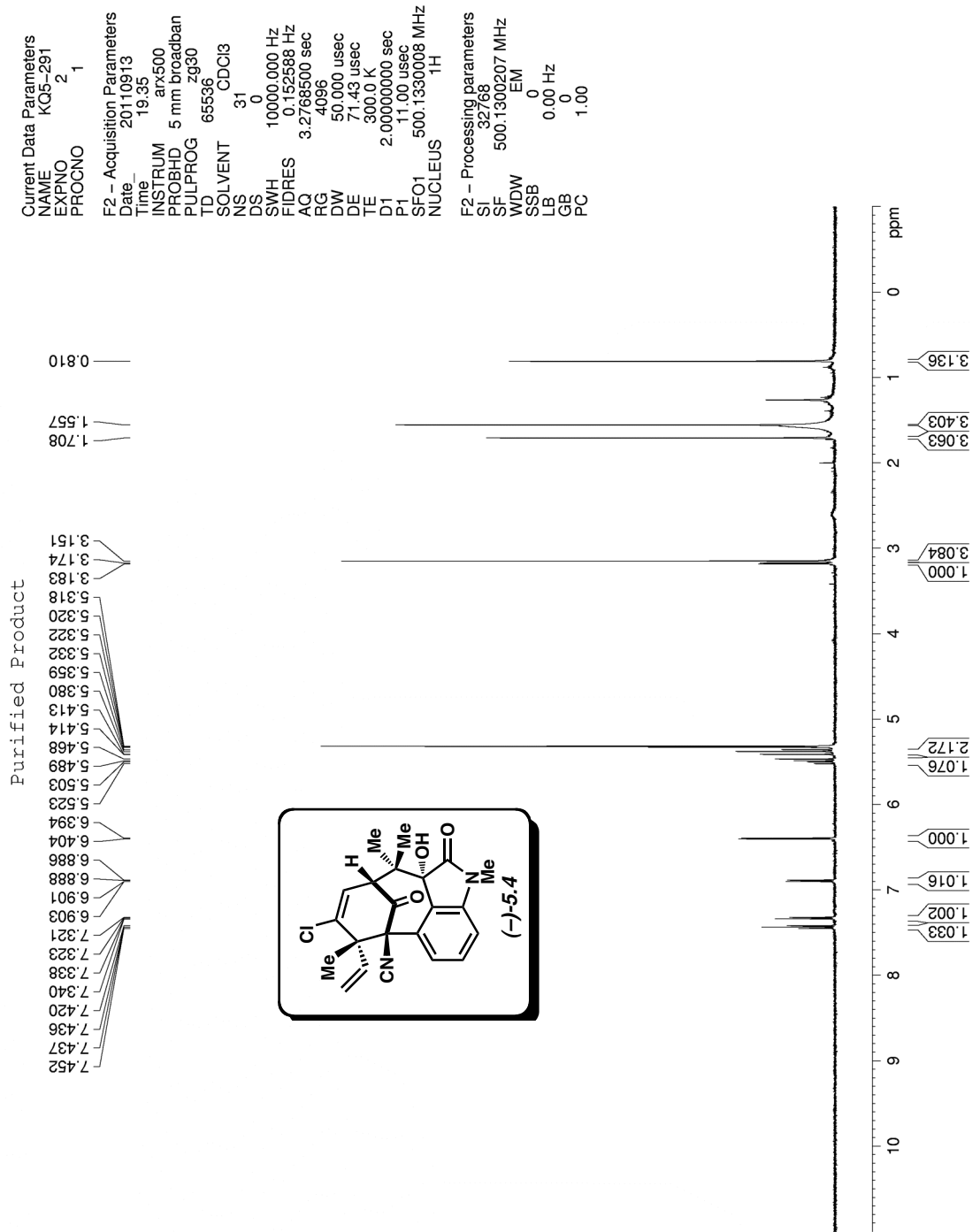


Figure A4.19 ¹H NMR (500 MHz, CD₂Cl₂) of compound 5.4.

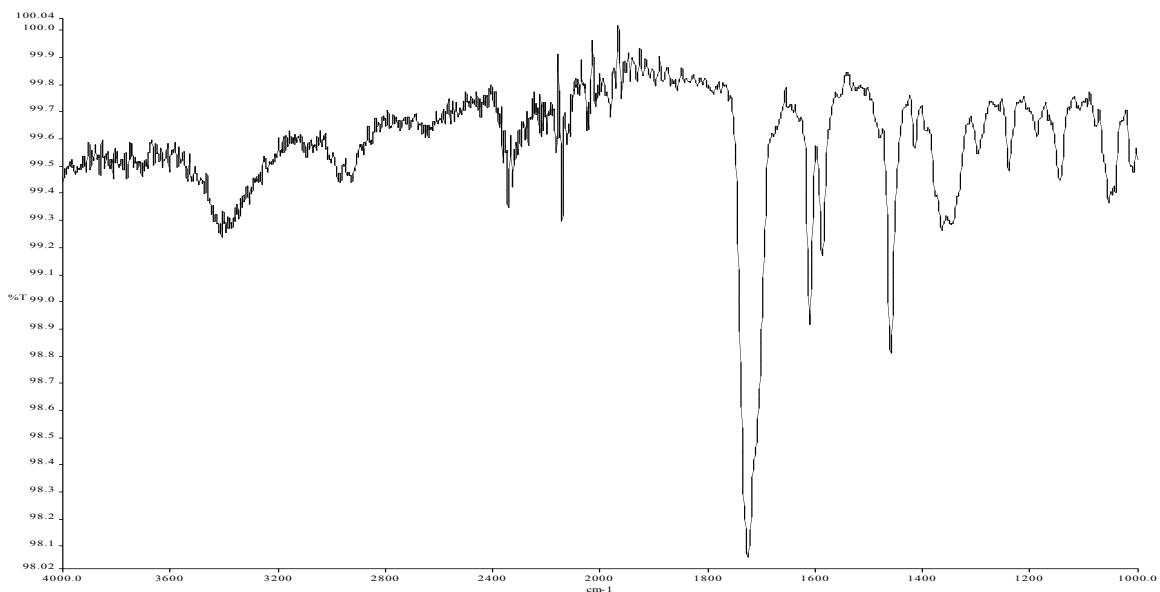


Figure A4.20 Infrared spectrum of compound **5.4**.

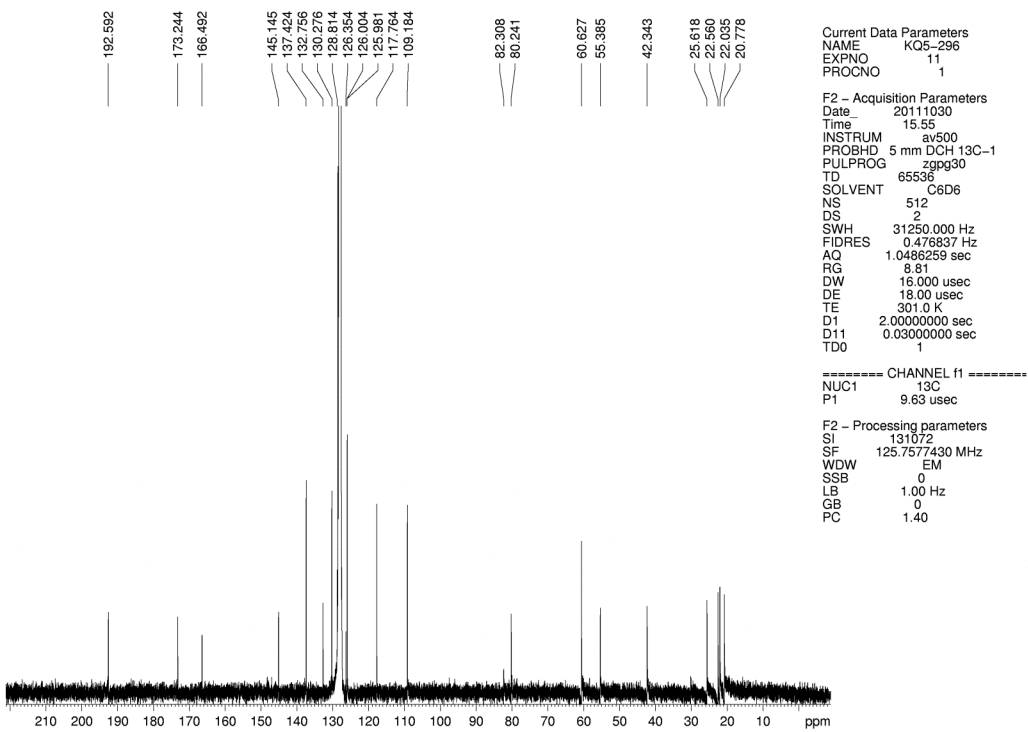


Figure A4.21 ¹³C NMR (125 MHz, C₆D₆) of compound **5.4**.

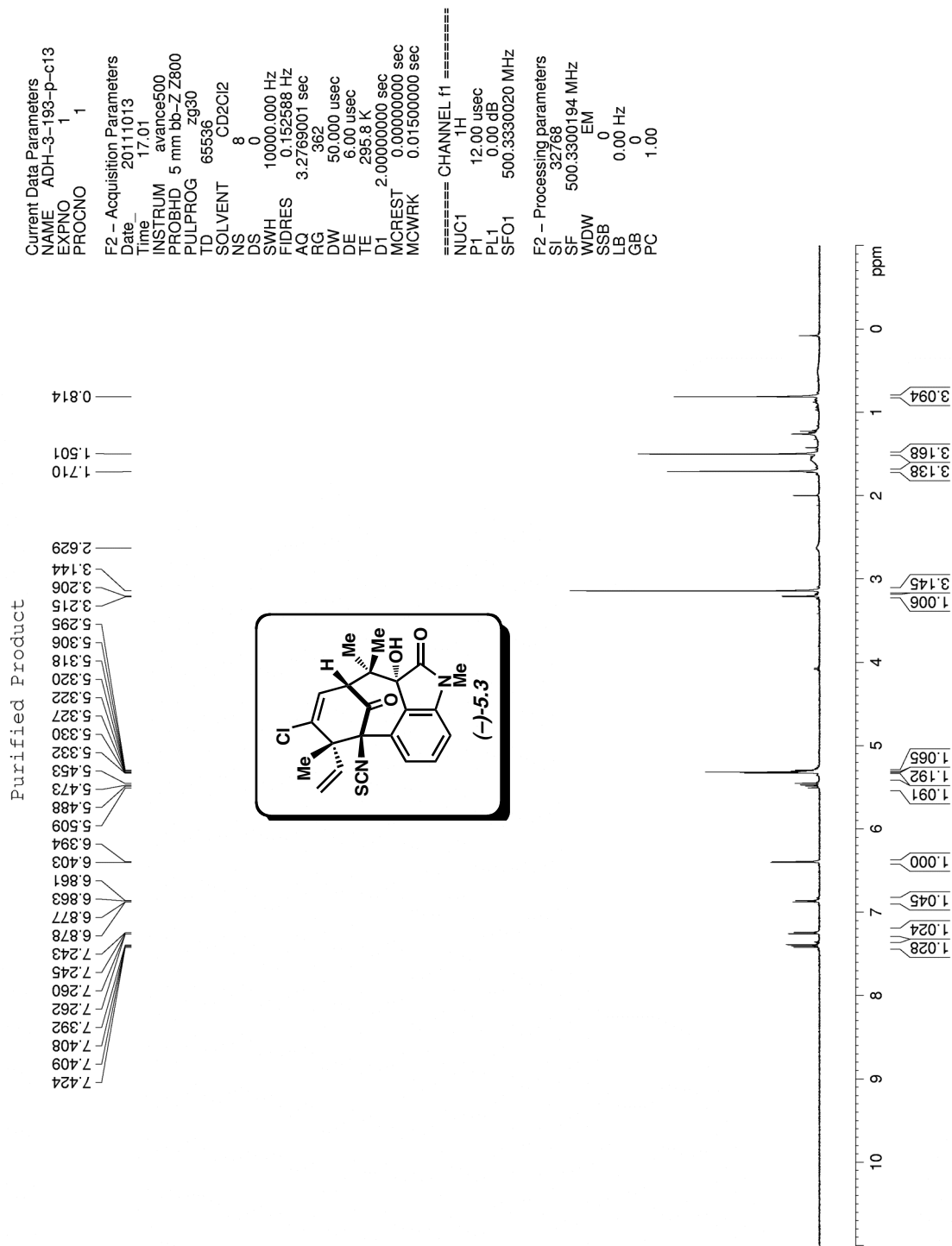


Figure A4.22 ^1H NMR (500 MHz, CD_2Cl_2) of compound **5.3**.

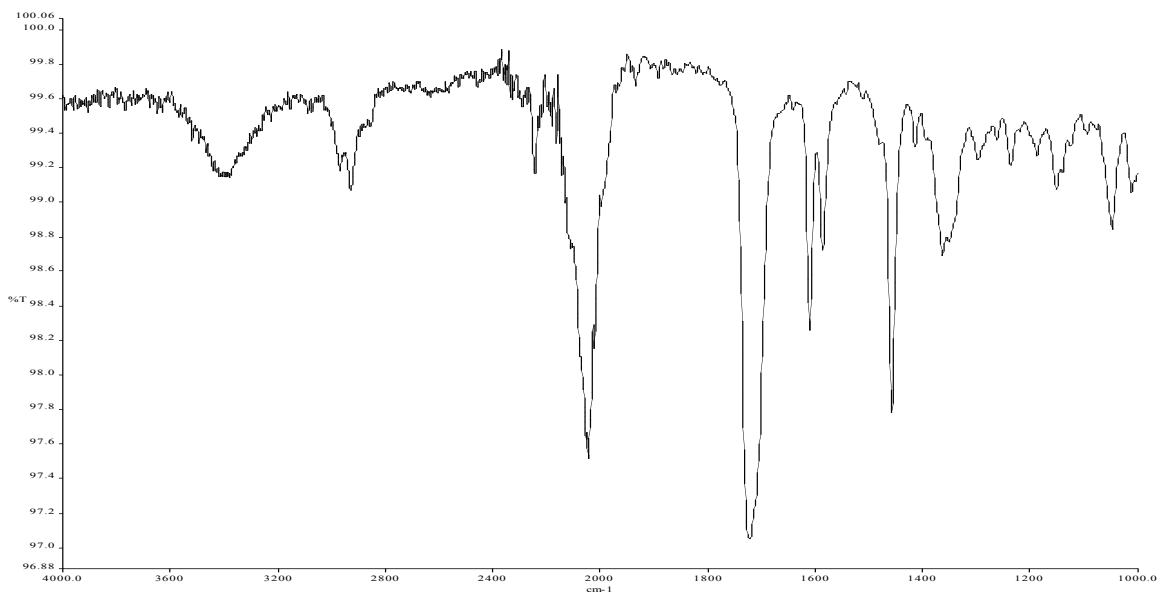


Figure A4.23 Infrared spectrum of compound **5.3**.

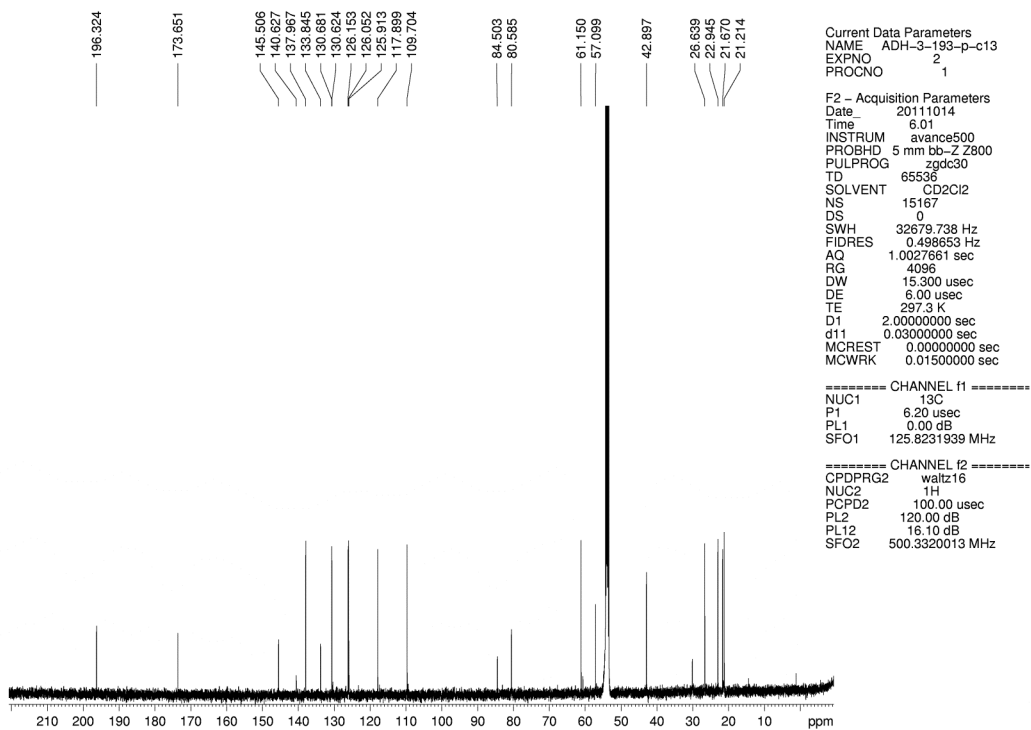


Figure A4.24 ^{13}C NMR (125 MHz, CD_2Cl_2) of compound **5.3**.

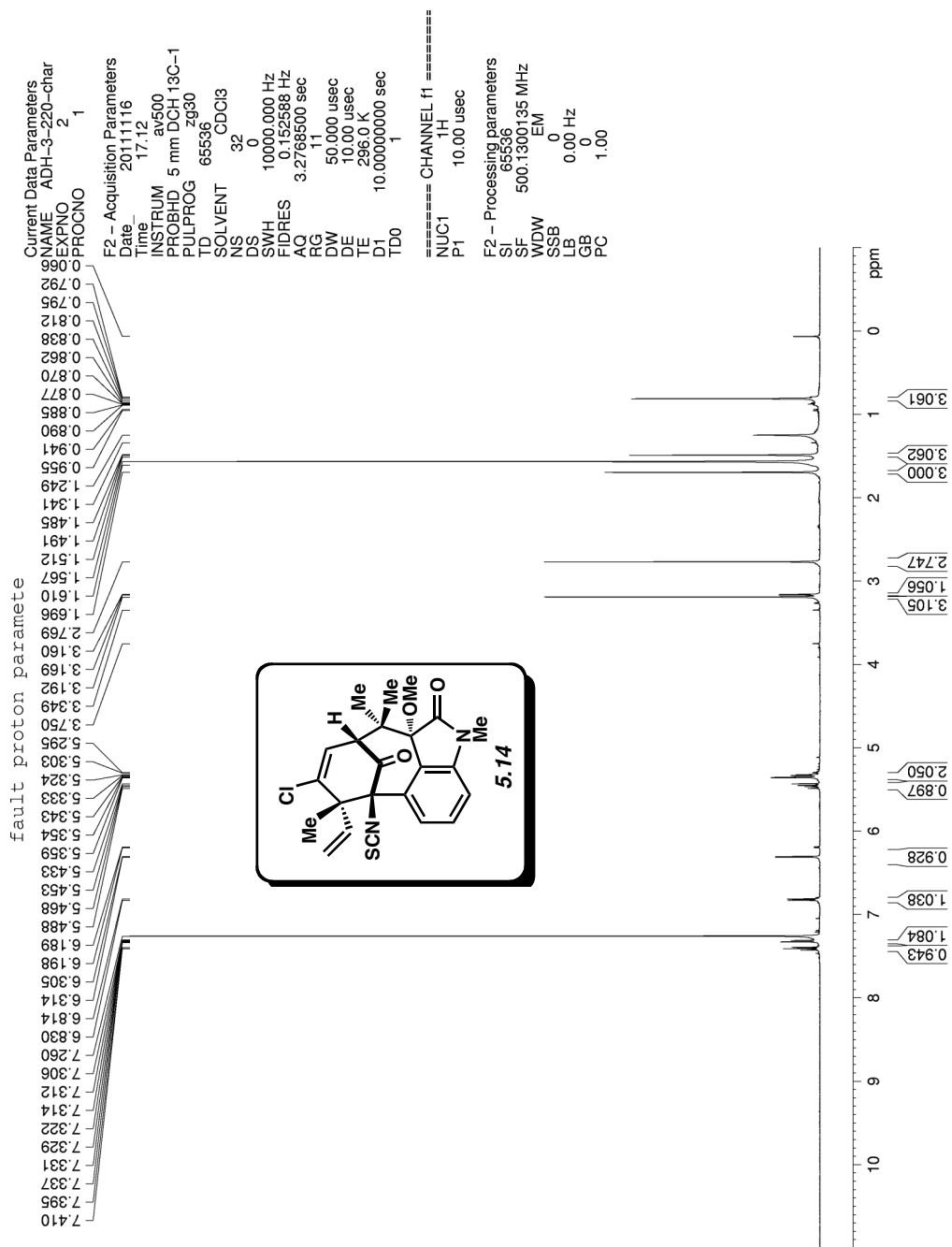


Figure A4.25 ^1H NMR (500 MHz, CDCl_3) of compound **5.14**.

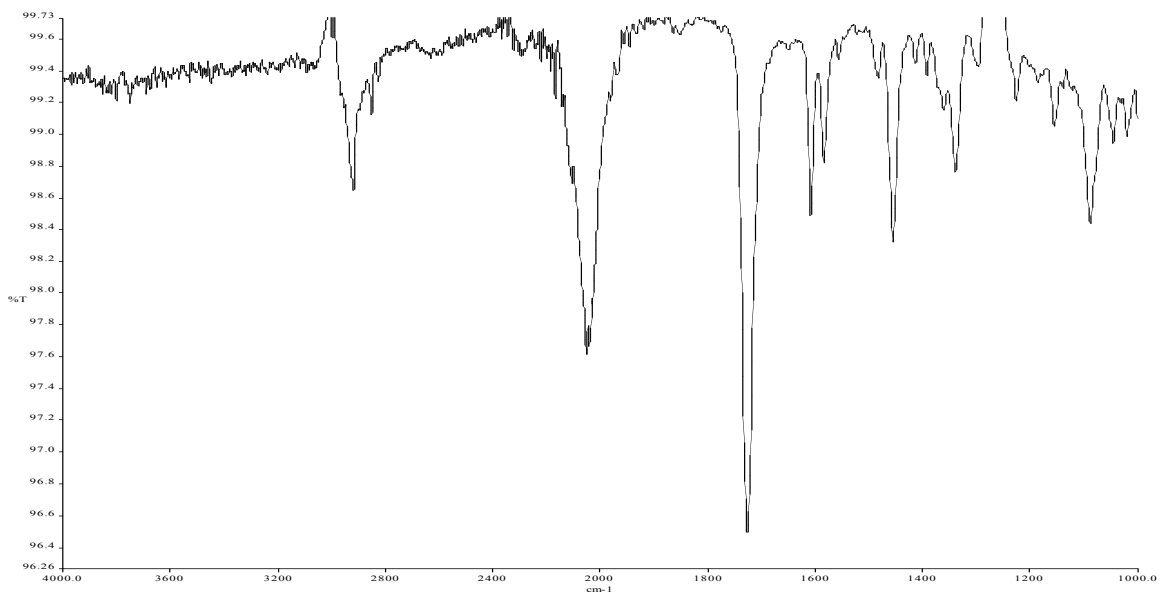


Figure A4.26 Infrared spectrum of compound **5.14**.

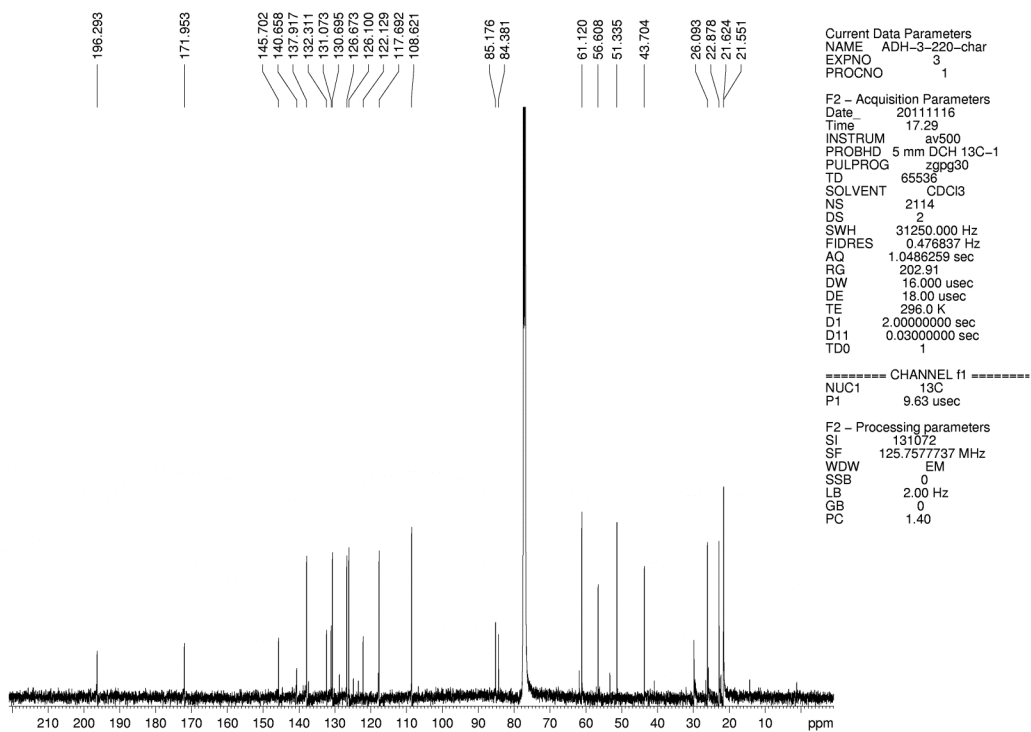


Figure A4.27 ¹³C NMR (125 MHz, CDCl₃) of compound **5.14**.